

ABSTRACT

CASE, SAMANTHA LEONG. Genetic Association Mapping of Agronomic, Fruit Quality, and Metabolic Traits in Blueberry and Broccoli. (Under the direction of Dr. Xu Li).

Eating more fruits and vegetables is widely known to provide numerous health benefits, and fruit and vegetable consumption should therefore increase as compared grains. Improving fruit and vegetable consumption entails increasing the agronomic supply while also improving the fruit quality and consumer appeal. Association mapping statistically links genetic variation with trait variation. The research goals of this dissertation are to identify important quantitative trait loci (QTLs) associated with agronomic and fruit quality traits as well as metabolic traits from metabolite profiling through association mapping for blueberry and broccoli.

Blueberries, *Vaccinium corymbosum*, are known for their potent antioxidant health benefits and unique color and taste. Blueberry buds undergo dormancy to protect the meristems from harsh conditions, and then dormancy break when favorable conditions return to resume meristem growth. The floral bud density and break efficiency is an important determinant of fruit yield. The Draper by Jewel (DxJ) mapping population is optimal for investigating agronomics and fruit quality because the parents represent the commercial growth range. With a DxJ specific tetraploid genetic map, biparental association mapping (BiPAM) using multiple different analyses was conducted on multiple growth and dormancy traits. The growth traits BiPAM results revealed multiple QTLs that are impacted by the location and year environmental variation. The dormancy break and flowering traits BiPAM results identified multiple QTLs that are strongly influenced by the yearly environmental variation. The past improvements in yield have sacrificed consumer-driven fruit quality, like texture, flavor, and nutrition, due to the breeding selection for industry-driven fruit quality that decreased metabolite diversity. The BiPAM results for ripening and consumer-driven fruit quality traits in DxJ revealed that the majority of QTLs impact firmness regardless of environmental variation. The remaining fruit quality QTLs influence fruit color, flavor, and nutrition regardless of environmental variation.

Investigating the blueberry metabolite diversity through metabolite profiling provides insight into the different metabolic pathways contributing to fruit quality and

nutrition. The metabolite profiling of the DxJ population detected and annotated 23 anthocyanin peaks using targeted HPLC-QTOFMS, and 29 other metabolite peaks using non-targeted ¹H NMR. Multiple anthocyanin correlations across the population revealed two subsets: one subset accumulates all the anthocyanin sugar moieties, while the other subset accumulates only two. The LC-MS anthocyanins BiPAM results reveal multiple QTLs, especially for acylated-glucosides. The ¹H NMR metabolites' BiPAM results revealed multiple QTLs with putative candidate genes for amino acid biosynthesis, sugar signaling, and phenolic acid biosynthesis. The antioxidant capacity BiPAM results identified QTLs with putative candidate genes from the shikimic, phenylpropanoid, flavonoid, and anthocyanin diversification pathways.

Broccoli, *Brassica oleracea* var. *italica*, has recently been shown to exhibit potent anticarcinogenic health benefits, resulting in an increased demand. High-yield broccoli cultivars exhibit low specialized metabolite diversity, which decreases broccoli health benefits and endogenous pathogen resistance. With a broccoli-specific genetic map, genome-wide association mapping (GWAS) was conducted on a global diversity population to investigate agronomic traits for harvest, growth, and pathogen resistance. The harvest GWAS QTLs revealed candidate genes involved in photoperiodism and floral meristem regulation. The multiple pathogen-related GWAS QTLs revealed candidate genes involved in each stage of pathogen resistance: recognition, signaling, and physiological response.

The identification of significant QTLs for blueberry growth and dormancy, as well as broccoli harvest will allow for elucidation of the multiple pathways involved in regulating floral bud development to improve future blueberry and broccoli production. Along with the BiPAM QTLs for consumer-driven fruit quality traits like texture and nutrition, the blueberry metabolic profiling and putative candidate genes underneath the QTLs will provide important foundational knowledge for blueberry metabolic pathways, and aid in future breeding strategies to develop blueberry cultivars with enhanced fruit quality and health benefits.

© Copyright 2019 by Samantha Leong Case

All Rights Reserved

Genetic Association Mapping of Agronomic, Fruit Quality, and Metabolic Traits in
Blueberry and Broccoli

by
Samantha Leong Case

A dissertation submitted to the Graduate Faculty of
North Carolina State University
in partial fulfillment of the
requirements for the Degree of
Doctor of Philosophy

Plant Biology

Raleigh, North Carolina
2019

APPROVED BY:

Dr. Xu Li
Committee Chair

Dr. Jose Alonso

Dr. Tzung-Fu Hsieh

Dr. Mary Ann Lila

Dr. Massimo Iorizzo

Dr. Robert Reid
External Member

DEDICATION

To all the family, friends, and colleagues who gave their steadfast support.

BIOGRAPHY

Samantha Leong Case was born in Washington, D.C. to the Case family who love learning, sports, and music. Her two older sisters should have never tricked her into eating dirt and her little brother should have not shown her earthworms as it may have inspired her future love for nature and plants. Samantha's inspiration to pursue science and music was ignited in her environmental science class and wind ensemble trombone part at Langley High School. Samantha decided to attend the liberal arts college Denison University in Granville, OH so she could learn a multitude of different subjects while pursuing biology and music degrees. In her pursuit of a Bachelor of Science in Biology, Samantha tried to take an oceanography class, but was default enrolled in the plant evolution and reproduction course with Dr. Andrew McCall. Little did she know that Dr. McCall's love and enthusiasm for plants would inspire the rest of Samantha's career. Luckily, Dr. McCall had on-going research that allowed Samantha to pursue a senior research project on prior floral damage inducing resistance in leaves or late flowers in wild radish. Through her senior research and biochemistry class, Samantha was inspired to also graduate with a chemistry minor. Samantha graduated from Denison University in 2012 with a Bachelor of Science in Biology, minor in chemistry, and minor in music performance.

To discover more about plant ecology, Samantha worked three months with the Great Basin Institute Nevada Conservation Corps, a part of Americorps, to rehabilitate trails and habitats, but soon realized she loved plant biochemistry and decided to further her education with a graduate degree. In 2013, Samantha interviewed for Ph.D. programs and was excited to receive an offer from the Department of Plant and Microbial Biology as a graduate research assistant working in the Plant Pathways Elucidation Project (P²EP) at North Carolina State University. The summer before her first semester of classes, Samantha moved to Kannapolis, NC to start the first P²EP undergraduate summer internship program. It was a whirlwind of excitement and frustration as Samantha, along with four other new graduate students, were tasked with each leading a team of 4-5 undergraduate students through a summer research project.

Samantha took an over-loaded and condensed class schedule for three semesters in Raleigh, NC at main campus, while summers were completely occupied

developing, managing, and mentoring the P²EP undergraduate summer internship program. In 2015, Samantha began her Ph.D. research full-time under the advisement of Dr. Xu Li and other committee members as part of the P²EP research program in Kannapolis, NC at the Plants for Human Health Institute (PHHI). The multidisciplinary environment of the PHHI and other universities at the North Carolina Research Campus allowed Samantha to develop her dissertation research to associate important agronomic, fruit quality, and metabolite characteristics with genomic regions in blueberry and broccoli. Throughout her Ph.D., Samantha directly mentored 28 undergraduate students during the summer internship program, which helped her develop valuable leadership, team dynamic, and program management skills. To aid the undergraduates with communication and presentation skills, the P²EP program showcased the summer research with a research symposium. At least one intern each summer utilized part of the summer research for further research projects at their respective school. Now as Samantha is finishing her studies, she is excited to begin applying all that she has learned into innovative plant research. Samantha hopes to gain further knowledge and experience in emerging technologies and research to help develop sustainable food that promote human health.

ACKNOWLEDGMENTS

At many points, working towards a Ph.D. was an unpredictable, stressful endeavor that seemed like an impossible venture. But friends and family provided unwavering support to lead me through. My wonderful husband, Evan, was my most ardent supporter with his motivation and optimism. I am eternally grateful to have you with me. Thank you to all my family – Dad, Mama, Jessica, Claiborne, Amanda, David, and Davey – for being great examples of lifelong learners and for constantly bringing joy and positivity to my life. You were all essential to keeping my spirits up and directly maintaining my sanity during this adventure

To my advisors and committee members, thank you for your advice and support throughout the frustrations and achievements of my research. This Ph.D. research and environment was a once in a lifetime opportunity to learn about and be a part of innovative research while also giving back to others through mentoring students throughout this experience. Thank you for everything you have taught me.

To everyone in the Li lab – Han-yi, Amanda, Chinmayee, and Xin – it was great to work with you all for over five years. Thank you for teaching me and helping me learn how to be a researcher.

To everyone in the Lila lab – Mary, Renee, Lorie, and Charles – it was amazing to also work alongside you all for over five years. Thank you for teaching and helping me work through the large samples of berries. I loved our very fun conversations in between sample prep or runs.

Thank you to everyone involved in the development and growing of the Draper by Jewel (DxJ) mapping population. A special thank you to Dr. Jim Hancock, Dr. Jozer Mangandi, Dr. Michael Timmers, and Ed Wheeler from Berry Blue Farms and Nursery, LLC for helping with the blueberry harvesting and guidance throughout the DxJ research. Thank you to Dr. Chad Finn and his lab for population growth and sampling as well as Dr. Nahla Bassil and her lab for genetic marker and genotype analysis from the Horticultural Crops Research group and National Clonal Germplasm Repository at the USDA-Agriculture Research Service. Thank you to Dr. Jim Olmstead and his lab at the University of Florida for DxJ population growth and phenotyping.

Thank you to all the professors and staff in the Department of Plant and Microbial Biology for teaching and guiding me through the wonderful world of plants. A special thank you to Dr. Blanton for supporting me throughout, especially during my transitions and distance between Raleigh and Kannapolis.

To everyone involved in the Plant Pathways Elucidation Project, there have been so many great memories from this program. It was an honor to be part of developing, mentoring, and growing such an amazing program as a graduate student. I am excited to utilize these program development and management skills throughout my career. Thank you to Tara, Susan, Claire, Aubrey, and Megan as the P²EP support team for managing the program throughout the years. A very special thank you to Ebony as the P²EP internship program manager as your confidence and encouragement brought about improvements throughout the internship program, and inspired determination in me to continually accomplish my goals in research and life. Thank you to the P²EP industry partners - Eric Jackson, Corey Scott, and Nick Gillet - whose advice showcased the applicability and big picture of P²EP research. A very special thank you to my fellow P²EP graduate mentors – Scott, Richard, Weston, Neha, Yu-Hung, Shawn, Adriano, Koyt, Jaime, Kelsey, Bryan, and Aaron. Your constant support and lively discussion kept everyone grounded and positive. It was amazing to share this graduate school experience with everyone.

Thank you to the University of North Carolina – Charlotte Bioinformatics Services Division, especially Dr. Brouwer, Rob, Jeremy, and Steven. I truly appreciate your easy acceptance of me as part of the group from the beginning, even though my computer skills were laughable. Your drive for to learn and constantly improving your skills deeply inspires me to continue learning throughout life, especially in computers.

Thank you to Dr. Kevin Knagge and his metabolomics-analytic science research team at the David H. Murdock Research Institute (DHMRI) at the NCRC for assisting with running and software analysis of the ¹H NMR non-targeted profiling of blueberry extracts.

Finally, thank you to all of the amazing undergraduate student that worked with me during the P²EP summer internship program. Teaching, coaching, learning, and working with you all was an unforgettable experience that will guide me throughout my

career. Thank you Kevon Stanford, Kiristin Klement, Amber Williamson, Jordan Hartman, Tamara Marlowe, and Christian Krzykwa; Titus Hunt, Fernando Guerrero-Nava, Daniel Sanchez, Stephany Daniel-Lopez, Austin Gibbs, Alexis Brown; Doriane Taylor, Zjanazja Cornwall, Jonathan Fabish, James Lohr; Ashley Wagoner, Jordan Hunt, Bryan Morris, Estefania Castro-Vazquez; Accola Hudson, Roa Saleh, Alexa Marcy, and Angeli Gupta for helping me grow and challenging me to be better.

TABLE OF CONTENTS

LIST OF ABBREVIATIONS	xii
LIST OF TABLES	xv
LIST OF FIGURES.....	xviii
Chapter 1. Genetic Association Mapping in Crops Improves Selective Breeding for Enhanced Agronomic and Fruit Quality Traits	1
1.1. Introduction	2
1.2. Traditional Selective Breeding in Plants.....	5
1.3. Successes in Utilizing Traditional Selective Breeding in Plants.....	7
1.4. Drawback to Traditional Selective Breeding: Decrease in Metabolites.....	12
1.5. Improvements in Breeding Capabilities.....	14
1.5.1. Marker Assisted Selection (MAS).....	16
1.5.2. Biparental Association Mapping (BiPAM).....	17
1.5.3. Genome-Wide Association Mapping (GWAS).....	19
1.6. Successes in Association Mapping and MAS for Crop Improvement.....	21
1.7. Research Program and Dissertation Objectives	24
REFERENCES.....	27
Chapter 2. Blueberry Agronomic and Fruit Quality Biparental Association Mapping	35
2.1. Abstract.....	36
2.2. Introduction	37
2.2.1. Blueberry Crop History and Agronomics	38
2.2.2. Blueberry Dormancy and Flowering	42
2.2.2.1. Endodormancy Induction	44
2.2.2.2. Endodormancy to Ecodormancy Release Progression	47
2.2.2.3. Flowering after Floral Bud Burst	52
2.2.3. Blueberry Berry Development and Ripening	55
2.2.3.1. Cell Wall Matrix Modifications and Sugar Signaling	57
2.2.3.2. Pigment Accumulation – Phenolic Acids	59
2.2.4. Consumer-Driven Fruit Quality and Blueberries	62
2.2.4.1. Perception of Flavor	63
2.2.4.2. Sensory Evaluations	64
2.2.4.3. Flavor Mechanism	65
2.2.4.4. Voluntary Blueberry Survey	67
2.2.4.5. Fruit Quality, Its Changes and Research	68
2.2.5. Blueberry Genomic Resource	72
2.3. Materials and Methods.....	74
2.3.1. Plant Material	74
2.3.2. Genotypic Data	74
2.3.3. Phenotypic Data	75
2.3.4. Biparental Association Mapping (BiPAM).....	77
2.4. Results	79
2.4.1. Genetic Map	79
2.4.2. Phenotype Results	81

2.4.3. Biparental Association Mapping (BiPAM) Results	88
2.5. Discussion	101
2.5.1. Agronomic Growth Regulation	104
2.5.1.1. Growth Traits QTLs and Overlapping QTL Regions	106
2.5.2. Dormancy Break and Flowering Regulation	116
2.5.2.1. Dormancy Break and Flowering Traits QTLs and Overlapping QTL Regions	117
2.5.3. Fruit Quality Regulation	122
2.5.3.1. Fruit Quality Traits QTLs and Overlapping QTL Regions	125
2.6. Conclusion	138
2.7. Acknowledgments	146
REFERENCES	147

Chapter 3. Blueberry Metabolite Profiling and Biparental Association

Mapping to Identify QTLs and Putative Candidate Genes	169
3.1. Abstract	170
3.2. Introduction	171
3.2.1. Plant Metabolite Profiling	174
3.2.2. Plant Metabolites and Human Health	178
3.2.3. Antioxidant Capacity	181
3.2.4. Blueberry Metabolites	186
3.3. Materials and Methods	192
3.3.1. Plant Material	192
3.3.2. Extraction	193
3.3.3. ¹ H NMR Analysis	193
3.3.4. HPLC-QTOFMS Analysis	194
3.3.5. Antioxidant Capacity – DPPH Scavenging Assay	195
3.3.6. Genotypic Data	196
3.3.7. Biparental Association Mapping (BiPAM)	197
3.3.8. Putative Candidate Gene Identification	198
3.4. Results	200
3.4.1. ¹ H NMR Metabolite Features	200
3.4.1.1. ¹ H NMR Known Metabolites Phenotype Description	201
3.4.1.2. ¹ H NMR Known Metabolites Distribution	205
3.4.1.3. ¹ H NMR Known Metabolites Correlations	212
3.4.1.3.1. TCA Acids	212
3.4.1.3.2. Amino Acids	213
3.4.1.3.3. Sugars	218
3.4.1.3.4. Phenolic Acids	220
3.4.2. HPLC-QTOFMS Metabolite Features	223
3.4.2.1. Anthocyanin Phenotype Description (DAD)	223
3.4.2.2. Anthocyanin Phenotype Description (EIC)	234
3.4.2.3. Anthocyanins (DAD) Correlations	245
3.4.2.4. Anthocyanins (EIC) Correlations	250
3.4.2.5. Anthocyanin Detection Comparison Correlations	255
3.4.3. Antioxidant Capacity through DPPH Scavenging Assay	259

3.4.4. BiPAM QTLs from CIM Analysis	264
3.4.4.1. ¹ H NMR Known Metabolites	264
3.4.4.2. Anthocyanin (DAD) Metabolites and DPPH-Antioxidant Capacity	266
3.4.5. Putative Candidate Gene Analysis of Significant QTL Regions	276
3.4.5.1. ¹ H NMR Known Metabolites and DPPH-Antioxidant Capacity	276
3.5. Discussion	289
3.5.1. Metabolite Profiling with ¹ H NMR Analysis	290
3.5.2. Metabolite Profiling with HPLC-QTOFMS Analysis	293
3.5.3. DPPH Assay for Antioxidant Capacity	304
3.5.4. TCA Cycle and Amino Acid Significant QTLs and Putative Candidate Genes	305
3.5.4.1. TCA Cycle Pathway	305
3.5.4.2. Glutamine Branch Pathway	308
3.5.4.3. Branch-Chain Branch Pathway	311
3.5.4.4. Aspartate Branch Pathway	313
3.5.5. Sugar Pathway Significant QTLs and Putative Candidate Genes	315
3.5.5.1. Fructose and Glucose	315
3.5.5.2. Sucrose, Maltose, and Maltitol	317
3.5.5.3. Galactose, Xylose, and Arabinose	320
3.5.6. Phenolic Acid Pathway Significant QTLs and Putative Candidate Genes	324
3.5.6.1. Shikimic Acid Pathway and Phenylalanine Synthesis	324
3.5.6.2. Phenylpropanoid Pathway	326
3.5.6.3. Flavonoid Pathway	329
3.5.7. DPPH –Antioxidant Capacity Assay Significant QTLs and Putative Candidate Genes	333
3.6. Conclusion	335
3.7. Acknowledgments	343
REFERENCES	344

Chapter 4. Identification of QTLs and Putative Candidate Genes Associated with Agronomic Traits in <i>Brassica oleracea</i> var. <i>italica</i>	359
4.1. Abstract	360
4.2. Introduction	361
4.2.1. Genome-Wide Association Mapping	363
4.3. Materials and Methods	364
4.3.1. Plant Population Material	364
4.3.2. Phenotypic Data	365
4.3.3. Genotypic Data and Genetic Map	365
4.3.4. Genome-Wide Association Mapping	366
4.3.5. Quantitative Trait Loci and Putative Candidate Gene Identification	367
4.4. Results	370
4.4.1. Genetic Map	370
4.4.2. Agronomic Phenotypes	372
4.4.3. Linkage Disequilibrium	375
4.4.4. Principle Component Analysis	376

4.4.5. Kinship Analysis and Relationship Matrix	377
4.4.6. Multivariate Correlation	380
4.4.7. Quantitative Trait Loci from Association Mapping	380
4.4.8. Putative Candidate Gene Identification	386
4.5. Discussion	392
4.5.1. Broccoli Traits with Putative Candidate Genes for Improving Harvest and Productivity	392
4.5.2. Broccoli Pathogen-Related Traits for Improving Pathogen Resistance	396
4.5.2.1. Pathogen Recognition Putative Candidate Genes	396
4.5.2.2. Pathogen Attack Signal Transduction Putative Candidate Genes	398
4.5.2.3. Pathogen Resistance Response Putative Candidate Genes	402
4.6. Conclusion	404
4.7. Acknowledgments	407
REFERENCES	408
Chapter 5. Improving Our Understanding of Agronomic, Fruit Quality, and Metabolic Traits in Blueberry and Broccoli	426
5.1. Blueberry Agronomic Growth, Dormancy, and Fruit Quality Traits Associated with Multiple Genetic Regions	428
5.2. Blueberry Metabolic Profiling and Associated Genetic Regions Contain Possible Regulatory Genes	434
5.3. Broccoli Agronomic Associated Genetic Regions Contain Possible Regulatory Genes	443
REFERENCES.....	447

LIST OF ABBREVIATIONS

P²EP = Plant Pathways Elucidation Project
NHB = Northern High-Bush
SHB = Southern High-Bush
DxJ = Draper by Jewel
QTL = Quantitative Trait Loci
BiPAM = Biparental Association Mapping
GWAS = Genome-Wide Association Mapping Studies
SNP = Single Nucleotide Polymorphism
MAS = Marker Assisted Selection
OR = Odds Ratio
cM = centimorgan
LOD = Logarithm of Odds
IM = Interval Mapping
CIM = Composite Interval Mapping
EM = Estimated Maximum-likelihood
MIM = Multiple Interval Mapping

KEGG = Kyoto Encyclopedia of Genes and Genomes
NMR = Nuclear magnetic resonance
GC-MS = Gas Chromatography-Mass spectrometry
HPLC-MS = High-Pressure liquid chromatography-Mass spectrometry
DAD = Diode array detector
TOFMS = Time-of-flight mass spectrometry
EIC = Extracted ion count
SS = Soluble Solids
TA = Titratable Acidity
DPPH = 2,3-diphenyl-1-picrylhydrazyl
TCA = Tricarboxylic Acid
GABA = γ -aminobutyric acid

Hormones:
ABA = Abscisic Acid
NCED = 9-cis-epoxycarotenoid dioxygenase
PYR = Pyrabactin resistance
PYL = PYR-like
PP2C = Protein phosphatase 2C
SnRK = Sucrose non-fermented 1-related kinase
ABI = ABA-insensitive protein
GA = Gibberellin
GID = GA insensitive dwarf
DELLA = GA-response inhibitor proteins
GAI = GA-insensitive
RGA = Repressor of GA
RGL = RGA-like

ET = Ethylene
ACC = 1-aminocyclopropane-1-carboxylate
ACS = ACC synthase
ACO = ACC oxidase
EIN = ET-insensitive
CTR = Constitutive triple response
EIL = EIN-like
EBF = EIN3-binding F-box protein
ERF = ET response factor

Sugars:

SUS = sucrose synthase
INV = Invertase
G1P = Glucose-1-phosphate
G6P = Glucose-6-phosphate
F6P = Fructose-6-phosphate
PPP = Pentose phosphate pathway
UDP = Uridine Diphosphate
T6P = Trehalose-6-phosphate
TPS = T6P synthase
TPP = T6P phosphatase
SnRK = Sucrose non-fermented 1-related kinase
HXK = Hexokinase

Oxidative Signaling:

ROS = Reactive oxygen species
RNS = Reactive nitrogen species
GSH = Glutathione
APX = Ascorbate peroxidase
MDAR = Monodehydroascorbate reductase
DHAR = Dehydroascorbate reductase
GSSG = Glutathione oxidized
GR = Glutathione reductase
GST = Glutathione-S-transferase

Phenolic Acids:

PAL = Phenylalanine ammonia lyase
C4H = Cinnamate-4-hydrolase
CoA = Coenzyme A
HCT = Hydroxycinnamoyl-CoA:quinate/shikimate hydroxycinnamoyltransferase
C3'H = p-coumaroyl quinate/shikimate 3'-hydroxylase
CHS = Naringenin-Chalcone synthase
CHI = Chalcone-flavanone isomerase
F3'5'H = Flavonoid 3'-/3',5'-hydroxylase
F3'H = Flavanone 3-dioxygenase
FLS = Flavonol synthase

DFR = Dihydroflavonol 4-reductase
ANR = Anthocyanidin reductase
ANS = Anthocyanidin synthase
OMT = O-methyltransferase
UFGT = UDP-sugar:flavonoid glucosyltransferases

LIST OF TABLES

Table 2.1	Summary statistics for overall genetic map for Draper x Jewel tetraploid mapping population	80
Table 2.2	Summary statistics of linkage groups for DxJ tetraploid genetic map	81
Table 2.3	Phenotype summary statistics for the 30 traits.....	83
Table 2.4	Total genome-wide significant QTLs for each trait when separated into the individual phenotypes from each location and year.....	91
Table 2.5	Total genome-wide significant QTLs for each trait when grouped together into location-specific, year-specific, and cofactor-specific analyses	92
Table 2.6	Overlapping QTL regions containing at least three significant QTLs from different CIM analyses for the growth traits.....	93
Table 2.7	Overlapping QTL regions containing at least three significant QTLs from different CIM analyses for the dormancy break and flowering traits.....	97
Table 2.8	Overlapping QTL regions containing at least three significant QTLs from different CIM analyses for the fruit quality traits	97
Table 3.1	Reaction schemes for possible non-enzymatic antioxidants when scavenging ROS-RNS.....	183
Table 3.2	HPLC-QTOFMS solvent gradient for optimized anthocyanin separation.....	194
Table 3.3	Metabolite features from non-targeted profiling with ¹ H NMR	200
Table 3.4	Accumulation and annotation summary data for TCA acids and amino acids from ¹ H NMR non-targeted profiling	203
Table 3.5	Accumulation and annotation summary data for sugars from ¹ H NMR non-targeted profiling	204
Table 3.6	Accumulation and annotation summary data for phenolic acids from ¹ H NMR non-targeted profiling	205
Table 3.7	Accumulation and annotation summary data for anthocyanins detected using DAD from targeted profiling with HPLC-QTOFMS.....	225

Table 3.8	Summary and total composition data for anthocyanin summation groups from the DAD detected anthocyanins	232
Table 3.9	Individual anthocyanin composition summary data using the DAD detected anthocyanins and summation groups.....	233
Table 3.10	Accumulation and annotation summary data for anthocyanins detected using EIC from targeted profiling with HPLC-QTOFMS	235
Table 3.11	Summary and total composition data for anthocyanin summation groups from EIC detected anthocyanins	242
Table 3.12	Individual anthocyanin composition summary data using the EIC detected anthocyanins and summation groups.....	244
Table 3.13	Summary data for DPPH antioxidant capacity assay for two years	259
Table 3.14	Summary of significant QTLs, genome-wide, for TCA acids and amino acids from ¹ H NMR non-targeted profiling	265
Table 3.15	Summary of significant QTLs, genome-wide, for individual sugars from ¹ H NMR non-targeted profiling	265
Table 3.16	Summary of significant QTLs, genome-wide, for phenolic acids from ¹ H NMR non-targeted profiling	265
Table 3.17	Summary of significant QTLs, genome-wide, for the individual anthocyanins and summation groups from DAD-detection by HPLC-QTOFMS targeted profiling	267
Table 3.18	Summary of significant QTLs, genome-wide, for anthocyanin ratios from DAD-detection by HPLC-QTOFMS targeted profiling	267
Table 3.19	A subset of significant QTLs with overlapping genetic regions for DAD-detected individual anthocyanins, summation groups, and ratios from HPLC-QTOFMS targeted profiling	269
Table 3.20	A subset of significant QTLs for TCA acids and amino acids from ¹ H NMR non-targeted profiling with corresponding putative candidate genes found within the genetic region.....	278
Table 3.21	A subset of significant QTLs for sugars from ¹ H NMR non-targeted profiling with corresponding putative candidate genes found within the genetic region.....	281

Table 3.22	A subset of significant QTLs for phenolic and ascorbic acid from ¹ H NMR non-targeted profiling with corresponding putative candidate genes found within the genetic region	284
Table 3.23	A subset of significant QTLs for DPPH-antioxidant capacity with corresponding putative candidate genes found within the genetic region	288
Table 4.1	Summary statistics of individual linkage groups for the broccoli high-density genetic map	372
Table 4.2	Summary statistics for two years of broccoli agronomic phenotypes.....	372
Table 4.3	Correlation statistics for the multivariate analysis of PCA and Kinship population structure variables	380
Table 4.4	Summary of significant QTLs for year 1 and year 2 GWAS analysis	382
Table 4.5	Putative candidate genes for days to harvest (year 1) significant QTLs.....	387
Table 4.6	Putative candidate genes for days to harvest (year 2) significant QTLs.....	387
Table 4.7	Putative candidate genes for multiple pathogen-related traits for a subset of overlapping, significant QTLs called pathogen-related 'hotspots'	388

LIST OF FIGURES

Figure 2.1	Anthocyanin molecular structure and diversity in blueberry	62
Figure 2.2	Draper x Jewel tetraploid genetic map	80
Figure 2.3	Distribution histograms for growth traits	85
Figure 2.4	Distribution histograms for dormancy break and flowering traits	86
Figure 2.5	Distribution histograms for fruit quality traits	87
Figure 3.1	Anthocyanin molecular structure and diversity in blueberry	187
Figure 3.2	Distribution histograms for total TCA acids and specific TCA acids from ¹ H NMR non-targeted profiling	208
Figure 3.3	Distribution histograms for the 11 amino acids from ¹ H NMR non- targeted profiling	209
Figure 3.4	Distribution histograms for total sugars and individual sugars from ¹ H NMR non-targeted profiling	210
Figure 3.5	Distribution histograms for the phenolic acids from ¹ H NMR non- targeted profiling	211
Figure 3.6	Correlations showing the relationship between the TCA Acids	212
Figure 3.7	Correlations showing the relationship between the different amino acid branches and total amino acids, as well as between each other	214
Figure 3.8	Correlations showing the relationship between the individual amino acids in the glutamine branch with the total glutamine branch and with each other	215
Figure 3.9	Correlations showing the relationship between the individual amino acids in the branch-chain branch with the total branch-chain branch and with each other	216
Figure 3.10	Correlations showing the relationship between the individual amino acids in the aspartate branch with total aspartate branch and with each other	217
Figure 3.11	Correlations showing the relationship between the individual sugars with total sugar	219

Figure 3.12	Correlations showing the relationship between the individual sugars.....	220
Figure 3.13	Correlations showing the relationship between the individual phenolic acids with total phenolic acids and with each other.....	222
Figure 3.14	Distribution histograms for the 17 individual anthocyanins detected and annotated by the DAD from targeted profiling with HPLC-QTOFMS.....	227
Figure 3.15	Distribution histograms for the anthocyanidin summation groups detected and annotated by the DAD from targeted profiling with HPLC-QTOFMS.....	230
Figure 3.16	Distribution histograms for the sugar moiety summation groups detected and annotated by the DAD from targeted profiling with HPLC-QTOFMS.....	231
Figure 3.17	Distribution histograms for the 23 individual anthocyanins detected and annotated by the EIC from targeted profiling with HPLC-QTOFMS.....	238
Figure 3.18	Distribution histograms for the anthocyanidin summation groups detected and annotated by the EIC from targeted profiling with HPLC-QTOFMS.....	240
Figure 3.19	Distribution histograms for the sugar moiety summation groups detected and annotated by the EIC from targeted profiling with HPLC-QTOFMS.....	241
Figure 3.20	Correlations showing the relationship between the DAD detected total anthocyanins with the summation groups.....	247
Figure 3.21	Correlations showing the relationship between the DAD detected total sugar moiety summation groups.....	248
Figure 3.22	Hierarchical clustering of the 17 individual DAD detected anthocyanins.....	249
Figure 3.23	Correlations showing the relationship between the EIC detected total anthocyanins with the anthocyanidin summation groups.....	250
Figure 3.24	Correlations showing the relationship between the EIC detected total anthocyanins with the sugar moiety summation groups.....	252
Figure 3.25	Correlations showing the relationship between the EIC detected total sugar moiety summation groups.....	253

Figure 3.26	Hierarchical clustering of the 23 individual EIC detected anthocyanins	255
Figure 3.27	Correlations showing the relationship between the summation groups detected by either DAD or EIC	256
Figure 3.28	Correlations showing the relationship between the delphinidin anthocyanins detected by either DAD or EIC	257
Figure 3.29	Correlations showing the relationship between the petunidin anthocyanins detected by either DAD or EIC	257
Figure 3.30	Correlations showing the relationship between the malvidin anthocyanins detected by either DAD or EIC	258
Figure 3.31	Correlations showing the relationship between the cyanidin and peonidin anthocyanins detected by either DAD or EIC	258
Figure 3.32	Distribution histograms for DPPH-antioxidant capacity for two years as well as both years merged together	259
Figure 3.33	Correlations showing the relationship between DPPH-antioxidant capacity and different summation groups or individual anthocyanins detected with DAD	261
Figure 3.34	Correlations showing the relationship between DPPH-antioxidant capacity and different summation groups or individual anthocyanins detected with EIC	262
Figure 3.35	Correlations showing the relationship between DPPH-antioxidant capacity and phenolic acids from the non-targeted profiling with ¹ H NMR	263
Figure 3.36	Anthocyanin spectra from the HPLC-QTOFMS with peaks representing the relative locations of the individual anthocyanins detected using DAD and EIC	299
Figure 4.1	Flow diagram outlining the putative candidate gene identification process	369
Figure 4.2	The high-density genetic linkage map of <i>Brassica oleracea</i> var. <i>italica</i>	371
Figure 4.3	Distribution histograms for the days to harvest trait for both years	373
Figure 4.4	Distribution histograms for the pathogen-related traits for both years	374

Figure 4.5	Waterfall scatterplot representing linkage disequilibrium (R^2)	375
Figure 4.6	Scatterplots and histograms representing each pairwise comparison of the first five principal components.....	376
Figure 4.7	Heat map representing the hierarchical clustering analysis of the diversity broccoli lines based on pair-wise identity by state similarity matrix	378
Figure 4.8	Scatterplots and histograms representing each pairwise comparison of the first five principal components dur to kinship	379
Figure 4.9	Manhattan plot of the days to harvest trait (year 2) for linkage group four.....	383
Figure 4.10	Manhattan plot of the days to harvest trait for both years for linkage group eight.....	383
Figure 4.11	Manhattan plot of the days to harvest trait (year 1) for linkage group nine	384
Figure 4.12	Manhattan plot of multiple pathogen-related traits for both years for linkage group two.....	384
Figure 4.13	Manhattan plot of multiple pathogen-related traits for both years for linkage group four	385
Figure 4.14	Manhattan plot of multiple pathogen-related traits for year 2 for linkage group eight.....	385

**Chapter 1. Genetic Association Mapping in Crops Improves Selective Breeding
for Enhanced Agronomic and Fruit Quality Traits**

1.1. Introduction

Everyone has learned at some point that eating more fruits and vegetables is good for their health, but if fruits and vegetables are not available and appealing to the consumers, then consumers are not going to readily consume them. As the human population increases significantly and the acreage of arable land decreases, the strain of creating enough supply to meet the demand for food is critical. At present, the agriculture industry aggressively researches and pursues innovation to increase food production. For example, one focus of research is increasing the yield per crop. There is also a focus on decreasing the inputs the crop requires to maintain a certain yield, thus reducing the amount of fertilizer, herbicide, and pesticide needed. Another focus is improving harvest efficiency through developing crops that easily detach from the plant, as well as more robust fruits or vegetables that can withstand mechanical harvesting.

Crop research must also incorporate consumer preference as the profits fuel growers, industry and research. Consumers decide to purchase, therefore consume, specific foods based on the perceived quality of the food. The crop's fruit quality is also an important aspect of consumer preference. Unfortunately, industry and consumers prioritize different fruit quality characteristics. Industry works to improve harvestability, transport, and shelf-life, which prioritizes fruit quality characteristics like firmness and slow ripening rate (Grunert, 2005; Kader, 2008; Klee, 2010; Kyriacou & Roupael, 2018). Consumers prioritize fruit quality characteristics that conform to an ideal image of the fruit or vegetable like visual, texture, and taste traits (Grunert, 2005; Kader, 2008; Klee, 2010; Kyriacou & Roupael, 2018). Industry fruit quality characteristics have been the primary focus of selection, but consumer awareness is shifting breeding selection and research towards crops with improved consumer fruit quality and nutrition. The commercial tomato is an example of conflicting fruit quality breeding selection. Tomato breeding in the past selected for yield and shelf-life, which resulted in current cultivars that are very firm and ripen very slowly (Azzi et al., 2015; Kramer & Redenbaugh, 1994; Passam, Karapanos, Bebeli, & Savvas, 2007). These cultivars reduced tomato crop loss as less tomatoes were damaged during harvest and transport, and lasted longer on market shelves (Azzi et al., 2015; Foolad & Panthee, 2012; Kramer & Redenbaugh, 1994; Mehta et al., 2002; Passam et al., 2007; Seymour, Chapman, Chew, & Rose,

2013). Although these industry cultivars were initially considered a success, consumers exhibited a preference for other tomato varieties rather than the industry cultivars (Azzi et al., 2015; Kramer & Redenbaugh, 1994; Mehta et al., 2002; Tieman et al., 2012). The firm, slow ripening industry cultivars had very little taste and an undesirable texture, and both of those characteristics are important to consumer preference (Kramer & Redenbaugh, 1994; Mehta et al., 2002; Tieman et al., 2012). The reduced taste and texture are a result of slow ripening, as many ripening enzymes breakdown complex polysaccharides to simple sugars that contribute to taste and texture (Azzi et al., 2015; Kramer & Redenbaugh, 1994; Mehta et al., 2002; Seymour, Chapman, et al., 2013; Tieman et al., 2012). Thus, both industry and consumer fruit quality characteristics must accommodate each other and incorporate the compromise into crop breeding strategies in order to produce a successful new crop cultivar.

The current societal climate emphasizes the importance of incorporating nutritional benefits as a consumer fruit quality characteristic. The increase in shared and publicized nutritional research of fruits and vegetable consumption has educated consumers of the benefits of fruit and vegetable consumption (Betoret, Betoret, Vidal, & Fito, 2011; Kearney, 2010; Sam Saguy, 2011; Tobey & Manore, 2014). For example, fruits or vegetables labeled as a “super food”, like pomegranates or acai berries, resulted in widespread publicity and a dramatic increase in sales and consumption of those products (Betoret et al., 2011; Biltekoff, 2010; Kearney, 2010; Sam Saguy, 2011; Tobey & Manore, 2014). As another example, carrots consumption has increased because more consumers are learning of the health benefits, resulting in a change in breeding strategies to enhance certain metabolites (Betoret et al., 2011; Sharma, Karki, Thakur, & Attri, 2012). Orange carrots contain β -carotene, and when research revealed β -carotene as a vital provitamin A for human health, consumption drastically increased (Gul et al., 2015; Sharma et al., 2012). Further research into carrot diversity revealed at least three different colored carrot varieties, yellow, pink, and purple (Gul et al., 2015; Sharma et al., 2012). The different colored carrots still contain β -carotene, but also contain other pigment metabolites that are associated with health benefits (Gul et al., 2015; Sharma et al., 2012). With the current rapid dissemination of food and nutrition information, consumers awareness of the health benefits surrounding rainbow carrots

drove an increase in demand, thus resulting in the majority of markets now offering rainbow carrots (Betoret et al., 2011; Biltekoff, 2010; Gul et al., 2015; Kearney, 2010; Sharma et al., 2012; Tobey & Manore, 2014). Therefore, the ideal crop cultivars balance agronomic and industry fruit quality traits like yield, firmness, and pathogen resistance, along with consumer fruit quality traits like flavor, texture, and nutrition.

The overarching research goal of this dissertation is to gain a greater understanding of the genetic components linked with agronomic, fruit quality, and metabolic traits in blueberry and broccoli. This research will aid future selective breeding programs to improve harvest, fruit quality, and nutrition in blueberry and broccoli. Complementary techniques were utilized for genetic association mapping and for metabolic profiling to identify important genetic regions that may affect harvest, growth, taste, appearance, and nutrition. The genetic association mapping of blueberry agronomic traits identified 27 genetic regions associated with efficient floral bud breaking and flowering to aid in reducing floral bud tissue damage and improve fruit harvest. Genetic association mapping of blueberry fruit quality traits identified 38 genetic regions associated with 11 characteristics that contribute to fruit color, texture, and taste. The targeted and non-targeted metabolic profiling of blueberries identified 46 annotated metabolites consisting of amino acids, sugars, phenolic acids, and anthocyanins. Phenolic acids and anthocyanins have been consistently associated with antioxidant health benefits like reducing oxidative stress, reducing inflammation, reducing neurodegeneration, and reducing carcinogenic progression. Genetic association mapping of 46 annotated metabolites identified over 300 significant quantitative trait loci (QTL) with 196 significant QTLs showing genetic regions containing putative candidate genes with biosynthesis or regulatory functions in either amino acid, sugar, or phenolic acid pathways. The antioxidant capacity of the blueberry extracts was also conducted, and genetic association mapping revealed two significant QTL regions containing mainly phenolic acid synthesis genes. The genetic association mapping of broccoli for agronomic traits identified over ten genetic regions associated with harvest and disease resistance. Most of the identified genetic regions contained candidate genes that have been shown by published literature to have a role in regulating the biosynthesis, metabolism, or signaling cascade of the associated trait.

These results can be applied to future work on characterizing the regulatory functions of the identified candidate genes and identifying specific breeding parents with genetic variation for the important QTLs to be utilized for selective breeding. The significant markers found through QTL mapping can be used to better select which parents are the best cross to produce the best progeny. The markers can also be used to screen for multiple traits at a time using a single genetic sample for each line. The markers can also be utilized to eliminate unsuitable lines early on in plant growth and population development to perform early generation or tandem selection. This allows for researchers to focus time and resources on the most promising material.

1.2. Traditional Selective Breeding in Plants

Over hundreds of years, society has used selective breeding to promote the prevalence of specific attributes in specific plants, which over time has resulted in a drastic change between the ancestor and current crop. Traditional selective breeding is summarized as choosing two parents with a desirable trait, crossing them to produce offspring, then selecting from the progeny which one has the desirable trait to propagate and maintain for the next generation (Bernardo, 2008; Collard, Jahufer, Brouwer, & Pang, 2005). The differences between ancestral teosintes and currently, cultivated maize is an example of selective plant breeding for traits like yield, crop harvestability, and crop size (Meyer & Purugganan, 2013).

Traditional selective breeding in plants typically requires multiple crosses and progeny generations to produce a genotype line that stably inherits the desirable trait improvements (Bernardo, 2008; Collard et al., 2005; Jannink, Lorenz, & Iwata, 2010; M. S. Kang, 2002; Meyer & Purugganan, 2013; Xu, 2010). After selecting the progeny exhibiting the desirable trait attributes, the progeny must grow to reproductive maturity in order to conduct the next cross and propagate the desirable trait into the next generation. Some plant species reach reproductive maturity quickly, while others can take years. For example, after an apple tree cross, phenotyping the next generation must wait at least five years before the tree is at reproductive and fruiting maturity (Koutinas, Pepelyankov, & Lichev, 2010; Melke, 2015).

Fortunately, many plants are self-compatible, meaning the ovule can be fertilized by the sperm of the same genotype, which allows for quicker selective breeding of

desirable trait while also breeding out the undesirable, background trait variations (Buchanan, Grussem, & Jones, 2012; M. S. Kang, 2002; Xu, 2010). Multiple generations of selfing results in inbred lines, and after eight or more inbred generations, the genotype lines are termed recombinant inbred lines (M. S. Kang, 2002; Xu, 2010). Unfortunately, only some selfing species can tolerate the extensive inbreeding for recombinant inbred lines. Most selfing species allow only a few generations of selfing before the population exhibits inbreeding depression. Inbreeding depression is the accumulation of deleterious or lethal alleles, or the expression of rare minor alleles due to lack of genetic diversity in genotype line (M. S. Kang, 2002; Xu, 2010). For example, purebred dog breeds continually undergo extensive inbreeding, which accelerates the selective breeding, for very specific characteristics to conform with the breed's ideal image, like the flat-faced pug (Sutter & Ostrander, 2004). Consequently, many purebred breeds are exhibiting inbreeding depression and the prevalence of rare genetic disorders and malformations like epilepsy and hip dysplasia (Sutter & Ostrander, 2004). Inbreeding tolerant crops like wheat and corn have allowed for quick selection and development of different genotype lines or cultivars with specific adaptations like pathogen resistance or climate change (Al-Khayri, Jain, & Johnson, 2015; C. Li et al., 2018; Miedaner & Korzun, 2012; Rasheed et al., 2017). Since most crops do not allow for extensive inbreeding, other breeding crosses like backcross or test cross are utilized to maintain the desirable trait while reducing background trait variation (M. S. Kang, 2002; Xu, 2010).

When traditional selective breeding in plants started, the desirable traits to select for were limited to only visual characteristics because molecular technology was very limited. Color of crop is a prime example of a visual trait used for selection that is still used today as breeders select for redder tomatoes and apples (Foolad & Panthee, 2012; Musacchi & Serra, 2018; Seymour, Chapman, et al., 2013; Toivonen & Brummell, 2008). Yield is another example as ears of corn or apples per tree is a visual trait easily differentiated and measured. Initially, the first few crosses and generations exhibit visually distinguishable differences in phenotypes, like red or yellow tomatoes. As selection continues, the phenotypic variation becomes less visually distinguishable, like dark or medium red tomatoes. The steady advancements over time in molecular

technology have allowed for improved quantification of phenotypic variation, like spectroscopy and chromatography (Cruz et al., 2016; Furbank & Tester, 2011; Houle, Govindaraju, & Omholt, 2010; Langridge & Fleury, 2011). Proper quantification of the phenotype is imperative for further breeding selection. If the more desirable trait is not selected for because it is indistinguishable, then the cross will not pass on the appropriate genetic information, which would result in an inefficient cross for the next generation.

1.3. Successes Utilizing Traditional Selective Breeding in Plants

Traditional selective breeding in plants has produced many successful crop cultivars with improved agricultural productivity (Bernardo, 2008; Collard et al., 2005; Fuller, Allaby, & Stevens, 2010; M. S. Kang, 2002; Meyer & Purugganan, 2013; Tzarfati et al., 2013; Zhang, Mittal, Leamy, Barazani, & Song, 2017). Using yield as an example, yield can be improved through increasing density of crop plant per acre and increasing yield per plant (Fischer & Edmeades, 2010; Hashemi, Herbert, & Putnam, 2005; Jannink et al., 2010; Lee & Tollenaar, 2007; Weiner & Freckleton, 2010; Zhang et al., 2017). Due to the great success in selective breeding, US crop productivity has at least doubled from 1997 to 2012 (USDA, 2012). This productivity and food supply increase is reflected in the continual increase in food consumption per person worldwide (Kearney, 2010; Tester & Langridge, 2010). With the exponentially increasing population, food production will also need to increase as well (Kearney, 2010; Tester & Langridge, 2010). The Declaration of the World Summit on Food Security proposes food production needs to increase by 70% by 2050, which is an average annual production increase of 44 million metric tons per year (Tester & Langridge, 2010). This is an increase of 38% over past breeding improvements, indicating traditional selective breeding in plants needs to become more efficient in producing more productive cultivars (Tester & Langridge, 2010).

The recent cultivars developed through traditional selective breeding exhibit some yield improvement, but the increased productivity is not the substantial 38% improvement needed (Tester & Langridge, 2010). Most breeding programs focused on improving yield promote the selection pressure to reallocate more resources towards yield, which reduces the resources needed for other major processes and tissues

(Bennett, Roberts, & Wagstaff, 2012; Deng et al., 2012; Fischer & Edmeades, 2010; Gambín & Borrás, 2010; Lee & Tollenaar, 2007; O. Sadras & F. Denison, 2009). The improvement gains in yield have decreased because the other major processes vital to plant fitness are starting to falter with the very limited resources, thus other regulatory pathways are induced to rebalance resource allocation (Bennett et al., 2012; Deng et al., 2012; Fischer & Edmeades, 2010; Gambín & Borrás, 2010; Lee & Tollenaar, 2007; O. Sadras & F. Denison, 2009). But, further selection for yield will eventually select against the rebalancing and lead to yield gains sacrificing overall plant fitness (Bennett et al., 2012; Deng et al., 2012; Fischer & Edmeades, 2010; Gambín & Borrás, 2010; Lee & Tollenaar, 2007; O. Sadras & F. Denison, 2009). For example, extensive selective breeding of corn has successfully increased ear and kernel size when compared to ancestral maize due to the selection shifting resource allocation to increasing storage compounds (Bennett et al., 2012; Gambín & Borrás, 2010; Lee & Tollenaar, 2007). The minimal yield improvements in recent corn cultivars through ear and kernel size is due to inadequate resources allocated to other tissues because most is directed to the ear and kernel (Bennett et al., 2012; Gambín & Borrás, 2010; Lee & Tollenaar, 2007; Weiner & Freckleton, 2010). The shortage of resources limits cell wall reinforcement of the elongated stem supporting the larger, heavier ear of corn (Gambín & Borrás, 2010; Hashemi et al., 2005; Lee & Tollenaar, 2007; Sher, Khan, Ashraf, Liu, & Li, 2018; Weiner & Freckleton, 2010). This leads to a weaker stem and subsequent stem buckling under the ear weight and strong turgor pressure, which results in a decrease in yield or entire ear necrosis (Gambín & Borrás, 2010; Hashemi et al., 2005; Sher et al., 2018).

Initially, increasing plant density tolerance did improve the overall crop yield as more crop was harvested per acre (Deng et al., 2012; Hashemi et al., 2005; Lee & Tollenaar, 2007). But, the continued selection for increased plant density has led to overcrowding, which results in an overall decrease in yield. The increase in plant density results in an increase in competition for nutrients due to overlapping root systems, thus resulting in an overall decrease in crop growth and yield, or increase in fertilizer supplementation. The reduced nutrient uptake due to overcrowded root systems further decreases the resources allocated to other processes, thus increasing

the occurrence of biomass damage (Deng et al., 2012; Hashemi et al., 2005; Lee & Tollenaar, 2007). The increase in plant density also decreases overall yield because it enhances pathogen spread and infection (Gambín & Borrás, 2010; Hashemi et al., 2005; Sher et al., 2018; Weiner & Freckleton, 2010). The dense foliage provides very favorable conditions for pathogens because it is dark and cool with more humidity and stagnant air flow (Gambín & Borrás, 2010; Hashemi et al., 2005; Sher et al., 2018; Weiner & Freckleton, 2010). The endogenous plant pathogen resistance is further reduced due to the limited resources and skewed allocation reducing the development of physical and metabolite deterrents (Bennett et al., 2012; Gambín & Borrás, 2010; Weiner & Freckleton, 2010). Researchers need to further elucidate the pathways involved in resource allocation, nutrient absorption, and pathogen resistance, to more efficiently select for improvements in yield without sacrificing vital developmental and defense processes.

Traditional selective breeding in plants has also been successful in improving the shelf-life of many fruits and vegetables (Jenks & Bebeli, 2011; X. Li, Xu, Korban, & Chen, 2010; Matas, Gapper, Chung, Giovannoni, & Rose, 2009; Seymour, Chapman, et al., 2013; Toivonen & Brummell, 2008). Initially, these successes focused on selecting specific plants that slowed the ripening process, specifically, unripe crops reached the ripe stage slower (J. Giovannoni, 2001; J. J. Giovannoni, 2004; Matas et al., 2009; Passam et al., 2007; V. Prasanna, Prabha, & Tharanathan, 2007). This increase in time period for the transition from unripe to ripe allowed for the crop to fully ripen either during transport or while on the market shelves (Matas et al., 2009; Passam et al., 2007). For example, cultivated strawberries ripen much slower than wild strawberry varieties, which greatly reduces crop waste from over-ripe and rotten strawberries (Ayub et al., 2016; Posé, Nieves, Quesada, & Mercado, 2011). Further success in improving shelf-life occurred when researchers determined the role and effect ethylene has in the climacteric ripening pathway (Abe & Watada, 1991; Matas et al., 2009; Passam et al., 2007; Seymour, Chapman, et al., 2013). In climacteric fruit and vegetables, ripening is induced when ethylene receptors sense a spike in ethylene (Abe & Watada, 1991; Osorio, Scossa, & Fernie, 2013; Passam et al., 2007; Seymour, Chapman, et al., 2013; Seymour, Østergaard, Chapman, Knapp, & Martin, 2013). This knowledge allowed

researchers to determine that exogenous ethylene can also trigger climacteric ripening (Abe & Watada, 1991; Matas et al., 2009; Passam et al., 2007; Seymour, Chapman, et al., 2013). The role of ethylene in ripening was a vital breakthrough because climacteric fruits and vegetables can be harvested and stored at an unripe stage, and then ripening induced through exogenous ethylene gas application. For example, bananas are a climacteric fruit that is currently harvested at an unripe green stage and is triggered to fully ripen through exposure to exogenous ethylene gas (Passam et al., 2007; V. Prasanna et al., 2007). Storing and transporting bananas at an unripe stage drastically reduces crop loss because the unripe peels are tougher and more resistant to bruising (Passam et al., 2007; V. Prasanna et al., 2007). Tomatoes are also a climacteric fruit that is more resistant to damage at an unripe stage. Tomatoes are harvested at the unripe stage because it improves transport and storage, and then treated with ethylene to induce ripening during transport and market shelves (Azzi et al., 2015; Osorio et al., 2013; Passam et al., 2007; Seymour, Chapman, et al., 2013). The successful application of pathway research for climacteric ripening not only resulted in great improvements for climacteric fruits and vegetables, but also reduced interest in elucidating the ripening pathway that is not induced by ethylene (Azzi et al., 2015; Jenks & Bebeli, 2011; Kyriacou & Roupael, 2018; Osorio et al., 2013; Seymour, Østergaard, et al., 2013). Therefore, it is still unclear if non-climacteric ripening can be induced by a single compound or condition. Non-climacteric crops like citrus and berries would greatly benefit from most research as current harvesting involves picking at the ripe stage, which results in a short shelf-life.

Another major success utilizing traditional selective breeding was the improvement of fruit and vegetable harvestability. Along with the previously mentioned improvements in transportability, improving harvestability will enhance the availability and consumption of fruits and vegetables. Since cereal grains and rice are vital economic resources and allow for extensive inbreeding, harvestability was rapidly improved through selection for non-shattering varieties (Fischer & Edmeades, 2010; Fuller, 2007; Fuller et al., 2010; Weiner & Freckleton, 2010). Shattering is the natural release of the mature seeds from the crop's spike, which allows for seed dispersal (Fuller, 2007; Fuller et al., 2010). For grain crops, non-shattering varieties allowed for

mature seeds to remain attached until the vast majority of ears were mature so the crop could be efficiently harvested in bulk (Fuller, 2007; Fuller et al., 2010). To further improve harvestability, breeders selected for more efficient threshing and winnowing, which made removing the grain from the remaining husk and grain chaff easier (Fischer & Edmeades, 2010; Fu, Chen, Han, & Ren, 2018; Fuller et al., 2010; Tzarfati et al., 2013; Weiner & Freckleton, 2010). Threshing and winnowing were further selected for when mechanical harvesting with the combine harvester was designed for drastically improved harvest efficiency (Fu et al., 2018; Tzarfati et al., 2013).

Traditional selective breeding to improve harvestability in fruits and vegetables has exhibited slower progress than cereal grains due to the varying fruit architecture and breeding genetics. One aspect that would improve harvestability of fruits and vegetables is easier detachment of fruit or organ abscission (Gulfishan, Jahan, Bhat, & Sahab, 2019). Initially, fruits were selectively bred for delayed pedicle abscission to reduce ripe fruit drop (Estornell, Agustí, Merelo, Talón, & Tadeo, 2013). Similar to grains, decreasing abscission will keep the ripe fruit attached longer while more fruit ripen, which allows for more ripe fruit harvested in one session (Estornell et al., 2013; Fuller et al., 2010; Gulfishan et al., 2019; Tzarfati et al., 2013). Although decreasing abscission may increase the accumulation of sugars, nutrients, and water in the fruit by remaining attached for longer, the increase in plant's fruit number may limit the resources allocated to each fruit and overall decrease fruit quality (Estornell et al., 2013; Gulfishan et al., 2019). Decreasing the abscission may also increase manual labor because more effort is needed to detach the fruit and may require shears to remove (Estornell et al., 2013; Gulfishan et al., 2019). Therefore, fruit abscission selection requires fruit-specific breeding strategies that optimize fruit quality improvements and detachment ease for labor and mechanical harvesting (Estornell et al., 2013; Gulfishan et al., 2019; P. Li, Lee, & Hsu, 2011; Matas et al., 2009).

Harvestability of fruits and vegetables can also be improved through improving their resilience to mechanical harvesting. Most of the consumed fruits and vegetables are soft and fleshy, therefore, they are easily damaged by mechanical harvesting (Estornell et al., 2013; Gulfishan et al., 2019; P. Li et al., 2011). Initially, the selective breeding focused on increasing the overall firmness to reduce potential bruising when

the fruit impacted the harvesting machine (Estornell et al., 2013; Gulfishan et al., 2019; Konarska, 2015; P. Li et al., 2011; Moggia, Graell, Lara, González, & Lobos, 2017). However, consumers disapproved of the very firm fruit texture, which decreases economic profits (Barrett, Beaulieu, & Shewfelt, 2010; Blaker, Plotto, Baldwin, & Olmstead, 2014; X. Li et al., 2010). Consequently, current selective breeding efforts are focused on increasing the firmness of the fruit skin, peel, or cuticle, rather than the whole fruit (Blaker et al., 2014; Choi, Wiersma, Toivonen, & Kappel, 2002; Fasoli et al., 2018; Giongo, Poncetta, Loretto, & Costa, 2013; Matas et al., 2009; Seymour, Chapman, et al., 2013). In conjunction, researchers are also starting to elucidate more fruit development and maturation pathways to determine tissue specific processes and regulation (J. J. Giovannoni, 2004; Kader, 2008; Serrano et al., 2017; Seymour, Østergaard, et al., 2013; Toivonen & Brummell, 2008). At present, fruit and vegetable research elucidating fruit development, ripening, and harvestability requires much more research to efficiently improve growth and yield.

1.4. Drawback to Traditional Selective Breeding: Decrease in Metabolites

Although the aim of traditional selective breeding in plants is to integrate trait improvements into specific cultivars, some of those improvements have led to negative effects in the long term. In particular, the extensive selective breeding for overall productivity has significantly decreased the diversity of endogenous compounds (Chandrasekhar, Shavit, Distelfeld, Christensen, & Tzin, 2018; Meyer & Purugganan, 2013; Ulrich & Olbricht, 2014; Wang et al., 2017; Zeiss, Mhlongo, Tugizimana, Steenkamp, & Dubery, 2018; Zhang et al., 2017). A large diversity of compounds is strongly associated with an increase pathogen resistance, fruit quality, and nutrition (Chandrasekhar et al., 2018; Ulrich & Olbricht, 2014; Wang et al., 2017; Zeiss et al., 2018; Zhang et al., 2017). Since breeding efforts are not directly addressing the reduced metabolite diversity, pathogens and diseases are rapidly evolving resistance to the limited plant-endogenous resistance metabolites as well as resistance to exogenous, commercial pesticides, thus increasing plant susceptibility (Chandrasekhar et al., 2018; Wang et al., 2017; Zeiss et al., 2018; Zhang et al., 2017). This evolutionary “arms-race” to adapt to resistance is similar to the “antibiotic resistance race” faced by pharmacologists. For example, wild soybean varieties accumulate a great diversity of

metabolites as well as exhibit resistance to a wide range of pathogens (Gardner, Heinz, Wang, & Mitchum, 2017; Zhang et al., 2017).

After soybean domestication, the subsequent intensive selective breeding for the extremely high yield in current commercial soybean varieties allocated the vast majority of energy resources towards bean productivity (Gardner et al., 2017; Zhang et al., 2017). Along with the application of pesticides, the soybean plant has neither the energy resources available for synthesis of many endogenous metabolites nor the selection pressures to maintain production of a wide diversity of metabolites. Therefore, commercial soybean varieties produce a very limited diversity of metabolites (Gardner et al., 2017; Zhang et al., 2017). In conjunction with the reduction of metabolite diversity, pathogens, like cyst nematodes, are continually evolving resistance to endogenous metabolites and exogenous pesticide (Gardner et al., 2017; Klink & Matthews, 2009; Zhang et al., 2017). The current race of cyst nematodes has evolved resistance to the majority of exogenous pesticides and causes over \$1.2 billion profit loss annually (Gardner et al., 2017; Klink & Matthews, 2009; Mitchum, 2016). With the reduced metabolite diversity, current soybean cultivars have very little endogenous pathogen resistance metabolites to combat the cyst nematodes (Gardner et al., 2017; Klink & Matthews, 2009). Fortunately, researchers are utilizing the wild soybean germplasm to identify potential endogenous pathogen resistance compounds that can be incorporated through selective breeding into current cultivars (Gardner et al., 2017; Klink & Matthews, 2009; Zhang et al., 2017).

The extensive selective breeding for crop productivity and the subsequent decrease in metabolite diversity also decreased the crop's fruit quality and nutrition for the consumer (Biltekoff, 2010; Gul et al., 2015; Ulrich & Olbricht, 2014; Wang et al., 2017; Zhang et al., 2017). The primary fruit quality characteristics that are important to consumers are color, texture, and taste. The selective breeding of grapes for both the fresh market and wine industry is an example of the decreased metabolite diversity resulting in a decreased in fruit quality and nutrition (Fasoli et al., 2018; Pagliarini, Laureati, & Gaeta, 2013; Pinasseau et al., 2017; Pinu, Pinu, & R, 2018; Roubelakis-Angelakis, n.d.; Serrano et al., 2017). The richness and different shade coloration of green and red grapes depends on the diversity of carotenoids and flavonoids that

accumulate in the berry fruit skin, thus the reduced metabolite diversity reduces the richness and stability of grape coloration (Fasoli et al., 2018; Pagliarini et al., 2013; Pinasseau et al., 2017; Pinu et al., 2018; Roubelakis-Angelakis, n.d.; Serrano et al., 2017). The decrease in carotenoids and flavonoids also reduces the health benefits of grapes because carotenoids and flavonoids have been shown to reduce the risk of cardiovascular disease and many other chronic inflammation ailments (Ahmadinejad, Geir Møller, Hashemzadeh-Chaleshtori, Bidkhor, & Jami, 2017; Chiva-Blanch & Visioli, 2012; Gul et al., 2015; Khoo, Azlan, Tang, & Lim, 2017; Lin et al., 2016; Nile & Park, 2014). Both texture and taste characteristics for fruits and vegetables are also affected by the decrease in metabolite diversity (Kader, 2008; X. Li et al., 2010; V. Prasanna et al., 2007; Schwab, Davidovich-Rikanati, & Lewinsohn, 2008; Varela & Ares, 2012). Some of the ripening enzymes also catalyze volatile metabolite production, thus a decrease in metabolite diversity decreases the diversity of volatiles released for retro-nasal flavor (Goff & Klee, 2006; Klee, 2010; Schwab et al., 2008). Therefore, the reduction of metabolite diversity in tomato has affected both texture and taste, thus resulting in a decrease in fruit quality, nutrition, and consumer preference.

Utilizing traditional selective breeding to improve the overall metabolite diversity would further deplete the already strained energy resources within the plant as metabolite synthesis and regulation can be energetically costly. Furthermore, metabolites are not a visual characteristic, thus their quantification requires large resource investments to appropriately determine the metabolites. The recent advancements in molecular biology and computing have greatly improved breeding capabilities that mitigate many of the limitations of traditional selective breeding and allow for more efficient and cost-effective breeding strategies and programs.

1.5. Improvements in Breeding Capabilities

A vital advancement in molecular biology has been the development and use of markers to represent a trait rather than the trait itself, which allows for earlier detection and selection (Bernardo, 2008; Garrido-Cardenas, Mesa-Valle, & Manzano-Agugliaro, 2018; M. S. Kang, 2002; Winter & Kahl, 1995). The use of markers allows for selection of individuals during early growth, which saves the time and resources usually spent on growing until maturation (Bernardo, 2008; Garrido-Cardenas et al., 2018; M. S. Kang,

2002; Winter & Kahl, 1995). In general, a marker can be a morphological, molecular, or genetic characteristic that is highly linked to variation in the desirable trait. An example of a morphological marker is the morphological curling of densely packed leaves around the shoot meristems as the curling is associated with pathogen infection of the shoot meristem (Bernardo, 2008; Garrido-Cardenas et al., 2018; M. S. Kang, 2002; Winter & Kahl, 1995). An example of a molecular marker is the ultraviolet-visual wavelength (UV-Vis) absorption reading of a specific tissue as the absorption is linked to the presence or absence of specific compounds that exhibit different UV spectra (Howard, Brownmiller, Mauromoustakos, & Prior, 2016). The utilization of UV-Vis spectrum as a marker for specific metabolites is a quick, cost-effective method for determining certain metabolites (Furbank & Tester, 2011; Howard et al., 2016; Muleke et al., 2017). For example, the UV-Vis spectra at specific wavelengths for fruit or root tissue provides a representation of different phenolic acid levels quicker than the analytical chemistry extraction and quantification methods (Howard et al., 2016; Muleke et al., 2017).

The development and utilization of genetic markers has been the major advancement in advancing breeding capabilities because the genetic markers link the genome to the desirable trait (Bernardo, 2008; Garrido-Cardenas et al., 2018; M. S. Kang, 2002; Rafalski, 2010; Xu, 2010). Specifically, a genetic marker is a short DNA sequence that exhibits some variation between different individuals and represents a larger region or location on the genome due to linkage (Bernardo, 2008; Garrido-Cardenas et al., 2018; M. S. Kang, 2002; Rafalski, 2010; Xu, 2010). Genetic linkage occurs when DNA regions in close proximity are inherited together due to a lack of cross over events during meiosis recombination (Bernardo, 2008; Garrido-Cardenas et al., 2018; M. S. Kang, 2002; Rafalski, 2010; Xu, 2010). Since the DNA sequences can show different variations, there are several types of genetic markers. For example, simple sequence repeat (SSR) markers are regions with multiple repeats of the same short nucleotide sequence (Collard et al., 2005; Collard & Mackill, 2008; Jannink et al., 2010). The SSR marker represent genetic variation when the number of repeats differs between different individuals (Collard et al., 2005; Collard & Mackill, 2008; Jannink et al., 2010). Initially, the development of genetic markers was slow, tedious, and expensive, which resulted in limited use and downstream application (Bernardo, 2008;

Collard et al., 2005; Collard & Mackill, 2008). However, the innovations in DNA sequencing in the last decade have advanced genetic marker research, development, and application (Bernardo, 2008; Rasheed et al., 2017). Now, hundreds of thousands of genetic markers can be identified in months for a fraction of the cost to develop only a hundred genetic markers a decade ago. The next-generation sequencing not only allows for faster, more accurate identification of more traditional genetic markers like SSRs, but also can identify more abundant markers like single nucleotide polymorphisms (SNPs) (Bernardo, 2008; Nielsen, Paul, Albrechtsen, & Song, 2011; Poland & Rife, 2012). SNP genetic markers represent the variation of a single nucleotide between two individuals (Bernardo, 2008; Nielsen et al., 2011; Poland & Rife, 2012). The ease and accuracy of developing markers, especially genetic markers, has pushed plant selective breeding towards the development and application of marker-assisted selection (MAS).

1.5.1. Marker-Assisted Selection (MAS)

Marker-assisted selection (MAS) uses markers closely associated with desirable traits to more efficiently select the individuals to cross and specific progeny to maintain for the next generation (Foolad & Panthee, 2012; Rafalski, 2010; Singh & Singh, 2015; Xu, 2010). The markers allow for a dramatic decrease in breeding and selection time because the breeder no longer has to wait for crop maturity to measure the desirable trait and can more accurately determine the trait's heritability (Bernardo, 2008; Foolad & Panthee, 2012; Hospital, 2009; Singh & Singh, 2015; Xu, 2010). For example, if a SNP genetic marker represents green or yellow pea traits through its variation of A vs. B, then a breeder could analyze a seedling's DNA sequence at that specific SNP genetic marker region to determine which SNP allele, A or B, is present. The breeder would then keep the individuals with the A allele as it is strongly linked to producing green peas when mature. Once the selected individual has reached maturity and the green pea trait confirmed, the breeder could further the green pea trait to the next generation by crossing the selected individual with another individual, thus passing the A allele to the progeny. Once the DNA sequences for the SNP allele are analyzed in the seedling progenies, the inheritance and segregation patterns can be determined for this specific SNP allele (Garrido-Cardenas et al., 2018; Nielsen et al., 2011). When one gene,

usually represented by a specific genetic marker, is the main regulatory component of a trait, the gene exhibits Mendelian genetics (M. S. Kang, 2002; Xu, 2010). Although there are some Mendelian genetic traits, the vast majority of visual traits are complex, therefore are regulated by a combination of multiple regulatory genes (Bernardo, 2008; Collard & Mackill, 2008; Heslot, Yang, Sorrells, & Jannink, 2012; Hospital, 2009; Singh & Singh, 2015). The advancements in bioinformatics has allowed for thousands of genetic markers to be tracked and analyzed for trait associations (Cabrera-Bosquet, Crossa, von Zitzewitz, Serret, & Luis Araus, 2012; Collard & Mackill, 2008; Nielsen et al., 2011; Rafalski, 2010; Rasheed et al., 2017; Schaart, van de Wiel, Lotz, & Smulders, 2016; Singh & Singh, 2015). Identifying multiple genetic markers associated with a single trait allows for efficient MAS so that the multiple genetic markers can be tracked and selected in the subsequent generations of MAS (Rafalski, 2010).

1.5.2. Biparental Association Mapping (BiPAM)

Implementing MAS requires the identification of quantitative trait loci (QTL) with association mapping through statistically associating genetic markers with a specific trait variation (Collard et al., 2005; M. S. Kang, 2002; Xu, 2010). In this dissertation, association mapping is used as an overarching term and is separated into the two main methodologies: biparental and genome-wide mapping. As a general matter, biparental association mapping was the first method of association mapping developed and is commonly called “QTL mapping” (Collard et al., 2005; M. S. Kang, 2002; Xu, 2010). The terminology “QTL mapping” is ambiguous because the genome-wide method also identifies QTLs through association mapping. Thus, this dissertation will use biparental association mapping (BiPAM) to describe more traditional association mapping. BiPAM is a powerful tool for identifying QTLs that are co-segregating with a trait because the population is derived from mating two parents to create a mapping population (Borevitz & Chory, 2004; Jannink et al., 2010; M. S. Kang, 2002; Rafalski, 2010; Xu, 2010). This allowed researchers to incorporate predicted recombination frequencies and segregation ratios into the analysis to address any population structure. In simplistic terms, the genetic marker is associated with variation in a trait by calculating the odds ratio (OR) (Borevitz & Chory, 2004; Jannink et al., 2010; M. S. Kang, 2002; Rafalski, 2010; Xu, 2010). The OR calculates the odds the variation in the phenotype will occur

given the variation in the genetic marker, compared to the odds of the phenotype occurring without the variation in the genetic marker. A significantly high OR is interpreted as the genetic marker variation is statistically associated with the trait variation, thus a significant QTL (Borevitz & Chory, 2004; Jannink et al., 2010; M. S. Kang, 2002; Rafalski, 2010; Xu, 2010).

Unfortunately, there are limitations to BiPAM. One limitation is that the trait analyzed must show distinct variation between the two individuals crossed as the “parents”, as well as exhibit some segregation across the progeny (Jannink et al., 2010; M. S. Kang, 2002; Rafalski, 2010; Xu, 2010). This is important because the progeny will inherit only the allelic diversity that is present in the parents, thus regulate the variation in the phenotype exhibited between the parents and progeny (Collard et al., 2005; Jannink et al., 2010; M. S. Kang, 2002; Rafalski, 2010; Xu, 2010). Any BiPAM concerning other traits may not produce adequate results, as the allelic diversity may not statistically associate with the specific variation in the trait, or produce a false positive (Collard et al., 2005; Jannink et al., 2010; M. S. Kang, 2002; Rafalski, 2010; Xu, 2010). Another limitation to BiPAM is it requires the development of a mapping population (Al-Khayri et al., 2015; Collard et al., 2005; M. S. Kang, 2002; Singh & Singh, 2015). Mapping populations are developed by crossing two specific individuals as parents, and then selecting and structuring specific crosses between the progenies over multiple generations (Borevitz & Chory, 2004; Collard et al., 2005; M. S. Kang, 2002; Rafalski, 2010). Since each generation must be maintained to maturity to allow for crosses, mapping population development requires years of time commitment and extensive resources to grow and select the individuals (Jannink et al., 2010; Xu, 2010). BiPAM is also limited by the relatively low number of recombination events that occur throughout mapping population development (Heslot et al., 2012; Jannink et al., 2010; M. S. Kang, 2002; Rafalski, 2010; Xu, 2010). Some plant species allow the development of inbred mapping populations, which can be advantageous because the limited recombination events and allelic diversity will be very strongly associated with the specific phenotypic variation (Chaffin et al., 2016; Collard et al., 2005; M. S. Kang, 2002; C. Li et al., 2018; Singh & Singh, 2015). Unfortunately, the limited recombination events from too much inbreeding also reduces the resolution of a genetic map built from

the inbred population, which results in large QTL regions (Chaffin et al., 2016; Collard et al., 2005; M. S. Kang, 2002; Singh & Singh, 2015). For well-known and simple traits, large QTL regions do not hinder further candidate gene analysis because pathways and regulatory genes have been elucidated and can be identified quickly (Bernardo, 2008; Chaffin et al., 2016; Collard et al., 2005; Hedley et al., 2010; Russell et al., 2011). Conversely, the large QTL regions make it nearly impossible to find novel regulatory candidate genes because the region would contain too many plausible genes. Although there are limitations, BiPAM is powerful in identifying QTLs as long as the mapping population is well designed to maintain a balance of recombination events and allelic diversity to minimize the limitations.

1.5.3. Genome-Wide Association Mapping (GWAS)

Since mapping populations are costly, time-consuming, and sometimes impossible for self-incompatible species, genome-wide association mapping studies (GWAS) were developed to conduct association mapping while mitigating some of the BiPAM limitations. GWAS was initially developed for association mapping of humans because developing a mapping population is unrealistic (Gibson, 2018; Korte & Farlow, 2013; Meyer & Purugganan, 2013; Visscher et al., 2017). Over the past decade of GWASs with human datasets, researchers are improving the algorithms and analyses of GWASs, which has resulted in a plethora of more robust results that have also been functionally validated (Gibson, 2018; Korte & Farlow, 2013; Visscher et al., 2017). For example, multiple GWASs for type-2 diabetes, insulin resistance, consistently identified a QTL region that contained a putative candidate gene for a pancreatic-specific zinc transporter (Visscher et al., 2017). The putative candidate gene was functionally validated through resequencing as a loss-of-function mutation, and has led to pharma companies developing an antagonist that targets this specific pancreatic zinc transporter (Visscher et al., 2017). Also, these type-2 diabetes GWASs show QTL and putative candidate gene results that implicate insulin secretion regulation as a major player in type-2 diabetes risk, thus redirecting treatment research (Visscher et al., 2017). A GWAS analyzes an unrelated population that does not exhibit a distinct kinship like a BiPAM mapping population and statistically associates the genetic variation with phenotypic variation to identify QTL regions (Atwell et al., 2010; Gibson, 2018; Korte &

Farlow, 2013; Riedelsheimer et al., 2012; Visscher, Brown, McCarthy, & Yang, 2012; Visscher et al., 2017). Unlike BiPAM, the unrelated population for GWAS can analyze multiple different traits from the same population dataset because the unrelated populations exhibit much greater allelic diversity. Although drastically more genetic data is needed, the greater number of recombination events within an unrelated population can increase the mapping resolution along with decrease the size of potential QTL regions, which improves the GWAS results and putative candidate gene list (Atwell et al., 2010; H M Kang et al., 2008; Korte & Farlow, 2013; Riedelsheimer et al., 2012; Visscher et al., 2012, 2017).

Unfortunately, there are also limitations to conducting a GWAS. Although the genetic and allelic diversity is a positive advantage, the large volume of genetic data from the GWAS population as well as the extensive diversity from an unrelated population can lead to inadequately analyzed data (Atwell et al., 2010; H M Kang et al., 2008; Hyun Min Kang et al., 2010; Korte & Farlow, 2013; Visscher et al., 2012, 2017). To represent this extensive diversity, GWAS research requires a very large number of genetic markers, which subsequently needs more investment and initial analyses to appropriately genotype the population. Another limitation is the variation of genetic linkage often changes between large, diverse populations, which makes comparisons between different populations and GWASs difficult. Genetic linkage or linkage disequilibrium is the distance at which linkage decays, thus each population needs to calculate its specific linkage disequilibrium (Gibson, 2018; Korte & Farlow, 2013; Visscher et al., 2012, 2017). Calculating linkage disequilibrium requires a greater density of genetic markers across a much larger population for greater statistical power (Atwell et al., 2010; H M Kang et al., 2008; Korte & Farlow, 2013; Riedelsheimer et al., 2012; Visscher et al., 2012, 2017). The larger population increases the power of the statistical associations because the associations are determined based on allele frequencies, not structured recombination frequencies. Consequently, the above-mentioned limitations can be mitigated through designing a GWAS with a large population that is genotyped for a large number of genetic markers (Atwell et al., 2010; Korte & Farlow, 2013; Riedelsheimer et al., 2012; Visscher et al., 2012, 2017).

Another limitation is that diverse populations can also exhibit underlying population structure. Population structure is the distribution and relationship of the genetic variation irrespectively of the traits being analyzed (H M Kang et al., 2008; Hyun Min Kang et al., 2010; Korte & Farlow, 2013; Visscher et al., 2017). For example, in a classroom of random children, there is variation in their genetics and height. Since the children have different ancestry, there will also be some population structure because the children descendant from northern Europe will have some similar historic genetic variation patterns that are different from children descendant from Asia. If the historic genetic variation patterns are not appropriately accounted for, then the GWAS statistics could associate the historic genetic patterns, population structure, as height regulatory QTLs when the QTLs may have no regulatory role on height. This false positive occurs because those historical genetic patterns do statistically occur more often in relation to variation in height, but are not the major regulators for height variation and may mask the identification of an important QTL. Therefore, appropriately accounting for population structure is vital to designing and conducting quality GWAS as it drastically reduces false-positive associations (H M Kang et al., 2008; Hyun Min Kang et al., 2010; Korte & Farlow, 2013; Visscher et al., 2017). Even though there are limitations to conducting a GWAS, it has become a powerful tool for identifying QTLs.

1.6. Successes in Association Mapping and MAS for Crop Improvement

The ability of BiPAM and GWAS to identify multiple QTLs for multiple traits allows for MAS to selectively breed for multiple, desirable traits. Through rigorous breeding strategy development, MAS can integrate multiple QTLs that would regulate different facets a single complex trait, or multiple QTLs that regulate multiple traits into the next generations (Bernardo, 2008; Garrido-Cardenas et al., 2018; Heslot et al., 2012; Hospital, 2009; Singh & Singh, 2015; Tester & Langridge, 2010; Xu & Crouch, 2008). Since improvements in complex traits like yield require differential regulation of multiple processes and pathways, MAS allows for more efficient and successful integration of the multiple regulatory QTLs into the next generation (Al-Khayri et al., 2015; Bernardo, 2008; Collard et al., 2005; Collard & Mackill, 2008; Visscher et al., 2017; Weiner & Freckleton, 2010). Application of MAS into crop breeding is extremely important in

improving food resources because it can not only maintain or improve agronomic productivity, but also improve the fruit quality and nutrition of crops.

MAS has been most successful in improving elite cultivars through the selection and stable incorporation of very specific gene sets (Das, Patra, & Baek, 2017; Foolad & Panthee, 2012; Hanson et al., 2016; Ishii & Araki, 2016; Jannink et al., 2010; C. Li et al., 2018; Miedaner & Korzun, 2012; H. C. Prasanna et al., 2015; Rafalski, 2010). The incorporation of disease resistance gene sets into important cultivars has been very successful in integrating stable resistance (Bradshaw, Hackett, Pande, Waugh, & Bryan, 2008; Lee & Tollenaar, 2007; Miedaner & Korzun, 2012; Schönhals et al., 2017; Zhang et al., 2017). The most routinely applied MAS improvement in cereal breeding programs is the resistance to Fusarium head blight (FHB) in wheat (Miedaner & Korzun, 2012). The two different QTLs identified for Fusarium resistance explained at least 20% of the phenotypic variation for different populations, and was successfully integrated into multiple different elite cultivars across different growing conditions as well as performed by different research groups. Each set of resulting progeny from the different locations and researchers showed significant improvement to FHB resistance, which is a clear indication of stable inheritance of FHB resistance. Enhancing FHB resistance in wheat will reduce wheat biomass loss and improve wheat overall harvest (Miedaner & Korzun, 2012). The incorporation of fungal resistance to barley mild mosaic virus (BaMMV) and barley yellow mosaic virus type 1 (BaYMV-1) in barley cultivars is another great example of incorporating MAS gene sets to improve disease resistance (Heslot et al., 2012; Miedaner & Korzun, 2012). Initial efforts through traditional selective breeding struggled to identify and separate resistance QTLs because the resistance genes exhibit recessive inheritance. Through meticulous breeding strategy development, QTLs for multiple different resistance genes were successfully identified through backcrossing and fine-tuned marker development. The majority of current elite barley cultivars show significant improvements in resistance to both mosaic viruses through successful MAS breeding (Heslot et al., 2012; Miedaner & Korzun, 2012).

The popularity and robust genomic resources for tomato breeding have allowed many association mapping studies to identify a large diversity of QTLs as well as integrate some of the significant QTLs into successful MAS programs (Bernardo, 2008;

Collard et al., 2005; Foolad & Panthee, 2012; Hanson et al., 2016; H. C. Prasanna et al., 2015). For example, many fields and greenhouses lose substantial yield to the late blight fungal pathogen, but a few resistance genes have been identified through association mapping (Foolad & Panthee, 2012; Hanson et al., 2016). With physical mapping and validation across multiple diverse population, the third resistance gene was strongly linked with a specific marker and exhibited good broad-spectrum resistance. Although MAS has successfully screened and integrated this broad-spectrum late blight resistance, parallel integration of the second resistance gene along with the third has resulted in the strongest broad-spectrum late blight resistance and has been readily applied to MAS breeding programs and taken to market (Foolad & Panthee, 2012; Hanson et al., 2016). Utilizing MAS and markers allows for early screening of seedlings for both resistance markers, thus saving time and resources (Bernardo, 2008; Collard et al., 2005; Foolad & Panthee, 2012; Hanson et al., 2016; H. C. Prasanna et al., 2015). Recently, MAS was successful in developing a few cultivars that incorporate resistance QTLs for six different pathogens (Hanson et al., 2016). Although these cultivars need to be further tested across different environmental conditions, these cultivars show a significant increase in yield (Hanson et al., 2016).

Although tomatoes have been a model for researching fleshy fruit development, ripening, and quality, the research has shown that the regulation of these processes is extremely complex (Azzi et al., 2015; Duangjit, Causse, & Sauvage, 2016; Osorio et al., 2013; Seymour, Chapman, et al., 2013). Since the fleshy fruit characteristics are multifaceted, the plethora of identified QTLs based on these characteristics are usually not specific or narrow enough for QTL or candidate gene functional validation (Klee, 2010; Osorio et al., 2013; Passam et al., 2007; Rolin, Teyssier, Hong, & Gallusci, 2015; Seymour, Chapman, et al., 2013). For tomato fruit size, one QTL, also associated with Brix sugar content, has a functionally validated candidate gene, a fruit-specific invertase, that has been proposed to regulate the fruit organ sink strength (Duangjit et al., 2016; Passam et al., 2007; Rolin et al., 2015). Improving the association mapping and subsequent MAS of fruit characteristics requires further elucidation of the fleshy fruit characteristics into more specific aspects that contribute to the overall fruit phenotype. For example, the overall fruit flavor phenotype can be separated into more

specific aspects like each of the five tastes, the ratio of specific tastes, and retronasal olfaction of volatiles (Kader, 2008; Klee, 2010; McGinn, 2015; Spence, 2015). These more specific phenotypes can result in narrow QTL regions containing more specific, regulatory candidate genes that will be more applicable to MAS breeding.

1.7. Research Program and Dissertation Objectives

The overarching research objective of this dissertation is to gain a greater understanding of and improve the genomic and metabolic resources for blueberry and broccoli crops, which coincides with the goals of the Plants for Human Health Institute initiative, the Plant Pathways Elucidation Project (P²EP). The P²EP is a multidisciplinary consortium of multiple universities and industry partners working together to improve human health through accomplishing the program's three goals: science, knowledgebase, and education. The scientific goal is to answer three questions: What do plants make? How do they make them? and how do those compounds benefit human health? Although the questions seem simple, the answers are extremely complex and require a highly collaborative environment across multiple disciplines. The knowledgebase goal is to develop a platform, accessible to a diversity of expertise, that compiles the known information from multiple databases and current P²EP data on phytochemical pathways and human health. The platform transforms into a knowledgebase when researchers curate and interact with the data through queries and knowledgebase discoveries to aid in generating new hypotheses for future research. The education goal is to train Ph.D. students for both industry and academic research, as well as provide undergraduate research opportunities. The training Ph.D. students receive is unique because it allows the student to experience all aspects of research in both an industry and academic environment. Canonical Ph.D. students are primarily to research limited to the academia environment. The program strives to produce well-rounded Ph.D. students trained in both team and project management skills. The Ph.D. students achieve this by balancing industry and academia research as well as developing and executing the internship research programs for undergraduates.

The undergraduate internship research program occurs during the summer over 10-11 weeks where the undergraduates gain experience in cutting edge research as well as professional development and networking skills. The P²EP Ph.D. students

became Ph.D. mentors for the undergraduate students and coach them throughout the summer. The Ph.D. mentors are responsible for: developing a conclusive project with a deliverable at program's end, developing modules and lectures to educate the undergraduates in advanced research concepts and professional skills, training undergraduates on advanced research techniques, and managing the team work environment to complete and present the project's end deliverable. The specific projects for the undergraduate interns are developed to be an aspect of the Ph.D. mentor's dissertation that has been scaled for 3-5 undergraduate students with varying schooling experience and can be completed in the internship program with a professionally presented poster and oral presentation.

In keeping with the goals of P²EP, the overarching objective for this research is to improve the foundational knowledge of the genetic components associated with agronomic, fruit quality, and metabolic traits in blueberry and broccoli. The results of this research will contribute to and improve the genomic and metabolic resources available for blueberry and broccoli, and aid the blueberry and broccoli research communities in future research. The QTLs and putative candidate genes identified in this research can be fine-tuned for more efficient application in breeding strategies through functional validation and allelic specific marker development. Functional validation will showcase the effect the QTL marker variation has on the associated trait. Developing allelic specific markers will create new markers that are more strongly links the marker and trait variation. Improvements to the QTL markers and candidate genes will improve MAS application through screening efficiency of the population as well as selection accuracy of parents and progeny. The identified putative candidate genes provide important preliminary insight into the trait's regulatory genes and pathways, which focuses the future research on validating the regulatory effect and specificity of the gene and allele variation. Overall, the results of this research will be utilized to improve MAS breeding strategies for more productive and nutritious crops that more of society will consume.

This research was separated into 3 aims. Aim 1 is to identify QTLs associated with agronomic and fruit quality traits in blueberry through biparental association mapping (BiPAM). Aim 2 is to conduct metabolic profiling to determine a diversity of

metabolites within blueberries, and utilize the metabolic profile for genetic association mapping to identify QTLs and putative candidate genes linked with important metabolites. Aim 3 is to identify QTLs and putative candidate genes associated with agronomic traits in broccoli through genome-wide association mapping

REFERENCES

- Abe, K., & Watada, A. E. (1991). Ethylene Absorbent to Maintain Quality of Lightly Processed Fruits and Vegetables. *Journal of Food Science*, 56(6), 1589–1592.
- Ahmadinejad, F., Geir Møller, S., Hashemzadeh-Chaleshtori, M., Bidkhorji, G., & Jami, M.-S. (2017). Molecular Mechanisms behind Free Radical Scavengers Function against Oxidative Stress. *Antioxidants*, 6(3), 51.
- Al-Khayri, J. M., Jain, S. M., & Johnson, D. V. (2015). *Advances in Plant Breeding Strategies: Breeding, Biotechnology and Molecular Tools*. Cham: Springer International Publishing.
- Atwell, S., Huang, Y. S., Vilhjálmsson, B. J., Willems, G., Horton, M., Li, Y., ... Nordborg, M. (2010). Genome-wide association study of 107 phenotypes in *Arabidopsis thaliana* inbred lines. *Nature*, 465(7298), 627–631.
- Ayub, R. A., Bosetto, L., Galvão, C. W., Etto, R. M., Inaba, J., & Lopes, P. Z. (2016). Abscisic acid involvement on expression of related gene and phytochemicals during ripening in strawberry fruit *Fragaria × ananassa* cv. Camino Real. *Scientia Horticulturae*, 203, 178–184.
- Azzi, L., Deluche, C., Gévaudant, F., Frangne, N., Delmas, F., Hernould, M., & Chevalier, C. (2015). Fruit growth-related genes in tomato. *Journal of Experimental Botany*, 66(4), 1075–1086.
- Barrett, D. M., Beaulieu, J. C., & Shewfelt, R. (2010). Color, flavor, texture, and nutritional quality of fresh-cut fruits and vegetables: Desirable levels, instrumental and sensory measurement, and the effects of processing. *Critical Reviews in Food Science and Nutrition*, 50(5), 369–389.
- Bennett, E., Roberts, J. A., & Wagstaff, C. (2012). Manipulating resource allocation in plants. *Journal of Experimental Botany*, 63(9), 3391–3400.
- Bernardo, R. (2008). Molecular markers and selection for complex traits in plants: Learning from the last 20 years. *Crop Science*, 48(5), 1649–1664.
- Betoret, E., Betoret, N., Vidal, D., & Fito, P. (2011). Functional foods development: Trends and technologies. *Trends in Food Science and Technology*, 22(9), 498–508.
- Biltekoff, C. (2010). Consumer response: The paradoxes of food and health. *Annals of the New York Academy of Sciences*, 1190, 174–178.
- Blaker, K. M., Plotto, A., Baldwin, E. A., & Olmstead, J. W. (2014). Correlation between sensory and instrumental measurements of standard and crisp-texture southern highbush blueberries (*Vaccinium corymbosum* L. interspecific hybrids): Southern highbush blueberry texture. *Journal of the Science of Food and Agriculture*, 94(13), 2785–2793.
- Borevitz, J. O., & Chory, J. (2004). Genomics tools for QTL analysis and gene discovery. *Current Opinion in Plant Biology*, 7(2), 132–136.
- Bradshaw, J. E., Hackett, C. A., Pande, B., Waugh, R., & Bryan, G. J. (2008). QTL mapping of yield, agronomic and quality traits in tetraploid potato (*Solanum tuberosum* subsp. *tuberosum*). *Theoretical and Applied Genetics*, 116(2), 193–211.
- Buchanan, B. B., Gruissem, W., & Jones, R. L. (2012). *Biochemistry & Molecular Biology of Plants*. American Society of Plant Biologists: 15501 Monona Drive, Rockville, MD 20855-2768 USA; Markono Print Media Pte Ltd.
- Cabrera-Bosquet, L., Crossa, J., von Zitzewitz, J., Serret, M. D., & Luis Araus, J. (2012). High-throughput Phenotyping and Genomic Selection: The Frontiers of Crop

- Breeding Converge. *Journal of Integrative Plant Biology*, 54(5), 312–320.
- Chaffin, A. S., Huang, Y.-F., Smith, S., Bekele, W. A., Babiker, E., Gnanesh, B. N., ... Tinker, N. A. (2016). A Consensus Map in Cultivated Hexaploid Oat Revealed Conserved Grass Synteny with Substantial Sub-Genome Rearrangement. *The Plant Genome*, 9(2), 0.
- Chandrasekhar, K., Shavit, R., Distelfeld, A., Christensen, S. A., & Tzin, V. (2018). Exploring the metabolic variation between domesticated and wild tetraploid wheat genotypes in response to corn leaf aphid infestation. *Plant Signaling and Behavior*, 13(6), 1–5.
- Chiva-Blanch, G., & Visioli, F. (2012). Polyphenols and health: Moving beyond antioxidants. *Journal of Berry Research*, 2(2), 63–71.
- Choi, C., Wiersma, P. A., Toivonen, P., & Kappel, F. (2002). Fruit growth, firmness and cell wall hydrolytic enzyme activity during development of sweet cherry fruit treated with gibberellic acid (GA3). *Journal of Horticultural Science and Biotechnology*, 77(5), 615–621.
- Collard, B. C. Y., Jahufer, M. Z. Z., Brouwer, J. B., & Pang, E. C. K. (2005). An introduction to markers, quantitative trait loci (QTL) mapping and marker-assisted selection for crop improvement: The basic concepts. *Euphytica*, 142(1–2), 169–196.
- Collard, B. C. Y., & Mackill, D. J. (2008). Marker-assisted selection: an approach for precision plant breeding in the twenty-first century. *Philosophical Transactions of the Royal Society B: Biological Sciences*, 363(1491), 557–572.
- Cruz, J. A., Yin, X., Liu, X., Imran, S. M., Morris, D. D., Kramer, D. M., & Chen, J. (2016). Multi-modality imagery database for plant phenotyping. *Machine Vision and Applications*, 27(5), 735–749.
- Das, G., Patra, J. K., & Baek, K.-H. (2017). Insight into MAS: A Molecular Tool for Development of Stress Resistant and Quality of Rice through Gene Stacking. *Frontiers in Plant Science*, 8.
- Deng, J., Ran, J., Wang, Z., Fan, Z., Wang, G., Ji, M., ... Brown, J. H. (2012). Models and tests of optimal density and maximal yield for crop plants. *Proceedings of the National Academy of Sciences*, 109(39), 15823–15828.
- Duangjit, J., Causse, M., & Sauvage, C. (2016). Efficiency of genomic selection for tomato fruit quality. *Molecular Breeding*, 36(3), 1–16.
- Estornell, L. H., Agustí, J., Merelo, P., Talón, M., & Tadeo, F. R. (2013). Elucidating mechanisms underlying organ abscission. *Plant Science*, 199–200, 48–60.
- Fasoli, M., Richter, C. L., Zenoni, S., Bertini, E., Vitulo, N., Dal Santo, S., ... Tornielli, G. B. (2018). Timing and order of the molecular events marking the onset of berry ripening in grapevine. *Plant Physiology*, pp.00559.2018.
- Fischer, R. A., & Edmeades, G. O. (2010). Breeding and cereal yield progress. *Crop Science*, 50(April), S-85-S-98.
- Foolad, M. R., & Panthee, D. R. (2012). Marker-Assisted Selection in Tomato Breeding. *Critical Reviews in Plant Sciences*, 31(2), 93–123.
- Fu, J., Chen, Z., Han, L. J., & Ren, L. Q. (2018). Review of grain threshing theory and technology. *International Journal of Agricultural and Biological Engineering*, 11(3), 12–20.
- Fuller, D. Q. (2007). Contrasting patterns in crop domestication and domestication

- rates: Recent archaeobotanical insights from the old world. *Annals of Botany*, 100(5), 903–924.
- Fuller, D. Q., Allaby, R. G., & Stevens, C. (2010). Domestication as innovation: The entanglement of techniques, technology and chance in the domestication of cereal crops. *World Archaeology*, 42(1), 13–28.
- Furbank, R. T., & Tester, M. (2011). Phenomics – technologies to relieve the phenotyping bottleneck. *Trends in Plant Science*, 16(12), 635–644.
- Gambín, B. L., & Borrás, L. (2010). Resource distribution and the trade-off between seed number and seed weight: A comparison across crop species. *Annals of Applied Biology*, 156(1), 91–102.
- Gardner, M., Heinz, R., Wang, J., & Mitchum, M. G. (2017). Genetics and Adaptation of Soybean Cyst Nematode to Broad Spectrum Soybean Resistance. *G3; Genes|Genomes|Genetics*, 7(3), 835–841.
- Garrido-Cardenas, J. A., Mesa-Valle, C., & Manzano-Agugliaro, F. (2018). Trends in plant research using molecular markers. *Planta*, 247(3), 543–557.
- Gibson, G. (2018). Population genetics and GWAS: A primer. *PLoS Biology*, 16(3), 1–6.
- Giongo, L., Poncetta, P., Loretto, P., & Costa, F. (2013). Texture profiling of blueberries (*Vaccinium* spp.) during fruit development, ripening and storage. *Postharvest Biology and Technology*, 76, 34–39.
- Giovannoni, J. (2001). Molecular Biology of Fruit Maturation and Ripening. *Annual Review of Plant Physiology and Plant Molecular Biology*, 52, 725–749.
- Giovannoni, J. J. (2004). Genetic Regulation of Fruit Development and Ripening. *The Plant Cell*, 16, S170–S180.
- Goff, S. A., & Klee, H. J. (2006). Plant Volatile Compounds: Sensory Cues for Health and Nutritional Value? *Science, New Series*, 311(5762), 815–819.
- Grunert, K. G. (2005). Food quality and safety: Consumer perception and demand. *European Review of Agricultural Economics*, 32(3), 369–391.
- Gul, K., Tak, A., Singh, A. K., Singh, P., Yousuf, B., & Wani, A. A. (2015). Chemistry, encapsulation, and health benefits of B-carotene - A review. *Cogent Food & Agriculture*, 1(1), 1–12.
- Gulfishan, M., Jahan, A., Bhat, T. A., & Sahab, D. (2019). Plant Senescence and Organ Abscission. *Senescence Signalling and Control in Plants*, 255–272.
- Hanson, P., Lu, S. F., Wang, J. F., Chen, W., Kenyon, L., Tan, C. W., ... Yang, R. Y. (2016). Conventional and molecular marker-assisted selection and pyramiding of genes for multiple disease resistance in tomato. *Scientia Horticulturae*, 201, 346–354.
- Hashemi, A. M., Herbert, S. J., & Putnam, D. H. (2005). Yield response of corn to crowding stress. *Agronomy Journal*, 97(3), 839–846.
- Hedley, P. E., Russell, J. R., Jorgensen, L., Gordon, S., Morris, J. A., Hackett, C. A., ... Brennan, R. (2010). Candidate genes associated with bud dormancy release in blackcurrant (*Ribes nigrum* L.). *BMC Plant Biol*, 10, 1–13.
- Heslot, N., Yang, H.-P., Sorrells, M. E., & Jannink, J.-L. (2012). Genomic Selection in Plant Breeding: A Comparison of Models. *Crop Science*, 52(1), 146.
- Hospital, F. (2009). Challenges for effective marker-assisted selection in plants. *Genetica*, 136(2), 303–310.
- Houle, D., Govindaraju, D. R., & Omholt, S. (2010). Phenomics: the next challenge.

- Nature Reviews Genetics*, 11(12), 855–866.
- Howard, L. R., Brownmiller, C., Mauromoustakos, A., & Prior, R. L. (2016). Improved stability of blueberry juice anthocyanins by acidification and refrigeration. *Journal of Berry Research*, 6(2), 189–201.
- Ishii, T., & Araki, M. (2016). Consumer acceptance of food crops developed by genome editing. *Plant Cell Reports*, 35(7), 1507–1518.
- Jannink, J.-L., Lorenz, A. J., & Iwata, H. (2010). Genomic selection in plant breeding: from theory to practice. *Briefings in Functional Genomics*, 9(2), 166–177.
- Jenks, M. A., & Bebeli, P. J. (2011). *Breeding for Fruit Quality*. West Sussex: John Wiley & Sons, Inc.
- Kader, A. A. (2008). Flavor quality of fruits and vegetables. *Journal of the Science of Food and Agriculture*, 88(11), 1863–1868.
- Kang, H M, Zaitlen, N. A., Wade, C. M., Kirby, A., Heckerman, D., Daly, M. J., & Eskin, E. (2008). Efficient Control of Population Structure in Model Organism Association Mapping. *Genetics*, 178(3), 1709–1723.
- Kang, Hyun Min, Sul, J. H., Service, S. K., Zaitlen, N. A., Kong, S., Freimer, N. B., ... Eskin, E. (2010). Variance component model to account for sample structure in genome-wide association studies. *Nature Genetics*, 42(4), 348–354.
- Kang, M. S. (2002). *Quantitative genetics, genomics and plant breeding*. New York: CABI Publishing.
- Kearney, J. (2010). Food consumption trends and drivers. *Philosophical Transactions of the Royal Society B: Biological Sciences*, 365(1554), 2793–2807.
- Khoo, H. E., Azlan, A., Tang, S. T., & Lim, S. M. (2017). Anthocyanidins and anthocyanins: colored pigments as food, pharmaceutical ingredients, and the potential health benefits. *Food & Nutrition Research*, 61(1), 1–21.
- Klee, H. J. (2010). Improving the flavor of fresh fruits: Genomics, biochemistry, and biotechnology. *New Phytologist*, 187(1), 44–56.
- Klink, V. P., & Matthews, B. F. (2009). Emerging Approaches to Broaden Resistance of Soybean to Soybean Cyst Nematode as Supported by Gene Expression Studies. *Plant Physiology*, 151(3), 1017–1022.
- Konarska, A. (2015). Development of fruit quality traits and comparison of the fruit structure of two *Vaccinium corymbosum* (L.) cultivars. *Scientia Horticulturae*, 194, 79–90.
- Korte, A., & Farlow, A. (2013). The advantages and limitations of trait analysis with GWAS: a review. *Plant Methods*, 9(1), 1.
- Koutinas, N., Pepelyankov, G., & Lichev, V. (2010). Flower induction and flower bud development in apple and sweet cherry. *Biotechnology and Biotechnological Equipment*, 24(1), 1549–1558.
- Kramer, M. G., & Redenbaugh, K. (1994). Commercialization of a tomato with an antisense polygalacturonase gene: The FLAVR SAVR™ tomato story. *Euphytica*, 79(3), 293–297.
- Kyriacou, M. C., & Roupael, Y. (2018). Towards a new definition of quality for fresh fruits and vegetables. *Scientia Horticulturae*, 234(August 2017), 463–469.
- Langridge, P., & Fleury, D. (2011). Making the most of 'omics' for crop breeding. *Trends in Biotechnology*, 29(1), 33–40.
- Lee, E. A., & Tollenaar, M. (2007). Physiological basis of successful breeding strategies

- for maize grain yield. *Crop Science*, 47(SUPPL. DEC.).
- Li, C., Xu, W., Guo, R., Zhang, J., Qi, X., Hu, L., & Zhao, M. (2018). Molecular marker assisted breeding and genome composition analysis of Zhengmai 7698, an elite winter wheat cultivar. *Scientific Reports*, 8(1).
- Li, P., Lee, S. H., & Hsu, H. Y. (2011). Review on fruit harvesting method for potential use of automatic fruit harvesting systems. *Procedia Engineering*, 23, 351–366.
- Li, X., Xu, C., Korban, S. S., & Chen, K. (2010). Regulatory mechanisms of textural changes in ripening fruits. *Critical Reviews in Plant Sciences*, 29(4), 222–243.
- Lin, D., Xiao, M., Zhao, J., Li, Z., Xing, B., Li, X., ... Chen, S. (2016). An overview of plant phenolic compounds and their importance in human nutrition and management of type 2 diabetes. *Molecules*, 21(10).
- Matas, A. J., Gapper, N. E., Chung, M. Y., Giovannoni, J. J., & Rose, J. K. (2009). Biology and genetic engineering of fruit maturation for enhanced quality and shelf-life. *Current Opinion in Biotechnology*, 20(2), 197–203.
- McGinn, C. (2015). The science of taste. *Metaphilosophy*, 46(1), 84–103.
- Mehta, R. A., Cassol, T., Li, N., Ali, N., Handa, A. K., & Mattoo, A. K. (2002). Engineered polyamine accumulation in tomato enhances phytonutrient content, juice quality, and vine life. *Nature Biotechnology*, 20(6), 613–618.
- Melke, A. (2015). The Physiology of Chilling Temperature Requirements for Dormancy Release and Bud-break in Temperate Fruit Trees Grown at Mild Winter Tropical Climate. *Journal of Plant Studies*, 4(2), 110–156.
- Meyer, R. S., & Purugganan, M. D. (2013). Evolution of crop species: Genetics of domestication and diversification. *Nature Reviews Genetics*, 14(12), 840–852.
- Miedaner, T., & Korzun, V. (2012). Marker-Assisted Selection for Disease Resistance in Wheat and Barley Breeding. *Phytopathology*, 102(6), 560–566.
- Mitchum, M. G. (2016). Soybean resistance to the soybean cyst nematode *Heterodera glycines*: an update. *Phytopathology*, 106(12), 1–29.
- Moggia, C., Graell, J., Lara, I., González, G., & Lobos, G. A. (2017). Firmness at Harvest Impacts Postharvest Fruit Softening and Internal Browning Development in Mechanically Damaged and Non-damaged Highbush Blueberries (*Vaccinium corymbosum* L.). *Frontiers in Plant Science*, 8(April), 1–11.
- Muleke, E. M., Fan, L., Wang, Y., Xu, L., Zhu, X., Zhang, W., ... Liu, L. (2017). Coordinated Regulation of Anthocyanin Biosynthesis Genes Confers Varied Phenotypic and Spatial-Temporal Anthocyanin Accumulation in Radish (*Raphanus sativus* L.). *Frontiers in Plant Science*, 8(July), 1–17.
- Musacchi, S., & Serra, S. (2018). Apple fruit quality: Overview on pre-harvest factors. *Scientia Horticulturae*, 234(December 2017), 409–430.
- Nielsen, R., Paul, J. S., Albrechtsen, A., & Song, Y. S. (2011). Genotype and SNP calling from next-generation sequencing data. *Nature Reviews Genetics*, 12(6), 443–451.
- Nile, S. H., & Park, S. W. (2014). Edible berries: Bioactive components and their effect on human health. *Nutrition*, 30(2), 134–144.
- O. Sadras, V., & F. Denison, R. (2009). Do plant parts compete for resources? An evolutionary viewpoint. *New Phytologist*, 183(3), 565–574.
- Osorio, S., Scossa, F., & Fernie, A. R. (2013). Molecular regulation of fruit ripening. *Frontiers in Plant Science*, 4(June 2013).

- Pagliarini, E., Laureati, M., & Gaeta, D. (2013). Sensory descriptors, hedonic perception and consumer's attitudes to Sangiovese red wine deriving from organically and conventionally grown grapes. *Frontiers in Psychology*, 4(NOV), 1–7.
- Passam, H. C., Karapanos, I. C., Bebeli, P. J., & Savvas, D. (2007). A review of recent research on tomato nutrition, breeding and post-harvest technology with reference to fruit quality. *The European Journal of Plant Science and Biotechnology*, 1 (1), 1–21.
- Pinasseau, L., Vallverdú-Queralt, A., Verbaere, A., Roques, M., Meudec, E., Le Cunff, L., ... Cheynier, V. (2017). Cultivar Diversity of Grape Skin Polyphenol Composition and Changes in Response to Drought Investigated by LC-MS Based Metabolomics. *Frontiers in Plant Science*, 8(October), 1–24.
- Pinu, F., Pinu, & R, F. (2018). Grape and Wine Metabolomics to Develop New Insights Using Untargeted and Targeted Approaches. *Fermentation*, 4(4), 92.
- Poland, J. A., & Rife, T. W. (2012). Genotyping-by-Sequencing for Plant Breeding and Genetics. *The Plant Genome Journal*, 5(3), 92.
- Posé, S., Nieves, J. a G., Quesada, F. P. M. a, & Mercado, J. a. (2011). Strawberry Fruit Softening : Role of Cell Wall Disassembly and its Manipulation in Transgenic Plants. *Genes, Genomes and Genomics*, 5, 40–48.
- Prasanna, H. C., Kashyap, S. P., Krishna, R., Sinha, D. P., Reddy, S., & Malathi, V. G. (2015). Marker assisted selection of Ty-2 and Ty-3 carrying tomato lines and their implications in breeding tomato leaf curl disease resistant hybrids. *Euphytica*, 204(2), 407–418.
- Prasanna, V., Prabha, T. N., & Tharanathan, R. N. (2007). Fruit ripening phenomena-an overview. *Critical Reviews in Food Science and Nutrition*, 47(1), 1–19.
- Rafalski, J. A. (2010). Association genetics in crop improvement. *Current Opinion in Plant Biology*, 13(2), 174–180.
- Rasheed, A., Hao, Y., Xia, X., Khan, A., Xu, Y., Varshney, R. K., & He, Z. (2017). Crop Breeding Chips and Genotyping Platforms: Progress, Challenges, and Perspectives. *Molecular Plant*, 10(8), 1047–1064.
- Riedelsheimer, C., Lisec, J., Czedik-Eysenberg, A., Sulpice, R., Flis, A., Grieder, C., ... Melchinger, A. E. (2012). Genome-wide association mapping of leaf metabolic profiles for dissecting complex traits in maize. *Proceedings of the National Academy of Sciences*, 109(23), 8872–8877.
- Rolin, D., Teyssier, E., Hong, Y., & Gallusci, P. (2015). *Tomato fruit quality improvement facing the functional genomics revolution. Applied Plant Genomics and Biotechnology*. Elsevier Ltd.
- Roubelakis-Angelakis, K. A. (n.d.). *Grapevine Molecular Physiology & Biotechnology*.
- Russell, J. R., Bayer, M., Booth, C., Cardle, L., Hackett, C. A., Hedley, P. E., ... Brennan, R. M. (2011). Identification, utilisation and mapping of novel transcriptome-based markers from blackcurrant (*Ribes nigrum*). *BMC Plant Biology*, 11(1), 147.
- Sam Saguy, I. (2011). Paradigm shifts in academia and the food industry required to meet innovation challenges. *Trends in Food Science and Technology*, 22(9), 467–475.
- Schaart, J. G., van de Wiel, C. C. M., Lotz, L. A. P., & Smulders, M. J. M. (2016). Opportunities for Products of New Plant Breeding Techniques. *Trends in Plant*

- Science*, 21(5), 438–449.
- Schönhals, E. M., Ding, J., Ritter, E., Paulo, M. J., Cara, N., Tacke, E., ... Gebhardt, C. (2017). Physical mapping of QTL for tuber yield, starch content and starch yield in tetraploid potato (*Solanum tuberosum* L.) by means of genome wide genotyping by sequencing and the 8.3 K SolCAP SNP array. *BMC Genomics*, 18(1).
- Schwab, W., Davidovich-Rikanati, R., & Lewinsohn, E. (2008). Biosynthesis of plant-derived flavor compounds. *Plant Journal*, 54(4), 712–732.
- Serrano, A., Espinoza, C., Armijo, G., Inostroza-Blancheteau, C., Pobleto, E., Meyer-Regueiro, C., ... Arce-Johnson, P. (2017). Omics Approaches for Understanding Grapevine Berry Development: Regulatory Networks Associated with Endogenous Processes and Environmental Responses. *Frontiers in Plant Science*, 8(September), 1–15.
- Seymour, G. B., Chapman, N. H., Chew, B. L., & Rose, J. K. C. (2013). Regulation of ripening and opportunities for control in tomato and other fruits. *Plant Biotechnology Journal*, 11(3), 269–278.
- Seymour, G. B., Østergaard, L., Chapman, N. H., Knapp, S., & Martin, C. (2013). Fruit Development and Ripening. *Annual Review of Plant Biology*, 64(1), 219–241.
- Sharma, K. D., Karki, S., Thakur, N. S., & Attri, S. (2012). Chemical composition, functional properties and processing of carrot-a review. *Journal of Food Science and Technology*, 49(1), 22–32.
- Sher, A., Khan, A., Ashraf, U., Liu, H. H., & Li, J. C. (2018). Characterization of the Effect of Increased Plant Density on Canopy Morphology and Stalk Lodging Risk. *Frontiers in Plant Science*, 9(September), 1–12.
- Singh, B. D., & Singh, A. K. (2015). *Marker-Assisted Plant Breeding: Principles and Practices*. New Delhi: Springer India.
- Spence, C. (2015). Multisensory flavor Perception. *Cell*, 161(1), 24–35.
- Sutter, N. B., & Ostrander, E. A. (2004). Dog star rising: The canine genetic system. *Nature Reviews Genetics*, 5(12), 900–910.
- Tester, M., & Langridge, P. (2010). Breeding Technologies to Increase Crop Production in a Changing World. *Science*, 327(5967), 818–822.
- Tieman, D., Bliss, P., McIntyre, L. M. M., Blandon-Ubeda, A., Bies, D., Odabasi, A. Z. Z., ... Klee, H. J. J. (2012). The chemical interactions underlying tomato flavor preferences. *Current Biology*, 22(11), 1035–1039.
- Tobey, L. N., & Manore, M. M. (2014). Social media and nutrition education: The food hero experience. *Journal of Nutrition Education and Behavior*, 46(2), 128–133.
- Toivonen, P. M. A. A., & Brummell, D. A. (2008). Biochemical bases of appearance and texture changes in fresh-cut fruit and vegetables. *Postharvest Biology and Technology*, 48(1), 1–14.
- Tzarfati, R., Saranga, Y., Barak, V., Gopher, A., Korol, A. B., & Abbo, S. (2013). Threshing efficiency as an incentive for rapid domestication of emmer wheat. *Annals of Botany*, 112(5), 829–837.
- Ulrich, D., & Olbricht, K. (2014). Diversity of metabolite patterns and sensory characters in wild and cultivated strawberries¹. *Journal of Berry Research*, 4(1), 11–17.
- USDA, N. A. S. S. (2012). *Census of Agriculture: US National Level Data*.
- Varela, P., & Ares, G. (2012). Sensory profiling, the blurred line between sensory and consumer science. A review of novel methods for product characterization. *Food*

- Research International*, 48(2), 893–908.
- Visscher, P. M., Brown, M. A., McCarthy, M. I., & Yang, J. (2012). Five years of GWAS discovery. *American Journal of Human Genetics*, 90(1), 7–24.
- Visscher, P. M., Wray, N. R., Zhang, Q., Sklar, P., McCarthy, M. I., Brown, M. A., & Yang, J. (2017). 10 Years of GWAS Discovery: Biology, Function, and Translation. *American Journal of Human Genetics*, 101(1), 5–22.
- Wang, S., Yang, C., Tu, H., Zhou, J., Liu, X., Cheng, Y., ... Xu, J. (2017). Characterization and Metabolic Diversity of Flavonoids in Citrus Species. *Scientific Reports*, 7(1), 1–10.
- Weiner, J., & Freckleton, R. P. (2010). Constant Final Yield. *Annual Review of Ecology, Evolution, and Systematics*, 41(1), 173–192.
- Winter, P., & Kahl, G. (1995). Molecular Marker Technologies for Plant Improvement. *World Journal of Microbiology & Biotechnology*, 11(4), 438–448.
- Xu, Y. (2010). *Molecular Plant Breeding*. New York: CABI Publishing.
- Xu, Y., & Crouch, J. H. (2008). Marker-Assisted Selection in Plant Breeding: From Publications to Practice. *Crop Science*, 48(2), 391.
- Zeiss, D. R., Mhlongo, M. I., Tugizimana, F., Steenkamp, P. A., & Dubery, I. A. (2018). Comparative metabolic phenotyping of tomato (*Solanum lycopersicum*) for the identification of metabolic signatures in cultivars differing in resistance to *Ralstonia solanacearum*. *International Journal of Molecular Sciences*, 19(9).
- Zhang, H., Mittal, N., Leamy, L. J., Barazani, O., & Song, B. H. (2017). Back into the wild—Apply untapped genetic diversity of wild relatives for crop improvement. *Evolutionary Applications*, 10(1), 5–24.

**Chapter 2. Blueberry Agronomic and Fruit Quality Biparental Association
Mapping**

2.1. Abstract

Perennial plants undergo dormancy, an arrest of active meristem growth, to protect the meristems during harsh conditions until favorable conditions return to cycle the meristems out of dormancy, into dormancy break, and the resumption of active growth. The fitness of blueberry floral buds to progress through dormancy break largely contributes to subsequent blueberry fruit yield. The Draper by Jewel (DxJ) mapping population was developed with parents adapted to the commercial habitat extremes in order to investigate blueberry growth, dormancy efficiency, and fruit quality. For 100 DxJ individuals, genotype marker information and multiple agronomic and fruit phenotypes were collected for two years at two locations. A DxJ specific genetic map was developed from the genetic markers to conduct bi-parental association mapping (BiPAM) of the growth, dormancy, and fruit quality traits. This was to identify quantitative trait loci (QTLs) for location-specific, year-specific, and both location and year -specific QTLs. The BiPAM results for the growth traits revealed many QTL regions for bud meristem development. The growth traits identified the largest number of location-specific and year-specific QTLs, which indicates the environmental variation from the locations and years impact the growth traits. Upon further investigation of all the QTLs, many overlapping QTL regions contained at least three QTLs from different analyses of the same trait, supporting the association between the trait and QTL. The majority of the growth traits' overlapping QTL regions contained QTLs for bud density and plant vigor traits. The dormancy break and flowering BiPAM results identified one chill requirement QTL, and four overlapping QTL regions for the two dormancy break traits. Fruit ripening and consumer-driven quality characteristics were also collected across the population to investigate the regulation and enhancement of blueberry texture, flavor, and nutrition. The fruit quality BiPAM results identified the largest number of QTLs and overlapping QTL regions. While half of the overlapping QTL regions contained specific blueberry firmness QTLs, the other half contained QTLs involved in regulating color, flavor, and firmness. The significant QTLs identified in this research can be utilized to further elucidate the pathways regulating blueberry bud meristem density, dormancy break, and fruit quality, as well as aid future breeding strategies in improving blueberry floral buds density and yield of blueberries with enhanced fruit quality and nutrition.

2.2. Introduction

Blueberry consumption and research has exponentially increased in the past few years due to its plethora of health benefits and recent labeling as a “super food” (S. Silva, Costa, Veiga, Morais, & Pintado, 2018). With its increase in popularity, the blueberry industry in the US in 2016 increased total production from 2015 by 5% to a total of 593.6 million pounds (Eklund, 2016). The blueberry industry is projected to continue increasing as blueberry harvest is increasing to over 200 lbs/acre, and demand continues to push research innovation (Eklund, 2016). When compared to the recommend daily values for an average adult, the consumption of only 1 cup of fresh blueberries provides 14% of the recommended dietary fiber and 21.6% of the recommended manganese intake (FDA, 2019; NIH, 2019; USDA, 2018). Dietary fiber is essential for maintaining a healthy digestive system, and manganese is essential for processing cholesterol and proteins (FDA, 2019; Kader, 2008; Kearney, 2010; Nile & Park, 2014). The 1 cup of blueberries also provides 16% of the recommended vitamin C and 23.8% of the recommended vitamin K intake (NIH, 2019; USDA, 2018). Vitamin C is an essential antioxidant in the body because it reduces the effect of oxidative stress (Buchanan, Gruisse, & Jones, 2012; Foyer & Noctor, 2011; Jenks & Bebeli, 2011; Nile & Park, 2014). Vitamin K is also essential to the body as it regulates blood clotting and bone health (Buchanan et al., 2012; Jenks & Bebeli, 2011; Nile & Park, 2014). Even though blueberries provide a diversity of essential nutrients, blueberries were designated a “super food” after a plethora of research showed its potent antioxidant capacity (Betoret, Betoret, Vidal, & Fito, 2011; Biltekoff, 2010; Kearney, 2010). In brief, antioxidant compounds neutralize free-radical compounds when there is an overabundance of free-radicals within the body. An overabundance of free-radicals causes oxidative stress, which has been closely linked to causing chronic inflammation, heart disease, and Alzheimer’s (Edirisinghe & Burton-Freeman, 2016; Giacalone et al., 2011; D. Lin et al., 2016; Lobo, Patil, Phatak, & Chandra, 2010; Ma et al., 2018). A detailed description of antioxidant mechanisms is in Chapter 3. Since the US is the leading blueberry producer, blueberries are an affordable, natural source of essential nutrients and antioxidant health benefits.

Although blueberry production has increased, blueberry breeding still strives to improve agronomic traits like yield, growth range, and bud hardiness in order to meet the continually increasing demand for blueberries. Unfortunately, blueberry breeding faces challenges because a blueberry bush reaches fruiting maturity after 3 years, and exhibits inbreeding depression (J F Hancock et al., 2008; Trehane, 2004). Inbreeding depression occurs when the offspring show reduced biological fitness after multiple generations of parents undergo self-fertilization (J F Hancock et al., 2008; Trehane, 2004). Therefore, blueberry breeders are unable to produce inbred lines, which are commonly produced for grain breeding and research (Fischer & Edmeades, 2010; Jim F Hancock, 2008; Hospital, 2009; Jannink, Lorenz, & Iwata, 2010; Trehane, 2004). An inbred line is a specific group of individuals that have undergone extensive inbreeding to select for variation only at a specific location while the rest of the genome is nearly identical (Fischer & Edmeades, 2010; M. S. Kang, 2002; Xu, 2010). The inbred line shows the link between variation at that specific genetic region and variation in the desirable trait (Fischer & Edmeades, 2010; M. S. Kang, 2002; Xu, 2010). Thus, blueberry breeding must utilize different breeding strategies, like crossing the progeny back to one of the parents, which will unfortunately require multiple generations, more time, and more resources to obtain progeny with the appropriate genetic variation (M. S. Kang, 2002; B. D. Singh & Singh, 2015; Xu, 2010). The recent advancements in bioinformatics and genomics has rapidly improved the efficiency of both population genetics and selective breeding (Al-Khayri, Jain, & Johnson, 2015; Garrido-Cardenas, Mesa-Valle, & Manzano-Agugliaro, 2018; Schaart, van de Wiel, Lotz, & Smulders, 2016; Sehgal, Singh, & Rajpal, 2016; B. D. Singh & Singh, 2015; H. Zhang, Mittal, Leamy, Barazani, & Song, 2017). Utilizing over 60 years of blueberry breeding knowledge with the improved genetics and breeding strategies has allowed for more efficient blueberry breeding.

2.2.1 Blueberry Crop History and Agronomics

The blueberry usually found at the stores and most consumed in North America is *Vaccinium corymbosum* (Mark K Ehlenfeldt, 1994; J F Hancock et al., 2008; Trehane, 2004). The *Vaccinium* genus is so large and diverse that researchers are still unsure the phylogenetic classification of *Vaccinium* species. Molecular phylogenetics will aid in

elucidating the phylogenetics and provide greater insight as to the evolutionary domestication of *Vaccinium* crops. *Vaccinium* is divided into 2 subgenera, *Oxycoccus* and *Vaccinium* (Mark K Ehlenfeldt, 1994; J F Hancock et al., 2008; Trehane, 2004). *Oxycoccus* is well known for containing the common and American cranberry (J F Hancock et al., 2008; Trehane, 2004). The *Vaccinium* subgenera is further divided into sections to aid in classifying species. The *myrtillus* section groups together bilberry varieties, huckleberry varieties, and southeast Asia blueberries. The *cyanococcus* section groups together most of the blueberry varieties (Mark K Ehlenfeldt, 1994; J F Hancock et al., 2008; Trehane, 2004).

The blueberry crop can be classified into three different categories: rabbiteye, low-bush, and high-bush (Mark K Ehlenfeldt, 1994; J F Hancock et al., 2008; Trehane, 2004). Rabbiteye blueberries are cultivars that thrive in the southern US. Since rabbiteye blueberries are hexaploids, 6 sets of chromosomes, selective breeding is complicated and very variable (Mark K Ehlenfeldt, 1994; J F Hancock et al., 2008; Trehane, 2004). Low-bush blueberries are traditionally described as only wild blueberries, which can exhibit multiple different ploidy levels. But as recent breeding is starting to incorporate wild blueberries, which would expand low-bush blueberries classification to include those breeding progeny. Some of these varieties can grow in severe habitats like Alaska and Maine. Some researchers have proposed that wild blueberries may exhibit more potent health benefits due to their greater diversity of metabolites (J F Hancock et al., 2008; Trehane, 2004; Whyte, Schafer, & Williams, 2016).

High-bush blueberries were initially cultivated to make productive commercial varieties. The high-bush blueberries originally started in the northern US, but are being cultivated worldwide (J F Hancock et al., 2008; Trehane, 2004). In 2008, highbush blueberries were grown in 37 US states, 6 Canadian provinces, Australia, Chile, Argentina, New Zealand, and many European countries (J F Hancock et al., 2008; Trehane, 2004). These high-bush blueberries are either diploid or tetraploid, two or four sets of chromosomes (J F Hancock et al., 2008; Trehane, 2004). Since the high-bush varieties are very productive, multiple breeding initiatives in the southern US hybridized the high-bush blueberry with native, wild blueberry species to expand the high-bush

growing range. The hybridizations lead to the development of southern high-bush varieties (SHB) (Gilbert, Schwieterman, Colquhoun, Clark, & Olmstead, 2013; J F Hancock et al., 2008; Trehane, 2004). The northern high-bush (NHB) blueberries require over 600 hours of chilling under 7°C, whereas the new southern high-bush varieties require less than 600 hours of chilling under 7°C (Mark K Ehlenfeldt, 2003; Mark K Ehlenfeldt, Rowland, Ogden, & Vinyard, 2007; Gilbert et al., 2013; J F Hancock et al., 2008; Kovaleski, Williamson, Olmstead, & Darnell, 2015; Timmers, Grace, Yousef, & Lila, 2017; Trehane, 2004). Although there are many varieties of SHB, the NHB varieties are still more hardy and productive. Most abundant NHB crops in US are Michigan, New Jersey, North Carolina, Oregon, and Washington (J F Hancock et al., 2008; Trehane, 2004). Most abundant SHB crops in US are from Georgia, Florida, and California (J F Hancock et al., 2008; Trehane, 2004).

In a brief synopsis of blueberry breeding history, blueberry crop breeding began with the first NHB hybrid cultivar release by Frederick Coville of the USDA in the early 1900s (J F Hancock et al., 2008; Trehane, 2004). Dr. Coville released many NHB hybrids that are still planted over 75% of the US blueberry fields. After Dr. Coville, Dr. Darrow and then Dr. Draper continued breeding NHB blueberries to improve crop hardiness as well as fruit productivity, color, firmness, and scars through collaborative programs all across the US. Southern high-bush (SHB) breeding began later in the 1950s with Dr. Sharp in FL. Majority of SHB cultivars are derived from Dr. Sharp's cultivated *V. darrowii*. Also, in the 1950s, NHB breeding in MI started to incorporate *V. angustifolium* genes to improve cold tolerance, which produced "half-high" cultivars. "Half-high" cultivars have also be produced through lowbush hybridization to increase yield and berry size from lowbush, and protect from extreme cold and snow with lower stature (J F Hancock et al., 2008; Trehane, 2004). Rabbiteye breeding began between 1920-1930s with the collection of wild species from multiple SE states and planted across different SE states (M K Ehlenfeldt & Rowland, 2006; J F Hancock et al., 2008; L J Rowland, 2000; Trehane, 2004). Breeding efforts have improved fruit color, size, texture, and appearance. Lowbush blueberry breeding has been spearheaded in Canada with a recent release of a hybrid that spreads by rhizomes and produces large berries. Current breeding programs are focused on disease-pest resistance, expanded

harvest season, machine harvestability, longer storage-life, and flavor (J F Hancock et al., 2008; Trehane, 2004).

When grown in their native habitat, blueberries exhibit resistance to multiple different diseases and pests (J F Hancock et al., 2008; Trehane, 2004). Since breeding has expanded their growing range, blueberry pathogen resistance has decreased, especially when grown at its range extremes and with increasing climate change. Many of the blueberry diseases infect the soft tissues of buds or the fleshy fruit, which reduces blueberry fitness and berry yield (J F Hancock et al., 2008; Trehane, 2004). For the majority of blueberry diseases, resistant or tolerant genotypes have been identified, but resistance incorporation is difficult due to the polyploidy genomes and limited genetic resources for understanding the resistance's genetic regulation and developing specific transformation systems (J F Hancock et al., 2008; Trehane, 2004). Blueberry pests attack the buds, stems, and fruit as the tissues contain the greatest sugar content (J F Hancock et al., 2008; Trehane, 2004). Similar to disease resistance, genotypes have been found for many of the pests, but breeding it into productive cultivars is difficult. Improving the genomic resources available for blueberry genetics will be vital for efficiently studying and incorporating disease or pest resistance into commercial cultivars (J F Hancock et al., 2008; Trehane, 2004).

Blueberry cultivation season generally spans from May to September (J F Hancock et al., 2008; G. A. Lobos, Callow, & Hancock, 2014; Routray & Orsat, 2011; Scalzo, Stevenson, & Hedderley, 2013; Trehane, 2004). Harvest generally occurs between August and September (J F Hancock et al., 2008; G. A. Lobos et al., 2014; Routray & Orsat, 2011; Scalzo et al., 2013; Trehane, 2004). Harvesting blueberries is a tedious task as normally they are hand-picked and unripe blueberries that ripen after picking exhibit less sweetness and softer texture when the unripe eventually change color and look ripe (Gilbert et al., 2015; J F Hancock et al., 2008; Trehane, 2004). This along with the different ripening rates means multiple picking sessions are required during each harvest season to clean the bushes off. The 4-6 week harvest season for NHB requires at least four picking sessions. The first harvest session usually occurs when 25% of the bush has ripe, blueberries and is hand-picked to ensure the other unripe berries are minimally disturbed (J F Hancock et al., 2008; Trehane, 2004). The

second harvest occurs when 75% of the bush has ripe, blue berries (J F Hancock et al., 2008; Trehane, 2004). If machine harvesting is feasible, this session is when the first of two machine harvests occurs because most of the fruit are ripe and the remaining unripe fruit are close to the cluster stem and less likely to be damaged from the machine harvesting (J F Hancock et al., 2008; Moggia, Graell, Lara, González, & Lobos, 2017; Trehane, 2004). The timing of the remaining harvest session are less structured since most of the blueberries are harvested. Since blueberry flowering and fruiting occurs rapidly in very early spring, the timing and signaling of the environmental and biological signals must be very efficient so that delicate reproductive tissues are not exposed to winter conditions through too early flowering.

2.2.2. Blueberry Dormancy and Flowering

Blueberries are perennial shrubs that undergo dormancy to protect developing tissues during harsh conditions (J F Hancock et al., 2008; Trehane, 2004). All perennial plants exhibit the seasonal cycling into dormancy when environmental stresses threaten tissue damage, as well as out of dormancy to resume active growth when conditions are favorable (Arora, Rowland, & Tanino, 2003; Considine & Considine, 2016; D. P. Horvath, Anderson, Chao, & Foley, 2003; Rohde & Bhalerao, 2007; Shim et al., 2014; Wisniewski et al., 2003). Dormancy has been traditionally defined as the temporary suspension of visible growth of any plant structure containing a meristem (Hussain, Niu, Yang, Hussain, & Teng, 2015; Rohde & Bhalerao, 2007; S. K. Yadav, 2010). Canonically, dormancy is classified into three categories: paradormancy, ecodormancy, and endodormancy (Arora et al., 2003; Rohde & Bhalerao, 2007; Wisniewski et al., 2003). Paradormancy occurs when another part of plant inhibits growth, for example, axillary buds exhibit paradormancy while apical buds are present (Considine & Considine, 2016; Cooke, Eriksson, & Junttila, 2012; Pletsers, Caffarra, Kelleher, & Donnelly, 2015; van der Schoot & Rinne, 2011). Ecodormancy occurs when growth is inhibited by unfavorable environmental conditions, but growth resumption occurs when favorable conditions return (Arora et al., 2003; Rohde & Bhalerao, 2007; Wisniewski et al., 2003). Endodormancy occurs when growth is inhibited by the dormant structure itself and requires specific signals to release inhibition (Arora et al., 2003; Rohde & Bhalerao, 2007; Wisniewski et al., 2003). Most temperate, perennial plants undergo

endodormancy during the winter months to protect floral and vegetative buds from harsh freezing conditions (Considine & Considine, 2016; Cooke et al., 2012; Rohde & Bhalerao, 2007; van der Schoot & Rinne, 2011). The traditional dormancy definitions rely on the bud's visual changes, which does not appropriately represent the dynamics of dormancy as all the changes occur within the bud's cells at a genetic and metabolic level.

Many researchers are now accepting the modified dormancy definition as the inability of a meristem to resume growth under favorable conditions (Cooke et al., 2012; Rohde & Bhalerao, 2007). This definition addresses the state of dormancy exhibited by the meristem, whereas the traditional definition stresses the source of the cues for imposing dormancy (Cooke et al., 2012; Rohde & Bhalerao, 2007). This definition also proposes that the inhibited growth capacity cannot be relieved until a specific signal removes the inhibition to restore growth capacity within the meristem. The categories are still commonly used but are interpreted slightly differently. Paradormancy in axillary meristems have no growth capacity even when conditions are conducive because of the inhibition by the other organ or apical bud meristem (D. P. Horvath et al., 2003; Rohde & Bhalerao, 2007). It is not until the growth inhibitor is removed that growth capacity is restored and growth can occur when conditions become favorable. Endodormancy, like in winter dormancy, occurs when the meristems have no growth capacity even if the plant experienced warm, long day conditions because the growth inhibitor is still present (Considine & Considine, 2016; Cooke et al., 2012; Pletsers et al., 2015; van der Schoot & Rinne, 2011). Ecodormancy is not included within the new definition because the meristems can resume growth under favorable conditions. Many recent studies are distinguishing endodormancy and ecodormancy stages within the traditional dormancy exhibiting by temperate perennial plants (Beauvieux, Wenden, & Dirlewanger, 2018; Considine & Considine, 2016; Lloret, Badenes, & Ríos, 2018; Malyshev, Shelyakin, & Golovko, 2016; Signorelli, Agudelo-Romero, Meitha, Foyer, & Considine, 2018). For this thesis, endodormancy is when the meristems cannot resume growth until the chilling requirement is fulfilled. This transitions the buds into endodormancy release where growth capacity is re-activated. Once re-activated, the buds are in ecodormancy where meristem cells are active by quiescence and waiting for favorable conditions to resume

growth (Beauvieux et al., 2018; Considine & Considine, 2016; Lloret et al., 2018; Malyshev et al., 2016; Signorelli et al., 2018). Of the categories mentioned previously, the emerging model proposes that the general term dormancy release is a progression: from endodormancy to endodormancy release to ecodormancy to ecodormancy release, which results in growth resumption and subsequent bud burst (Beauvieux et al., 2018; Malyshev et al., 2016; Meitha et al., 2015; Ophir et al., 2009; Signorelli et al., 2018; Vergara, Noriega, Aravena, Prieto, & Pérez, 2017; Zheng et al., 2018). Once favorable conditions are signaled, rapid growth occurs to achieve bud burst. Due to the annual life-style of the major model plants, there is very limited research and characterization studies concerning dormancy.

2.2.2.1. Endodormancy Induction

Endodormancy is induced by either shortening day length, decreasing temperatures, or a combination of both. Day length is sensed through light-activated photoperiod proteins, which transduce the light signal to start a signaling cascade (Basler & Körner, 2012, 2014; Linkosalo & Lechowicz, 2006; Melke, 2015; Pletsers et al., 2015; Reddy, Holalu, Casal, & Finlayson, 2013; Signorelli et al., 2018; R. K. Singh, Svystun, AlDahmash, Jonsson, & Bhalerao, 2017). The signaling mechanism for sensing low temperature is very poorly understood. Although the effect of photoperiod versus temperature varies with species and genotype, the stimuli induces many physiological and metabolic changes. For the temperate woody perennials like trees, grape vine, and blueberries, induction re-directs resources to bud tissue formation, to bud set, and sugar storage (Beauvieux et al., 2018; Fadón, Herrero, & Rodrigo, 2018; Gubler, Hughes, Waterhouse, & Jacobsen, 2008; D. Horvath, 2009; Lloret et al., 2018; Stephenson, Fankhauser, & Terry, 2009; van der Schoot & Rinne, 2011; Z. Zhang et al., 2018). Photosynthesis and protein synthesis are very gradually reduced while current sugar and energy production redirected to the buds (Fadón et al., 2018; L. Lin, Liu, & Yin, 2018; Lloret et al., 2018; Signorelli et al., 2018). As enzymes and proteins are decommissioned, the amino acids and other nutrients are being recycled into more storage compounds (Beauvieux et al., 2018; Malyshev et al., 2016; Meitha et al., 2018; Miura & Furumoto, 2013; Ophir et al., 2009; Stephenson et al., 2009). Modifications to the cell walls and membranes are also induced to increase fluidity (Buchanan et al.,

2012; Shim et al., 2014). These metabolic changes provide the energy and carbohydrates for storage during bud formation.

Buds are meristematic regions that continue growth soon after deposition, or enter a dormant phase to resume growth later (Arora et al., 2003; D. P. Horvath et al., 2003; Kovaleski et al., 2015; Shim et al., 2014; Signorelli et al., 2018; van der Schoot & Rinne, 2011; Wisniewski et al., 2003). Buds are located along stems at either axillary junctures or terminal ends. Axillary buds usually differentiate into just vegetative meristems, whereas terminal buds can differentiate into vegetative or floral meristems (Arora et al., 2003; Beauvieux et al., 2018; D. P. Horvath et al., 2003; Kovaleski et al., 2015; Shim et al., 2014; Signorelli et al., 2018; van der Schoot & Rinne, 2011). Bud fate is mostly determined during dormancy induction as either floral or vegetative cells (Kovaleski et al., 2015). Floral buds tend to be larger and rounder than leaf buds due to more partially differentiated cells (Kovaleski et al., 2015). If the bud is going dormant, bud scales, bracts, or other protective casings develop around the delicate meristems for protection (Considine & Considine, 2016; Fennell, 2004; D. Horvath, 2009; Signorelli et al., 2018).

Recent research into blueberry buds formation and development revealed blueberries undergo five stages of bud development (Arora & Rowland, 2011; Dhanaraj et al., 2007; Die, Arora, & Rowland, 2016; M. Ehlenfeldt, 2012; Mark K Ehlenfeldt et al., 2007; Kovaleski et al., 2015; Malyshev et al., 2016). Stage 1 consists of buds showing only one vegetative meristem that remains in stage 1 throughout winter dormancy, termed dormancy for rest of thesis. Stage 2 is determined by the developing inflorescence meristem differentiating two flanking lateral, floral meristems along with developing outer and inner bracts. Stage 3 consists of individual floral meristems clearly differentiating and forming sepals, along with the bract covered floral bud broadening to accommodate the developing inflorescence. Stage 4 contains a distinct inflorescence bud with distinct flowers containing petals, sepals, anthers, and pistils underneath the bud scales and bracts. Both the bud scales and bracts are fully developed and sealed to protect everything as bud growth arrests at this stage to go fully dormant (Kovaleski et al., 2015). Before going dormant, some buds can reach stage 5 where there is some expansion of the pedicel, peduncle, stamen, pistil, and flowers (Kovaleski et al., 2015).

Blueberry floral buds are large and round, whereas blueberry vegetative buds are narrow and pointed (Kovaleski et al., 2015; Trehane, 2004). Usually once stage 4 is reached, buds are considered “set” because the meristem activity is arrested and are ready for endodormancy (Arora & Rowland, 2011; Kovaleski et al., 2015; Trehane, 2004). Once buds are established, meristem activity is arrested and endodormancy begins.

Soon after endodormancy begins, cold acclimation also starts as it improves the bud’s cold tolerance (Miura & Furumoto, 2013; Rihan, Al-Issawi, & Fuller, 2017). Cold acclimation is the exposure of plants to repeated low non-freezing temperatures to induce metabolic changes that will improve cold tolerance (Arora & Rowland, 2011; Kovaleski et al., 2015; Miura & Furumoto, 2013; Rihan et al., 2017; Trehane, 2004). Although most metabolic activity is arrested, cold acclimation induces the synthesis of more abscisic acid (ABA), the production of more osmolytes, and the activity of some cell wall and membrane modifiers (Arora & Rowland, 2011; M. Ehlenfeldt, 2012; Miura & Furumoto, 2013; Rihan et al., 2017). Cold acclimation induces increased levels of ABA to maintain cessation of the cell cycle (Cooke et al., 2012; Del Pozo, Lopez-Matas, Ramirez-Parra, & Gutierrez, 2005; Vergara et al., 2017). ABA levels continue to increase during endodormancy and reaches a maximum when dormancy is deepest (J. Li et al., 2018; Vergara et al., 2017; Zheng et al., 2015).

Osmolytes are certain solutes, like soluble sugars or sugar alcohols, that can accumulate in the cytoplasm in high concentrations to increase solute potential and reduce water loss (Buchanan et al., 2012; Rihan et al., 2017). The deposition of callose, 1,3-linked glucose chains, in plasmodesmata blocks transport between cells to reduce water loss and prevent spread of damage or ice (Pagter, Andersen, & Andersen, 2015; Pearce, 2001; P. L. Rinne & Schoot, 2003; van der Schoot & Rinne, 2011; Z. Zhang et al., 2018; Zheng et al., 2018). The desaturation of membrane lipids increases membrane fluidity (Pagter et al., 2015; Pearce, 2001; P. L. Rinne & Schoot, 2003; van der Schoot & Rinne, 2011). Membrane fluidity aids in maintaining cell shape, preventing membrane destabilization, reducing ice-dehydration damage, and improving chill tolerance (Beauvieux et al., 2018; Buchanan et al., 2012; Fennell, 2004; Pearce, 2001).

Endodormancy induction also increases a rapid accumulation of carbon reserves like starch and soluble sugars (Buchanan et al., 2012). Starch is composed of long chains of glucose molecules bound by 1,4 linkages, and is the primary storage carbohydrate. Soluble sugars can be mono- or disaccharides involved not only in cell structure, but also carbon-energy homeostasis. The most common soluble sugars are glucose and sucrose, but other soluble sugars include fructose, mannose, and trehalose (Buchanan et al., 2012; Lunn, Delorge, Figueroa, Van Dijck, & Stitt, 2014; O'Hara, Paul, & Wingler, 2013). During cold acclimation in endodormancy, some of the starch reserves and sucrose are slowly degraded into soluble sugars to act as osmolytes until the freezing tolerance of the cells adequately lowers the freezing point of the water and disrupts potential ice crystal formation (H. Ben Mohamed, Vadel, Geuns, & Khemira, 2012; Fennell, 2004; Pagter et al., 2015; Z. Zhang et al., 2018). Starch is broken down into glucose or maltose soluble sugars, whereas sucrose, the main transport sugar, is broken down into glucose and fructose. The level of glucose accumulation corresponds to the available carbon resource that can be utilized for energy conversion or polysaccharide synthesis. Trehalose and sucrose signaling regulates carbon resource availability, which is vital for tissue survival because premature carbon depletion before completing a developmental transition usually results in tissue or organ death (Couée, Sulmon, Gouesbet, & El Amrani, 2006; Fadón et al., 2018; Kulik, Wawer, Krzywińska, Bucholc, & Dobrowolska, 2011; Lunn et al., 2014; O'Hara et al., 2013; Pagter et al., 2015; Tsai & Gazzarrini, 2014; Wingler, 2017).

2.2.2.2. Endodormancy to Ecodormancy Release Progression

The emerging model proposes the progression from endodormancy to endodormancy release to ecodormancy to ecodormancy release, which results in growth resumption and subsequent bud burst (Beauvieux et al., 2018; Malyshev et al., 2016; Meitha et al., 2015; Ophir et al., 2009; Signorelli et al., 2018; Vergara et al., 2017; Zheng et al., 2018). Endodormancy is released and growth capacity reactivated when the appropriate stimuli starts the signaling cascade. Although there are many researchers studying and proposing multiple pathways regulating endodormancy release, there is not enough information to develop a comprehensive regulatory network as many biological processes intersect during endodormancy release (Beauvieux et al.,

2018; H. Ben Mohamed et al., 2012; Lloret et al., 2018; Malyshev et al., 2016; Meitha et al., 2018; Pagter et al., 2015; Pucciariello, Banti, & Perata, 2012; van der Schoot & Rinne, 2011; Vergara et al., 2017; Z. Zhang et al., 2018; Zheng et al., 2015; Zhuang et al., 2015). The most common signal to release endodormancy is the fulfillment of a chilling requirement threshold where a certain number of chilling hours must accumulate (Hussain et al., 2015; Leida et al., 2012; Miura & Furumoto, 2013; Ophir et al., 2009; Rohde & Bhalerao, 2007). For chilling units to accumulate efficiently, the plant must be exposed to uninterrupted hours of temperatures between 5-7.2°C (Hussain et al., 2015; Miura & Furumoto, 2013). The chilling requirement of a plant varies greatly between species, cultivars, and genotypes (Hussain et al., 2015; Miura & Furumoto, 2013). Not accumulating enough chilling hours results in irregular bud break that may lead to bud abortion (Hussain et al., 2015; Miura & Furumoto, 2013). Although chilling requirements for endodormancy release have been known for over 60 years, it is still unclear how exactly the low-chilling temperatures are sensed, how accumulation occurs, and what are the initiating signals for endodormancy release.

When metabolism is reactivated at the beginning of endodormancy release, the bud cells start operating at a hypoxic, low-oxygen state because the tight, overlapping bud scales prevent oxygen infiltration (Beauvieux et al., 2018; Malyshev et al., 2016; Meitha et al., 2018, 2015; Pucciariello et al., 2012; Suzuki, Koussevitzky, Mittler, & Miller, 2012; Vergara, Parada, Rubio, & Perez, 2012). The bud is also operating at an energy-depleted state due to the inhibition of mitochondrial respiration during endodormancy (Beauvieux et al., 2018; Malyshev et al., 2016; Meitha et al., 2018, 2015; Pucciariello et al., 2012; Suzuki et al., 2012; Vergara et al., 2012). Both hypoxic and respiratory stress result in an increase in reactive oxygen species (ROS) accumulation and oxidative signaling (Beauvieux et al., 2018). ROS are continually produced as byproducts of aerobic metabolism. Oxidative signaling is the fine-tuned regulation of ROS accumulation for signaling and transient oxidative stress as well as also regulating the activity of ROS detoxification enzymes and antioxidants (Beauvieux et al., 2018; Considine & Considine, 2016; Meitha et al., 2015; Reddy et al., 2013; Signorelli et al., 2018). When ROS accumulation exceeds ROS detoxification rates, oxidative damage occurs which can cause significant cellular damage that may result in cell death.

Multiple studies investigating dormancy regulation have emphasized that oxidative-ROS signaling plays a significant role in regulating dormancy progression and release (Beauvieux et al., 2018; Malyshev et al., 2016; Meitha et al., 2018; Pucciariello et al., 2012; Reddy et al., 2013; Signorelli et al., 2018; Suzuki et al., 2012; van der Schoot & Rinne, 2011; Vergara et al., 2012). These studies have shown an increase in multiple different ROS as well as an upregulation in ROS-detoxification enzymes (Beauvieux et al., 2018; Kumar & Trivedi, 2018; Malyshev et al., 2016; Meitha et al., 2018, 2015; Ophir et al., 2009; Vergara et al., 2012). Multiple studies have also shown that oxidative signaling also interacts with plant hormones to appropriately transduce signals like dormancy release (Beauvieux et al., 2018; Cooke et al., 2012; J. Li et al., 2018; B. Liu et al., 2016; Malyshev et al., 2016; Meitha et al., 2018; Ophir et al., 2009; Shu, Liu, Xie, & He, 2016; Stephenson et al., 2009; Vergara et al., 2012; Zheng et al., 2015).

The plant hormones, ABA, gibberellin (GA), and ethylene (ET), regulate and cross-talk between pathways to transduce or integrate multiple signals. As mentioned previously, ABA levels reach a maximum at the deepest stage of endodormancy (J. Li et al., 2018; Vergara et al., 2017; Zheng et al., 2015). Once the appropriate signals for endodormancy release are fulfilled, there is a rapid decrease in ABA accumulation (Z. Zhang et al., 2018; Zheng et al., 2015, 2018). Inversely, the lowest GA levels at maximum endodormancy are induced to rapidly increase when endodormancy release has been signaled (Patrick Achard & Davie, 2015; Lv, Huo, Wen, Gao, & Khalil-ur-Rehman, 2018; P. L. H. Rinne et al., 2011; Zheng et al., 2018; Zhuang et al., 2015). The discrepancies in research utilizing exogenous GA application on buds indicates that the effect of GA on endodormancy release depends on the dormancy stage of the dormant bud (Patrick Achard & Davie, 2015; Conti, 2017; Zheng et al., 2018; Zhuang et al., 2015). When dormant buds are treated with ET, dormancy release and bud break are induced rapidly (Alonso & Stepanova, 2004; Dubois, Van den Broeck, & Inzé, 2018; Ophir et al., 2009; Stepanova & Alonso, 2009; Vergara et al., 2012). The application of ET inhibitors results in an increase in ABA accumulation and delayed bud break (Ophir et al., 2009; Vergara et al., 2012; Zheng et al., 2015). This indicates that ET down-regulates ABA synthesis and up-regulates ABA catabolism. Ethylene application also increases gene expression of other important antioxidants (Beauvieux et al., 2018;

Ophir et al., 2009; Vergara et al., 2012). Ethylene is an important signal for endodormancy release as it transitions ABA to catabolism and induces antioxidants to detoxify ROS.

Overall, during endodormancy release, the accumulation of GA and decrease in ABA induces a rapid increase in storage carbohydrate degradation into soluble sugars to increase the carbon resources available for energy production and synthesis (H. Ben Mohamed et al., 2012; Fadón et al., 2018; Hussain et al., 2015; Kulik et al., 2011; O'Hara et al., 2013; Ophir et al., 2009; Pagter et al., 2015; Tsai & Gazzarrini, 2014; Wingler, 2017; Z. Zhang et al., 2018). There is also an increase in sugar signaling, sugar conversion, and alternative energy pathways like pentose phosphate pathways (PPP), glycolysis, and gluconeogenesis to maintain soluble sugar pools and provide reducing power (Buchanan et al., 2012). The increase in GA accumulation also induces the degradation of callose in the plasmodesmata (P. L. Rinne & Schoot, 2003; van der Schoot & Rinne, 2011). The re-opening of the plasmodesmata allows for transport of sugars and proteins between neighboring cells as well as over long distances through the phloem. The opened plasmodesmata also allows for transport of flowering proteins like flowering locus T (FT) from the leaves to the floral bud meristem (P. L. H. Rinne et al., 2011; P. L. Rinne & Schoot, 2003; van der Schoot & Rinne, 2011).

As endodormancy release progresses, sugars are continually degraded to produce energy, plasmodesmata are re-opened, and sucrose and ROS levels exhibit a net positive accumulation (Beauvieux et al., 2018; H. Ben Mohamed et al., 2012; Ophir et al., 2009; van der Schoot & Rinne, 2011). Although still unclear when, endodormancy transitions the bud to ecodormancy where growth capacity has been restored and the buds are “primed for rapid growth during bud bursting when conditions are favorable” (Beauvieux et al., 2018; Considine & Considine, 2016; Lloret et al., 2018). Ecodormancy is released when the bud tissues break through the bud scales, usually termed bud burst. Dormancy break will be used as a general term for the progression of endodormancy to ecodormancy to bud burst (Beauvieux et al., 2018; Couée et al., 2006; Meitha et al., 2018, 2015; Ophir et al., 2009; Vergara et al., 2012; Z. Zhang et al., 2018).

Since dormancy break is an important determining factor of vigor and yield for perennial plants like blueberries, improving our knowledge and elucidating the regulatory pathways is essential to improving blueberry productivity. Although the sequence of initial signals is still unclear, the majority of dormancy break research proposes oxidative, hormone, and sugar signaling are vital signaling pathways for the dormancy progression transition to dormancy break, therefore, the pathways could be important areas for improving blueberry dormancy (Anderson, 2015; Beauvieux et al., 2018; Considine & Considine, 2016; Lloret et al., 2018; Malyshev et al., 2016; Signorelli et al., 2018; Z. Zhang et al., 2018; Zheng et al., 2015; Zhuang et al., 2015). The appropriate balance between ROS signaling and ROS detoxification enzymes during endodormancy release allows for a net positive accumulation of ROS while up-regulating detoxification enzymes to mitigate oxidative damage (Beauvieux et al., 2018; Signorelli et al., 2018). Further research into the regulation of this balance will aid in efficiently signaling other pathways to promote progression, and reducing ROS after signal transduction to prevent rampant oxidative damage, thus optimizing dormancy and bud break (Beauvieux et al., 2018; Signorelli et al., 2018).

ABA is the main hormone regulating the maintenance of dormancy as sustained, high-levels of ABA from suppressed ABA catabolism represses the cell cycle (Cooke et al., 2012; Vergara et al., 2017; Xing et al., 2015). Differentially regulating ABA catabolism would optimize endodormancy release for cultivars in different locations. For example, NHB blueberries experience very long winters, therefore, maintaining ABA catabolism suppression would allow for ABA levels to stay high and delay endodormancy break for the later warmer weather (Cooke et al., 2012; Vergara et al., 2017; Xing et al., 2015). Conversely, SHB blueberries experience very short winters, therefore, releasing the suppression of or up-regulating ABA catabolism would decrease ABA levels and induce endodormancy break earlier when the warm weather begins cycle (Cooke et al., 2012; Vergara et al., 2017; Xing et al., 2015). GA works antagonistically with ABA during dormancy break as GA promotes cell cycle growth and plasmodesmata re-opening (Patrick Achard et al., 2009; De Lucas et al., 2008; P. L. H. Rinne et al., 2011; Zheng et al., 2018). For NHB blueberries, delaying an increase in GA accumulation until ABA levels start decreasing would delay bud meristem growth and

reduce bud damage from early spring frosts. For SHB blueberries, increasing GA accumulation as ABA levels decrease would promote bud meristem growth earlier with the warmer weather. Promoting GA accumulation also induces the re-opening of plasmodesmata channels by degrading callose deposits (P. L. H. Rinne et al., 2011; P. L. Rinne & Schoot, 2003; van der Schoot & Rinne, 2011). Improving the regulation of GA accumulation for plasmodesmata re-opening would allow for rapid transport of sugars and energy into the meristems cells to support the growth, but re-opening cannot occur during cold temperatures as ice and dehydration damage can spread quickly with open plasmodesmata (P. L. H. Rinne et al., 2011; P. L. Rinne & Schoot, 2003; van der Schoot & Rinne, 2011). Further research into regulating ABA catabolism and GA accumulation would improve the dormancy bud break efficiency through synchronizing the resumption of cell cycle growth and the re-opening of plasmodesmata transport.

Improvements the coordination dormancy bud break will reduce the frost damage from buds bursting too early and improve the number of viable buds that grow into mature leaves or flowers. Increasing the number of young leaves that break from vegetative buds will provide more photosynthetic energy to supply the rapid growth of leaves and flowers. For the floral buds, any frost damage at the end of dormancy break to the floral meristems or right after floral bud burst to the immature floral tissue results in a non-viable bud because floral tissue and organ differentiation is interrupted (Basler & Körner, 2014; J F Hancock et al., 2008; G. A. Lobos & Hancock, 2015; Lisa J Rowland et al., 2013; Trehane, 2004). Therefore, improving the survival of viable floral buds from dormancy break will greatly increase the number of mature flowers that will subsequently produce more blueberry berries and improve yield.

2.2.2.3. Flowering after Floral Bud Burst

The conclusion of dormancy break is the immature vegetative or floral tissues bursting from the bud scales. At this stage, the immature vegetative and floral tissues are extremely vulnerable to damage because they are exposed to the harsh environmental conditions and still contain large meristematic centers that have not yet differentiated (Brelsford & Robson, 2018; Costes et al., 2014; Díaz-Riquelme, Grimplet, Martínez-Zapater, & Carmona, 2012; Koutinas, Pepelyankov, & Lichev, 2010; R. Mohamed et al., 2010; Molinero-Rosales, Latorre, Jamilena, & Lozano, 2004; P. L. H.

Rinne et al., 2011; van der Schoot & Rinne, 2011; Vasconcelos, Greven, Winefield, Trought, & Raw, 2009). While the inner core of the buds may still be hypoxic, the vast majority of the bud cells are now exposed to ample oxygen and light to fuel rapid cell proliferation and differentiation (Meitha et al., 2018, 2015; Signorelli et al., 2018). The oxygen, light, and re-opened transport will continually supply and upregulate carbon and energy pathways, but will still need to be supplemented by storage starch degradation to support the rapid growth of leaves and flowers (Albani & Coupland, 2010; D. Horvath, 2009; Vasconcelos et al., 2009; Wilkie, Sedgley, & Olesen, 2008).

Right before floral bud burst, the induction of floral meristem differentiation occurs with the production and transport of flowering locus T through the plasmodesmata and into the meristem (Cooke et al., 2012; Ito et al., 2016; P. L. H. Rinne et al., 2011). The induction of flowering is best characterized for annual plants and consists of either positive regulation of two floral integrators, flowering locus T (FT) and suppressor of overexpression of constans1 (SOC1), or negative regulation of flowering locus C (FLC) to alleviate its repression of FT (Albani & Coupland, 2010; Conti, 2017; D. Horvath, 2009; Ionescu, Møller, & Sánchez-Pérez, 2016; Wilkie et al., 2008). The photoperiod pathway transduces the long daylength with phytochromes activating *giganta* (GI) and *constans* (CO) (Mishra & Panigrahi, 2015; Suarez-Lopez et al., 2001; Yu et al., 2009). GI and CO induce expression of FT in the leaves, which is then transported to the shoot apical meristem (SAM) (Cooke et al., 2012; Ito et al., 2016; P. L. H. Rinne et al., 2011). Once FT binds with flowering locus D (FD), the complex activates SOC1 and induces floral meristem identity genes (Mishra & Panigrahi, 2015; Suarez-Lopez et al., 2001; Yu et al., 2009). The vernalization pathway utilizes *frigida* (FRI) to epigenetically silence FLC to relieve its repression on FT (D.-H. Kim & Sung, 2014; Teotia & Tang, 2015). Flowering can also be regulated by microRNA, mainly through miR156 levels (D.-H. Kim & Sung, 2014; Teotia & Tang, 2015). As the plant ages, miR156 levels decrease and relieve its repression of squamosa promoter-binding protein-like (SPLs) (D.-H. Kim & Sung, 2014; Teotia & Tang, 2015). SPLs have been shown to promote expression of SOC1, FT, or floral meristem identity regulators (D.-H. Kim & Sung, 2014; Teotia & Tang, 2015). During ecodormancy release, parts of these pathways are induced so that flowering can occur

rapidly once the conducive, warm conditions return. GA has also been shown to positively regulate multiple flowering pathways, especially when the photoperiod pathway is not dominant (Albani & Coupland, 2010; Conti, 2017; Ionescu et al., 2016; Teotia & Tang, 2015; Wilkie et al., 2008). ABA signaling inhibitors have been implicated as negative regulators of flowering by binding to CO (Albani & Coupland, 2010; Conti, 2017; D. Horvath, 2009; Ionescu et al., 2016; Teotia & Tang, 2015). ABA can also negatively regulate flowering through ABA signaling inhibitors activating FLC (Conti, 2017; Teotia & Tang, 2015). ET has also been implicated as a negative regulator of flowering through ET reducing bioactive GA accumulation (Conti, 2017; Teotia & Tang, 2015).

After blueberry floral buds burst, the immature floral tissue grows, matures, and blooms into a cluster of 5-12 white to pink flowers with a corolla tube of five fused petals (Díaz-Riquelme et al., 2012; Kovaleski et al., 2015; Trehane, 2004). During the initial stages of flower expansion, the flower tissues are most susceptible to damage as early spring still has cold spells. Although the risk of sudden frosts is less at full bloom because flowers can tolerate temperatures -2.2°C , frost damage at this stage would cause great damage as the reproductive organs are only hidden by the flower petals (Trehane, 2004). Blueberries are primarily outcrossing as self-fertilization usually results in reduced fruit and seed set, smaller berry size, reduced germination rate, and weak seedling growth (Brevis, Bassil, Ballington, & Hancock, 2008; Die & Rowland, 2013; J F Hancock et al., 2008; Lisa J Rowland et al., 2012; Lisa J Rowland, Ogden, & Ehlenfeldt, 2010). The self-infertility commonly associated with blueberries is due to late-acting inbreeding depression, and the effect of the inbreeding depression varies greatly between species and genotypes (J F Hancock et al., 2008). This has resulted in blueberry plants being asexually propagated through cuttings or tissue culture (J F Hancock et al., 2008; Trehane, 2004). Once the flower is fertilized, growth is resumed through a decrease in ABA levels, and an increase in gibberellin (GA) to produce a fruit (Coombe & McCarthy, 2000; J. Giovannoni, 2001; Prasanna, Prabha, & Tharanathan, 2007).

2.2.3. Blueberry Berry Development and Ripening

Blueberry berries are simple fruit with a fleshy pericarp that contains 5 loculi (Cappai, Benevenuto, Ferrão, & Munoz, 2018; Moggia et al., 2017; Trehane, 2004). Fleshy fruit are greatly expanded ovaries, due to enhanced cell division and expansion, as well as wall thickening without lignification (J. Giovannoni, 2001; J. J. Giovannoni, 2004; Osorio, Scossa, & Fernie, 2013; Prasanna et al., 2007; Seymour, Østergaard, Chapman, Knapp, & Martin, 2013). The pericarp differentiates further into an exocarp or skin, roughly 3 layers cells thick, and a mesocarp called pulp or flesh that is roughly 25 cells deep (Cappai et al., 2018; Coombe & McCarthy, 2000; Moggia et al., 2017; Trehane, 2004). The characteristic blueberry blue color is due to the accumulation of anthocyanins in the skin (Cappai et al., 2018; Moggia et al., 2017; Routray & Orsat, 2011; Trehane, 2004). The skin is composed of a single cell layer of epidermis and 1-2 cell layer hypodermis (Cappai et al., 2018; Moggia et al., 2017; Trehane, 2004). The berry skin epidermis is coated by epicuticular wax that gives the characteristic “bloom” sheen, contains some anthocyanins, and has been proposed to aid in retaining blueberry firmness and reducing water loss (Chu, Gao, Chen, Fang, & Zheng, 2018; J F Hancock et al., 2008; Trehane, 2004). The hypodermis contains highest levels of anthocyanin and the colors carried from light pink to almost black (He et al., 2010; Konarska, 2015; Routray & Orsat, 2011; Yonekura-Sakakibara, Nakayama, Yamazaki, & Saito, 2009).

Fruit are classified into two categories depending on the ripening process. Climacteric fruit exhibit a respiratory burst and large increase in ethylene at ripening onset (J. Giovannoni, 2001; J. J. Giovannoni, 2004; Osorio et al., 2013; Prasanna et al., 2007; Seymour, Østergaard, et al., 2013). Non-climacteric fruit exhibit no substantial respiratory burst and no increase in ethylene at ripening onset (Klee, 2010; Osorio et al., 2013; Seymour, Østergaard, et al., 2013). Most fruit ripening research in the past has focused on dry fruit, due to Arabidopsis, or climacteric fleshy fruit due to tomato (Azzi et al., 2015; Seymour, Chapman, Chew, & Rose, 2013; Seymour, Østergaard, et al., 2013). Only within the last decade with the diversification of research into crops and accessibility of transcriptomics has non-climacteric ripening research increased. Strawberry and grapes are emerging as non-climacteric ripening models (Ayub et al.,

2016; Castellarin et al., 2016; Wang et al., 2017; Xi et al., 2017). Blueberries are non-climacteric fleshy fruit with each berry within the cluster of blueberries ripening at different rates so all stages of berry ripening are present in one cluster. NHB gradually ripens for about six to eight weeks, but timing can vary cultivar dependent (Cappai et al., 2018; Gündüz, Serçe, & Hancock, 2015; Trehane, 2004).

Blueberries exhibit a double sigmoid growth curve like grapes, which consists of two growth phases separated by a lag phase (Cappai et al., 2018; Coombe & McCarthy, 2000; Osorio et al., 2013; Prasanna et al., 2007; Serrano et al., 2017). Stage 1 occurs after fertilization and the ovaries mature with rapid cell proliferation and remaining differentiation (Castellarin et al., 2016; Konarska, 2015; Xi et al., 2017). During stage 1, the cell cycle is upregulated for rapid division, but cell expansion is reduced to allocate energy to division (Seymour, Østergaard, et al., 2013). After cell proliferation achieves the final fruit cell number, the fruit starts stage 2 where cell division and expansion stop to allow for seed maturation and preparation for fruit ripening to occur (Castellarin et al., 2016; Konarska, 2015; Xi et al., 2017). Genetic and metabolomic changes during fruit ripening onset and duration are described in more detail in the following sections. Overall, the walls thicken from pectin and hemicellulose, photosynthetic components are recycled from fruit tissue only, and phytohormones accumulate and start signaling cascades (Barrett, Beaulieu, & Shewfelt, 2010; Giongo, Poncetta, Loretto, & Costa, 2013; X. Li, Xu, Korban, & Chen, 2010; Osorio et al., 2013; Seymour, Østergaard, et al., 2013). The walls thicken for protection from pests and diseases, and to accommodate the rapid expansion that occurs in stage 3 (Castellarin et al., 2016; Pilati et al., 2014; Serrano et al., 2017; Seymour, Østergaard, et al., 2013; Xi et al., 2017). Chlorophyll and other photosynthesis proteins are degraded and recycled to provide synthesis substrates and to accommodate increasing solutes (Azzi et al., 2015; Prasanna et al., 2007). Phytohormones like ABA, GA, and auxin regulate each other to trigger the onset of ripening (Castellarin et al., 2016; Coombe & McCarthy, 2000; Seymour, Chapman, et al., 2013). Stage 3 is the onset of ripening when the rapid cell expansion, but no division, results in the berry doubling in size as well as gradual softening, sugars accumulate in supply energy and increase water content, and pigment accumulates (Castellarin et al., 2016; Konarska, 2015; Xi et al., 2017).

2.2.3.1. Cell Wall Matrix Modifications and Sugar Signaling

As mentioned previously, fruit development and ripening requires extensive cell division with the synthesis of new cell wall matrix components and rapid expansion through modifications of existing cell wall matrix components to accommodate turgor increases (Castellarin et al., 2016; X. Li et al., 2010; Posé, Nieves, Quesada, & Mercado, 2011; Toivonen & Brummell, 2008) . Fruit softening is the decrease in fruit firmness and occurs when the turgor pressure decreases quickly and the expanded cell wall matrix is more easily degraded (Castellarin et al., 2016; Toivonen & Brummell, 2008). Researchers are still unsure whether the fruit softening process begins right before or right after the peak of fruit ripeness (Cappai et al., 2018; Choi, Wiersma, Toivonen, & Kappel, 2002; Coombe & McCarthy, 2000; Moggia et al., 2017; C. Paniagua et al., 2014; Pilati et al., 2014; Serrano et al., 2017; Wang et al., 2017; Xi et al., 2017).

The cell wall consists of a cellulose-hemicellulose glycan matrix embedded in pectin (Buchanan et al., 2012; Choi et al., 2002; Takatsuka & Umeda, 2014; Vicente et al., 2007). The cell expands through an upregulation of wall loosening enzymes and an increase in turgor pressure to push outwards (Azzi et al., 2015; Choi et al., 2002; De Lucas et al., 2008; J. J. Giovannoni, 2004; X. Li et al., 2010; Ozga & Reinecke, 2003; Posé et al., 2011). Auxin has been shown to induce wall loosening enzymes, stimulate water uptake, and induce cell wall acidification (Majda & Robert, 2018; Perrot-Rechenmann, 2010). If the disruptions to the cell wall matrix are not fixed through transferring important residues, the loosening could increase and result in greater changes in wall strength (Majda & Robert, 2018; Perrot-Rechenmann, 2010). The pectin matrix is also modified during fruit development and ripening through increasing calcium bridge formation or increasing wall porosity (Chen et al., 2015; Majda & Robert, 2018; C. Paniagua et al., 2014; Posé et al., 2011; Prasanna et al., 2007). Increasing the porosity provides easier access for degradation enzymes to the wall and pectin matrix (Choi et al., 2002; Majda & Robert, 2018; C. Paniagua et al., 2014; Posé et al., 2011). Pectin matrix modification also affects intercellular adhesion because pectin is the predominant polymer in the middle lamella (Majda & Robert, 2018; C. Paniagua et al., 2014; Posé et al., 2011). As the fruit ripens, the pectin degradation increases and allows

for not only separation of neighboring cells that creates air spaces, but also greater cell wall degradation. The combination of cell wall matrix degradation, turgor pressure reduction, and cell-to-cell separation results in a reduction in firmness and increase in softening (Castellarin et al., 2016; Majda & Robert, 2018; C. Paniagua et al., 2014; Posé et al., 2011).

Throughout fruit development and ripening, sugars are constantly transported into the fruit to supply carbon and energy (Castellarin et al., 2016; Choi et al., 2002; J. Giovannoni, 2001; Karppinen et al., 2013; Leng, Yuan, Guo, & Chen, 2014; Posé et al., 2011). But as the influx of sugars is constantly utilized for energy production and cell wall matrix synthesis, there is a low carbon energy signal that induces the down regulation of overall growth, up regulation of photosynthesis, and up regulation of storage catabolism and mobilization (Jia et al., 2017; Leng et al., 2014; O'Hara et al., 2013; Serrano et al., 2017; Tognetti, Pontis, & Martínez-Noël, 2013; Tsai & Gazzarrini, 2014; Wurzinger, Nukarinen, Nägele, Weckwerth, & Teige, 2018). During stage 2 of fruit development, the predominant sugar source shifts to sucrose while growth is suspended so that soluble sugars and precursor metabolites can gradually accumulate. At the onset of ripening at the beginning of stage 3, soluble sugars continue to accumulate even though some are utilized for specialized metabolite synthesis because sucrose influx continually increases, storage carbohydrates are broken down, and sugar alcohols are up-regulated in the ripening fruit tissue (Granot, David-Schwartz, & Kelly, 2013; Jia et al., 2013, 2017; Koyama, Sadamatsu, & Goto-Yamamoto, 2010; Osorio et al., 2013; C. Paniagua et al., 2014; Rapaille, Goosens, & Heume, 2003; Tsai & Gazzarrini, 2014).

Multiple studies have shown that non-climacteric fruit exhibit an increase in ABA accumulation at the onset of ripening (Ayub et al., 2016; Castellarin et al., 2016; J. J. Giovannoni, 2004; Karppinen et al., 2013; Leng et al., 2014; Moggia et al., 2017; Oh, Yu, Chung, Chea, & Lee, 2018; Osorio et al., 2013; Ren et al., 2011; Serrano et al., 2017; Toivonen & Brummell, 2008). ABA signaling genes are also up-regulated at ripening onset to induce an increase in sugar accumulation and pigment synthesis (Jia et al., 2017; Leng et al., 2014). Although ABA plays an important role, there is evidence that ABA is not the major inducer like ethylene is during climacteric fruit ripening, thus

other hormones or signaling molecules contribute (Seymour, Østergaard, et al., 2013). GA signaling is also implicated in regulating cell proliferation and growth in fruit development (Patrick Achard et al., 2009; Claeys, De Bodt, & Inzé, 2014; De Lucas et al., 2008). Auxin has also been implicated in regulating fruit development and ripening through not only inducing cyclins for cell division, but also inducing acidic cell expansion (Leyser, 2017; Majda & Robert, 2018; Perrot-Rechenmann, 2010; Takatsuka & Umeda, 2014). Acidic cell expansion increases the porosity of the wall matrix, which increases the accessibility for new component deposition and degradation enzymes during the rapid growth of stage 1 and 3 (Chen et al., 2015; Majda & Robert, 2018; C. Paniagua et al., 2014; Perrot-Rechenmann, 2010).

2.2.3.2. Pigment Accumulation – Phenolic Acids

The main pigment metabolites present in grapes and blueberries are anthocyanins, a large group of flavonoid metabolites (Ali Ghasemzadeh, 2011; He et al., 2010; Khoo, Azlan, Tang, & Lim, 2017; Muleke et al., 2017; Nakayama, Suzuki, & Nishino, 2003; Routray & Orsat, 2011; Sasaki, Nishizaki, Ozeki, & Miyahara, 2014). Anthocyanin biosynthesis is a branch off of the flavonoid pathway, which is a branch of the larger phenylpropanoid pathway (Ali Ghasemzadeh, 2011; He et al., 2010; Mattila, Hellström, & Törrönen, 2006; Routray & Orsat, 2011; Yonekura-Sakakibara et al., 2009). The phenylpropanoid pathway is part of the overarching phenolic acid pathway. The phenolic acid pathway begins with the shikimate pathway converting glycolysis and PPP products into shikimic acid and quinic acid (Kanehisa, Furumichi, Tanabe, Sato, & Morishima, 2017; T. Kim et al., 2017). Phenylalanine is one of the main products from the shikimate pathway and is the beginning substrate for phenylpropanoid acid synthesis (Kanehisa et al., 2017; T. Kim et al., 2017). The metabolite p-coumaroyl-CoA, produced from phenylalanine, is a branching point in the phenylpropanoid pathway to synthesize either phenylpropanoid acids or flavonoids (Khoo et al., 2017; Routray & Orsat, 2011). The phenylpropanoid acid biosynthesis pathway contains multiple enzyme isoforms that catalyze the use and production of caffeoyl-quinic acid, chlorogenic acid, or caffeoyl-shikimic acid (Ali Ghasemzadeh, 2011; He et al., 2010; Routray & Orsat, 2011; Yonekura-Sakakibara et al., 2009). While caffeoyl-shikimic acid can be converted to caffeic acid, caffeoyl-shikimic acid and chlorogenic acid are converted to caffeoyl-

CoA, which is a vital substrate for synthesis pathways of other phenylpropanoid acids and lignin (Kanehisa et al., 2017; T. Kim et al., 2017).

The flavonoid pathway begins at the p-coumaroyl-CoA branch where p-coumaroyl-CoA is converted to naringenin-chalcone (He et al., 2010; Routray & Orsat, 2011). After naringenin-chalcone is converted to naringenin, the flavonoid pathway splits into multiple branches (Kanehisa et al., 2017; T. Kim et al., 2017). Midway through the pathway, one of the branches produces multiple dihydroflavonols, like dihydroquercetin and dihydromyricetin (He et al., 2010; Kanehisa et al., 2017; Overall et al., 2017; Stevenson & Scalzo, 2012; Yonekura-Sakakibara et al., 2009). Dihydroquercetin and dihydromyricetin are converted to leucocyanidin and leucodelphinidin, respectively (He et al., 2010; Routray & Orsat, 2011). Leucocyanidin and leucodelphinidin can then be converted to either epicatechin and epigallocatechin, or cyanidin and delphinidin, respectively (He et al., 2010; Routray & Orsat, 2011).

The diversity of anthocyanins, exemplified by over 500 different anthocyanins reported, is due to the different sugars and functional groups modifications that can be added to the core structure (He et al., 2010; Khoo et al., 2017; Routray & Orsat, 2011; Sasaki et al., 2014; Wahyuningsih, Wulandari, Wartono, Munawaroh, & Ramelan, 2017; Yonekura-Sakakibara et al., 2009). The different modifications not only produce variation in the color hue, but also stabilize the anthocyanins when the pH changes while in the vacuole (He et al., 2010; Routray & Orsat, 2011; Yonekura-Sakakibara et al., 2009). The intensity of blue coloration characteristic of blueberries is due to the anthocyanin composition diversity and pH within the skin (Khoo et al., 2017; Routray & Orsat, 2011; Sasaki et al., 2014; Wahyuningsih et al., 2017; Yonekura-Sakakibara et al., 2009). Anthocyanins are composed of an anthocyanidin core and additional sidechains consisting of different glycosides and acyls (Figure 2.1) (Ali Ghasemzadeh, 2011; He et al., 2010; Khoo et al., 2017; Muleke et al., 2017; Nakayama et al., 2003; Routray & Orsat, 2011; Sasaki et al., 2014). The anthocyanin cores are initially the two anthocyanidins, cyanidin and delphinidin, that diversify to petunidin, malvidin, and peonidin through methylation at specific carbons (Khoo et al., 2017; Routray & Orsat, 2011; Sasaki et al., 2014; Yonekura-Sakakibara et al., 2009). Anthocyanin metabolites can be classified as either anthocyanidin glycosides or acylated anthocyanins (He et al.,

2010; Horbowicz, Grzesiuk, DEBski, & Kosson, 2008; Nakayama et al., 2003; Sasaki et al., 2014; Yonekura-Sakakibara et al., 2009). With either anthocyanidins or anthocyanins being the sugar acceptors, the sugar donors can be UDP-glucose, UDP-galactose, UDP-rhamnose, UDP-xylose, and UDP-arabinose (Yonekura-Sakakibara, 2009; Yonekura-Sakakibara et al., 2009). Glycosylation can occur at C3, C5, C7, C3', C4', and C5' hydroxyl groups (Yonekura-Sakakibara, 2009; Yonekura-Sakakibara et al., 2009). Blueberries usually have sugars added to only the C3, where grapes also accumulate anthocyanidin-3,5-O-diglucosides (Alcalde & Bogs, 2017; He et al., 2010; Muleke et al., 2017; Rinaldo et al., 2015; Routray & Orsat, 2011, 2014; Zorenc et al., 2017).

Acylation of anthocyanins adds either aromatic hydroxycinnamoyl groups, or aliphatic substituents usually bound to CoA (Khoo et al., 2017; Nakayama et al., 2003; Routray & Orsat, 2011; Sasaki et al., 2014; Wahyuningsih et al., 2017; Yonekura-Sakakibara et al., 2009). Acylation occurs primarily at the C6'' hydroxy group of the sugar moiety. Aliphatic acylation enhances the stability of the anthocyanins especially when densely accumulated or stacked, which intensifies the color. In grapes, the anthocyanin composition usually consists of multiple glucosides and acylation with a variety of substrates (Alcalde & Bogs, 2017; He et al., 2010; Khoo et al., 2017; Nakayama et al., 2003; Rinaldo et al., 2015; Sasaki et al., 2014; Wahyuningsih et al., 2017; Yonekura-Sakakibara et al., 2009). In blueberries, anthocyanin diversity usually consists of 3'-glycosylation with different sugars and limited acylation (Khoo et al., 2017; D. Li et al., 2017; Nakayama et al., 2003; Routray & Orsat, 2011, 2014; Sasaki et al., 2014; Yonekura-Sakakibara, 2009; Yonekura-Sakakibara et al., 2009; Zorenc et al., 2017)

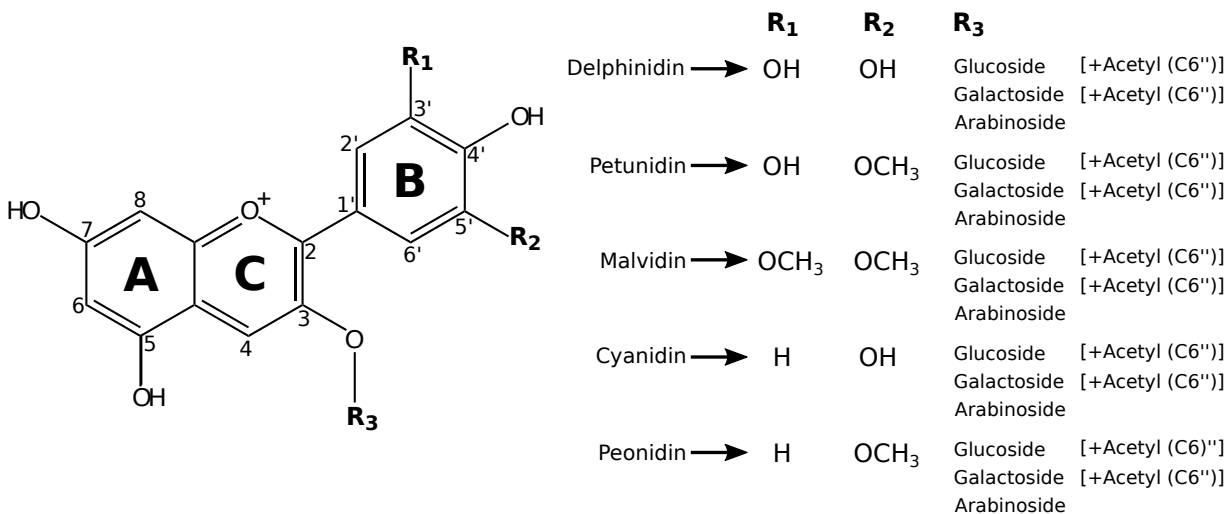


Figure 2.1 – Anthocyanin metabolite diversity in blueberry. Anthocyanidin core molecule consists of two 6-carbon rings (A and B) linked together by a 3-carbon and oxygen ring (C). The anthocyanidin diversity is due to the different functional groups at positions R₁ and R₂. The anthocyanin metabolite diversity is due to different combinations of different anthocyanidin cores with different sugar moieties and modifications at position R₃. The anthocyanins described in the figure represent the common anthocyanins found in blueberry.

2.2.4. Consumer-Driven Fruit Quality and Blueberries

Consumers purchase food based on what appeals to their senses best, meaning if they like it. Sensory traits are characteristics experienced through auditory, visual, olfactory, tactile, and gustatory stimuli (Barrett et al., 2010; Klee, 2010; McGinn, 2015; Musacchi & Serra, 2018; Pagliarini, Laureati, & Gaeta, 2013). For fruits and vegetables, auditory traits are not common. Common visual characteristics are color, size, and shape (Barrett et al., 2010; Gilbert et al., 2015, 2014; Pagliarini et al., 2013; Saftner, Polashock, Ehlenfeldt, & Vinyard, 2008; J. L. Silva, Marroquin, Matta, Garner, & Stojanovic, 2005). Olfactory or smell attributes consist of aroma and pungency (Barrett et al., 2010; Gilbert et al., 2015; Goff & Klee, 2006; Musacchi & Serra, 2018; Pagliarini et al., 2013). Tactile or texture characteristics include firm, smooth, and elastic (Barrett et al., 2010; Cappai et al., 2018; Gilbert et al., 2014; X. Li et al., 2010). Gustatory or taste attributes consist of the five main taste receptors, sweet, salty, bitter, sour, and umami (Barrett et al., 2010; Gilbert et al., 2014; McGinn, 2015; Pagliarini et al., 2013). Flavor is commonly used interchangeably with taste, but flavor incorporates more stimuli than taste.

2.2.4.1. Perception of Flavor

Flavor is determined through the sensations and perception of consuming the food (Barrett et al., 2010; Kader, 2008; Klee, 2010; McGinn, 2015; Schwab, Davidovich-Rikanati, & Lewinsohn, 2008; Spence, 2015). The sensations are the raw sensory traits experienced while eating (Barrett et al., 2010; Kader, 2008; Klee, 2010; McGinn, 2015; Schwab et al., 2008; Spence, 2015). The perception is the brain filtering and contextualizing the sensory traits, so they can be interpreted to determine if the sensory traits are meaningful (Grunert, 2005; McGinn, 2015; Pagliarini et al., 2013; Spence, 2015). The traits are assigned meaning when compare to our learned associations and expectations. Learned associations are a compilation of prior experiences that include our own experiences eating the food, other people sharing their experience, and ideal examples (Grunert, 2005; Pagliarini et al., 2013; Spence, 2015). The learned associations form an expectation for the sensory traits that should be experienced with that food. When faced with that food choice again, consumers will automatically compare against that expectation and quickly make a choice. Since everyone has different learned associations, there can be a large diversity of consumer expectations for each item (Grunert, 2005; Pagliarini et al., 2013; Spence, 2015). For example, consumer A developed an expectation for green apples that have a crunchy texture and tart taste, while consumer B has an expectation for red apples that have a mealy texture and sweet taste. When both consumers are faced with both types of apples, consumer A will not choose the red apples and preferentially choose the green apples, whereas consumer B will not choose the green apples and preferentially choose the red apples.

While eating, a consumer compares the current experience and flavor to the formed expectation for that food. Any attribute that does not conform to that expectation arouses suspicion, because the vast majority of consumers prefer the safety of conformity (McGinn, 2015; Pagliarini et al., 2013; Spence, 2015). For example, a common expectation for orange juice is orange colored liquid with an acidic taste. If presented an orange juice that is colored blue and tastes bitter, the consumer would distrust the designation of the liquid as orange juice. The extent of non-conformity from the expectation determines a consumer's choice (McGinn, 2015; Pagliarini et al., 2013; Spence, 2015). Some consumers can only accept minimal non-conformity before the

food becomes unacceptable (Grunert, 2005; Pagliarini et al., 2013; Spence, 2015). Other consumers can tolerate larger departures from the expectation. For example, when faced with choosing a banana at the market, the preference of the first consumer would be to only choose a banana that is colored a rich yellow and feels firm as that is a common expectation for a ripe banana. The preference of the second consumer would not be limited to a potentially small subset of bananas that narrowly conform, but would include bananas with a green tinge or brown spots because the consumer's tolerance for non-conformity is greater. Since everyone has different expectations and different tolerances for non-conformity, understanding and predicting consumer preferences is more complicated than originally thought.

2.2.4.2. Sensory Evaluations

Since consumers drive the food industry, gaining a greater understanding of the sensory traits the majority of consumers prefer would aid in developing fruits and vegetables more consumers would purchase and eat (Grunert, 2005; Kyriacou & Rouphael, 2018). Investigating sensory characteristics of food requires sensory evaluations, which can be conducted by trained panelists or consumers. Trained panelists provide fine-tuned and detailed descriptions of a food's sensory traits as they have training in discerning subtle differences and have experience with a greater variety of sensory experiences to compare with (Grunert, 2005; Kyriacou & Rouphael, 2018; Varela & Ares, 2012). During a sensory evaluation with trained panelists, tasting examples of both extremes for the evaluated characteristic are provided, as well as replicates of each test sample for ample comparison (Grunert, 2005; Kyriacou & Rouphael, 2018; Varela & Ares, 2012). The sensory evaluation results from trained panelists provide detailed information as well as less variability because of their training and experience, which reduces the number of panelists needed to obtain good results (Grunert, 2005; Kyriacou & Rouphael, 2018; Varela & Ares, 2012). Unfortunately, the high cost of hiring a trained sensory panel and the detailed discernment has decreased the demand for trained panelists because comparative studies have shown the common consumer does not taste subtle differences so trained panelist results do not accurately represent the preferences of consumers (Varela & Ares, 2012).

Sensory evaluations conducted by consumers require a different evaluation format and a very large number of consumers. The evaluations have to be very carefully worded so to not induce bias, and only have a ranking system for consumer results reporting (Grunert, 2005; Kyriacou & Rouphael, 2018; Varela & Ares, 2012). Well-designed sensory evaluations for consumers will also contain at least one example of the attribute's extreme for the consumer to experience and compare too. If physical examples are not possible due to evaluation circumstances, descriptive examples of the extremes have to be carefully chosen and provided for the consumer. The examples have to be something a majority of consumers know and have experience with the extreme attribute (Grunert, 2005; Varela & Ares, 2012). For example, the strong acidic and sour taste of lemons is a common example for taste sour attribute as majority of people have tasted a lemon. The large number of consumers is needed to account for the large variability of consumer panel results (Grunert, 2005; Kyriacou & Rouphael, 2018; Varela & Ares, 2012).

The large variability can come from the bias of strong opinions or inexperience. Consumer response platforms, like product reviews or voluntary surveys, tend to attract consumers with strong opinions because they want to share their opinion (Grunert, 2005; Varela & Ares, 2012). This would bias the results to cluster at the extremes or in distinct groups. One way to mitigate this bias would be to get participation from not-strongly opiated consumers through incentives like prizes. The inexperience bias occurs when the middle answer is chosen most often (Grunert, 2005; Varela & Ares, 2012). The middle answer is viewed as a neutral answer, and if the consumer does not understand or have experience with the extreme examples, then they are more likely to answer neutral. It is very difficult to distinguish this bias from the preference of the consumers for the middle result. A large consumer panel would provide a large dataset, and large datasets decrease skewing by outliers and increase statistical power (Grunert, 2005; Varela & Ares, 2012). Consumer sensory panel results provide direct insight into the sensory attributes and tolerance levels consumers prefer.

2.2.4.3. Flavor Mechanism

Since flavor is a vital characteristic for all foods, flavor, for this thesis, is the combination of specific texture attributes, aroma, and taste (Barrett et al., 2010; Kader,

2008; Klee, 2010; Schwab et al., 2008; Spence, 2015). For flavor, the specific texture attributes concern the sensation of masticating the food, like graininess, juiciness, or skin toughness (Barrett et al., 2010; Spence, 2015). Aroma attributes contribute to flavor because the majority of volatile compounds are released during chewing and saliva interaction (Goff & Klee, 2006; Spence, 2015). These released volatiles are sensed through retronasal olfaction. Taste attributes are the interaction of specific molecules with specific taste receptors (Barrett et al., 2010; Klee, 2010; McGinn, 2015; Spence, 2015). Multiple taste receptors are clustered into taste buds, which are located in varying densities along the tongue (McGinn, 2015). Each taste bud has multiple nerve terminals attached at the bottom to transduce the taste signal to the brain (McGinn, 2015). Sweet taste is induced by mono- and di-saccharides. Bitter taste is induced by alkaloid or nitrogen-containing compounds. Umami or savory taste is primarily induced by glutamate. Sweet, bitter and umami taste occurs when a G-protein coupled receptor is activated and transduces the signal to later induce an influx of Ca^{2+} to induce the vesicle-membrane fusion that releases neurotransmitters to activate the nerve terminal. Each nerve terminal is attached to a taste specific receptor, so activation of a sugar nerve terminal means a sugar compound was tasted. Sodium ions (Na^+) start the signal transduction of salty taste by Na^+ binds and open Na^+ -specific channels that allow the influx of positive ions, which triggers an action potential that will release neurotransmitters to activate the salty specific nerve terminal. Protons from acids induce a sour taste. The protons inhibit efflux of K^+ out of the cell, which leaves to a buildup of K^+ , which induces an action potential and the subsequent release of neurotransmitters to activate the sour specific nerve terminal (McGinn, 2015). Once the brain receives all the sensory data from eating, it perceives the taste, smell, and texture traits of the food (Barrett et al., 2010; Kader, 2008; Klee, 2010; Schwab et al., 2008; Spence, 2015).

Along with the flavor attributes, the visual and textural sensory data is interpreted and added to the expectation for the food. For blueberry consumer preference, some sensory traits are common for many consumers while other traits can vary (Cappai et al., 2018; Gilbert et al., 2015, 2014; Saftner et al., 2008; J. L. Silva et al., 2005). Some common visual traits for blueberry are a deep blue color, round in shape, and roughly nickel coin in size. Common textural traits are smooth, but waxy outer skin and a

medium-high firmness or turgidity of an overfilled water balloon. There is variability in firmness expectations as some consumers want high-firmness, while other consumers view high-firmness as un-ripe (Cappai et al., 2018; Gilbert et al., 2015, 2014; Saftner et al., 2008; J. L. Silva et al., 2005). Blueberry flavor consists of a sweet and mildly sour taste. The mildly sour or tart taste varies widely for consumer preference. Flavor also includes a juicy pulp with a good skin toughness, which is often described as high bursting energy, and minimal graininess or mealiness in pulp (Cappai et al., 2018; Gilbert et al., 2015, 2014; Saftner et al., 2008; J. L. Silva et al., 2005). The blueberry aroma is constantly described as “fresh green, grassy, fruity, floral, and blueberry-like” by trained panelists (Cappai et al., 2018; Gilbert et al., 2015, 2014; Saftner et al., 2008; J. L. Silva et al., 2005). Whereas consumers describe aroma in more general terms, thus consumer usually describe blueberry aroma as sweet and tart or citrus.

2.2.4.4. Voluntary Blueberry Survey

A voluntary survey was conducted by a Plant Pathways Elucidation Project (P²EP) summer undergraduate intern Ashley Wagoner at Catawba College to investigate the consumer’s perception of blueberries. The survey was available for a two-week period with extra credit incentives from some professors to encourage participation. Overall, 300 people from the Catawba College campus community provided responses. The ranking of preferred blueberry color on a scale of 1-5 (1-dark blue and 5-magenta) resulted in 38.7% choosing dark blue and 68% choosing dark and medium blue. When ranking preference of blueberry size, the larger than average blueberries were chosen, but no distinct answer was significantly picked over the other large options. The preference for blueberry firmness (1-soft/squishy and 5-firm/dense) showed 43% chose middle firmness and 40.7% chose middle-high firmness, which supports the common expectation that blueberries should be firm, but not too firm as that is an unripe indicator. Even though this survey did not provide physical examples for questions or address many other sensory attributes of blueberry, it is still valuable information. Sensory evaluations, even if they are simplistic like the above-mentioned survey, are vital for providing fundamental knowledge on blueberry sensory characteristics that are preferred by consumers. More consumer sensory evaluations need to be conducted to gain a better understanding of important sensory traits that can

be utilized in the near future for selective breeding for a more ideal blueberry. Enhancing the flavor of blueberries would entice more consumption, and increased blueberry consumption will improve the consumer's health.

2.2.4.5. Fruit Quality, Its Changes and Research

In simplistic terms, fruit quality is defined as a set of attributes that make a fruit good (Barrett et al., 2010; Grunert, 2005; Kader, 2008; Kyriacou & Roupael, 2018; Musacchi & Serra, 2018; Pagliarini et al., 2013; Varela & Ares, 2012). But the fruit quality definition is drastically changing because of consumer input. This has led to controversy as who or what gets to decide the attributes and goodness defining quality since it is food that every human eats. Traditionally, fruit quality was dictated by visual and texture attributes like color and firmness (Grunert, 2005; Kyriacou & Roupael, 2018; Varela & Ares, 2012). Standardizing the visual appearance of the "ripe" fruit or vegetable streamlined the harvest and transport packing process. Workers could easily compare to the "ripe" standard and pick or pack only the "ripe" ones. This efficiency leads to food markets filled with fruits and vegetables that all looked the same. Reducing the deformities or damage caused by harvest, storage, transport, and shelf-life was also a high priority, so firmness became a fruit quality attribute to increase (Grunert, 2005; Kyriacou & Roupael, 2018; Varela & Ares, 2012). Initially, improving fruit quality attributes did a great job to improve transportability and shelf-life. The increase in firmness improved fruit quality from mechanical harvesting and different storage conditions.

The mechanical harvestability of blueberries has received recent attention from researchers to aid in lowering costs (Cappai et al., 2018; Moggia et al., 2017; Olmstead, Armenta, & Lyrene, 2013). The proposed mechanical harvesting utilizes a tree shaker with trays below to catch the fruit (Cappai et al., 2018; Moggia et al., 2017; Olmstead et al., 2013). The ease at which the ripe blueberry detaches from the cluster is an important factor for improving hand and mechanical harvesting. The compactness of the flower cluster, and later blueberry cluster, is an important factor for agronomic and fruit quality that needs further research. Compact berry clusters lead to misshapen fruit and an ideal environment for pests, fungus, and diseases (J F Hancock et al., 2008; Olmstead et al., 2013; Trehane, 2004). Blueberries in a compact cluster impedes berry

detachment, so improvements towards opening the flower clusters with longer pedicels would be important research, especially for mechanical harvesting (Cappai et al., 2018; J F Hancock et al., 2008; Moggia et al., 2017; Olmstead et al., 2013). Increasing a ripe berry's firmness without sacrificing texture or flavor will drastically improve mechanical harvesting of blueberries because the ripe berries are dropping from the bushes, which can cause bruising or splitting if too soft. Increasing the firmness will also aid in prolonging storage life span as bruising, crushing, and moisture loss will decrease. But the intense, continued selection for firmness and reduced softening caused a decrease in flavor and nutritional compounds (Barrett et al., 2010; Grunert, 2005; Kader, 2008; Kyriacou & Roupael, 2018; X. Li et al., 2010; Pagliarini et al., 2013; Schwab et al., 2008; Varela & Ares, 2012).

The effect of increasing firmness and reducing softening, thus extending shelf-life, while sacrificing flavor became most apparent with the release of the Flavr Savr tomato (Kramer & Redenbaugh, 1994). The Flavr Savr tomato reduced the production of polygalacturonase through genetic modification, which should have reduced softening, increased ripe firmness, and increased shelf-life (Kramer & Redenbaugh, 1994). Although there was success with reducing softening and extending shelf-life, the tomatoes exhibited very little taste and consumers were extremely displeased (Kramer & Redenbaugh, 1994). This startled consumers into realizing how much fruits and vegetables have changed, especially in the flavor attributes. After the consumer outcry, sensory evaluations of fruit and vegetables increased to determine important fruit quality traits (Barrett et al., 2010; Gilbert et al., 2014; Kader, 2008; Klee, 2010; Kramer & Redenbaugh, 1994; Kyriacou & Roupael, 2018; X. Li et al., 2010; McGinn, 2015; Schwab et al., 2008; Spence, 2015). Overall, consumers indicated the fruit quality needs to include taste, aroma, and texture, which are all components of flavor. Flavr Savr taste was reduced probably due to the decrease in diverse compounds interacting with the taste buds and reduced metabolism of complex sugars into mono- or disaccharides (Klee, 2010; McGinn, 2015; Spence, 2015). Since aroma largely contributes to the taste experience, the Flavr Savr aroma was also reduced due to the decrease in released volatile compounds that would interact through retronasal olfaction (Goff & Klee, 2006; Schwab et al., 2008; Spence, 2015). The release of volatile

compounds would normally occur during the ripening process, but the lack of polygalacturonase activity would disrupt proper ripening, resulting in a reduction of volatiles (Goff & Klee, 2006; Schwab et al., 2008; Spence, 2015). The Flavr Savr tomato improved one texture attribute of flavor by reducing softening, but fruit texture also consists of crispness or juiciness (Kramer & Redenbaugh, 1994; X. Li et al., 2010). The decrease in polygalacturonase activity would decrease the solute concentration, which would not induce increased water uptake, and would decrease wall expansion capabilities, which would not allow for increased water retention (Chen et al., 2015; Choi et al., 2002; D'Ovidio, Mattei, Roberti, & Bellincampi, 2004; C. Paniagua et al., 2014). The increase in sensory analyses conducted on different fruits and vegetables shows that consumers want fruit flavor to be included with fruit quality characteristics (Barrett et al., 2010; Gilbert et al., 2015, 2014; Kader, 2008; Klee, 2010; Konarska, 2015; Kyriacou & Rouphael, 2018; McGinn, 2015; Schwab et al., 2008; Spence, 2015; Varela & Ares, 2012).

Selective breeding to improve fruit quality characteristics has been difficult because most of the consumer sensory analyses report the data as distinct rankings rather than quantitative measurements (Barrett et al., 2010; Gilbert et al., 2015, 2014; Saftner et al., 2008). The distinct rankings do not measure small variations in the phenotype, which limits the association mapping ability to identify QTLs. The current technological advancements in laboratory quantification has allowed for thorough quantification of sensory trait rankings, as the rankings correlate with the quantification, thus allowing for improved association mapping of consumer sensory characteristics (Barrett et al., 2010; Gilbert et al., 2015, 2014; Saftner et al., 2008). Described below are some examples of instrumentation that can quantitatively measure sensory attributes. Color can be quantified through wavelength absorption by a spectrophotometer (Barrett et al., 2010; Gilbert et al., 2015, 2014; Saftner et al., 2008). Aroma can be measured through volatile analyses like GC-MS or headspace-extraction (Barrett et al., 2010; Du & Rouseff, 2014; Gilbert et al., 2015, 2014; Saftner et al., 2008). Firmness can be quantified by force-deformation responses, bursting energy, and force-rupture responses (Cappai et al., 2018). Juiciness can also be an attribute of texture, which can be quantified through weight and water loss. Taste can be measured through

quantifying compounds within the fruit, like soluble solids (SS) represents sugars while titratable acidity (TA) and pH measures acids (Barrett et al., 2010; Gilbert et al., 2015, 2014; Saftner et al., 2008). Recent research indicated that taste is a ratio or mixture of compounds interacting with taste buds (Barrett et al., 2010; Gilbert et al., 2015, 2014; Saftner et al., 2008). SS:TA ratio is often used to represent taste. If the food taste is more complicated than sugars to acids, an HPLC-MS can quantify and identify a large diversity of compounds. Quantification of consumer-driven fruit quality traits allows for researchers to statistically find and analyze differences between traits, which improves breeding efficiency (Schaart et al., 2016; Sehgal et al., 2016; B. D. Singh & Singh, 2015). Although the difference in a trait may be statistically significant, too small a difference may be imperceptible to the consumer. Thus, it is still important to conduct consumer sensory evaluations to understand the thresholds and distinctions consumers can detect and prefer.

The consumer-driven fruit quality traits have recently started to include nutrition as an important attribute due to an increase in chronic diseases globally (Barrett et al., 2010; Gilbert et al., 2014; Kyriacou & Rouphael, 2018; Spence, 2015; Varela & Ares, 2012). A multitude of research has consistently shown that a greater consumption of fruits and vegetables decreases chronic diseases because of their nutrients and phytochemicals (Ali Ghasemzadeh, 2011; Castellarin & Di Gaspero, 2007; De Souza et al., 2014; Horbowicz et al., 2008; Khoo et al., 2017; Kraujalyte, Venskutonis, Pukalskas, Česonienė, & Daubaras, 2015; D. Li et al., 2017; Lila, Burton-Freeman, Grace, & Kalt, 2016). Antioxidants are very important phytochemicals found in fruits and vegetables and have been consistently shown to reduce chronic diseases by decreasing oxidative stress within the body (Ali Ghasemzadeh, 2011; Castellarin & Di Gaspero, 2007; De Souza et al., 2014; Horbowicz et al., 2008; Khoo et al., 2017; Kraujalyte et al., 2015; D. Li et al., 2017; Lila et al., 2016). The antioxidant capacity from blueberries and other fruits with anthocyanins have been shown to reduce cardiovascular strain, reduce inflammation, and reduce oxidative injury of nerve cells, especially in the brain (Khoo et al., 2017; Lila et al., 2016). Anthocyanins have been shown to reduce neurodegeneration diseases and improve retina health more effectively than other antioxidants (Khoo et al., 2017; Lila et al., 2016; D. Lin et al., 2016). Anthocyanins have

also been shown to reduce cancer cell proliferation, suppress angiogenesis of tumors, and induce insulin secretion (Khoo et al., 2017; Lila et al., 2016). Some researchers have implicated anthocyanins in regulating adipocyte dysfunctions to aid in obesity (Lila et al., 2016; D. Lin et al., 2016). Even though anthocyanins are associated with great health benefits, the regulatory mechanisms are still unclear and need further investigation.

Unfortunately, many phytochemicals with potent nutritional qualities are associated with off-tastes, resulting in a consumer conflict of whether nutritional quality or flavor is more important. Anthocyanins, along with other antioxidants, have been associated with sour and tart, while anti-carcinogenic metabolites like glucosinolate and isothiocyanate metabolites in broccoli and Brussel sprouts have been associated with an extremely bitter flavor (Drewnowski & Gomez-Carneros, 2000; Fenwick, Griffiths, & Heaney, 1983). Recently, the focus on nutritional quality by consumers has altered the priorities within consumer-driven fruit quality traits as nutrition is of equal importance as flavor (Cappai et al., 2018; Gilbert et al., 2015, 2014; Konarska, 2015; G. A. Lobos et al., 2014; Saftner et al., 2008). For example, consumers are indicating that the tart flavor, commonly associated with the anthocyanins and phenolic acids, is expected and pleasing to some consumers when consuming blueberries (Gilbert et al., 2015, 2014). Consumer sensory evaluations have also indicated that the unique blueberry flavor is the balance of the tart skin to the sweet pulp (Cappai et al., 2018; Gilbert et al., 2015, 2014; Konarska, 2015; G. A. Lobos et al., 2014; Saftner et al., 2008). Blueberry consumer-driven fruit quality traits consist of color, texture, flavor, and nutrition. Color and nutritional fruit quality signify anthocyanin accumulation through a darker blue color and potent antioxidant activity. Textural fruit quality consists of a medium-high firmness. Flavor fruit quality incorporates bursting energy texture for skin toughness and pulp juiciness, and tart and sweet taste for anthocyanins in skin and sugars in pulp (Cappai et al., 2018; Gilbert et al., 2015, 2014; Konarska, 2015; G. A. Lobos et al., 2014; Saftner et al., 2008).

2.2.5. Blueberry Genomic Resource

Since developing a stable blueberry breeding population is difficult due to inbreeding depression and ploidy, blueberry selective breeding has been successful

with improving yield and growth. Unfortunately, the gains in improvements have decreased due to cross incompatibility and lack of genetic resources to fine-tune breeding strategies. With the recent advancements in genomic sequencing and molecular breeding, association mapping in polyploid species is now possible (Cabrera-Bosquet, Crossa, von Zitzewitz, Serret, & Luis Araus, 2012; Carreno-Quintero, Bouwmeester, & Keurentjes, 2013; Foolad & Panthee, 2012; Langridge & Fleury, 2011). The high-throughput, affordable sequencing of a vast amount of genetic data has made it possible to generate enough genetic markers for large, polyploid genomes (Gardner et al., 2014; Lu et al., 2013; Schönhals et al., 2017). The computing power and development of advanced statistical software to analyze the complex algorithms and predictive modeling has also made it possible to calculate and model bigger, more complex breeding populations (Carreno-Quintero et al., 2013; Gardner et al., 2014; Garrido-Cardenas et al., 2018; Lu et al., 2013; Schönhals et al., 2017). Consequently, an autotetraploid blueberry genetic map has been developed for the Draper and Jewel mapping population (Die & Rowland, 2013; McCallum et al., 2016).

The development of the Draper by Jewel (DxJ) mapping population was initiated through the Specialty Crop Research Initiative (SCRI) of the USDA-NIFA (James F. Hancock et al., 2018; McCallum et al., 2016). This brought together a collaboration between the USDA, Michigan State University, University of Oregon, and University Florida with the goal to generate DNA diagnostic markers that could be used by the blueberry breeding community for marker assisted breeding (James F. Hancock et al., 2018; McCallum et al., 2016). The Draper cultivar was chosen as a parent because it is a NHB with high yield, firm and sweet berries, and good shelf-life. The Jewel cultivar was chosen as the other parent because it is a SHB with relatively high yield and very large and tart berries. A main objective of choosing Draper and Jewel was to improve the range of chill requirement thresholds in the offspring (James F. Hancock et al., 2018; McCallum et al., 2016). The tetraploid genetic maps for Draper and Jewel utilized 233 offspring to incorporate 1,794 markers across 12 linkage groups (James F. Hancock et al., 2018; McCallum et al., 2016).

The Draper and Jewel genetic map accomplished the first goal of the SCRI. The other two goals are to phenotypically evaluate the DxJ offspring for horticulturally

important traits associated with development, chilling response, and fruit quality, and to conduct QTL analysis to identify key DNA diagnostics makers for use in future MAS efforts. The phenotypic evaluation was conducted by the collaboration between Michigan State University and University of Florida (Draper & Hancock, 2003; Finn, Hancock, T. Mackey, & Serce, 2003; James F. Hancock et al., 2018). An in-depth analysis of the phenotypic data was published by Hancock et al (2018), but will be summarized in the methods and results section of this Chapter (James F. Hancock et al., 2018). The multiple association mapping analyses of the agronomic and fruit quality phenotypic traits and the resulting QTLs are described in this Chapter.

The objective of this research is to identify QTL markers for important agronomic and fruit quality traits in the tetraploid blueberry population DxJ. The identification of these QTLs will not only assist future MAS for improved blueberries, but also aid in improving our understanding of these trait's regulation through putative candidate gene identification.

2.3. Materials and Methods

2.3.1. Plant Material

The DxJ mapping population used in this research consists of the 4 year old plants from the original 99 individual propagated in the Michigan State University (MSU) greenhouse (James F. Hancock et al., 2018). After 2 years of growth, the genotypes were transplanted in a randomized design across 4 different field environments that represent the typical range of high-bush blueberry commercial growing conditions (James F. Hancock et al., 2018). The Gainesville, FL location typically experiences 250-350 chilling hours. The Waycross, GA location typically experiences 500-600 chilling hours. The Corvallis, OR location typically experiences over 800 chilling hours. The Grand Junction, MI location typically experiences over 800 chilling hours with winter temperatures often below -20°C (James F. Hancock et al., 2018).

2.3.2. Genotypic Data

The genotypic data and SNP marker information was conducted and published by the USDA-ARS labs of Dr. Rowland and Dr. Bassil, and McCallum lab at the James Hutton Institute (McCallum et al., 2016). Both the USDA-ARS and McCallum lab

graciously provided the population genotype and SNP marker data for this research (McCallum et al., 2016). The separate Draper and Jewel tetraploid genetic maps were published by McCallum, et al. (McCallum et al., 2016).

A modified mapping procedure described by Oliver et al. was used to develop a high-density linkage map of the highbush blueberry Draper × Jewel (*Vaccinium corymbosum*) mapping population (Oliver et al., 2013). In brief, single nucleotide polymorphism (SNP) loci derived from genotype-by-sequencing (GBS) were assembled into maps for each parental line using the MultiPoint package (MultiQTL Ltd., Haifa, Israel). Preliminary grouping and ordering of the genotypic matrices were done at a recombination fraction (rf) = 0.15 and loci with $rf = 0$ were assigned to a binned group. A single locus or “delegate” was then chosen to represent each bin based on data quality and strength of position using a likelihood of odds approach. The preliminary marker orders within each group were refined using a jackknife approach where the probability of the marker order was estimated based on 30 iterations with a 0.10 random hold out of individual in the population. Unstable orders were refined by identification and removal of problematic loci using the order variance, segregation ratio, and the rf with nearby markers. Once stable orders were generated, linkage groups were merged end-to-end by incrementally increasing rf by 0.05 up to a final rf of 0.3. Alignment of the two parental maps was made on the basis of best fit of the shared loci and linkages to double-simplex markers segregating in both parents as described by McCallum et al (McCallum et al., 2016).

2.3.3. Phenotypic Data

The phenotypic data was collected for both 2011 and 2012 by University of Florida, Berry Blue industries, Michigan State University, University of Oregon, and USDA-ARI for the three locations, FL, GA, and OR (Blaker, Plotto, Baldwin, & Olmstead, 2014; Finn, Hancock, T. Mackey, et al., 2003; Gilbert et al., 2015, 2014, 2013; James F. Hancock et al., 2018; McCallum et al., 2016; Lisa J Rowland et al., 2012). A detailed phenotypic description and cultivar performance analysis of the 30 traits measured in the DxJ mapping population can be found in the publication by Hancock et al. (James F. Hancock et al., 2018). As a brief summary of the phenotype descriptions and analysis published by Hancock et al., the 30 different traits measured

multiple growth, developmental, and fruit quality characteristics (James F. Hancock et al., 2018). Bush size, height and width, was measured at the end of the growing season. The crop potential was estimated on a 1-9 scale through counting the number of floral buds on the three largest canes. Flower bud development was measured weekly when majority of buds were at bud break and full bloom. Leaf bud development was also scored weekly for early green tip, late green tip, and shoot expansion according to MSU specific tables ([2016](#)) (James F. Hancock et al., 2018). The proportion of vegetative buds that broke was evaluated on a 1-9 scale after the new growth ceased. After fruiting, the strength of leafing and overall vigor was rated on a 1-9 scale. Fruit development was measured when the fruit began coloring and when 50% of the bush turned blue (James F. Hancock et al., 2018). Flower and fruit development period was estimated as days between bud break and full bloom, and full bloom and 50% blue fruit. Subjective ratings were collected after the bush contained 50% blue fruit and were on a 1-9 scale. Color rating ranged from dark blue to powder blue. Firmness ratings ranged from soft to very firm. Flavor ratings ranged from poor to excellent. The fruit quality traits of berries from both years for GA and FL were also quantified when at least 30% of the bush contained ripe, blue fruit (James F. Hancock et al., 2018). Fruit weight was an average of 50 random ripe berries. Berry firmness (g/mm deflection) and equatorial width of 25 random berries were measured using the FirmTech2 instrument (BioWorks, Inc., Wamego, KS). SS, pH, TA, and total anthocyanins were measured from an extract made from frozen, thawed, blended, and strained blueberries. Total SS was quantified with a digital hand-held “pocket” refractometer PAL-1 (Atago Bellevue, WA). pH and TA were measured with a Mettler DL15 Auto-Titrator (Columbus, OH). Total anthocyanin content was quantified as cited in Hancock et al (James F. Hancock et al., 2018).

The 30 traits were categorized in this research into three groups, which consisted of: growth, dormancy break and flowering time, and fruit quality. The growth group consisted of the traits: bush height, bush width, yield estimate rating, vigor rating, leafing strength, % broken vegetative buds rating, leaf:fruit ratio rating, and floral buds per cane. The dormancy break and flowering time group consisted of the traits: vegetative chill requirement, floral chill requirement, floral chill rating, days until shoot expansion,

days until early green tip, days until floral bud break, days until full bloom, and days between floral bud break to full bloom. The fruit quality group consisted of the traits: days between full bloom and blue fruit, days until blue fruit, fruit color rating, fruit scar rating, fruit firmness rating, fruit flavor rating, berry weight, berry firmness, % juice, pH, SS, TA, SS:TA ratio, and total anthocyanin content. The distribution of each phenotype was analyzed for a statistical deviation from normality throughout the population using JMP Professional (13.1) (James F. Hancock et al., 2018).

2.3.4. Biparental Association Mapping (BiPAM)

The BiPAM was conducted using JMP Genomics 7 (JMP[®], SAS Institute Inc.). The genotypic and phenotypic data was merged together to make a geno-pheno file that had stacked genotypic information to account for the individual lines replicated across the years and locations (James F. Hancock et al., 2018). This allowed for year and location to become a factor that could be utilized as a cofactor to account for the year or location effects. Each trait consisted of individual phenotypes for each location and year, for example, the growth trait of bush height consisted of six individual phenotypes for the three locations (FL, GA, and OR) and two years (2011 and 2012) (Table 2.4). The genotypes were filtered for a minimum proportion of non-missing genotypes of 0.6. A genotype probability data table was built using the Kosambi map function. The genotype probability data table utilized the cross information to calculate recombination frequencies and the relationship between markers. When the gap between markers was larger than 2 cM, pseudo-markers were created, and recombination frequencies predicted. This develops a denser genetic map to allow for finer association mapping to identify smaller QTL regions. The cross type selected was T(B2)SF_n indicating a test-backcross with parent 2 with a selfing genotype generation of n. For the DxJ mapping, parent 2 is Draper and the self-genotype generation is 1 because the offspring are the F1 generation.

The DxJ specific tetraploid genetic map was incorporated as the annotation file with the genetic map linkage groups designated as chromosomes, and the genetic map consensus position designated as chromosome position. The number of distinct genotypes was 2 for each marker because the marker was either D/J - D/D or D/J - J/J. The QTL test step was 2 cM to refine the association mapping. The conventional LOD

threshold of 3 was used to determine significant QTLs. Interval mapping (IM) and composite interval mapping (CIM) was conducted with the EM, estimated maximum-likelihood, algorithm for modeling. For the CIM method, 5 control markers and a 5 cM test window was utilized to refine the interval mapping window. The control markers were selected using a stepwise regression with a 0.35 significance level for entry into the model, and a 0.05 significance level for staying in the model as a control marker. Multiple interval mapping (MIM) was also conducted on the traits to determine possible interacting and secondary QTLs that may have an indirect role on regulating the trait that could only be detected once the variation of the major QTLs are accounted for during the mapping (Bernardo, 2008; Feenstra, 2006; Hackett, Bradshaw, & McNicol, 2001; Kao, 2000; H. Li, Ye, & Wang, 2006; Mayer, 2005).

BiPAM using CIM was conducted on all the different phenotypic data because CIM identifies multiple QTLs across the genome while also accounting for the effect of QTLs on other significant QTLs (Bernardo, 2008; Feenstra, 2006; Hackett et al., 2001; Kao, 2000; H. Li et al., 2006; Mayer, 2005). For each of the 30 traits, there were four to six individual phenotypes that were CIM mapped separately. Association CIM mapping was also conducted for each trait when the specific locations were grouped separately into FL, GA, or OR -specific traits, and was designated as location-specific analyses. Association CIM mapping was also conducted for each trait when the specific years were grouped separately into 2011 or 2012, and was designated as year-specific analyses. Association CIM mapping was also conducted on all the phenotypic data together to investigate the 30 traits overall by using the categorical variables location, year, and the combination of “both location and year” as cofactors, and was designated as the three cofactor analyses. Using the categorical co-factors for CIM association mapping accounted for phenotypic variation possibly caused by the environmental variation from the locations or years (Bernardo, 2008; Collard, Jahufer, Brouwer, & Pang, 2005; James F. Hancock et al., 2018; H. Li et al., 2006).

2.4. Results

2.4.1. Genetic Map

The DxJ specific tetraploid genetic map was constructed utilizing the genotypic information from the McCallum lab at the James Hutton Institute (McCallum et al., 2016). The tetraploid genetic maps for the Draper and Jewel parents were published by MaCallum et al. (McCallum et al., 2016). This DxJ genetic map has 12 total linkage groups, which is the predicted chromosome number for haploid blueberry (McCallum et al., 2016). This DxJ genetic map also has two large linkage group fragments, 6.5 and 11.5, that may align with linkage groups 6 and 11, respectively, but further research is required to link the fragments to linkage groups (Figure 2.2). Summary statistics for the DxJ genetic map are shown in Table 2.1. The whole genetic map without the fragments has an average density of 1.51 cM per locus and an average gap of 1.50 cM. The genetic map has only 1 gap greater than 20 cM. Linkage group twelve has the greatest number of markers, 139, and the smallest average density of 1.16 cM per locus. Linkage group seven has the least number of markers, 47, and greatest average density of 3.53 cM per locus. Further summary statistics of individual linkage groups are in Table 2.2.

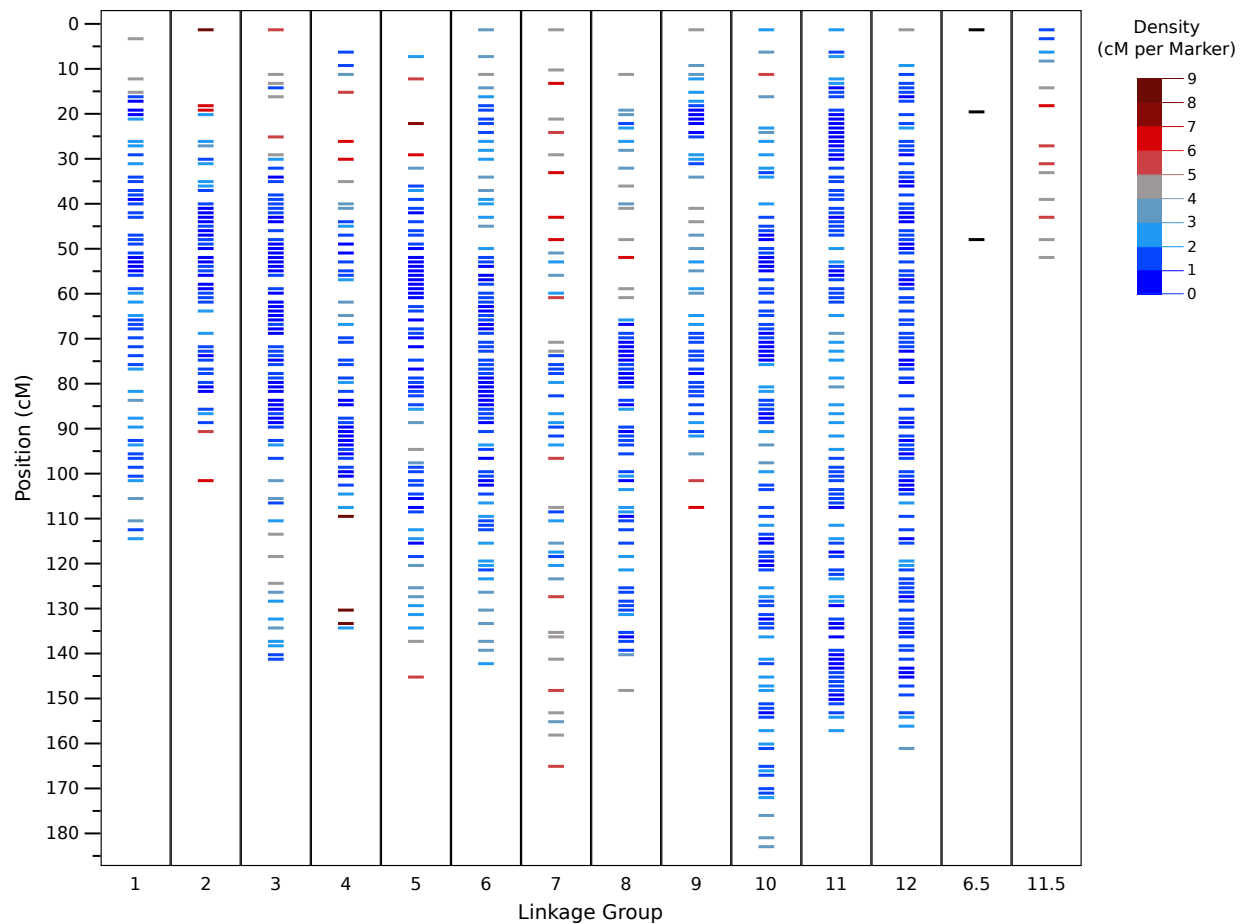


Figure 2.2 – Draper x Jewel (DxJ) tetraploid genetic map, including fragments 6.5 and 11.5. The darker the blue color, the less dense cM per markers in the area. The darker the red color, the less dense and further away the markers are in the area. The black color markers on fragment 6.5 indicate the markers are further apart then 10.

Table 2.1 – Summary statistics for overall genetic map for Draper x Jewel tetraploid mapping population.

	Total Markers	Total Distance	Average Density (cM/Locus)	Average Gap (cM)	Gap >10	Gap >15	Gap >20
Without Fragments	1,117	1,698	1.510	1.4996	9	2	1
With Fragments	1,133	1,795	1.576	1.5640	11	4	2

Table 2.2 – Summary statistics of linkage groups for DxJ tetraploid genetic map.

Linkage Group	Total Markers	Total Distance	Average Density (cM/Locus)	Average Gap (cM)	Gap >10	Gap >15	Gap >20
1	72	114	1.576	1.5556	0	0	0
2	66	101	1.551	1.5303	2	1	0
3	118	141	1.211	1.1949	1	0	0
4	67	134	1.938	1.9254	2	1	1
5	105	145	1.3238	1.3238	1	0	0
6	97	142	1.473	1.4639	0	0	0
7	47	165	3.528	3.5106	3	0	0
8	87	148	1.588	1.5862	0	0	0
9	61	107	1.776	1.7541	0	0	0
10	124	183	1.487	1.4758	0	0	0
11	134	157	1.175	1.1716	0	0	0
12	139	161	1.164	1.1583	0	0	0
6.5	3	46	15.778	15.3333	2	2	1
11.5	10	51	3.962	3.9231	0	0	0

2.4.2. Phenotype Results

Each trait had phenotypic data obtained for both 2011 and 2012 years. Some phenotypes could not be collected for all three locations, which was further described in methodologies of the previously published research by Hancock et al. (Blaker et al., 2014; Finn, Hancock, T. Mackey, et al., 2003; Gilbert et al., 2015, 2014, 2013; James F. Hancock et al., 2018; McCallum et al., 2016; Lisa J Rowland et al., 2012) (Table 2.3). The three traits: chill requirement vegetative, chill requirement floral, and floral chill rating, had phenotype data collected in only one location for one year. Nine of the 30 traits had phenotypes measured in the two FL and GA locations. The remaining 18 traits had phenotypes measured in the three FL, GA, and OR locations. Therefore, each trait had individual phenotypes for each location for each year, which resulted in 147 individual phenotypes. To investigate location specificity, the individual phenotypes were grouped into location-specific phenotypes for FL, GA, and OR locations, which resulted in 72 location-specific phenotypes. To investigate year specificity, the individual phenotypes were also grouped into year-specific phenotypes for 2011 or 2012 years, which resulted in 54 year-specific phenotypes. To investigate the overall traits, the individual phenotypes were grouped all together with the specific location and year

information for each individual phenotype incorporated as additional variables or cofactors.

The 30 traits were subdivided into three categories: growth, dormancy break and flowering, and fruit quality. The eight growth traits focused on overall plant agronomics and included: bush height, bush width, vigor rating, leafing strength, % broken vegetative buds rating, leaf:fruit ratio rating, floral buds per cane, and yield estimate rating. The eight dormancy break and flowering traits focused on the developmental transitions of dormancy break and flowering and included: chill requirement vegetative, chill requirement floral, floral chill rating, days until shoot expansion, days until early green tip, days until floral bud break, days until full bloom, and days between floral bud break and full bloom. The 14 fruit quality traits focused on fruit development and ripening as well as blueberry fruit characteristics and included: days between full bloom and blue fruit, days until blue fruit, fruit color rating, fruit scar rating, fruit firmness rating, fruit flavor rating, berry weight, berry firmness, % juice, pH, SS, TA, SS:TA ratio, and total anthocyanin content.

The distribution of each phenotype was analyzed for goodness of fit to a normal distribution, as indicated by the red line in each of the histograms in Figures 2.3, 2.4, and 2.5 (James F. Hancock et al., 2018). If the p-value was less than 0.05, then the phenotype across the population does not follow a normal distribution. Only berry weight, days between full bloom and blue fruit, and SS follow a normal distribution. The traits bush height, % vegetative buds that broken rating, days until shoot expansion, days between floral bud break and full bloom, days until full bloom, days until blue fruit, fruit firmness rating, and % juice showed two distinct peaks or binominal distribution.

Table 2.3 – Phenotype summary statistics for the 30 DxJ traits.

	Location Number	Total Individuals (N) (Years+Location)	Mean ± Standard Error Mean	Goodness of Fit to a Normal Distribution
Growth Traits				
Bush Height (cm)	3	503	83.87±1.84	<0.0001
Bush Width (cm)	3	502	84.24±1.97	<0.0001
Leafing Strength	3	505	5.58±0.098	<0.0001
% Broken Vegetative Buds Rating	3	508	4.73±0.099	<0.0001
Leaf:Fruit Ratio Rating	3	503	6.14±0.092	<0.0001
Yield Estimate Rating	3	488	4.45±0.099	<0.0001
Floral Buds per Cane	2	309	94.03±4.27	<0.0001
Vigor Rating	3	506	5.80±0.077	<0.0001
Dormancy Break and Flowering Traits				
Chill Requirement Vegetative	1	65	576.15±12.06	<0.0001
Chill Requirement Floral	1	74	436.49±11.44	<0.0001
Floral Chill Rating	1	74	1.72±0.07	<0.0001
Days until Early Green Tip	3	408	53.43±0.59	<0.0001
Days until Shoot Expansion	3	489	75.88±0.66	<0.0001
Days until Floral Bud Break	3	463	46.53±0.79	<0.0001
Days until Full Bloom	3	438	94.15±1.65	<0.0001
Days Between Floral Bud Break to Full Bloom	3	425	45.76±1.29	<0.0001
Fruit Quality Traits				
Days Between Full Bloom to Blue Fruit	3	422	60.67±0.60	0.032
Days until Blue Fruit	3	460	146.74±1.75	<0.0001
Fruit Scar Rating	3	436	5.80±0.12	<0.0001
Fruit Color Rating	3	438	6.20±0.08	<0.0001
Fruit Firmness Rating	3	436	4.86±0.12	<0.0001
Fruit Flavor Rating	3	373	4.89±0.12	<0.0001
Berry Weight (g)	2	297	2.15±0.029	0.089
Berry Firmness (N)	2	300	204.83±1.73	<0.0001

Table 2.3 – (continued).

% Juice	2	292	35.86±0.45	0.0029
pH	2	295	3.30±0.016	0.0012
Titrateable Acidity (TA)	2	292	0.67±0.017	<0.0001
Soluble Solids (SS)	2	292	11.21±0.86	0.0924
SS:TA Ratio	2	287	19.45±0.55	<0.0001
Total Anthocyanin Content (mg cyn-3-glu/g fw)	2	288	132.22±3.65	0.0012

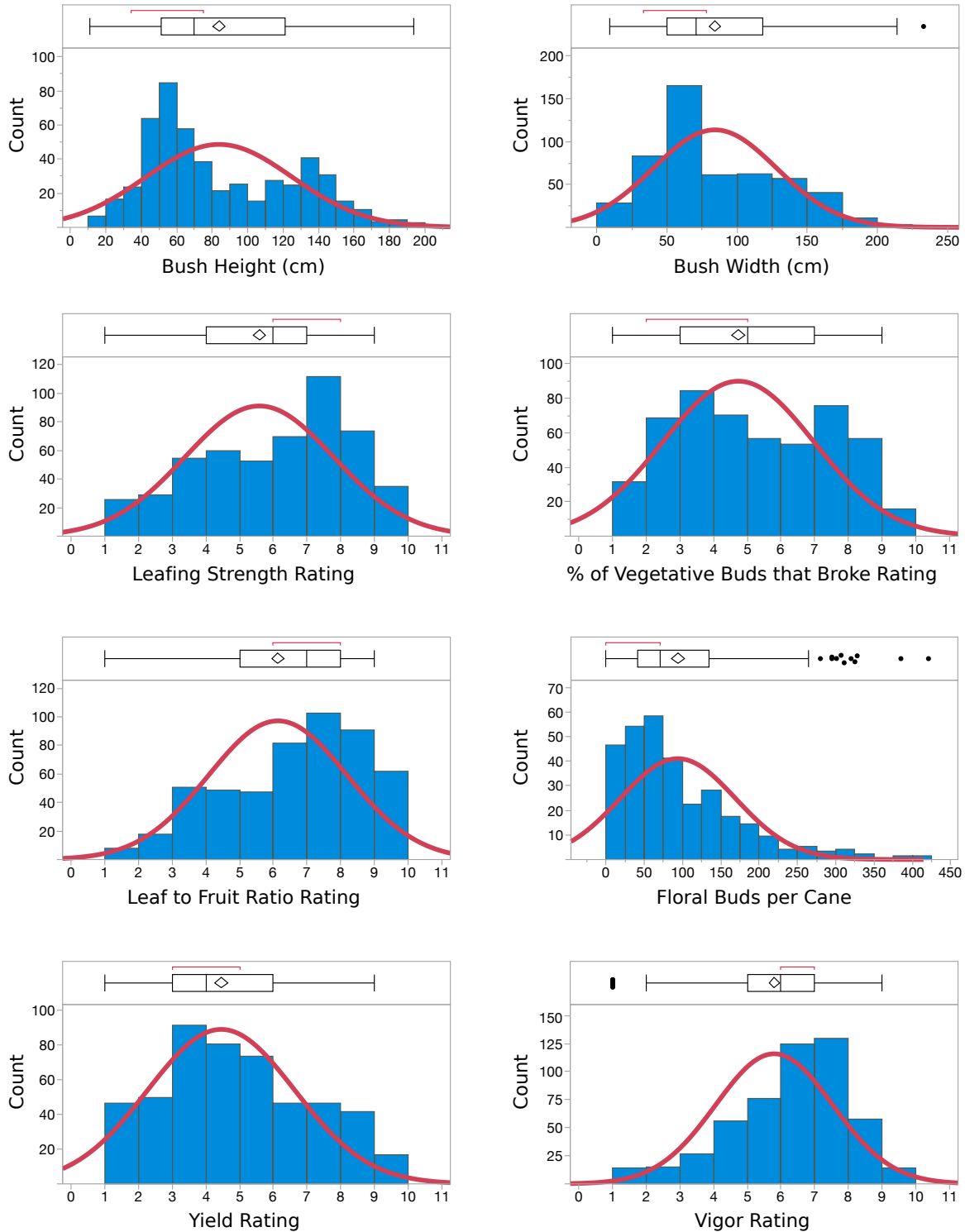


Figure 2.3 – Distribution histograms for growth traits. The red line indicates a normal distribution. The box plot shows the mean, quartiles, and interquartile range, as well as possible outliers as dots.

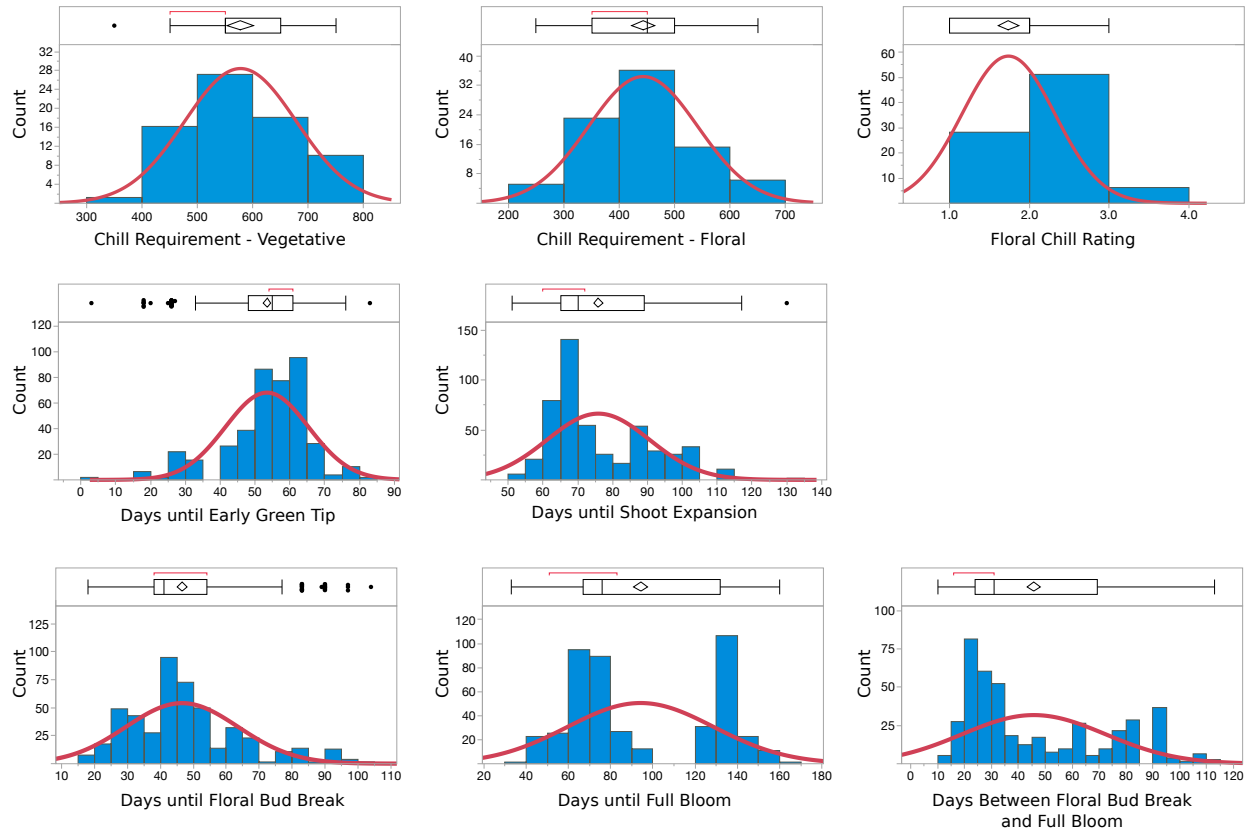


Figure 2.4 – Distribution histograms for dormancy break and flowering traits. The red line indicates a normal distribution. The box plot shows the mean, quartiles, and interquartile range, as well as possible outliers as dots.

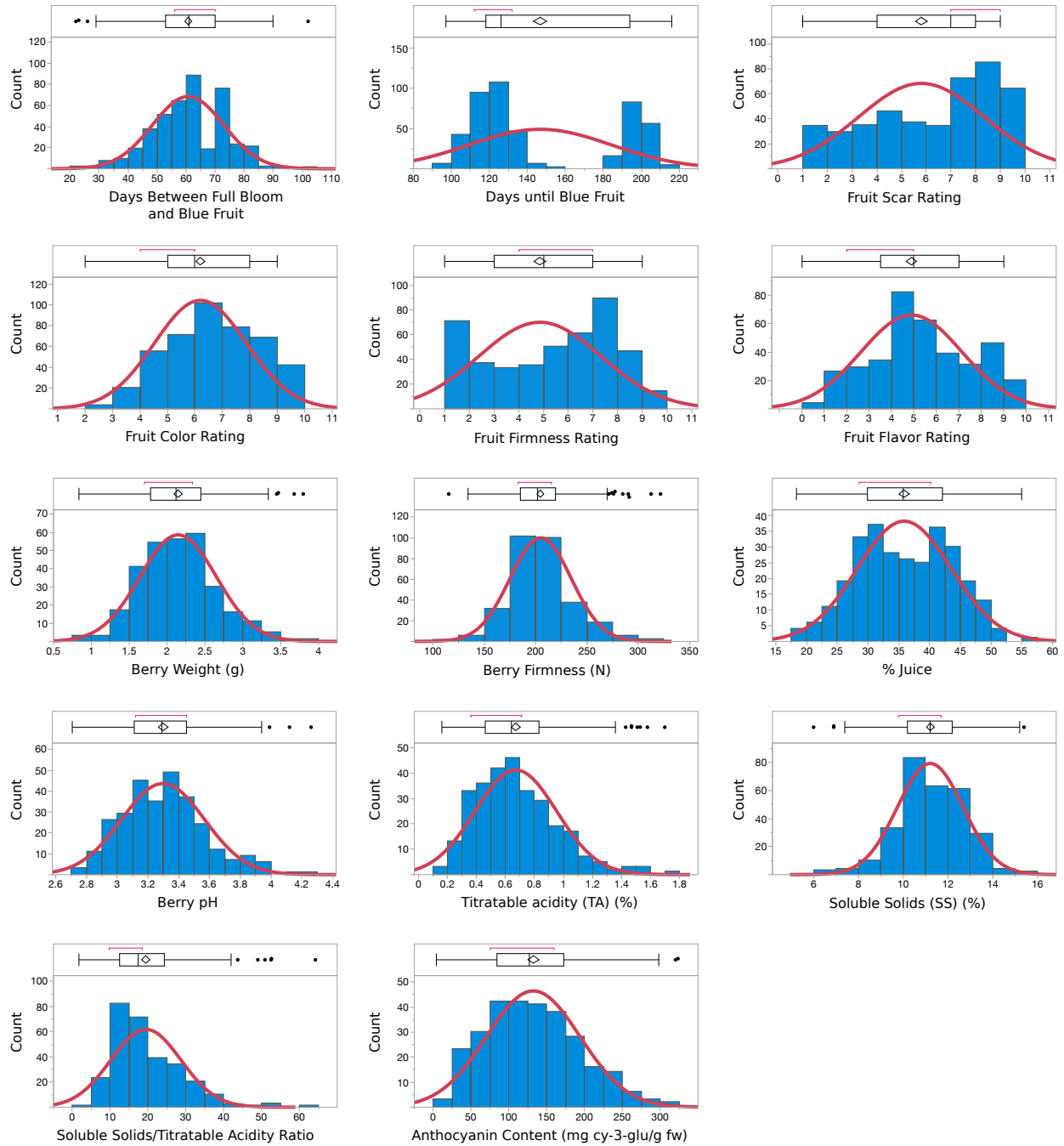


Figure 2.5 – Distribution histograms for fruit quality traits. The red line indicates a normal distribution. The box plot shows the mean, quartiles, and interquartile range, as well as possible outliers as dots.

Since 10 of the 30 traits are qualitative rankings, some of the correlations between quantitative and qualitative traits were difficult, as discussed in the previously published paper by Hancock et al. (James F. Hancock et al., 2018). As a brief summary of the correlations from the Hancock et al. published research, the yield rating was correlated with bush height, bush width, and floral buds per cane. Conversely, yield rating showed a strong, negative correlation with the leaf to fruit ratio rating. Bush height and bush width showed a strong, positive correlation. Vigor rating showed a strong, positive correlation with leafing strength rating. Leafing strength rating exhibited a strong, positive correlation with % vegetative buds that broke rating. For the dormancy break and flowering traits, the days until early green tip was negatively correlated with the days between full bud break to full bloom. The days until floral bud break showed a strong, positive correlation with the days until full bloom. The days until full bloom was also highly correlated with the days between floral bud break and full bloom. The days between floral bud break and full bloom was also positively correlated with days between full bloom to blue fruit transition. The days until full bloom showed a high, positive correlation with the days until blue fruit. The days until blue fruit was strongly correlated with the days between floral bud break and full bloom, as well as days between full bloom and blue fruit transition. For the fruit quality traits, berry firmness quantified in the lab showed a positive correlation with fruit firmness ratings from consumers. Berry firmness also showed a positive correlation with TA. TA showed a very strong, positive correlation with pH. pH showed a strong, positive correlation with SS:TA ratio. SS:TA ratio showed a very strong, negative correlation with TA. SS showed a positive correlation with SS:TA ratio. % juice showed a positive correlation with pH and total anthocyanin content. Fruit color rating by consumers showed no correlation with the total anthocyanin content. Specific details for phenotype correlations can be found in Hancock et al. (James F. Hancock et al., 2018).

2.4.3. Biparental association mapping (BiPAM) results

The BiPAM of the 30 agronomic traits used IM and CIM methods for analyzing the 147 individual phenotypes, the 72 location-specific, the 54 year-specific, and 30 overall traits (Tables 2.4 and 2.5). The 30 total traits were also analyzed with CIM using the location and year variables as cofactors, which resulted in three more analyses: just

location cofactor, just year cofactor, and both location and year cofactors (Table 2.5). BiPAM using MIM was also conducted on the 30 total traits. The results reported and discussed for the remainder of this chapter are from all the CIM method because the CIM method uses multiple regression to account for the effect of other QTLs (Bernardo, 2008; Feenstra, 2006; Hackett et al., 2001; Kao, 2000; H. Li et al., 2006; Mayer, 2005).

Association mapping of all the individual phenotypes resulted in 226 significant QTLs with 42.9% of the QTLs significant for growth traits, 23.9% significant for dormancy break and flowering, and 33.2% of the QTLs significant for fruit quality traits (Table 2.4). The leafing strength trait and days until early green tip trait resulted in the highest number of significant QTLs (Table 2.4). Vegetative chill requirement, floral chill requirement, and days between full bloom and blue fruit traits did not produce any significant QTLs (Table 2.4).

When analyzing the locations separately, there were 178 total significant QTLs as 46.1% were significant for growth, 12.9% for dormancy break and flowering, and 41.0% for fruit quality traits (Table 2.5). Of these 178 total significant QTLs, 29.2% were significant specifically for FL, 29.8% were specifically significant for GA, and 41.0% were significant for OR (Table 2.5). The FL location mapping identified 52 total significant QTLs with 34.6% for growth traits, 7.7% for dormancy break and flowering traits, and 57.7% for fruit quality traits. The GA location mapping identified 53 total significant QTLs with 17.0% for growth traits, 24.5% for dormancy break and flowering traits, and 58.5% for fruit quality traits. The OR location mapping identified 73 total significant QTLs with 75.3% for growth traits, 8.3% for dormancy break and flowering, and 16.4% for fruit quality traits.

Association mapping of the total traits with location as a cofactor resulted in 116 total significant QTLs with growth traits constituting 43.1%, dormancy break and flowering constituting 3.5%, and fruit quality constituting 53.4% of the total QTLs (Table 2.5). The floral buds per cane trait resulted in the largest number of significant QTLs with location as a cofactor (Table 2.5).

When analyzing the years separately, there were 68 total significant QTLs with growth traits constituting 54.4%, dormancy break and flowering traits constituting 4.4%, and fruit quality constituting 41.2% (Table 2.5). Of those 68 significant QTLs, 51.5%

were significant for 2011 and 48.5% were significant for 2012 (Table 2.5). In 2011, the growth traits accounted for 45.7%, dormancy break and flowering traits accounted for 8.6%, and fruit quality traits accounted for 45.7% of the 35 total significant QTLs (Table 2.5). Whereas, in 2012, growth traits accounted for 63.6%, dormancy break and flowering traits accounted for 0%, fruit quality traits accounted for 46.4% of the 33 total significant QTLs (Table 2.5).

Association mapping of the overall traits with year as a cofactor resulted in 106 total significant QTLs with 42.5% of the QTLs significant for growth traits, 8.5% significant for dormancy break and flowering traits, and 49.0% significant for fruit quality traits (Table 2.5). Using both location and year as cofactors for association mapping resulted in 359 total significant QTLs with 44.8% of the QTLs significant for growth traits, 5.6% significant for dormancy break and flowering, and 49.6% significant for fruit quality (Table 2.5). The vigor rating trait resulted in the highest number of significant QTLs for 2012 in the years separately mapping and in the year cofactor mapping (Table 2.5).

All of the significant QTLs for each trait were further investigated for overlap with other significant QTLs from the other mapping analyses. An overlapping QTL region was determined when three or more significant QTLs from different mapping analyses are in the same significant QTL region (Tables 2.6, 2.7, 2.8). For the 30 traits, the 14 mapping analyses resulted in 98 overlapping QTL regions with growth traits accounting for 43.9% of the regions, dormancy break and flowering accounting for 4.1%, and fruit quality traits accounting for 52.0% of the QTLs (Tables 2.6, 2.7, 2.8).

Table 2.4 – Total genome-wide significant QTLs for each trait when separated into the individual phenotypes from each location and year.

Individual Phenotypes						
Location	FL		GA		OR	
Year	11	12	11	12	11	12
Growth						
Bush Height (cm)	9	2	0	0	0	0
Bush Width (cm)	0	6	0	0	0	1
Leafing Strength	0	3	2	0	12	8
% Broken Veg. Buds Rating	0	2	1	5	3	5
Leaf:Fruit Ratio Rating	2	0	0	2	4	3
Yield Estimate Rating	0	1	0	1	0	1
Floral Buds per Cane	0	1	2	6	-	-
Vigor Rating	0	3	1	0	3	8
Dormancy Break and Flowering						
Chill Requirement Vegetative	0	-	-	-	-	-
Chill Requirement Floral	0	-	-	-	-	-
Floral Chill Rating	1	-	-	-	-	-
Days until Shoot Expansion	1	0	0	2	2	0
Days until Early Green Tip	0	12	4	9	0	0
Days until Floral Bud Break	0	0	0	10	1	2
Days until Full Bloom	0	2	1	0	0	0
Days Between Floral Bud Break and Full Bloom	0	1	1	2	2	1
Fruit Quality						
Days Between Full Bloom and Blue Fruit	0	0	0	0	0	0
Days until Blue Fruit	5	1	0	1	7	2
Fruit Scar Rating	0	3	0	1	0	2
Fruit Color Rating	1	4	2	0	0	2
Fruit Firmness Rating	1	1	0	0	0	0
Fruit Flavor Rating	1	0	0	2	2	0
Berry Weight (g)	2	0	1	2	-	-
Berry Firmness (N)	1	4	0	1	-	-
Percent (%) Juice	0	1	0	3	-	-
pH	0	2	0	0	-	-
Titrateable Acidity (TA)	1	0	0	0	-	-
Soluble Solids (SS)	0	0	1	4	-	-
SS:TA Ratio	6	5	0	0	-	-
Total Anthocyanin Content (mg cyn-3-glu/ g fw)	1	2	0	0	-	-

Table 2.5 – Total genome-wide significant QTLs for each trait when grouped together into location-specific, year-specific, and cofactor-specific analyses.

	Location-Specific			Year-Specific		Cofactor-Specific		
	FL	GA	OR	2011	2012	Loc	YR	Both
Growth								
Bush Height (cm)	6	0	6	0	0	0	0	4
Bush Width (cm)	2	0	14	0	0	2	1	3
Leafing Strength	0	0	13	4	7	5	4	11
% Broken Veg. Buds Rating	1	1	12	0	0	0	0	0
Leaf:Fruit Ratio Rating	0	2	2	0	1	4	1	4
Yield Estimate Rating	1	2	0	2	0	7	7	8
Floral Buds per Cane	7	3	-	5	4	17	12	17
Vigor Rating	1	0	10	5	9	15	20	19
Dormancy and Flowering Time								
Days until Shoot Expansion	0	0	0	1	0	0	1	0
Days until Early Green Tip	1	9	3	1	0	2	4	5
Days until Floral Bud Break	0	0	0	1	0	2	4	2
Days until Full Bloom	2	0	0	0	0	0	0	0
Days Between Floral Bud Break and Full Bloom	1	4	3	0	0	0	0	0
Fruit Quality								
Days Between Full Bloom and Blue Fruit	1	1	0	0	0	1	1	1
Days until Blue Fruit	2	5	6	0	0	0	0	0
Fruit Scar Rating	0	0	1	0	0	0	0	0
Fruit Color Rating	6	0	4	1	0	2	2	2
Fruit Firmness Rating	0	0	1	0	0	1	0	1
Fruit Flavor Rating	0	0	0	0	0	0	0	0
Berry Weight (g)	4	8	-	7	3	11	12	12
Berry Firmness (N)	1	2	-	2	4	11	11	11
Percent (%) Juice	0	2	-	1	0	4	4	4
pH	8	3	-	0	3	4	0	5
Titrateable Acidity (TA)	3	2	-	0	0	12	9	12
Soluble Solids (SS)	0	2	-	0	1	3	3	3
SS:TA Ratio	5	6	-	4	1	9	6	9
Total Anthocyanin Content (mg cyn-3-glu/ g fw)	0	0	-	1	0	4	4	4

Table 2.6 – Overlapping QTL regions containing at least three significant QTLs from different CIM analyses for the growth traits.

	LG	Position (cM)	CIM Analyses of the Significant QTLs	LOD	% Variation Explained
Height	5	10-19	Both Loc(FL) Ind. -FL_11	4.25 5.04 5.80	3.82 13.58 28.09
	5	124	Both Loc(FL) Ind. -FL_11	3.22 4.54 5.76	2.91 12.32 27.91
Width	5	15-17	Both & Loc Loc(FL) & (OR) Ind. -FL_12 & -OR_12	3.78 & 3.53 4.03 & 5.92 7.81 & 3.20	3.41 & 3.18 11.14 & 14.06 36.94 & 15.28
	5	117	Both & Loc & YR	4.56 & 4.45 & 3.26	4.10 & 4.00 & 2.95
	5	124-125	Both Loc(OR) Ind. -FL_12	3.18 4.02 4.20	2.87 9.78 21.97
Leafing Strength Rating	3	130	Both Loc(OR) YR(12) Ind. -OR_12	3.04 5.31 3.63 3.02	2.73 12.77 6.41 14.31
	5	15-19	Both & Loc & YR Loc(OR) YR(12) Ind. -FL_12, -OR_11, -OR_12	6.19 & 5.46 & 5.01 9.71 5.23 3.90 & 9.71 & 13.71	5.48 & 4.86 & 4.46 35.09 9.12 20.12 & 38.83 & 50.41
	5	124-125	Both & Loc & YR Loc(OR) YR(12) Ind. -FL_12, -OR_11, -OR_12	5.50 & 4.65 & 4.60 5.61 5.05 3.42 & 6.59 & 4.93	4.89 & 4.16 & 4.11 13.44 8.82 17.87 & 28.37 & 22.30
	6	38-41	Both Loc(OR) YR(11)	3.38 3.25 3.16	3.04 8.02 5.58

Table 2.6 – (continued).

	10	50	Both & Loc & YR YR(12)	4.43 & 3.70 & 3.99 3.23	3.96 & 3.31 & 3.57 5.73
	10	59-61	Both & Loc & YR	3.93 & 3.28 & 3.52	3.52 & 2.95 & 3.16
	12	78	Both YR(12) Ind. -OR_11	3.22 3.33 3.67	2.90 5.91 16.93
Leaf:Fruit Ratio	12	78	Both & Loc & YR	3.47 & 3.30 & 3.03	3.13 & 2.97 & 2.74
Yield Rating	3	87	Both & Loc & YR	3.78 & 3.66 & 3.32	3.51 & 3.40 & 3.08
	5	13-17	Both & Loc & YR YR(11)	4.06 & 3.82 & 4.21 3.18	3.76 & 3.54 & 3.90 5.78
	5	58	Both & Loc & YR	3.44 & 3.35 & 3.05	3.19 & 3.11 & 2.84
	5	60	Both & Loc & YR Loc(GA)	3.64 & 3.52 & 3.32 3.11	3.38 & 3.27 & 3.09 8.51
	5	124-125	Both & Loc & YR YR(11)	4.15 & 3.95 & 4.25 4.44	3.84 & 3.66 & 3.93 7.98
	11	80	Both & Loc & YR	3.31 & 3.21 & 3.10	3.07 & 2.99 & 2.89
Floral Buds per Cane	2	11	Both & Loc & YR YR(11) Ind. -GA_12	5.14 & 5.51 & 6.60 3.38 3.96	7.37 & 7.89 & 9.36 9.56 20.61
	4	18-24	Both & Loc & YR Loc(FL) YR(11) Ind. -GA_12	6.04 & 6.54 & 7.36 4.48 3.64 3.54	8.61 & 9.28 & 10.39 12.63 10.25 18.65
	4	130-134	Both & Loc & YR Loc(FL) & (GA) YR(12) Ind. -GA_12	6.31 & 7.01 & 7.56 3.28 & 4.10 6.35 3.52	8.97 & 9.92 & 10.66 9.40 & 11.41 17.29 18.57
	6.5	0-10	Both & Loc & YR YR(11) Ind. -GA_11	3.39 & 3.28 & 9.48 7.08 3.51	4.92 & 4.77 & 13.17 18.98 18.73
	9	93	Both & Loc & YR Loc(FL)	4.47 & 4.33 & 3.31 3.61	6.45 & 6.25 & 4.81 10.30

Table 2.6 – (continued).

	11	25	Both & Loc & YR Loc(GA)	3.79 & 3.74 & 3.20 3.71	5.49 & 5.43 & 4.65 10.37
	11	80	Both & Loc & YR Loc(FL)	4.30 & 4.28 & 3.38 3.72	6.21 & 6.17 & 4.91 10.59
	12	42	Both & Loc & YR Loc(FL)	4.39 & 4.38 & 3.49 4.29	6.33 & 6.32 & 5.07 12.11
Vigor Rating	4	83	Both & Loc & YR	3.98 & 3.39 & 3.90	3.56 & 3.04 & 3.49
	4	95	Both & Loc & YR	3.67 & 3.10 & 3.44	3.23 & 2.78 & 3.08
	5	17-19	Both & Loc & YR Loc(FL) & (OR) YR(11) & (12) Ind. -FL_12, -OR_11, -OR_12	14.27 & 12.86 & 12.60 3.99 & 13.10 4.83 & 8.48 5.89 & 6.25 & 8.96	12.18 & 11.05 & 10.83 10.79 & 28.35 8.38 & 14.35 28.78 & 27.11 & 36.77
	5	46	Both & Loc & YR	5.21 & 4.23 & 5.03	4.63 & 3.78 & 4.48
	5	58	Both & Loc & YR YR(12)	5.37 & 4.45 & 5.16 3.50	4.77 & 3.96 & 4.59 6.19
	5	60	Both & Loc & YR	4.57 & 3.72 & 4.39	4.07 & 3.33 & 3.92
	5	114	Both & Loc & YR YR(11) & (12)	6.82 & 5.56 & 6.38 3.90 & 3.06	6.02 & 4.94 & 5.64 6.83 & 5.44
	5	117	Both & Loc & YR Loc(OR)	7.02 & 5.86 & 6.74 3.56	6.19 & 5.20 & 5.95 8.67
	5	122-124	Both & Loc & YR Loc(OR) YR(11) & (12) Ind. -FL_12, -OR_11, -OR_12	11.24 & 9.34 & 10.48 8.30 4.50 & 6.20 4.34 & 7.44 & 4.36	9.72 & 8.15 & 9.10 19.04 7.84 & 10.71 22.09 & 31.36 & 19.97
	6	55	Both & Loc & YR Loc(OR) YR(12)	6.23 & 6.07 & 5.39 4.31 3.91	5.52 & 5.37 & 4.78 10.40 6.89
	10	50	Both & Loc & YR	3.97 & 3.23 & 3.83	3.55 & 2.92 & 3.42
	11	34	Both & Loc & YR	3.84 & 3.25 & 3.58	3.43 & 2.91 & 3.21
	12	49	Both & Loc & YR Loc(OR) YR(11)	5.99 & 5.17 & 5.90 3.94 5.50	5.31 & 4.59 & 5.23 9.53 9.49

Table 2.6 – (continued).

	12	78	Both & Loc & YR Loc(OR) YR(11) & (12) Ind. -FL_12	7.59 & 6.31 & 7.27 3.40 3.07 & 4.75 3.83	6.67 & 5.58 & 6.40 9.67 5.41 & 8.32 19.79
	12	95-96	Both & Loc & YR Loc(OR) YR(12)	5.71 & 4.77 & 5.56 4.36 4.87	5.06 & 4.25 & 4.94 10.51 8.52
	12	161	Both & Loc & YR	4.55 & 3.73 & 4.59	4.06 & 3.34 & 4.10

LG – Linkage group

LOD – Logarithm of Odds value with significance threshold at 3

Both – Cofactor analysis using “both location and year” as a cofactor

Loc – Cofactor analysis using just location as a cofactor

YR – Cofactor analysis using just year as a cofactor

Loc(FL, GA, or OR) – Location-specific analysis

YR(11 or 12) – Year-specific analysis

Ind. – Analysis of individual phenotype from the specified location (FL, GA, or OR) and year (_11 or _12)

Table 2.7 – Overlapping QTL regions containing at least three significant QTLs from different CIM analyses for the dormancy break and flowering traits.

	LG	Position (cM)	CIM Analyses of the Significant QTLs	LOD	% Variation Explained
Days until Early Green Tip	2	30-32	Both & Loc & YR Loc(GA) YR(11) Ind. -FL_12	4.51 & 5.28 & 9.49 7.38 6.85 7.83	4.96 & 5.78 & 10.16 26.57 11.77 64.29
	2	38	Both & Loc & YR	4.97 & 6.35 & 11.16	5.45 & 6.92 & 11.84
Days until Floral Bud Break	3	84	Both & Loc Ind. -OR_11	3.04 & 3.05 3.33	2.98 & 2.99 16.50
	10	75	Both & Loc & YR	3.74 & 3.73 & 3.26	3.65 & 3.64 & 3.19

LG – Linkage group

LOD – Logarithm of Odds value with significance threshold at 3

Both – Cofactor analysis using “both location and year” as a cofactor

Loc – Cofactor analysis using just location as a cofactor

YR – Cofactor analysis using just year as a cofactor

Loc(FL, GA, or OR) – Location-specific analysis

YR(11 or 12) – Year-specific analysis

Ind. – Analysis of individual phenotype from the specified location (FL, GA, or OR) and year (_11 or _12)

Table 2.8 – Overlapping QTL regions containing at least three significant QTLs from different CIM analyses for the fruit quality traits.

	LG	Position (cM)	CIM Analyses of the Significant QTLs	LOD	% Variation Explained
Days between Full Bloom and Blue Fruit	1	87	Both & Loc & YR	4.13 & 3.68 & 3.28	4.41 & 3.94 & 3.51
Fruit Color Rating	1	110-114	Both & Loc & YR YR(11)	3.19 & 3.17 & 3.51 3.08	3.30 & 3.28 & 3.62 6.13
	2	57	Both & Loc & YR	4.17 & 3.16 & 3.82	4.29 & 4.28 & 3.93
Fruit Firmness Rating	1	55	Both & Loc Loc(OR)	3.21 & 3.21 3.16	3.33 & 3.33 9.48

Table 2.8 – (continued).

Berry Weight	1	13-15	Both & Loc & YR Loc(FL) & (GA) YR(11)	7.19 & 6.81 & 7.19 4.41 & 5.73 4.11	10.54 & 10.03 & 10.55 13.33 & 15.65 11.63	
	1	18-19	Both & Loc & YR Loc(FL) & (GA) YR(11)	7.32 & 6.87 & 7.34 4.18 & 5.06 4.46	10.72 & 10.11 & 10.76 12.69 & 13.95 12.56	
	1	33	Both & Loc & YR Loc(GA) YR(11) Ind. -GA_11, -GA_12	6.81 & 6.41 & 6.81 6.01 4.29 3.87 & 3.18	10.02 & 9.46 & 10.02 16.34 12.12 20.19 & 16.94	
	1	52	Both & Loc & YR Loc(GA) YR(11)	6.04 & 5.87 & 6.03 4.99 3.44	8.94 & 8.70 & 8.93 13.78 9.84	
	1	61-63	Both & Loc & YR Loc(FL) & (GA) YR(11) & (12)	8.11 & 8.55 & 8.10 4.98 & 4.42 3.36 & 3.75	11.81 & 12.42 & 11.80 14.91 & 12.30 9.61 & 11.31	
	1	87	Both & Loc & YR	4.95 & 4.49 & 4.90	7.39 & 6.72 & 7.32	
	1	92	Both & Loc & YR	3.68 & 3.37 & 3.66	5.55 & 5.10 & 5.52	
	2	58-59	Both & YR Loc(FL) YR(11) Ind. -FL_11	3.22 & 3.19 3.65 3.44 3.11	4.88 & 4.83 11.15 9.84 17.39	
	7	32	Both & Loc & YR	3.37 & 3.10 & 3.39	5.09 & 4.69 & 5.12	
	11	31-34	Both & Loc & YR Loc(GA)	3.84 & 3.64 & 3.82 3.11	5.78 & 5.49 & 5.74 8.81	
	11	48-49	Both & Loc & YR	4.18 & 3.77 & 4.19	6.28 & 5.68 & 6.28	
	12	154	Both & Loc & YR Loc(GA)	3.53 & 3.13 & 3.52 3.65	5.32 & 4.74 & 5.31 10.28	
	Berry Firmness	1	41	Both & Loc & YR	3.54 & 3.52 & 3.65	5.29 & 5.26 & 5.45
		1	47	Both & Loc & YR YR(12)	3.69 & 3.69 & 3.72 3.50	5.50 & 5.51 & 5.56 10.45

Table 2.8 – (continued).

	1	55	Both & Loc & YR YR(12)	4.09 & 4.09 & 4.03 3.06	6.08 & 6.09 & 6.00 9.19
	3	50-52	Both & Loc & YR Ind. -FL_11	3.37 & 3.31 & 3.31 3.03	5.04 & 4.95 & 4.96 17.00
	3	106	Both & Loc & YR Loc(GA)	3.91 & 3.93 & 3.96 3.90	5.82 & 5.85 & 5.89 10.80
	4	130-134	Both & Loc & YR Loc(GA) YR(11)	4.15 & 4.15 & 4.20 3.33 4.02	6.18 & 6.17 & 6.24 9.31 9.80
	7	57-59	Both & Loc & YR	3.31 & 3.27 & 3.27	4.95 & 4.90 & 4.90
	12	104	Both & Loc & YR	3.07 & 3.08 & 3.05	4.60 & 4.62 & 4.58
% Juice	3	55	Both & Loc & YR	3.70 & 3.54 & 3.56	5.67 & 5.43 & 5.45
	5	60	Both & Loc & YR	3.44 & 3.25 & 3.34	5.28 & 4.99 & 5.13
	8	40	Both & Loc & YR	5.22 & 5.02 & 4.80	7.91 & 7.61 & 7.29
	10	86	Both & Loc & YR Loc(GA)	4.38 & 4.18 & 4.14 5.96	6.68 & 6.38 & 6.31 16.53
pH	4	64	Both & Loc Loc(FL) YR(12)	3.20 & 3.04 3.47 3.21	4.87 & 4.63 10.71 9.74
TA	4	38	Both & Loc & YR Loc(FL) Ind. -FL_11	3.96 & 3.94 & 4.49 3.22 3.16	6.05 & 6.03 & 6.83 10.06 18.53
	4	64	Both & Loc & YR Loc(FL)	4.44 & 4.42 & 3.80 3.21	6.77 & 6.73 & 5.81 10.01
	5	60	Both & Loc & YR	3.98 & 3.96 & 3.70	6.08 & 6.06 & 5.66
	5	79	Both & Loc & YR	3.76 & 3.75 & 3.35	5.75 & 5.74 & 5.15
	5	94	Both & Loc & YR Loc(FL)	5.01 & 5.02 & 4.15 5.13	7.59 & 7.61 & 6.34 15.53
	8	82	Both & Loc & YR	3.21 & 3.19 & 3.01	4.94 & 4.90 & 4.64
	8	89	Both & Loc & YR	3.77 & 3.77 & 3.30	5.78 & 5.77 & 5.08
	8	95	Both & Loc & YR	3.41 & 3.39 & 3.00	5.24 & 5.21 & 4.63
	9	76	Both & Loc & YR	3.74 & 3.73 & 3.95	5.72 & 5.71 & 4.69

Table 2.8 – (continued).

SS	3	86	Both & Loc & YR	4.72 & 4.71 & 4.54	7.17 & 7.16 & 6.90
	8	40-46	Both & Loc & YR Loc(GA)	3.63 & 3.59 & 3.58 3.01	5.56 & 5.50 & 5.48 8.72
	10	163	Both & Loc & YR	4.01 & 3.99 & 3.89	6.13 & 6.10 & 5.95
SS:TA Ratio	2	38	Both & Loc & YR	3.96 & 4.26 & 3.90	6.16 & 6.61 & 6.06
	2	83	Both & Loc & YR	3.70 & 3.87 & 4.08	5.77 & 6.02 & 6.34
	4	20-22	Both & Loc & YR YR(11)	6.24 & 6.59 & 5.52 4.12	9.53 & 10.02 & 8.48 11.97
	8	82-83	Both & Loc Loc(FL) Ind. -FL_11	3.17 & 3.04 & 3.13 4.40 3.86	4.97 & 4.76 & 4.90 13.85 21.90
	8	89	Both & Loc & YR Loc(FL)	4.25 & 4.12 & 3.78 3.63	6.58 & 6.40 & 5.89 11.57
	11	103	Both & Loc & YR	3.60 & 3.57 & 3.07	5.61 & 5.56 & 4.80
	12	68	Both & Loc Loc(GA) YR(11)	3.14 & 3.14 3.89 3.01	4.92 & 4.92 11.19 8.87
Total Anthocyanin Content	6	111-114	Both & Loc & YR	3.33 & 3.29 & 3.14	5.18 & 5.12 & 4.89
	8	80-84	Both & Loc & YR YR(11)	3.80 & 3.75 & 3.57 3.41	5.90 & 5.82 & 5.55 9.81
	12	34-39	Both & Loc & YR	4.76 & 4.21 & 4.73	7.33 & 6.51 & 7.29

LG – Linkage group

LOD – Logarithm of Odds value with significance threshold at 3

Both – Cofactor analysis using “both location and year” as a cofactor

Loc – Cofactor analysis using just location as a cofactor

YR – Cofactor analysis using just year as a cofactor

Loc(FL, GA, or OR) – Location-specific analysis

YR(11 or 12) – Year-specific analysis

Ind. – Analysis of individual phenotype from the specified location (FL, GA, or OR) and year (_11 or _12)

2.5. Discussion

The Draper x Jewel (DxJ) mapping population represents a cross between two commercial blueberry cultivars grown in the US: the northern highbush (NHB) and the southern high bush (SHB) (Draper & Hancock, 2003; James F. Hancock et al., 2018). These parents exhibit different chill requirement hours and dormancy break timing, as Draper needs over 600 hours of chilling, whereas Jewel needs much less than 600 hours of chilling (Draper & Hancock, 2003; James F. Hancock et al., 2018). The progeny of DxJ cross exhibit a variety of distributions for agronomic growth, dormancy break, and fruit quality traits like vigor, flowering, and fruit ripening (James F. Hancock et al., 2018). What constitutes fruit quality has traditionally been dictated by the needs of industry, such as post-harvest processing hardiness (Barrett et al., 2010; Jenks & Bebeli, 2011; Kyriacou & Rouphael, 2018; P. Li, Lee, & Hsu, 2011; Moggia et al., 2017). Today, consumer opinion insists upon other fruit quality traits like taste, texture, and nutrition (Gilbert et al., 2015, 2014; James F. Hancock et al., 2018; Klee, 2010). The DxJ progeny show a variety of distributions for multiple fruit quality traits that address the concerns of both post-harvest processing hardiness, as well as consumer-driven fruit quality (Barrett et al., 2010; Gilbert et al., 2014; Grunert, 2005; James F. Hancock et al., 2018; Kader, 2008; Kyriacou & Rouphael, 2018; Pagliarini et al., 2013).

The main purpose of this part of the research is to identify important quantitative trait loci (QTLs) associated with agronomic and fruit quality traits. The phenotypic data consists of the 30 agronomic and fruit quality traits, and was collected by Dr. Hancock's research team at Berry Blue Industries and Michigan State University, Dr. Finn's research lab at University of Oregon and USDA-ARI, and Dr. Olmstead's research lab at University of Florida (Blaker et al., 2014; Finn, Hancock, T. Mackey, et al., 2003; Gilbert et al., 2015, 2014, 2013; James F. Hancock et al., 2018; McCallum et al., 2016; Lisa J Rowland et al., 2012). The collected phenotype data from two years at two or three locations was consolidated into specific traits (James F. Hancock et al., 2018). A detailed description and analysis of each trait's phenotypic data was published by Hancock et al. (James F. Hancock et al., 2018). In order to conduct association mapping on the 30 traits, the DxJ population needs a DxJ genetic map.

The DxJ genetic map was developed for this specific mapping population by merging the previously published Draper and Jewel genetic maps made by McCallum et al. (James F. Hancock et al., 2018; McCallum et al., 2016). This DxJ genetic merged map is the first tetraploid map for a blueberry mapping population (Figure 2.1). One caveat of this genetic map, however, is the genetic markers were filtered to only include markers acting as diploids since no allele dosage information for the markers is available. This filtering reduces the number of markers available for mapping, and therefore, reduces mapping resolution (Al-Khayri et al., 2015; Rasheed et al., 2017; Sehgal et al., 2016; B. D. Singh & Singh, 2015). Obtaining allele dosage information for the original markers would refine the recombination frequencies and improve the marker density of the tetraploid DxJ genetic map (Al-Khayri et al., 2015; Rasheed et al., 2017; Sehgal et al., 2016; B. D. Singh & Singh, 2015).

Improving the marker density of the DxJ genetic map will improve bi-parental association mapping (BiPAM) because denser markers will increase the mapping resolution and decrease the linkage distance (Bernardo, 2008; Bradshaw, Hackett, Pande, Waugh, & Bryan, 2008; Collard et al., 2005; Hackett et al., 2001; Heslot, Yang, Sorrells, & Jannink, 2012; M. S. Kang, 2002; Mayer, 2005; Rafalski, 2010). Increasing the population size of genotyped DxJ progeny will also improve BiPAM through improving the predicted recombination frequencies, which increases mapping resolution and statistical power (Bernardo, 2008; Bradshaw et al., 2008; Collard et al., 2005; Korte & Farlow, 2013; Rafalski, 2010; Lisa J Rowland et al., 2014). The increases in marker density and population size will also allow for permutations to be conducted during the BiPAM so that specific LOD significance thresholds for the specific phenotypes can be calculated. Permutations are often utilized to determine phenotype-specific LOD thresholds to account for the number of independent tests conducted and reduce false positives (Bernardo, 2008; Bradshaw et al., 2008; Collard et al., 2005; Hackett et al., 2001; Heslot et al., 2012; M. S. Kang, 2002; Mayer, 2005; Rafalski, 2010). Although the above limitations exist, the results of the BiPAM research will provide vital foundational knowledge of potential QTL regions that can be further investigated to refine the QTL regions and to characterize candidate genes with the genomic regions.

The overall purpose of BiPAM is to statistically associate variation in a trait to the genome through the variation in a genetic marker. As previously discussed, BiPAM is utilized to investigate agronomic traits because most agronomic traits are regulated by multiple genes and pathways, and BiPAM is able to identify multiple significant QTLs that contribute to the trait's variation (Bernardo, 2008; Collard et al., 2005; M. S. Kang, 2002; Xu, 2010). The result of conducting BiPAM is a quantitative trait loci (QTL), which is a genetic marker that is linked to a genetic sequence. The QTL result has a significance threshold when the LOD value is above 3 (Bernardo, 2008; Collard et al., 2005; M. S. Kang, 2002; Xu, 2010). Each significant QTL has a corresponding significant QTL region that is dictated by the LOD value of the neighboring markers. The boundaries of a significant QTL region are designated by the centimorgan (cM) position of the closest neighboring markers with an LOD value below 3. BiPAM was conducted on all the DxJ agronomic and fruit quality trait data using IM, CIM, and MIM analyses. BiPAM using CIM identifies multiple QTLs across the genome while also accounting for the effect of QTLs on other significant QTLs (Bernardo, 2008; Feenstra, 2006; Hackett et al., 2001; Kao, 2000; H. Li et al., 2006; Mayer, 2005).

As described previously in the results, the CIM method was conducted on the 30 traits for each individual phenotype, for location-specific phenotypes, and for year-specific phenotypes. The location-specific CIM method reveals if environmental variation from specific locations contribute to an association of trait variation with genetic variation (Table 2.5). For example, locations with longer days and summers may contribute to variation in vegetative growth traits as more photosynthesis can occur, which would identify some QTLs that are different from other locations with shorter photosynthetic periods (Bernardo, 2008; Hospital, 2009; M. S. Kang, 2002; Meyer & Purugganan, 2013; Winter & Kahl, 1995). Identifying location-specific QTLs may be beneficial for breeding strategies focused on optimizing blueberry growth or harvest in a specific location. The year-specific CIM method reveals if environmental variation from the 2011 or 2012 years contribute to an association of trait variation with genetic variation (Table 2.5). For example, one year with more precipitation will increase the soil water content and may contribute to variation in overall growth traits, which would identify some QTLs that are different from other years with less precipitation

(Bernardo, 2008; Buchanan et al., 2012; Hospital, 2009; M. S. Kang, 2002; Meyer & Purugganan, 2013; Winter & Kahl, 1995). Identifying year-specific QTLs may be beneficial for breeding strategies focused on optimizing blueberry growth or harvest for a specific set of environmental conditions exhibited during that specific year.

The CIM method was also conducted on the 30 traits using the location cofactor, the year cofactor, and both location and year cofactors (Table 2.5). Utilizing location as a cofactor allows for the CIM mapping to account for location-specific variation so that the significant QTL is primarily associated with the variation in the trait, not location. Similarly, the CIM mapping with year as a cofactor accounts for year-specific variation so the significant QTL is primarily associated with trait variation, not year-specific environments. When both location and year cofactors are utilized in the CIM mapping, the significant QTL is only associated with variation of the trait.

Furthermore, all the significant QTLs for each trait were investigated for overlapping QTL regions. Overlapping QTL regions were determined as regions with multiple significant QTLs from at least three different mapping analyses for the same trait (Tables 2.6, 2.7, 2.8). Identifying the same QTL region with different mapping analyses supports the association between the trait's variation and the genetic variation. To further discuss the results and implications of the overlapping QTL regions for each trait, the 30 traits were categorized into three groups: growth, dormancy break and flowering, and fruit quality.

2.5.1. Agronomic Growth Regulation

Investigating overall plant growth involves elucidating the complex signaling and coordination of many different pathways that promote cell proliferation and differentiation (Patrick Achard et al., 2009; Buchanan et al., 2012; Del Pozo et al., 2005; Durbak & Tax, 2011; Gutierrez, 2009; Mert, Barut, & Ipek, 2013; Takatsuka & Umeda, 2014). While cell proliferation induces cell division and expansion pathways like cell wall matrix synthesis and modifications, cell differentiation induces specific tissue-identity pathways so that an appropriate tissue can be developed (Buchanan et al., 2012; Del Pozo et al., 2005; Durbak & Tax, 2011; Gutierrez, 2009; Majda & Robert, 2018; Mert et al., 2013; Perrot-Rechenmann, 2010; Takatsuka & Umeda, 2014). This coordination is especially important in meristem centers as they are constantly transitioning cells from

division to expansion to differentiation (Bar & Ori, 2014; Considine & Considine, 2016; Costes et al., 2014; Koutinas et al., 2010; Lloret et al., 2018; Tsai & Gazzarrini, 2014; van der Schoot & Rinne, 2011).

As discussed previously, plant hormones are the main signal transducers that mediate the cross-talk between the multitude of pathways (Patrick Achard & Davie, 2015; Del Pozo et al., 2005; Lau & Deng, 2010; Majda & Robert, 2018; Reddy et al., 2013; A. P. Singh & Savaldi-Goldstein, 2015; Stepanova & Alonso, 2009; Vergara et al., 2017; Xing et al., 2015; Yang & Jiao, 2016). Cytokinins primarily regulate the cell cycle, as well as work with auxin to signal stem and root differentiation (Buchanan et al., 2012; Del Pozo et al., 2005; Gray & Brady, 2016; Lau & Deng, 2010; Takatsuka & Umeda, 2014; Yang & Jiao, 2016). Auxin also regulates growth through inducing cell wall matrix loosening factors, which allows for cell elongation and expansion (Leyser, 2017; Majda & Robert, 2018; Perrot-Rechenmann, 2010; Posé et al., 2011; Swarup & Péret, 2012; Takatsuka & Umeda, 2014; Yang & Jiao, 2016). The cross-talk between auxin and ethylene is important for regulating apical dominance of the shoot apical meristem (P. Achard et al., 2007; Development, 2010; Dubois et al., 2018; Guo et al., 2018; Leyser, 2017; Ozga & Reinecke, 2003; Stepanova & Alonso, 2009; van der Schoot & Rinne, 2011; Yang & Jiao, 2016). Auxin and GA signaling also exhibits some cross-talk during the alleviation of ABA growth inhibition during dormancy (Beauvieux et al., 2018; Kovaleski et al., 2015; J. Li et al., 2018; Reddy et al., 2013; van der Schoot & Rinne, 2011; Vergara et al., 2017; Z. Zhang et al., 2018; Zheng et al., 2015; Zhuang et al., 2015). The significant QTLs identified through association mapping of different aspects of growth may reveal important stages of regulation where multiple pathways converge to impact overall plant growth.

Another important aspect for regulating growth is the appropriate allocation and signaling of resources, such as carbon and energy (Baena-González, Rolland, Thevelein, & Sheen, 2007; Bennett, Roberts, & Wagstaff, 2012; O. Sadras & F. Denison, 2009; Ruan, 2014; Wingler, 2017). To support the metabolic and structural changes during growth, resources must be allocated and transported to the active growth areas (Bennett et al., 2012; Gambín & Borrás, 2010; Granot et al., 2013; Gray & Brady, 2016; Y. Kang, Khan, & Ma, 2009; O. Sadras & F. Denison, 2009; Reddy et al.,

2013). Concurrently, the availability of specific resources must also be signaled so that major processes are not prematurely ended due to insufficient resources (Baena-González et al., 2007; Bennett et al., 2012; Fischer & Edmeades, 2010; Granot et al., 2013; O. Sadras & F. Denison, 2009; Pagter et al., 2015; Rolland, Moore, & Sheen, 2002; Ruan, 2014; Wingler, 2017). Efficient resource allocation is especially important for perennial crops like blueberries because resources must be promptly reallocated towards replenishing resource storage and preparing for cycling into dormancy, even though resources were depleted by the development and ripening of fruit (Beauvieux et al., 2018; Bennett et al., 2012; Fischer & Edmeades, 2010; Granot et al., 2013; Pagter et al., 2015; Reddy et al., 2013; Rolland et al., 2002; Wingler, 2017). Consequently, some agronomic growth traits are measured after fruit ripening and harvest to gain insight into resource allocation efficiency (Bennett et al., 2012; Granot et al., 2013; Jenks & Bebeli, 2011; Y. Kang et al., 2009; O. Sadras & F. Denison, 2009; Rolin, Teyssier, Hong, & Gallusci, 2015; Ruan, 2014; Weiner & Freckleton, 2010; Wingler, 2017). Identifying significant QTLs from association mapping of different agronomic growth traits will reveal important regulatory regions of blueberry growth at different developmental stages.

2.5.1.1. Growth Traits QTLs and Overlapping QTL Regions

The eight growth traits represent multiple processes of overall plant growth and includes bush height, bush width, leafing strength, % broken vegetative buds, leaf:fruit ratio, yield estimate rating, floral buds per cane, and vigor rating (James F. Hancock et al., 2018). The association mapping of the growth trait of % broken vegetative buds did not identify any significant QTLs (Table 2.4 and 2.5). Turning to the remaining growth traits, the association mapping results for the growth trait of bush height revealed two overlapping QTL regions that contain significant QTLs for: the “both location and year” cofactor analysis, the FL-specific location, and the individual phenotype for -FL-2011 (Table 2.6). For the two QTL regions, the FL-specific location and individual phenotype -FL-2011 are more significant than the “both location and year” cofactors analysis QTL, due to the higher LOD value for the FL-specific and FL-2011 QTLs (Table 2.6). This indicates that those QTL regions are strongly influenced by the FL location and year, but the significant QTL for “both location and year” cofactors analysis suggests these

two QTL regions can still impact bush height for other locations and years. The genes within the two genetic regions corresponding to the overlapping QTL regions are most likely involved in pathways like auxin signaling with other hormones for apical dominance and phototropism (Patrick Achard & Davie, 2015; Patrick Achard et al., 2009; Rabot et al., 2012; Reddy et al., 2013; P. L. H. Rinne et al., 2011; van der Schoot & Rinne, 2011; Vergara et al., 2017; Wingler, 2017; Yang & Jiao, 2016). The strong influence of the FL location on these QTL regions suggests that further gene research should be focused on auxin signaling with other hormones that regulate apical and phototropic growth since the FL location is the blueberry growth extreme for harsh light and long seasons (Draper & Hancock, 2003; Finn, Hancock, Mackey, & Serce, 2003; James F. Hancock et al., 2018; Trehane, 2004). These QTL regions can also be utilized in future breeding strategies to improve bush height and growth in warmer locations.

The results of association mapping of the growth trait of bush width identified three overlapping QTL regions (Table 2.6). First, the overlapping QTL region on linkage group five between 124-125cM contains significant QTLs for: the “both location and year” cofactors analysis, OR-specific location, and individual phenotype for -FL-2012. Both the OR-specific and individual phenotype -FL-2012 are more significant than the “both location and year” cofactors analysis QTL. This indicates that this QTL region is strongly influenced by the specific locations and years, but the significant QTL for “both location and year” cofactors analysis suggests this QTL region can still be a QTL region that impacts bush width for other locations and years. Second, the overlapping QTL region on linkage group five between 15-17cM contains significant QTLs for: the “both location and year” cofactor analysis, location cofactor analysis, FL-specific, OR-specific, and multiple individual phenotypes. Similar to the previously mentioned QTL region, the location specific and individual phenotypes are more significant than the cofactor analyses QTLs. This indicates that this QTL region is strongly influenced by specific locations and years for bush width, but the two cofactor QTLs suggest this region can still impact bush width for other locations and years. Third, the overlapping QTL region on linkage group five at 117cM contains significant QTLs for all three cofactor analyses, which strongly indicates that this QTL region is an important region for bush width regulation, regardless of location or year. The first two above mentioned overlapping

QTL regions for bush width that are strongly influenced by location may contain genes involved in phototropic growth or the auxin-ethylene ratio in axillary meristems as OR and FL are very different climates (Considine & Considine, 2016; Hao et al., 2017; R. Mohamed et al., 2010; Reddy et al., 2013; Signorelli et al., 2018; Yang & Jiao, 2016). Since OR and FL represent the environmental range of efficient commercial blueberry growth, investigating the genetic regions for the location specific QTLs would provide insight into QTLs that would improve blueberry bush width and growth in diverse locations. Further research into the genetic regions for the QTL not specific for locations would provide insight into the regulation of bush width growth irrespective of environmental conditions.

The growth trait of leafing strength represents the leaf development and expansion (Buchanan et al., 2012; James F. Hancock et al., 2018). The association mapping results of the leafing strength trait revealed seven overlapping QTL regions with four of the QTL regions containing significant QTLs for all three of the cofactor analyses (Table 2.6). The overlapping QTL region on linkage group 12 at 78cM contains significant QTLs for: the “both location and year” cofactors analysis and the 2012 year. The 2012 year QTL has a greater LOD significance than the “both location and year” cofactors analysis QTL, which indicates the 2012 year has a strong influence on the QTL region, but the significant both location and year cofactors analysis QTL suggests the QTL region may still be important for leafing strength regulation for other locations and years. The overlapping QTL region on linkage group three at 130cM contains significant QTLs for: the “both location and year” cofactor analysis, the OR-specific location, the 2012 specific year, and the individual phenotype -OR-2012. The OR-specific and 2012 year QTLs are more significant than the “both location and year” cofactors analysis QTL, which indicates this QTL region is strongly influenced by specific locations and years for leafing strength. The overlapping QTL regions on linkage group five between 15-19cM and between 124-125cM contain significant QTLs for: all three cofactor analyses, OR-specific location, and the 2012 year. For these two QTL regions, the OR-specific QTL has the strongest LOD significance value, which indicates these QTL regions are strongly influenced by the OR location for leafing strength. But the three significant cofactor QTLs also in these QTL regions suggest that

these QTL regions may still be important for regulating leafing strength regardless of location or year. Within the genetic regions impacted by environmental variation, the genes are probably involved in regulating chlorophyll and stomata density to reduce UV and water stress (Patrick Achard et al., 2009; Bar & Ori, 2014; Bennett et al., 2012; S. J. Kim, Yu, Kim, & Lee, 2011; Linkosalo & Lechowicz, 2006; C. Liu, Callow, Rowland, Hancock, & Song, 2010; P. Liu et al., 2014; Mathan, Bhattacharya, & Ranjan, 2016; Vishwakarma et al., 2017).

The remaining overlapping QTL regions for the growth traits of leafing strength contain a significant QTL for the “both location and year” cofactor analysis that is more significant than the other analyses QTLs (Table 2.6). The overlapping QTL region on linkage group six between 38-41cM contains significant QTLs for the “both location and year” cofactor analysis, the OR-specific location, and the 2011 year. The OR-specific and 2011 year QTLs are less significant than the “both location and year” cofactor QTL, which suggests this QTL region may be partially influenced by the location and year, but is more important as a QTL region for leafing strength regulation regardless of location and year. The overlapping QTL region on linkage group 10 at 50cM contained significant QTLs for all three cofactor analyses and the 2012 year. Also, the overlapping QTL region on linkage group 10 between 59-61cM contains significant QTLs for all three cofactor analyses. For the two overlapping QTL regions on linkage group 10, the “both location and year” cofactors QTLs are the most significant QTLs. The genes within the genetic regions regulating leafing strength regardless of environmental variation are most likely involved in the overall development and expansion of leaf architecture (Bar & Ori, 2014; Buchanan et al., 2012; Grant, Dami, Ji, Scurlock, & Streeter, 2009). For the leafing strength trait, the influence of specific locations or years depends on the specific overlapping QTL region. This indicates that different overlapping regions and their corresponding genetic regions contain specific genes that either regulate leafing strength irrespective of the environmental variation, or differentially regulate leafing strength due to the environmental variation (Patrick Achard et al., 2009; Bar & Ori, 2014; Bennett et al., 2012; Linkosalo & Lechowicz, 2006; C. Liu et al., 2010; P. Liu et al., 2014; Mathan et al., 2016). Future breeding strategies could utilize this information

and specific QTL regions to improve leafing strength across different or specifically optimized for locations or years.

The growth trait of leaf to fruit ratio represents the differentiation process between vegetative and floral buds (James F. Hancock et al., 2018; Kovaleski et al., 2015). The association mapping of leaf to fruit ratio identified only one overlapping QTL region on linkage group 12 at 78cM that contains significant QTLs for all three cofactor analyses (Table 2.6). The genes within this genetic region are most likely involved in regulating the differentiation of a vegetative meristem to a floral meristem (D. P. Horvath et al., 2003; Kovaleski et al., 2015; Mert et al., 2013; R. Mohamed et al., 2010; van der Schoot & Rinne, 2011). There is limited knowledge for perennial plants about the signals that induce the meristem transition from vegetative to floral (Buchanan et al., 2012; D. P. Horvath et al., 2003; Kovaleski et al., 2015; Mert et al., 2013; R. Mohamed et al., 2010; van der Schoot & Rinne, 2011). Some research suggests it is a combination of hormone signaling and resource availability that promotes the floral differentiation (Ito et al., 2015; Kovaleski et al., 2015; Mert et al., 2013; R. Mohamed et al., 2010; Reddy et al., 2013; van der Schoot & Rinne, 2011; Xing et al., 2015; Yang & Jiao, 2016). A main component during floral differentiation is the induction of floral meristem identity genes (P. Achard et al., 2007; Amasino & Michaels, 2010; Conti, 2017; R. Mohamed et al., 2010; P. L. H. Rinne et al., 2011; Wilkie et al., 2008). If the floral identity meristem genes are not induced, the bud meristems remain vegetative meristems (P. Achard et al., 2007; Conti, 2017; D. Horvath, 2009; R. Mohamed et al., 2010; Wilkie et al., 2008; Yang & Jiao, 2016). Future gene research will start to elucidate the regulation of bud differentiation, which could be utilized along with the QTL region in future breeding strategies to increase the floral buds and subsequent fruit production.

The growth trait of yield estimate rating represents the blueberry crop potential through the overall density of floral buds per bush right before dormancy break (James F. Hancock et al., 2018). The association mapping results of the yield estimate rating revealed six overlapping QTL regions that all contain significant QTLs for all three cofactor analyses (Table 2.6). The overlapping QTL regions on linkage group five between 13-17cM and between 124-125cM contain significant QTLs for the 2011 year

along with the three cofactor analyses QTLs. Since the 2011 year QTL is more significant than the cofactor analyses QTLs, this indicates the 2011 year strongly influences these QTL regions, but the three significant cofactor analyses QTLs suggest these QTL regions can still impact yield for other locations and years. In other words, the greater significance of the 2011 year suggests that the 2011 year environmental variation more strongly influenced floral bud development across differences in location. The overlapping QTL region on linkage group five at 60cM also contains a significant QTL for the GA-specific location, which is less significant than the three cofactor analyses QTLs. This suggests that the QTL region is slightly influenced by the GA location, but the QTL region is more important as a QTL region for yield estimation regardless of location or year. The remaining three overlapping QTL regions contain all three cofactor analyses QTLs with the both location and year cofactors analysis QTL showing the highest significance. This indicates that the genes within these corresponding genetic regions regulate the yield estimate rating regardless of environmental variation from location or year. Since the yield estimation trait is a better representation of growth and development of floral buds rather than fruit development and ripening, the genetic regions for these overlapping QTLs probably contain genes involved in floral bud development and differentiation (Costes et al., 2014; D. Horvath, 2009; Mert et al., 2013; van der Schoot & Rinne, 2011). Future breeding strategies could utilize these QTL regions to optimize floral bud differentiation and density for specific environmental variation or for diverse environmental conditions while further gene research will elucidate the signaling and regulation of floral bud differentiation.

The growth trait of floral buds per cane is the quantification of floral buds on the three largest canes, rather than the subjective rating of floral buds for the yield estimate trait (James F. Hancock et al., 2018). Since the floral buds per cane trait is a continuous variable that can measure small variations, the association mapping often identifies a larger number of significant QTLs (Bernardo, 2008; Hospital, 2009; M. S. Kang, 2002; Winter & Kahl, 1995; Xu, 2010). The association mapping results of the floral buds per cane trait identified the eight overlapping QTL regions that all contained significant QTLs for all three of the cofactor analyses (Table 2.6). The overlapping QTL regions on linkage group two at 11cM and linkage fragment 6.5 between 0-10cM also contain

significant QTLs for the 2011 year. The overlapping QTL region on linkage group four between 18-24cM contains significant QTLs for: the 2011 year as well as the FL-specific location. The overlapping QTL region on linkage group four between 130-134cM contains significant QTLs for: the FL-specific location, the GA- specific location, and the 2012 year. The year cofactor QTL in the four above-mentioned QTL regions is more significant than the other QTLs, which indicates that these QTL regions are highly impacted by the environmental variation from the years. The genes within the genetic regions for these corresponding QTL regions are most likely involved in pathways regulating floral bud differentiation like energy and storage availability signaling because floral buds only differentiate when ample resources are available to support the transition (P. Achard et al., 2007; Conti, 2017; D. Horvath, 2009; Ionescu et al., 2016; Ito et al., 2015; Lloret et al., 2018; Molinero-Rosales et al., 2004; O'Hara et al., 2013; Vasconcelos et al., 2009).

The other four overlapping regions for the floral buds per cane trait contain significant QTLs for all three of the cofactor analyses and for specific locations (Table 2.6). The overlapping QTL region on linkage group 11 at 25cM contains a significant QTL for the GA-specific location, whereas the overlapping regions on linkage groups nine, 11 and 12 at 93cM, 80cM, and 42cM, respectively, contain significant QTLs for the FL-specific location. The LOD significance values for the GA-specific and FL-specific QTLs in those regions are less than the three cofactor analyses QTLs, which indicates the QTL regions may be partially influenced by specific locations. But the QTL regions are more important as QTL regions for floral buds per cane regulation regardless of location or year. The genes within these corresponding genetic regions are primarily not influenced by location environmental variation and may be involved in regulating overall bud formation or floral meristem identity genes (Arora et al., 2003; Beauvieux et al., 2018; Cooke et al., 2012; Díaz-Riquelme et al., 2012; Koutinas et al., 2010; Lloret et al., 2018; Mert et al., 2013; Xing et al., 2015; Zheng et al., 2015). Overall, future breeding strategies could utilize these eight QTL regions across different locations to improve floral bud differentiation and density while further gene research will provide more information on the signaling and regulation of floral bud differentiation.

The growth trait of vigor rating represents the overall robustness of the blueberry bush after fruiting, which is especially important for efficiently preparing for and transitioning to dormancy (James F. Hancock et al., 2018). The association mapping results of the vigor rating trait identified 16 overlapping QTL regions with all the QTL regions containing significant QTLs for all three cofactor analyses (Table 2.6). The overlapping QTL region on linkage group five at 58cM also contains a significant QTL for the 2012 year, which is less significant than the three cofactor analyses QTLs. This suggests that the QTL region may be slightly influenced by the 2012 year, but this region is more important as a QTL region for regulating vigor regardless of location and year. The overlapping QTL region on linkage group five at 114cM also contains significant QTLs for both 2011 and 2012 years. Similar to above, this QTL region may be partially influenced by the years, but is more important as a regulator of vigor regardless of location and year.

The remaining overlapping QTL regions for the growth trait of vigor rating all contain significant QTLs for all three cofactor analyses with the “both location and year” cofactor analysis QTL having the highest significance value (Table 2.6). The overlapping region on linkage group five at 117cM contains an additional significant QTL for the OR-specific location along with the three cofactor analyses QTLs. The OR-specific QTL is less significant than the three cofactor analyses QTLs, which indicates that the QTL region may be slightly influenced by the OR-specific location, but the QTL region is more important as a regulator of vigor irrespective of location or year. The overlapping QTL region on linkage group 12 at 49cM contains significant QTLs for the OR-specific location and the 2011 year. The overlapping QTL regions on linkage group six at 55cM and linkage group 12 between 95-96cM also contain significant QTLs for the OR-specific location and the 2012 year. For the QTL regions on linkage group six and 12, the LOD significance values for the cofactor analyses QTLs are greater than the OR-specific or year QTLs. This indicates that those QTL regions may be influenced by the OR-location or year, but is a more important as a QTL region for vigor regulation irrespective of location or year. The overlapping QTL regions on linkage group five between 122-124cM and linkage group 12 at 78cM contain significant QTLs for: the OR-specific location, and the 2011 and 2012 years. Similar to the previously discussed QTL

regions, the cofactor analyses QTLs are more significant than the other analyses, which indicates some influence of the OR-location and years, but the QTL regions are more important regardless of location or year. The overlapping QTL region on linkage group five between 17-19cM contains similar significant QTLs with an additional significant QTL for the FL-specific location. Also similar to the previously discussed QTL regions, the cofactor analyses QTLs are more significant than the other QTLs, which indicates that locations and years may have a slight influence on the QTL region, but the QTL region is more important as a regulator of vigor irrespective of location and year. Overall, the overlapping QTL regions for the vigor rating trait are more significant for the cofactor analyses than the specific location or year QTLs, which indicates these QTLs can be utilized in future breeding strategies across other locations with different environmental variation to improve blueberry plant vigor. The genes within the corresponding genetic regions for the QTL regions are most likely involved in processes like cell proliferation regulation with auxin-cytokinin-ethylene, or leaf development and expansion (Bar & Ori, 2014; Daviere & Achard, 2013; Del Pozo et al., 2005; Lau & Deng, 2010; Lloret et al., 2018; Ophir et al., 2009; Perrot-Rechenmann, 2010; Ruan, 2014; Signorelli et al., 2018; Takatsuka & Umeda, 2014; Wingler, 2017; Yang & Jiao, 2016; Zheng et al., 2015).

To expand the analysis individual growth traits, when the overlapping QTL regions for each growth trait were compared to regions for another growth trait, seven multi-trait overlapping regions were revealed. There are four overlapping QTL regions on linkage group five that contain significant QTLs for multiple growth traits. The overlapping regions between 10-19cM and between 124-125cM both contain multiple significant QTLs for bush height, bush width, vigor rating, leafing strength, and yield estimate. The genes within those genetic regions are most likely involved in regulating vegetative growth like leaf development or photosynthetic capacity (Bar & Ori, 2014; Ghelardini, Santini, Black-Samuelsson, Myking, & Falusi, 2009; Granot et al., 2013; Grant et al., 2009; Inostroza-Blancheteau et al., 2016; Mathan et al., 2016; Rho, Yu, Kim, & Lee, 2012; Rosa et al., 2009; Wingler, 2017). The overlapping QTL region between 58-60cM contains significant QTLs for vigor rating and yield estimate. The genes within this genetic region most likely regulate overall growth processes like cell

division and expansion (Del Pozo et al., 2005; Majda & Robert, 2018; Perrot-Rechenmann, 2010; Takatsuka & Umeda, 2014). The overlapping QTL region at 117cM contains significant QTLs for bush width and vigor rating. This genetic region most likely contains genes involved in regulating branching and axillary growth (Considine & Considine, 2016; Reddy et al., 2013; Signorelli et al., 2018; Yang & Jiao, 2016). The overlapping QTL region on linkage group 10 at 50cM contains significant QTLs for vigor rating and leafing strength, which suggests this genetic region contains genes involved in leaf development and expansion (Bar & Ori, 2014; Granot et al., 2013; Grant et al., 2009; Linkosalo & Lechowicz, 2006; Majda & Robert, 2018; O'Hara et al., 2013; Perrot-Rechenmann, 2010; Zhiponova et al., 2013). The overlapping QTL region on linkage group 11 at 80cM contains significant QTLs for floral buds per cane and yield estimate rating. Since both traits measure floral bud numbers, the genes within this genetic region most likely regulate floral bud differentiation and development (Arora et al., 2003; Koutinas et al., 2010; Lloret et al., 2018; Mert et al., 2013; van der Schoot & Rinne, 2011). The overlapping QTL region on linkage group 12 at 78cM contains significant QTLs for vigor rating, leafing strength, and leaf to fruit ratio. The genes within this genetic region are most likely involved in regulating leaf density like phyllotaxy and leaf development (Bar & Ori, 2014; Buchanan et al., 2012; Leyser, 2017; Molinero-Rosales et al., 2004; Swarup & Péret, 2012).

In summary, the eight growth traits represent multiple aspects of blueberry agronomics, including bush growth, leaf development, and floral bud development (James F. Hancock et al., 2018). The association mapping of the individual phenotypes for the eight growth traits identified 97 total significant QTLs (Table 2.4). The association mapping of the eight growth traits for the specific locations revealed 82 total significant QTLs, with 22.0% of the total for FL, 11.0% for GA, and 67.0% for OR locations (Table 2.5). When the eight growth traits were association mapped for specifically the 2011 and 2012 years, the mapping identified 37 significant QTLs, with 43.2% of the total for 2011 and 56.8% for 2012 (Table 2.5). Overall, the eight growth traits identified more OR-specific QTLs than the other locations or years, which suggests the OR location exhibits a strong influence on blueberry growth (Table 2.5). The eight growth traits when association mapped with the location cofactor, year cofactor, and “both location and

year” cofactors revealed 161 total significant QTLs (Table 2.5). Of the 161 significant QTLs for all the cofactor analyses, 31.0% were for the location cofactor, 28.0% for the year cofactor, and 41.0% for both location and year cofactors (Table 2.5). Further analysis of all the significant QTLs revealed 43 overlapping QTL regions where three or more significant QTLs from different analyses were in the same QTL region (Table 2.6). Of the 43 overlapping QTL regions, 25.6% of the QTL regions contained significant QTLs for the location or year -specific analyses that were more significant than the cofactor analyses, which suggests these QTL regions are strongly impacted by the environmental variation from location or year (Table 2.6). The 74.4% of the total QTL regions that was more significant for the cofactor analyses indicates that these QTL regions are important for regulating the growth traits regardless of the environmental variation from location or year (Table 2.6). Although there are some QTL regions that will be more beneficial for future breeding strategies at specific locations or climates, the majority of QTL regions identified with the eight growth traits can be utilized in future breeding strategies to improve growth across different environmental conditions.

2.5.2. Dormancy Break and Flowering Regulation

Since blueberries are perennial shrubs, they undergo dormancy to protect the delicate floral and vegetative buds from harsh winter conditions, and then resume active growth once favorable spring conditions return (Arora et al., 2003; Beauvieux et al., 2018; Considine & Considine, 2016; Cooke et al., 2012; D. P. Horvath et al., 2003; Pagter et al., 2015; Rohde & Bhalerao, 2007; Shim et al., 2014; Signorelli et al., 2018; Wisniewski et al., 2003). As described in the introduction, the cycling of dormancy involves the signaling and coordination of multiple processes to transition the inactive meristems to active growth (Arora et al., 2003; Beauvieux et al., 2018; Considine & Considine, 2016; D. P. Horvath et al., 2003; Pagter et al., 2015; Rohde & Bhalerao, 2007; Shim et al., 2014; Signorelli et al., 2018; Wisniewski et al., 2003). Gaining a greater understanding of dormancy regulation will improve blueberry yield because more floral buds will progress through dormancy break at the appropriate time and reduce the number of damaged buds from breaking too early or late (Mark K Ehlenfeldt et al., 2007; Kovaleski et al., 2015; L J Rowland, Mehra, & Arora, 2003; Lisa J Rowland et al., 2014; Lisa J Rowland, Ogden, Ehlenfeldt, & Arora, 2008). A greater number of

floral buds means there will be more mature flowers available for fertilization, allowing for fruits to subsequently develop (Ito et al., 2015; Kovaleski et al., 2015; Mert et al., 2013; Salvo et al., 2012).

2.5.2.1. Dormancy Break and Flowering Traits QTLs and Overlapping QTL Regions

The eight dormancy break and flowering traits consist of three chill requirement traits, five dormancy break and flowering traits. The three chill requirement traits are chill requirement vegetative, chill requirement floral, and floral chill rating traits with the chill requirement vegetative and chill requirement floral traits identifying no significant QTL regions. The five dormancy break and flowering traits consist of the days until early green tip, days until shoot expansion, days until floral bud break, days until full bloom, and days between floral bud break and full bloom. The main factor inducing dormancy break is fulfilling the chill requirement threshold, which means the blueberry bush accumulates a certain number of hours below 7°C (Hussain et al., 2015; Leida et al., 2012; Miura & Furumoto, 2013; Ophir et al., 2009; Rohde & Bhalerao, 2007). Of the three chill requirement traits, the association mapping results identified only one significant QTL for floral chill rating on linkage group six at 111cM with an LOD of 3.96 and 21.9% of the variation explained (Table 2.4). Further research into the genetic region may reveal important genes that regulate the chill requirement signal, which could aid future breeders in improving the growth range through optimization of the chill requirement for that area (Arora et al., 2003; Die et al., 2016; Mark K Ehlenfeldt et al., 2007; Hussain et al., 2015; Leida et al., 2012; L J Rowland et al., 2003; Lisa J Rowland et al., 2014).

The dormancy break and flowering trait of days until early green tip assesses the timing and regulation of dormancy break for vegetative buds (Bar & Ori, 2014; Considine & Considine, 2016; Grant et al., 2009; James F. Hancock et al., 2018; Hedley et al., 2010; C. Liu et al., 2010; Zhiponova et al., 2013). The association mapping results of the days until early green tip trait revealed two overlapping QTL regions on linkage group two that both contain significant QTLs for the three cofactor analyses: location, year, and “both location and year” cofactors (Table 2.7). The overlapping QTL region on linkage group two between 30-32cM also contains significant QTLs for GA-

specific location and 2011 year mapping (Table 2.7). The large LOD significance values for the GA-specific and 2011 year QTLs indicate that this QTL region is strongly influenced by specific locations and years. The year cofactor QTL in the two QTL regions have the largest LOD significance values, which indicates that year strongly affects these QTL regions for days until early green tip. However, these QTL regions also contain significant QTLs for the other two cofactor analyses, which suggests these QTL regions can still impact and regulate days until early green tip for other locations and years. Further research into the genetic region for these QTLs may reveal genes involved in oxidative signaling, cell wall matrix regulation, or sugar signaling as multiple studies have implicated these pathways in regulating the dormancy break progression (Beauvieux et al., 2018; Malyshev et al., 2016; Meitha et al., 2018; Signorelli et al., 2018; Z. Zhang et al., 2018). Future breeding strategies can utilize these QTLs to improve the dormancy break efficiency of vegetative buds and allow for rapid photosynthetic energy production for rapid growth after dormancy break, thus improving blueberry growth range (Arora & Rowland, 2011; Basler & Körner, 2014; Die et al., 2016; Ghelardini et al., 2009; Rihan et al., 2017; Suzuki et al., 2012; Trehane, 2004).

The dormancy break and flowering trait of days until floral bud break represents the timing and regulation of dormancy break for floral buds (James F. Hancock et al., 2018). The association mapping results of the days until floral bud break trait also revealed two overlapping QTL regions (Table 2.7). The overlapping QTL region on linkage group 10 at 75cM contains significant QTLs for all three cofactor analyses, which indicates that this QTL region is important for regulating days until floral bud break regardless of location or year (Table 2.7). The genes within this genetic region are most likely involved in sugar conversions and signaling to allow for the reopening of plasmodesmata and transport of flowering locus T (P. L. H. Rinne et al., 2011; P. L. Rinne & Schoot, 2003; van der Schoot & Rinne, 2011). The other overlapping region on linkage group three at 84cM contains significant QTLs for: the “both location and year” cofactors analysis, the location cofactor analysis, and the individual phenotype for OR-2011 (Table 2.7). The OR-2011 individual phenotype is more significant than the two cofactor QTLs, which suggests the QTL region is strongly impacted by the OR location and 2011 year. The genes within this genetic region are most likely involved in the

signaling of environmental conditions specific to the OR-location that induce the start of dormancy break like photoperiod or chill sensing (Arora & Rowland, 2011; Arora et al., 2003; Basler & Körner, 2012; Cooke et al., 2012; Ghelardini et al., 2009; Pletsers et al., 2015; R. K. Singh et al., 2017). The days until floral bud break trait also revealed a QTL region where only two significant QTLs overlapped, specifically on linkage group one at 6cM. The two significant QTLs are for the year cofactor analysis and the 2011 year, which suggests that this QTL region is very strongly influenced by the environmental variation from the 2011 year. All the other significant QTLs for days until floral bud break did not overlap for different mapping analyses and were distinctly separated by location or individual phenotypes. Even though the overlapping QTL region on linkage group 10 is minimally influenced by environmental variation from location or year, the many other, non-overlapping significant QTLs strongly suggest the days until floral bud break trait is heavily impacted by environmental variation from location or year. Within these genetic regions, the genes are most likely involved in regulating photoperiod, oxidative signaling or hormone signaling since they are influenced by environmental variation (Anderson, 2015; Basler & Körner, 2014; Beauvieux et al., 2018; Fadón et al., 2018; Lloret et al., 2018; Malyshev et al., 2016; Meitha et al., 2018; Zheng et al., 2015). Further gene research into these genetic regions will elucidate the regulatory pathways for floral bud dormancy break, and can be utilized in future breeding strategies to improve blueberry growth range with optimization of floral bud dormancy break for that region (Anderson, 2015; Basler & Körner, 2014; Beauvieux et al., 2018; Fadón et al., 2018; Jim F Hancock, 2008; Hanson, Berkheimer, & Hancock, 2007; Lloret et al., 2018; Malyshev et al., 2016; Meitha et al., 2018; Trehane, 2004; Zheng et al., 2015).

The dormancy break and flowering trait of days until shoot expansion assesses the timing and development of vegetative buds into young, delicate leaves and the induction of shoot growth (Patrick Achard et al., 2009; Bar & Ori, 2014; Brelsford & Robson, 2018; James F. Hancock et al., 2018). The association mapping results of the days until shoot expansion trait did not reveal any overlapping QTL regions containing significant QTLs for three or more mapping analyses. There is a QTL region on linkage group one at 8cM that contains only two significant QTLs for the 2011 year and year cofactor, which indicates that this QTL region is heavily influenced by the 2011

year. The significant QTLs for the other mapping analyses did not overlap with each other, thus it is difficult to determine whether the association of the QTL represents the trait rather than the environmental variation of location or year. The genes within this region may be involved in regulating leaf cell expansion (Patrick Achard et al., 2009; Bar & Ori, 2014; Majda & Robert, 2018; Mathan et al., 2016; Zhiponova et al., 2013). Further gene research will provide important knowledge towards the differentiation and expansion of leaves soon after dormancy break, and can be utilized along with the QTLs to improve the rapid growth soon after dormancy break (Patrick Achard et al., 2009; Bar & Ori, 2014; Claeys et al., 2014; Cooke et al., 2012; Daviere & Achard, 2013; Meitha et al., 2018, 2015).

The dormancy break and flowering trait of days until full bloom represents the timing and development of mature, blooming flowers from dormant floral buds, thus includes dormancy break, floral organ differentiation, flower growth, and blooming processes (James F. Hancock et al., 2018; Ito et al., 2015; P. L. H. Rinne et al., 2011). The association mapping results of the days until full bloom trait also did not reveal any overlapping QTL regions. The significant QTLs from the other mapping analyses did reveal that the FL location heavily influences the trait (Table 2.4 and 2.5). This suggests that the genes within the genetic regions are probably involved in signaling environmental conditions like long daylength through photoperiodism and carbon signaling (H. Ben Mohamed et al., 2012; Ghelardini et al., 2009; D. P. Horvath et al., 2003; Ito et al., 2015; Krieger, Lippman, & Zamir, 2010; Melke, 2015; Pagter et al., 2015; Rihan et al., 2017; Wilkie et al., 2008; Z. Zhang et al., 2018; Zhuang et al., 2015).

The dormancy break and flowering trait of days between floral bud break and full bloom specifically assesses the development of the mature, blooming flower from floral buds after dormancy break (James F. Hancock et al., 2018). Although the association mapping results of the days between floral bud break and full bloom trait identified many significant QTLs for the different mapping analyses, none of the QTLs overlapped across analyses. These significant QTLs were distinctly separated by location or individual phenotypes, which suggest that the days between floral bud break and full bloom is strongly impacted by environmental variation from location or year (Table 2.4 and 2.5). This indicates that the genes within the corresponding genetic regions may be

involved in regulating hormone cross-talk like cytokinin-auxin for differentiation for maturity and auxin-ABA for cell expansion for division and blooming (Conti, 2017; D. Horvath, 2009; Ionescu et al., 2016; Ito et al., 2015; Lau & Deng, 2010; Takatsuka & Umeda, 2014; Vasconcelos et al., 2009; Wilkie et al., 2008; Xing et al., 2015). Further gene research will elucidate the transition between floral buds and mature flowers for specific environmental conditions (Amasino & Michaels, 2010; Conti, 2017; Ionescu et al., 2016; Ito et al., 2015; Koutinas et al., 2010; Krieger et al., 2010; Vasconcelos et al., 2009; Wilkie et al., 2008). These QTL regions can be utilized in future breeding strategies to improve floral bud maturation into flowers when optimized for specific environmental conditions.

In summary, the eight dormancy break and flowering traits represent the main transition processes from dormancy break induction to leaf and flower maturation (James F. Hancock et al., 2018). The association mapping of the individual phenotypes for the eight dormancy break and flowering traits identified 54 total significant QTLs (Table 2.4). The three chill requirement traits identified only one significant QTL for the floral chill rating trait. This chill requirement QTL region can be utilized for further gene research to investigate the regulation of fulfilling the chill requirement, and for future breeding strategies to improve the growth range of blueberries (Arora & Rowland, 2011; Arora et al., 2003; Die et al., 2016; M. Ehlenfeldt, 2012; Jim F Hancock, 2008; Kovaleski et al., 2015; Melke, 2015; Lisa J Rowland et al., 2014, 2008; Trehane, 2004). The association mapping of the five dormancy and flowering traits for the specific locations revealed 23 total significant QTLs with 17.4% for FL, 56.5% for GA, and 26.1% for OR locations (Table 2.5). When the five dormancy break and flowering traits were association mapped for specifically the 2011 and 2012 years, the mapping identified three significant QTLs with 100% for 2011 and none for 2012 (Table 2.5). Since the year mapping identified significant QTLs in only 2011, this suggests that the 2011 year may also influence the dormancy and flowering traits. The five dormancy break and flowering traits revealed 23 significant QTLs when the association mapping included the location cofactor, year cofactor, and both location and year cofactors. Of the 23 significant QTLs for all the cofactor analyses, 20.0% were for the location cofactor, 45.0% for the year cofactor, and 35.0% for “both location and year” cofactors (Table

2.5). The comparison of all the significant QTLs for all the different analyses for the five dormancy break and flowering traits revealed only four overlapping QTL regions (Table 2.7). Three of the four overlapping QTL regions contain significant QTLs for location or year -specific that are more significant than the cofactor analyses, which indicates these QTL regions are highly impacted by the environmental variation from location or year. Furthermore, the many non-overlapping significant QTLs for the location and year -specific analyses indicates that the five dormancy break and flower traits are impacted by different environmental conditions. Future research and breeding strategies will elucidate the regulatory processes of dormancy break and flowering to improve blueberry growth range and productivity (Arora et al., 2003; M. Ehlenfeldt, 2012; Jim F Hancock, 2008; Kovaleski et al., 2015; G. A. Lobos & Hancock, 2015; Melke, 2015; Lisa J Rowland et al., 2008; Trehane, 2004).

2.5.3. Fruit Quality Regulation

Blueberry berries develop and ripen similarly to grapes through double sigmoid growth and non-climacteric ripening (Castellarin et al., 2016; Konarska, 2015; Xi et al., 2017). As previously described in the introduction, double sigmoid growth undergoes two growth stages separated by a lag stage (Castellarin et al., 2016; Konarska, 2015; Xi et al., 2017). The growth stages exhibit rapid cell proliferation and expansion so that the berry grows in size and weight (Cappai et al., 2018; Coombe & McCarthy, 2000; Osorio et al., 2013; Serrano et al., 2017). The lag stage primarily accumulates soluble sugars and precursor metabolites so that the berry is prepared for the induction of ripening (Cappai et al., 2018; Coombe & McCarthy, 2000; Osorio et al., 2013; Serrano et al., 2017). Ripening occurs during the last growth stage where the berry achieves final size and accumulates pigment (Coombe & McCarthy, 2000; J. Giovannoni, 2001; Osorio et al., 2013; Serrano et al., 2017; Seymour, Østergaard, et al., 2013).

The signaling pathways at the onset of ripening categorize fruits into climacteric and non-climacteric (Buchanan et al., 2012; Osorio et al., 2013). Non-climacteric fruit like blueberries do not exhibit a respiratory burst and ethylene accumulation spike to trigger the induction of ripening (Coombe & McCarthy, 2000; J. Giovannoni, 2001; Osorio et al., 2013; Serrano et al., 2017). Multiple studies have implicated ABA accumulation and soluble sugar signaling as important factors for non-climacteric

ripening as it induces cell wall matrix modifications and pigment accumulation (Ayub et al., 2016; Castellarin et al., 2016; Gambetta, Matthews, Shaghasi, McElrone, & Castellarin, 2010; J. J. Giovannoni, 2004; Jia et al., 2017; Karppinen et al., 2013; Leng et al., 2014; Moggia et al., 2017; Oh et al., 2018; Osorio et al., 2013; Ren et al., 2011; Serrano et al., 2017; Toivonen & Brummell, 2008). Breeding cultivars with efficient coordination and regulation of blueberry ripening pathways will increase blueberry berry yield and improve consumer-driven fruit quality characteristics like dark blue color, firm and juicy texture, sweet and tart taste, and enhanced nutrition (Cappai et al., 2018; Gilbert et al., 2015, 2014; Saftner et al., 2008; J. L. Silva et al., 2005).

The blue color of blueberries is from the accumulation and stabilization of anthocyanin metabolites in acidic conditions (Khoo et al., 2017; Routray & Orsat, 2011, 2014; Sasaki et al., 2014; Trehane, 2004; Wahyuningsih et al., 2017; Yonekura-Sakakibara et al., 2009). The dark blue color preferred by consumers is a result of blueberry skin cells accumulating a diversity of anthocyanins (He et al., 2010; Khoo et al., 2017; Routray & Orsat, 2011, 2014; Sasaki et al., 2014; Wahyuningsih et al., 2017; Yonekura-Sakakibara et al., 2009). The acidity needed for anthocyanins also contributes to regulating the firmness and juice content of blueberries through affecting cell wall modifications and turgor pressure (Castellarin et al., 2016; Gould et al., 2013; Majda & Robert, 2018; Perrot-Rechenmann, 2010; Wahyuningsih et al., 2017). As previously described in the introduction, acidic cell expansion aids rapid cell growth by allowing cell wall matrix modification enzymes to increase the relative flexibility of the cell wall matrix (Buchanan et al., 2012; Chen et al., 2015; Majda & Robert, 2018; C. Paniagua et al., 2014; Perrot-Rechenmann, 2010). This relative flexibility allows for an increase in turgor pressure to expand the cell, which is quickly followed by the induction of cell wall matrix stiffening processes to stiffen the newly-expanded cell wall matrix (Buchanan et al., 2012; Cappai et al., 2018; Castellarin et al., 2016; Chen et al., 2015; Choi et al., 2002; X. Li et al., 2010; Posé et al., 2011; Vicente et al., 2007). The increase in turgor pressure is induced by the increase in tonicity or acidity and soluble solid content within the cell, which directs the osmotic flow into the cell (Castellarin et al., 2016; Gould et al., 2013; Koyama et al., 2010; Toivonen & Brummell, 2008; A. K. Yadav & Singh, 2014).

Therefore, firm and juicy blueberries are a balance of cell wall matrix modifications to allow for maximum turgor pressure (Castellarin et al., 2016; Choi et al., 2002; Gould et al., 2013; Koyama et al., 2010; X. Li et al., 2010; Prasanna et al., 2007; Toivonen & Brummell, 2008; A. K. Yadav & Singh, 2014). Low firmness and softening occurs when the turgor pressure is not increased to push against the cell wall matrix, thus the matrix and membranes become flaccid (Buchanan et al., 2012; Cappai et al., 2018; Chen et al., 2015; Choi et al., 2002; X. Li et al., 2010; Moggia et al., 2017; A. C. Paniagua, East, Hindmarsh, & Heyes, 2013; C. Paniagua et al., 2014; Posé et al., 2011; Prasanna et al., 2007; Vicente et al., 2007). If the cell wall matrix modification enzymes are not appropriately regulated to allow for the subsequent stiffening, then the cell wall matrix degrades and becomes more flaccid (Cappai et al., 2018; Chen et al., 2015; Choi et al., 2002; X. Li et al., 2010; Moggia et al., 2017; A. C. Paniagua et al., 2013; C. Paniagua et al., 2014; Posé et al., 2011; Prasanna et al., 2007; Vicente et al., 2007).

The soluble sugar content and acidity contributes to the turgor pressure and to the taste of blueberries with sugars providing sweetness and acids, especially organic acids, providing tartness (Etienne, Génard, Lobit, Mbéguié-A-Mbéguié, & Bugaud, 2013; Gilbert et al., 2015, 2014, 2013; Gündüz et al., 2015; Tieman et al., 2012; Zeiss, Mhlongo, Tugizimana, Steenkamp, & Dubery, 2018). Many consumer preference studies have proposed that the appealing flavor of fruits is from the ratio between sweet and tart rather than just a sweet taste (Biltekoff, 2010; Cappai et al., 2018; Gilbert et al., 2015, 2014; Klee, 2010; McGinn, 2015; Pagliarini et al., 2013; Schwab et al., 2008; Spence, 2015; Tieman et al., 2012; Ulrich & Olbricht, 2014; Varela & Ares, 2012). The health benefits of blueberries are from the potent antioxidant properties of anthocyanins and phenolic acids, which can be improved concurrently with the other fruit quality characteristics important for blueberries (Bornsek et al., 2012; Brito, Areche, Sepúlveda, Kennelly, & Simirgiotis, 2014; Khoo et al., 2017; D. Li et al., 2017; Lila et al., 2016; Montecchiarini et al., 2018; Oh et al., 2018; Reque et al., 2014; S. Silva et al., 2018; Yousuf, Gul, Wani, & Singh, 2016). The significant QTLs from the association mapping of blueberry fruit quality traits will provide insight into potential regulatory regions involved in fruit development and ripening pathways like cell wall matrix modifications, sugar signaling, and phenolic acid accumulation (Cappai et al., 2018; Castellarin et al.,

2016; Giongo et al., 2013; Jia et al., 2017; Konarska, 2015; Nguyen et al., 2018; Oh et al., 2018; Osorio et al., 2013; Serrano et al., 2017; Seymour, Chapman, et al., 2013; Seymour, Østergaard, et al., 2013; Xi et al., 2017).

2.5.3.1. Fruit Quality Traits QTLs and Overlapping QTL Regions

The 14 fruit quality traits represent fruit development, ripening, and consumer-drive fruit quality and consist of: days between full bloom and blue fruit, days until blue fruit, fruit color rating, fruit scar rating, fruit firmness rating, fruit flavor rating, berry weight, berry firmness, % juice, pH, SS, TA, SS:TA ratio, and total anthocyanin content (Table 2.4 and 2.5). The fruit quality trait of days between full bloom and blue fruit represents the fruit development and ripening processes, whereas the fruit quality trait of days until blue fruit represents the overarching processes from dormancy break to flowering to fruit development and ripening (James F. Hancock et al., 2018). The association mapping results of the days between full bloom and blue fruit trait identified one overlapping QTL region on linkage group one at 87cM (Table 2.8). The overlapping QTL region contains significant QTLs for all three cofactor mapping analyses with the “both location and year” cofactors analysis QTL showing the highest LOD significance value, which indicates that this QTL region is an important QTL for days between full bloom and blue fruit irrespective of location or year. The genes within this genetic region are most likely involved in regulating fruit development and ripening like cell division and expansion for rapid growth, ABA accumulation for induction, or pigment synthesis (Cappai et al., 2018; Castellarin et al., 2016; Giongo et al., 2013; Jia et al., 2017; Konarska, 2015; Nguyen et al., 2018; Oh et al., 2018; Osorio et al., 2013; Serrano et al., 2017; Seymour, Chapman, et al., 2013; Seymour, Østergaard, et al., 2013; Xi et al., 2017). Further research into this genetic region will elucidate important pathways for fruit development and ripening, which will aid future breeding strategies for improving blueberry harvest across different environmental conditions. The fruit quality trait of days until blue fruit trait did not reveal any overlapping QTL regions as the significant QTLs for the different mapping analyses were distinctly separated by location or individual phenotypes, which suggests that the overarching processes are strongly impacted by environmental conditions.

The fruit quality trait of fruit color rating represents the pigment accumulation of ripe blueberries (James F. Hancock et al., 2018). Fruit color is an important fruit quality characteristic as consumers prefer the dark blue blueberries and the health benefits of the blue pigment metabolites, anthocyanins, for their potent antioxidant properties (Cappai et al., 2018; Gilbert et al., 2015, 2014; Konarska, 2015; G. A. Lobos et al., 2014; Saftner et al., 2008; J. L. Silva et al., 2005). The association mapping results of the fruit color rating trait identified two overlapping QTL regions that contained significant QTLs for all three cofactor mapping analyses (Table 2.8). The overlapping region on linkage group one between 110-114cM also contained a significant QTL for the 2011 year. The 2011 year QTL in this QTL region is less significant than the three cofactor analyses QTLs, due to the lower LOD value for the 2011 year QTL (Table 2.8). This indicates that this QTL region for fruit color may be slightly influenced by the 2011 year, but the QTL region is more important as a QTL that impacts fruit color irrespective of location or year. The other overlapping QTL region on linkage group two at 57cM contains significant QTLs for all three cofactor analyses with the “both location and year” cofactor analysis QTL showing the highest significance. This indicates that this QTL region impacts fruit color irrespective of location or year environmental variation. The genes within these genetic regions corresponding to the two QTL regions are most likely involved in regulating anthocyanin synthesis and diversification (Howard, Brownmiller, Mauromoustakos, & Prior, 2016; Khoo et al., 2017; Montecchiarini et al., 2018; Muleke et al., 2017; Oh et al., 2018; Overall et al., 2017; Sasaki et al., 2014; Stevenson & Scalzo, 2012; Timmers et al., 2017; Wahyuningsih et al., 2017). Further gene research into these genetic regions will elucidate blueberry specific anthocyanin synthesis and diversification pathways, which will aid future breeding strategies in improving fruit quality, consumer appeal, and nutrition of blueberries.

The fruit quality trait of fruit firmness rating assesses the overall firmness texture of a ripe blueberry (James F. Hancock et al., 2018). Fruit firmness is another important fruit quality characteristic because industry and consumers prefer firm texture blueberries, as industry favors the resistance to bruising, while consumers prefer the firm texture for consumption (Barrett et al., 2010; Blacker, 2013; Blaker & Olmstead, 2015; Cappai et al., 2018; Choi et al., 2002; Giongo et al., 2013; X. Li et al., 2010; C.

Paniagua et al., 2014; Toivonen & Brummell, 2008). The association mapping results of the fruit firmness rating trait revealed only one overlapping QTL region that contained significant QTLs for: the “both location and year” cofactors, location cofactor, and OR-specific location mapping (Table 2.8). The OR-specific QTL is less significant than the cofactor analyses QTLs, which indicates that this QTL region may be partially influenced by the OR location for fruit firmness, but is more important as a QTL region that impacts fruit firmness regulation, regardless of location or year. The genes within this genetic region are most likely involved in regulating the cell wall matrix modifications and turgor pressure balance (Cappai et al., 2018; Castellarin et al., 2016; Giongo et al., 2013; A. C. Paniagua et al., 2013; C. Paniagua et al., 2014). Gaining a greater understanding of the genes within the genetic regions of the QTLs will aid future research and breeding strategies for regulating fruit firmness and improving fruit quality.

The fruit quality trait of berry weight represents the turgor pressure, tonicity, soluble solids, and metabolite content of a ripe blueberry (Castellarin et al., 2016; Choi et al., 2002; Gould et al., 2013; James F. Hancock et al., 2018; T. E. Lobos et al., 2018; Toivonen & Brummell, 2008; A. K. Yadav & Singh, 2014). Berry weight is another important fruit quality characteristic as consumers prefer heavier berries as it implies more juice and sugar (Blacker, 2013; Castellarin et al., 2016; Gould et al., 2013; Toivonen & Brummell, 2008; A. K. Yadav & Singh, 2014). The association mapping results of berry weight identified 12 overlapping QTL regions with 11 of the 12 overlapping regions containing significant QTLs for all three cofactor mapping analyses (Table 2.8). The overlapping region on linkage group two between 59-59cM contains significant QTLs for: the “both location and year” cofactor, the year cofactor, the FL-specific location, and the 2011 year (Table 2.8). The FL-specific and 2011 QTLs are more significant than the cofactor analyses, which indicates this QTL region is strongly impacted by the environmental variation from location and year. The overlapping region on linkage group 12 at 154cM contains significant QTLs for all the cofactor analyses and for the GA-specific location (Table 2.8). Since the GA-specific QTL is more significant than the cofactor analyses, this indicates this QTL region is strongly influenced by the environmental variation from the GA location. The genes within these genetic regions are probably involved in the ABA regulation of turgor pressure and

metabolite accumulation (Blacker, 2013; Cappai et al., 2018; Castellarin et al., 2016; Gambetta et al., 2010; Pilati et al., 2017; Toivonen & Brummell, 2008; A. K. Yadav & Singh, 2014).

The remaining 10 overlapping QTL regions for the berry weight trait all contain significant QTLs for all three cofactor analyses (Table 2.8). The overlapping QTL regions on linkage group one at 87cM and 92cM, and on linkage group seven at 32cM contain the “both location and year” cofactors analysis QTL that is more significant than the other cofactors QTLs, which indicates that these QTL regions are important for regulating berry weight regardless of location and year. The overlapping region on linkage group 11 between 31-34cM also contains a significant QTL for the GA-specific location, which is more significant than the three cofactor analyses QTLs. This indicates this QTL region may be slightly influenced by the GA location for berry weight, but is more important as a QTL region that impacts and regulates berry weight regardless of location and year. The overlapping QTL regions on linkage group one at 33cM and 52cM also contain significant QTLs for GA-specific location and the year 2011. For these two QTL regions, the three cofactor analyses QTLs are more significant than the GA-specific and 2011 year QTLs, which strongly suggests that these QTL regions are important for regulating berry weight regardless of location or year. The overlapping QTL regions on linkage group one between 13-15cM and between 18-19cM contain significant QTLs for: the three cofactor analyses, GA-specific location, 2011 year, and the FL-specific location. The three cofactor analyses QTLs are more significant than the other analyses QTLs, which strongly suggests that these QTL regions are important regions for berry weight regulation regardless of location and year. The overlapping region on linkage group one between 61-63cM contains significant QTLs for: all three cofactor analyses, FL-specific location, GA-specific location, 2011 year, and 2012 year. Since the three cofactor analyses were the most significant QTLs, this indicates this QTL region aids in regulating berry weight irrespective of location or year. The majority of the overlapping QTL regions identified impact and regulate berry weight regardless of variation from location or year, thus the genes within the corresponding genetic regions are involved in regulating the overall turgor pressure and tonicity of the pulp tissue (Blacker, 2013; Cappai et al., 2018; Castellarin et al., 2016; Gambetta et al., 2010; Pilati

et al., 2017; Toivonen & Brummell, 2008; A. K. Yadav & Singh, 2014). Further gene research on these genetic regions will help clarify the regulation and signaling of pathways like turgor pressure and soluble solids for berry weight, which will aid future breeding strategies when these QTLs are utilized to improve blueberry fruit quality.

The fruit quality trait of berry firmness quantifies the force required to deform a ripe blueberry, which is an important characteristic for industry and consumer fruit quality (Barrett et al., 2010; Blacker, 2013; Blaker & Olmstead, 2015; Cappai et al., 2018; Choi et al., 2002; Giongo et al., 2013; X. Li et al., 2010; C. Paniagua et al., 2014; Toivonen & Brummell, 2008). Berry firmness is a different measure than fruit firmness rating. Berry firmness is a continuous variable that records small variations in firmness, rather than the categorical fruit firmness rating trait. Because berry firmness is a continuous variable, the association mapping often identifies a larger number of significant QTLs (Bernardo, 2008; Hospital, 2009; M. S. Kang, 2002; Winter & Kahl, 1995; Xu, 2010). The association mapping results of the berry firmness trait identified eight overlapping QTL regions that all contain significant QTLs for all three cofactor mapping analyses (Table 2.8). The overlapping QTL regions on linkage group one at 47cM and 55cM also contains a significant QTL for the year 2012. Since the 2012 QTL is less significant than the cofactor analyses, these QTL regions may be slightly influenced by the year 2012 for berry firmness, but the QTL regions are more important as QTL regions regulating berry firmness regardless of location or year. The overlapping QTL region on linkage group three at 106cM contains significant QTLs for the three cofactor analyses and the GA-specific location. The overlapping region on linkage group four between 130-134cM contains significant QTLs for: the three cofactor analyses, the GA-specific location, and the 2011 year. The GA-specific and 2011 year QTLs are less significant than the cofactor analyses QTLs, which indicates that GA and 2011 may have a slight influence on these QTL regions for berry firmness, but the QTL regions are more important for berry firmness regulation regardless of location or year. Overall, the overlapping QTLs for berry firmness are not substantially influenced by environmental variation from specific locations or years. Therefore, the genes within the corresponding genetic regions are involved in pathways like ABA and sugar signaling that regulate the turgor pressure and soluble sugars of berry skin and pulp cells

(Blacker, 2013; Cappai et al., 2018; Castellarin et al., 2016; Gambetta et al., 2010; Pilati et al., 2017; Toivonen & Brummell, 2008; A. K. Yadav & Singh, 2014). Further research into the genes within these genetic regions will elucidate regulation of berry firmness as well as aid future breeding for firmness through the incorporation of these QTLs to improve blueberry fruit quality and consumer appeal.

The fruit quality trait of percent (%) juice represents the turgor and turgor pressure of the fruit cells (Castellarin et al., 2016; James F. Hancock et al., 2018; Koyama et al., 2010; A. K. Yadav & Singh, 2014). The % juice of the blueberry is another important fruit quality trait as consumers prefer blueberries that are very juicy (Barrett et al., 2010; Gilbert et al., 2014; X. Li et al., 2010; Milić et al., 2018). The results from association mapping the % juice trait identified four overlapping QTL regions that all contained significant QTLs for all three cofactor analyses (Table 2.8). Since the QTL regions contain significant QTLs for all three cofactor analyses, the QTL regions strongly impact and regulate % juice in berries regardless of location or year. The overlapping region on linkage group 10 at 86cM also contains a significant QTL for the GA-specific location, which has a higher significance value than the three cofactor analyses QTLs. This indicates that this QTL region is strongly influenced by the GA location, but the cofactor analyses QTLs suggest the QTL region can still impact the % juice regardless of location or year. For this QTL region on linkage group 10, the genes within the genetic region most likely regulate a process like transpiration that can be strongly affected by environmental variation like the GA location (Buchanan et al., 2012; Wasilewska et al., 2008). The other three overlapping QTL regions show the highest significance for the “both location and year” cofactor QTLs, indicating the QTL regions impact the % juice irrespective of location or year. The genes within these corresponding genetic regions are probably involved in processes like turgor pressure and turgor pressure from soluble solids that can regulate % juice irrespective of environment variation from specific locations or years (Barrett et al., 2010; Castellarin et al., 2016; Gilbert et al., 2014; X. Li et al., 2010; Milić et al., 2018; A. K. Yadav & Singh, 2014). Further research into the genes within the genetic regions will elucidate the different processes regulating % juice as the knowledge is very limited. Utilizing this information

and QTLs in future breeding strategies will aid in improving the juiciness, consumer appeal, and overall fruit quality of blueberries.

The fruit quality trait of pH quantifies the hydrogen ions of the blueberry juice (James F. Hancock et al., 2018). The pH is an important fruit quality characteristic because pH contributes to acidity, which is involved in acidic cell expansion and improves the stability of anthocyanins (Horbowicz et al., 2008; Jia et al., 2017; Khoo et al., 2017; Koyama et al., 2010; Majda & Robert, 2018; Ozga & Reinecke, 2003; Perrot-Rechenmann, 2010; Wahyuningsih et al., 2017). The association mapping results of the pH trait identified one overlapping QTL region on linkage group four at 64cM (Table 2.8). This overlapping region contains significant QTLs for: the “both location and year” cofactors, the location cofactor, the FL-specific location, and the 2012 year. Both the FL-specific and 2012 year QTLs exhibit stronger LOD significance values than the cofactor QTLs, which indicates that this QTL region is strongly influenced by a specific location and year. However, the significant cofactor analyses QTLs suggest the QTL region can still be an important QTL region for regulating pH for other locations and years. Within this genetic region, the genes are most likely involved in pathways like acidic cell expansion and turgor pressure (Castellarin et al., 2016; Jia et al., 2017; Majda & Robert, 2018; Perrot-Rechenmann, 2010). Those processes can be strongly influenced by specific environmental conditions like FL or the 2012 year, but can also regulate berry pH in other environmental conditions. Further research on the genes within the region will elucidate the regulation and effects of blueberry acidity from pH. The incorporation of this QTL into future breeding strategies will aid in improving blueberry consumer appeal and nutrition because the pH acidity can impact berry firmness as well as stabilize the anthocyanin metabolites.

The fruit quality trait of titratable acidity (TA) quantifies the total acidity of the blueberry juice (James F. Hancock et al., 2018). TA is also an important fruit quality characteristic to consumers because TA better represents the organic acids that impact flavor, and TA represents the acidity that also aids in stabilizing anthocyanins (Choi et al., 2002; Gilbert et al., 2014; Klee, 2010; Konarska, 2015; Moggia et al., 2017; Osorio et al., 2013; Schwab et al., 2008; Wahyuningsih et al., 2017; Xi et al., 2017). The association mapping results of the TA trait identified nine overlapping QTL regions that

all contained significant QTLs for all three cofactor analyses (Table 2.8). The overlapping QTL regions on linkage group four at 38cM and 64cM, and linkage group five at 94cM also contains significant QTLs for the FL-specific location. The FL-specific QTL in the two overlapping QTL regions on linkage group four show an LOD significance value lower than the three cofactor analyses QTLs. This indicates the FL location may slightly influence these QTL regions, but the QTL regions are important regulators of TA irrespective of location or year. The FL-specific QTL in the overlapping region on linkage group five is more significant than the cofactor analyses QTLs, which indicates that this QTL region is strongly influenced by the FL location for TA, but can still impact TA regulation for other locations and years. For this QTL region, the genes within the genetic region are involved in pathways like phenylpropanoid acid and flavonoid synthesis that are strongly influenced by environmental variation from a specific location (Brito et al., 2014; He et al., 2010; Karppinen, Zoratti, Nguyenquynh, Häggman, & Jaakola, 2016; Koyama et al., 2010; Schwab et al., 2008; Zorenc et al., 2017). For the other six QTL regions that contain just the three cofactor analyses QTLs, the genes in the corresponding genetic regions regulate pathways like overall phenolic acid and TCA acid synthesis that are not influenced by environmental variation from specific locations or years (Ayub et al., 2016; Barrett et al., 2010; Cappai et al., 2018; Conde et al., 2015; Coombe & McCarthy, 2000; Gilbert et al., 2015, 2014; Giongo et al., 2013; Kader, 2008; Konarska, 2015; Leng et al., 2014; Moggia et al., 2017; Oh et al., 2018; Serrano et al., 2017). Further gene research on these genetic regions will elucidate TA regulation during blueberry ripening. Along with this knowledge, incorporating these QTLs into future breeding strategies will aid in improving blueberry fruit quality and consumer appeal through turgor firmness, tart taste, anthocyanin coloration, and nutrition.

The fruit quality trait of soluble solids (SS) represents the soluble sugar level within the blueberry juice, which is an important fruit quality characteristic to consumers as sugars content can impact blueberry sweetness and blueberry firmness (Castellarin et al., 2016; Choi et al., 2002; Gilbert et al., 2015, 2014; James F. Hancock et al., 2018; Tieman et al., 2012). The association mapping results of the SS trait identified three overlapping QTL regions that all contained significant QTLs for all three cofactor

mapping analyses (Table 2.8). The overlapping QTL region on linkage group eight between 40-46cM also contains a significant QTL for the GA-specific location, but the cofactor analyses QTLs exhibit a greater LOD significance value than the GA-location QTL. This indicates that this QTL region may be slightly influenced by the GA location for SS, but is more important as a QTL region for SS regulation regardless of location or year. For all three overlapping QTL regions, the “both location and year” cofactor analysis QTL is the most significant QTL. This indicates that the genes within the corresponding genetic regions are involved in pathways like sugar interconversions and turgor pressure that are not strongly influenced by environmental variation from specific locations or years (Castellarin et al., 2016; Conde et al., 2015; O’Hara et al., 2013; Posé et al., 2011; Wingler, 2017). The composition and accumulation of sugars are the main contributors to the sweet taste of blueberries (Cappai et al., 2018; Gilbert et al., 2015, 2014; Giongo et al., 2013; Konarska, 2015; Leiva-Valenzuela, Lu, & Aguilera, 2013; Pagliarini et al., 2013; Spence, 2015; Tieman et al., 2012). Further gene research on the genetic regions will elucidate soluble sugar regulation during blueberry fruit development and ripening, and the incorporation of these QTLs in future breeding strategies will improve blueberry fruit quality and consumer appeal in firmness and flavor.

The fruit quality trait of SS:TA ratio represents the sugar to acidity ratio in blueberry juice, which is a very important fruit quality characteristic because consumers prefer the blueberry taste to be a balance of sweet and tart (Gilbert et al., 2015, 2014, 2013; James F. Hancock et al., 2018). The results from association mapping SS:TA ratio identified seven overlapping QTL regions with five of the seven QTL regions containing significant QTLs for all three cofactor analyses (Table 2.8). The overlapping QTL region on linkage group four between 20-22cM contains significant QTLs for all three cofactor analyses and the 2011 year. Since the 2011 QTL is less significant than the three cofactor analyses QTLs, this suggests the QTL region may be slightly influenced by the year 2011 for SS:TA ratio, but is a more important QTL region for regulating SS:TA ratio irrespective of location or year. The overlapping QTL region on linkage group eight at 89cM contains significant QTLs for the three cofactor analyses and the for FL-specific location. Since the FL-specific QTL is less significant than the

three cofactor analysis QTLs, this suggests the QTL region may be slightly influenced by the FL location for SS:TA ratio, but is more important as a QTL region for SS:TA ratio regulation regardless of location or year. The overlapping QTL region on linkage group eight between 82-83cM contains significant QTLs for: the “both location and year” cofactors, the location cofactor, and the FL-specific location. The FL-specific QTL has a higher LOD significance than the three cofactor analyses QTLs, which indicates that this QTL region is strongly influenced by the FL location, but the three cofactor analyses QTLs indicates that the QTL region can still impact and regulate the SS:TA ratio irrespective of locations and years. The overlapping region on linkage group 12 at 68cM contains significant QTLs for: the “both location and year” cofactors, the location cofactor, the GA-specific location, and the 2011 year. The GA-specific location QTL is more significant than the other QTLs, which indicates the GA location strongly influences this QTL region for SS:TA ratio. The latter two described QTL regions contain FL-specific and GA-specific QTLs that are more significant than the other QTLs, thus the genes within those corresponding genetic regions are involved in pathways like sugar signaling or flavonoid synthesis that is strongly influenced by environmental variation from the specific locations (Couée et al., 2006; Gambetta et al., 2010; Jia et al., 2017; Konarska, 2015; Rabot et al., 2012; Serrano et al., 2017; Zifkin et al., 2012).

Of the remaining five regions for the SS:TA ratio trait, two of the QTL regions are more significant for the location cofactor QTL, one QTL region is more significant for the year cofactor QTL, and two QTL regions are more significant for the “both location and year cofactors” analysis QTL (Table 2.8). Overall, half of the overlapping QTL regions are strongly impacted by environmental variation from location or year, whereas the other half of the overlapping QTL regions influence the SS:TA ratio irrespective of the environmental variation. The genes within the corresponding genetic regions influenced by location or year variation are probably involved in hormone signaling of sugar and acid synthesis (Ayub et al., 2016; Jia et al., 2017; Osorio et al., 2013; Prasanna et al., 2007). Whereas, the genes within the corresponding genetic regions minimally influenced by environmental variation are most likely involved in the interconversion or biosynthesis pathways of sugars or acids (Coombe & McCarthy, 2000; Giongo et al., 2013; J. J. Giovannoni, 2004; Leiva-Valenzuela et al., 2013; X. Li et al., 2010; Matas,

Gapper, Chung, Giovannoni, & Rose, 2009; A. C. Paniagua et al., 2013; Posé et al., 2011; Zifkin et al., 2012). Further gene research on these genetic regions will elucidate the regulation of SS:TA ratio during blueberry ripening. Utilizing this knowledge along with incorporating these QTLs into future breeding strategies will aid in improving blueberry fruit quality and consumer appeal as the sugar to acid ratio is important to blueberry firmness, flavor, and anthocyanin synthesis signaling.

The total anthocyanin content trait quantifies the accumulation of anthocyanin metabolites, which is another very important fruit quality characteristic because anthocyanins are the dark blue color and nutritious antioxidants consumers prefer for blueberries (Grace, Xiong, Esposito, Ehlenfeldt, & Lila, 2018; James F. Hancock et al., 2018; Khoo et al., 2017; D. Li et al., 2017; Ma et al., 2018; Oh et al., 2018; S. Silva et al., 2018). The association mapping of total anthocyanin content identified three overlapping QTL regions that all contain significant QTLs for all three cofactor analyses (Table 2.8). The overlapping QTL region on linkage group eight between 80-84cM also contains a significant QTL for the 2011 year. Since the 2011 year QTL is less significant than the three cofactor analyses QTLs, this suggests this QTL region is partially influenced by the 2011 year for total anthocyanin content, but is more important as a QTL region for total anthocyanin regulation irrespective of location or year. The other overlapping QTL regions on linkage group six between 111-114cM and on linkage group 12 between 34-39cM contain significant QTLs for all three cofactor analyses with the “both location and year” cofactor analysis QTL showing the highest significance value, which indicates these QTL regions impact total anthocyanin content regardless of location or year. For all the QTL regions for total anthocyanin content, the genes within those corresponding genetic regions are involved in regulating anthocyanin accumulation through the shikimic acid, phenylpropanoid acid, or flavonoid synthesis pathways while not being substantially influenced by environmental variation from specific locations and years (Khoo et al., 2017; D. Li et al., 2017; Muleke et al., 2017; Oh et al., 2018; Overall et al., 2017; Scalzo, Stevenson, & Hedderley, 2015; S. Silva et al., 2018; Zorenc et al., 2017). Further gene research on these genetic regions will elucidate anthocyanin synthesis regulation at different stages of the overarching phenolic acid synthesis pathway as well as other signaling pathways during blueberry

ripening (Castellarin et al., 2016; Karppinen et al., 2013; Konarska, 2015; Oh et al., 2018; Xi et al., 2017; Zifkin et al., 2012). This knowledge can be utilized along with the QTL regions to inform future breeding strategies in improving blueberry fruit quality and health benefits through improving anthocyanin content, diversity, color, and nutrition.

When the overlapping QTL regions for each fruit quality trait were compared to regions for another fruit quality trait, eight multi-trait overlapping regions were revealed. The overlapping region on linkage group one at 87cM contains significant QTLs for days between full bloom and blue fruit and berry weight. The genes within this genetic region are most likely involved in regulating overall fruit development like cell division and transitions between fruit development stage 1 and 2 (Coombe & McCarthy, 2000; Godoy, Monterubbianesi, & Tognetti, 2008; Seymour, Østergaard, et al., 2013). The overlapping multi-trait region on linkage group eight at 89cM contains significant QTLs for TA and SS:TA ratio. The genes within this genetic region are most likely involved in regulating acidic metabolite accumulation and the ratio between acidic metabolites and sugars because it is the main contributor to consumer-drive blueberry flavor and induces for anthocyanin content (Barrett et al., 2010; Jeong et al., 2010; Jia et al., 2017; Kader, 2008; Pagliarini et al., 2013; Tieman et al., 2012; Wahyuningsih et al., 2017). The multi-trait overlapping QTL region on linkage group eight between 82-83cM contains significant QTLs for TA, SS:TA ratio, and total anthocyanin content. The genes within this genetic region are most likely involved in soluble sugar signaling to induce anthocyanin synthesis, phenolic acid synthesis to promote anthocyanin accumulation, and acidic metabolite accumulation to stabilize diverse anthocyanins (Couée et al., 2006; Gambetta et al., 2010; Jia et al., 2017; Konarska, 2015; Rabot et al., 2012; Serrano et al., 2017; Zifkin et al., 2012). The multi-trait overlapping QTL region on linkage group two between 57-59cM contains significant QTLs for fruit color rating and berry weight. The genes within this genetic region are mostly likely involved in regulating anthocyanin accumulation while concurrently regulating weight. This dual regulation could be due to either increasing the acidity so that anthocyanins stabilize and turgor increases, or increasing soluble sugar content so that anthocyanin synthesis is induced and tonicity increases the turgor pressure (Choi et al., 2002; Gilbert et al.,

2014; Klee, 2010; Konarska, 2015; Moggia et al., 2017; Osorio et al., 2013; Schwab et al., 2008; Wahyuningsih et al., 2017; Xi et al., 2017).

The other four multi-trait overlapping regions contain significant QTLs for traits involved in firmness and turgor pressure regulation. The multi-trait overlapping QTL region on linkage group one at 55cM contains significant QTLs for fruit firmness rating and berry firmness. The genes within this genetic region are most likely involved in regulating pathways like turgor pressure and berry skin strength (Blaker & Olmstead, 2015; Castellarin et al., 2016; Majda & Robert, 2018; Pilati et al., 2017; Toivonen & Brummell, 2008). The multi-trait overlapping QTL region on linkage group four at 64cM contains significant QTLs for pH and TA. The genetic region for this overlapping region probably contains genes involved in regulating acidity through TCA and phenolic acid synthesis pathways (Ayub et al., 2016; Barrett et al., 2010; Cappai et al., 2018; Conde et al., 2015; Coombe & McCarthy, 2000; Gilbert et al., 2015, 2014; Giongo et al., 2013; Kader, 2008; Konarska, 2015; Leng et al., 2014; Moggia et al., 2017; Oh et al., 2018; Serrano et al., 2017). The multi-trait overlapping QTL region on linkage group five at 60cM contains significant QTLs for % juice and TA. This genetic region probably contains genes involved in regulating acidity and turgor pressure (Castellarin et al., 2016; Jia et al., 2017; Majda & Robert, 2018; Perrot-Rechenmann, 2010). The multi-trait overlapping QTL region on linkage group eight between 40-46cM contains significant QTLs for % juice and SS. The genes within this genetic region are probably involved in regulating turgor pressure and soluble sugars (Castellarin et al., 2016; Conde et al., 2015; O'Hara et al., 2013; Posé et al., 2011; Wingler, 2017). Further gene research will investigate the genetic region for possible regulatory genes for turgor and sugar signaling, while future breeding strategies can utilize these QTLs to improve blueberry firmness without sacrificing juice or taste, which appeases both industry and consumer fruit quality preferences.

In summary, the 14 fruit quality traits represent many of the important processes occurring during blueberry fruit development and ripening (James F. Hancock et al., 2018). The association mapping of the individual phenotypes for the 14 fruit quality traits identified 75 total significant QTLs (Table 2.4). The association mapping of the 14 fruit quality traits for the specific locations revealed 73 total significant QTLs with 41.1% for

FL, 42.5% for GA, and 16.4% for OR locations (Table 2.5). When the 14 fruit quality traits were association mapped for specifically the 2011 and 2012 years, the mapping identified 28 significant QTLs with 57.1% for 2011 and 42.9% for 2012 (Table 2.5). Overall, the 14 fruit quality traits revealed similar numbers of significant QTLs for the FL and GA locations, which suggests both may influence fruit quality traits similarly (Table 2.5). The 14 fruit quality traits revealed 178 significant QTLs when the association mapping included the location cofactor, year cofactor, and both location and year cofactors (Table 2.5). Of the 178 significant QTLs for all the cofactor analyses, 34.8% were for the location cofactor, 29.2% for the year cofactor, and 36.0% for both location and year cofactors (Table 2.5). Further analysis of all the significant QTLs revealed the most, 51, overlapping QTL regions where three or more significant QTLs from different analyses were in the same region (Table 2.8). Of the 51 overlapping QTL regions, 25.5% of the regions contained significant QTLs for the location or year -specific analyses that were more significant, which suggests these regions are strongly impacted by the environmental variation from location or year (Table 2.8). The 74.5% of the total overlapping QTL regions that were more significant for the cofactor analyses, especially the “both location and year” cofactors QTLs, indicates that these QTL regions are important for regulating the fruit quality trait regardless of the environmental variation from location or year (Table 2.8). Although there are some QTL regions that will be more beneficial for future breeding strategies at specific locations or climates, the majority of the QTL regions identified with the 14 fruit quality traits can be utilized for breeding to improve fruit quality across different environmental conditions.

2.6. Conclusion

Blueberries, *Vaccinium corymbosum*, is an important fresh fruit crop given their recent publicity as a “super fruit” with very potent antioxidant properties (Betoret et al., 2011; Gowd, Jia, & Chen, 2017; McNamara et al., 2018; Morita, Naito, Yoshikawa, & Niki, 2017; Pan et al., 2017; N. Singh & Ghosh, 2019; Subash et al., 2014; Whyte et al., 2016). In particular, the antioxidant capacity of blueberries has been shown to reduce the oxidative stress of free radicals that increase the onset and progression of inflammation, heart disease, diabetes, neurological degeneration, and cancer (Gowd et

al., 2017; McNamara et al., 2018; Morita et al., 2017; Pan et al., 2017; N. Singh & Ghosh, 2019; Subash et al., 2014; Whyte et al., 2016). To increase production of blueberries, gaining a greater understanding of the different networks contributing to agronomic productivity will aid in fine-tuning selection for greater fruit production and longer harvest seasons. The advancements in bioinformatics computing allow for utilization of genomic datasets and statistics for genetic association mapping, which links variation in a trait to variation in a genetic marker (Borevitz & Chory, 2004; Chae, Kim, Nilo-Poyanco, & Rhee, 2014; Collard et al., 2005; Collard & Mackill, 2008; Kanehisa et al., 2017; M. S. Kang, 2002; T. Kim et al., 2017). The genetic association mapping identifies genetic regions or QTLs that are associated with differences in a quantitative trait because the genetic regions contain genetic variation that represents possible regulatory genes (Borevitz & Chory, 2004; Collard et al., 2005; M. S. Kang, 2002). The goal of this research was to identify significant QTLs associated with agronomic and fruit quality traits.

The DxJ mapping population is a valuable resource for investigating agronomic growth, dormancy break and flowering, and fruit quality characteristics because the Draper and Jewel cultivars are diverse commercial cultivars for NHB and SHB blueberries. Since Draper and Jewel cultivars are adapted to different environmental conditions, the DxJ progeny exhibit a wide range of growth traits, including leafing strength, floral bud density, and vigor. Plant growth regulation is a complex network of interacting signals, like hormones and sugars, that coordinate processes such as cell proliferation, cell differentiation, and resource allocation (Bennett et al., 2012; Buchanan et al., 2012; Del Pozo et al., 2005; O. Sadras & F. Denison, 2009; Takatsuka & Umeda, 2014; Xing et al., 2015).

Cell proliferation, cell differentiation, and resource allocation are all intertwined (Amasino & Michaels, 2010; Arora et al., 2003; Considine & Considine, 2016; Mathan et al., 2016; R. Mohamed et al., 2010; Signorelli et al., 2018; Swarup & Péret, 2012; van der Schoot & Rinne, 2011; Yang & Jiao, 2016). For example, resource allocation signaling regulates the transition from quiescent to active meristems, as well as the expansion of cells so they can differentiate into tissues (Patrick Achard et al., 2009; Bennett et al., 2012; Buchanan et al., 2012; Colebrook, Thomas, Phillips, & Hedden,

2014; R. Mohamed et al., 2010; O. Sadras & F. Denison, 2009; Reddy et al., 2013; Wasilewska et al., 2008; Yang & Jiao, 2016). The availability and signaling of resources is also very important in bud differentiation regulation as a depletion of resources results in the premature termination of the tissue (Bennett et al., 2012; Buchanan et al., 2012; Moghaddam & Ende, 2013; O'Hara et al., 2013; Ruan, 2014; Tsai & Gazzarrini, 2014; Wingler, 2017). The signaling and regulation of resource availability is essential for perennial plants because bud formation and differentiation as well as preparations for dormancy induction occurs after fruiting (Beauvieux et al., 2018; Considine & Considine, 2016; Cooke et al., 2012; Díaz-Riquelme et al., 2012; J. Li et al., 2018; Lloret et al., 2018; Malyshev et al., 2016; Rohde & Bhalerao, 2007; Shim et al., 2014; Vergara et al., 2017; Zheng et al., 2015).

The association mapping of the eight growth traits identified many significant QTLs using CIM for location-specific, year-specific, location cofactor, year cofactor, and “both location and year” cofactors analyses of vegetative meristem growth, bud meristem differentiation, and plant vigor traits. Of the multiple different mapping analyses conducted, the OR-specific location and 2012 year resulted in the most significant QTLs. The comparison of all the significant QTLs from all the different analyses revealed 43 overlapping QTL regions that contained at least three significant QTLs. While 12 of the 43 overlapping QTL regions are associated with vegetative meristem growth, 15 regions are associated specifically with bud meristem differentiation between vegetative and floral buds. Of the eight individual growth traits, the vigor rating trait identified the most overlapping QTL regions. Specifically the 16 overlapping QTL regions for this trait represents overall plant growth and efficient resource allocation after fruiting to prepare for dormancy (Bennett et al., 2012; Díaz-Riquelme et al., 2012; J. Li et al., 2018; O. Sadras & F. Denison, 2009; Xing et al., 2015).

To explore how the growth traits relate to one another, the overlapping QTL regions were analyzed further for multiple overlapping traits, which revealed seven multi-trait overlapping QTL regions. Three of the seven multi-trait regions contain significant QTLs for vegetative meristem growth, which indicates this region may regulate the induction of shoot apical and axillary meristem growth and rapid cell

differentiation and expansion into new vegetative tissue (Bar & Ori, 2014; Bennett et al., 2012; Considine & Considine, 2016; Signorelli et al., 2018; van der Schoot & Rinne, 2011). Two of the seven multi-trait regions contain significant QTLs for leafing strength and vigor after fruiting, which indicates these regions may regulate vegetative tissue expansion and density (Bar & Ori, 2014; Costes et al., 2014; Majda & Robert, 2018; Swarup & Péret, 2012). The remaining two multi-trait regions contain significant QTLs for bud meristem differentiation between vegetative and floral, which indicates these regions are most likely involved in signaling differentiation and resource availability signals as well as floral meristem identity genes (Bennett et al., 2012; Costes et al., 2014; R. Mohamed et al., 2010; Molinero-Rosales et al., 2004; O. Sadras & F. Denison, 2009; O'Hara et al., 2013; van der Schoot & Rinne, 2011; Wingler, 2017). Since there is limited information on floral bud differentiation from vegetative buds in perennial plants, further gene research within the genetic regions corresponding to these QTL regions will provide foundational knowledge for bud formation and differentiation (Costes et al., 2014; Meitha et al., 2018; Mert et al., 2013; R. Mohamed et al., 2010; Molinero-Rosales et al., 2004; van der Schoot & Rinne, 2011). Future breeding strategies can utilize this information and the identified QTL regions to improve meristem differentiation and floral bud density, which will subsequently improve blueberry yield per plant.

Since blueberries are woody, perennial shrubs, blueberry floral buds must overwinter and efficiently burst in early spring to produce blueberry fruit (Draper & Hancock, 2003; Lyrene, Journal, & Society, 2002; Trehane, 2004; Williamson & Lyrene, 2004). The coordination of floral bud dormancy break is a complex network that is essential for subsequent yield (Anderson, 2015; Beauvieux et al., 2018; Considine & Considine, 2016; Cooke et al., 2012; Die et al., 2016; Lloret et al., 2018; Z. Zhang et al., 2018). If the floral buds burst from dormancy too early, then there is a greater risk of frost damage to the delicate meristems (Buchanan et al., 2012; Trehane, 2004). If the floral buds burst from dormancy too late, then there is less pollination and fruit set due to competition with other plants (Buchanan et al., 2012; Trehane, 2004). Appropriately coordinating floral bud burst for different environments is the main issue inhibiting blueberry habitat expansion and productivity (J F Hancock et al., 2008; Trehane, 2004). Floral bud burst requires the coordination of multiple pathways (Anderson, 2015;

Beauvieux et al., 2018; Considine & Considine, 2016; Cooke et al., 2012; Die et al., 2016; Lloret et al., 2018; Malyshev et al., 2016; Lisa J Rowland et al., 2014; Yamane, 2014; Z. Zhang et al., 2018). The low oxygen and low carbon environment within the floral bud suggests the oxidative-ROS signaling and regulation pathways plays an important role in floral bud burst and flowering (Beauvieux et al., 2018; Lloret et al., 2018; Meitha et al., 2018; Signorelli et al., 2018). Sugar metabolism and signaling is another important pathway for dormancy break and flowering as the availability of carbon and energy is essential for a successful developmental transition to reproduction (Anderson, 2015; Beauvieux et al., 2018; Malyshev et al., 2016; Pagter et al., 2015; Z. Zhang et al., 2018).

The association mapping of the eight dormancy break and flowering traits identified many significant QTLs using CIM for location-specific, year-specific, location cofactor, year cofactor, and “both location and year” cofactors analyses. The GA-location and 2011 year resulted in the most significant QTLs. The comparison of all the significant QTLs from all the different analyses revealed four overlapping QTL regions that contained at least three significant QTLs. Of those four overlapping QTL regions, two of the overlapping QTL regions address the days until early green tip trait. In those two overlapping QTL regions, the year cofactor QTL was the most significant QTL, which indicates that the environmental variation between years strongly impacts leaf dormancy break. Of the four overlapping QTL regions, the other two overlapping QTL regions address the days until floral bud break trait. In those two overlapping QTL regions, the environmental variation from different locations strongly impacts the regulation of floral bud dormancy break. Since both bud dormancy break traits also contained significant QTLs for the “both location and year” cofactor analysis in the overlapping region, the corresponding genetic regions should be further investigated for regulatory genes in pathways like oxidative signaling, sugar signaling, or hormone regulation because multiple studies indicate they are vital in regulating bud dormancy break across a variety of environmental conditions (Beauvieux et al., 2018; Considine & Considine, 2016; Cooke et al., 2012; Díaz-Riquelme et al., 2012; J. Li et al., 2018; Lloret et al., 2018; Malyshev et al., 2016; van der Schoot & Rinne, 2011; Vergara et al., 2017; Z. Zhang et al., 2018; Zheng et al., 2015). The many other significant QTLs for the eight

dormancy break and flowering traits are also important for future gene research as the majority were significant for location or year -specific analyses, which supports the influence environmental conditions have on dormancy break and flowering regulation (Arora et al., 2003; Basler & Körner, 2012, 2014; Beauvieux et al., 2018; Cooke et al., 2012; Ghelardini et al., 2009; D. P. Horvath et al., 2003; Malyshev et al., 2016; Rohde & Bhalerao, 2007; Shim et al., 2014; R. K. Singh et al., 2017). Utilizing these dormancy break and flowering QTLs for future breeding strategies will aid in narrowing the QTL and genetic regions through fine-mapping and in improving the efficiency of dormancy break and floral maturation to increase blueberry's yield and productive growth range (Arora et al., 2003; M. Ehlenfeldt, 2012; Jim F Hancock, 2008; Kovaleski et al., 2015; G. A. Lobos & Hancock, 2015; Melke, 2015; Lisa J Rowland et al., 2008; Trehane, 2004).

Traditionally, fruit quality was determined by storage and shelf-life, leading to breeders selecting for fruits that ripened very slowly (Betoret et al., 2011; Biltekoff, 2010; Grunert, 2005; Kader, 2008; Kearney, 2010; Kyriacou & Roupheal, 2018). Unfortunately, this has led to many fruits and vegetables becoming too firm and tasteless, increasing consumer awareness of fruit quality perception discrepancies (Biltekoff, 2010; Kader, 2008; Kearney, 2010; Kyriacou & Roupheal, 2018; Sam Saguy, 2011; Tieman et al., 2012). For blueberries, good fruit quality characteristics from the consumer perspective consist of firm, juicy, sweet, and blue colored berries (Barrett et al., 2010; Cappai et al., 2018; Gilbert et al., 2014; Giongo et al., 2013; Kader, 2008; Leiva-Valenzuela et al., 2013; Matas et al., 2009; Saftner et al., 2008). Transport and processing companies deem firmness a good fruit quality characteristic because it reduces tissue damage, and thus reduces product loss (Barrett et al., 2010; Biltekoff, 2010; Gilbert et al., 2014; P. Li et al., 2011; X. Li et al., 2010; Matas et al., 2009; Sam Saguy, 2011).

The slower ripening process selected for by industry most likely differentially regulates the development and onset of ripening, which results in firmness and flavor that is unwanted by consumers (Giongo et al., 2013; X. Li et al., 2010; Matas et al., 2009; Prasanna et al., 2007). Blueberries exhibit double sigmoid fruit development and non-climacteric fruit ripening (Cappai et al., 2018; Coombe & McCarthy, 2000; Klee, 2010; Osorio et al., 2013; Prasanna et al., 2007; Serrano et al., 2017; Seymour,

Chapman, et al., 2013; Seymour, Østergaard, et al., 2013). Since double sigmoid development has two growth stages, the cell proliferation and expansion pathways are important regulators in the development of large, firm, weighty blueberries that consumers prefer (Castellarin et al., 2016; Coombe & McCarthy, 2000; Godoy et al., 2008; Serrano et al., 2017). In between the growth stages, there is a lag stage where fruit growth pauses so that the fruit can accumulate sugars and metabolite precursors to prepare for the subsequent growth stage and ripening (Castellarin et al., 2016; Coombe & McCarthy, 2000; Godoy et al., 2008; Serrano et al., 2017). Fruit ripening occurs at the beginning of the third stage and utilizes auxin, ABA, and GA to mediate the cross-talk between multiple pathways to induce rapid growth with acidic cell expansion, soluble sugar accumulation, turgor pressure, and pigment accumulation (Cappai et al., 2018; Castellarin et al., 2016; J. J. Giovannoni, 2004; Huan et al., 2016; Jia et al., 2017; Matas et al., 2009; Osorio et al., 2013; Prasanna et al., 2007; Seymour, Østergaard, et al., 2013). In order to investigate the multiple different pathways involved in fruit development and ripening, the 14 fruit quality traits in this research represent consumer-driven fruit quality characteristics like firmness, color, taste, and nutrition, while also representing the above-mentioned ripening regulatory pathways (Cappai et al., 2018; Gilbert et al., 2015, 2014; Saftner et al., 2008; J. L. Silva et al., 2005).

The association mapping of the 14 fruit quality traits identified many significant QTLs for fruit development, ripening, and quality using CIM and multiple different mapping analyses. Of all the different mapping analyses using CIM, the FL and GA - specific locations revealed the most significant QTLs. The comparison of all the significant QTLs from all the different analyses revealed 51 overlapping QTL regions that contained at least three significant QTLs. While one of the 51 overlapping QTL regions is associated with fruit development processes, five regions are specifically associated with color and anthocyanins. Of the 51 overlapping QTL regions, 25 overlapping regions are specifically associated with firmness and turgor pressure traits. The remaining 20 overlapping QTL regions are associated with the pH, SS, TA, and SS:TA ratio traits, which can contribute to regulating color, firmness, turgor, or flavor (Castellarin et al., 2016; Forney, Kalt, Jordan, Vinqvist-Tymchuk, & Fillmore, 2012; Gilbert et al., 2015, 2014; T. E. Lobos et al., 2018; Montecchiarini et al., 2018). When

the overlapping QTL regions were analyzed further for multiple overlapping traits, eight multi-trait overlapping QTL regions were revealed. One multi-trait region contained significant QTLs for TA, SS:TA ratio, and total anthocyanin content, which indicates this region may regulate anthocyanin accumulation as acidity and sugars induce anthocyanin diversity synthesis (Howard et al., 2016; Jia et al., 2017; Karppinen et al., 2013; Oh et al., 2018; Wahyuningsih et al., 2017). Another multi-trait region contained significant QTLs for TA and SS:TA ratio, which indicates this region may be important for regulating blueberry flavor (Barrett et al., 2010; Gilbert et al., 2015, 2014, 2013; Kader, 2008; Klee, 2010; Tieman et al., 2012). Four of the eight multi-trait regions contained significant QTLs for at least two traits involved in regulating firmness and turgor pressure, which strongly suggests that blueberry firmness and turgor pressure are closely associated within the DxJ population. Since there is limited information on the regulation of berry firmness and fruit turgor pressure, further gene research within the genetic regions of these QTL regions will provide foundational knowledge for berry firmness regulation (Castellarin et al., 2016; Giongo et al., 2013; Gould et al., 2013; Konarska, 2015; Montecchiarini et al., 2018; A. C. Paniagua et al., 2013; A. K. Yadav & Singh, 2014). Future breeding strategies can utilize this information and the identified QTL regions to improve berry firmness and turgor pressure while concurrently improving color, texture, flavor, and nutrition fruit quality.

The goal of this research was to identify important QTLs for different agronomic growth, dormancy break and flowering, and fruit quality traits. Improving the vegetative and floral bud growth along with the efficiency of bud dormancy break will increase bud density and reduce bud tissue damage. This will subsequently improve blueberry productivity and growth range. Through investigating the different fruit quality traits, future gene research can elucidate regulatory information while future breeding strategies can utilize the QTL regions to improve blueberry ripening along with fruit quality characteristics preferred by both industry and consumers. Overall, the results provide valuable foundational knowledge for blueberry resources to develop specific markers and breeding strategies for specific agronomic or fruit quality traits. As a result, more blueberries will be produced that more consumers will want to eat, and will benefit from their potent nutritious qualities.

2.7. Acknowledgments

This work was supported by both the Plant Pathways Elucidation Project through Dr. Lila and Dr. Li, and the NCSU faculty start-up funds from Dr. Li. A special thank you to Dr. Hancock, Dr. Finn, and Dr. Olmstead for coordinating and phenotyping the DxJ blueberries from FL, GA, and OR for both 2011 and 2012. Thank you to Dr. Nahla Bassil and her lab at the National Clonal Germplasm Repository at USDA-Agriculture Research Service for analyzing the DxJ genetic markers. A special thank you to Dr. Eric Jackson and Dr. Jaime Sheridan from General Mills for guiding and working with me to assemble the DxJ genetic map used throughout the DxJ association mapping. A special thank you to the P²EP summer undergraduate interns - Doriane Taylor, Zjanazja Cornwall, Jonathan Fabish, James Lohr, Ashley Wagoner, Jordan Hunt, Bryan Morris, Estefania Castro-Vazquez - for working with me to organize and conduct the biparental association mapping for all the agronomic and fruit quality traits.

REFERENCES

- Achard, P., Baghour, M., Chapple, A., Hedden, P., Van Der Straeten, D., Genschik, P., ... Harberd, N. P. (2007). The plant stress hormone ethylene controls floral transition via DELLA-dependent regulation of floral meristem-identity genes. *Proceedings of the National Academy of Sciences*, *104*(15), 6484–6489.
- Achard, Patrick, & Davie, J. (2015). A Pivotal Role of DELLAs in Regulating Multiple Hormone Signals.
- Achard, Patrick, Gusti, A., Cheminant, S., Alioua, M., Dhondt, S., Coppens, F., ... Genschik, P. (2009). Gibberellin Signaling Controls Cell Proliferation Rate in Arabidopsis. *Current Biology*, *19*(14), 1188–1193.
- Al-Khayri, J. M., Jain, S. M., & Johnson, D. V. (2015). *Advances in Plant Breeding Strategies: Breeding, Biotechnology and Molecular Tools*. Cham: Springer International Publishing.
- Albani, M. C., & Coupland, G. (2010). Comparative analysis of flowering in annual and perennial plants. *Current Topics in Developmental Biology*, *91*(C), 323–348.
- Alcalde, A., & Bogs, J. (2017). A group of grapevine MYBA transcription factors located in chromosome 14 control anthocyanin synthesis in vegetative organs with different specificities compared with the berry color locus, *5*, 220–236.
- Ali Ghasemzadeh. (2011). Flavonoids and phenolic acids: Role and biochemical activity in plants and human. *Journal of Medicinal Plants Research*, *5*(31), 6697–6703.
- Alonso, J. M., & Stepanova, A. N. (2004). The Ethylene Signaling Pathway. *Science*, *306*(5701), 1513–1515.
- Amasino, R. M., & Michaels, S. D. (2010). The Timing of Flowering. *Plant Physiology*, *154*(2), 516–520.
- Anderson, J. V. (2015). *Advances in plant dormancy*. (J. V. Anderson, Ed.). New York, NY: Springer Science+Business Media.
- Arora, R., & Rowland, L. J. (2011). Physiological research on winter-hardiness: deacclimation resistance, reacclimation ability, photoprotection strategies, and a cold acclimation protocol design. *HortScience*, *46*(8), 1070–1078.
- Arora, R., Rowland, L. J., & Tanino, K. (2003). Induction and release of bud dormancy in woody perennials: A science comes of age. *HortScience*, *38*(5), 911–921.
- Ayub, R. A., Bosetto, L., Galvão, C. W., Etto, R. M., Inaba, J., & Lopes, P. Z. (2016). Abscisic acid involvement on expression of related gene and phytochemicals during ripening in strawberry fruit *Fragaria × ananassa* cv. Camino Real. *Scientia Horticulturae*, *203*, 178–184.
- Azzi, L., Deluche, C., Gévaudant, F., Frangne, N., Delmas, F., Hernould, M., & Chevalier, C. (2015). Fruit growth-related genes in tomato. *Journal of Experimental Botany*, *66*(4), 1075–1086.
- Baena-González, E., Rolland, F., Thevelein, J. M., & Sheen, J. (2007). A central integrator of transcription networks in plant stress and energy signalling. *Nature*, *448*(7156), 938–942.
- Bar, M., & Ori, N. (2014). Leaf development and morphogenesis. *Development*, *141*(22), 4219–4230.
- Barrett, D. M., Beaulieu, J. C., & Shewfelt, R. (2010). Color, flavor, texture, and nutritional quality of fresh-cut fruits and vegetables: Desirable levels, instrumental and sensory measurement, and the effects of processing. *Critical Reviews in Food*

- Science and Nutrition*, 50(5), 369–389.
- Basler, D., & Körner, C. (2012). Photoperiod sensitivity of bud burst in 14 temperate forest tree species. *Agricultural and Forest Meteorology*, 165, 73–81.
- Basler, D., & Körner, C. (2014). Photoperiod and temperature responses of bud swelling and bud burst in four temperate forest tree species. *Tree Physiology*, 34(4), 377–388.
- Beauvieux, R., Wenden, B., & Dirlwanger, E. (2018). Bud Dormancy in Perennial Fruit Tree Species: A Pivotal Role for Oxidative Cues. *Frontiers in Plant Science*, 9(May), 1–13.
- Ben Mohamed, H., Vadel, A. M., Geuns, J. M. C., & Khemira, H. (2012). Carbohydrate changes during dormancy release in Superior Seedless grapevine cuttings following hydrogen cyanamide treatment. *Scientia Horticulturae*, 140, 19–25.
- Bennett, E., Roberts, J. A., & Wagstaff, C. (2012). Manipulating resource allocation in plants. *Journal of Experimental Botany*, 63(9), 3391–3400.
- Bernardo, R. (2008). Molecular markers and selection for complex traits in plants: Learning from the last 20 years. *Crop Science*, 48(5), 1649–1664.
- Betoret, E., Betoret, N., Vidal, D., & Fito, P. (2011). Functional foods development: Trends and technologies. *Trends in Food Science and Technology*, 22(9), 498–508.
- Biltekoff, C. (2010). Consumer response: The paradoxes of food and health. *Annals of the New York Academy of Sciences*, 1190, 174–178.
- Blaker, K. M. (2013). *Comparison of Crisp and Standard Fruit Texture in Southern Highbush Blueberry Using Instrumental and Sensory Panel Techniques*. University of Florida.
- Blaker, K. M., & Olmstead, J. W. (2015). Cell wall composition of the skin and flesh tissue of crisp and standard texture southern highbush blueberry genotypes. *Journal of Berry Research*, 5(1), 9–15.
- Blaker, K. M., Plotto, A., Baldwin, E. A., & Olmstead, J. W. (2014). Correlation between sensory and instrumental measurements of standard and crisp-texture southern highbush blueberries (*Vaccinium corymbosum* L. interspecific hybrids): Southern highbush blueberry texture. *Journal of the Science of Food and Agriculture*, 94(13), 2785–2793.
- Borevitz, J. O., & Chory, J. (2004). Genomics tools for QTL analysis and gene discovery. *Current Opinion in Plant Biology*, 7(2), 132–136.
- Bornsek, S. M., Ziberna, L., Polak, T., Vanzo, A., Ulrich, N. P., Abram, V., ... Passamonti, S. (2012). Bilberry and blueberry anthocyanins act as powerful intracellular antioxidants in mammalian cells. *Food Chemistry*, 134(4), 1878–1884.
- Bradshaw, J. E., Hackett, C. A., Pande, B., Waugh, R., & Bryan, G. J. (2008). QTL mapping of yield, agronomic and quality traits in tetraploid potato (*Solanum tuberosum* subsp. *tuberosum*). *Theoretical and Applied Genetics*, 116(2), 193–211.
- Brelsford, C. C., & Robson, T. M. (2018). Blue light advances bud burst in branches of three deciduous tree species under short-day conditions. *Trees - Structure and Function*, 32(4), 1157–1164.
- Brevis, P. A., Bassil, N. V., Ballington, J. R., & Hancock, J. F. (2008). Impact of wide hybridization on highbush blueberry breeding. *Journal of the American Society for Horticultural Science*, 133(3), 427–437.

- Brito, A., Areche, C., Sepúlveda, B., Kennelly, E. J., & Simirgiotis, M. J. (2014). Anthocyanin characterization, total phenolic quantification and antioxidant features of some Chilean edible berry extracts. *Molecules*, *19*(8), 10936–10955.
- Buchanan, B. B., Gruissem, W., & Jones, R. L. (2012). *Biochemistry & Molecular Biology of Plants*. American Society of Plant Biologists: 15501 Monona Drive, Rockville, MD 20855-2768 USA: Markono Print Media Pte Ltd.
- Cabrera-Bosquet, L., Crossa, J., von Zitzewitz, J., Serret, M. D., & Luis Araus, J. (2012). High-throughput Phenotyping and Genomic Selection: The Frontiers of Crop Breeding Converge. *Journal of Integrative Plant Biology*, *54*(5), 312–320.
- Cappai, F., Benevenuto, J., Ferrão, L., & Munoz, P. (2018). Molecular and Genetic Bases of Fruit Firmness Variation in Blueberry—A Review. *Agronomy*, *8*(9), 174.
- Carreno-Quintero, N., Bouwmeester, H. J., & Keurentjes, J. J. B. (2013). Genetic analysis of metabolome–phenotype interactions: from model to crop species. *Trends in Genetics*, *29*(1), 41–50.
- Castellarin, S. D., & Di Gaspero, G. (2007). Transcriptional control of anthocyanin biosynthetic genes in extreme phenotypes for berry pigmentation of naturally occurring grapevines. *BMC Plant Biology*, *7*, 1–10.
- Castellarin, S. D., Gambetta, G. A., Wada, H., Krasnow, M. N., Cramer, G. R., Peterlunger, E., ... Matthews, M. A. (2016). Characterization of major ripening events during softening in grape: Turgor, sugar accumulation, abscisic acid metabolism, colour development, and their relationship with growth. *Journal of Experimental Botany*, *67*(3), 709–722.
- Chae, L., Kim, T., Nilo-Poyanco, R., & Rhee, S. Y. (2014). Genomic Signatures of Specialized Metabolism in Plants. *Science*, *344*(May), 510–513.
- Chen, H., Cao, S., Fang, X., Mu, H., Yang, H., Wang, X., ... Gao, H. (2015). Changes in fruit firmness, cell wall composition and cell wall degrading enzymes in postharvest blueberries during storage. *Scientia Horticulturae*, *188*, 44–48.
- Choi, C., Wiersma, P. A., Toivonen, P., & Kappel, F. (2002). Fruit growth, firmness and cell wall hydrolytic enzyme activity during development of sweet cherry fruit treated with gibberellic acid (GA3). *Journal of Horticultural Science and Biotechnology*, *77*(5), 615–621.
- Chu, W., Gao, H., Chen, H., Fang, X., & Zheng, Y. (2018). Effects of cuticular wax on the postharvest quality of blueberry fruit. *Food Chemistry*, *239*, 68–74.
- Claeys, H., De Bodt, S., & Inzé, D. (2014). Gibberellins and DELLAs: Central nodes in growth regulatory networks. *Trends in Plant Science*, *19*(4), 231–239.
- Colebrook, E. H., Thomas, S. G., Phillips, A. L., & Hedden, P. (2014). The role of gibberellin signalling in plant responses to abiotic stress. *Journal of Experimental Biology*, *217*(1), 67–75.
- Collard, B. C. Y., Jahufer, M. Z. Z., Brouwer, J. B., & Pang, E. C. K. (2005). An introduction to markers, quantitative trait loci (QTL) mapping and marker-assisted selection for crop improvement: The basic concepts. *Euphytica*, *142*(1–2), 169–196.
- Collard, B. C. Y., & Mackill, D. J. (2008). Marker-assisted selection: an approach for precision plant breeding in the twenty-first century. *Philosophical Transactions of the Royal Society B: Biological Sciences*, *363*(1491), 557–572.
- Conde, A., Regalado, A., Rodrigues, D., Costa, J. M., Blumwald, E., Chaves, M. M., &

- Gerós, H. (2015). Polyols in grape berry: Transport and metabolic adjustments as a physiological strategy for water-deficit stress tolerance in grapevine. *Journal of Experimental Botany*, 66(3), 889–906.
- Considine, M. J., & Considine, J. A. (2016). On the language and physiology of dormancy and quiescence in plants. *Journal of Experimental Botany*, 67(11), 3189–3203.
- Conti, L. (2017). Hormonal control of the floral transition: Can one catch them all? *Developmental Biology*, 430(2), 288–301.
- Cooke, J. E. K., Eriksson, M. E., & Junttila, O. (2012). The dynamic nature of bud dormancy in trees: environmental control and molecular mechanisms. *Plant, Cell & Environment*, 35(10), 1707–1728.
- Coombe, B. G., & McCarthy, M. G. (2000). Dynamics of grape growth and physiology of ripening. *Australian Journal of Grape and Wine Research*, 6(2), 131–135.
- Costes, E., Crespel, L., Denoyes, B., Morel, P., Demene, M.-N., Lauri, P.-E., & Wenden, B. (2014). Bud structure, position and fate generate various branching patterns along shoots of closely related Rosaceae species: a review. *Frontiers in Plant Science*, 5(December), 1–11.
- Couée, I., Sulmon, C., Gouesbet, G., & El Amrani, A. (2006). Involvement of soluble sugars in reactive oxygen species balance and responses to oxidative stress in plants. *Journal of Experimental Botany*, 57(3), 449–459.
- D'Ovidio, R., Mattei, B., Roberti, S., & Bellincampi, D. (2004). Polygalacturonases, polygalacturonase-inhibiting proteins and pectic oligomers in plant–pathogen interactions. *Biochimica et Biophysica Acta (BBA) - Proteins and Proteomics*, 1696(2), 237–244.
- Daviere, J.-M., & Achard, P. (2013). Gibberellin signaling in plants. *Development*, 140(6), 1147–1151.
- De Lucas, M., Davière, J. M., Rodríguez-Falcón, M., Pontin, M., Iglesias-Pedraz, J. M., Lorrain, S., ... Prat, S. (2008). A molecular framework for light and gibberellin control of cell elongation. *Nature*, 451(7177), 480–484.
- De Souza, V. R., Pereira, P. A. P., Da Silva, T. L. T., De Oliveira Lima, L. C., Pio, R., & Queiroz, F. (2014). Determination of the bioactive compounds, antioxidant activity and chemical composition of Brazilian blackberry, red raspberry, strawberry, blueberry and sweet cherry fruits. *Food Chemistry*, 156, 362–368.
- Del Pozo, J. C., Lopez-Matas, M. A., Ramirez-Parra, E., & Gutierrez, C. (2005). Hormonal control of the plant cell cycle. *Physiologia Plantarum*, 123(2), 173–183.
- Development, R. (2010). *The Plant Hormone Ethylene. Annual Plant Reviews (Vol. 37)*.
- Dhanaraj, A. L., Alkharouf, N. W., Beard, H. S., Chouikha, I. B., Matthews, B. F., Wei, H., ... Rowland, L. J. (2007). Major differences observed in transcript profiles of blueberry during cold acclimation under field and cold room conditions. *Planta*, 225(3), 735–751.
- Díaz-Riquelme, J., Grimplet, J., Martínez-Zapater, J. M., & Carmona, M. J. (2012). Transcriptome variation along bud development in grapevine (*Vitis vinifera* L.). *BMC Plant Biology*, 12.
- Die, J. V., Arora, R., & Rowland, L. J. (2016). Global patterns of protein abundance during the development of cold hardiness in blueberry. *Environmental and Experimental Botany*, 124, 11–21.

- Die, J. V., & Rowland, L. J. (2013). Advent of genomics in blueberry. *Molecular Breeding*, 32(3), 493–504.
- Draper, A., & Hancock, J. F. (2003). Florida 4B: Native Blueberry with Exceptional Breeding Value. *Journal of the American Pomological Society*, 57(4), 138–141.
- Drewnowski, A., & Gomez-Carneros, C. (2000). Bitter taste, phytonutrients, and the consumer: a review. *The American Journal of Clinical Nutrition*, 72(6), 1424–1435.
- Du, X., & Rouseff, R. (2014). Aroma active volatiles in four southern highbush blueberry cultivars determined by gas chromatography-olfactometry (GC-O) and gas chromatography-mass spectrometry (GC-MS). *Journal of Agricultural and Food Chemistry*, 62(20), 4537–4543.
- Dubois, M., Van den Broeck, L., & Inzé, D. (2018). The Pivotal Role of Ethylene in Plant Growth. *Trends in Plant Science*, 23(4), 311–323.
- Durbak, A. R., & Tax, F. E. (2011). CLAVATA Signaling Pathway Receptors of Arabidopsis Regulate Cell Proliferation in Fruit Organ Formation as well as in Meristems. *Genetics*, 189(1), 177–194.
- Edirisinghe, I., & Burton-Freeman, B. (2016). Anti-diabetic actions of Berry polyphenols - Review on proposed mechanisms of action. *Journal of Berry Research*, 6(2), 237–250.
- Ehlenfeldt, M. (2012). Cold-hardiness, acclimation, and deacclimation among diverse blueberry genotypes. *Journal of the ...*, 137(1), 31–37.
- Ehlenfeldt, M K, & Rowland, L. J. (2006). Main content area Cold-hardiness of *Vaccinium ashei* and *V. constablaei* germplasm and the potential for northern-adapted rabbiteye cultivars. *Acta Horticulturae*, (715), 77–80.
- Ehlenfeldt, Mark K. (1994). The genetic composition and tetrasomic inbreeding coefficients of highbush blueberry cultivars. *HortScience*, 29(11), 1342–1345.
- Ehlenfeldt, Mark K. (2003). Investigations of Metaxenia in Northern Highbush Blueberry (*Vaccinium corymbosum* L.) Cultivars. *Journal of the American Pomological Society*, 57(1), 26–31.
- Ehlenfeldt, Mark K, Rowland, L. J., Ogden, E. L., & Vinyard, B. T. (2007). Floral bud cold hardiness of *Vaccinium ashei*, *V. constablaei*, and hybrid derivatives and the potential for producing northern-adapted rabbiteye cultivars. *HortScience*, 42(5), 1131–1134.
- Eklund, B. (2016). *2016 Blueberry Statistics - USDA*. Trenton.
- Etienne, A., Génard, M., Lobit, P., Mbeguié-A-Mbéguié, D., & Bugaud, C. (2013). What controls fleshy fruit acidity? A review of malate and citrate accumulation in fruit cells. *Journal of Experimental Botany*, 64(6), 1451–1469.
- Fadón, E., Herrero, M., & Rodrigo, J. (2018). Dormant Flower Buds Actively Accumulate Starch over Winter in Sweet Cherry. *Frontiers in Plant Science*, 9(February), 1–10.
- FDA. (2019). *Dietary Fiber - Interactive Nutrition Facts Label*.
- Feenstra, B. (2006). Mapping Quantitative Trait Loci by an Extension of the Haley-Knott Regression Method Using Estimating Equations. *Genetics*, 173(4), 2269–2282.
- Fennell, A. (2004). Freezing Tolerance and Injury in Grapevines. *Journal of Crop Improvement*, 10(1–2), 201–235.
- Fenwick, G. R., Griffiths, N. M., & Heaney, R. K. (1983). Bitterness in Brussels sprouts (*Brassica oleracea* L. var. *gemmifera*): the role of glucosinolates and their breakdown products. *Journal of the Science of Food and Agriculture*, 34(1), 73–80.

- Finn, C. E., Hancock, J. ., T. Mackey, & Serce, S. (2003). Genotype × Environment Interactions in Highbush Blueberry (*Vaccinium* sp . L .) Families Grown in Michigan and Oregon. *J Am Soc Hort Sci*, 128(2), 196–200.
- Finn, C. E., Hancock, J. F., Mackey, T., & Serce, S. (2003). GenotypeXEnvironment Interactions in Highbush Blueberry (*Vaccinium* sp. L.) Families Grown in Michigan and Oregon. *Journal of American Soci and Horticulture Science*, 128(2), 196–200.
- Fischer, R. A., & Edmeades, G. O. (2010). Breeding and cereal yield progress. *Crop Science*, 50(April), S-85-S-98.
- Foolad, M. R., & Panthee, D. R. (2012). Marker-Assisted Selection in Tomato Breeding. *Critical Reviews in Plant Sciences*, 31(2), 93–123.
- Forney, C. F., Kalt, W., Jordan, M. A., Vinqvist-Tymchuk, M. R., & Fillmore, S. A. E. (2012). Blueberry and cranberry fruit composition during development. *Journal of Berry Research*, 2(3), 169–177.
- Foyer, C. H., & Noctor, G. (2011). Ascorbate and Glutathione: The Heart of the Redox Hub. *Plant Physiology*, 155(1), 2–18.
- Gambetta, G. A., Matthews, M. A., Shaghasi, T. H., McElrone, A. J., & Castellarin, S. D. (2010). Sugar and abscisic acid signaling orthologs are activated at the onset of ripening in grape. *Planta*, 232(1), 219–234.
- Gambín, B. L., & Borrás, L. (2010). Resource distribution and the trade-off between seed number and seed weight: A comparison across crop species. *Annals of Applied Biology*, 156(1), 91–102.
- Gardner, K. M., Brown, P., Cooke, T. F., Cann, S., Costa, F., Bustamante, C., ... Myles, S. (2014). Fast and Cost-Effective Genetic Mapping in Apple Using Next-Generation Sequencing. *G3: Genes|Genomes|Genetics*, 4(9), 1681–1687.
- Garrido-Cardenas, J. A., Mesa-Valle, C., & Manzano-Agugliaro, F. (2018). Trends in plant research using molecular markers. *Planta*, 247(3), 543–557.
- Ghelardini, L., Santini, A., Black-Samuelsson, S., Myking, T., & Falusi, M. (2009). Bud dormancy release in elm (*Ulmus* spp.) clones - A case study of photoperiod and temperature responses. *Tree Physiology*, 30(2), 264–274.
- Giacalone, M., Di Sacco, F., Traupe, I., Topini, R., Forfori, F., & Giunta, F. (2011). Antioxidant and neuroprotective properties of blueberry polyphenols: a critical review. *Nutritional Neuroscience*, 14(3), 119–125.
- Gilbert, J. L., Guthart, M. J., Gezan, S. A., de Carvalho, M. P., Schwieterman, M. L., Colquhoun, T. A., ... Olmstead, J. W. (2015). Identifying breeding priorities for blueberry flavor using biochemical, sensory, and genotype by environment analyses. *PloS One*, 10(9), 1–21.
- Gilbert, J. L., Olmstead, J. W., Colquhoun, T. A., Levin, L. A., Clark, D. G., & Moskowitz, H. R. (2014). Consumer-assisted selection of blueberry fruit quality traits. *HortScience*, 49(7), 864–873.
- Gilbert, J. L., Schwieterman, M. L., Colquhoun, T. A., Clark, D. G., & Olmstead, J. W. (2013). Potential for increasing southern highbush blueberry flavor acceptance by breeding for major volatile components. *HortScience*, 48(7), 835–843.
- Giongo, L., Poncetta, P., Loretto, P., & Costa, F. (2013). Texture profiling of blueberries (*Vaccinium* spp.) during fruit development, ripening and storage. *Postharvest Biology and Technology*, 76, 34–39.

- Giovannoni, J. (2001). Molecular Biology of Fruit Maturation and Ripening. *Annual Review of Plant Physiology and Plant Molecular Biology*, 52, 725–749.
- Giovannoni, J. J. (2004). Genetic Regulation of Fruit Development and Ripening. *The Plant Cell*, 16, S170–S180.
- Godoy, C., Monterubbianesi, G., & Tognetti, J. (2008). Analysis of highbush blueberry (*Vaccinium corymbosum* L.) fruit growth with exponential mixed models. *Scientia Horticulturae*, 115(4), 368–376.
- Goff, S. A., & Klee, H. J. (2006). Plant Volatile Compounds: Sensory Cues for Health and Nutritional Value? *Science, New Series*, 311(5762), 815–819.
- Gould, N., Morrison, D. R., Clearwater, M. J., Ong, S., Boldingh, H. L., & Minchin, P. E. H. (2013). Elucidating the sugar import pathway into developing kiwifruit berries (*Actinidia deliciosa*). *New Zealand Journal of Crop and Horticultural Science*, 41(4), 189–206.
- Gowd, V., Jia, Z., & Chen, W. (2017). Anthocyanins as promising molecules and dietary bioactive components against diabetes – A review of recent advances. *Trends in Food Science and Technology*, 68, 1–13.
- Grace, M. H., Xiong, J., Esposito, D., Ehlenfeldt, M., & Lila, M. A. (2018). Simultaneous LC-MS quantification of anthocyanins and non-anthocyanin phenolics from blueberries with widely divergent profiles and biological activities. *Food Chemistry*.
- Granot, D., David-Schwartz, R., & Kelly, G. (2013). Hexose Kinases and Their Role in Sugar-Sensing and Plant Development. *Frontiers in Plant Science*, 4(March), 1–17.
- Grant, T. N., Dami, I. E., Ji, T., Scurlock, D., & Streeter, J. (2009). Variation leaf bud soluble sugar concentration among *Vitis* genotypes grown under two temperature regimes. *Canadian Journal of Plant Science*, 89, 961–968.
- Gray, S. B., & Brady, S. M. (2016). Plant developmental responses to climate change. *Developmental Biology*, 419(1), 64–77.
- Grunert, K. G. (2005). Food quality and safety: Consumer perception and demand. *European Review of Agricultural Economics*, 32(3), 369–391.
- Gubler, F., Hughes, T., Waterhouse, P., & Jacobsen, J. (2008). Regulation of Dormancy in Barley by Blue Light and After-Ripening: Effects on Abscisic Acid and Gibberellin Metabolism. *Plant Physiology*, 147(2), 886–896.
- Gündüz, K., Serçe, S., & Hancock, J. F. (2015). Variation among highbush and rabbiteye cultivars of blueberry for fruit quality and phytochemical characteristics. *Journal of Food Composition and Analysis*, 38, 69–79.
- Guo, J., Wang, S., Yu, X., Dong, R., Li, Y., Mei, X., & Shen, Y. (2018). Polyamines Regulate Strawberry Fruit Ripening by ABA, IAA, and Ethylene. *Plant Physiology*, 177(May), pp.00245.2018.
- Gutierrez, C. (2009). The Arabidopsis Cell Division Cycle. *The Arabidopsis Book*, 7, e0120.
- Hackett, C. A., Bradshaw, J. E., & McNicol, J. W. (2001). Interval mapping of quantitative trait loci in autotetraploid species. *Genetics*, 159(4), 1819–1832.
- Hancock, J F, Lyrene, P., Finn, C. E., Vorsa, N., Lobos, G. A., Building, S. S., ... Agronomia, D. (2008). Blueberries and Cranberries. In James F. Hancock (Ed.), *Temperate Fruit Crop Breeding: Germplasm to Genomics* (pp. 1–31). Dordrecht, The Netherlands: Springer, Kluwer Academic Publishers.
- Hancock, James F., Olmstead, J. W., Iltle, R. A., Callow, P. W., Neils-Kraft, S., Wheeler,

- E. J., ... Finn, C. E. (2018). Performance of an elite, hybrid family of a northern × southern highbush cross ('Draper' × 'Jewel'). *Euphytica*, 214(6), 1–16.
- Hancock, Jim F. (2008). *Temperate fruit crop breeding: germplasm to genomics*. (James F. Hancock, Ed.), *Temperate fruit crop. Germoplasm to genomics*. Springer Science+Business Media.
- Hanson, E. J., Berkheimer, S. F., & Hancock, J. F. (2007). Seasonal Changes in the Cold Hardiness of the Flower Buds of Highbush Blueberry with Varying Species Ancestry. *Journal of the American Pomological Society*, 61(1), 14–18.
- Hao, X., Yang, Y., Yue, C., Wang, L., Horvath, D. P., & Wang, X. (2017). Comprehensive Transcriptome Analyses Reveal Differential Gene Expression Profiles of *Camellia sinensis* Axillary Buds at Para-, Endo-, Ecodormancy, and Bud Flush Stages. *Frontiers in Plant Science*, 8(April), 1–19.
- He, F., Mu, L., Yan, G. L., Liang, N. N., Pan, Q. H., Wang, J., ... Duan, C. Q. (2010). Biosynthesis of anthocyanins and their regulation in colored grapes. *Molecules*, 15(12), 9057–9091.
- Hedley, P. E., Russell, J. R., Jorgensen, L., Gordon, S., Morris, J. A., Hackett, C. A., ... Brennan, R. (2010). Candidate genes associated with bud dormancy release in blackcurrant (*Ribes nigrum* L.). *BMC Plant Biol*, 10, 1–13.
- Heslot, N., Yang, H.-P., Sorrells, M. E., & Jannink, J.-L. (2012). Genomic Selection in Plant Breeding: A Comparison of Models. *Crop Science*, 52(1), 146.
- Horbowicz, M., Grzesiuk, A., DEBski, H., & Kosson, R. (2008). Anthocyanins of Fruits and Vegetables - Their Occurrence, Analysis and Role in Human. *Vegetable Crops Research Bulletin*, 68, 5–22.
- Horvath, D. (2009). Common mechanisms regulate flowering and dormancy. *Plant Science*, 177(6), 523–531.
- Horvath, D. P., Anderson, J. V., Chao, W. S., & Foley, M. E. (2003). Knowing when to grow: Signals regulating bud dormancy. *Trends in Plant Science*, 8(11), 534–540.
- Hospital, F. (2009). Challenges for effective marker-assisted selection in plants. *Genetica*, 136(2), 303–310.
- Howard, L. R., Brownmiller, C., Mauromoustakos, A., & Prior, R. L. (2016). Improved stability of blueberry juice anthocyanins by acidification and refrigeration. *Journal of Berry Research*, 6(2), 189–201.
- Huan, C., Jiang, L., An, X., Yu, M., Xu, Y., Ma, R., & Yu, Z. (2016). Potential role of reactive oxygen species and antioxidant genes in the regulation of peach fruit development and ripening. *Plant Physiology and Biochemistry*, 104, 294–303.
- Hussain, S., Niu, Q., Yang, F., Hussain, N., & Teng, Y. (2015). The possible role of chilling in floral and vegetative bud dormancy release in *Pyrus pyrifolia*. *Biologia Plantarum*, 59(4), 726–734.
- Inostroza-Blancheteau, C., Acevedo, P., Loyola, R., Arce-Johnson, P., Alberdi, M., & Reyes-Díaz, M. (2016). Short-term UV-B radiation affects photosynthetic performance and antioxidant gene expression in highbush blueberry leaves. *Plant Physiology and Biochemistry*, 107, 301–309.
- Ionescu, I. A., Møller, B. L., & Sánchez-Pérez, R. (2016). Chemical control of flowering time. *Journal of Experimental Botany*, 68(3), erw427.
- Ito, A., Saito, T., Sakamoto, D., Sugiura, T., Bai, S., & Moriguchi, T. (2015). Physiological differences between bud breaking and flowering after dormancy

- completion revealed by DAM and FT/TFL1 expression in Japanese pear (*Pyrus pyrifolia*). *Tree Physiology*, 36(1), 109–120.
- Ito, A., Saito, T., Sakamoto, D., Sugiura, T., Bai, S., & Moriguchi, T. (2016). Physiological differences between bud breaking and flowering after dormancy completion revealed by DAM and FT/TFL1 expression in Japanese pear (*Pyrus pyrifolia*). *Tree Physiology*, 36(1), 109–120.
- Jannink, J.-L., Lorenz, A. J., & Iwata, H. (2010). Genomic selection in plant breeding: from theory to practice. *Briefings in Functional Genomics*, 9(2), 166–177.
- Jenks, M. A., & Bebeli, P. J. (2011). *Breeding for Fruit Quality*. West Sussex: John Wiley & Sons, Inc.
- Jeong, S.-W., Das, P. K., Jeoung, S. C., Song, J.-Y., Lee, H. K., Kim, Y.-K., ... Park, Y.-I. (2010). Ethylene Suppression of Sugar-Induced Anthocyanin Pigmentation in *Arabidopsis*. *Plant Physiology*, 154(3), 1514–1531.
- Jia, H., Wang, Y., Sun, M., Li, B., Han, Y., Zhao, Y., ... Jia, W. (2013). Sucrose functions as a signal involved in the regulation of strawberry fruit development and ripening, 453–465.
- Jia, H., Xie, Z., Wang, C., Shangguan, L., Qian, N., Cui, M., ... Fang, J. (2017). Abscisic acid, sucrose, and auxin coordinately regulate berry ripening process of the Fujiminori grape. *Functional and Integrative Genomics*, 17(4), 441–457.
- Kader, A. A. (2008). Flavor quality of fruits and vegetables. *Journal of the Science of Food and Agriculture*, 88(11), 1863–1868.
- Kanehisa, M., Furumichi, M., Tanabe, M., Sato, Y., & Morishima, K. (2017). KEGG: New perspectives on genomes, pathways, diseases and drugs. *Nucleic Acids Research*, 45(D1), D353–D361.
- Kang, M. S. (2002). *Quantitative genetics, genomics and plant breeding*. New York: CABI Publishing.
- Kang, Y., Khan, S., & Ma, X. (2009). Climate change impacts on crop yield, crop water productivity and food security - A review. *Progress in Natural Science*, 19(12), 1665–1674.
- Kao, C.-H. (2000). On The Differences Between Maximum Likelihood and Regression Interval Mapping in the Analysis of Quantitative Trait Loci. *Genetics*, 156, 855–865.
- Karppinen, K., Hirvelä, E., Nevala, T., Sipari, N., Suokas, M., & Jaakola, L. (2013). Changes in the abscisic acid levels and related gene expression during fruit development and ripening in bilberry (*Vaccinium myrtillus* L.). *Phytochemistry*, 95, 127–134.
- Karppinen, K., Zoratti, L., Nguyenquynh, N., Häggman, H., & Jaakola, L. (2016). On the Developmental and Environmental Regulation of Secondary Metabolism in *Vaccinium* spp. Berries. *Frontiers in Plant Science*, 7(May), 1–9.
- Kearney, J. (2010). Food consumption trends and drivers. *Philosophical Transactions of the Royal Society B: Biological Sciences*, 365(1554), 2793–2807.
- Khoo, H. E., Azlan, A., Tang, S. T., & Lim, S. M. (2017). Anthocyanidins and anthocyanins: colored pigments as food, pharmaceutical ingredients, and the potential health benefits. *Food & Nutrition Research*, 61(1), 1–21.
- Kim, D.-H., & Sung, S. (2014). Genetic and Epigenetic Mechanisms Underlying Vernalization. *The Arabidopsis Book*, 12, e0171.
- Kim, S. J., Yu, D. J., Kim, T.-C. C., & Lee, H. J. (2011). Growth and photosynthetic

- characteristics of blueberry (*Vaccinium corymbosum* cv. Bluecrop) under various shade levels. *Scientia Horticulturae*, 129(3), 486–492.
- Kim, T., Banf, M., Kahn, D., Bernard, T., Dreher, K., Chavali, A. K., ... Zhang, P. (2017). Genome-Wide Prediction of Metabolic Enzymes, Pathways, and Gene Clusters in Plants. *Plant Physiology*, 173(4), 2041–2059.
- Klee, H. J. (2010). Improving the flavor of fresh fruits: Genomics, biochemistry, and biotechnology. *New Phytologist*, 187(1), 44–56.
- Konarska, A. (2015). Development of fruit quality traits and comparison of the fruit structure of two *Vaccinium corymbosum* (L.) cultivars. *Scientia Horticulturae*, 194, 79–90.
- Korte, A., & Farlow, A. (2013). The advantages and limitations of trait analysis with GWAS: a review. *Plant Methods*, 9(1), 1.
- Koutinas, N., Pepelyankov, G., & Lichev, V. (2010). Flower induction and flower bud development in apple and sweet cherry. *Biotechnology and Biotechnological Equipment*, 24(1), 1549–1558.
- Kovaleski, A. P., Williamson, J. G., Olmstead, J. W., & Darnell, R. L. (2015). Inflorescence Bud Initiation, Development, and Bloom in Two Southern Highbush Blueberry Cultivars. *Journal of American Soci and Horticulture Science*, 140(1), 38–44.
- Koyama, K., Sadamatsu, K., & Goto-Yamamoto, N. (2010). Abscisic acid stimulated ripening and gene expression in berry skins of the Cabernet Sauvignon grape. *Functional and Integrative Genomics*, 10(3), 367–381.
- Kramer, M. G., & Redenbaugh, K. (1994). Commercialization of a tomato with an antisense polygalacturonase gene: The FLAVR SAVR™ tomato story. *Euphytica*, 79(3), 293–297.
- Kraujalyte, V., Venskutonis, P. R., Pukalskas, A., Česonienė, L., & Daubaras, R. (2015). Antioxidant properties, phenolic composition and potentiometric sensor array evaluation of commercial and new blueberry (*Vaccinium corymbosum*) and bog blueberry (*Vaccinium uliginosum*) genotypes. *Food Chemistry*, 188, 583–590.
- Krieger, U., Lippman, Z. B., & Zamir, D. (2010). The flowering gene SINGLE FLOWER TRUSS drives heterosis for yield in tomato. *Nature Genetics*, 42(5), 459–463.
- Kulik, A., Wawer, I., Krzywińska, E., Bucholc, M., & Dobrowolska, G. (2011). SnRK2 Protein Kinases—Key Regulators of Plant Response to Abiotic Stresses. *OMICS: A Journal of Integrative Biology*, 15(12), 859–872.
- Kumar, S., & Trivedi, P. K. (2018). Glutathione S-Transferases: Role in Combating Abiotic Stresses Including Arsenic Detoxification in Plants. *Frontiers in Plant Science*, 9(June), 751.
- Kyriacou, M. C., & Roupheal, Y. (2018). Towards a new definition of quality for fresh fruits and vegetables. *Scientia Horticulturae*, 234(August 2017), 463–469.
- Langridge, P., & Fleury, D. (2011). Making the most of 'omics' for crop breeding. *Trends in Biotechnology*, 29(1), 33–40.
- Lau, O. S., & Deng, X. W. (2010). Plant hormone signaling lightens up: integrators of light and hormones. *Current Opinion in Plant Biology*, 13(5), 571–577.
- Leida, C., Conejero, A., Arbona, V., Gómez-Cadenas, A., Llácer, G., Badenes, M. L., & Ríos, G. (2012). Chilling-Dependent Release of Seed and Bud Dormancy in Peach Associates to Common Changes in Gene Expression. *PLoS ONE*, 7(5), e35777.

- Leiva-Valenzuela, G. A., Lu, R., & Aguilera, J. M. (2013). Prediction of firmness and soluble solids content of blueberries using hyperspectral reflectance imaging. *Journal of Food Engineering*, 115(1), 91–98.
- Leng, P., Yuan, B., Guo, Y., & Chen, P. (2014). The role of abscisic acid in fruit ripening and responses to abiotic stress. *Journal of Experimental Botany*, 65(16), 4577–4588.
- Leyser, O. (2017). Auxin Signaling. *Plant Physiology*, 176(January), pp.00765.2017.
- Li, D., Li, B., Ma, Y., Sun, X., Lin, Y., & Meng, X. (2017). Polyphenols, anthocyanins, and flavonoids contents and the antioxidant capacity of various cultivars of highbush and half-high blueberries. *Journal of Food Composition and Analysis*, 62, 84–93.
- Li, H., Ye, G., & Wang, J. (2006). A Modified Algorithm for the Improvement of Composite Interval Mapping. *Genetics*, 175(1), 361–374.
- Li, J., Xu, Y., Niu, Q., He, L., Teng, Y., & Bai, S. (2018). Abscisic acid (ABA) promotes the induction and maintenance of pear (*Pyrus pyrifolia* white pear group) flower bud endodormancy. *International Journal of Molecular Sciences*, 19(1).
- Li, P., Lee, S. H., & Hsu, H. Y. (2011). Review on fruit harvesting method for potential use of automatic fruit harvesting systems. *Procedia Engineering*, 23, 351–366.
- Li, X., Xu, C., Korban, S. S., & Chen, K. (2010). Regulatory mechanisms of textural changes in ripening fruits. *Critical Reviews in Plant Sciences*, 29(4), 222–243.
- Lila, M. A., Burton-Freeman, B., Grace, M., & Kalt, W. (2016). Unraveling Anthocyanin Bioavailability for Human Health. *Annual Review of Food Science and Technology*, 7(1), 375–393.
- Lin, D., Xiao, M., Zhao, J., Li, Z., Xing, B., Li, X., ... Chen, S. (2016). An overview of plant phenolic compounds and their importance in human nutrition and management of type 2 diabetes. *Molecules*, 21(10).
- Lin, L., Liu, X., & Yin, R. (2018). PIF3 Integrates Light and Low Temperature Signaling. *Trends in Plant Science*, 23(2), 93–95.
- Linkosalo, T., & Lechowicz, M. J. (2006). Twilight far-red treatment advances leaf bud-burst of silver birch (*Betula pendula*). *Tree Physiology*, 26(February), 1249–1256.
- Liu, B., Yang, Z., Gomez, A., Liu, B., Lin, C., & Oka, Y. (2016). Signaling mechanisms of plant cryptochromes in *Arabidopsis thaliana*. *Journal of Plant Research*, 129(2), 137–148.
- Liu, C., Callow, P., Rowland, L. J., Hancock, J. F., & Song, G. qing. (2010). Adventitious shoot regeneration from leaf explants of southern highbush blueberry cultivars. *Plant Cell, Tissue and Organ Culture*, 103(1), 137–144.
- Liu, P., Lindstedt, A., Markkinen, N., Sinkkonen, J., Suomela, J. P., & Yang, B. (2014). Characterization of metabolite profiles of leaves of bilberry (*Vaccinium myrtillus* L.) and lingonberry (*Vaccinium vitis-idaea* L.). *Journal of Agricultural and Food Chemistry*, 62(49), 12015–12026.
- Lloret, A., Badenes, M. L., & Ríos, G. (2018). Modulation of Dormancy and Growth Responses in Reproductive Buds of Temperate Trees. *Frontiers in Plant Science*, 9(September), 1368.
- Lobo, V., Patil, A., Phatak, A., & Chandra, N. (2010). Free radicals, antioxidants and functional foods: Impact on human health. *Pharmacognosy Reviews*, 4(8), 118.
- Lobos, G. A., Callow, P., & Hancock, J. F. (2014). The effect of delaying harvest date on

- fruit quality and storage of late highbush blueberry cultivars (*Vaccinium corymbosum* L.). *Postharvest Biology and Technology*, 87, 133–139.
- Lobos, G. A., & Hancock, J. F. (2015). Breeding blueberries for a changing global environment: a review. *Frontiers in Plant Science*, 6.
- Lobos, T. E., Retamales, J. B., Ortega-Farías, S., Hanson, E. J., López-Olivari, R., & Mora, M. L. (2018). Regulated deficit irrigation effects on physiological parameters, yield, fruit quality and antioxidants of *Vaccinium corymbosum* plants cv. Brigitta. *Irrigation Science*, 36(1), 49–60.
- Lu, F., Lipka, A. E., Glaubitz, J., Elshire, R., Cherney, J. H., Casler, M. D., ... Costich, D. E. (2013). Switchgrass Genomic Diversity, Ploidy, and Evolution: Novel Insights from a Network-Based SNP Discovery Protocol. *PLoS Genetics*, 9(1), e1003215.
- Lunn, J. E., Delorge, I., Figueroa, C. M., Van Dijck, P., & Stitt, M. (2014). Trehalose metabolism in plants. *The Plant Journal*, 79(4), 544–567.
- Lv, L., Huo, X., Wen, L., Gao, Z., & Khalil-ur-Rehman, M. (2018). Isolation and Role of PmRGL2 in GA-mediated Floral Bud Dormancy Release in Japanese Apricot (*Prunus mume* Siebold et Zucc.). *Frontiers in Plant Science*, 9(January), 1–13.
- Lyrene, P., Journal, P., & Society, A. P. (2002). Development of Highbush Blueberry Cultivars Adapted to Florida. *Journal of the American Pomological Society*, 56(2), 79–85.
- Ma, H., Johnson, S. L., Liu, W., Dasilva, N. A., Meschwitz, S., Dain, J. A., & Seeram, N. P. (2018). Evaluation of Polyphenol Anthocyanin-Enriched Extracts of Blackberry , Black Raspberry , Blueberry , Cranberry , Red Raspberry , and Strawberry for Free Radical Scavenging , Reactive Carbonyl Species Aggregation , and Microglial Neuroprotective Effects. *International Journal of Molecular Sciences*, 19(461), 1–19.
- Majda, M., & Robert, S. (2018). The role of auxin in cell wall expansion. *International Journal of Molecular Sciences*, 19(4).
- Malyshev, R. V., Shelyakin, M. A., & Golovko, T. K. (2016). Bud dormancy breaking affects respiration and energy balance of bilberry shoots in the initial stage of growth. *Russian Journal of Plant Physiology*, 63(3), 409–416.
- Matas, A. J., Gapper, N. E., Chung, M. Y., Giovannoni, J. J., & Rose, J. K. (2009). Biology and genetic engineering of fruit maturation for enhanced quality and shelf-life. *Current Opinion in Biotechnology*, 20(2), 197–203.
- Mathan, J., Bhattacharya, J., & Ranjan, A. (2016). Enhancing crop yield by optimizing plant developmental features. *Development*, 143(18), 3283–3294.
- Mattila, P., Hellström, J., & Törrönen, R. (2006). Phenolic acids in berries, fruits, and beverages. *Journal of Agricultural and Food Chemistry*, 54(19), 7193–7199.
- Mayer, M. (2005). A comparison of regression interval mapping and multiple interval mapping for linked QTL. *Heredity*, 94(6), 599–605.
- McCallum, S., Graham, J., Jorgensen, L., Rowland, L. J., Bassil, N. V., Hancock, J. F., ... Hackett, C. A. (2016). Construction of a SNP and SSR linkage map in autotetraploid blueberry using genotyping by sequencing. *Molecular Breeding*, 36(4).
- McGinn, C. (2015). The science of taste. *Metaphilosophy*, 46(1), 84–103.
- McNamara, R. K., Kalt, W., Shidler, M. D., McDonald, J., Summer, S. S., Stein, A. L., ... Krikorian, R. (2018). Cognitive response to fish oil, blueberry, and combined

- supplementation in older adults with subjective cognitive impairment. *Neurobiology of Aging*, 64, 147–156.
- Meitha, K., Agudelo-Romero, P., Signorelli, S., Gibbs, D. J., Considine, J. A., Foyer, C. H., & Considine, M. J. (2018). Developmental control of hypoxia during bud burst in grapevine. *Plant Cell and Environment*, 41(5), 1154–1170.
- Meitha, K., Konnerup, D., Colmer, T. D., Considine, J. A., Foyer, C. H., & Considine, M. J. (2015). Spatio-temporal relief from hypoxia and production of reactive oxygen species during bud burst in grapevine (*Vitis vinifera*). *Annals of Botany*, 116(4), 703–711.
- Melke, A. (2015). The Physiology of Chilling Temperature Requirements for Dormancy Release and Bud-break in Temperate Fruit Trees Grown at Mild Winter Tropical Climate. *Journal of Plant Studies*, 4(2), 110–156.
- Mert, C., Barut, E., & Ipek, A. (2013). Variation in Flower Bud Differentiation and Progression of Floral Organs with Respect to Crop Load in Olive. *Notulae Botanicae Horti Agrobotanici Cluj-Napoca*, 41(1), 79–85.
- Meyer, R. S., & Purugganan, M. D. (2013). Evolution of crop species: Genetics of domestication and diversification. *Nature Reviews Genetics*, 14(12), 840–852.
- Milić, B., Tarlanović, J., Keserović, Z., Magazin, N., Miodragović, M., & Popara, G. (2018). Bioregulators can improve fruit size, yield and plant growth of northern highbush blueberry (*Vaccinium corymbosum* L.). *Scientia Horticulturae*, 235(February), 214–220.
- Mishra, P., & Panigrahi, K. C. (2015). GIGANTEA an emerging story. *Frontiers in Plant Science*, 6.
- Miura, K., & Furumoto, T. (2013). Cold Signaling and Cold Response in Plants. *International Journal of Molecular Sciences*, 14(3), 5312–5337.
- Moggia, C., Graell, J., Lara, I., González, G., & Lobos, G. A. (2017). Firmness at Harvest Impacts Postharvest Fruit Softening and Internal Browning Development in Mechanically Damaged and Non-damaged Highbush Blueberries (*Vaccinium corymbosum* L.). *Frontiers in Plant Science*, 8(April), 1–11.
- Moghaddam, M. R. B., & Ende, W. Van den. (2013). Sugars, the clock and transition to flowering. *Frontiers in Plant Science*, 4(February), 1–6.
- Mohamed, R., Wang, C. T., Ma, C., Shevchenko, O., Dye, S. J., Puzey, J. R., ... Brunner, A. M. (2010). *Populus* CEN/TFL1 regulates first onset of flowering, axillary meristem identity and dormancy release in *Populus*. *Plant Journal*, 62(4), 674–688.
- Molinero-Rosales, N., Latorre, A., Jamilena, M., & Lozano, R. (2004). SINGLE FLOWER TRUSS regulates the transition and maintenance of flowering in tomato. *Planta*, 218(3), 427–434.
- Montecchiarini, M. L., Bello, F., Rivadeneira, M. F., Vázquez, D., Podestá, F. E., & Tripodi, K. E. J. (2018). Metabolic and physiologic profile during the fruit ripening of three blueberries highbush (*Vaccinium corymbosum*) cultivars. *Journal of Berry Research*, 8(3), 177–192.
- Morita, M., Naito, Y., Yoshikawa, T., & Niki, E. (2017). Antioxidant capacity of blueberry extracts: Peroxyl radical scavenging and inhibition of plasma lipid oxidation induced by multiple oxidants. *Journal of Berry Research*, 7(1), 1–9.
- Muleke, E. M., Fan, L., Wang, Y., Xu, L., Zhu, X., Zhang, W., ... Liu, L. (2017). Coordinated Regulation of Anthocyanin Biosynthesis Genes Confers Varied

- Phenotypic and Spatial-Temporal Anthocyanin Accumulation in Radish (*Raphanus sativus* L.). *Frontiers in Plant Science*, 8(July), 1–17.
- Musacchi, S., & Serra, S. (2018). Apple fruit quality: Overview on pre-harvest factors. *Scientia Horticulturae*, 234(December 2017), 409–430.
- Nakayama, T., Suzuki, H., & Nishino, T. (2003). Anthocyanin acyltransferases: Specificities, mechanism, phylogenetics, and applications. *Journal of Molecular Catalysis B: Enzymatic*, 23(2–6), 117–132.
- Nguyen, N., Suokas, M., Karppinen, K., Vuosku, J., Jaakola, L., & Häggman, H. (2018). Recognition of candidate transcription factors related to bilberry fruit ripening by de novo transcriptome and qRT-PCR analyses. *Scientific Reports*, 8(1), 1–12.
- NIH. (2019). *Labeling Daily Values - Dietary Supplement Label Database*.
- Nile, S. H., & Park, S. W. (2014). Edible berries: Bioactive components and their effect on human health. *Nutrition*, 30(2), 134–144.
- O. Sadras, V., & F. Denison, R. (2009). Do plant parts compete for resources? An evolutionary viewpoint. *New Phytologist*, 183(3), 565–574.
- O'Hara, L. E., Paul, M. J., & Wingler, A. (2013). How do sugars regulate plant growth and development? new insight into the role of trehalose-6-phosphate. *Molecular Plant*, 6(2), 261–274.
- Oh, H. D., Yu, D. J., Chung, S. W., Chea, S., & Lee, H. J. (2018). Abscisic acid stimulates anthocyanin accumulation in 'Jersey' highbush blueberry fruits during ripening. *Food Chemistry*, 244(June 2017), 403–407.
- Oliver, R. E., Tinker, N. A., Lazo, G. R., Chao, S., Jellen, E. N., Carson, M. L., ... Jackson, E. W. (2013). SNP Discovery and Chromosome Anchoring Provide the First Physically-Anchored Hexaploid Oat Map and Reveal Synteny with Model Species. *PLoS ONE*, 8(3).
- Olmstead, J. W., Armenta, H. P. R., & Lyrene, P. M. (2013). Using sparkleberry as a genetic source for machine harvest traits for southern highbush blueberry. *HortTechnology*, 23(4), 419–424.
- Ophir, R., Pang, X., Halaly, T., Venkateswari, J., Lavee, S., Galbraith, D., & Or, E. (2009). Gene-expression profiling of grape bud response to two alternative dormancy-release stimuli expose possible links between impaired mitochondrial activity, hypoxia, ethylene-ABA interplay and cell enlargement. *Plant Molecular Biology*, 71(4–5), 403–423.
- Osorio, S., Scossa, F., & Fernie, A. R. (2013). Molecular regulation of fruit ripening. *Frontiers in Plant Science*, 4(June 2013).
- Overall, J., Bonney, S. A., Wilson, M., Beermann, A., Grace, M. H., Esposito, D., ... Komarnytsky, S. (2017). Metabolic effects of berries with structurally diverse anthocyanins. *International Journal of Molecular Sciences*, 18(2).
- Ozga, J. A., & Reinecke, D. M. (2003). Hormonal Interactions in Fruit Development. *Journal of Plant Growth Regulation*, 22(73), 73–81.
- Pagliarini, E., Laureati, M., & Gaeta, D. (2013). Sensory descriptors, hedonic perception and consumer's attitudes to Sangiovese red wine deriving from organically and conventionally grown grapes. *Frontiers in Psychology*, 4(NOV), 1–7.
- Pagter, M., Andersen, U. B., & Andersen, L. (2015). Winter warming delays dormancy release, advances budburst, alters carbohydrate metabolism and reduces yield in a temperate shrub. *AoB PLANTS*, 7(1), 1–15.

- Pan, P., Skaer, C., Yu, J., Zhao, H., Ren, H., Oshima, K., & Wang, L. S. (2017). Berries and other natural products in pancreatic cancer chemoprevention in human clinical trials. *Journal of Berry Research*, 7(3), 147–161.
- Paniagua, A. C., East, A. R., Hindmarsh, J. P., & Heyes, J. A. (2013). Moisture loss is the major cause of firmness change during postharvest storage of blueberry. *Postharvest Biology and Technology*, 79, 13–19.
- Paniagua, C., Posé, S., Morris, V. J., Kirby, A. R., Quesada, M. A., & Mercado, J. A. (2014). Fruit softening and pectin disassembly: An overview of nanostructural pectin modifications assessed by atomic force microscopy. *Annals of Botany*, 114(6),
- Pearce, R. S. (2001). Plant freezing and damage. *Annals of Botany*, 87(4), 417–424.
- Perrot-Rechenmann, C. (2010). Cellular responses to auxin: division versus expansion. *Cold Spring Harbor Perspectives in Biology*, 2(5), 1–15.
- Pilati, S., Bagagli, G., Sonogo, P., Moretto, M., Brazzale, D., Castorina, G., ... Moser, C. (2017). Abscisic Acid Is a Major Regulator of Grape Berry Ripening Onset: New Insights into ABA Signaling Network. *Frontiers in Plant Science*, 8(June), 1–16.
- Pilati, S., Brazzale, D., Guella, G., Milli, A., Ruberti, C., Biasioli, F., ... Moser, C. (2014). The onset of grapevine berry ripening is characterized by ROS accumulation and lipoxygenase-mediated membrane peroxidation in the skin. *BMC Plant Biology*, 14(1), 1–15.
- Pletsers, A., Caffarra, A., Kelleher, C. T., & Donnelly, A. (2015). Chilling temperature and photoperiod influence the timing of bud burst in juvenile *Betula pubescens* Ehrh. and *Populus tremula* L. trees. *Annals of Forest Science*, 72(7), 941–953.
- Posé, S., Nieves, J. a G., Quesada, F. P. M. a, & Mercado, J. a. (2011). Strawberry Fruit Softening : Role of Cell Wall Disassembly and its Manipulation in Transgenic Plants. *Genes, Genomes and Genomics*, 5, 40–48.
- Prasanna, V., Prabha, T. N., & Tharanathan, R. N. (2007). Fruit ripening phenomena-an overview. *Critical Reviews in Food Science and Nutrition*, 47(1), 1–19.
- Pucciariello, C., Banti, V., & Perata, P. (2012). ROS signaling as common element in low oxygen and heat stresses. *Plant Physiology and Biochemistry*, 59, 3–10.
- Rabot, A., Henry, C., Baaziz, K. Ben, Mortreau, E., Azri, W., Lothier, J., ... Sakr, S. (2012). Insight into the role of sugars in bud burst under light in the rose. *Plant and Cell Physiology*, 53(6), 1068–1082.
- Rafalski, J. A. (2010). Association genetics in crop improvement. *Current Opinion in Plant Biology*, 13(2), 174–180.
- Rapaille, A., Goosens, J., & Heume, M. (2003). Sugar Alcohols. *Encyclopedia of Food Sciences and Nutrition*, 5665–5671.
- Rasheed, A., Hao, Y., Xia, X., Khan, A., Xu, Y., Varshney, R. K., & He, Z. (2017). Crop Breeding Chips and Genotyping Platforms: Progress, Challenges, and Perspectives. *Molecular Plant*, 10(8), 1047–1064.
- Reddy, S. K., Holalu, S. V., Casal, J. J., & Finlayson, S. A. (2013). Abscisic Acid Regulates Axillary Bud Outgrowth Responses to the Ratio of Red to Far-Red Light. *Plant Physiology*, 163(2), 1047–1058.
- Ren, J., Chen, P., Dai, S. J., Li, P., Li, Q., Ji, K., ... Leng, P. (2011). Role of abscisic acid and ethylene in sweet cherry fruit maturation: Molecular aspects. *New Zealand Journal of Crop and Horticultural Science*, 39(3), 161–174.

- Reque, P. M., Steffens, R. S., Jablonski, A., Flôres, S. H., Rios, A. de O., & de Jong, E. V. (2014). Cold storage of blueberry (*Vaccinium* spp.) fruits and juice: Anthocyanin stability and antioxidant activity. *Journal of Food Composition and Analysis*, 33(1), 111–116.
- Rho, H., Yu, D. J., Kim, S. J., & Lee, H. J. (2012). Limitation factors for photosynthesis in 'Bluecrop' highbush blueberry (*Vaccinium corymbosum*) leaves in response to moderate water stress. *Journal of Plant Biology*, 55(6), 450–457.
- Rihan, H. Z., Al-Issawi, M., & Fuller, M. P. (2017). Advances in physiological and molecular aspects of plant cold tolerance. *Journal of Plant Interactions*, 12(1), 143–157.
- Rinaldo, A., Cavallini, E., Jia, Y., Moss, S. M. A., McDavid, D. A. J., Hooper, L. C., ... Walker, A. R. (2015). A grapevine anthocyanin acyltransferase, transcriptionally regulated by VvMYBA, can produce most acylated anthocyanins present in grape skins. *Plant Physiology*, 169(November), pp.01255.2015.
- Rinne, P. L. H., Welling, A., Vahala, J., Ripel, L., Ruonala, R., Kangasjärvi, J., & van der Schoot, C. (2011). Chilling of Dormant Buds Hyperinduces *FLOWERING LOCUS T* and Recruits GA-Inducible 1,3- β -Glucanases to Reopen Signal Conduits and Release Dormancy in *Populus*. *The Plant Cell*, 23(1), 130–146.
- Rinne, P. L., & Schoot, C. van der. (2003). Plasmodesmata at the crossroads between development, dormancy, and defense. *Canadian Journal of Botany*, 81(12), 1182–1197.
- Rohde, A., & Bhalerao, R. P. (2007). Plant dormancy in the perennial context. *Trends in Plant Science*, 12(5), 217–223.
- Rolin, D., Teyssier, E., Hong, Y., & Gallusci, P. (2015). *Tomato fruit quality improvement facing the functional genomics revolution. Applied Plant Genomics and Biotechnology*. Elsevier Ltd.
- Rolland, F., Moore, B., & Sheen, J. (2002). Sugar Sensing 2002 Rolland. *The Plant Cell*, 185–205.
- Rosa, M., Prado, C., Podazza, G., Interdonato, R., González, J. A., Hilal, M., & Prado, F. E. (2009). Soluble sugars-metabolism, sensing and abiotic stress a complex network in the life of plants. *Plant Signaling and Behavior*, 4(5), 388–393.
- Routray, W., & Orsat, V. (2011). Blueberries and Their Anthocyanins: Factors Affecting Biosynthesis and Properties. *Comprehensive Reviews in Food Science and Food Safety*, 10(6), 303–320.
- Routray, W., & Orsat, V. (2014). Variation of phenolic profile and antioxidant activity of North American highbush blueberry leaves with variation of time of harvest and cultivar. *Industrial Crops and Products*, 62, 147–155.
- Rowland, L J. (2000). Germplasm and the Potential for Northern-Adapted Rabbiteye Cultivars, 77–80.
- Rowland, L J, Mehra, S., & Arora, R. (2003). Identification of molecular markers associated with cold tolerance in blueberry. *Acta Horticulturae*, 626, 59–69.
- Rowland, Lisa J, Bell, D. J., Alkharouf, N., Bassil, N. V, Drummond, F. A., Beers, L., ... Main, D. (2012). Generating Genomic Tools for Blueberry Improvement. *International Journal of Fruit Science*, 12(1–3), 276–287.
- Rowland, Lisa J, Ogden, E. L., Bassil, N., Buck, E. J., McCallum, S., Graham, J., ... Vinyard, B. T. (2014). Construction of a genetic linkage map of an interspecific

- diploid blueberry population and identification of QTL for chilling requirement and cold hardiness. *Molecular Breeding*, 34(4), 2033–2048.
- Rowland, Lisa J, Ogden, E. L., & Ehlenfeldt, M. K. (2010). EST-PCR markers developed for highbush blueberry are also useful for genetic fingerprinting and relationship studies in rabbiteye blueberry. *Scientia Horticulturae*, 125(4), 779–784.
- Rowland, Lisa J, Ogden, E. L., Ehlenfeldt, M. K., & Arora, R. (2008). Cold tolerance of blueberry genotypes throughout the dormant period from acclimation to deacclimation. *HortScience*, 43(7), 1970–1974.
- Rowland, Lisa J, Ogden, E. L., Takeda, F., Glenn, D. M., Ehlenfeldt, M. K., & Vinyard, B. T. (2013). Variation among highbush blueberry cultivars for frost tolerance of open flowers. *HortScience*, 48(6), 692–695.
- Ruan, Y.-L. (2014). Sucrose Metabolism: Gateway to Diverse Carbon Use and Sugar Signaling. *Annual Review of Plant Biology*, 65(1), 33–67.
- Saftner, R., Polashock, J., Ehlenfeldt, M., & Vinyard, B. (2008). Instrumental and sensory quality characteristics of blueberry fruit from twelve cultivars. *Postharvest Biology and Technology*, 49(1), 19–26.
- Salvo, S., Muñoz, C., Ávila, J., Bustos, J., Ramírez-Valdivia, M., Silva, C., & Vivallo, G. (2012). An estimate of potential blueberry yield using regression models that relate the number of fruits to the number of flower buds and to climatic variables. *Scientia Horticulturae*, 133(1), 56–63.
- Sam Saguy, I. (2011). Paradigm shifts in academia and the food industry required to meet innovation challenges. *Trends in Food Science and Technology*, 22(9), 467–475.
- Sasaki, N., Nishizaki, Y., Ozeki, Y., & Miyahara, T. (2014). The role of acyl-glucose in anthocyanin modifications. *Molecules*, 19(11), 18747–18766.
- Scalzo, J., Stevenson, D., & Hedderley, D. (2013). Blueberry estimated harvest from seven new cultivars: Fruit and anthocyanins. *Food Chemistry*, 139(1–4), 44–50.
- Scalzo, J., Stevenson, D., & Hedderley, D. (2015). Polyphenol compounds and other quality traits in blueberry cultivars. *Journal of Berry Research*, 5(3), 117–130.
- Schaart, J. G., van de Wiel, C. C. M., Lotz, L. A. P., & Smulders, M. J. M. (2016). Opportunities for Products of New Plant Breeding Techniques. *Trends in Plant Science*, 21(5), 438–449.
- Schönhals, E. M., Ding, J., Ritter, E., Paulo, M. J., Cara, N., Tacke, E., ... Gebhardt, C. (2017). Physical mapping of QTL for tuber yield, starch content and starch yield in tetraploid potato (*Solanum tuberosum* L.) by means of genome wide genotyping by sequencing and the 8.3 K SolCAP SNP array. *BMC Genomics*, 18(1).
- Schwab, W., Davidovich-Rikanati, R., & Lewinsohn, E. (2008). Biosynthesis of plant-derived flavor compounds. *Plant Journal*, 54(4), 712–732.
- Sehgal, D., Singh, R., & Rajpal, V. R. (2016). Molecular Breeding for Sustainable Crop Improvement, 11, 31–60.
- Serrano, A., Espinoza, C., Armijo, G., Inostroza-Blancheteau, C., Poblete, E., Meyer-Regueiro, C., ... Arce-Johnson, P. (2017). Omics Approaches for Understanding Grapevine Berry Development: Regulatory Networks Associated with Endogenous Processes and Environmental Responses. *Frontiers in Plant Science*, 8(September), 1–15.
- Seymour, G. B., Chapman, N. H., Chew, B. L., & Rose, J. K. C. (2013). Regulation of

- ripening and opportunities for control in tomato and other fruits. *Plant Biotechnology Journal*, 11(3), 269–278.
- Seymour, G. B., Østergaard, L., Chapman, N. H., Knapp, S., & Martin, C. (2013). Fruit Development and Ripening. *Annual Review of Plant Biology*, 64(1), 219–241.
- Shim, D., Ko, J.-H. H., Kim, W.-C. C., Wang, Q., Keathley, D. E., & Han, K.-H. H. (2014). A molecular framework for seasonal growth-dormancy regulation in perennial plants. *Horticulture Research*, 1(1), 1–9.
- Shu, K., Liu, X. D., Xie, Q., & He, Z. H. (2016). Two Faces of One Seed: Hormonal Regulation of Dormancy and Germination. *Molecular Plant*, 9(1), 34–45.
- Signorelli, S., Agudelo-Romero, P., Meitha, K., Foyer, C. H., & Considine, M. J. (2018). Roles for Light, Energy, and Oxygen in the Fate of Quiescent Axillary Buds. *Plant Physiology*, 176(2), 1171–1181.
- Silva, J. L., Marroquin, E., Matta, F. B., Garner, J. O., & Stojanovic, J. (2005). Physicochemical, carbohydrate and sensory characteristics of highbush and rabbiteye blueberry cultivars. *Journal of the Science of Food and Agriculture*, 85(11), 1815–1821.
- Silva, S., Costa, E. M., Veiga, M., Morais, R. M., & Pintado, M. (2018). Health promoting properties of blueberries : a review. *Critical Reviews in Food Science and Nutrition*, 0(0), 1–20.
- Singh, A. P., & Savaldi-Goldstein, S. (2015). Growth control: Brassinosteroid activity gets context. *Journal of Experimental Botany*, 66(4), 1123–1132.
- Singh, B. D., & Singh, A. K. (2015). *Marker-Assisted Plant Breeding: Principles and Practices*. New Delhi: Springer India.
- Singh, N., & Ghosh, K. K. (2019). Recent Advances in the Antioxidant Therapies for Alzheimer's Disease: Emphasis on Natural Antioxidants. In S. Singh & N. Joshi (Eds.), *Pathology, Prevention, and Therapeutics of Neurodegenerative Disease* (pp. 253–263).
- Singh, R. K., Svystun, T., AlDahmash, B., Jonsson, A. M., & Bhalerao, R. P. (2017). Photoperiod- and temperature-mediated control of phenology in trees – a molecular perspective. *New Phytologist*, 213(2), 511–524.
- Spence, C. (2015). Multisensory flavor Perception. *Cell*, 161(1), 24–35.
- Stepanova, A. N., & Alonso, J. M. (2009). Ethylene signaling and response: where different regulatory modules meet. *Current Opinion in Plant Biology*, 12(5), 548–555.
- Stephenson, P. G., Fankhauser, C., & Terry, M. J. (2009). PIF3 is a repressor of chloroplast development. *Proceedings of the National Academy of Sciences of the United States of America*, 106(18), 7654–7659.
- Stevenson, D., & Scalzo, J. (2012). Anthocyanin composition and content of blueberries from around the world. *Journal of Berry Research*, 2(4), 179–189.
- Suarez-Lopez, P., Wheatley, K., Robson, F., Onouchi, H., Valverde, F., & Coupland, G. (2001). *CONSTANS* mediates between the circadian clock and the control of flowering in arabidopsis. *Nature*, 410(April), 1116–1120.
- Subash, S., Essa, M. M., Al-adawi, S., Memon, M. A., Manivasagam, T., & Akbar, M. (2014). Neuroprotective effects of berry fruits on neurodegenerative diseases. *Neural Regeneration Research*, 9(16), 1557–1566.
- Suzuki, N., Koussevitzky, S., Mittler, R., & Miller, G. (2012). ROS and redox signalling in

- the response of plants to abiotic stress. *Plant, Cell and Environment*, 35(2), 259–270.
- Swarup, R., & Péret, B. (2012). AUX/LAX family of auxin influx carriers—an overview. *Frontiers in Plant Science*, 3(October), 1–11.
- Takatsuka, H., & Umeda, M. (2014). Hormonal control of cell division and elongation along differentiation trajectories in roots. *Journal of Experimental Botany*, 65(10), 2633–2643.
- Teotia, S., & Tang, G. (2015). To bloom or not to bloom: Role of micrnas in plant flowering. *Molecular Plant*, 8(3), 359–377.
- Tieman, D., Bliss, P., McIntyre, L. M. M., Blandon-Ubeda, A., Bies, D., Odabasi, A. Z. Z., ... Klee, H. J. J. (2012). The chemical interactions underlying tomato flavor preferences. *Current Biology*, 22(11), 1035–1039.
- Timmers, M. A., Grace, M. H., Yousef, G. G., & Lila, M. A. (2017). Inter- and intra-seasonal changes in anthocyanin accumulation and global metabolite profiling of six blueberry genotypes. *Journal of Food Composition and Analysis*, 59, 105–110.
- Tognetti, J. A., Pontis, H. G., & Martínez-Noël, G. M. A. (2013). Sucrose signaling in plants: A world yet to be explored. *Plant Signaling and Behavior*, 8(3).
- Toivonen, P. M. A. A., & Brummell, D. A. (2008). Biochemical bases of appearance and texture changes in fresh-cut fruit and vegetables. *Postharvest Biology and Technology*, 48(1), 1–14.
- Trehane, J. (2004). *Blueberries, Cranberries, and Other Vacciniums*. Portland, OR: Royal Horticultural Society.
- Tsai, A. Y.-L., & Gazzarrini, S. (2014). Trehalose-6-phosphate and SnRK1 kinases in plant development and signaling: the emerging picture. *Frontiers in Plant Science*, 5(April), 1–11.
- Ulrich, D., & Olbricht, K. (2014). Diversity of metabolite patterns and sensory characters in wild and cultivated strawberries1. *Journal of Berry Research*, 4(1), 11–17.
- USDA. (2018). *Blueberries, Raw - National Nutrient Database for Standard Reference*.
- van der Schoot, C., & Rinne, P. L. H. (2011). Dormancy cycling at the shoot apical meristem: Transitioning between self-organization and self-arrest. *Plant Science*, 180(1), 120–131.
- Varela, P., & Ares, G. (2012). Sensory profiling, the blurred line between sensory and consumer science. A review of novel methods for product characterization. *Food Research International*, 48(2), 893–908.
- Vasconcelos, M. C., Greven, M., Winefield, C. S., Trought, M. C. T., & Raw, V. (2009). The Flowering Process of *Vitis vinifera*: A Review. *American Society of Enology and Viticulture*, 4, 411–434.
- Vergara, R., Noriega, X., Aravena, K., Prieto, H., & Pérez, F. J. (2017). ABA Represses the Expression of Cell Cycle Genes and May Modulate the Development of Endodormancy in Grapevine Buds. *Frontiers in Plant Science*, 8(May), 1–10.
- Vergara, R., Parada, F., Rubio, S., & Perez, F. J. (2012). Hypoxia induces H₂O₂ production and activates Antioxidant defense system in grapevine buds through mediation of H₂O₂ and ethylene. *Journal of Experimental Botany*, 63(11), 4123–4131.
- Vicente, A. R., Ortugno, C., Rosli, H., Powell, A. L. T., Greve, L. C., & Labavitch, J. M. (2007). Temporal sequence of cell wall disassembly events in developing fruits. 2.

- Analysis of blueberry (*Vaccinium* species). *Journal of Agricultural and Food Chemistry*, 55(10), 4125–4130.
- Vishwakarma, K., Upadhyay, N., Kumar, N., Yadav, G., Singh, J., Mishra, R. K., ... Sharma, S. (2017). Abscisic Acid Signaling and Abiotic Stress Tolerance in Plants: A Review on Current Knowledge and Future Prospects. *Frontiers in Plant Science*, 08(February), 1–12.
- Wahyuningsih, S., Wulandari, L., Wartono, M. W., Munawaroh, H., & Ramelan, A. H. (2017). The Effect of pH and Color Stability of Anthocyanin on Food Colorant. *IOP Conference Series: Materials Science and Engineering*, 193(1), 12047.
- Wang, Q.-H., Zhao, C., Zhang, M., Li, Y.-Z., Shen, Y.-Y., & Guo, J.-X. (2017). Transcriptome analysis around the onset of strawberry fruit ripening uncovers an important role of oxidative phosphorylation in ripening. *Scientific Reports*, 7(November 2016), 41477.
- Wasilewska, A., Vlad, F., Sirichandra, C., Redko, Y., Jammes, F., Valon, C., ... Leung, J. (2008). An Update on Abscisic Acid Signaling in Plants and More *Molecular Plant*, 1(2), 198–217.
- Weiner, J., & Freckleton, R. P. (2010). Constant Final Yield. *Annual Review of Ecology, Evolution, and Systematics*, 41(1), 173–192.
- Whyte, A. R., Schafer, G., & Williams, C. M. (2016). Cognitive effects following acute wild blueberry supplementation in 7- to 10-year-old children. *European Journal of Nutrition*, 55(6), 2151–2162.
- Wilkie, J. D., Sedgley, M., & Olesen, T. (2008). Regulation of floral initiation in horticultural trees. *Journal of Experimental Botany*, 59(12), 3215–3228.
- Williamson, J. G., & Lyrene, P. M. (2004). Blueberry varieties for Florida (HS967), 1–9.
- Wingler, A. (2017). Transitioning to the next phase: the role of sugar signaling throughout the plant life cycle. *Plant Physiology*, 176(February), pp.01229.2017.
- Winter, P., & Kahl, G. (1995). Molecular Marker Technologies for Plant Improvement. *World Journal of Microbiology & Biotechnology*, 11(4), 438–448.
- Wisniewski, M., Bassett, C., Gusta, L. V., Li, P., Fuchigami, L., Quamme, H., ... Mcleester, R. (2003). An overview of cold hardiness in woody plants: Seeing the forest through the trees. *Hortscience*, 38(5), 952–959.
- Wurzinger, B., Nukarinen, E., Nägele, T., Weckwerth, W., & Teige, M. (2018). The SnRK1 kinase as central mediator of energy signalling between different organelles. *Plant Physiology*, 176(February), pp.01404.2017.
- Xi, F. F., Guo, L. L., Yu, Y. H., Wang, Y., Li, Q., Zhao, H. L., ... Guo, D. L. (2017). Comparison of reactive oxygen species metabolism during grape berry development between 'Kyoho' and its early ripening bud mutant 'Fengzao.' *Plant Physiology and Biochemistry*, 118, 634–642.
- Xing, L. B., Zhang, D., Li, Y. M., Shen, Y. W., Zhao, C. P., Ma, J. J., ... Han, M. Y. (2015). Transcription profiles reveal sugar and hormone signaling pathways mediating flower induction in apple (*Malus domestica* Borkh.). *Plant and Cell Physiology*, 56(10), 2052–2068.
- Xu, Y. (2010). *Molecular Plant Breeding*. New York: CABI Publishing.
- Yadav, A. K., & Singh, S. V. (2014). Osmotic dehydration of fruits and vegetables: a review. *Journal of Food Science and Technology*, 51(9), 1654–1673.
- Yadav, S. K. (2010). Cold stress tolerance mechanisms in plants. A review. *Agronomy*

- for *Sustainable Development*, 30(3), 515–527.
- Yamane, H. (2014). Regulation of Bud Dormancy and Bud Break in Japanese Apricot (*Prunus mume* Siebold & Zucc.) and Peach [*Prunus persica* (L.) Batsch]: A Summary of Recent Studies. *Journal of the Japanese Society for Horticultural Science*, 83(3), 187–202.
- Yang, M., & Jiao, Y. (2016). Regulation of Axillary Meristem Initiation by Transcription Factors and Plant Hormones. *Frontiers in Plant Science*, 7(February), 1–6.
- Yonekura-Sakakibara, K. (2009). Functional genomics of family 1 glycosyltransferases in *Arabidopsis*. *Plant Biotechnology*, 26(3), 267–274.
- Yonekura-Sakakibara, K., Nakayama, T., Yamazaki, M., & Saito, K. (2009). Modification and Stabilization of Anthocyanins. In C. S. Winefield, K. Davies, & K. Gould (Eds.), *Anthocyanins* (pp. 169–190). New York: Springer Science+Business Media.
- Yousuf, B., Gul, K., Wani, A. A., & Singh, P. (2016). Health Benefits of Anthocyanins and Their Encapsulation for Potential Use in Food Systems: A Review. *Critical Reviews in Food Science and Nutrition*, 56(13), 2223–2230.
- Yu, J., Rubio, V., Lee, N., Bai, S., Lee, S., Kim, S., ... Deng, X. W. (2009). COP1 and ELF3 control circadian function and photoperiodic flowering by regulating GI stability. *Plant Cell*, 21(5), 617–630.
- Zeiss, D. R., Mhlongo, M. I., Tugizimana, F., Steenkamp, P. A., & Dubery, I. A. (2018). Comparative metabolic phenotyping of tomato (*Solanum lycopersicum*) for the identification of metabolic signatures in cultivars differing in resistance to *Ralstonia solanacearum*. *International Journal of Molecular Sciences*, 19(9).
- Zhang, H., Mittal, N., Leamy, L. J., Barazani, O., & Song, B. H. (2017). Back into the wild—Apply untapped genetic diversity of wild relatives for crop improvement. *Evolutionary Applications*, 10(1), 5–24.
- Zhang, Z., Zhuo, X., Zhao, K., Zheng, T., Han, Y., Yuan, C., & Zhang, Q. (2018). Transcriptome Profiles Reveal the Crucial Roles of Hormone and Sugar in the Bud Dormancy of *Prunus mume*. *Scientific Reports*, 8(1).
- Zheng, C., Halaly, T., Acheampong, A. K., Takebayashi, Y., Jikumaru, Y., Kamiya, Y., & Or, E. (2015). Abscisic acid (ABA) regulates grape bud dormancy, and dormancy release stimuli may act through modification of ABA metabolism. *Journal of Experimental Botany*, 66(5), 1527–1542.
- Zheng, C., Kwame Acheampong, A., Shi, Z., Halaly, T., Kamiya, Y., Ophir, R., ... Or, E. (2018). Distinct gibberellin functions during and after grapevine bud dormancy release. *Journal of Experimental Botany*, 69(7), 1635–1648.
- Zhiponova, M. K., Vanhoutte, I., Boudolf, V., Betti, C., Dhondt, S., Coppens, F., ... Russinova, E. (2013). Brassinosteroid production and signaling differentially control cell division and expansion in the leaf. *New Phytologist*, 197(2), 490–502.
- Zhuang, W., Gao, Z., Wen, L., Huo, X., Cai, B., & Zhang, Z. (2015). Metabolic changes upon flower bud break in Japanese apricot are enhanced by exogenous GA4. *Horticulture Research*, 2.
- Zifkin, M., Jin, A., Ozga, J. A., Zaharia, L. I., Scherthaner, J. P., Gesell, A., ... Constabel, C. P. (2012). Gene expression and metabolite profiling of developing highbush blueberry fruit indicates transcriptional regulation of flavonoid metabolism and activation of abscisic acid metabolism. *Plant Physiology*, 158(1), 200–224.
- Zorenc, Z., Veberic, R., Slatnar, A., Koron, D., Miosic, S., Chen, M. H., ... Mikulic-

Petkovsek, M. (2017). A wild 'albino' bilberry (*Vaccinium myrtillus* L.) from Slovenia shows three bottlenecks in the anthocyanin pathway and significant differences in the expression of several regulatory genes compared to the common blue berry type. *PLoS ONE*, 12(12), 1–14.

**Chapter 3. Blueberry Metabolite Profiling and Biparental Association Mapping to
Identify QTLs and Putative Candidate Genes**

3.1. Abstract

The elucidation of metabolites in fruits and vegetables produces essential foundational knowledge researchers utilize to improve the nutrition and health benefits of crops. Blueberries are consistently linked to providing potent health benefits, but only a few metabolites have been thoroughly characterized from fruit extracts. Metabolite profiling can detect and annotate either diverse metabolite groups, like amino acids, or specific metabolites, like anthocyanins, through non-targeted or targeted approaches, respectively. Both non-targeted and targeted metabolite profiling were conducted on acidified extracts of the tetraploid Draper by Jewel (DxJ) mapping population. The non-targeted profiling used ^1H NMR to measure and annotate 192 metabolite features that condensed into 29 known metabolite peaks. The targeted profiling used HPLC-QTOFMS to measure and annotate 23 anthocyanin metabolites. Multiple anthocyanin correlations showed two subsets in the DxJ population. One subset accumulates all the different anthocyanin sugar moieties, while the other subset accumulates only two. Biparental association mapping (BiPAM) was performed on the accumulation of the 29 known metabolites measured by ^1H NMR to identify significant QTL regions and to identify putative candidate genes involved in biosynthesis or regulatory pathways. The BiPAM results for the 11 amino acids revealed primarily biosynthesis putative candidate genes, while the BiPAM results for the eight sugars revealed interconversion and polysaccharide degradation putative candidate genes. The five phenolic acids reveal BiPAM results containing putative candidate genes from multiple steps in the overarching phenolic acid pathway, including epicatechin synthesis. The BiPAM results for the targeted LC-MS anthocyanins revealed multiple QTLs, especially glucoside acylation, that future breeding strategies can utilize to improve anthocyanin accumulation and antioxidant capacity. The antioxidant capacity was also quantified and BiPAM results revealed two QTL regions with putative candidate genes involving in shikimic, phenylpropanoid, flavonoid, and anthocyanin diversification pathways. The metabolic profiling and BiPAM results can be built upon to further elucidate the important metabolic pathways in blueberries, as well as utilized by in future blueberry breeding strategies to develop blueberries with enhanced fruit quality, nutrition, and health benefits.

3.2. Introduction

Plant metabolites are chemical compounds synthesized through metabolic pathways that exhibit essential and specific functions. Metabolites have been traditionally categorized as either primary or secondary due to the limited knowledge researchers had on the diversity and function of metabolites in plants. Primary metabolites are traditionally defined as compounds necessary for the survival of the organism or cell, like nucleic acids, lipids, and amino acids (Buchanan, Grissem, & Jones, 2012). Secondary metabolites are traditionally defined as compounds not necessary for the survival of the organism or cell, like phenolic acids (Buchanan et al., 2012). A plethora of recent research concerning metabolite functions and signaling in plants challenges the traditional definitions as some traditionally secondary metabolites are extremely important for the survival and reproduction of the plant (Chae, Kim, Nilo-Poyanco, & Rhee, 2014; Okazaki & Saito, 2012; Sumner, Lei, Nikolau, & Saito, 2015). For example, plant hormones like salicylic acid are vital for appropriately signaling environmental stresses and pathogen attack (An & Mou, 2011; Klessig & Malamy, 1994; Vlot, Dempsey, & Klessig, 2009). Plant hormones are essential for plant growth and development, but have not been traditionally categorized as a primary metabolite.

A more current definition of primary metabolites are compounds accumulated in almost every cell, all the time, across the majority of plant species (Buchanan et al., 2012; Chae et al., 2014; Hirai et al., 2005; Okazaki & Saito, 2012; Saito & Matsuda, 2010; Sumner et al., 2015; Weng, 2014). This definition still includes nucleic acids, lipids, and amino acids, but also includes vital metabolites like hormones. Secondary metabolites are commonly re-termed as specialized metabolites with a current definition as compounds that are expressed and accumulated in specific cells during specific times, and usually have evolved in select phylogenetic clades (Buchanan et al., 2012; Chae et al., 2014; Hirai et al., 2005; Okazaki & Saito, 2012; Saito & Matsuda, 2010; Sumner et al., 2015; Weng, 2014). A classic example of specialized metabolites are glucosinolate compounds as they are not synthesized in every plant cell and only evolved in the Brassicales order with the function to deter pests and provide some pathogen resistance (Traka & Mithen, 2009). Although these current definitions more appropriately categorize the diversity of metabolites in plants, future research

characterizing the function of more metabolites will bring about modifications to or new definitions in the future.

Even though plant metabolites are vital for energy and nutrition, only a relatively few plant metabolites have been thoroughly characterized. The lack of characterized plant metabolites is due to the limited foundational knowledge and difficulty extracting an appropriate metabolite sample (Scalbert et al., 2009; Sumner et al., 2015). The comprehensive development of an extraction approach is vital for any subsequent metabolite analyses because a great extraction will minimize undesirable structural changes, interactions, or contaminant metabolites in the resulting extract, which would interfere with the quality of metabolite detection analyses (Okazaki & Saito, 2012; Saito & Matsuda, 2010; Theodoridis, Gika, & Wilson, 2008). Developing the thorough extraction approach for the metabolite or metabolites of interest depends on the amount of known information and research focus (Fernie & Schauer, 2009; Matsuda, 2016; Theodoridis et al., 2008). The two main approaches are targeted or non-targeted extractions.

Targeted extractions are utilized when there is a substantial collection of known information about the metabolite so that specific solvents are selected to primarily extract the desired metabolite (Scalbert et al., 2009; Sumner et al., 2015; Weng, 2014). Targeted extractions can focus on either a specific metabolite or a specific metabolite group (Scalbert et al., 2009; Sumner et al., 2015; Weng, 2014). If the research focus of the targeted extraction is a specific metabolite, much more known information is needed to appropriately select extraction solutions and purification methods that differentiate from other similar metabolites (Matsuda, 2016; Saito & Matsuda, 2010; Scalbert et al., 2009; Sumner et al., 2015; Theodoridis et al., 2008). For example, a targeted extraction approach can be developed to extract for the specific glucoraphanin metabolite or a group of metabolites like glucosinolates. Since glucoraphanin is a specific glucosinolate metabolite, a lot of detailed information about glucoraphanin is needed for the targeted extraction in order to select extraction solutions that will only extract the glucoraphanin rather than other similar glucosinolates. A targeted extraction approach for the glucosinolate metabolite group still requires a bunch of previously known information to select extraction solutions that will extract only glucosinolates and not other sulfur and

nitrogen containing metabolites. An ideal targeted extraction will extract the metabolite or metabolite group at the expense of all other metabolites, thus resulting in an extract with very minimal impurities (Matsuda, 2016; Okazaki & Saito, 2012; Saito & Matsuda, 2010; Theodoridis et al., 2008). Unfortunately, the limited knowledge of plant metabolites makes developing targeted extractions with resulting quality extracts very time consuming and costly due to the optimization and instrumentation needed to gain the necessary extraction specificity knowledge (Okazaki & Saito, 2012; Saito & Matsuda, 2010; Theodoridis et al., 2008). But continued metabolite characterization research and advancements in metabolite filtering and detection technology are gradually improving plant metabolite foundational knowledge.

Non-targeted extractions are utilized when there is minimal known information about the metabolite so extraction solutions are selected to extract a group or class of metabolites (Okazaki & Saito, 2012; Saito & Matsuda, 2010; Theodoridis et al., 2008). Since not enough information is known, non-targeted extractions are usually focused on groups of metabolites, like flavonoids (Matsuda, 2016; Saito & Matsuda, 2010; Scalbert et al., 2009; Sumner et al., 2015; Theodoridis et al., 2008). Some non-targeted extraction approaches use few very extraction solutions, often termed crude extracts, that are focused on very broad metabolite groups like phenolic acids or sugars (French, Harvey, & McCullagh, 2018; Matsuda, 2016). Some metabolite assays and kits are non-targeted extractions because they extract for broader metabolite groups, like carbohydrate content (French et al., 2018; Matsuda, 2016; Okazaki & Saito, 2012; Scalbert et al., 2009). The results from non-targeted extractions can be very non-specific, which makes annotation difficult, but can contribute to foundational metabolite knowledge to be utilized for development of targeted extraction approaches for future characterization research (French et al., 2018; Matsuda, 2016; Okazaki & Saito, 2012; Scalbert et al., 2009). With the advancements in computing, bioinformatics, and compound detection, metabolomics and metabolite profiling research has greatly increased, which provides more information on plant metabolites that can be utilized in future research.

3.2.1. Plant Metabolite Profiling

Metabolite profiling is the quantification and identification of metabolites within an extract utilizing highly-sensitive detectors (Saito & Matsuda, 2010; Wolfender, Marti, Thomas, & Bertrand, 2015). Gaining a greater understanding of plant metabolites through metabolite profiling will provide vital information for current and future research on elucidating the complex pathways and interactions that regulate and signal a multitude of processes in plants (Buchanan et al., 2012; Saito & Matsuda, 2010; Wolfender et al., 2015). With the rapid advancements in chromatography, spectrometry, and bioinformatics in the last few decades, metabolite profiling instrumentation has drastically improved in both sensitivity and resolution, which allows for more extensive metabolite profiling (Alonso, Marsal, & Juliá, 2015; Bingol, 2018; Pinu, Pinu, & R, 2018; Sumner et al., 2015; Wolfender et al., 2015; Hengyou Zhang, Mittal, Leamy, Barazani, & Song, 2017). A higher sensitivity allows for the detection of very small quantities and accumulation differences (Alonso et al., 2015; Bingol, 2018; Sumner et al., 2015; Wolfender et al., 2015). A higher resolution allows for the detectors to differentiate between multiple isoforms as well as different stereochemical conformations (Alonso et al., 2015; Bingol, 2018; Sumner et al., 2015; Wolfender et al., 2015). For example, the glucosinolate metabolite class consists of 132 compounds that primarily show diversification at only 1 position (Fernie & Schauer, 2009; Halkier & Gershenzon, 2006; Søndersby, Geu-Flores, & Halkier, 2010; Sumner et al., 2015; Traka & Mithen, 2009). Thorough metabolite profiling of glucosinolates led to the identification of glucoraphanin, which further research has shown to be a very potent anti-carcinogen (Fernie & Schauer, 2009; Halkier & Gershenzon, 2006; Søndersby et al., 2010; Sumner et al., 2015; Traka & Mithen, 2009). Although identifying and quantifying the diversity of metabolites is valuable foundational knowledge, elucidating the regulatory pathways for those metabolites is also vital for a greater understanding of plant metabolites (Alonso et al., 2015; Bingol, 2018; Okazaki & Saito, 2012; Pinu et al., 2018; Saito & Matsuda, 2010; Sumner et al., 2015; Wolfender et al., 2015).

The diversification and accumulation of many specialized metabolites has been attributed to exposure to different selection pressures and stresses, thus stress signaling interacts with the metabolite's regulatory pathway (Buchanan et al., 2012;

Weng, 2014). For example, exposure to harsh light results in flavonoids and anthocyanins accumulation, which indicates the UV stress signaling interacts with and induces flavonoid and anthocyanin biosynthesis (Grace, Xiong, Esposito, Ehlenfeldt, & Lila, 2018; Okazaki & Saito, 2012; Pinasseau et al., 2017; Pinu et al., 2018; Saito & Matsuda, 2010). Primary metabolite regulation is also responsive to stress signaling and can interact with specialized metabolite regulation (Buchanan et al., 2012; Weng, 2014). It is this complexity in signaling and metabolite accumulation that necessitates detection of both high-sensitivity and high-resolution for thorough metabolomics research through targeted and non-targeted profiling.

Targeted and non-targeted profiling utilizes the available known information of plant metabolites to analyze and identify the metabolites within sample extracts. Targeted profiling requires a lot of known information about the metabolite or group of metabolites of interest to configure the detectors for optimal detection (Bingol, 2018; French et al., 2018). A plethora of known information is needed to develop a standard for a metabolite that is of high-quality and pure (Bingol, 2018; Matsuda, 2016; Pinu et al., 2018; Scalbert et al., 2009). Analyzing a purified standard of the metabolite of interest in parallel with profiling the extract provides a very robust identification of the metabolite (Bingol, 2018; Matsuda, 2016; Pinu et al., 2018; Scalbert et al., 2009). Unfortunately, very few plant metabolites have enough information for the development of a purified standard (Bingol, 2018; Matsuda, 2016; Pinu et al., 2018; Scalbert et al., 2009). Other specific characteristics like UV absorbance can be utilized for identification in targeted profiling because only specific metabolites exhibit a UV trace at specific wavelengths (Bingol, 2018; French et al., 2018; Matsuda, 2016; Scalbert et al., 2009; Theodoridis et al., 2008). Although targeted profiling provides high-quality data about a metabolite, the cost and tediousness along with the lack of knowledge hinders the frequency of targeted profiling in research.

Non-targeted profiling requires a minimal amount of known information about a metabolite group of interest in order to provide data on a general metabolite group or a wide array of metabolites, which aids in identification (Bingol, 2018; French et al., 2018; Matsuda, 2016; Scalbert et al., 2009; Theodoridis et al., 2008). One way the detectors for non-targeted profiling can be configured is for a range of detection across narrow

conditions (Bingol, 2018; Matsuda, 2016; Pinu et al., 2018; Scalbert et al., 2009). For example, configuring the UV detector for a range of wavelengths while the extract conditions slightly change in acidity, thus allowing the detection of multiple different metabolites (He et al., 2010; K. D. Sharma, Karki, Thakur, & Attri, 2012; Wahyuningsih, Wulandari, Wartono, Munawaroh, & Ramelan, 2017). Another way the detectors for non-targeted profiling can be configured is for narrow detection across a range of conditions (Bingol, 2018; Matsuda, 2016; Pinu et al., 2018; Scalbert et al., 2009). For example, configuring the UV detector for a specific wavelength while the extract conditions range from slightly acidic to very acidic pH (He et al., 2010; K. D. Sharma et al., 2012; Wahyuningsih et al., 2017). The non-targeted profiling results in many detected metabolites that are compared to known metabolite data (Bingol, 2018; Matsuda, 2016; Pinu et al., 2018; Scalbert et al., 2009). If a detected metabolite is very similar to a well characterized metabolite, like an amino acid, then the detected metabolite is identified as the characterized metabolite (Bingol, 2018; Matsuda, 2016; Pinu et al., 2018; Scalbert et al., 2009). If a detected metabolite shows some similarity to characterized metabolites, then the detected metabolite is annotated as the characterized and requires further research to support or change the annotation (Alonso et al., 2015; Bingol, 2018; Carreno-Quintero, Bouwmeester, & Keurentjes, 2013; Fernie & Schauer, 2009; Matsuda, 2016; Saito & Matsuda, 2010; Scalbert et al., 2009; Sumner et al., 2015; Theodoridis et al., 2008). If the detected metabolite shows no similarity to characterized metabolites, the detected metabolite is an unknown and provides the basis for novel metabolite discovery (Alonso et al., 2015; Bingol, 2018; Carreno-Quintero et al., 2013; Fernie & Schauer, 2009; Matsuda, 2016; Saito & Matsuda, 2010; Scalbert et al., 2009; Sumner et al., 2015; Theodoridis et al., 2008).

Nuclear Magnetic Resonance (NMR) spectroscopy is frequently utilized for metabolite profiling for both targeted and non-targeted analyses. Proton NMR (^1H NMR) determines the chemical shift (ppm) of each hydrogen nuclei within a metabolite (Bingol, 2018; Buchanan et al., 2012; French et al., 2018). The chemical shift of a hydrogen varies depending on the metabolites composition, structure, and proximity to other elements (Bingol, 2018; Buchanan et al., 2012; French et al., 2018). Deuterium (^2H) is a hydrogen isotope that is commonly used in the extract solvent to differentiate solvent

hydrogens from the hydrogens in metabolites of interest (Bingol, 2018; Buchanan et al., 2012; French et al., 2018). When compared to ^2H and known peak spin-spin couplings, the chemical shifts of the metabolite hydrogens provide valuable data for determining metabolite structure and identification (Bingol, 2018; Buchanan et al., 2012; French et al., 2018). ^1H NMR is commonly used to determine compound structure for targeted extractions (Bingol, 2018; Buchanan et al., 2012; French et al., 2018). When analyzing non-targeted extractions, ^1H NMR identifies high abundance compounds due to the peak signals of other metabolites getting muddled with other peaks or noise (Bingol, 2018; Buchanan et al., 2012; French et al., 2018).

High-pressure liquid chromatography (HPLC) coupled with mass spectrometry (MS) is also frequently utilized for metabolite profiling on targeted and non-targeted extractions. The HPLC utilizes highly-specific columns and liquid chromatography to separate metabolites within an aqueous extract for detection by either UV/Vis spectrometry or mass spectrometry (MS) (Bingol, 2018; Matsuda, 2016; Scalbert et al., 2009; Sumner et al., 2015; Theodoridis et al., 2008). UV/Vis spectrometry measures the absorption or reflectance of compounds with photodetectors when exposed to different light wavelengths (Bingol, 2018; Matsuda, 2016; Pinasseau et al., 2017; Scalbert et al., 2009; Sumner et al., 2015; Theodoridis et al., 2008). As the sample run progresses, the sample is exposed to multiple wavelengths and the photodetectors measure the responses to produce a UV trace spectra for the sample (Bingol, 2018; Matsuda, 2016; Pinasseau et al., 2017; Scalbert et al., 2009; Sumner et al., 2015; Theodoridis et al., 2008). Specific metabolites absorb or reflect specific wavelengths, which allows for UV/Vis detection to measure specific metabolites in a mixture (Bingol, 2018; Matsuda, 2016; Scalbert et al., 2009; Sumner et al., 2015; Theodoridis et al., 2008). The separated metabolites from HPLC can also be directly injected into an MS for ion detection (LC-MS) (Bingol, 2018; Matsuda, 2016; Scalbert et al., 2009; Sumner et al., 2015; Theodoridis et al., 2008). In summary, the separated metabolites are ionized, accelerated by magnetic fields, and detected with highly-sensitive ion detectors to determine the mass-to-charge ratio (m/z) (Bingol, 2018; Matsuda, 2016; Scalbert et al., 2009; Sumner et al., 2015; Theodoridis et al., 2008). For time-of-flight MS (TOFMS), the metabolite m/z is determined by the time it takes for the individual metabolite ion to hit

to the detector under a constant magnetic field (Bingol, 2018; Matsuda, 2016; Pinasseau et al., 2017; Scalbert et al., 2009; Sumner et al., 2015; Theodoridis et al., 2008). The detector differentiates the different metabolites because metabolites with a small m/z travel faster to the detector than metabolites with large m/z (Bingol, 2018; Matsuda, 2016; Scalbert et al., 2009; Sumner et al., 2015; Theodoridis et al., 2008). Due to the separation specificity of HPLC and detection sensitivity of MS, a multitude of metabolite features can be detected, thus only small amounts of quality sample are needed for metabolite quantification and annotation.

Before databases were prevalent for “-omics” data, metabolite annotations and pathway analysis required great expertise and background knowledge specific for that pathway. The compilation of metabolomics and metabolite pathway data into user-friendly databases has greatly enhanced metabolite annotations and analysis. The Kyoto Encyclopedia of Genes and Genomes (KEGG) database is one of the main compilation databases that contains not only metabolomic data, but also genomic and other high-throughput data technologies (Kanehisa, Furumichi, Tanabe, Sato, & Morishima, 2017). With the KEGG database exponentially increasing, it has been separated into 16 different databases focused on either systems, genomic, chemical, or health information. The KEGG pathway database provides metabolite, enzyme, and reaction information represented in manually drawn pathway maps (Kanehisa et al., 2017). Along with KEGG, the plant metabolic network (PMN) is another main compilation database comprised of information from 350 plant species (Chae et al., 2014). PMN contains species specific databases as well as the PlantCyc database, which combines multiple species to form reference pathways and enzymes (Chae et al., 2014). PlantCyc has over 1,000 pathways with the majority of enzymes and metabolites being curated from experimental literature (Chae et al., 2014). KEGG and PlantCyc are a wealth of knowledge and resources that is open to the public and has truly change metabolomics and metabolite pathway analysis for years to come.

3.2.2. Plant Metabolites and Human Health

Eating plants provides all the essential nutrients: fats, proteins, amino acids, carbohydrates, and other vitamins and minerals. Humans cannot fully synthesize nine of the 20 amino acids needed for complete protein synthesis (Buchanan et al., 2012;

Kader, 2008). These nine amino acids (methionine, valine, leucine, isoleucine, threonine, lysine, histidine, phenylalanine, and tryptophan) are labeled essential amino acids and must be obtained through diet (Buchanan et al., 2012; Kader, 2008). Foods that contain good proportions of the essential amino acids are termed “complete protein” sources (Barrett, Beaulieu, & Shewfelt, 2010; Buchanan et al., 2012; Prasanna, Prabha, & Tharanathan, 2007). Animal products high in protein like meat, poultry, eggs, milk, cheese, and yogurt are considered “complete protein” sources. The best non-animal “complete protein” sources are plant crops with high protein content, especially beans like soybeans and grains like quinoa. Of the remaining 11 amino acids, six are labeled as conditional due to the limited synthesis in humans during stress or illness, with an emphasis on obtaining more through diet (arginine, cysteine, glycine, glutamine, proline, and tyrosine) (Barrett et al., 2010; Buchanan et al., 2012; Prasanna et al., 2007). Consuming more of these amino acids will aid in the body fighting the sickness and other stresses because it not only supplies protein synthesis but also allows the body to reserve energy to fight the sickness more.

In addition to providing vital nutrients, plants have been constantly utilized for medicinal benefits. For example, ginger root, *Zingiber officinale*, has been utilized as a medicinal remedy for a plethora of ailments for thousands of years (Butt & Sultan, 2011). The phytochemicals with health benefits consists mainly of gingerols and volatile sesquiterpene and monoterpenes (Butt & Sultan, 2011). Gingerols are phenols with unbranched alkyl chains that are hydrated into shogaols, which also hydrates shogaols into paradol and other derivatives (Butt & Sultan, 2011). Gingerol alone shows strong antioxidant activity in vitro (Butt & Sultan, 2011) and any consumption of antioxidants improves the reduction of oxidative stress. There is strong evidence supporting ginger reducing cancer onset, preventing tumor growth, inhibiting rapid proliferation, inducing apoptosis, and inducing detoxification pathway genes (Butt & Sultan, 2011).

The story of discovering and developing aspirin from a plant metabolite is a well-known success story (Buchanan et al., 2012; Gul et al., 2015; Hernández-Sotomayor et al., 2018; Kumar et al., 2015; Weng, 2014; Wolfender et al., 2015). Throughout history, willow bark was used as a strong remedy for pain and inflammation (Buchanan et al., 2012; Kumar et al., 2015). By the nineteenth century, chemical research dramatically

advanced and determined the compound salicylic acid and its derivatives were the active metabolite in willow extract (Kumar et al., 2015). Pharmaceutical companies utilized this knowledge to investigate salicylic acid derivatives and artificial synthesis to determine their effectiveness on treating inflammation (Buchanan et al., 2012; Kumar et al., 2015). After further research and artificial synthesis optimization, acetylsalicylic acid was developed as a less-irritating anti-inflammatory and branded aspirin by Bayer in 1899 (Kumar et al., 2015). Aspirin is used globally as a pain-reliever and anti-inflammatory (Kumar et al., 2015; Okazaki & Saito, 2012; Weng, 2014; Wolfender et al., 2015). Recent research shows aspirin reducing heart attacks and strokes through decreasing blood platelet aggregation (Kumar et al., 2015; Weng, 2014; Wolfender et al., 2015). The great success of aspirin from willow bark sparked research initiatives to discover more plant metabolites that benefit human health.

Another well-known plant metabolite with great health benefits is paclitaxel, also known as taxol. Paclitaxel was discovered and isolated from pacific yew tree, *Taxus brevifolia*, extracts (Buchanan et al., 2012; Kumar et al., 2015). Both in cell culture and cancer patients, paclitaxel is a potent chemotherapy metabolite (Kumar et al., 2015). The paclitaxel mechanism involves interfering with a microtubule function and chromosome segregation during mitosis, thus inhibiting mitosis progression (Kumar et al., 2015). When cells do not complete proper mitotic checkpoints, apoptosis of the cell is triggered (Buchanan et al., 2012). Paclitaxel is now synthesized in cell culture and has become a vital chemotherapy drug (Kumar et al., 2015). The digitalin metabolite is also another plant metabolite that was discovered to have important health benefits. Digitalin was isolated from the *Digitalis* genus, commonly known as foxglove (Buchanan et al., 2012). In patients with cardiac arrhythmia and congestive heart failure, digitalin has been shown to steady the patient's heart rate by strengthening the hearts contractibility (Kumar et al., 2015). Digitalin works by inhibiting sodium-potassium ATPases pumps in the heart, which increases the sodium and calcium gradient across the cell membrane (Kumar et al., 2015). This results in improved contractibility of heart muscles (Kumar et al., 2015). Taxol and digitalin are metabolites that are extracted from the plants and turned into very important cancer and heart drugs.

The medicinal story for glucosinolates provides hope that within human cultivated fruits and vegetables, humans are constantly consuming small amounts of anticarcinogens and antioxidants that will protect against future illnesses. Brassicaceae vegetables have been important vegetables in the human diet for thousands of years due to their distinctive flavor. The discovery and elucidation of glucosinolates was originally focused on reducing off flavors in *Brassica rapeseed* oil (Kumar et al., 2015; Saban, 2018; Traka & Mithen, 2009). It wasn't until much later after most of the *Arabidopsis thaliana* glucosinolate pathway was characterized to further reduce the flavor, when a plethora of research focused on the anticarcinogenic properties emerged (Kumar et al., 2015; Saban, 2018; Traka & Mithen, 2009). Soon after the initial studies, multiple labs started working on glucosinolate biosynthesis and its effect of cancer cell lines (Kumar et al., 2015; Saban, 2018; Traka & Mithen, 2009). This led to the discovery that the potent anticarcinogenic compound is not glucosinolates, but the degradation products, isothiocyanates. The conversion of glucosinolates to isothiocyanates is catalyzed by myrosinase, which is released from its compartmentalization to interact with other glucosinolates. After investigating a multitude of *Brassica* vegetables and relatives, broccoli was shown to accumulate high levels of the glucosinolate, glucoraphanin, which produces sulforaphan after myrosinase conversion (Kumar et al., 2015; Saban, 2018; Traka & Mithen, 2009). Therefore, optimal sulforaphan conversion by myrosinase in broccoli consists of heating broccoli to inactivate competitive degradation enzymes and chewing broccoli to allow myrosinase interaction (Matusheski, Juvik, & Jeffery, 2004; Rungapamestry, Duncan, Fuller, & Ratcliffe, 2008; Song & Thornalley, 2007; Van Eylen, Oey, Hendrickx, & Van Loey, 2007).

3.2.3. Antioxidant Capacity

Researchers consistently see a strongly link between antioxidants and numerous health benefits like anticancer, anti-bacterial, anti-inflammatory, cardioprotective, and neuroprotective, as well as therapeutic for diabetes, osteoporosis, arthritis, and retinal degeneration (Alam, Bristi, & Rafiquzzaman, 2013; Aurelia Magdalena Pisoschi, Aneta Pop, Carmen Cimpeanu, & Gabriel Predoi, 2016; Galano et al., 2016; Huang, Ou, & Prior, 2005; Moharram & Youssef, 2014; Niki, 2011; S. Singh & Singh, 2008). These health benefits have been tightly associated with the antioxidants reducing oxidative

stress, because prolonged oxidative stress has been shown to accelerate the onset and progression of the above mentioned diseases (R. L. Prior, Sintara, & Chang, 2016; Silva, Costa, Veiga, Morais, & Pintado, 2018; N. Singh & Ghosh, 2019; Subash et al., 2014). Oxidative stress is an imbalance of free radicals and antioxidants (Galano et al., 2016; Huang et al., 2005; Lobo, Patil, Phatak, & Chandra, 2010; Mishra, Ojha, & Chaudhury, 2012; Moharram & Youssef, 2014; O. P. Sharma & Bhat, 2009; S. Singh & Singh, 2008). Free radicals are any metabolite that contains an unpaired electron, which can be donated or accepted by another metabolite, thus acting as an oxidant or reductant, respectively (R. L. Prior et al., 2016; Silva et al., 2018; N. Singh & Ghosh, 2019; Subash et al., 2014). Free radicals can be reactive oxygen species (ROS) or reactive nitrogen species (RNS), and are a natural byproduct of respiration as well as environmental stresses respectively (Ahmadinejad, Geir Møller, Hashemzadeh-Chaleshtori, Bidkhorji, & Jami, 2017; Foyer & Noctor, 2011; Huang et al., 2005; Lobo et al., 2010). During oxidative stress, there is an accumulation of ROS-RNS that are not scavenged and perpetuate oxidative reaction chains that cause oxidative damage to important macromolecules (Ahmadinejad et al., 2017; Foyer & Noctor, 2011; Huang et al., 2005; Lobo et al., 2010; S. Singh & Singh, 2008). ROS have been shown to damage lipids, proteins, and DNA.

The dynamic equilibrium between ROS-RNS and antioxidants provides vital signaling and defense responses for plants and humans. Antioxidants are compounds that quench the ROS-RNS and oxidative reactions through enzymatic and non-enzymatic reactions while maintaining its own stability (Lobo et al., 2010; Suzuki, Koussevitzky, Mittler, & Miller, 2012; S. Y. Wang & Jiao, 2000). Antioxidants are only effective if the subsequent antioxidant radical formed after neutralizing the original ROS is less reactive and more stable than the ROS-RNS (Aurelia Magdalena Pisoschi et al., 2016; Foyer & Noctor, 2011; Galano et al., 2016; Huang et al., 2005; Mishra et al., 2012; Moharram & Youssef, 2014). Enzymatic antioxidants convert the multiple different ROS-RNS to hydrogen peroxide, which is then further converted to water (Galano et al., 2016; Saito & Matsuda, 2010). Common enzymatic antioxidants are catalases and peroxidases. The ascorbic acid-glutathione cycle combines both enzymatic and non-

enzymatic antioxidants to recycle antioxidant capacity (Foyer & Noctor, 2011; Galano et al., 2016; Saito & Matsuda, 2010).

Non-enzymatic antioxidants interact with the ROS to neutralize the free radical reactivity (Galano et al., 2016; Saito & Matsuda, 2010). These antioxidants break the radical chain reaction through different combinations of proton or electron transfers. The reaction schemes described below and in Table 1 are possible mechanisms for phenolic acids, hydroxycinnamic acids, flavonoids, and anthocyanins (Chiva-Blanch & Visioli, 2012; Giacalone et al., 2011; Kraujalyte, Venskutonis, Pukalskas, Česonienė, & Daubaras, 2015). The simplest reaction scheme (Table 3.1), hydrogen-atom transfer (HAT), transfers in one step a single hydrogen atom entity, which contains a proton and electron (Galano et al., 2016; Saito & Matsuda, 2010). In a two-step process, sequential proton-loss electron transfer (SPLET) (Table 3.1) first transfers a proton, and then transfers an electron to the radical. Sequential electron proton transfer (SEPT) is the reverse of SPLET with an electron transferred first to the radical, then a proton is transferred (Table 3.1). Sequential proton-loss hydrogen-atom transfer (SPLHAT) also involves two steps with first a transfer of a proton, and then a transfer of a hydrogen atom (Table 3.1).

Table 3.1 – Reaction schemes for possible non-enzymatic antioxidants when scavenging ROS-RNS.

	Reaction Scheme
HAT	$H_nA + R^\bullet \rightarrow H_{n-1}A^\bullet + HR$
SPLET	1) $H_nA \rightarrow H_{n-1}A^- + H^+$ 2) $H_{n-1}A^- + R^\bullet \rightarrow H_{n-1}A^{\bullet-} + R^-$
SEPT	1) $H_nA + R^\bullet \rightarrow H_{n-1}A^{\bullet+} + R^-$ 2) $H_{n-1}A^{\bullet+} \rightarrow H_{n-1}A^\bullet + H^+$
SPLHAT	1) $H_nA \rightarrow H_{n-1}A^- + H^+$ 2) $H_{n-1}A^- + R^\bullet \rightarrow H_{n-2}A^{\bullet-} + HR$

(Table adapted from reaction equations Galano et al 2016).

- H_nA represents the number of hydrogens bound to the antioxidant (A)

- \bullet represents the unpaired electron

- R represents the radical

- $^+$ or $^-$ represents compound charge

There are multiple *in vitro* assays that measure a sample's antioxidant or free radical scavenging capacity (Moharram & Youssef, 2014; S. Singh & Singh, 2008). The main limitation to all *in vitro* antioxidant capacity assays is the translation and applicability to biological systems. Antioxidant capacity data obtained in cell culture and *in vivo* provides the best biologically relevant data. Unfortunately, cell culture and *in vivo* assays are expensive, time-consuming, and require ample training to produce quality data. *In vitro* assays are focused primarily on the reaction chemistry, but must be optimized for substrate-reaction efficiency and reproducibility without sacrificing translatability to biological context (Moharram & Youssef, 2014; S. Singh & Singh, 2008). The four antioxidant capacity assays described below are simple, sensitive, quick, and inexpensive assays, which are important factors for phenotyping a large population, and utilize trolox, a vitamin E analog, as an antioxidant standard control (Ahmadinejad et al., 2017; Aurelia Magdalena Pisoschi et al., 2016; Galano et al., 2016; Himamura et al., 2014; Huang et al., 2005; Kedare & Singh, 2011; Mishra et al., 2012; Niki, 2011; O. P. Sharma & Bhat, 2009).

The oxygen radical absorbance capacity (ORAC) assay measures the reduction in fluorescence as the fluorescent molecule degrades (Aurelia Magdalena Pisoschi et al., 2016; Huang et al., 2005; Mishra et al., 2012; Moharram & Youssef, 2014). Without an antioxidant, free peroxy or hydroxyl radicals degrade the fluorescent molecule. With an antioxidant, the free radicals are scavenged, which minimizes the degradation of the fluorescent molecule. ORAC results also provide information on both inhibition time and inhibition degree. Utilizing fluorescent probes for detection eliminates any interference from the extract's color, which can be an issue for UV spectrometry assays. Unfortunately, the fluorescent molecule does not resemble any natural metabolite, thus the antioxidant activity does not translate well to a biological system. There is also a lack of strong evidence for efficient production of free radicals during the assay to effect the fluorescent molecule, and for the involvement of scavenging the free radicals in reducing the fluorescent molecule degradation (Aurelia Magdalena Pisoschi et al., 2016; Huang et al., 2005; Mishra et al., 2012; Moharram & Youssef, 2014).

The ABTS (2,2'-azino-bis(3-ethylbenzothiazoline-6-sulphonic acid)) assay and DPPH (2,3-diphenyl-1-picrylhydrazyl) assay measure the antioxidant capacity through

decolorization because the antioxidants change the assay solution's color, which can be quantified through UV spectrometry at wavelengths 415nm and 520nm, respectively (Himamura et al., 2014; Huang et al., 2005; Kedare & Singh, 2011; Mishra et al., 2012; Moharram & Youssef, 2014; Niki, 2011; O. P. Sharma & Bhat, 2009; S. Singh & Singh, 2008). Although the ABTS assay can be performed in a range of pHs and provide some rate data, ABTS requires pre-generation of the ABTS radical, which can show batch variation, and results are very time interval sensitive (Ahmadinejad et al., 2017; Huang et al., 2005; Moharram & Youssef, 2014; Niki, 2011; S. Singh & Singh, 2008). The DPPH assay utilizes the stable DPPH radical that is probably scavenged through HAT/SPLHAT mechanism. DPPH is light sensitive and requires hydrophilic conditions. The DPPH assay is simple, easy, sensitive, and cost effective, which is all ideal for phenotyping across large samples like a mapping population (Ahmadinejad et al., 2017; Himamura et al., 2014; Huang et al., 2005; Kedare & Singh, 2011; Mishra et al., 2012; Moharram & Youssef, 2014; Niki, 2011; O. P. Sharma & Bhat, 2009). The FRAP (ferric reducing/antioxidant power) assay measures coloration at 593nm wavelength when exposed to antioxidants (Aurelia Magdalena Pisoschi et al., 2016; Huang et al., 2005; Mishra et al., 2012; Moharram & Youssef, 2014). The antioxidant reduces through electron transfer ferric tripyridyltriazine complex (Fe^{3+} -TPTZ) to ferrous complex (Fe^{2+} -TPTZ) under acidic conditions. Although FRAP is very reproducible, the low pH restriction limits its physiological application and does not provide chain-breaking or preventative activity information with no oxidizable substrate. Although each antioxidant capacity assay has its limitations, an appropriate assay can still provide useful foundational knowledge, especially when the limitations are reduced or not applicable for the research. A thorough quantification of antioxidant capacity and free radical scavenging occurs when multiple *in vitro* and *in vivo* assays are conducted on the particular extract.

As mentioned previously, antioxidants can be enzymes or metabolites so that there is a constant balancing of ROS-RNS with antioxidants (Lobo et al., 2010; Suzuki et al., 2012; S. Y. Wang & Jiao, 2000). Phenolic acids have been constantly linked to antioxidant properties of food as phenolic acids contain at least one phenol moiety and one carboxylic acid functional group (Aurelia Magdalena Pisoschi et al., 2016; Chiva-

Blanch & Visioli, 2012; Galano et al., 2016; Himamura et al., 2014; Huang et al., 2005; Lobo et al., 2010; Niki, 2011). Phenolic acids is a general classification of aromatic acids that includes gallic, quinic, shikimic, chorismic, chlorogenic, caffeic, and benzoic acids, along with polyphenols like flavonoids (Aurelia Magdalena Pisoschi et al., 2016; Chiva-Blanch & Visioli, 2012; Kanehisa et al., 2017). Polyphenols branch off from the central intermediate in the phenylpropanoid pathway, p-coumaroyl-CoA (Chae et al., 2014; Kanehisa et al., 2017). Polyphenols contain two phenol rings linked by an oxygen pyran ring (Figure 3.1). Of the polyphenols, flavonoids and their derivatives like flavonols and anthocyanins exhibit strong antioxidant properties and are found in high quantities in fruits and vegetables (Chiva-Blanch & Visioli, 2012; Galano et al., 2016).

3.2.4. Blueberry Metabolites

Blueberries are an important fresh berry crop that is shipped globally and has increased in consumption, production, and demand due to society spreading the news on blueberries exhibiting potent antioxidant health benefits (Eklund, 2016). Blueberry background and agronomic information is described in detail in Chapter 2. Anthocyanins are responsible for the blue, dark purple coloration of blueberry skins (Ferreira, Castro, Carrasco, Pinto-Carnide, & Arroyo-García, 2018; Forney, Kalt, Jordan, Vinqvist-Tymchuk, & Fillmore, 2012). Anthocyanins are phenolic phytochemicals synthesized from phenylalanine through the flavonoid biosynthesis pathway and branching off to an anthocyanin specific pathway (He et al., 2010; Horbowicz, Grzesiuk, DEBski, & Kosson, 2008; Khoo, Azlan, Tang, & Lim, 2017; Routray & Orsat, 2011; Scalzo, Stevenson, & Hedderley, 2015). Anthocyanins consist of an anthocyanidin core structure with different sugar moieties and other sugar modifications at specific positions (He et al., 2010; Khoo et al., 2017; Routray & Orsat, 2011; Yonekura-Sakakibara, Nakayama, Yamazaki, & Saito, 2009). The anthocyanidin core is a polyphenol with two 6-carbon rings (A and B) linked together by a 3-carbon and oxygen ring (C) (Figure 3.1) (He et al., 2010; Khoo et al., 2017; Routray & Orsat, 2011; Yonekura-Sakakibara et al., 2009). The anthocyanidin core is in dynamic equilibrium with four different forms: flavylium cation, quinonodial structure, hemiketal form, and chalcone forms. The flavylium cation is predominant when pH is 1-3 (Routray & Orsat, 2011; Yonekura-Sakakibara et al., 2009). As pH increases, equilibrium shifts to hemiketal/hydrated flavylium cation, to quinonoidal

structures, then chalcone forms (Routray & Orsat, 2011; Yonekura-Sakakibara et al., 2009). Due to the low pH of blueberry fruit, anthocyanidins are predominantly in flavyium cation, which has a dark purple color (Horbowicz et al., 2008; Nakayama, Suzuki, & Nishino, 2003; Routray & Orsat, 2011; Scalzo, Stevenson, & Hedderley, 2013; Yonekura-Sakakibara et al., 2009).

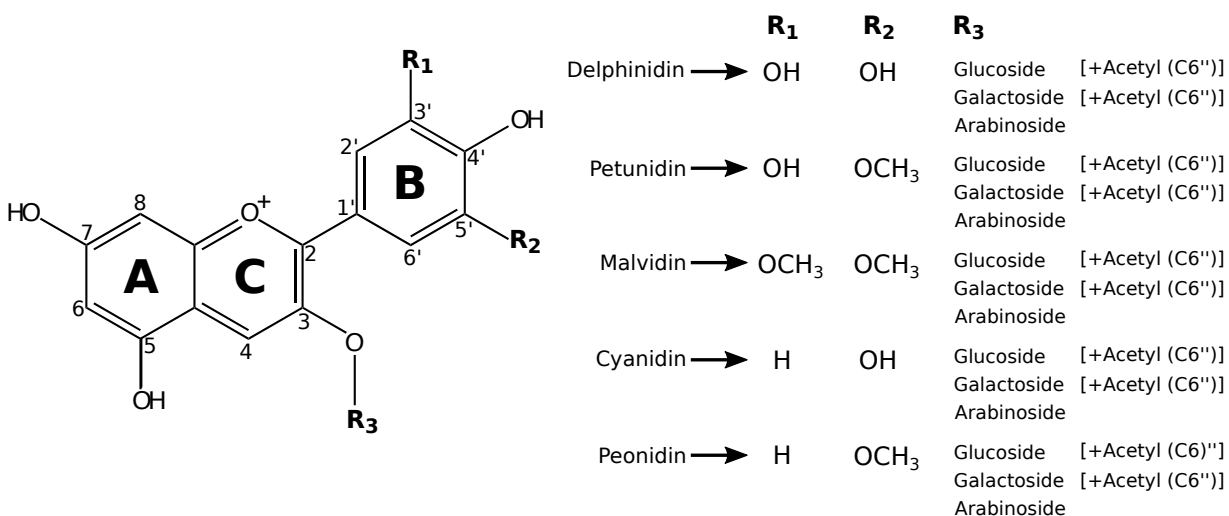


Figure 3.1 – Anthocyanin metabolite diversity in blueberry. Anthocyanidin core molecule consists of two 6-carbon rings (A and B) linked together by a 3-carbon and oxygen ring (C). The anthocyanidin diversity is due to the different functional groups at positions R₁ and R₂. The anthocyanin metabolite diversity is due to different combinations of different anthocyanidin cores with different sugar moieties and modifications at position R₃. The anthocyanidins described in the figure represent the common anthocyanidins found in blueberry.

The five main anthocyanidin cores found in blueberry berries are delphinidin, petunidin, malvidin, cyanidin, and peonidin. Petunidin and malvidin are methylated derivatives of delphinidin, whereas peonidin is a methylated derivative of cyanidin, shown with R₁ and R₂ in Figure 3.1. Delphinidin and cyanidin branched from each other during flavonoid biosynthesis when dihydroquercetin could be either converted to leucocyanidin or dihydromyricetin, which then converts to leucodelphinidin (He et al., 2010; Jaakola, 2002; Khoo et al., 2017; Routray & Orsat, 2011; Scalzo et al., 2015; Stevenson & Scalzo, 2012; Yonekura-Sakakibara et al., 2009). The delphinidin anthocyanidin contains hydroxyl groups at the 3' (R₁) and 5' (R₂) positions, whereas cyanidin contains a hydroxyl group at only 3' (R₁) position (Figure 3.1). Methylation at

the 3' (R_1) hydroxyl group of delphinidin and cyanidin produce the anthocyanidins, petunidin and peonidin, respectively (Figure 3.1). The anthocyanidin, malvidin, is produced from delphinidin methylated at both the 3' (R_1) and the 5' (R_2) hydroxyl group (Figure 3.1) (Routray & Orsat, 2011; Yonekura-Sakakibara et al., 2009). Although not found in blueberries, pelargonidin is another anthocyanidin core that is neither hydroxylated nor methylated (Chae et al., 2014; Kanehisa et al., 2017).

Due to the diversity of sugars moieties and other modifications that can be added to the anthocyanidins, over 500 different anthocyanins have been identified (D. Li et al., 2017; Routray & Orsat, 2011; Wahyuningsih et al., 2017; Yonekura-Sakakibara et al., 2009). According to anthocyanin literature, anthocyanins are broadly categorized as either anthocyanidin glycosides, which is termed an anthocyanin, or acylated anthocyanins (Khoo et al., 2017; Nakayama et al., 2003; Rinaldo et al., 2015; Routray & Orsat, 2011; Sasaki, Nishizaki, Ozeki, & Miyahara, 2014; Skates et al., 2018; Wahyuningsih et al., 2017; Yonekura-Sakakibara, 2009). Glycosylation of the anthocyanidin predominantly occurs at the 3 (R_3) position of ring C (Figure 3.1). The different sugar moieties usually found in blueberry anthocyanins are glucoside, galactoside, arabinoside, and xyloside (Figure 3.1). Anthocyanin sugar moieties can also be a rutinoside, sambubioside, rhamnoside, or di-glucoside (Routray & Orsat, 2011; Yonekura-Sakakibara et al., 2009). The glycoside can also be further modified through additional glycosylation or acylation with different acids (Khoo et al., 2017; Nakayama et al., 2003; Rinaldo et al., 2015; Sasaki et al., 2014; Skates et al., 2018; Wahyuningsih et al., 2017; Yonekura-Sakakibara, 2009). Acylation with aliphatic acids like acetic, malic, and succinic acids has been shown for anthocyanins (Khoo et al., 2017; Nakayama et al., 2003; Rinaldo et al., 2015; Routray & Orsat, 2011; Sasaki et al., 2014; Yonekura-Sakakibara et al., 2009). Acylation with aromatic acids like p-coumaric, caffeic, or gallic acid has also been shown for anthocyanins (Khoo et al., 2017; Nakayama et al., 2003; Rinaldo et al., 2015; Routray & Orsat, 2011; Sasaki et al., 2014; Yonekura-Sakakibara et al., 2009). In blueberries, acylation with acetic acid at the glycoside's 6-OH is more common (Figure 3.1) (Nakayama et al., 2003; Overall et al., 2017; Rinaldo et al., 2015; Sasaki et al., 2014). Glycosylation and acylation of anthocyanins has been shown increase anthocyanin stability and coloration through

intramolecular H-bonding (Khoo et al., 2017; Nakayama et al., 2003; Rinaldo et al., 2015; Routray & Orsat, 2011; Sasaki et al., 2014; Skates et al., 2018; Wahyuningsih et al., 2017; Yonekura-Sakakibara, 2009; Yonekura-Sakakibara et al., 2009).

The high phenolic acid content along with the anthocyanins has gained blueberries the spotlight in crop nutrition research. Blueberry phenolics have been strongly associated with reducing oxidative stress, preventing cardiovascular disease, protecting neurological function, managing diabetes pathways, and reducing cancer tumor growth (Aqil et al., 2016; Edirisinghe & Burton-Freeman, 2016; Gowd, Jia, & Chen, 2017; Klimis-Zacas, Vendrame, & Kristo, 2016; Lin et al., 2016; Pan et al., 2018, 2017; Sarkar et al., 2017; Silva et al., 2018; N. Singh & Ghosh, 2019; Whyte, Schafer, & Williams, 2016; Xi et al., 2017). Blueberry phenolics have been shown by multiple researchers to exhibit potent antioxidant characteristics, particularly the anthocyanins (McNamara et al., 2018; Prencipe et al., 2014; Rodriguez-Mateos, Feliciano, Cifuentes-Gomez, & Spencer, 2016; Rodriguez-Mateos et al., 2013; Routray & Orsat, 2011; Silva et al., 2018; N. Singh & Ghosh, 2019; Subash et al., 2014; Willig, 2009). Not only do blueberry extracts with their high phenolic acid content and anthocyanins scavenge ROS-RNS radicals, but they also induce other antioxidants like glutathione and ascorbate (Aurelia Magdalena Pisoschi et al., 2016; Chiva-Blanch & Visioli, 2012; Foyer & Noctor, 2011; Galano et al., 2016; Lobo et al., 2010; S. Y. Wang, Chen, Camp, & Ehlenfeldt, 2012). Anthocyanins, along with other flavonoids, are very strong ROS-RNS scavengers because the unpaired electron can be spread out over the resonance structures of the 3 phenolic rings, and shielded by the electronegativity of the hydroxyl groups (Ahmadinejad et al., 2017; Galano et al., 2016; Huang et al., 2005; S. Y. Wang & Jiao, 2000). The potent antioxidant capacity of blueberry phenolics and anthocyanins plays a significant role in the anti-inflammation benefits.

Chronic inflammation and oxidative stress have been shown to drastically increase arthritis onset, the risk of cardiovascular disease, and developing metabolic syndrome (Ahmadinejad et al., 2017; Edirisinghe & Burton-Freeman, 2016; Klimis-Zacas et al., 2016; Lobo et al., 2010; Mykkänen et al., 2014; Neto, 2007). Blueberry extracts containing phenolics like gallic and chlorogenic acid, and enriched anthocyanins have been shown to reduce inflammation through either inducing anti-

inflammatory genes or reducing oxidative stress (Ahmadinejad et al., 2017; Edirisinghe & Burton-Freeman, 2016; Klimis-Zacas et al., 2016; Lobo et al., 2010; Mykkänen et al., 2014; Neto, 2007). Blueberry extracts have also been shown in both mice and teenagers to reduce the inflammation and degradation of joints commonly found in arthritis (Ahmadinejad et al., 2017; Edirisinghe & Burton-Freeman, 2016; Klimis-Zacas et al., 2016; Lobo et al., 2010; Mykkänen et al., 2014; Neto, 2007; Silva et al., 2018). Flavonoids have been shown to improve blood flow and vascular endothelial function, which reduces the risk of heart attack and cardiovascular disease (Ali Ghasemzadeh, 2011; Bornsek et al., 2012; Khoo et al., 2017; Klimis-Zacas et al., 2016; Lila, Burton-Freeman, Grace, & Kalt, 2016; Overall et al., 2017; Raskin I, Yousef GG, 2013; Rodriguez-Mateos et al., 2013). When treated with the anthocyanin malvidin, umbilical cord vascular endothelial cells showed a decrease in ROS as well as an increase in superoxide dismutase (SOD), which indicates the mechanism involves reducing oxidative stress (Ali Ghasemzadeh, 2011; Bornsek et al., 2012; Khoo et al., 2017; Klimis-Zacas et al., 2016; Lila et al., 2016; Overall et al., 2017; Raskin I, Yousef GG, 2013; Rodriguez-Mateos et al., 2013; Silva et al., 2018).

The regulation and improvement of vascular endothelial functions not only helps reduce cardiovascular issues, but also aids in regulating metabolic syndrome. Metabolic syndrome occurs when multiple metabolic processes are dysfunctional and result in central obesity, high blood pressure, high blood sugar, high serum triglycerides, and low serum high-density lipoprotein (Ali Ghasemzadeh, 2011; Bornsek et al., 2012; Khoo et al., 2017; Klimis-Zacas et al., 2016; Lila et al., 2016; Overall et al., 2017; Raskin I, Yousef GG, 2013; Rodriguez-Mateos et al., 2013; Silva et al., 2018). Upon blueberry consumption, adults with metabolic syndrome saw improved endothelial function and reduced inflammation markers. The proposed mechanism is that anthocyanins stimulate the energy homeostasis regulator, peroxisome proliferator-activated receptor, which results in improved insulin resistance, upregulated fat metabolites, and reduced fat storage (Ali Ghasemzadeh, 2011; Bornsek et al., 2012; Khoo et al., 2017; Klimis-Zacas et al., 2016; Lila et al., 2016; Overall et al., 2017; Raskin I, Yousef GG, 2013; Rodriguez-Mateos et al., 2013; Silva et al., 2018). Diabetes is an increasingly prevalent condition where the body cannot produce or recognize insulin, resulting in high blood

glucose levels (Blueberry et al., 2010; Edirisinghe & Burton-Freeman, 2016; Gowd et al., 2017; Lin et al., 2016; Sarkar et al., 2017; Silva et al., 2018). Diabetes patients supplemented with blueberry extracts showed enhanced glucose tolerance, normalized glucose metabolism, and enhanced insulin sensitivity (Blueberry et al., 2010; Edirisinghe & Burton-Freeman, 2016; Gowd et al., 2017; Lin et al., 2016; Sarkar et al., 2017; Silva et al., 2018). Gaining a greater understanding of the mechanism by which blueberry phenolics and anthocyanins are able to regulate and reduce metabolic syndrome and diabetes will allow for better treatment development.

Inflammation and oxidative stress are also main contributors to neurological deterioration. Researchers are finding that anthocyanins can pass the blood-brain barrier and localize in cerebral regions for cognitive function like the hippocampus and neocortex (Ahmadinejad et al., 2017; Giacalone et al., 2011; Ma et al., 2018; McNamara et al., 2018; Neto, 2007; N. Singh & Ghosh, 2019; Subash et al., 2014). Blueberry supplementation to older animal diets resulted in enhanced motor and memory performance. Blueberry consumption reduced inflammation from kainic acid in the hippocampus. Due to the reduced inflammation and oxidative stress, mice show steady if not improved learning and memory capabilities during aging. In older animals, the normal cognitive decline in object recognition was reversed when supplemented with blueberry extract. When rats are injected with kainic acid into hippocampus and fed a blueberry supplemented diet for two months afterwards, there was reduced inflammation, reduced neuron loss, and alleviated reduction in learning and memory abilities. Blueberry consumption over a few months also improved the memory capabilities in older adults. Even though the mechanisms are not elucidated, the phenolics and anthocyanins in blueberry extracts reduce oxidative stress and inflammation through scavenging ROS-RNS, upregulating antioxidant enzymes, and upregulating anti-inflammation regulatory genes.

Blueberry extracts and anthocyanins have been shown to reduce tumor development (Ali Ghasemzadeh, 2011; Aqil et al., 2016; Neto, 2007; Nile & Park, 2014; Pan et al., 2018, 2017; Prencipe et al., 2014; Willig, 2009). The antioxidant capacity of blueberries and anthocyanins also aids, either directly or indirectly, in protecting and repairing DNA mutations that are often present in early tumor development. Multiple

studies have shown the treatment of cancer cells with blueberry phenolics or anthocyanins reduces cell proliferation and induces apoptosis (Ali Ghasemzadeh, 2011; Aqil et al., 2016; Neto, 2007; Nile & Park, 2014; Pan et al., 2018, 2017; Prencipe et al., 2014; Silva et al., 2018; Willig, 2009). Other researchers have also shown reduced tumor development or growth for different types of cancer in mice (Ali Ghasemzadeh, 2011; Aqil et al., 2016; Neto, 2007; Nile & Park, 2014; Pan et al., 2018, 2017; Prencipe et al., 2014; Willig, 2009). The complexity of cancer development and regulation makes determining a mechanism for blueberry phenolics difficult, as some researchers propose an indirect effect on signaling while others propose a more direct effect on gene expression.

With the plethora of health benefits strongly associated with blueberry phenolics and anthocyanins, there is less information on other metabolites present in blueberry berries. Gaining the foundational knowledge of the diversity of metabolites in blueberries will provide vital information on primary metabolite composition and proportions along with specialized metabolites that may contribute to the health benefits associated with anthocyanins. Once metabolite diversity is determined, identifying important QTLs and determining putative candidate genes that effect the variation of a specific metabolite's accumulation aids in elucidating metabolite pathways and potential regulatory mechanisms. There are two main research objectives addressed in this chapter. One objective is to profile a diversity of metabolites in blueberry fruit utilizing both a targeted and non-targeted approach. The second objective is to identify important QTLs associated with metabolites linked to consumer aesthetics and nutritional quality traits, and identified putative candidate genes that may regulate metabolites of interest.

3.3. Materials and Methods

3.3.1. Plant Material

The DxJ blueberries were harvested for two years (2015 and 2016) for two different locations (GA and OR). Berries were harvested at the ripe stage and picked randomly from different locations on the bush. For 2015, berries were picked for 212 lines. For 2016, berries were picked for 190 lines. The harvested berries were

transported on ice to collection centers and frozen to -80°C in freezer. Once frozen, the berries were transported on dry ice to Plants for Human Health Institute, Kannapolis, NC.

3.3.2. Extraction

The blueberries were completely re-frozen to -80°C to aid in efficiently lyophilizing the berries. The freeze-drying aids in stabilizing some of the metabolites within the berries as they can no longer interact with water. Initially, the blueberries were freeze-dried for five days. The weights of the samples before and after 5 days of freeze-drying were recorded to determine if 75-80% of the total weight decreased after freeze-drying. The 75-80% decrease in the blueberry sample weight after freeze-drying indicates that almost all of the 75-80% water content in blueberries was removed during freeze-drying. If the blueberry sample did not achieve 75-80% weight loss, then all the water was not removed, thus, the blueberry sample was freeze-dried again until the weight decreased 75-80%. Once the berries were dried, 1.25-1.5g of dried berries from each unique line were separated into separate tubes and homogenized with a falcon test tube blender in acidified 70% methanol with 0.5% formic acid. The slurry was centrifuged and supernatant decanted into 50mL volumetric flasks. The supernatant was poured through glass wool to filter out large cell debris. The pellet was re-extracted 2 more times and brought up to 50mL at the end. From each line's extraction stock, a 1mL aliquot was made for ^1H NMR analysis and 0.5mL aliquot was made for HPLC-QTOFMS analysis.

3.3.3. ^1H NMR Analysis

Sample extracts were dried down using a nitrogen evaporator. Buffer and internal controls were added to suspend the dried extract. An aliquot from random samples was selected for quality control pooled samples. ^1H NMR was conducted on a Bruker 700MHz Avance III spectrometer. A noesypr1d experiment was performed on all samples using a sweepwidth of 12ppm, delay of 2 seconds, noesy mixing time of 100msec. Total point collected was 65536 with 256 scans. All quality control pooled samples were compared to judge the reproducibility of the NMR analysis. One quality control pooled sample was also analyzed using ^{13}C , HSQC, HMBC, and COSY experiments for future structural elucidation information.

The raw data was converted to spectra using Bruker Topspin software (Version 2.1) and 0.5 Hz line broadening to eliminate noise. Spectra was phased, and base corrected manually using a zero order correction. Spectra peaks were aligned by setting the DSS peak chemical shift to 0.0. Using Mestronova software (version 11.0.3), metabolite feature peaks were determined using quality control pooled samples, and then determined in extract samples. Metabolite feature peaks were integrated, and then normalized by the DSS peak area. Metabolite feature peak areas were further normalized by extract concentration. Fully normalized metabolite feature peaks were annotated with Chenomx software and Chenomx libraries. Annotated metabolite feature peaks were designated as “known metabolites” and un-annotated metabolite features labeled as “unknown metabolites”. All of the metabolite features determined for extracts from years 1 and 2 were later merged to create a ‘both-YRs’ dataset through integrating each dataset peaks at 0.01 ppm increments. Common chemical shift (ppm) ranges across both year 1 and 2 datasets further supported annotations in both year dataset as “known metabolites”.

3.3.4. HPLC-QTOFMS Analysis

The blueberry extract samples for HPLC-QTOFMS were stored in -80°C while the analysis method was optimized. The HPLC solvent gradient consisted of decreasing solvent A, 5% formic acid in water (Fisher Scientific), by increasing solvent B, 100% methanol, at a flow rate of 1mL/min over 30 mins (Table 3.2).

Table 3.2 – HPLC-QTOFMS solvent gradient for optimized anthocyanin separation.

Time (min)	% Solvent B
0	5
2.5	15
7.5	20
10	25
12.5	30
22.5	60
25	100
27.5	100
28	5
30	5

An Eclipse Plus C18 3.0x100mm, 1.8um, 600bar column was used to separate the acidified metabolites in the extracts (Agilent). The UV/Vis absorbance of the extract was measured using a diode array detector (DAD) that was set at to a 5 step scan with a range between 220nm and 800nm. Before injection into the QTOFMS, the elute from the HPLC was diluted 5-fold to a 1.0% formic acid extract with an auxiliary pump and post-column splitter because long-term exposure of the mass detector to high acid would result in damage and reduced sensitivity (VersaGrad Dual-piston Pump-model prep 36). The QTOFMS was run in positive mode and tuned with positive mode specific tuning solution. Reference metabolites at 121.0509 m/z and 922.0098 m/z were analyzed with every sample to monitor detector sensitivity. A standard mix specifically for positive mode was optimized to separate and span the detection run and stay within the detection limits. It contained proline, leucine, lysine, phenylalanine, tyrosine, NALL, and NALI. Blank and standard mix samples were analyzed at the beginning and end of each batch run to monitor detector sensitivity and consistency.

The blueberry extract samples were further filtered into HPLC vials with reusable caps (Agilent) using 0.2 um regenerated cellulose filters (Fisher Scientific) to remove any cellular debris. Since the blueberry extracts are a complex mixture of metabolites, the sample batch threshold before detector sensitivity reduced by 95% was 10. Before each batch, the HPLC was purged with both solutions to wash out any lingering debris or bubbles, and the source of the QTOFMS was manually cleaned to prevent by-product buildup. The raw spectra data was analyzed using Agilent MassHunter Qualitative Analysis B.06.00 software (Agilent). Anthocyanins peak data, from the DAD1 detector scan at 520nm, was integrated and annotated using the m/z and elution times from previously published literature by Grace et al. (2009) as a guide. Anthocyanins peaks from the QTOFMS were also annotated using the previously published m/z and elution times through extracted ion count (EIC).

3.3.5. Antioxidant Capacity - DPPH Scavenging Assay

The DPPH antioxidant capacity assay was chosen for all the DxJ blueberry sample extracts due to the sensitivity and reproducibility for phenotyping across a mapping population (Ahmadinejad et al., 2017; Kedare & Singh, 2011; O. P. Sharma & Bhat, 2009). The assay was optimized for the extract's acidity by optimizing the range of

the Trolox concentrations for the standard curve. The standard curve utilized Trolox concentrations of 20 μ M, 160 μ M, 300 μ M, 460 μ M, 600 μ M, and 700 μ M. Trolox was used for the antioxidant standard as Trolox is a vitamin E analog, thus exhibits good radical scavenging capacity. The assay was conducted in a 96-well plate using the SpectraMax 384Plus UV/Vis Microplate Reader set at 517nm wavelength (Molecular Devices). The DPPH solution at 150 μ M was made fresh every day and kept in the dark until application into each well. Each extract was replicated across 4 wells and 2 interns for a total of 8 well replicates. On each plate, blanks of water and 80% MeOH were replicated across 4 wells, and negative controls with water and DPPH were also replicated across 4 wells. After the assay incubated for 40mins, the absorbance values were read directly from the microplate reader, and were compiled in the SoftMax Pro software to be exported into excel for further analyses. The 8 replicates for each extract were filtered so the range was either within 0.02 or only 4 wells remained for averaging. The standard curve was run multiple times per day. The final standard utilized for trolox equivalence calculations was an average of all standard curve replicates.

3.3.6. Genotypic Data

The genotypic data and SNP marker information was conducted and published by the USDA-ARS labs of Dr. Rowland and Dr. Bassil, and McCallum lab at the James Hutton Institute (McCallum et al., 2016). Both the USDA-ARS and McCallum lab graciously provided the population genotype and SNP marker data for this research (McCallum et al., 2016). The separate Draper and Jewel tetraploid genetic maps were published by McCallum, et al. (McCallum et al., 2016).

A modified mapping procedure described by Oliver et al. was used to develop a high-density linkage map of the highbush blueberry Draper \times Jewel (*Vaccinium corymbosum*) mapping population (Oliver et al., 2013). In brief, single nucleotide polymorphism (SNP) loci derived from genotype-by-sequencing (GBS) were assembled into maps for each parental line using the MultiPoint package (MultiQTL Ltd., Haifa, Israel). Preliminary grouping and ordering of the genotypic matrices were done at a recombination fraction (rf) = 0.15 and loci with rf = 0 were assigned to a binned group. A single locus or “delegate” was then chosen to represent each bin based on data quality and strength of position using a likelihood of odds approach. The preliminary marker

orders within each group were refined using a jackknife approach where the probability of the marker order was estimated based on 30 iterations with a 0.10 random hold out of individual in the population. Unstable orders were refined by identification and removal of problematic loci using the order variance, segregation ratio, and the *rf* with nearby markers. Once stable orders were generated, linkage groups were merged end-to-end by incrementally increasing *rf* by 0.05 up to a final *rf* of 0.3. Alignment of the two parental maps was made on the basis of best fit of the shared loci and linkages to double-simplex markers segregating in both parents as described by McCallum et al (McCallum et al., 2016). A detailed analysis of the DxJ-specific tetraploid genetic map can be found in Chapter 2 of this dissertation in the results and discussion sections (Figure 2.2, and Tables 2.1 and 2.2).

3.3.7. Biparental Association Mapping (BiPAM)

The BiPAM was conducted using JMP Genomics 7 (JMP[®], SAS Institute Inc.). The genotypic and phenotypic data was merged together to make a geno-pheno file that had stacked genotypic information to account for the individual lines replicated across the years and locations (Hancock et al., 2018). This allowed for year and location to become a factor that could be utilized as a cofactor to account for the year or location effects. Each trait consisted of individual phenotypes for each location and year, for example, the growth trait of bush height consisted of six individual phenotypes for the three locations (FL, GA, and OR) and two years (2011 and 2012) (Table 2.4). The genotypes were filtered for a minimum proportion of non-missing genotypes of 0.6. A genotype probability data table was built using the Kosambi map function. The genotype probability data table utilized the cross information to calculate recombination frequencies and the relationship between markers. When the gap between markers was larger than 2 cM, pseudo-markers were created, and recombination frequencies predicted. This develops a denser genetic map to allow for finer association mapping to identify smaller QTL regions. The cross type selected was T(B2)SF_n indicating a test-backcross with parent 2 with a selfing genotype generation of *n*. For the DxJ mapping, parent 2 is Draper and the self-genotype generation is 1 because the offspring are the F1 generation.

The DxJ specific tetraploid genetic map was incorporated as the annotation file with the genetic map linkage groups designated as chromosomes, and the genetic map consensus position designated as chromosome position. The number of distinct genotypes was 2 for each marker because the marker was either D/J - D/D or D/J - J/J. The QTL test step was 2 cM to refine the association mapping. The conventional LOD threshold of 3 was used to determine significant QTLs. Interval mapping (IM) and composite interval mapping (CIM) was conducted with the EM, estimated maximum-likelihood, algorithm for modeling. For the CIM method, 5 control makers and a 5 cM test window was utilized to refine the interval mapping window. The control markers were selected using a stepwise regression with a 0.35 significance level for entry into the model, and a 0.05 significance level for staying in the model as a control marker. Multiple interval mapping (MIM) was also conducted on the traits to determine possible interacting and secondary QTLs that may have an indirect role on regulating the trait that could only be detected once the variation of the major QTLs are accounted for during the mapping (Bernardo, 2008; Feenstra, 2006; Hackett, Bradshaw, & McNicol, 2001; Kao, 2000; H. Li, Ye, & Wang, 2006; Mayer, 2005). BiPAM using CIM was conducted on all the different phenotypic data because CIM identifies multiple QTLs across the genome while also accounting for the effect of QTLs on other significant QTLs (Bernardo, 2008; Feenstra, 2006; Hackett et al., 2001; Kao, 2000; H. Li et al., 2006; Mayer, 2005).

3.3.8. Putative Candidate Gene Identification

The QTL result has a significance threshold when the LOD value is above 3 (Bernardo, 2008; Collard, Jahufer, Brouwer, & Pang, 2005; Kang, 2002; Xu, 2010). Each significant QTL has a corresponding significant QTL region that is dictated by the LOD value of the neighboring markers. The boundaries of a significant QTL region are designated by the centimorgan (cM) position of the closest neighboring markers with an LOD value below 3. The sequence tags associated with the DxJ genetic markers were aligned to genome assembly scaffolds of a blueberry draft genome currently being assembled and curated by Dr. Iorizzo's lab at North Carolina State University's Plants for Human Health Institute (Iorizzo et al., 2018). For each trait, the significant QTL regions were aligned to the DxJ genetic map as well as the corresponding draft genome

scaffolds to determine rearrangements in the genetic map and any overlapping QTL regions showcased by the draft genome scaffolds. The genomic sequences underneath the significant QTL regions for specific traits were separated for gene sequence comparison.

The putative candidate genes were selected based on previously published literature that proposed catalytical activity or other regulatory functions for the gene in the specific biosynthesis or catabolism pathways. The metabolite and pathway databases from KEGG and PlantCyc were utilized extensively to prioritize and cross-reference pathways and metabolite interactions (Chae et al., 2014; Kanehisa et al., 2017). Gene sequence information was obtained from KEGG and PlantCyc for genes in the metabolite biosynthesis pathways for: TCA acid synthesis, specific amino acid synthesis, sugar interconversions, sugar signaling, shikimic acid, phenylpropanoid, flavonoid, and anthocyanin synthesis (Chae et al., 2014; Kanehisa et al., 2017). The gene information for genes in the ascorbate-glutathione cycling pathway and cell wall matrix modifications pathways were also obtained for sequence comparisons because many studies propose oxidative stress detoxification and cell wall matrix modifications contribute to regulating fruit ripening and quality (Cappai, Benevenuto, Ferrão, & Munoz, 2018; Castellarin et al., 2016; Paniagua et al., 2014; Pilati et al., 2014; Serrano et al., 2017; Xi et al., 2017). cDNA sequence information for tomato, *Solanum lycopersicum*, was obtained from the public databases and was preferentially chosen over other species' cDNA sequences due to the close phylogenetic relationship with blueberry and robust functional characterizations of many pathways.

These nucleotide gene sequences along with the nucleotide sequences of the significant QTLs were translated into protein sequences for all three frames. Using blastp, the protein gene sequences were aligned the protein sequences for the significant QTL regions from the draft genome scaffolds. The blastp result were considered significant potential putative candidate genes if the E-value was lower than E-10, and the percent alignment length was greater than 50%. The % alignment length was utilized to see how much of the whole gene aligns to genomic sequence from the scaffold. This aided in eliminating small gene fragments with high sequence similarity. Alignment results with lower E-values and higher % alignment lengths were prioritized

as more important potential putative candidate genes. The potential putative candidate genes within a genetic region were aligned in order along the genomic scaffold to determine overlap between the potential putative candidate gene sequences. If there was overlap between potential putative candidate genes sequences, then one was chosen for that area based on a combination of best E-value, best % alignment length, and multiple studies supporting the genes involvement in regulating the specific pathway and associated significant metabolite peak. After this manual curation of the potential putative candidate genes so that there were no overlapping sequences within the genetic region, the putative candidate genes were prioritized based on proximity to the position of the significant genetic marker and involvement from literature in regulating the pathway. The putative candidate genes reported for each significant QTL region in the following results and discussion sections were chosen because of the proximity to the significant marker and the involvement of the gene in regulating the associated metabolite as supported by pathway databases and published research.

3.4. Results

3.4.1. ¹H NMR Metabolite Features

The non-targeted profiling using ¹H NMR found over 900 metabolite features for both years that were annotated as either unknown or known metabolites (Table 3.3). Of the 943 metabolite features, 751 metabolite features were annotated as unknowns (Table 3.3). The 192 metabolite features annotated as known metabolite features were condensed into 29 metabolite peaks since metabolite features from the same metabolite annotation are different hydrogens from the same metabolite. This condensation did not occur with the unknown metabolite features because the features were unknown with not enough information to determine which ones come from the same metabolite.

Table 3.3 – Detected metabolite features from non-targeted profiling with ¹H NMR.

Extract Year	Total Metabolite Features	Known Metabolites	Unknown Metabolites
1	188	48	140
2	191	91	100
Both Years	943	192	751

3.4.1.1. ¹H NMR Known Metabolites Phenotype Description

The TCA acids annotated from the metabolite profile are citric acid, succinic acid +others, and malic acid (Table 3.4). Citric acid comprised the vast majority of the total TCA acid content. The metabolite feature peaks that had a “ +others” indicated the overall peak contained a known metabolite feature and another metabolite peak that cannot be separated into distinct peaks. The amino acids annotated consisted of glutamine, γ -aminobutyric acid (GABA), arginine, isoleucine, valine, isopropylmalic acid, leucine, aspartate, asparagine, threonine, and alanine (Table 3.4). The annotated amino acids were further categorized for this research into the glutamine branch, branch-chain branch, and aspartate branch based on their biosynthesis pathways branching from the TCA cycle. Although there are other amino acids within the biosynthesis pathway branches, their metabolite peaks were not annotated within the ¹H NMR data and are therefore not discussed within the scope of this research.

The glutamine branch category consists of glutamine, GABA, and arginine as their biosynthesis branches from the TCA cycle when 2-oxoglutarate is interconverted with glutamate by glutamate dehydrogenase (Kanehisa et al., 2017). Glutamate is then either interconverted with glutamine, converted to GABA, or converted to N-acetylglutamate to start arginine biosynthesis. The summation of the glutamate branch metabolite peaks constitutes 24.40% of the total amino acid content. Of the total glutamine branch content, glutamine constitutes 16.89%, GABA accounts for 44.77%, and arginine accounts for 38.31% (Table 3.4).

The branch-chain branch category consists of isoleucine, valine, isopropylmalic acid, and leucine because parts of their biosynthesis pathways utilize the same enzymes (Kanehisa et al., 2017). Valine, isopropylmalic acid, and leucine biosynthesis branches from TCA when pyruvate, the precursor to the TCA cycle, is converted acetolactate by acetolactate synthase. Although isoleucine biosynthesis starts with aspartate biosynthesis from fumarate or oxaloacetate at the TCA cycle, isoleucine biosynthesis shares four main enzymes, including acetolactate synthase, with threonine as a precursor. The summation of the branch-chain branch metabolite peaks accounts for 6.21% of the total amino acids. Of the total branch-chain branch content, isoleucine

constitutes 24.10%, valine is 41.44%, isopropylmalic acid is 17.67%, and leucine constitutes 16.90% (Table 3.4).

The aspartate branch category consists of aspartate, asparagine, threonine, and alanine as their biosynthesis branches from the TCA cycle when fumarate or oxaloacetate is converted to aspartate (Kanehisa et al., 2017). Aspartate can be interconverted with asparagine by asparagine synthase. Aspartate can also be converted with multiple steps and branching points to threonine, cysteine, serine, glycine, and alanine. The aspartate branch accounts for 69.39% of the total amino acid content. Aspartate and asparagine constitute 48.36% and 40.12%, respectively, of the total aspartate branch content. Threonine accounts for 4.16% and alanine accounts for 7.36% of the total aspartate branch content (Table 3.4). Aspartate contributed the most to the total amino acid content compared to the other individual amino acids.

Table 3.4 –Accumulation and annotation summary data for TCA acids and amino acids from ¹H NMR non-targeted profiling.

Metabolite – TCA-Amino Acid	Shift (ppm)		Mean [◇]	Standard Error Mean	Draper	Jewel	% of Total
Total TCA acids			38.06	2.19	78.86	38.37	-
Citric Acid	2.5	2.6	34.17	2.08	72.30	33.75	89.78
Succinate +others	2.39	2.40	0.91	0.031	1.62	1.09	2.39
Malic Acid	2.36	2.38	2.98	0.14	4.94	3.53	7.83
			*4.97	*0.16			-
Total Amino Acids			147.74	5.08	105.75	129.98	-
Glutamine	2.42	2.47	6.09	0.21	6.84	11.47	4.12
GABA	2.98	3.03	16.14	1.60	34.35	6.94	10.92
			*7.00	0.152			-
Arginine	1.68	1.77	13.81	0.35	20.90	14.16	9.35
Isoleucine	0.92	0.94	2.21	0.064	2.48	2.74	1.50
	1.01	1.02					
Valine	0.98	1.05	3.80	0.14	3.18	5.11	2.57
Isopropylmalic Acid	0.86	0.91	1.62	0.03	2.57	1.47	1.10
Leucine	0.95	0.97	1.55	0.07	1.41	2.51	1.05
Aspartate	2.78	2.81	49.58	2.62	12.04	40.27	33.56
			*86.27	*2.88			-
Asparagine	2.91	2.94	41.13	2.43	5.55	35.52	27.84
			*77.03	*2.95			-
Threonine	1.3	1.35	4.26	0.02	5.86	3.43	2.88
Alanine	1.45	1.5	7.55	0.20	10.60	6.35	5.11
Total Glutamine Branch			36.05	1.65	62.09	32.58	24.40
Total Branch-Chain Branch			9.17	0.28	9.62	11.84	6.21
Total Aspartate Branch			102.52	4.70	34.04	85.57	69.39

◇ - indicates the annotated metabolite accumulations are relative measurements of peak area from peak integration and do not have units

* - indicates values from another distribution analysis on a subset of the population as described below

“+others” – indicates specified annotated metabolite and the presence of other metabolites that could not be separated into another distinct peak

The sugars annotated from the metabolite profile are fructose, glucose, sucrose, maltose, maltitol, galactose, xylose, and arabinose +others (Table 3.5). Maltitol is the sugar alcohol composed of a glucose and a glucitol. There was also a peak annotated “other sugars” as it contained peaks for galactose, xylose, and other 6-C sugars that

could not be separated into distinct peaks. Glucose and fructose contributed over 90% of the total sugar content.

Table 3.5—Accumulation and annotation summary data for sugars from ¹H NMR non-targeted profiling.

Metabolite - Sugars	Shift (ppm)		Mean [◇]	Standard Error Mean	Draper	Jewel	% of Total
Total Sugars			5627.93	76.18	6266.49	5808.29	-
Fructose	3.52 3.99	3.61 4.14	2652.72	37.20	2946.11	2635.13	47.14
Sucrose	4.21 5.4 5.49	4.23 5.42 5.5	27.66	0.82	25.68	25.51	0.49
Glucose	3.21 3.38 4.62 5.22	3.26 3.51 4.68 5.25	2917.38	38.93	3238.51	3121.29	51.84
Maltose	5.20	5.21	2.15	0.060	2.55	2.36	0.14
Maltitol	5.09	5.11	5.66	103.55	11.32	5.57	
Galactose	5.25	5.26	1.12	0.022	1.44	0.89	0.40
Other Sugars (Galactose, Xylose)	4.55	4.58	5.92	0.039	7.94	5.92	
Xylose	5.17	5.2	4.20	0.015	8.49	3.55	
Arabinose +others	4.52	4.53	11.12	0.23	24.47	8.06	

◇ - indicates the annotated metabolite accumulations are relative measurements of peak area from peak integration and do not have units

“+others” – indicates specified annotated metabolite and the presence of other metabolites that could not be separated into another distinct peak

The phenolic acids annotated consist of gallic acid, quinic acid, chlorogenic acid, caffeic acid +others, and epicatechin (Table 3.6). Chlorogenic acid contributed the most to the total phenolic acid content compared to the other phenolic acids. Although ascorbate is synthesized from galactose, the ascorbate +others metabolite peak was associated with the phenolic acid grouping for this thesis as ascorbate functions as an antioxidant.

Table 3.6 –Accumulation and annotation summary data for phenolic acids from ¹H NMR non-targeted profiling.

Metabolite – Phenolic Acids	Shift (ppm)		Mean [◇]	Standard Error Mean	Draper	Jewel	% of Total
Total Phenolic Acids			64.92	1.69	120.79	46.76	-
Gallic Acid	6.97	7.02	5.76	0.017	6.93	4.50	8.87
Quinic Acid	1.83 1.95	1.88 1.98	22.03	1.23	53.35	16.85	33.93
Chlorogenic Acid	6.25 7.1 7.49	6.3 7.21 7.67	23.48	0.51	40.43	16.03	36.17
Caffeic Acid+ Others	6.31	6.36	4.30	0.20	4.16	2.48	6.62
Epicatechin	6.1 6.92	6.24 6.96	9.35	0.22	15.91	6.90	14.40
Ascorbic +others	4.49	4.51	8.36	0.23	17.95	4.51	-

[◇] - indicates the annotated metabolite accumulations are relative measurements of peak area from peak integration and do not have units

“+others” – indicates specified annotated metabolite and the presence of other metabolites that could not be separated into another distinct peak

3.4.1.2. ¹H NMR Known Metabolites Distributions

The distributions of the TCA acids all showed severe right-skewed distributions and with none following a normal distribution (Figure 3.2). A normal distribution is shown by the red line in each distribution histogram. The right-skewing of malic is severe as 190 (46.57%) of the individuals have malic acid amounts less than 1, which is 5.5% of the maximum or 33.6% of overall mean. The remaining 218 individual show only a slight right-skewed distribution with a mean of 4.97 and standard error mean of 0.16. A distribution analysis was conducted on the population subsets when the original distribution showed on bin with over 40% of the population while the remainder of the population shows a trend for a normal distribution. The distribution of the percent of total TCA acid content for citric acid, succinic acid +others, and malic acid are shown in the histograms to the right of each TCA acid.

The distributions of the 11 amino acids annotated show either a distinct bimodal shape or dramatic right-skewing (Figure 3.3). In Figure 3.3, the glutamine branch distributions are shown in section A, the aspartate branch distributions are shown in section B, and the branch-chain branch distributions are shown in section C. Total

amino acids, total aspartate branch, aspartate, and asparagine show the distinct bimodal shape. For total aspartate branch, the first distinct peak contains 168 (41.18%) individuals that have a total aspartate branch content less than 25, which is 5.79% of maximum and 24.39% of the overall mean (Figure 3.3). A separate distribution analysis of the 168 individuals showed normal distribution with a mean of 15.46. The second peak, containing 240 individuals, has a mean of 163.46. For aspartate, the first peak constitutes 179 (43.87%) individuals that have aspartate amounts less than 5, which is 2.2% of the maximum or 10.1% of the overall mean, show an almost normal distribution with a mean of 2.65. The second peak constitutes 229 individuals with an almost normal distribution and mean of 86.37 (Figure 3.3). For asparagine, the first peak consists of 194 (47.55%) individuals with asparagine amounts less than 5, which is 2.4% of the maximum or 12.2% of the overall mean, and have a subset mean of 1.55. The second peak has 214 individuals with a mean of 77.03 (Figure 3.3). The distribution of total glutamine branch and GABA show extreme right skewing (Figure 3.3). The distribution of total glutamine branch shows 51 individuals severely skewing the data and the remaining 357 individuals accumulating under 50. A separate distribution of the 357 individuals shows a broad distribution with a mean of 26.15. The distribution of GABA shows 46 individuals severely skewing the data while 362 individuals accumulate under 20. A separate distribution of the 362 individuals shows a right-skewed distribution with a mean of 7.003. Glutamine, arginine, threonine, alanine, total branch-chain branch, isoleucine, valine, isopropylmalic acid, and leucine all exhibit right-skewed distribution histograms (Figure 3.3). The distribution of each amino acid percentage of the total amino acid content is shown in the histograms to the right of each corresponding amino acid (Figure 3.3).

The distributions of the nine sugars annotated showed primarily slightly right-skewed distributions with sucrose showing a more dramatic skewing with a longer right-tail (Figure 3.4). Only xylose showed a bimodal distribution with two distinct peaks, with 174 individuals composing the first peak and 234 individuals in the second peak. The distribution of each sugar's percentage of the total sugar content is shown in the histograms to the right of each corresponding sugar (Figure 3.4).

The distributions of the six phenolic acids show varying degrees of right-skewed histograms (Figure 3.5). Gallic acid shows only slight right-skewed, whereas total phenolic acids, chlorogenic acid, and epicatechin show more prominent right-skewed distributions. Caffeic acid +others shows severe right-skewed distribution as 192 (47.06%) of individuals have a caffeic acid +others amount less than 2, which is 9.8% of the maximum or 46.6% of overall mean. The distribution of the 192 individuals barely shows right-skewing with a mean of 0.97, whereas the remaining 216 individuals show a slight right-skewed distribution with a mean of 7.25. Quinic acid exhibits a very severe right-skewed distribution as 267 (65.4%) of individuals have quinic acid amounts less than 20, which is 7.8% of maximum but 90.8% of overall mean. The distribution of the 267 individuals shows a slight right-skewing with a mean of 10.86, whereas the 141 other individuals shows a very right skewed distribution with a mean of 43.18. The distribution of each phenolic acids' percentage of the total phenolic acid content is shown in the histograms to the right of each corresponding phenolic acid (Figure 3.5).

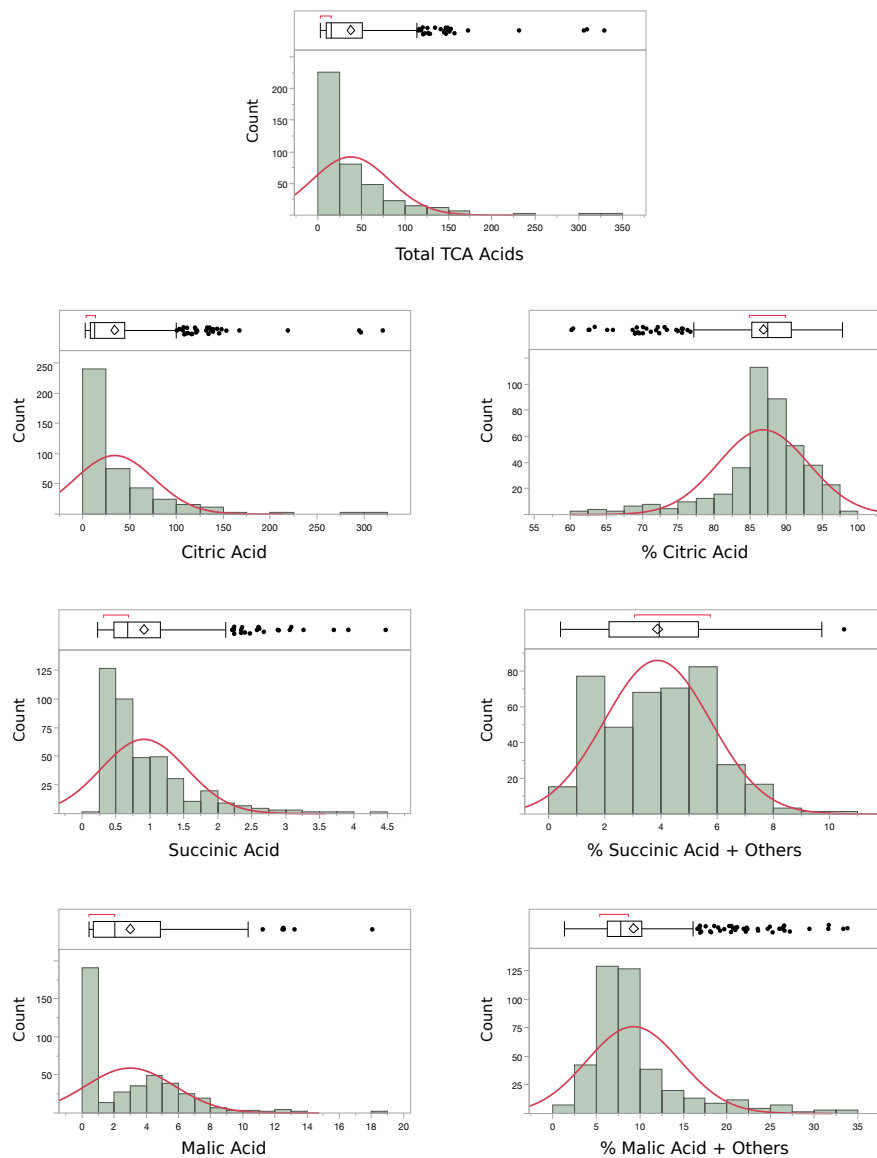


Figure 3.2 – Distribution histograms for total TCA acids and specific TCA acids from ^1H NMR non-targeted profiling. The distribution histogram of % TCA acid to total TCA acids for each individual TCA acid is to the right of the corresponding TCA acid. The red line indicates a normal distribution. The box plot shows the mean, quartiles, and interquartile range, as well as possible outliers as dots.

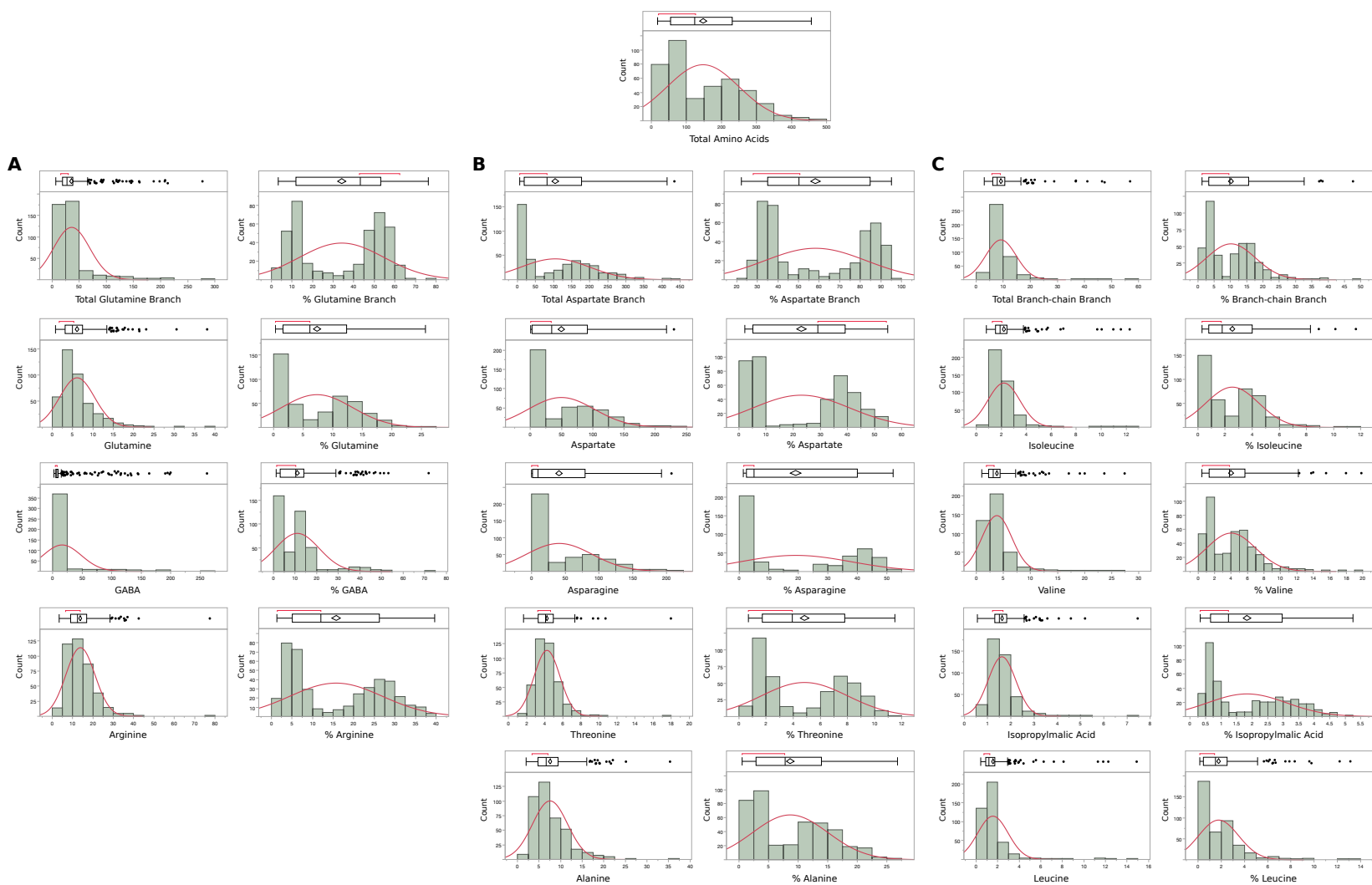


Figure 3.3 – Distribution histograms for the 11 amino acids from ^1H NMR non-targeted profiling. The total amino acids distribution is the top most histogram. The % of the corresponding total summation is to the right of each amino acid. The glutamine branch distributions are the left two (Section A), while the aspartate branch distributions are the middle two (Section B), and the branch-chain branch distributions are the right two (Section C). The red line indicates a normal distribution. The box plot shows the mean, quartiles, and interquartile range, as well as possible outliers as dots.

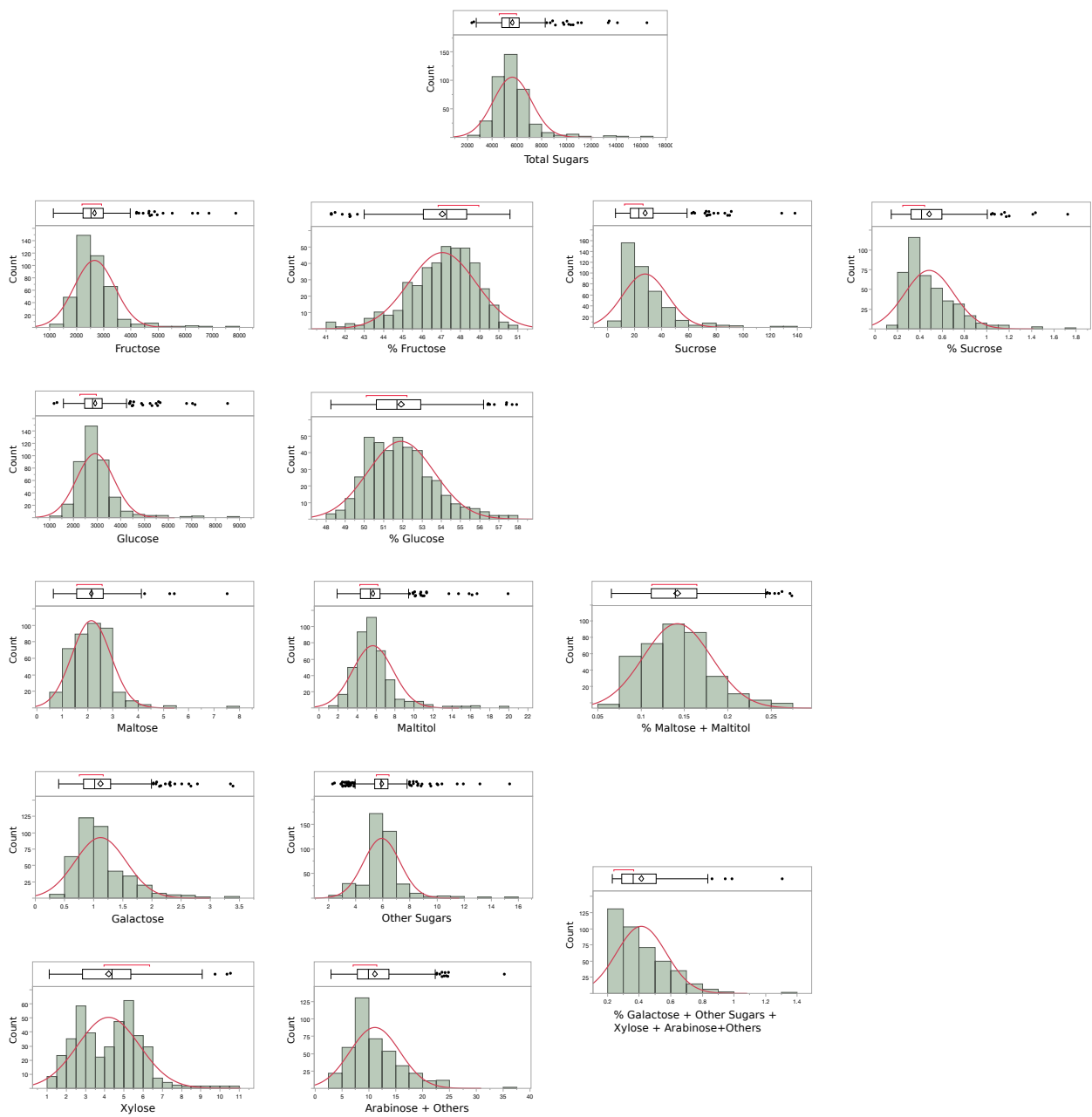


Figure 3.4 – Distribution histograms + box plots for total sugars and individual sugars from ^1H NMR non-targeted profiling. For fructose, glucose, and sucrose, the % of total sugars is to the right of the corresponding sugar. Maltose and maltitol were summed together for % of total sugar since accumulation was very low and the metabolites are related. Galactose, other sugars, xylose, and arabinose +others were summed together as well for % of total sugar since accumulation was low. The red line indicates a normal distribution. The box plot shows the mean, quartiles, and interquartile range, as well as possible outliers as dots.

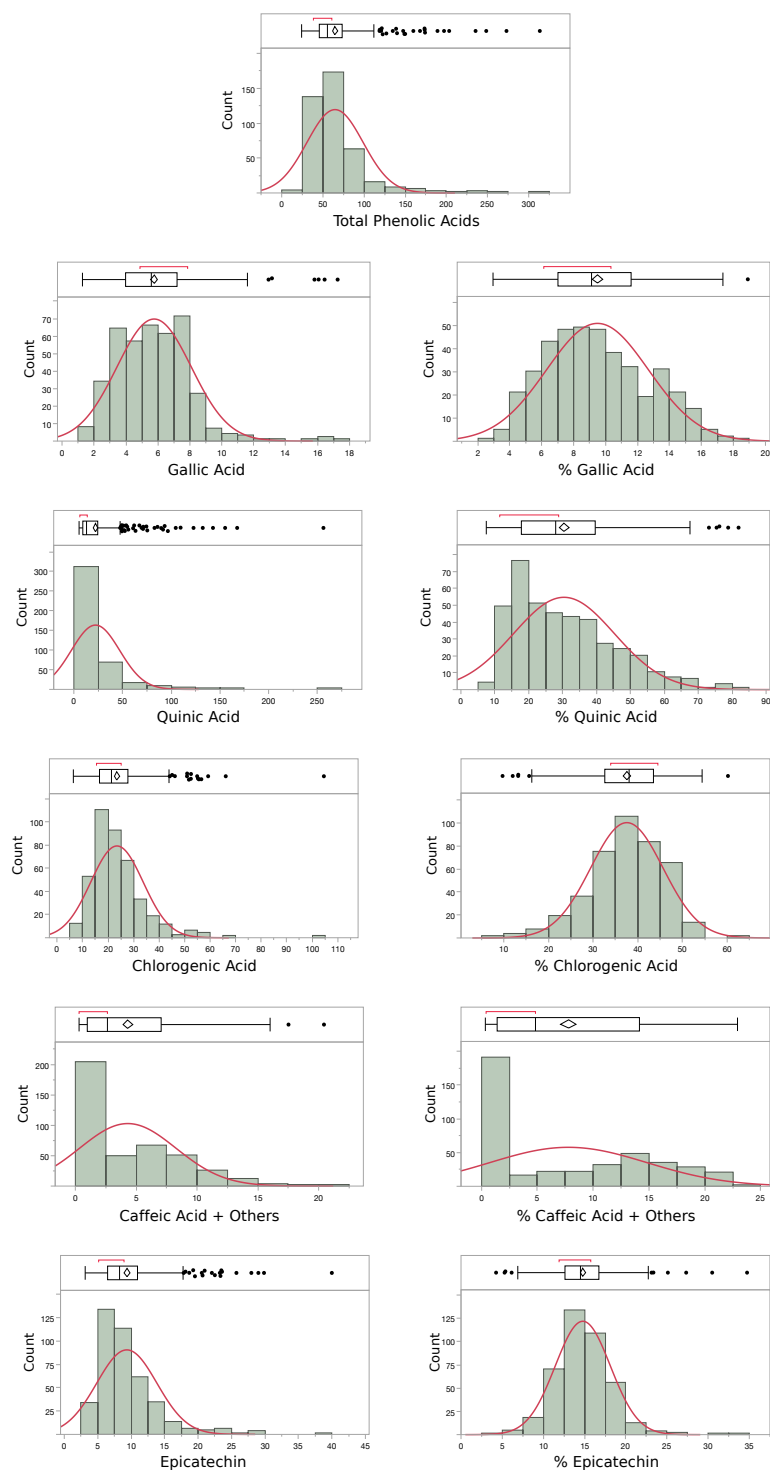


Figure 3.5 – Distribution histograms for phenolic acids from ^1H NMR non-targeted profiling. The distribution histogram of total phenolic acids is the topmost histogram, while the different phenolic acids are below on the left. The % of total phenolic acids distribution histogram for each phenolic acid is to the right of the corresponding phenolic acid. The red line indicates a normal distribution. The box plot shows the mean, quartiles, and interquartile range, as well as possible outliers as dots.

3.4.1.3. ¹H NMR Known Metabolites Correlations

3.4.1.3.1. TCA acids

Citric acid is very strongly correlated with total TCA acids ($R^2 = 0.997$), due to citric acid constituting over 85% of the total (Figure 3.6). Succinic acid +others and malic acid show weak, positive correlations with total TCA acid content ($R^2 = 0.453$ and $= 0.446$, respectively). Citric Acid shows no correlation with succinic acid +others and malic acid (Figure 3.6). Malic acid and succinic acid +others exhibit a strong positive correlation ($R^2 = 0.695$) (Figure 3.6).

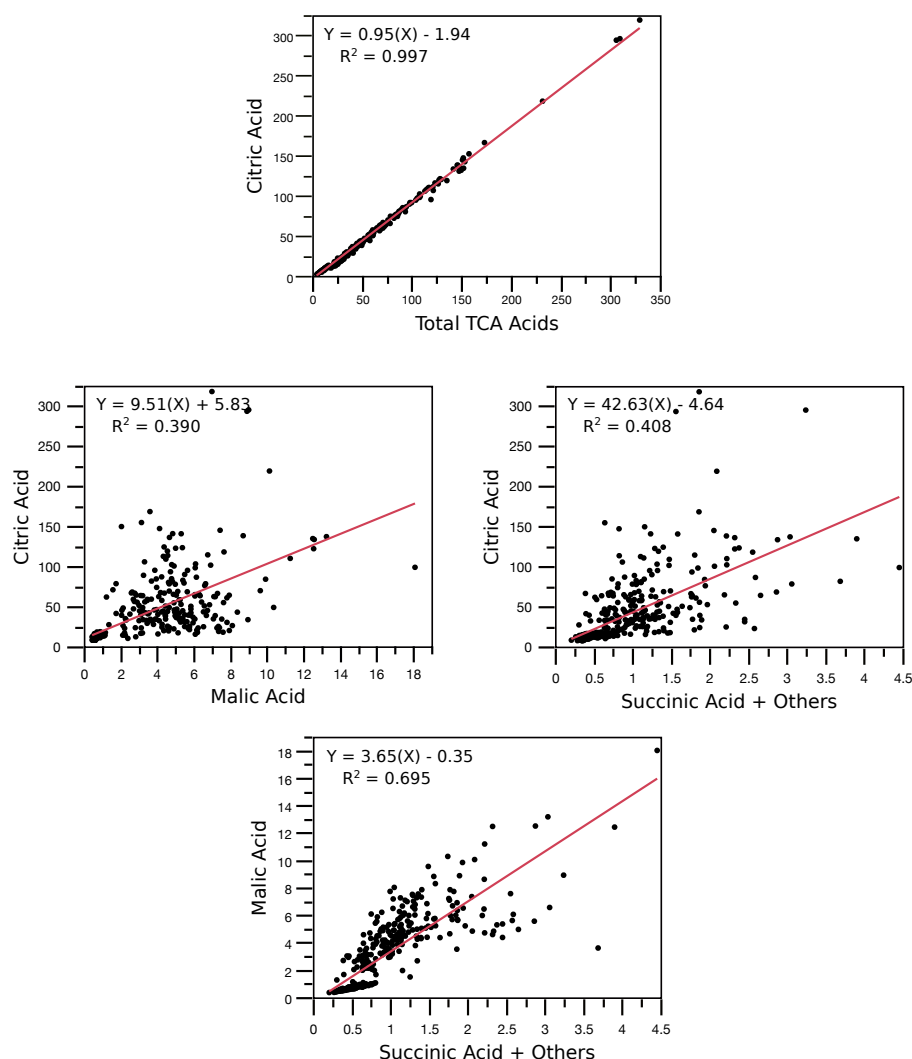


Figure 3.6 – Correlations showing the relationship between TCA acids. The best fit line (red line) equation and R^2 value is within each of the corresponding correlations.

3.4.1.3.2. Amino Acids

The correlations between total amino acids and the different amino acid branches all show a two split pattern, but with slight differences (Figure 3.7, section A). The total amino acid correlation with total glutamine branch shows a two split pattern with one correlation showing both increasing ($R^2 = 0.919$) while the other correlation showing only total amino acids increasing ($R^2 = 0.072$). A similar two split pattern is shown in the correlation between total amino acids and total branch-chain branch. There is a strong correlation between total amino acids and total aspartate branch ($R^2 = 0.887$), but there is also a narrow two split pattern with one correlation showing both proportionally increasing ($R^2 = 0.961$) and the other correlation showing total amino acids increasing twice as fast ($R^2 = 0.946$). When the amino acid branches are correlated with each other, they also all show a two split pattern that varies (Figure 3.7, section B). For the aspartate and glutamine branch correlation, one split show both increasing ($R^2 = 0.812$) while the other split shows aspartate branch increasing while glutamine branches changes very little ($R^2 = 0.001$). The aspartate and branch-chain branch correlation, the split pattern is slightly different because as branch-chains increase there is little change in aspartates ($R^2 = 0.511$), and as aspartates increase there is little change in branch-chains ($R^2 = 0.033$). The branch-chain and glutamine branch correlation shows a different two split pattern where the split can only be distinguished at higher amounts of each branch, but the two correlations could not be separated.

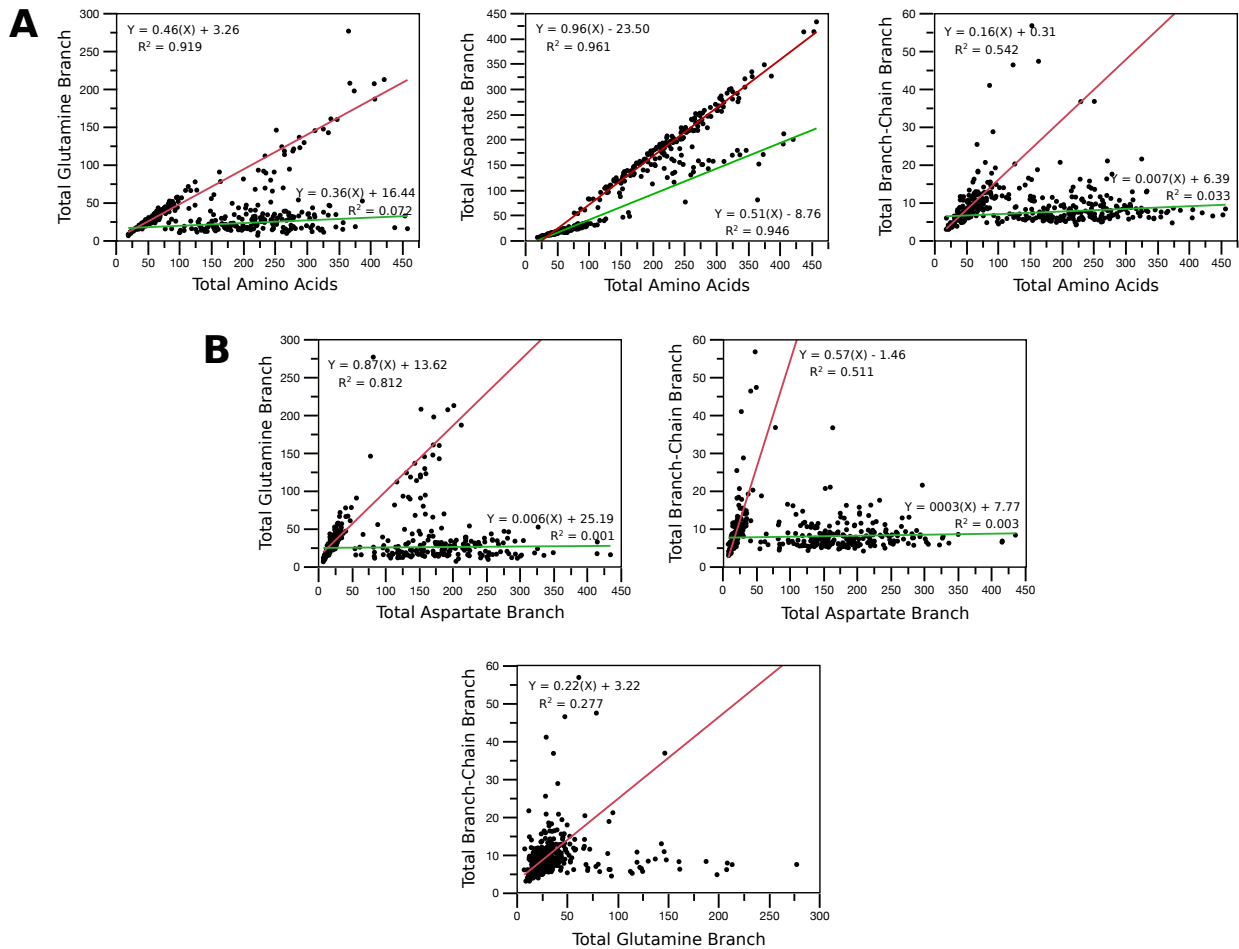


Figure 3.7 – Correlations showing the relationships between the different amino acid branches and total amino acids (Section A) and between each other (Section B). The best fit lines are shown with red and green lines, with the corresponding equations and R^2 values within each of the correlations.

The total glutamine branch shows a strong correlation with GABA ($R^2 = 0.894$), while glutamine and arginine show a two-split pattern (Figure 3.8). The correlations between glutamine and GABA, as well as arginine and GABA show a distinct two split pattern. Glutamine and arginine show a strong positive correlation ($R^2 = 0.623$).

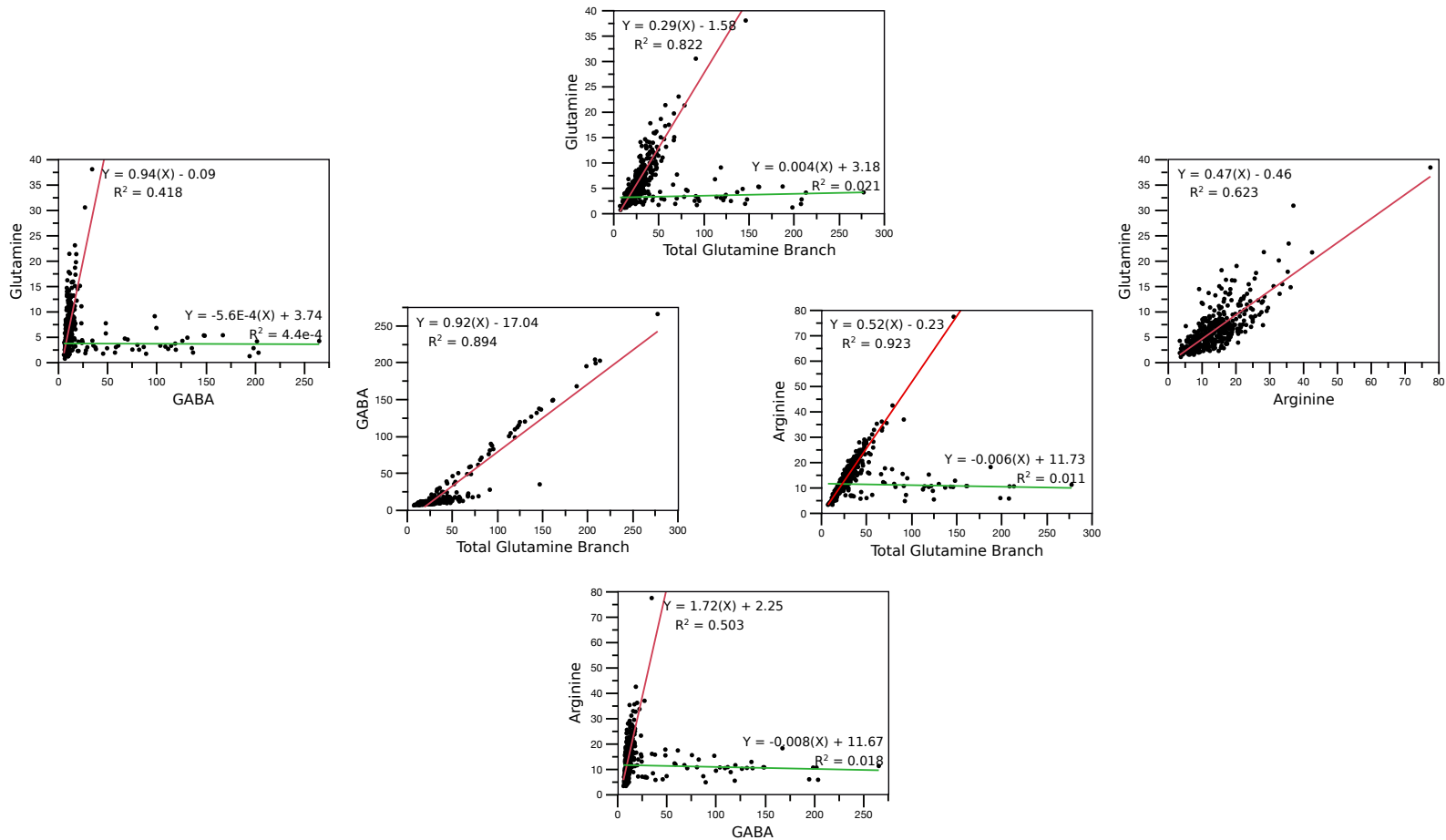


Figure 3.8 – Correlations showing the relationships between the individual amino acids in the glutamine branch with total glutamine branch and with each other. The equations for the best fit lines (red and green lines) and corresponding R^2 values are within each of the corresponding correlations.

The total branch-chain branch shows strong positive correlations with isoleucine, valine, and leucine ($R^2 = 0.929$, 0.926 , and 0.930 , respectively) (Figure 3.9). Isopropylmalic acid shows a weak, positive correlation with total branch-chain branch, probably due to the tentative split at high concentrations. Isoleucine shows a strong positive correlation with valine and leucine ($R^2 = 0.744$ and 0.910 , respectively). Leucine and valine show a strong positive correlation ($R^2 = 0.810$). Isopropylmalic acid and leucine correlation shows a low R^2 due to the tentative split at high concentrations that could not be separated into two correlations.

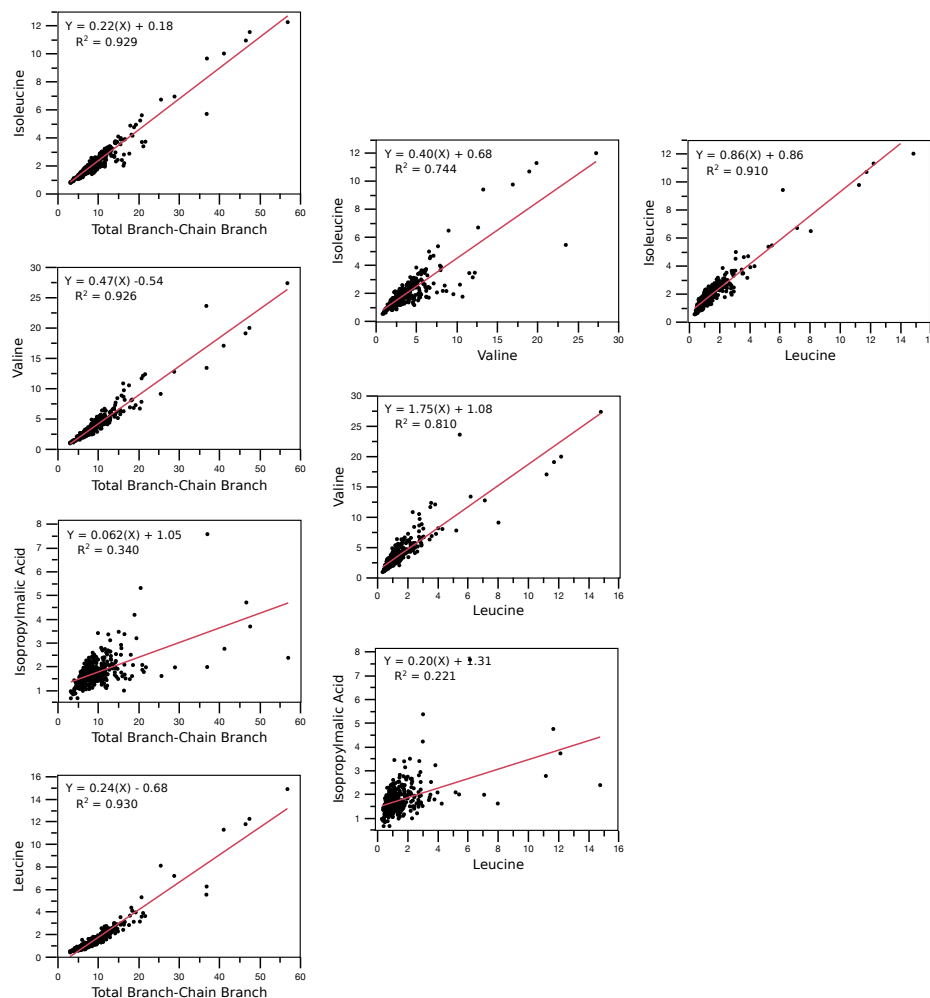


Figure 3.9 – Correlations showing the relationships between the individual amino acids in the branch-chain branch with total branch-chain branch and with each other. The equation for the best fit line (red line) and corresponding R^2 value is within each of the corresponding correlations.

Total aspartate branch shows strong correlations with aspartate ($R^2 = 0.893$) as well as the narrow two split pattern seen with asparagine ($R^2 = 0.915$ and 0.763) (Figure 3.10). Aspartate and asparagine show a two split pattern with one correlation showing a proportional increase while the other shows a greater aspartate increase ($R^2 = 0.945$ and 0.566 , respectively). Both threonine and alanine show very similar two split patterns when correlated with total aspartate branch as well as with aspartate and asparagine. Threonine shows a positive correlation with alanine ($R^2 = 0.567$).

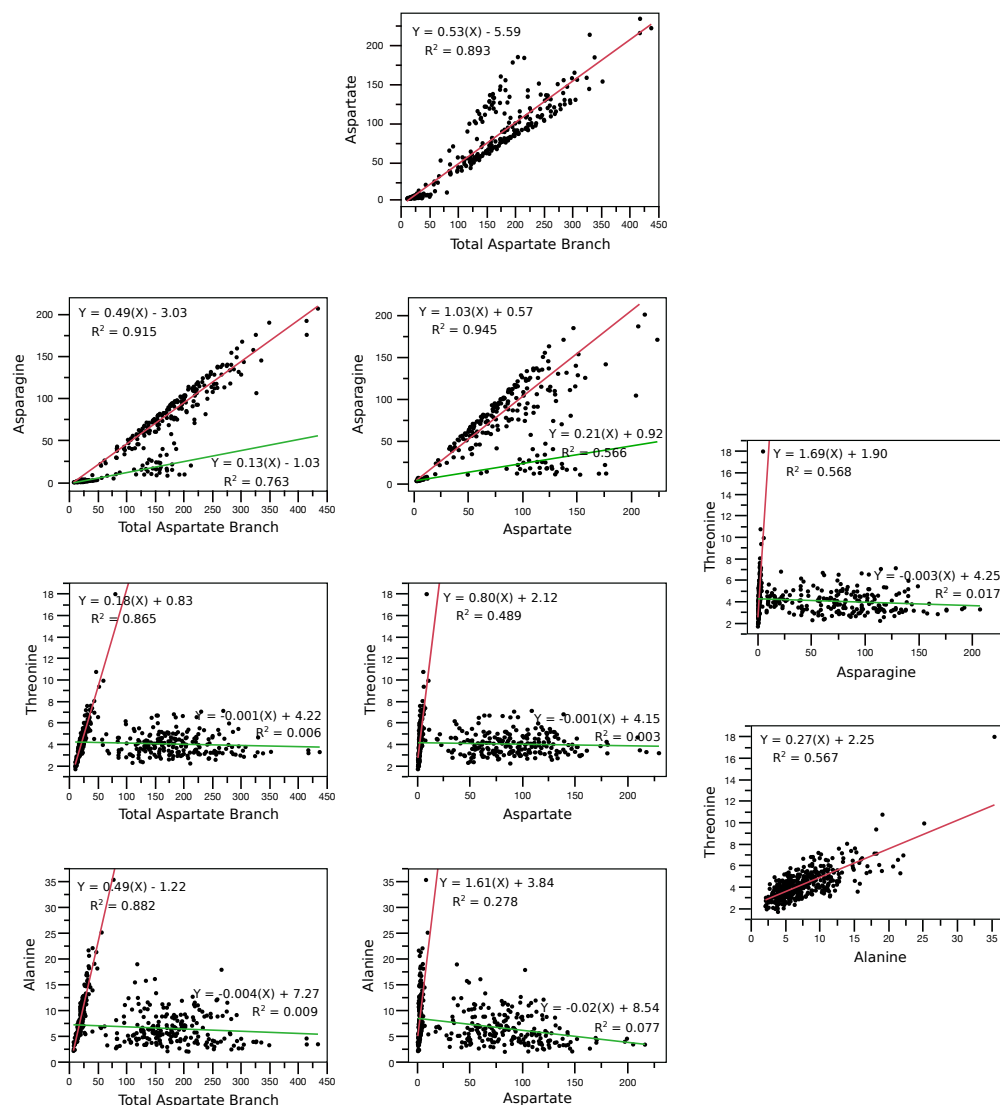


Figure 3.10 – Correlations showing the relationships between the individual amino acids in the aspartate branch with total aspartate branch and with each other. The equations for the best fit lines (red and green lines) and corresponding R^2 values are within each of the corresponding correlations.

3.4.1.3.3. Sugars

Fructose, glucose, and “other sugars” show strong, positive correlations with total sugar content ($R^2 = 0.985, 0.986, \text{ and } 0.615$). Sucrose and maltitol show weak, but positive correlations with total sugar. Maltose, galactose, xylose, and arabinose +others exhibit a split pattern into 2 distinct branches when correlated with total sugar (Figure 3.11). The correlations between the different sugars are shown in Figure 3.12. Glucose and fructose have a very strong positive correlation ($R^2 = 0.944$) (Figure 3.12, section A). The correlation between sucrose and glucose, as well as sucrose and fructose show a weak, positive correlation ($R^2 = 0.264 \text{ and } 0.298$, respectively), due to a split into 3 at high concentrations. The glucose and maltose correlation shows an overall positive correlation with a two split pattern, while the glucose and maltitol correlation shows a weak, positive correlation ($R^2 = 0.341$). Sucrose does not show a correlation with maltose or maltitol. The correlation between maltose and maltitol shows a weak R^2 value due to a two split pattern that could not be separated into distinct correlations. Interestingly, maltose shows a strong correlation with xylose ($R^2 = 0.687$).

The correlation between glucose and galactose, epimers of each other, shows a low R^2 value due to the nice two split pattern that could not be separated into distinct correlations (Figure 3.12, section B). Arabinose +others shows a very similar two split pattern with correlated with glucose as the galactose-glucose correlation. The glucose correlation with xylose also shows a two split pattern that could be separated into two correlations. The galactose with xylose and galactose with arabinose +others both show positive correlations ($R^2 = 0.347 \text{ and } 0.433$, respectively). Xylose and arabinose +other show a strong, positive correlation ($R^2 = 0.615$). Glucose shows the strongest correlation with “other sugars”, while xylose shows a weak, positive correlation ($R^2 = 0.604 \text{ and } 0.353$, respectively) (Figure 3.12).

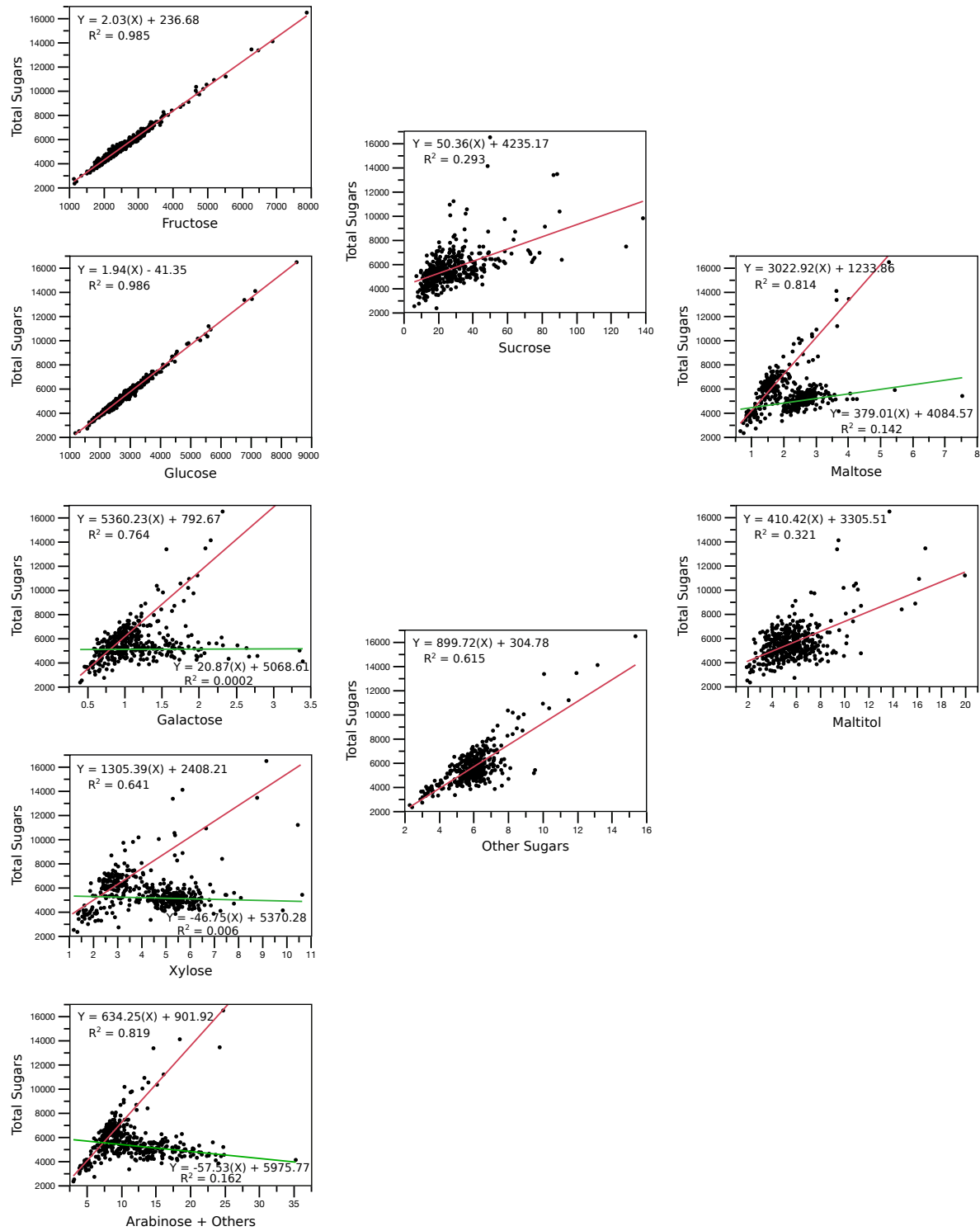


Figure 3.11 – Correlations showing the relationships between the individual sugars and total sugars. The equations for the best fit lines (red and green lines) and corresponding R^2 values are within each of the corresponding correlations

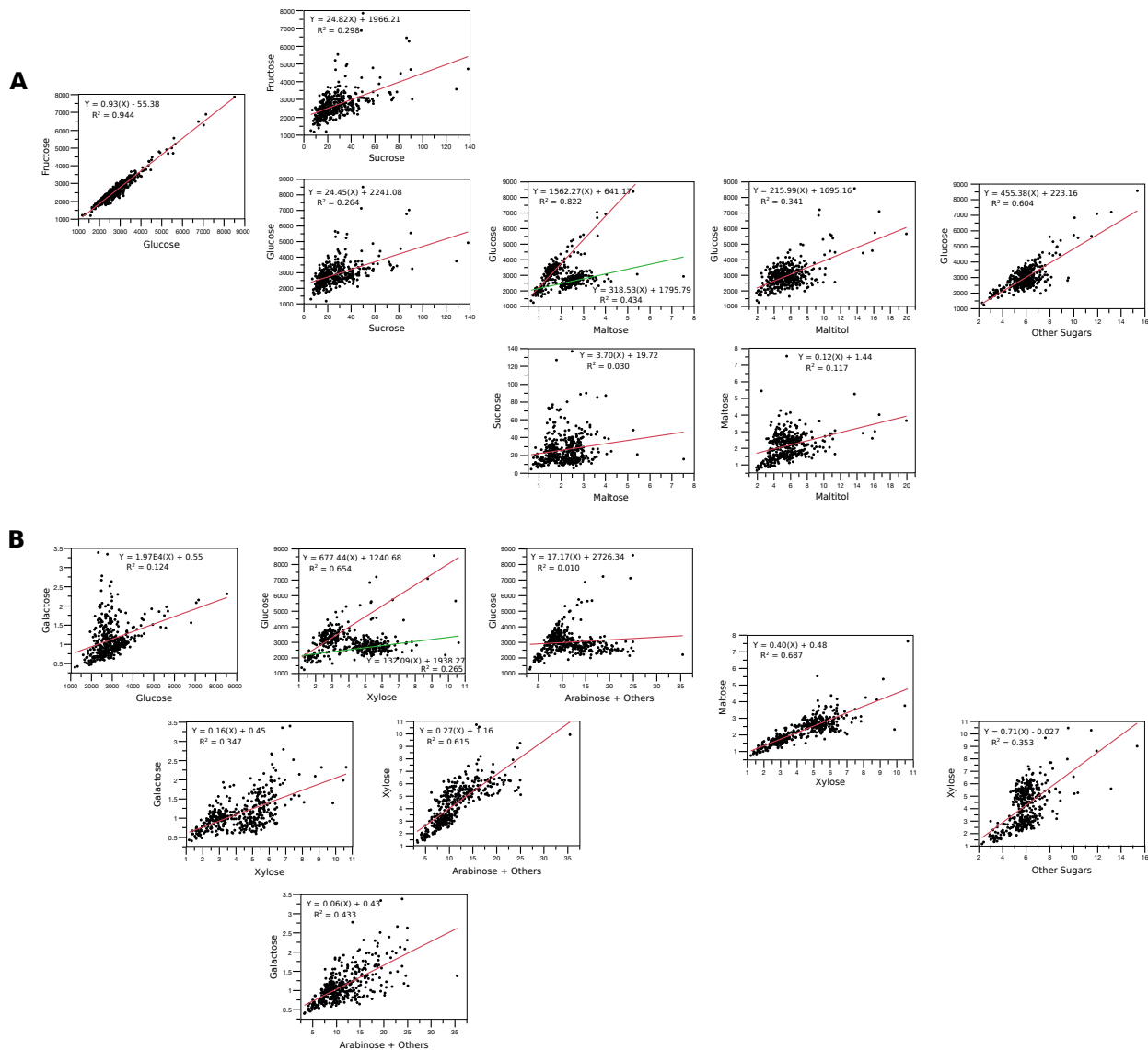


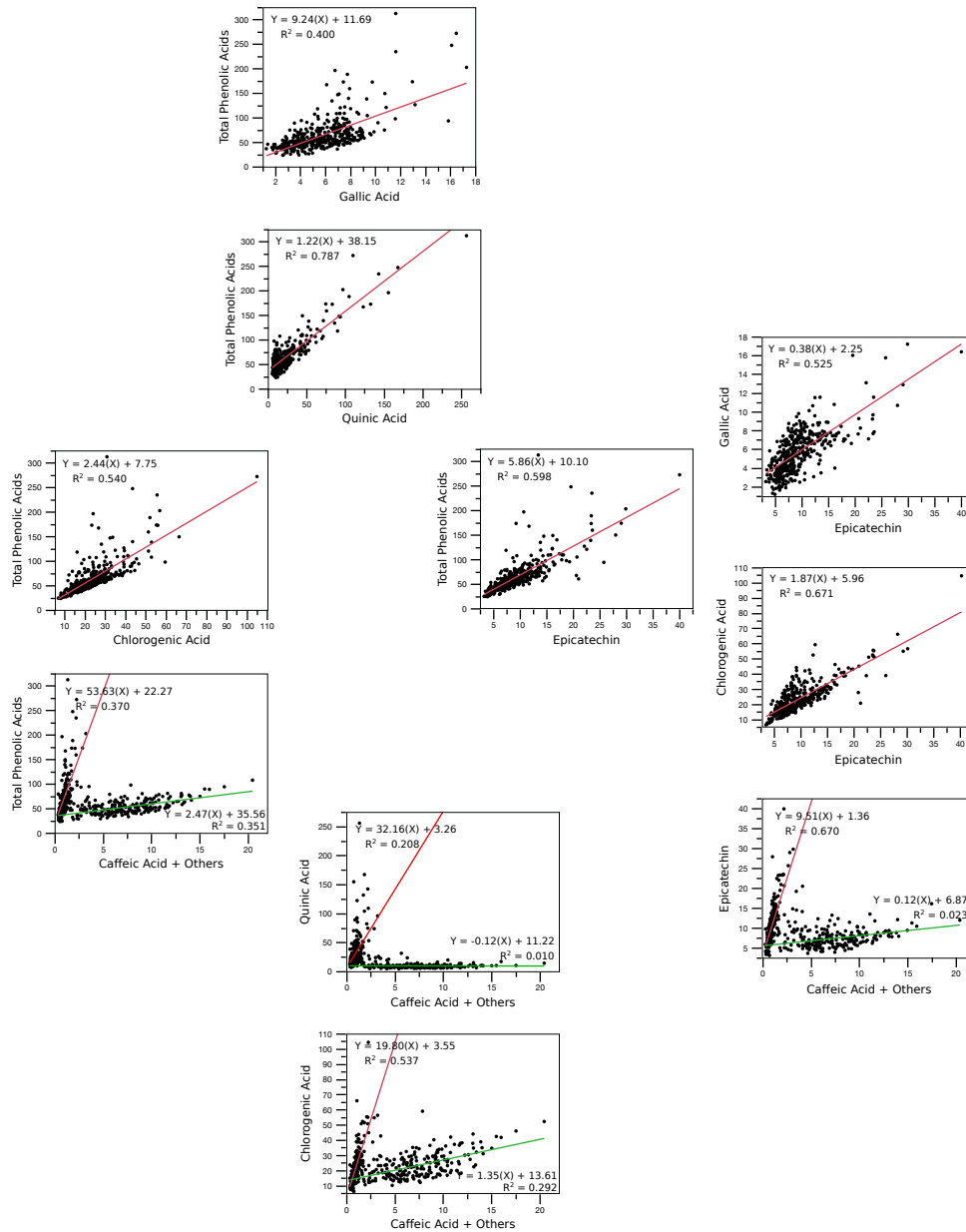
Figure 3.12 – Correlations showing the relationships between the individual sugars. Section A includes Glucose, fructose, sucrose, maltose, maltitol, and other sugars. Section B includes Galactose, xylose, arabinose +others and other sugars. Poor correlations are not shown. The equations for the best fit lines (red and green lines) and corresponding R^2 values are within each of the corresponding correlations

3.4.1.3.4. Phenolic acids

Total phenolic acids shows a strong, positive correlation with quinic acid ($R^2 = 0.787$) (Figure 3.13, section A). Total phenolic acids also shows a positive correlation with gallic acid, chlorogenic acid, and epicatechin ($R^2 = 0.400, 0.540, \text{ and } 0.598$, respectively). Chlorogenic acid and epicatechin show a strong positive correlation ($R^2 =$

0.671), while epicatechin and gallic acid also show a positive correlation ($R^2 = 0.525$). Total phenolic acids show a two split pattern when correlated with caffeic acid +others (Figure 3.13, section A) and ascorbic acid +others (Figure 3.13, section B). When caffeic acid +others is correlated with quinic acid, chlorogenic acid, and epicatechin, they show distinct two split patterns. When ascorbic acid +others is correlated with quinic acid and epicatechin, there is a weak two split pattern (Figure 3.13, section B). There is a positive correlation between ascorbic acid +others and caffeic acid +others ($R^2 = 0.580$).

A



B

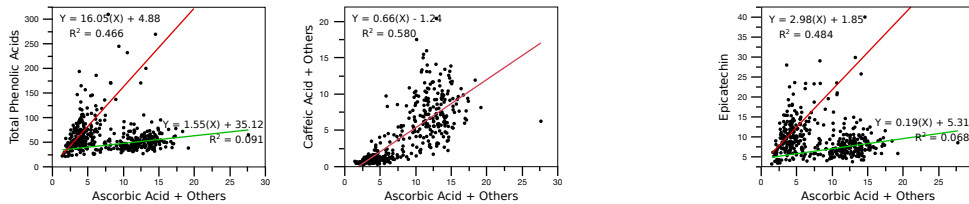


Figure 3.13 – Correlations showing the relationships between the individual phenolic acids with total phenolic acids and with each other (Section A). Total phenolic acids and individual phenolic acids are also correlated with ascorbic +others (Section B). The equations for the best fit lines (red and green lines) and corresponding R² values are within each of the corresponding correlations. Poor correlations not shown.

3.4.2. HPLC-QTOFMS Metabolite Features

The optimized LC-MS method detected anthocyanins utilizing both a DAD detector in the HPLC and the ion detector in the QTOFMS. The optimized method separated the extracted anthocyanins so that 17 anthocyanins were detected by DAD and 23 anthocyanins were detected by the ion detector. The difference in detected anthocyanins is due to some anthocyanins with overlapping peaks and some accumulating below the detection limit of the DAD, as discussed further in the discussion section (Figure 3.36). Both analyses detected and measured the five anthocyanidins commonly found in blueberries, delphinidin, petunidin, malvidin, cyanidin, and peonidin. The three sugar moieties annotated by both analyses were glucoside, galactoside, and arabinoside. The anthocyanins were also annotated with a sugar modification, acetylation, which is described as a separate sugar moiety for the results. The DAD detector only annotated acetyl-glucosides, whereas the MS also indicates acetyl-galactosides. The anthocyanins annotated by DAD are described first, followed by EIC annotated anthocyanins.

3.4.2.1. Anthocyanin Phenotype Description (DAD)

The 17 anthocyanins annotated by the DAD at wavelength 520nm in the 210 DxJ blueberry samples are listed in Table 3.7 along with other phenotypic characteristics. The anthocyanins with multiple rows, glucosides and acetyl-glucosides showed distributions with two different peaks were the distribution of each peak subset was analyzed separately. The distributions of the 17 anthocyanins across the population are seen in Figure 3.14. A normal distribution is shown by the red line in each distribution histogram (Figure 3.14). The distribution of delphinidin-arabinoside exhibits a normal distribution, whereas the rest of the galactosides and arabinosides show slight right-tailed skewing (Figure 3.14). Anthocyanins containing a glucoside, including acetyl-glucosides, exhibit bimodal distributions as two distinct peaks are present.

The distribution of each peak within the binomial distribution was separately analyzed to determine shape and normality of each peak. Delphinidin-glucoside, petunidin-glucoside, and malvidin-glucoside had two distribution peaks with 110 and 100 individuals showing distributions close to normal (Table 3.7). The cyanidin-glucoside distribution showed 36% of the individuals had 0 accumulation, which would

skew the overall cyanidin-glucoside mean (Table 3.7). All the acetyl-glucoside distributions showed one peak consisting of over 50% of the individuals with a 0 accumulation (Table 3.7).

Table 3.7 – Accumulation and annotation summary data for anthocyanins detected using DAD from targeted profiling with HPLC-QTOFMS.

Detected Anthocyanins (DAD)	m/z	RT (min)	N	Mean [◇]	Standard Error Mean	Draper	Jewel
Delphinidin-3 -glucoside	465.104	11.40	210	21123.6	1458.4	1312.8	1678.6
			110 [#]	38784.7	1369.4		
			100 [#]	1888.8	88.4		
Delphinidin-3 -galactoside	465.104	10.49	210	73758.8	1853.1	70435.4	79754.9
Delphinidin-3 -arabinoside	435.076	12.63	210	41211.0	735.0	38332.2	44888.5
Delphinidin-6-acetyl- 3-glucoside	507.115	18.19	210	1150.2	141.6	0	0
			68 [#]	3569.0	257.0		
			142 [#]	0	0		
Petunidin-3 -glucoside	479.119	14.44	210	15876.4	1077.6	1117.3	1352.9
			110 [#]	29019.8	988.7		
			100 [#]	1564.3	61.1		
Petunidin-3 -galactoside	479.119	13.71	210	38191.2	1031.5	40839.2	41620.9
Petunidin-3 -arabinoside	449.109	15.46	210	18310.0	353.7	19991.1	20468.5
Petunidin- 6-acetyl- 3-glucoside	521.130	19.73	210	821.2	99.9	0	0
			70 [#]	2475.4	179.7		
			140 [#]	0	0		
Malvidin-3 -glucoside	493.135	16.49	210	25475.3	1775.2	0	0
			110 [#]	46634.4	1733.3		
			100 [#]	2417.1	272.2		
Malvidin-3 -galactoside	493.136	15.95	210	64950.3	2032.6	68110.6	60613.8
Malvidin-3 -arabinoside	463.125	17.28	210	31194.1	857.6	33622.2	30210.3
Malvidin- 6-acetyl- 3-glucoside	535.146	20.72	210	914.9	107.6	0	0
			71 [#]	2718.8	182.1		
			139 [#]	0	0		

Table 3.7 – (continued).

Cyanidin-3 -glucoside	449.109	13.16	210	2652.1	206.5	0	0
			135 [#]	4145.2	241.4		
			75 [#]	0	0		
Cyanidin-3 -galactoside	449.108	12.21	210	10816.0	418.5	16320.4	11651.7
Peonidin-3 -galactoside	463.125	15.08	210	3407.7	164.0	5078.7	4151.5
Cyanidin-3 -arabinoside	419.099	14.14	210	4855.7	167.4	7088.7	5635.6
Cyanidin- 6-acetyl- 3-glucoside	491.119	19.26	210	302.8	45.0	0	0
			46 [#]	1388.8	99.1		
			164 [#]	0	0		

m/z – indicates exact mass predicted for that specific anthocyanin

RT – indicates the average retention time in minutes the anthocyanin peak was detected

N – indicates the number of samples included in the distribution analysis of the total population (210) or a subset.

- indicates the separate analyses of the two peaks from the binomial distributions

◇ - indicates the annotated metabolite accumulations are relative measurements of peak area from peak integration and do not have units

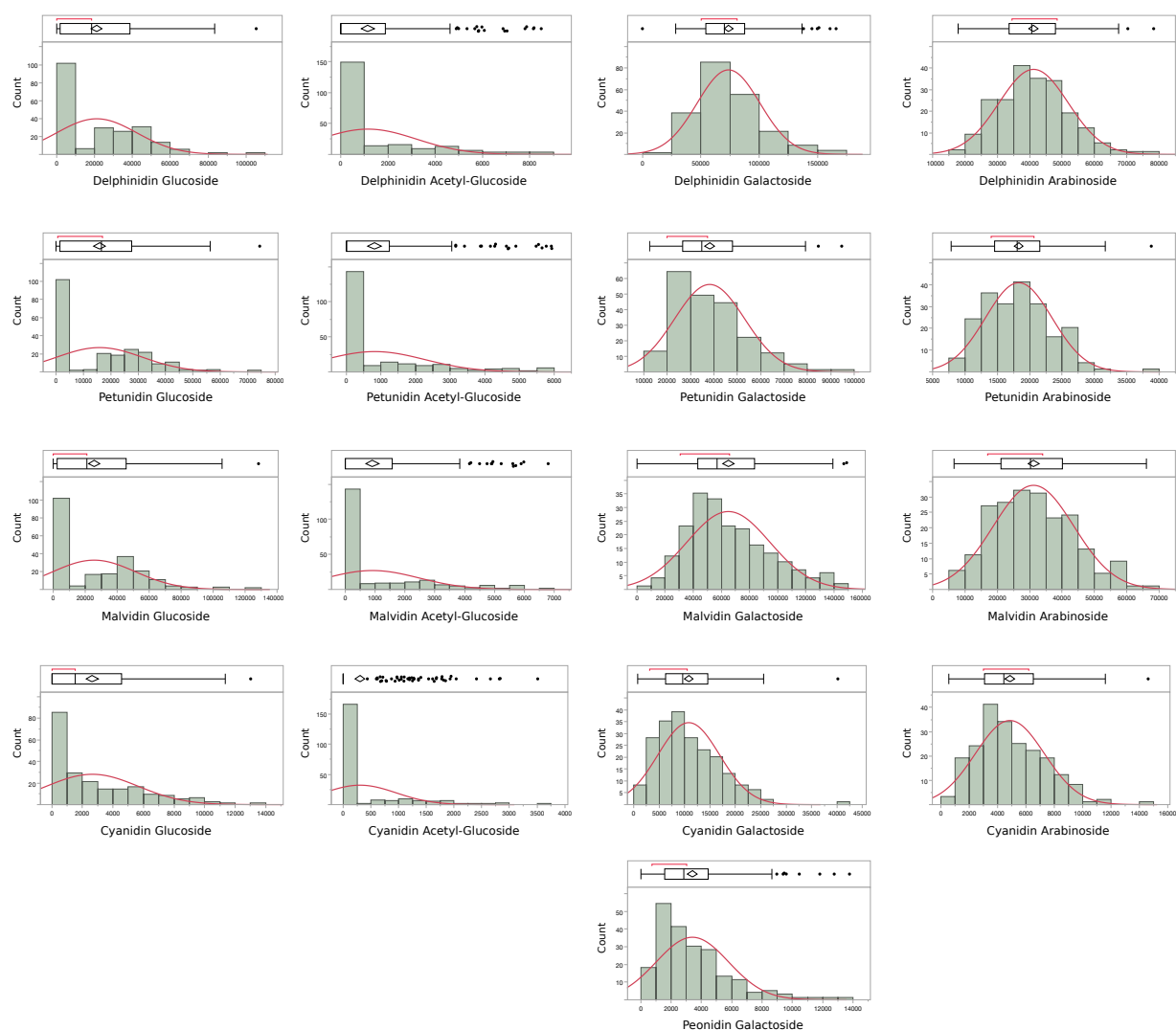


Figure 3.14 – Distribution histograms for the 17 individual anthocyanins detected and annotated by the DAD from targeted profiling with HPLC-QTOFMS. The red line indicates a normal distribution. The box plot shows the mean, quartiles, and interquartile range, as well as possible outliers as dots.

The 17 anthocyanins were grouped together in different combinations to produce broader summation groups to aid in investigating anthocyanin composition (Figure 3.15, 3.16, and Table 3.8). The first grouping, total anthocyanins, is the summation of the 17 annotated anthocyanins. The distribution of total anthocyanins is very close to following a normal distribution, but still has a very slight right-tailed skewing (Figure 3.15 with blue bars). To investigate the relative composition of anthocyanins in blueberries, the percent

of total anthocyanins was calculated for each of the subsequent summation groupings and their distribution shown in Figures 3.15 and 3.16 directly to the right of each corresponding summation grouping.

The second grouping is based on the four anthocyanidin core structures to investigate differences in anthocyanidin core accumulation. These groupings utilize “all” to distinguish from the third summation groups. The second grouping consists of “all delphinidins”, “all petunidins”, “all malvidins”, and “all cyanidins”. The distributions of these anthocyanidins groups show non-normal distributions and slight right-tailed skewing (Figure 3.15). The summation group “all delphinidins” represents the summation of each anthocyanin with a delphinidin anthocyanidin core, and shows the highest accumulation constituting 38.72% of total anthocyanins (Table 3.8). The all cyanidin grouping represents the summation of each anthocyanin with a cyanidin anthocyanidin cores, and shows the lowest accumulation with only 5.40% of total anthocyanins. These summation groups were also combined into either “all delphinidin derivatives” or “all cyanidin derivatives” to further investigate differences in the anthocyanidin core accumulation. The anthocyanidin core is a product of the flavonoid biosynthesis pathway. Midway through flavonoid biosynthesis, the pathway branches to produce multiple dihydroflavonols, including dihydroquercetin and dihydromyricetin (He et al., 2010; Kanehisa et al., 2017; Overall et al., 2017; Stevenson & Scalzo, 2012; Yonekura-Sakakibara et al., 2009). The production of dihydromyricetin and dihydroquercetin is the branch point that separates the biosynthesis pathways for the different anthocyanidins cores, delphinidins or cyanidins, respectively. From the delphinidin anthocyanidin core, petunidin and malvidin cores are produced. Therefore, delphinidin, petunidin, and malvidin summation groups were combined into the “all delphinidin derivative” group. From the cyanidin anthocyanidin core, peonidin is produced, thus the cyanidin and peonidin summation group were combined into the “all cyanidin derivative” group. The distributions of these larger anthocyanidin groups also show non-normal distributions and slight right-tailed skewing (Figure 3.15). The delphinidin derivatives accounted for 93.62% of total anthocyanin content, whereas cyanidin derivatives only accounted for 6.38% (Table 3.8).

The third grouping is based on the four sugar moieties to investigate differences in sugar moiety accumulation. These groupings utilize “total” to distinguish from the second summation group. The third grouping consists of “total glucosides”, “total acetyl-glucosides”, “total glucoside + total acetyl-glucoside”, “total galactosides”, “total arabinosides”, and “total galactoside + total arabinosides” (Figure 3.16). The distributions of total glucosides, total acetyl-glucosides, and the summation of glucosides and acetyl-glucosides showed similar binomial distributions as the individual anthocyanin glucosides and acetyl-glucosides (Figure 3.16). Total galactosides follow a non-normal distribution with a very slight right-tailed skewing, whereas total arabinosides follow a normal distribution. The summation of the galactoside sugar moiety, total galactosides, accounted for 53.77% of total anthocyanins, and the summation of galactosides and arabinosides accounted for 80.75% of total anthocyanins (Table 3.8). Total glucosides accounted for 18.42%, whereas total acetyl-glucosides accounted for only 0.89% of total anthocyanins (Table 3.8). The distribution of the % contribution of all anthocyanidin and total sugar moiety summation groups to total anthocyanins across the population is shown as histograms to the right of the corresponding summation group histograms (Figures 3.15 and 3.16).

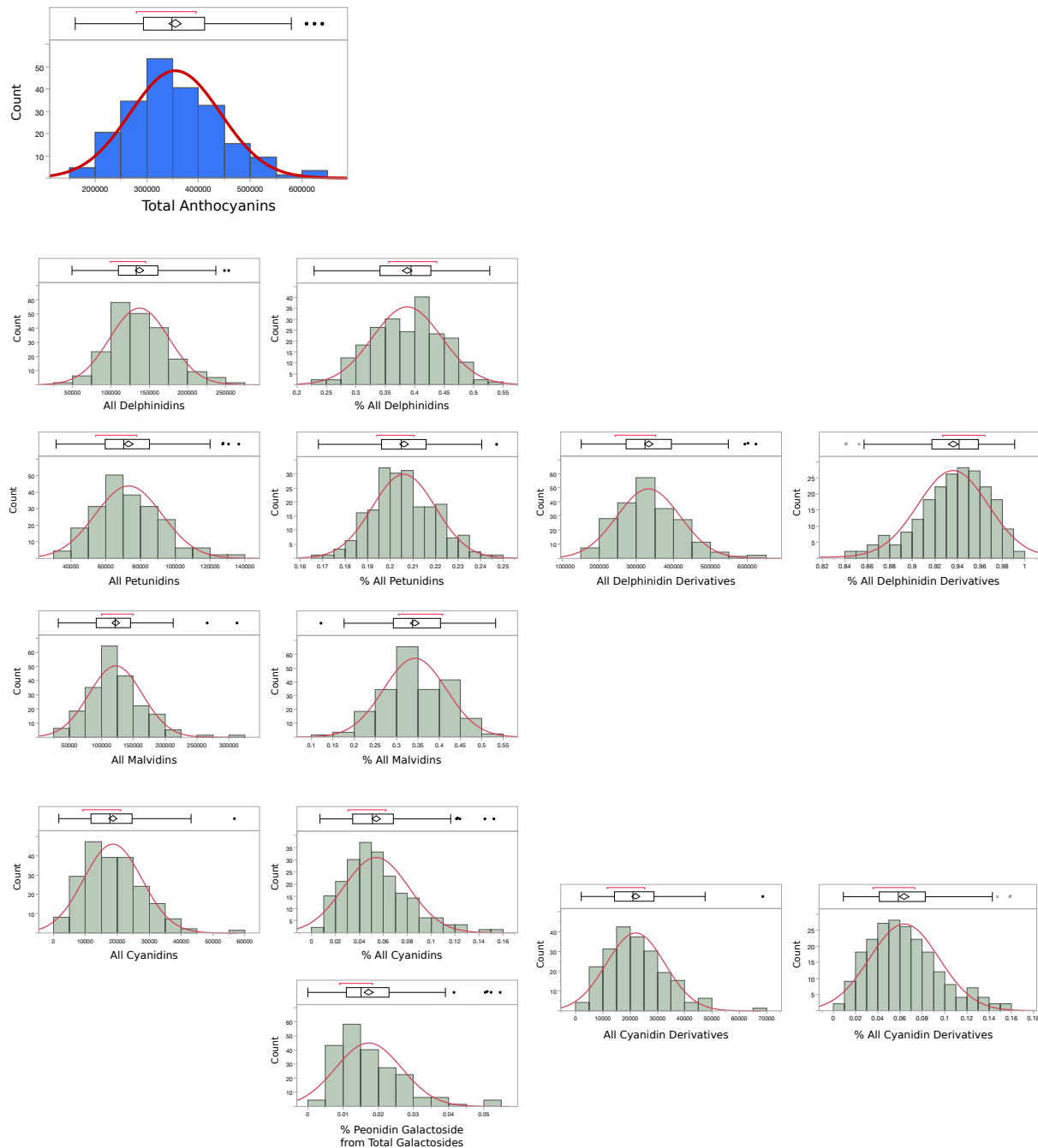


Figure 3.15 – Distribution histograms for the anthocyanidin summation groups of the 17 individual anthocyanins detected and annotated by the DAD from targeted profiling with HPLC-QTOFMS. The total anthocyanins distribution has blue histogram bars. The % of total anthocyanins for each of the anthocyanidin summation groups is to the right of the corresponding anthocyanidin group. The red line indicates a normal distribution. The box plot shows the mean, quartiles, and interquartile range, as well as possible outliers as dots.

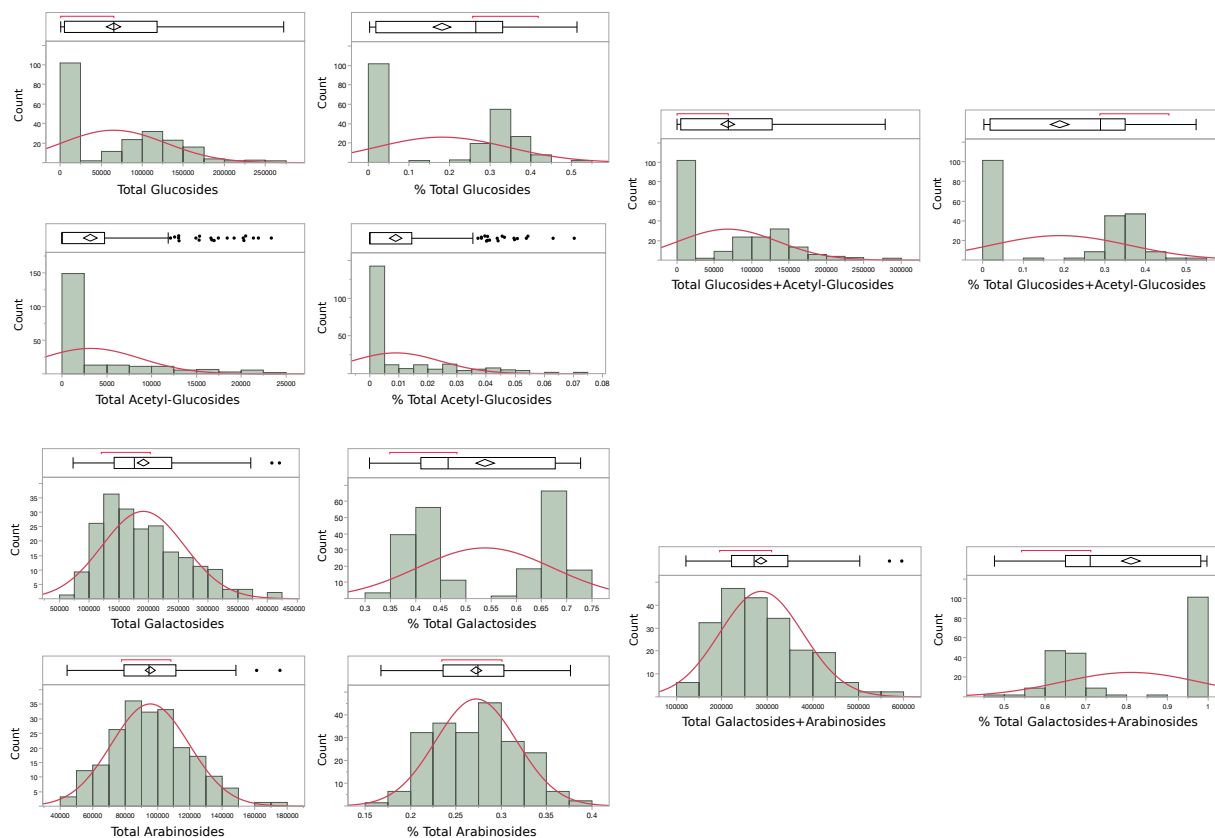


Figure 3.16 – Distribution histograms for the sugar moiety summation groups of the 17 individual anthocyanins detected and annotated by the DAD from targeted profiling with HPLC-QTOFMS. The % of total anthocyanins for each of the sugar moiety summation groups is to the right of the corresponding sugar moiety group. The red line indicates a normal distribution. The box plot shows the mean, quartiles, and interquartile range, as well as possible outliers as dots.

Table 3.8 – Summary and total composition data for anthocyanin summation groups from the DAD detected anthocyanins.

Anthocyanin Summation Groups (DAD)	Mean[◇]	Standard Error Mean	Draper	Jewel	% of Total Anthocyanin
Total Anthocyanins	355011.1	6009.2	302248.6	302027.2	-
All Delphinidins	137243.6	2668.9	110080.4	126322.1	38.72
All Petunidins	73198.8	1323.4	61947.6	63442.2	20.60
All Malvidins	122534.6	2871.9	101732.8	90824.1	34.30
All Delphinidin Derivatives	332976.9	5884.8	273760.8	280588.4	93.62
All Cyanidins	18626.6	628.7	23409.1	17287.3	5.40
All Cyanidin Derivatives	22034.2	736.7	28487.8	21438.8	6.38
Total Glucosides	65404.3	4384.9	2430.1	3031.5	18.42
	119268.5 [#]	3790.7			33.60
	6153.6 [#]	375.8			1.73
Total Acetyl-Glucosides	3204.3	386.0	0	0	0.90
	8738.9 [#]	693.6			2.46
	0 [#]	0			0
Total Glucosides + Total Acetyl-Glucosides	68608.5	4591.6	2430.1	3031.5	19.33
	125320.1 [#]	3884.1			35.30
	6225.8 [#]	387.2			1.75
Total Galactosides	191124.0	4778.6	200784.3	197792.9	53.77
Total Arabinosides	95570.6	1650.8	99034.2	101202.9	27.24
Total Galactosides + Total Arabinosides	286667.0	6320.9	299818.6	298995.7	80.75

◇ - indicates the annotated metabolite accumulations are relative measurements of peak area from peak integration and do not have units

- indicates the separate analyses of the two peaks from the binomial distributions

The % contribution of each anthocyanin to total anthocyanins was determined to see the specific anthocyanin composition of blueberries (Table 3.9). The highest accumulating anthocyanin is delphinidin-galactoside at 20.78% of total anthocyanins. The lowest accumulating anthocyanin is cyanidin-acetyl-glucoside at 0.09% of total anthocyanins. Each anthocyanin % contribution was also determined for the other summation groups to see if the summation groups appropriately summarize the differences in the anthocyanins (Table 3.9). The galactoside sugar moiety is the highest % across all the anthocyanidin cores (% of all anthocyanidins), which is consistent with total galactosides also showing the highest % for total anthocyanins. The delphinidin anthocyanidin is the highest % across all the sugar moieties (% of total sugar moiety), which is consistent with all delphinidins also showing the highest % for total anthocyanins. Although all malvidin shows second highest % of total anthocyanins, the petunidin anthocyanidin shows the second highest % for glucosides, galactosides, and arabinosides rather than malvidin.

Table 3.9 – Individual anthocyanin composition summary data using the DAD detected anthocyanins and summation groups.

Individual Anthocyanins (DAD)	% of Total Anthocyanins	% of Corresp. "All" Anthocyanidin Core	% of Corresp. "Total" Sugar Moieties
Delphinidin-3 -glucoside	5.95	15.39	32.43
	10.93 [#]	28.26	32.52
	0.53 [#]	1.38	30.69
Delphinidin-3 -galactoside	20.78	53.74	38.59
Delphinidin-3 -arabinoside	11.61	30.03	43.12
Delphinidin -6-acetyl- 3-glucoside	0.32	0.84	36.07
	1.07 [#]	2.77	36.62
	0 [#]	0	0
Petunidin-3 -glucoside	4.47	21.69	24.38
	8.17 [#]	39.65	24.33
	0.44 [#]	2.14	25.42
Petunidin-3 -galactoside	10.76	52.18	19.98
Petunidin-3 -arabinoside	5.16	25.01	19.16
Petunidin -6-acetyl- 3-glucoside	0.23	1.12	25.75
	0.71 [#]	3.42	24.11
	0 [#]	0	0
Malvidin-3 -glucoside	7.18	20.79	7.18
	13.14 [#]	38.06	13.14
	0.68 [#]	1.97	39.28

Table 3.9 – (continued).

Malvidin-3 -galactoside	18.30	53.01	18.30
Malvidin-3 -arabinoside	8.79	25.46	8.79
Malvidin -6-acetyl- 3-glucoside	0.26	0.75	28.69
	0.78 [#]	2.27	26.80
	0 [#]	0	0
Cyanidin-3 -glucoside	0.75	14.24	4.07
	1.23 [#]	23.53	3.68
	0 [#]	0	0
Cyanidin-3 -galactoside	3.05	58.07	5.66
Peonidin-3 -galactoside	0.96	-	1.78
Cyanidin-3 -arabinoside	1.37	26.07	5.08
Cyanidin -6-acetyl- 3-glucoside	0.09	1.63	9.49
	0.39 [#]	7.46	13.37
	0 [#]	0	0

Corresp. – abbreviation for corresponding

[#] - indicates the separate analyses of the two peaks from the binomial distributions

3.4.2.2. Anthocyanin Phenotype Description (EIC)

The 23 anthocyanins annotated by the EIC in the 210 DxJ blueberry samples are listed in Table 3.10 along with other phenotypic characteristics. The anthocyanins with multiple rows showed distributions usually with two different peaks, similarly to the DAD anthocyanins. The distributions of the 23 anthocyanins across the population are seen in Figure 3.17. A normal distribution is indicated by the red line in each distribution histogram (Figure 3.17). The delphinidin, petunidin, and malvidin -glucoside anthocyanins exhibit the bimodal distribution with two distinct peaks, thus the distribution of each peak was also analyzed separately (Table 3.10). Each of the -acetyl-glucosides and each of the -acetyl-galactoside exhibited severe right-tailed skewing (Figure 3.17). These distributions showed that over 50% of the population has a mean of less than 15% of the total population's mean for that anthocyanin. Thus, the majority bar and right-tail bars were also analyzed separately (Table 3.10). Both petunidin-arabinoside and malvidin arabinoside exhibit a normal distribution. The remaining anthocyanins show distributions with slight right-tailed skewing and non-normal distributions.

Table 3.10 – Accumulation and annotation summary data for anthocyanins detected using EIC from targeted profiling with HPLC-QTOFMS.

Detected Anthocyanins (EIC)	m/z	RT (min)	N	Mean[◇]	Standard Error Mean	Draper	Jewel
Delphinidin -3 - glucoside	465.104	11.45	210	926809760.3	58476167.5	82991702.1	128306793.9
			120 [#]	1526877234.4	58579868.5		
			90 [#]	126719794.7	5634074.5		
Delphinidin -3 - galactoside	465.104	10.52	210	2555301353.6	84677386.0	2097346391.5	3051465437.8
Delphinidin -3 - arabinoside	435.076	12.68	210	2082666103.5	47022947.2	1449591052.4	2162162410.1
Delphinidin -6 - acetyl- 3-glucoside	507.115	18.26	210	90454271.1	9629701.6	0	0
			71 [#]	241385976.6	17955084.6		
			139 [#]	13359659.0	1122096.8		
Delphinidin -6 - acetyl- 3-galactoside*	507.115	16.60	210	21028273.7	2022580.1	1911430.6	1054932.9
			102 [#]	40887656.0	3125626.7		
			108 [#]	2272190.5	242404.4		
Petunidin -3 - glucoside	479.119	14.50	210	999039414.1	63063835.2	105074551.0	147113885.9
			122 [#]	1616938147.2	65430237.2		
			88 [#]	142407079.6	5101448.2		
Petunidin -3 - galactoside	479.119	13.77	210	1997742517.2	58610682.8	1730162834.2	2302158030.8
Petunidin -3 - arabinoside	449.109	15.51	210	1344485665.8	35576578.6	1169724477.4	1531994728.5
Petunidin -6 -acetyl- 3-glucoside	521.130	19.80	210	107070166.4	11533550.9	0	0
			74 [#]	276613236.9	21633485.8		
			136 [#]	14818789.9	1182449.9		
Petunidin -6 -acetyl- 3-galactoside*	521.130	18.39	210	17533111.2	1638544.4	1480845.0	0
			115 [#]	31323167.3	2300258.5		
			95 [#]	839885.4	119489.9		

Table 3.10 – (continued).

Malvidin -3 -glucoside	493.135	16.54	210	1854868819.7	112622188.6	240943667.5	289413766.8
			132 [#]	2774235447.2	121495262.9		
			78 [#]	299017603.9	13270381.8		
Malvidin -3 -galactoside	493.136	16.01	210	3610230665.6	105703171.8	3209176477.9	3824650145.1
Malvidin -3 -arabinoside	463.125	17.35	210	2813561922.6	82230784.4	2481898136.2	2983456403.5
Malvidin -6 -acetyl-3-glucoside	535.146	20.84	210	162015677.8	16682699.9	0	56727.0
			67 [#]	448311289.3	30275580.2		
			143 [#]	27877174.5	2187825.0		
Malvidin -6 -acetyl-3-galactoside*	535.146	19.61	210	37510101.1	3668484.1	1109107.8	0
			100 [#]	74453168.8	5750598.0		
			110 [#]	3925494.0	476650.0		
Cyanidin -3 -glucoside	449.109	13.23	210	239058500.6	16068986.0	51327167.0	51305895.9
			130 [#]	387843027.3	19625650.9		
			92 [#]	48226172.9	2511930.1		
Cyanidin -3 -galactoside	449.109	12.27	210	670377781.8	26152664.8	789622182.0	789113358.0
Cyanidin -3 -arabinoside	419.099	14.20	210	473661698.5	17653797.5	518934936.5	565321460.2
Cyanidin -6 -acetyl-3-glucoside	491.119	19.33	210	41469225.6	4951701.4	1469863.5	0
			64 [#]	122448540.8	10748573.0		
			146 [#]	5971443.6	561172.5		
Cyanidin -6 -acetyl-3-galactoside*	491.119	17.68	210	8790831.2	889145.7	1149624.9	0
			94 [#]	18805723.2	1410732.5		
			116 [#]	675315.4	132036.0		
Peonidin -3 -glucoside	463.125	15.89	210	187031551.8	13279960.2	40135876.9	50463834.6
			139 [#]	278252491.0	14975299.1		
			71 [#]	8444079.5	1875604.1		
Peonidin -3 -galactoside	463.125	15.14	210	469579694.5	21554824.3	480500738.0	586636288.6

Table 3.10 – (continued).

Peonidin -3 - arabinoside	433.115	16.70	210	270351828.4	14125822.6	321968695.9	410074893.7
------------------------------	---------	-------	-----	-------------	------------	-------------	-------------

* - indicates “putative” annotation assigned due to m/z charge, RT, and limited published literature

-m/z – indicates exact mass predicted for that specific anthocyanin

-RT – indicates the average retention time in minutes the anthocyanin peak was detected

-N – indicates the number of samples included in the distribution analysis of the total population (210) or a subset.

- indicates the separate distribution analyses for either binomial or severe right-tail skewed distributions

◇ - indicates the annotated metabolite accumulations are relative measurements of peak area from peak integration and do not have units

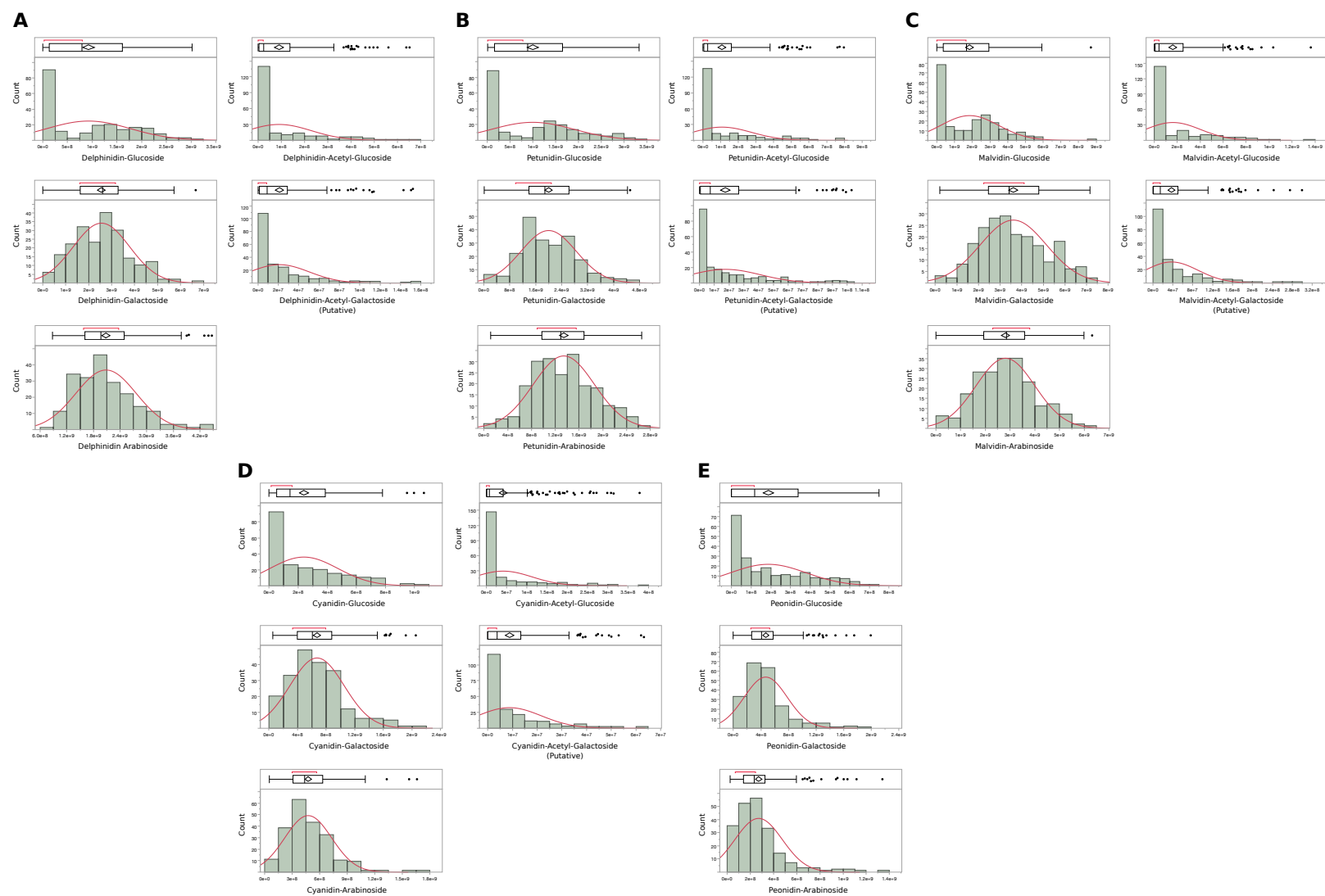


Figure 3.17 – Distribution histograms for the 23 individual anthocyanins detected and annotated by the EIC from HPLC-QTOFMS targeted profiling. The red line indicates a normal distribution. Delphinidin anthocyanins (Section A), Petunidin anthocyanins (Section B), Malvidin anthocyanins (Section C), Cyanidin anthocyanins (Section D), Peonidin anthocyanins (Section E). The box plot shows the mean, quartiles, and interquartile range, as well as possible outliers as dots.

The 23 anthocyanins detected with EIC were also categorized into three summation groups using the same pattern as the DAD anthocyanins. The first summation group, total anthocyanins, summed all the 23 anthocyanins and almost follows a normal distribution (Figure 3.18 with blue bars). To investigate the relative composition of anthocyanins in blueberries, the percent of total anthocyanins was calculated for each of the subsequent summation groupings and their distribution shown in Figures 3.18 and 3.19 directly to the right of each corresponding summation grouping.

The second summation grouping is the same as the DAD-anthocyanin groupings, which is biased on the four anthocyanidin cores and larger anthocyanidin derivative group. The distributions of all delphinidin derivatives, all delphinidins, all petunidins, and all malvidins followed a normal distribution. The all malvidin group represents the summation of each anthocyanin with a malvidin anthocyanidin core, and constitutes 40.57% of the total anthocyanidin (Table 3.11). The all delphinidin derivative group accounts for 88.34% of the total anthocyanins (Table 3.11). The all cyanidin derivatives, all cyanidins, and all peonidins showed right-tailed skewing (Figure 3.18). The all peonidin group represents the summation of each anthocyanin with a peonidin anthocyanidin core, and accounts for only 4.57% of total anthocyanins (Table 3.11).

The third summation grouping is the same as the DAD-anthocyanin groupings, which was based on the sugar moieties, with the addition of a “total acetyl-galactoside” group. The distributions of total glucosides and total glucoside + total acetyl-glucosides show a binomial distribution (Figure 3.19). Total glucosides accounts for 20.19%, total acetyl-glucosides accounts for 1.87%, and total glucosides + total acetyl-glucosides accounts for 22.06% of total anthocyanins. Total galactosides, total arabinosides, and total galactoside + total arabinoside follow a normal distribution (Figure 3.19). Total acetyl-galactoside exhibits a severe right-tailed skewed distribution (Figure 3.19). The total galactoside group is the summation of the anthocyanins with galactoside sugar moieties, and accounts for 45.03% of total anthocyanins (Table 3.11). The summation grouping of total galactosides + total arabinosides + total acetyl-galactosides accounts for 78.90% of the total anthocyanins (Table 3.11).

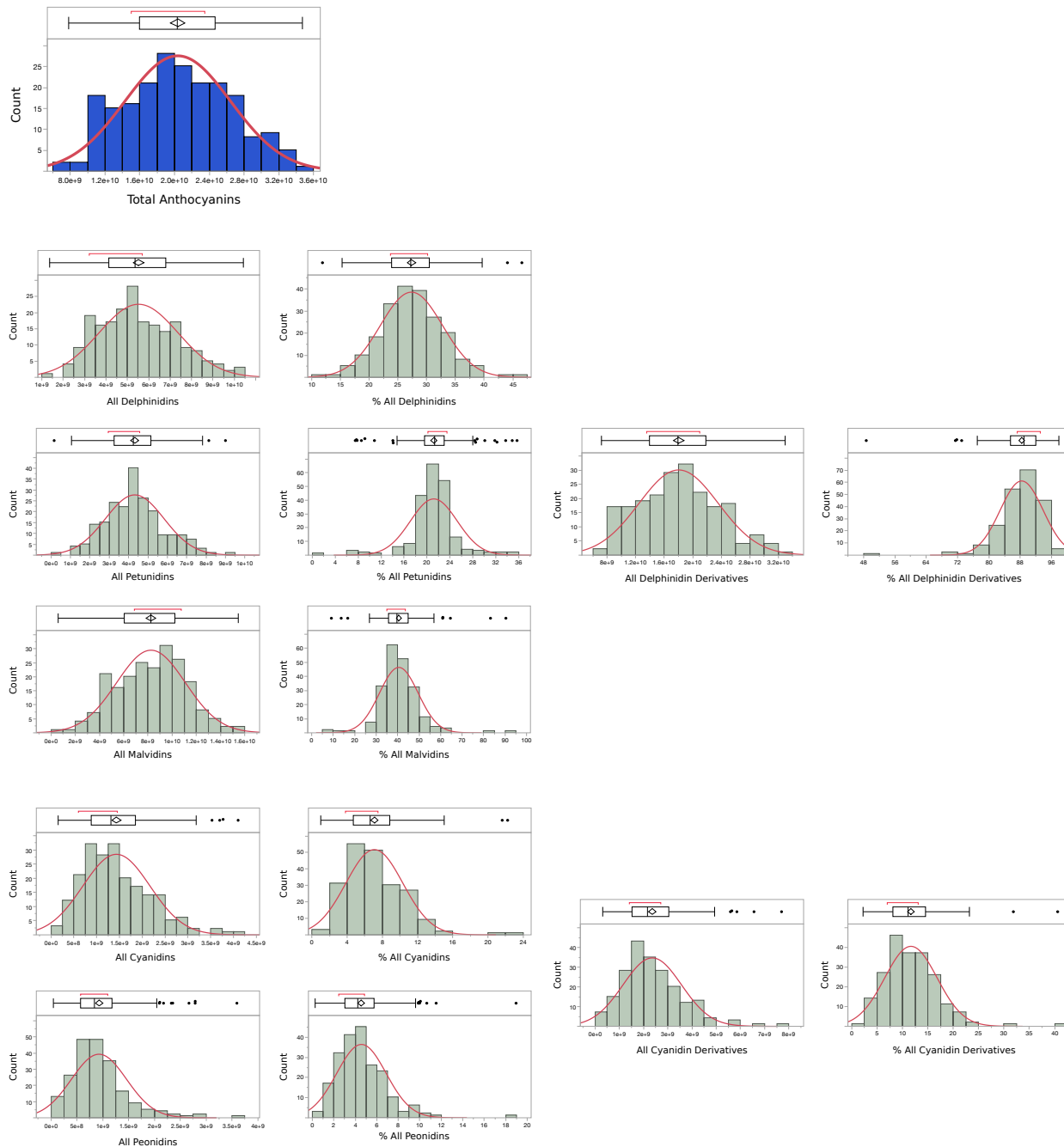


Figure 3.18 – Distribution histograms for the anthocyanidin summation groups of the 23 individual anthocyanins detected and annotated by the EIC from targeted profiling with HPLC-QTOFMS. The total anthocyanins distribution has blue histogram bars. The % of total anthocyanins for each of the anthocyanidin summation groups is to the right of the corresponding anthocyanidin group. The red line indicates a normal distribution. The box plot shows the mean, quartiles, and interquartile range, as well as possible outliers as dots.

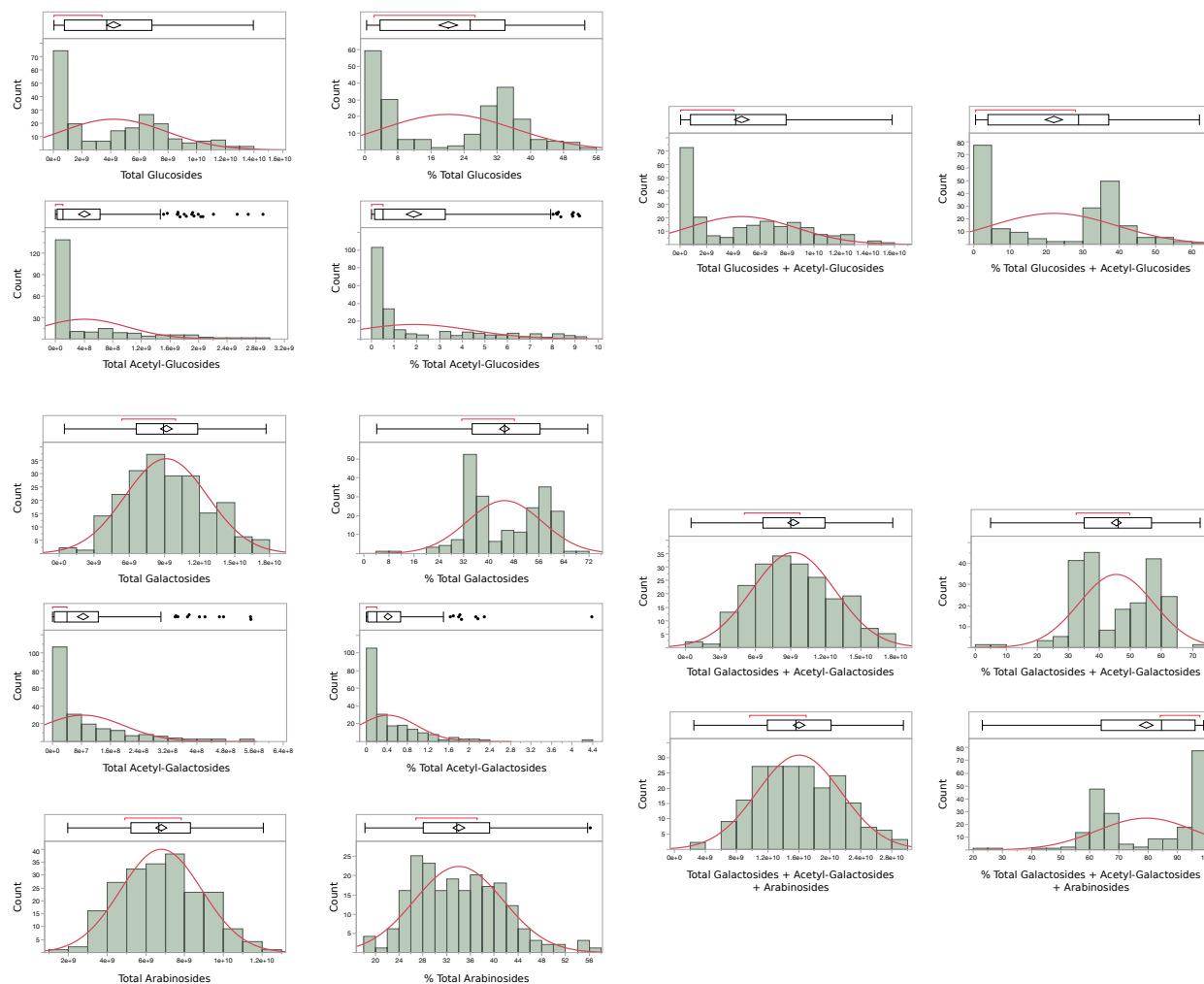


Figure 3.19 – Distribution histograms for the sugar moiety summation groups of the 23 individual anthocyanins detected and annotated by the EIC from targeted profiling with HPLC-QTOFMS. The % of total anthocyanins for each of the sugar moiety summation groups is to the right of the corresponding sugar moiety group. The red line indicates a normal distribution. The box plot shows the mean, quartiles, and interquartile range, as well as possible outliers as dots.

Table 3.11 – Summary and total composition data for anthocyanin summation groups from EIC detected anthocyanins.

Anthocyanin Summation Groups (EIC)	Mean[◇]	Standard Error Mean	Draper	Jewel	% of Total Anthocyanin
Total Anthocyanins	20373337667.6	419301344.6	14776519758.3	18874748993.3	-
All Delphinidins	5523970853.8	128059398.5	3631840576.6	5342989574.8	27.36
All Petunidins	4317680798.9	104272022.4	3006442707.6	3981266645.2	21.20
All Malvidins	8252026180.3	196169073.0	5933127389.4	7097577042.4	40.57
All Delphinidin Derivatives	18023974091.9	384393911.8	12571410673.6	16421833262.4	88.34
All Cyanidins	1433358037.7	50821757.6	1362503773.9	1405740714.0	7.09
All Peonidins	926963074.7	36798904.7	842605310.9	1047175017.0	4.57
All Cyanidin Derivatives	2360321112.4	83294436.1	2205109084.7	2452915731.0	11.66
Total Glucosides	4206808046.5	250648016.3	520472964.6	666604177.1	20.19
	6155325489.3 [#]	264951866.1			30.21
	625748962.6 [#]	24234711.4			3.07
Total Acetyl-Glucosides	401009341.0	41829097.5	1469863.5	56727.0	1.87
	954691498.5 [#]	74606415.1			4.69
	53348451.3 [#]	4270014.2			0.26
Total Glucosides + Total Acetyl-Glucosides	4607817387.5	276206275.4	521942828.1	666660904.1	22.06
	6671883009.2 [#]	293645274.6			32.75
	651691612.6 [#]	25592798.6			3.20
Total Galactosides	9163464845.3	243536181.1	8306808623.7	10554023260.4	45.03
Total Arabinosides	6795022287.3	144703838.3	5942117298.3	7653009896.0	34.04
Total Acetyl-Galactosides*	84862317.2	7786877.1	5651008.3	1054932.9	0.42
	162924603.8 [#]	11406941.5			0.80
	8272904.0 [#]	1035255.0			0.04
Total Galactosides + Total Arabinosides	15958487132.5	372802661.6	14248925821.9	18207033156.4	78.90
Total Galactosides + Total Acetyl-Galactosides	9247294938.5	245212534.7	8312459631.9	10555078193.3	45.44

Table 3.11 – (continued).

Total Galactosides + Total Arabinosides + Total Acetyl-Galactosides	16042317225.8	374520006.8	14254576930.2	18208088089.2	79.31
---	---------------	-------------	---------------	---------------	-------

- indicates the separate distribution analyses for either binomial or severe right-tail skewed distributions

◇ - indicates the annotated metabolite accumulations are relative measurements of peak area from peak integration and do not have units

The % contribution of each anthocyanin to total anthocyanins, as well as the other summation groups, was determined to see the specific anthocyanin composition of blueberries (Table 3.12). The highest accumulating anthocyanin is malvidin-galactoside at 17.72% of total anthocyanins. The lowest accumulating anthocyanin is cyanidin acetyl-galactoside at 0.04% of total anthocyanins. The galactoside sugar moiety is the highest % across all the anthocyanidin cores (% of all anthocyanidins), which is consistent with total galactosides also showing the highest % for total anthocyanins. The malvidin anthocyanidin is the highest % across all the sugar moieties (% of total sugar moiety), which is consistent with all malvidins also showing the highest % for total anthocyanins.

Table 3.12 – Individual anthocyanin composition summary data using the EIC detected anthocyanins and summation groups.

Individual Anthocyanins (EIC)	% of Total Anthocyanins	% of Corresp. “All” Anthocyanidin Core	% of Corresp. “Total” Sugar Moieties
Delphinidin -3 -glucoside	4.55	16.78	22.03
	7.49 [#]	27.64	24.81
	0.62 [#]	2.29	20.25
Delphinidin-3 -galactoside	12.54	46.26	27.89
Delphinidin-3 -arabinoside	10.22	37.70	30.65
Delphinidin -6 -acetyl- 3-glucoside	0.44	1.64	22.56
	1.19 [#]	4.37	25.28
	0.07 [#]	0.24	25.04
Delphinidin -6 -acetyl- 3-galactoside*	0.10	0.38	24.78
	0.20 [#]	0.74	25.10
	0.01 [#]	0.04	27.47
Petunidin -3 -glucoside	4.90	23.14	23.75
	7.94 [#]	37.45	26.27
	0.70 [#]	3.30	22.76
Petunidin -3 -galactoside	9.81	46.27	21.80
Petunidin -3 -arabinoside	6.60	31.14	19.79
Petunidin -6 -acetyl- 3-glucoside	0.53	2.48	26.70
	1.36 [#]	6.41	28.97
	0.07 [#]	0.34	27.78
Petunidin -6 -acetyl- 3-galactoside*	0.09	0.41	20.66
	0.15 [#]	0.73	19.23
	0 [#]	0.02	10.15

Table 3.12 – (continued).

Malvidin -3 -glucoside	9.10	22.48	44.09
	13.62 [#]	33.62	45.07
	1.47 [#]	3.62	47.79
Malvidin -3 -galactoside	17.72	43.75	39.40
Malvidin -3 -arabinoside	13.81	34.10	41.41
Malvidin -6 -acetyl- 3- glucoside	0.80	1.96	40.40
	2.20 [#]	5.43	46.96
	0.14 [#]	0.34	52.25
Malvidin -6 -acetyl- 3- galactoside*	0.18	0.46	44.20
	0.37 [#]	0.90	45.70
	0.02 [#]	0.05	47.45
Cyanidin -3 -glucoside	1.17	16.68	5.68
	1.9 [#]	27.06	6.30
	0.24 [#]	3.36	7.71
Cyanidin -3 -galactoside	3.29	46.77	7.32
Cyanidin -3 -arabinoside	2.33	33.05	6.97
Cyanidin -6 -acetyl- 3- glucoside	0.20	2.89	10.34
	0.60 [#]	8.54	12.83
	0.03 [#]	0.42	11.19
Cyanidin -6 -acetyl- 3- galactoside*	0.04	0.61	10.36
	0.09 [#]	1.31	11.54
	0 [#]	0.05	8.16
Peonidin -3 -glucoside	0.92	20.18	4.45
	1.37 [#]	30.02	4.52
	0.04 [#]	0.91	1.35
Peonidin -3 -galactoside	2.31	50.66	5.12
Peonidin -3 -arabinoside	1.33	29.17	3.98

-Corresp. – abbreviation for corresponding

- indicates the separate distribution analyses for either binomial or severe right-tail skewed distributions

3.4.2.3. Anthocyanins (DAD) Correlations

Correlations between total anthocyanins and the summation groups for the anthocyanidins or total sugar moieties are shown in Figure 3.20 as sections A or B, respectively. When correlating total anthocyanins and anthocyanidins, there is a strong, positive correlation with the delphinidin derivative anthocyanidins, with petunidin showing the best correlation ($R^2 = 0.934$) (Figure 3.20). The cyanidin anthocyanidin showed no correlation with total anthocyanins. The correlation between total anthocyanins and total glucosides shows a distinctive “2-group” pattern that can be

separated into two correlations (Figure 3.20). One correlation, indicated with the red line, shows both total anthocyanins and total glucosides increasing ($R^2 = 0.781$). The other correlation, indicated with the green line, shows total anthocyanins increasing while there is very little to no change in the total glucoside accumulation ($R^2 = 0.435$). The correlation between total anthocyanins and total galactosides shows an overall positive correlation ($R^2 = 0.468$), but shows a distinctive split into two branches (Figure 3.20). This narrow split pattern reveals one correlation showing total anthocyanins is increasing twice as fast as total galactosides ($R^2 = 0.877$), whereas the other correlation shows total anthocyanins and total galactosides increasing more proportionally ($R^2 = 0.986$). Total anthocyanins show a strong correlation with total arabinosides ($R^2 = 0.607$) (Figure 3.20). When glucosides and acetyl-glucosides are summed together to account for all glucosides present, the correlation with total anthocyanins shows the similar “2-group” pattern ($R^2 = 0.864$ and 0.270) (Figure 3.20). When galactosides and arabinosides are summed together to account for sugars other than glucosides, the correlation with total anthocyanins shows the similar narrow, split pattern, but with even tighter branches ($R^2 = 0.924$ and 0.997) (Figure 3.20).

The correlations between the anthocyanin sugar moieties provides more information on the relationship between different anthocyanins. The DAD-anthocyanin sugar moiety correlations for the total summation groups are shown in Figure 3.21, and are very representative of the correlation patterns seen when comparing the individual anthocyanins. Total glucosides exhibit the “2-group” pattern when correlated with total galactosides (Figure 3.21). One correlation, red line, shows both glucosides and galactosides increasing almost proportionally ($R^2 = 0.619$), whereas the other correlation, green line, shows only galactosides increasing with no accumulation change for glucosides ($R^2 = 0.218$). A very similar “2-group” pattern is seen when total glucosides is correlated with total arabinosides ($R^2 = 0.514$ and 0.195) (Figure 3.21). Total galactoside and total arabinoside show a strong positive correlation ($R^2 = 0.789$) (Figure 3.21). The correlation between glucosides-acetyl-glucosides and galactosides-arabinosides shows again the “2-group” pattern ($R^2 = 0.627$ and 0.220) (Figure 3.21).

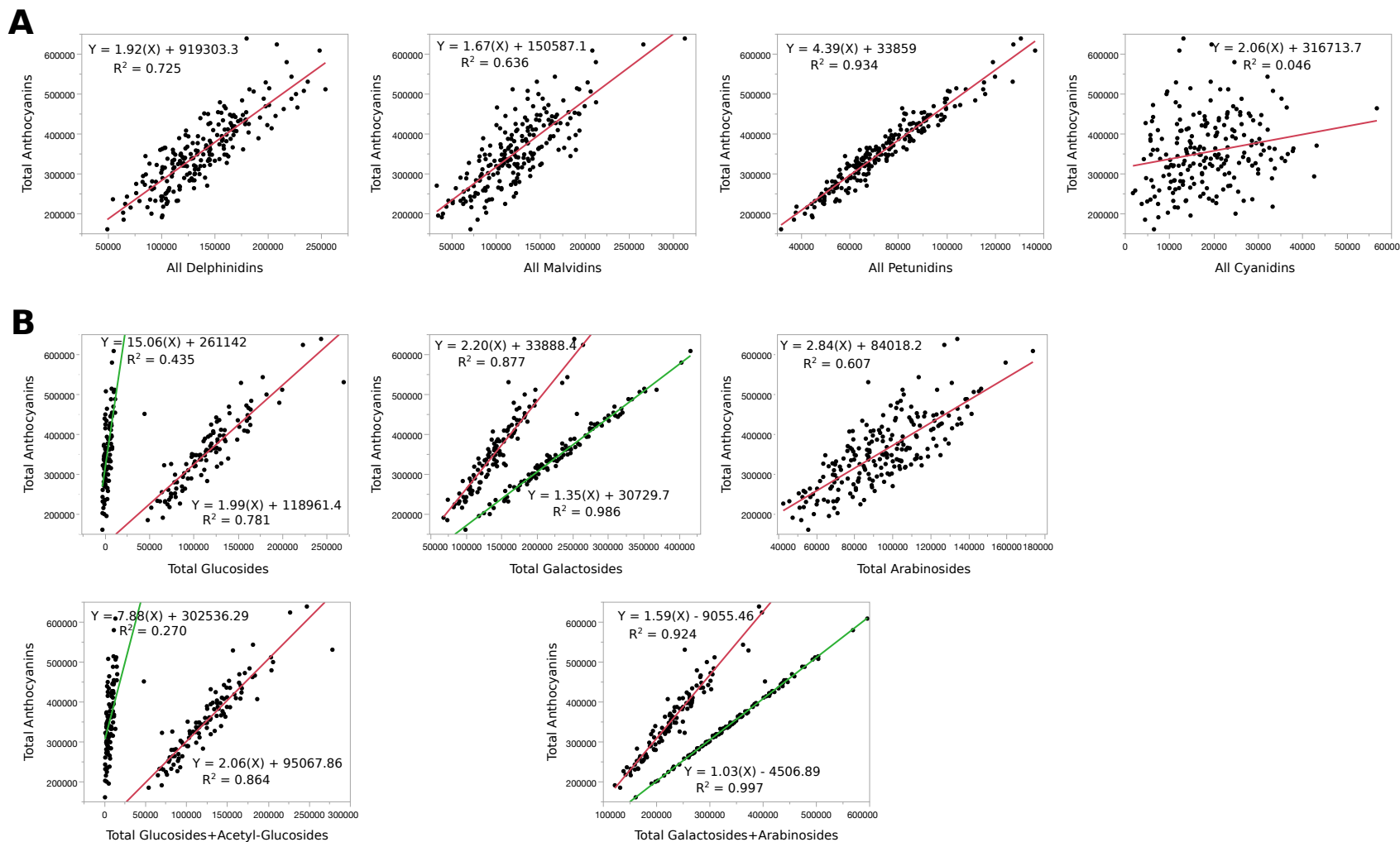


Figure 3.20 – Correlations showing the relationships between the DAD detected total anthocyanins and anthocyanidin summations (Section A) or sugar moiety summations (Section B). The equations for the best fit lines (red and green lines) and corresponding R² values are within each of the corresponding correlations.

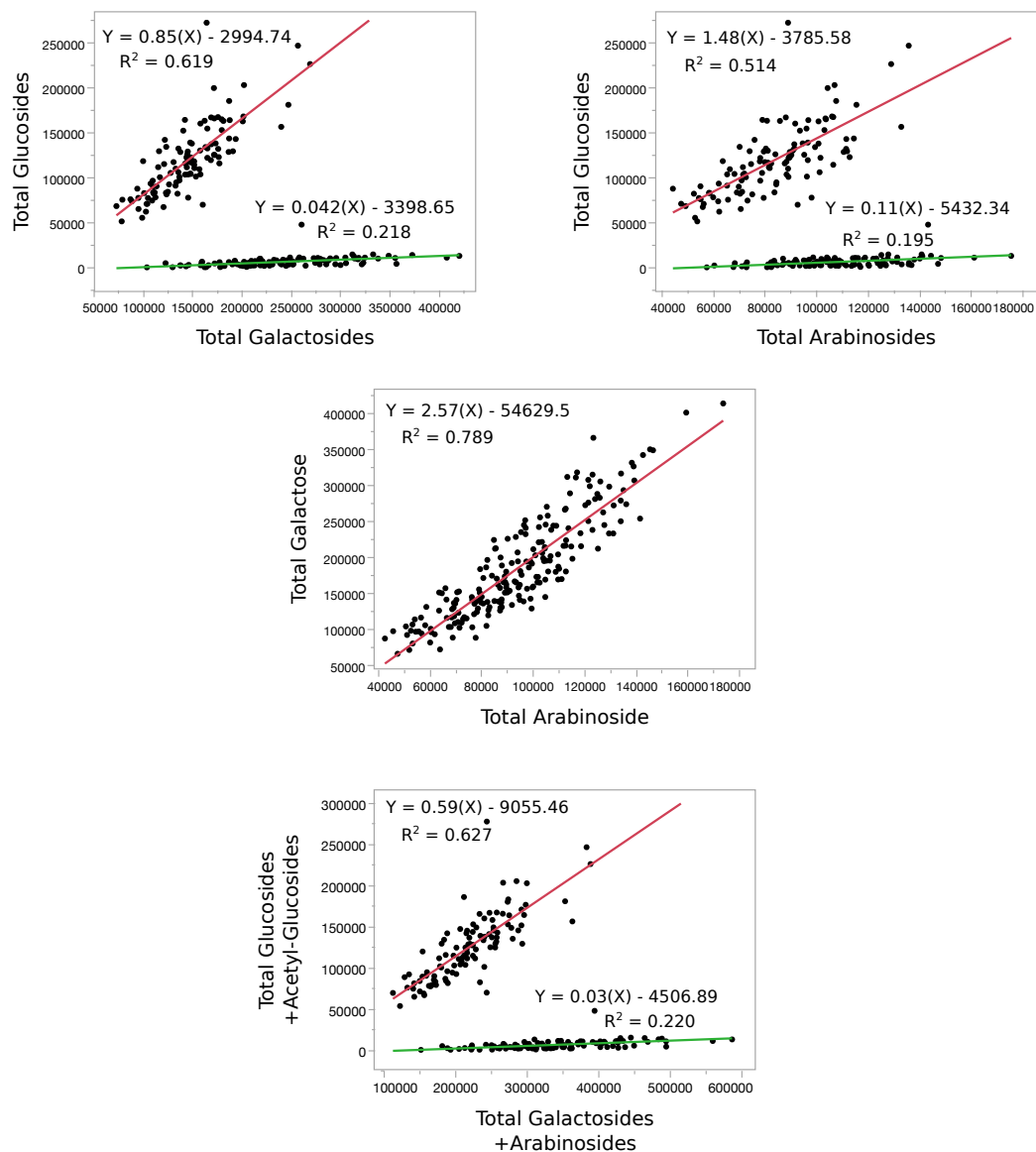


Figure 3.21 – Correlations showing the relationships between the DAD detected total sugar moiety summations. The equations for the best fit lines (red and green lines) and corresponding R^2 values are within each of the corresponding correlations.

Hierarchical clustering of the individual DAD-anthocyanins shows the population grouping into 14 clusters while the anthocyanins show four clusters based on maximum likelihood and distance (Figure 3.22). Anthocyanin cluster A includes delphinidin derivative galactosides and arabinosides, which supports the strong correlation between delphinidin derivative anthocyanidins as well as between galactosides and arabinosides. Anthocyanin cluster B includes cyanidin-galactoside, cyanidin-

arabinoxide, and peonidin-galactoside, which supports the strong correlation between cyanidin derivative anthocyanidins and further supports the correlation between galactosides and arabinosides. Anthocyanin cluster C consists of all the glucosides, and anthocyanin cluster D consists of acetyl-glucosides, which supports the separation of glucosides from galactosides and arabinosides.

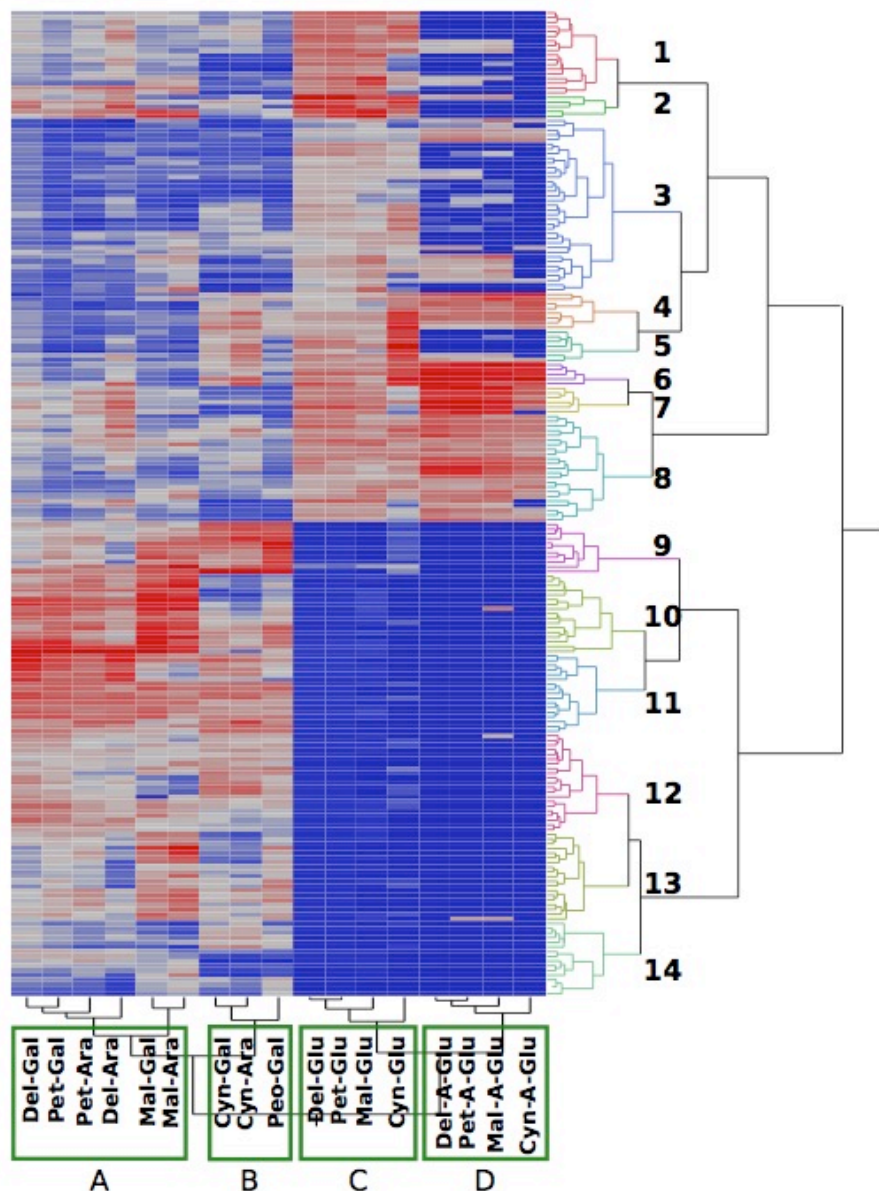


Figure 3.22 – Hierarchical clustering of the 17 individual DAD detected anthocyanins. The dendrogram on the right shows the relationship within the DxJ population that clusters into 14 clusters. The clustering on the bottom (A through D) shows the relationship within the population between the individual anthocyanins.

3.4.2.4. Anthocyanins (EIC) Correlations

The correlations between total anthocyanins and the summation groups of the anthocyanidins and total sugar moieties are shown in Figures 3.23 and 3.24, respectively. The delphinidin derivative anthocyanidins shows strong positive correlations with total anthocyanins, with the petunidin anthocyanidin showing the strongest correlation ($R^2 = 0.960$ and 0.756 , respectively) (Figure 3.23). The cyanidin and peonidin anthocyanidins show weak, positive correlations with total anthocyanins ($R^2 = 0.272$ and 0.214 , respectively).

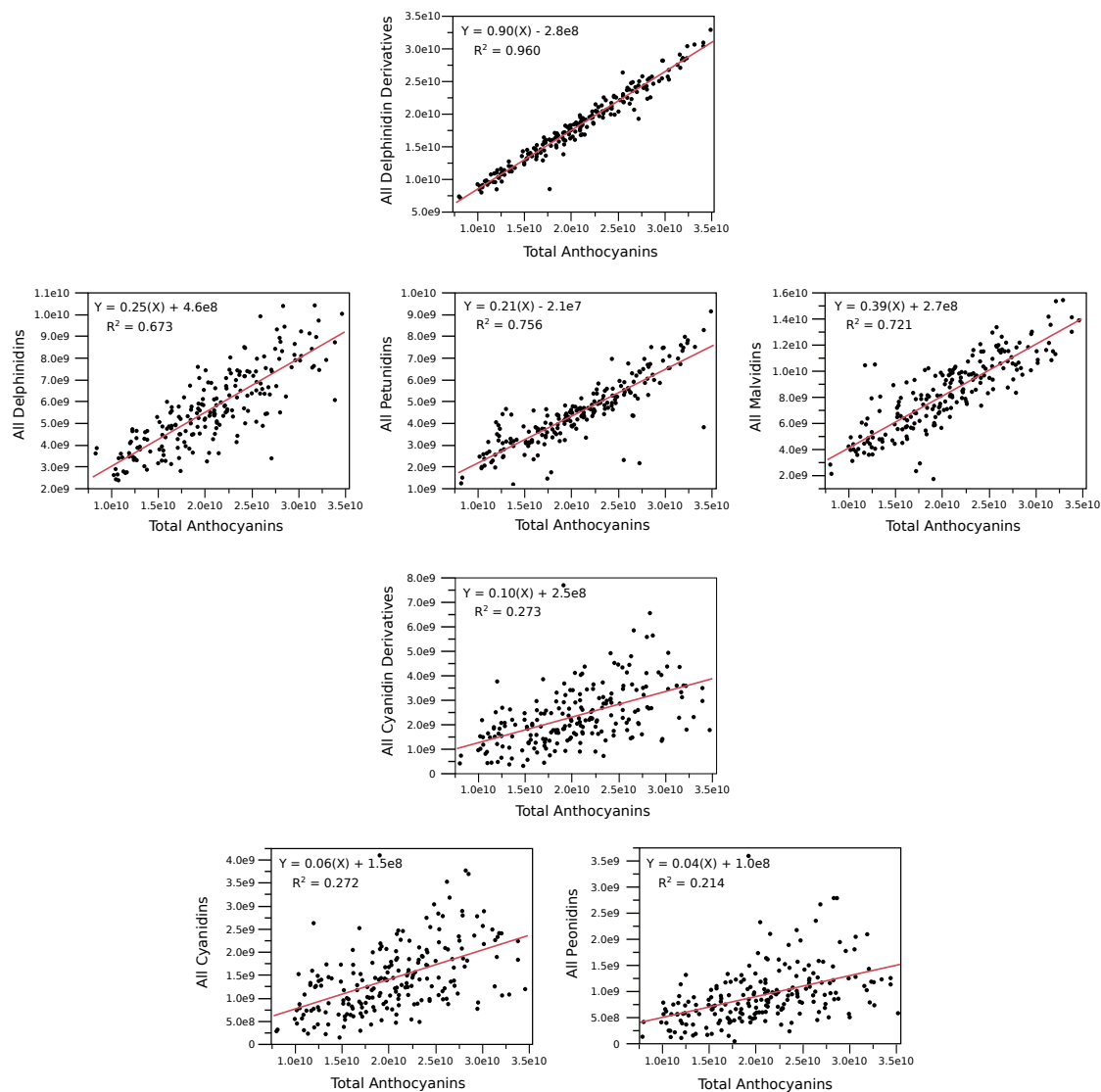


Figure 3.23 – Correlations showing the relationships between the EIC detected total anthocyanins and anthocyanidin summations. The equation for the best fit line (red line) and corresponding R^2 value is within each of the corresponding correlations.

The correlations between total anthocyanins and total glucosides, as well as total acetyl-glucoside and their summation together, shows the distinctive “2-group” pattern (Figure 3.24). One correlation shows both total anthocyanins and total glucosides increasing at a proportional one-third rate ($R^2 = 0.722$). The other correlation shows total anthocyanins increasing while there is very little to no change in the total glucoside accumulation ($R^2 = 0.162$). The correlation between total anthocyanins and total galactosides shows an overall positive correlation ($R^2 = 0.520$), but does show the narrow two-split pattern. Unfortunately, the narrow two split pattern could not be separated into two distinctive split into two branches. Total anthocyanin shows no correlation with total acetyl-galactosides. There is a positive correlation seen between total anthocyanins and total arabinoside ($R^2 = 0.604$). Total anthocyanins show the narrow two-split pattern when correlated with total galactosides and acetyl-galactosides ($R^2 = 0.525$). When arabinosides are added to galactosides and acetyl-galactosides, they correlate with total anthocyanins strongly and show a narrow and distinct split ($R^2 = 0.973$ and 0.927).

The correlations between the total sugar moieties from the EIC anthocyanins are shown in Figure 3.25. A strong, distinct “2-group” pattern is also seen when correlating total glucosides with total galactosides, and total glucosides with total arabinosides. There is also a good positive correlation between total galactoside and total arabinoside ($R^2 = 0.694$). A very strong “2-group” pattern is also seen when correlating total acetyl-glucosides and total acetyl-galactosides, as well as total glucosides with total acetyl-glucosides and total galactoside with total acetyl-galactoside and total arabinoside.

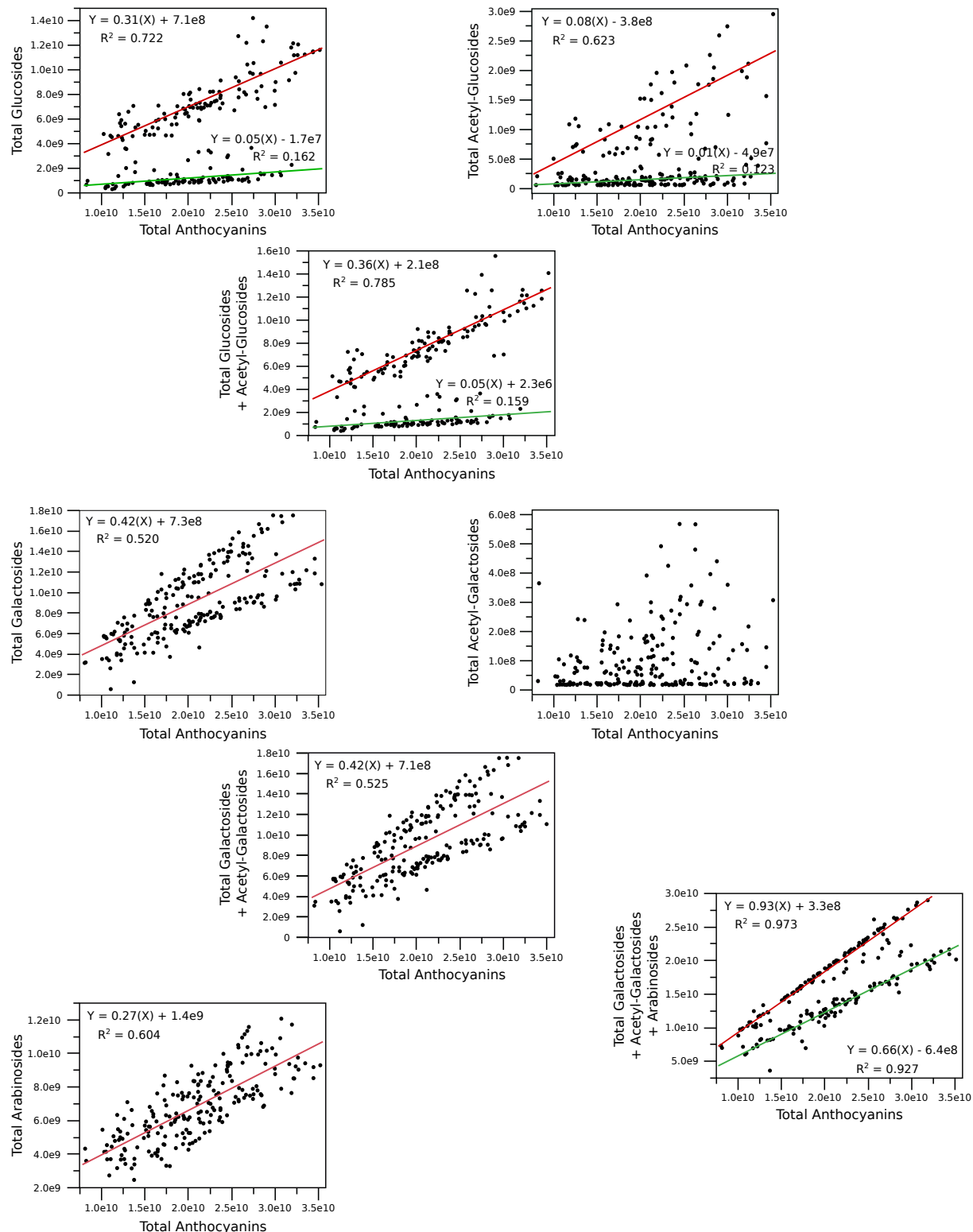


Figure 3.24 – Correlations showing the relationships between the EIC detected total anthocyanins and sugar moiety summations. The equations for the best fit lines (red and green lines) and corresponding R^2 values are within each of the corresponding correlations.

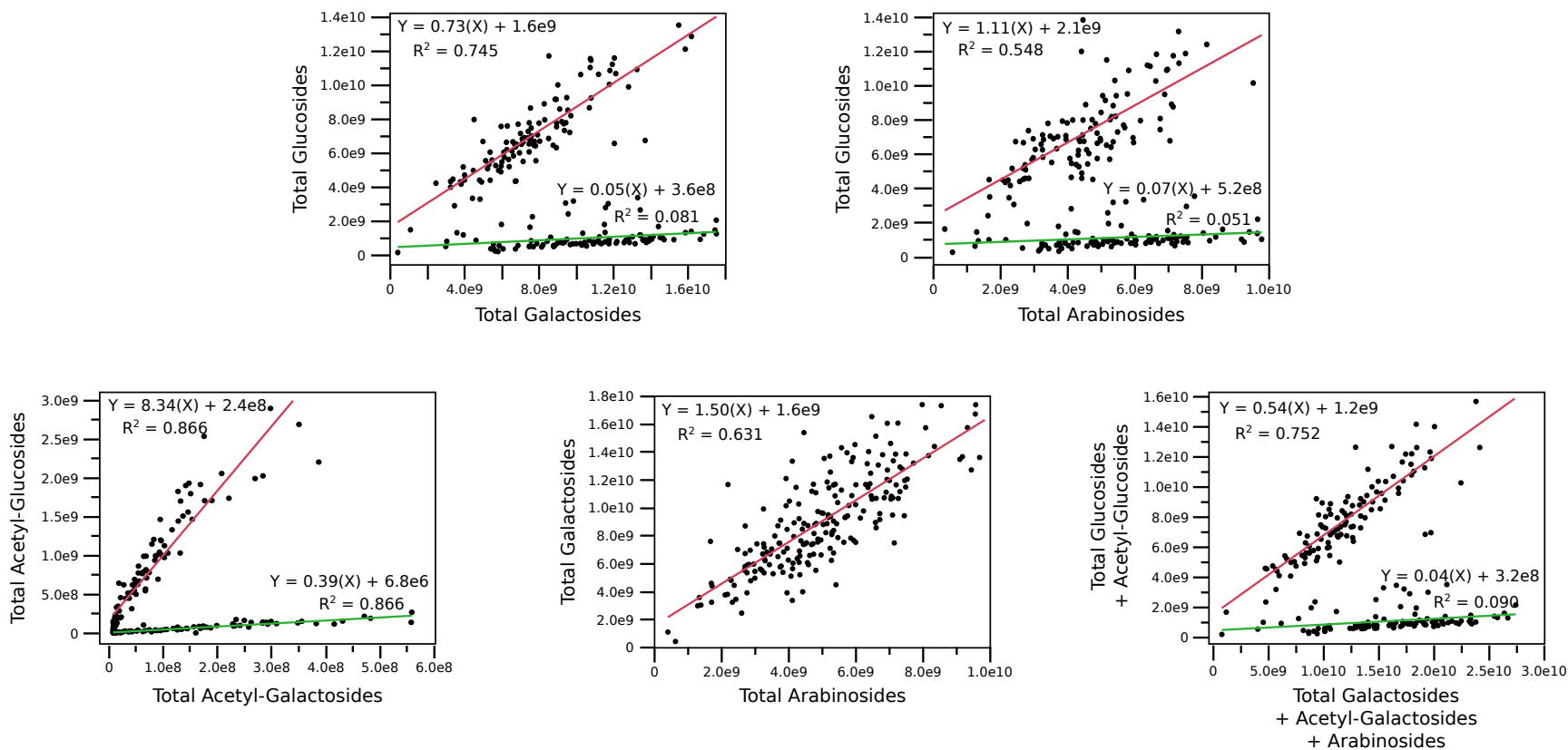


Figure 3.25 – Correlations showing the relationships between the EIC detected sugar moiety summations. The equations for the best fit lines (red and green lines) and corresponding R^2 values are within each of the corresponding correlations.

Hierarchical clustering of the 23 EIC anthocyanins show the population also grouping into 14 clusters while the anthocyanins form five clusters based on maximum likelihood and distance (Figure 3.26). Anthocyanin cluster A include cyanidin derivative galactosides and arabinosides, further supporting the strong correlations between cyanidin derivative anthocyanidins. Anthocyanin cluster B consists of the delphinidin derivative galactosides and arabinosides, which supports the strong correlation between delphinidin derivative anthocyanidins. Both cluster A and B further support the correlation between galactosides and arabinosides. Cluster C consists of all the acetyl-galactosides, which suggests some distinction from galactosides but not similar to acetyl-glucosides. Anthocyanin cluster D consists of all the glucosides with cyanidin and peonidin clustering separately from delphinidin derivative glucosides. This supports the distinctive separation of glucosides from the other anthocyanins as well as anthocyanidins. Anthocyanin cluster E consists of all the acetyl-glucosides.

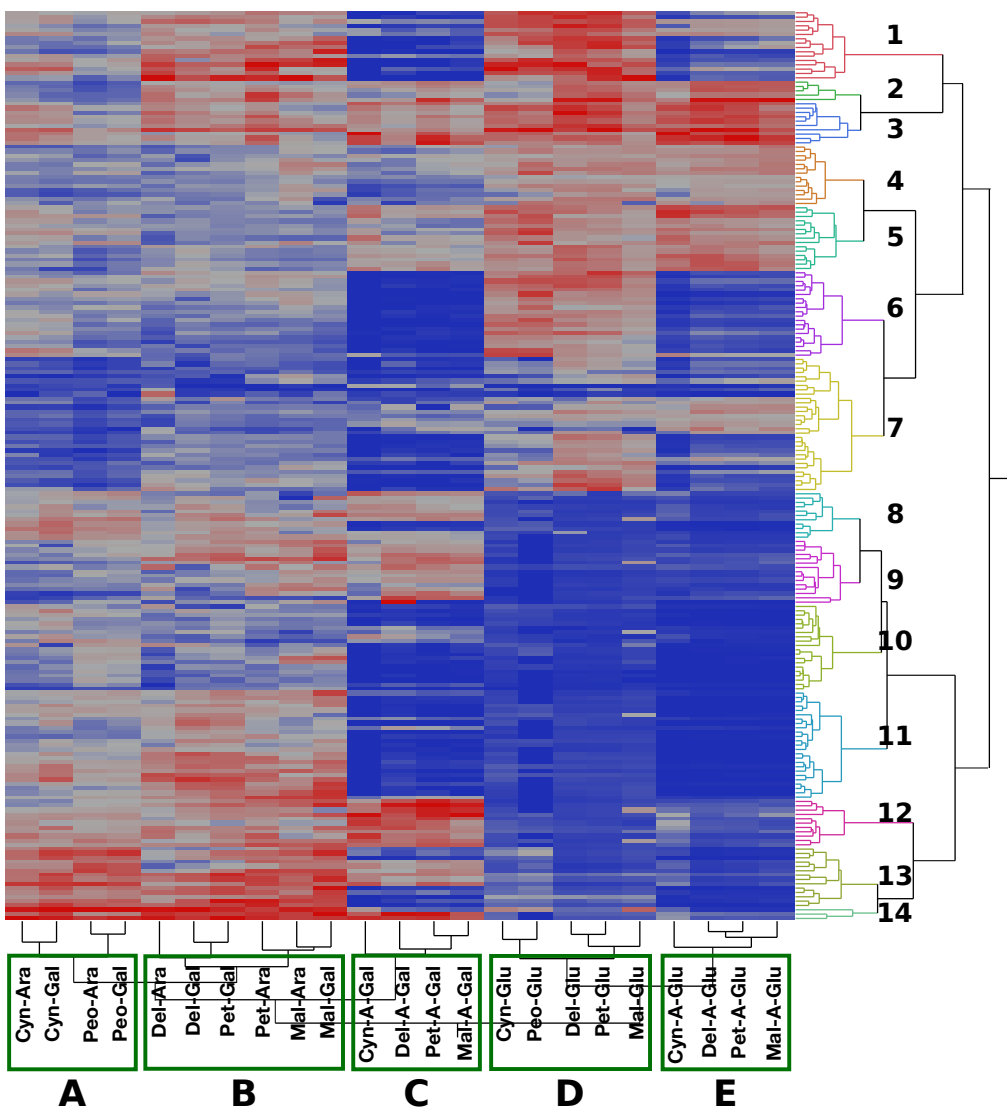


Figure 3.26 – Hierarchical clustering of the 23 individual EIC detected anthocyanins. The dendrogram on the right shows the relationship within the DxJ population that clusters into 14 clusters. The clustering on the bottom (A through E) shows the relationship within the population between the individual anthocyanins.

3.4.2.5. Anthocyanin Detection Comparison Correlations

The similar distribution and correlation patterns suggest a good correlation between the DAD annotated and EIC annotated anthocyanins (Figures 3.27, 3.28, 3.29, 3.30, and 3.31). Both total anthocyanins and all delphinidin derivatives show a weak positive correlation ($R^2 = 0.333$ and 0.353 , respectively) (Figure 3.27). All cyanidin derivatives exhibit a positive correlation ($R^2 = 0.507$). Total glucosides, total acetyl-

glucosides, and total glucosides +acetyl-glucosides show strong positive correlations ($R^2 = 0.780, 0.836,$ and $0.785,$ respectively). Both total galactosides and arabinosides correlations show a weak positive correlation ($R^2 = 0.407$ and $0.317,$ respectively). The individual anthocyanin correlations and anthocyanidin correlations are grouped together by anthocyanidin core with delphinidins shown in Figure 3.28, petunidins shown in Figure 3.29, malvidins shown in Figure 3.30, and cyanidins and peonidins shown in Figure 3.31. Overall, the cyanidin anthocyanidins exhibit the strongest and best correlations between DAD and EIC detection methods (Figure 3.31). The individual anthocyanin correlations also show that the glucosides and acetyl-glucosides exhibit the best and strongest correlations.

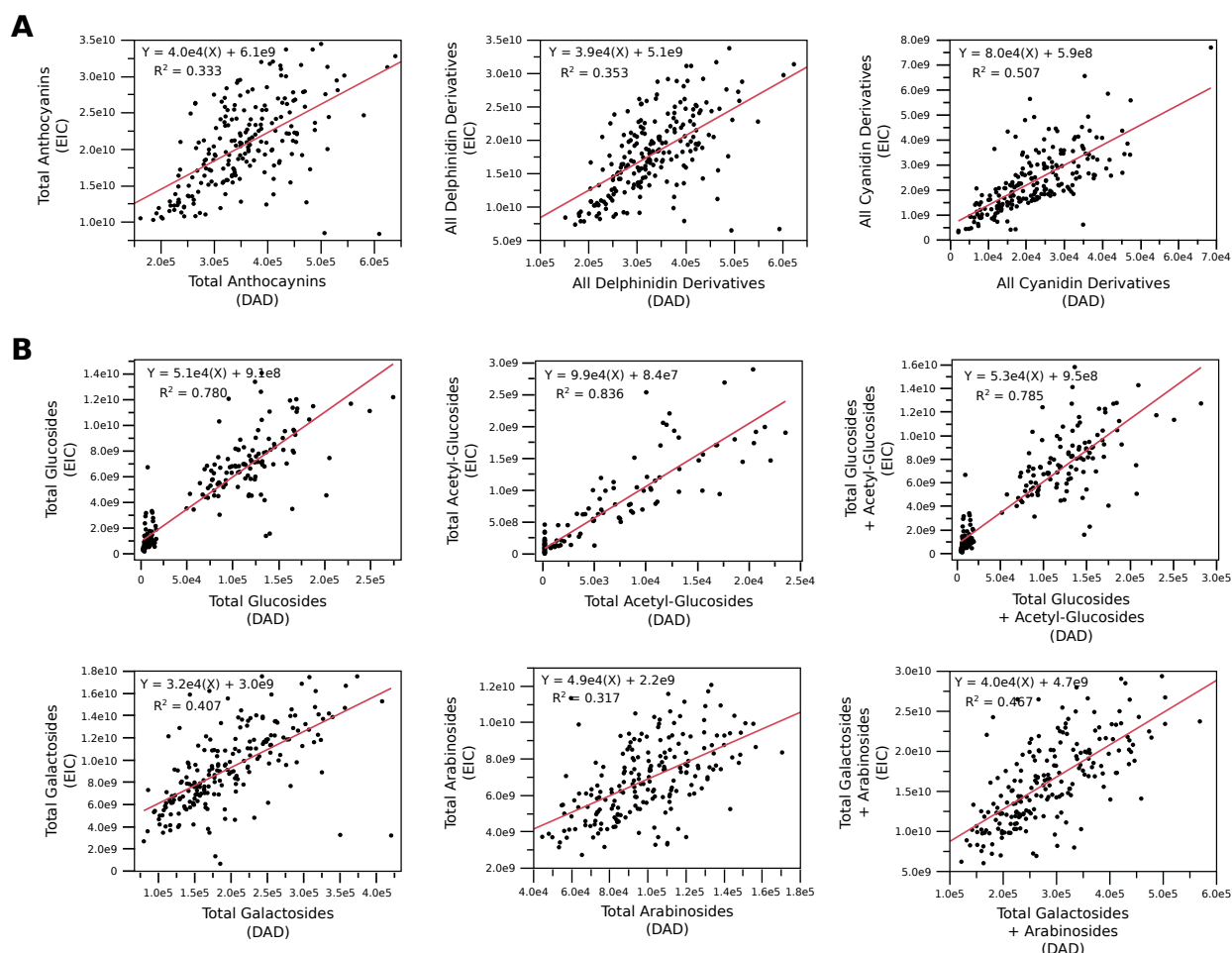


Figure 3.27 – Correlations showing the relationships between DAD and EIC detection for the large anthocyanidin summation groups, (Section A) and sugar moiety summation groups (Section B). The equation for the best fit line (red line) and corresponding R^2 value is within each of the corresponding correlations.

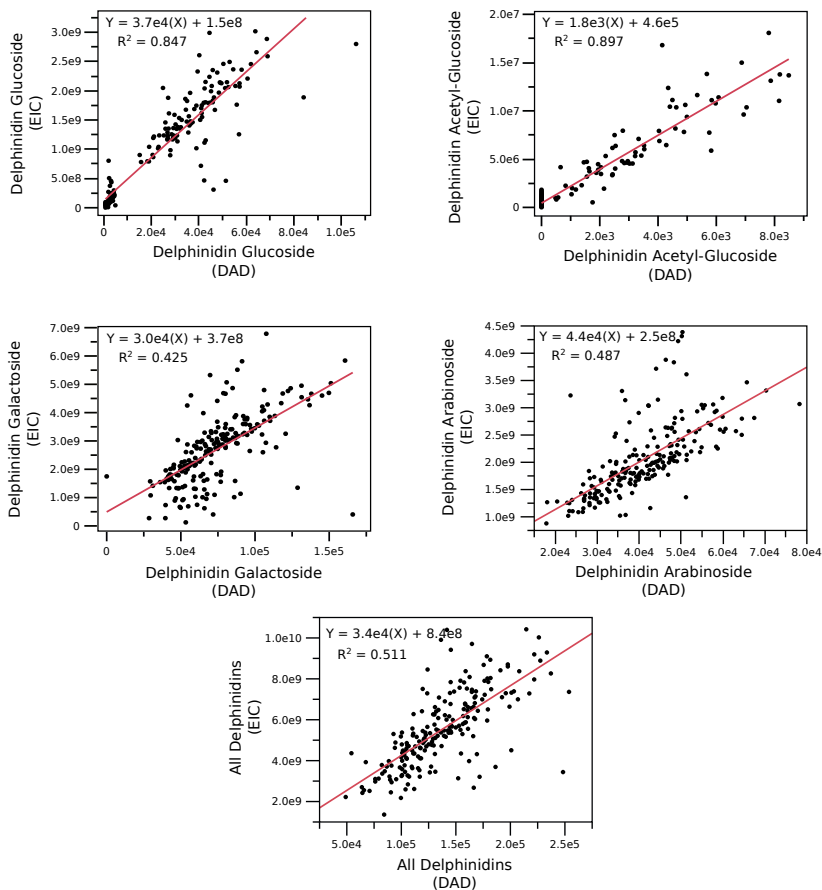


Figure 3.28 – Correlations showing the relationships between the delphinidin anthocyanins detected by either DAD or EIC. The equation for the best fit line (red line) and corresponding R^2 value is within each of the corresponding correlations.

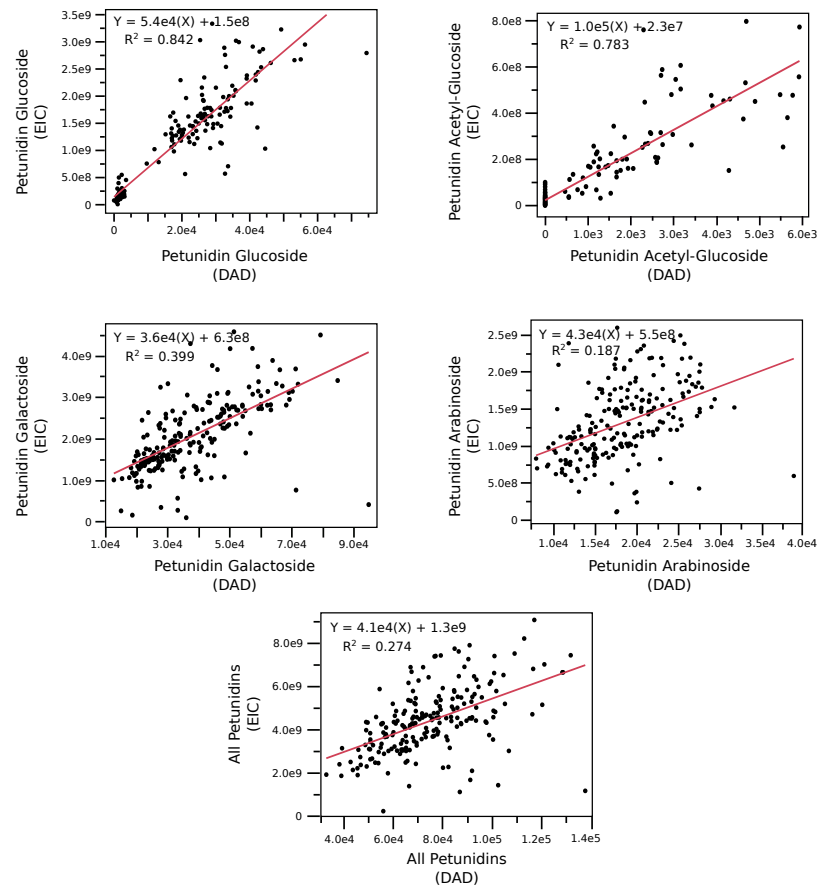


Figure 3.29 – Correlations showing the relationships between the petunidin anthocyanins detected by either DAD or EIC. The equation for the best fit line (red line) and corresponding R^2 value is within each of the corresponding correlations.

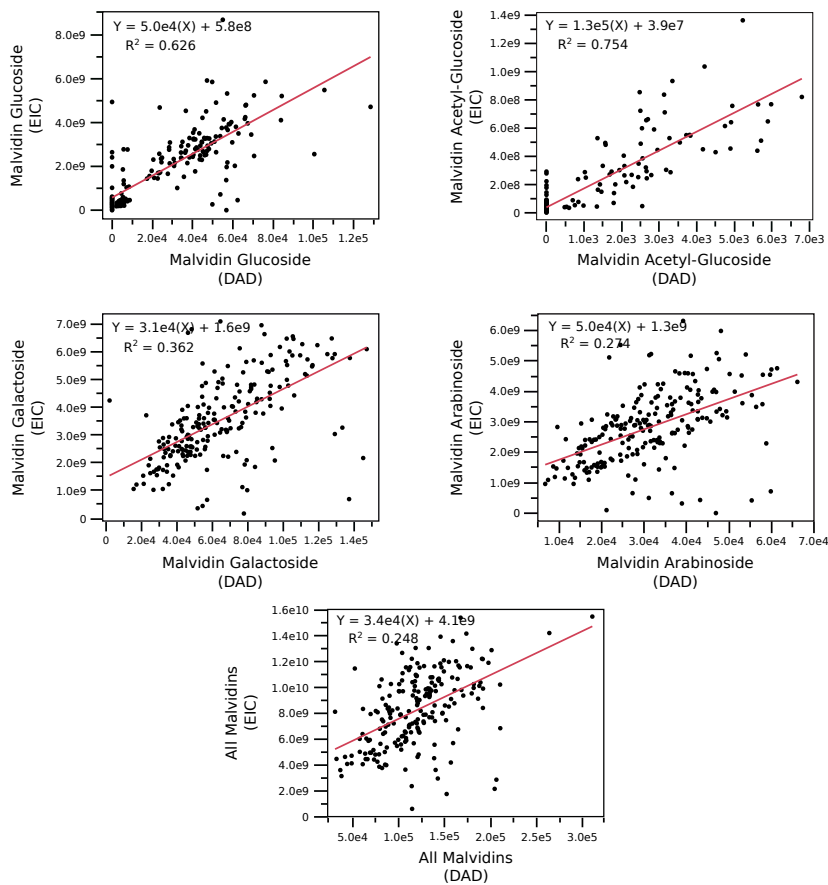


Figure 3.30 – Correlations showing the relationships between the malvidin anthocyanins detected by either DAD or EIC. The equation for the best fit line (red line) and corresponding R^2 value is within each of the corresponding correlations.

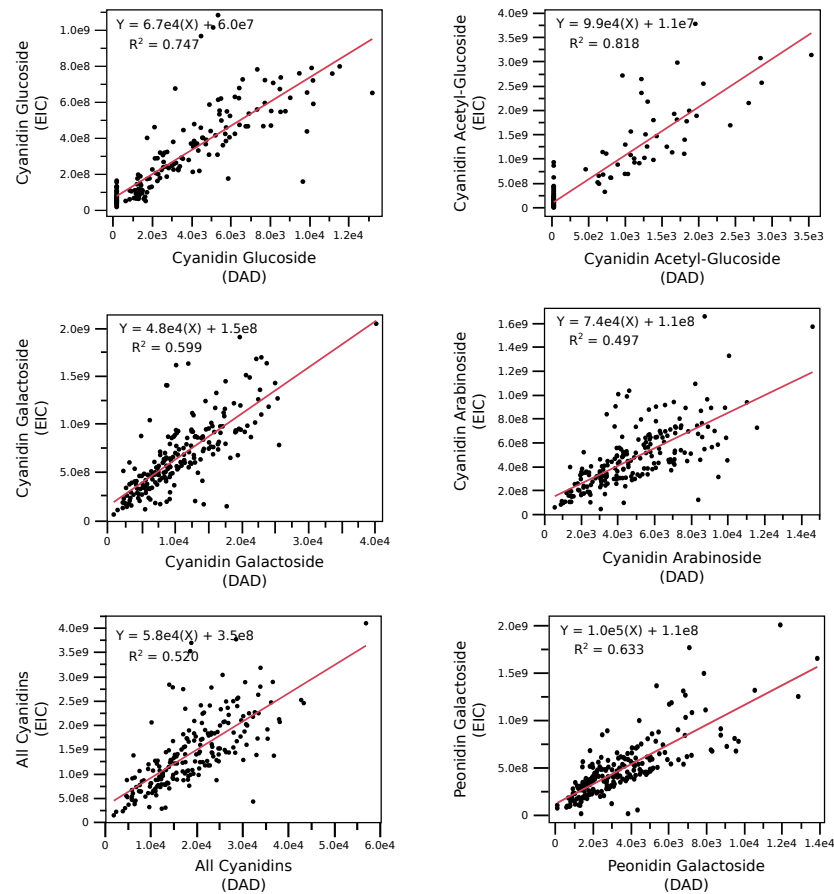


Figure 3.31 – Correlations showing the relationships between the cyanidin and peonidin anthocyanins detected by either DAD or EIC. The equation for the best fit line (red line) and corresponding R^2 value is within each of the corresponding correlations.

3.4.3. Antioxidant Capacity through DPPH Scavenging Assay

The blueberry extracts for both years were analyzed with the DPPH scavenging assay to estimate the antioxidant capacity of the extracts. The final trolox standard curve was an average of 108 individual standard curves. The best fit line equation utilized to calculate the Trolox equivalence values, termed DPPH-antioxidant capacity for thesis, was: $Y = 0.1417(\text{DPPH}) + 3.9551$ with an $R^2 = 0.9791$. The phenotypic summary for each year as well as both years combined are shown in Table 3.13. The distributions for the three DPPH phenotypes are show left-tailed skewing (Figure 3.32).

Table 3.13 – Summary data for DPPH antioxidant capacity assay for two years.

DPPH	Mean	Standard Error Mean	Draper	Jewel
Year 1	521.18	2.78	534.06	529.73
Year 2	534.34	3.12	512.38	561.24
Both Years	527.42	2.11	-	-

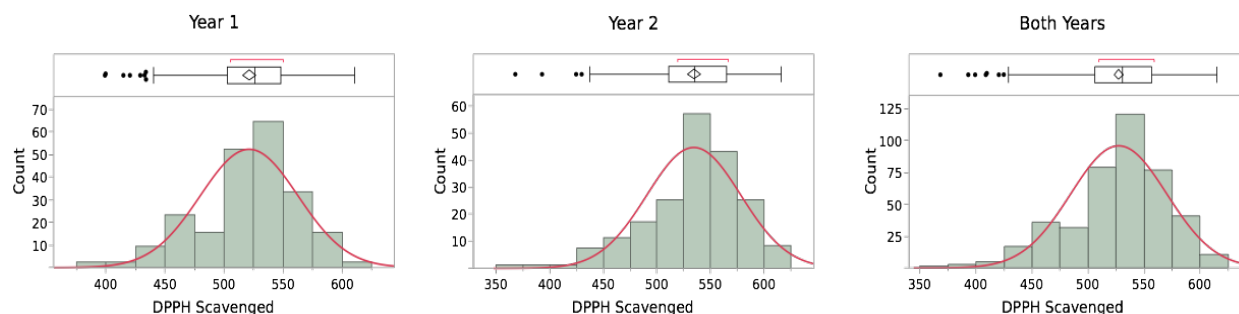


Figure 3.32 – Distribution histograms for DPPH-antioxidant capacity for two years as well as both years merged together. The red line indicates a normal distribution. The box plot shows the mean, quartiles, and interquartile range, as well as possible outliers as dots.

The DPPH results reveal a strong, positive correlation with DAD-total anthocyanin content ($R^2=0.791$) (Figure 3.33). The anthocyanidin, petunidin, shows the strongest, positive correlation with DPPH ($R^2 = 0.730$), whereas delphinidin shows only a good correlation ($R^2 = 0.556$) (Figure 3.33). Delphinidin-arabinoside exhibits the strongest correlation with DPPH when compared to each anthocyanin ($R^2 = 0.507$) (Figure 3.33). Petunidin-glucoside shows the most distinct “2-group” pattern when

compared the other individual anthocyanins ($R^2 = 0.614$ and 0.189) (Figure 3.33). Total glucosides and total acetyl-glucosides both show good, distinct “2-group” patterns when correlated with DPPH (Figure 3.33). Total arabinoside exhibits the strongest, positive correlation with DPPH ($R^2 = 0.551$), whereas total glucosides and total galactoside, arabinoside, and their summation show a weak positive correlation ($R^2 = 0.462$, 0.551 , and 0.506 respectively), due to the split pattern (Figure 3.33).

The EIC anthocyanins overall show weaker correlations with DPPH than the DAD detected anthocyanins. The EIC total anthocyanins exhibit a positive correlation with DPPH ($R^2 = 0.472$) (Figure 3.34). Of the anthocyanidin summation groups, all delphinidins showed the best correlation with DPPH ($R^2 = 0.450$) (Figure 3.34). The best individual anthocyanin correlation with DPPH is delphinidin-arabinoside ($R^2 = 0.364$) (Figure 3.34). Of the sugar moiety summation groups, total galactosides showed the best correlation with DPPH ($R^2 = 0.417$), while total galactosides + acetyl-galactosides + arabinosides shows a mediocre positive correlation with DPPH ($R^2 = 0.360$) (Figure 3.34).

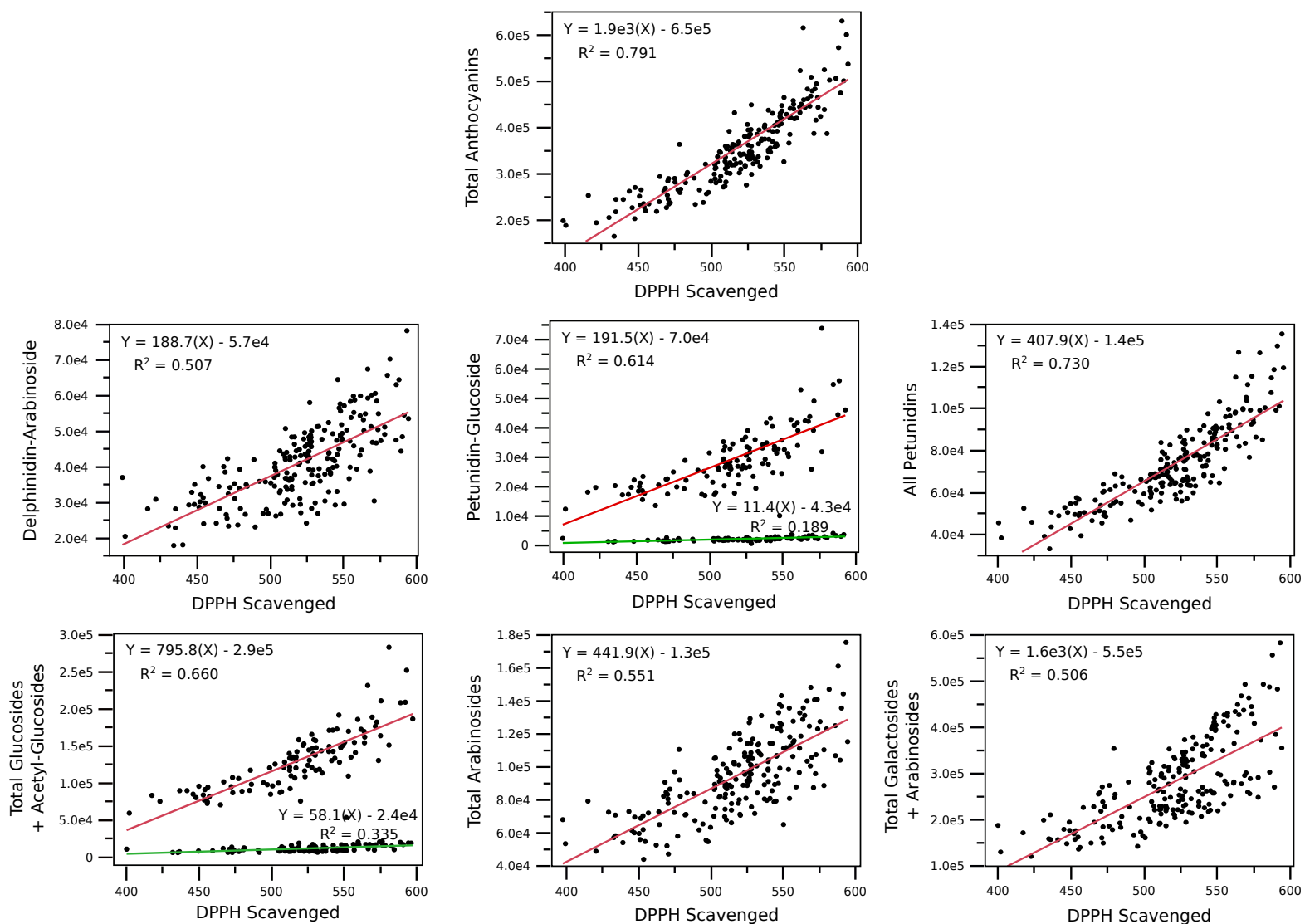


Figure 3.33 – Correlations showing the relationships between DPPH-antioxidant capacity and different summation groups or individual anthocyanins detected using DAD. Poor or no correlations are not shown. The equations for the best fit lines (red and green lines) and corresponding R² values are within each of the corresponding correlation.

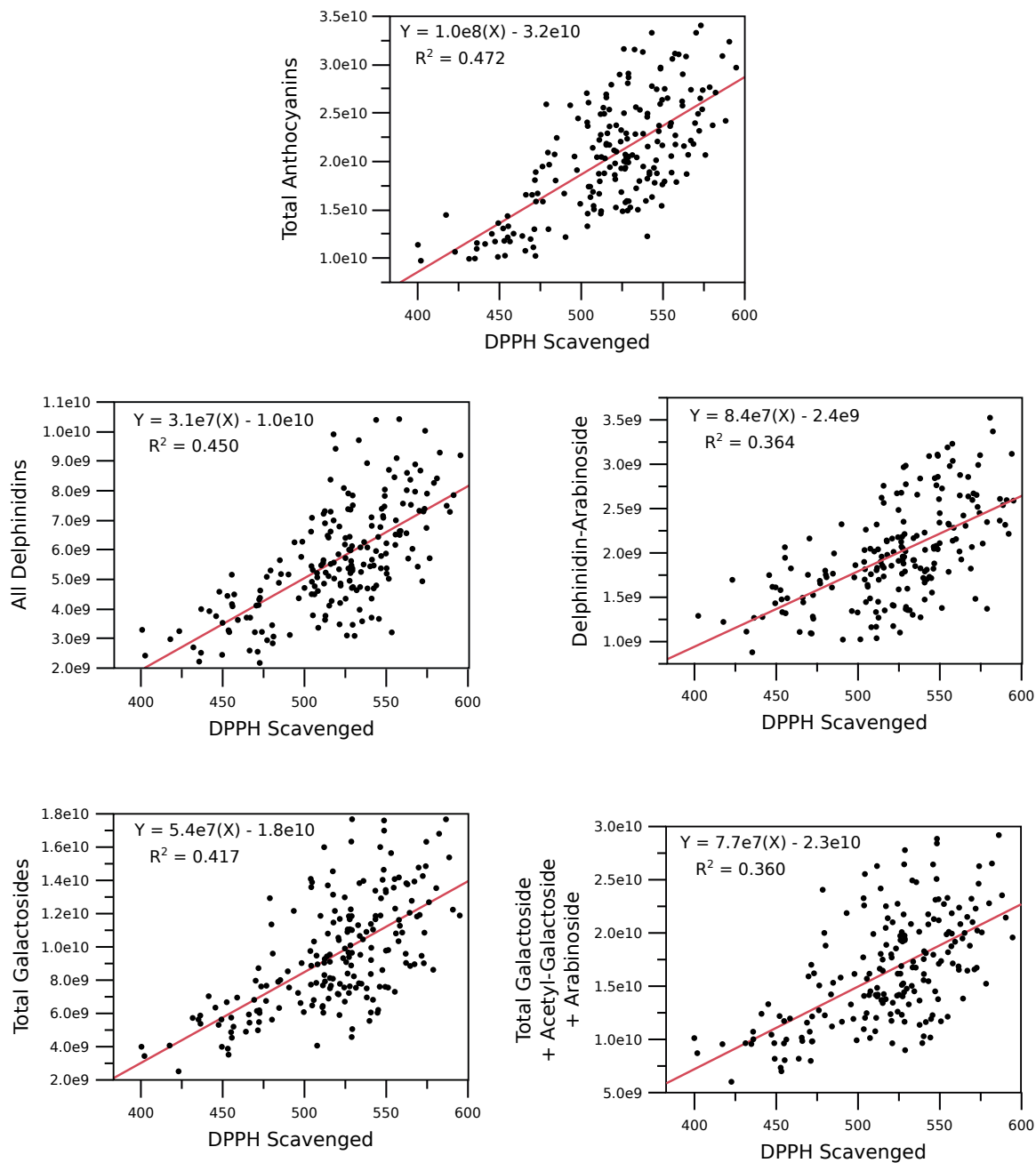


Figure 3.34 – Correlations showing the relationships between DPPH-antioxidant capacity and different summation groups or individual anthocyanins detected using EIC. Poor or no correlations are not shown. The equations for the best fit lines (red line) and corresponding R^2 values are within each of the corresponding correlations.

The DPPH results also show a positive correlation with select phenolic acids from ^1H NMR annotated metabolite features (Figure 3.35). Epicatechin and gallic acid show positive correlations with DPPH ($R^2 = 0.459$ and 0.455 , respectively) (Figure 3.35). Chlorogenic acid shows a weak, positive correlation with DPPH ($R^2 = 0.363$) (Figure 3.35).

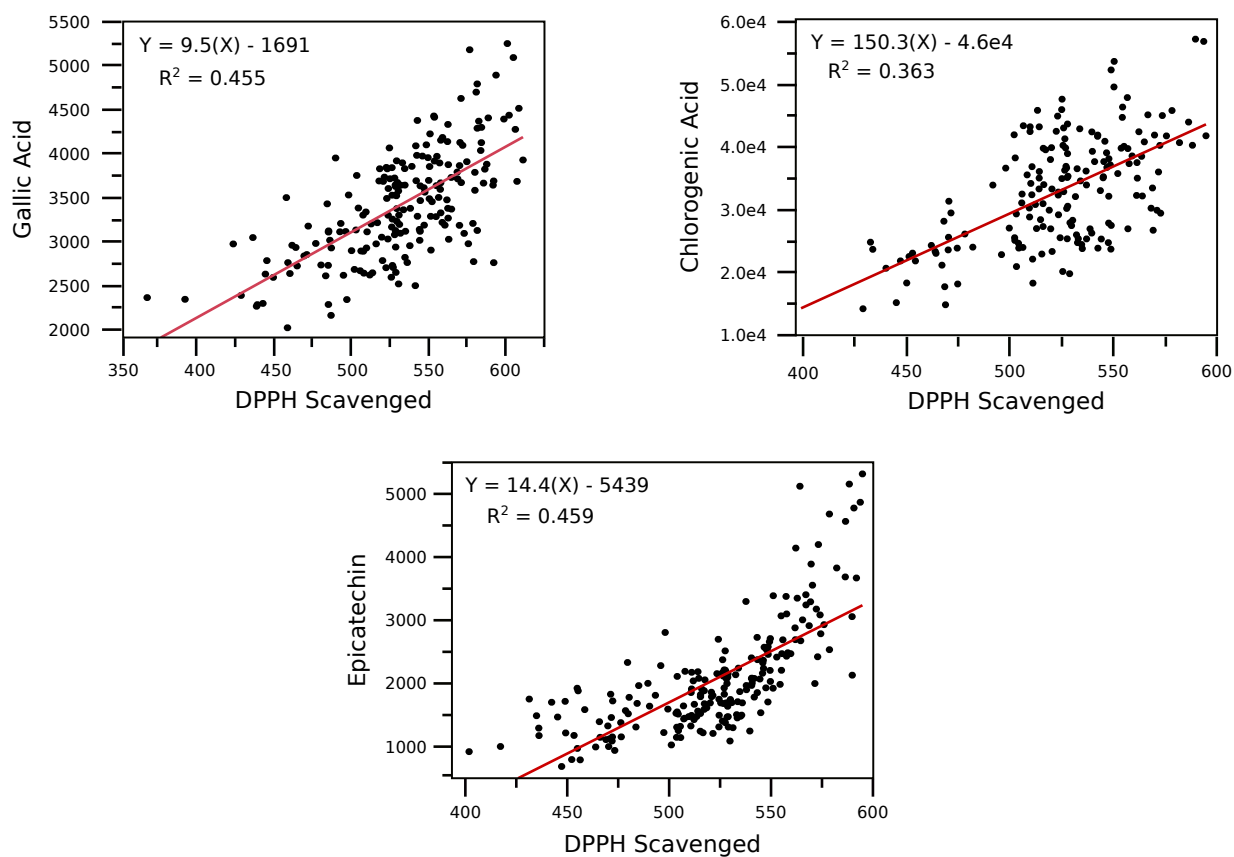


Figure 3.35 – Correlations showing the relationships between DPPH-antioxidant capacity and phenolic acids from the non-targeted profiling on ^1H NMR. Poor or no correlations are not shown. The equations for the best fit lines (red and green lines) and corresponding R^2 values are within each of the corresponding correlations.

3.4.4. BiPAM QTLs from CIM analysis

3.4.4.1. ¹H NMR Known Metabolites

BiPAM was conducted for each of the known-annotated metabolites using IM and CIM. The two different years were initially QTL mapped separately due to the time gap between receiving each year's samples and conducting the metabolite profiling. The raw metabolite profiling data was merged together to create the final dataset and then also QTL mapped. The summation phenotypes utilized for correlations (total amino acids, total TCA acids, total glutamine branch, total aspartate branch, total branch-chain branch, total sugars, and total phenolic acids) were not QTL mapped since the summation does not represent all the metabolites within that specific pathway. The QTL regions were determined significant if the LOD value was above the LOD threshold of 3.0. If multiple markers and pseudo-markers were not separated by non-significant markers, they were collapsed into one single QTL region. The significant QTLs for year 1 and year 2 for the annotated metabolite peaks are summarized in Tables 3.14, 3.15, and 3.16. Merging the datasets for both years provided more replicates for each line, which improves the power of the QTL mapping. The significant QTLs for the merged year data are also summarized in Table 3.14, 3.15, and 3.16. It is the merged years significant QTLs that were utilized for further putative candidate gene analysis. Of the TCA acids and amino acids, succinic +others mapped to the most QTL regions, 13 in total (Table 3.14). GABA, valine, and isopropylmalic acid each mapped to 11 QTL regions (Table 3.14). Leucine mapped to the least number of QTLs, four in total (Table 3.14). Of the sugars and all the annotated metabolites, xylose mapped to a total of 21 QTL regions (Table 3.15). Sucrose mapped to the least number of QTLs, four in total (Table 3.15). Of the phenolic acids, quinic acid mapped to most QTL regions, 12, whereas gallic acid mapped to the least QTL regions, 4 in total (Table 3.16).

Table 3.14 – Summary of significant QTLs genome wide for TCA acids and amino acids from ¹H NMR non-targeted profiling.

TCA Acids & Amino Acids	Total QTLs (Year 1)	Total QTLs (Year 2)	Total QTLs (Merged Years)
Citric Acid	1	4	6
Succinic +others	-	4	13
Malic Acid	-	3	8
Glutamine	4	0	9
γ-Aminobutyric Acid (GABA)	-	1	11
Arginine	8	0	6
Isoleucine	7	4	7
Valine	5	3	11
Isopropylmalic Acid	-	5	11
Leucine	6	3	4
Aspartate	-	3	5
Asparagine	-	5	7
Threonine	2	1	9
Alanine	10	5	9

Table 3.15 – Summary of significant QTLs genome wide for individual sugars from ¹H NMR non-targeted profiling.

Sugars	Total QTLs (Year 1)	Total QTLs (Year 2)	Total QTLs (Merged Years)
Fructose	4	4	5
Glucose	3	4	5
Galactose	-	0	7
Xylose	-	14	21
Arabinose +others	-	0	12
Other sugars (galactose, xylose)	-	2	9
Sucrose	1	7	4
Maltose	-	1	13
Maltitol	-	0	12

Table 3.16 – Summary of significant QTLs genome wide for phenolic acids from ¹H NMR non-targeted profiling.

Phenolic Acids	Total QTLs (Year 1)	Total QTLs (Year 2)	Total QTLs (Merged Years)
Gallic Acid	-	0	5
Quinic Acid	7	11	12
Chlorogenic Acid	8	7	10
Caffeic Acid +others	-	1	7
Epicatechin	10	-	10
Ascorbic +others	-	3	11

3.4.4.2. Anthocyanin (DAD) Metabolites and DPPH-Antioxidant Capacity

The anthocyanin metabolites annotated using the DAD detector were utilized for QTL mapping because the DAD-anthocyanin data is cleaner and shows cleaner correlations with other metabolites and DPPH-antioxidant capacity. The significant QTL regions for the anthocyanins are summarized in Table 3.17. Cyanidin acetyl-glucoside mapped to 12 QTL regions. The acetyl-glucoside anthocyanins revealed eight significant QTL regions that overlapped for cyanidin acetyl-glucoside as well as two other delphinidin derivative acetyl-glucosides. The anthocyanin QTL mapping also revealed three QTL regions that showed overlap for only cyanidin derivative anthocyanins. Due to the distinctive “2-group” pattern seen in the anthocyanin correlations, the ratio between galactosides-arabinosides to glucosides-acetyl-glucosides were also mapped, which revealed eight significant QTL regions.

The composition of individual anthocyanins was also investigated through the development of and BiPAM mapping of different ratios of individual anthocyanins and summation groups. Ratios with total anthocyanins investigated overall composition, whereas ratios like delphinidin-glucoside to petunidin-glucoside investigated the anthocyanidin composition specificity. Overall, the acetyl-anthocyanins resulted in the most significant QTLs, therefore, specific ratios for acetyl-anthocyanins like total acetyl-glucosides to total glucosides were also BiPAM mapped. Since the sugar moiety correlations exhibited a distinctive “2-group” pattern, ratios between the different sugar moieties like total arabinosides + galactosides to total glucosides + acetyl-glucosides were also calculated and BiPAM mapped. Although there are many other ratios analyzed with BiPAM, only the ratios with significant QTLs are summarized in Table 3.18. A subset of significant QTLs for the individual anthocyanins, summation groups, and ratios that have overlapping genetic regions are reported in detail in Table 3.19.

The DPPH-antioxidant capacity assay was conducted for year 1 and year 2 extract samples, and were QTL mapped as separate phenotypes. Similar to ¹H NMR datasets, the two DPPH datasets were merged into a single dataset and also QTL mapped. When the two years were mapped separately, there were no significant QTLs found. With the merged DPPH dataset, there were two significant QTLs found and are discussed in more detail with the putative candidate gene section (Table 3.23).

Table 3.17 – Summary of significant QTLs genome wide for individual anthocyanins and summation groups from DAD-detection by HPLC-QTOFMS targeted profiling.

Anthocyanins (DAD)	Total QTLs
Delphinidin-3-galactoside	1
Delphinidin-3-glucoside	0
Cyanidin-3-galactoside	2
Delphinidin-3-arabinoside	0
Cyanidin-3-glucoside	7
Petunidin-3-galactoside	1
Cyanidin-3-arabinoside	3
Petunidin-3-glucoside	0
Peonidin-3-galactoside	2
Petunidin-3-arabinoside	0
Malvidin-3-galactoside	2
Malvidin-3-glucoside	1
Malvidin-3-arabinoside	0
Delphinidin-6-acetyl- 3-glucoside	9
Cyanidin-6-acetyl- 3-glucoside	12
Petunidin-6-acetyl- 3-glucoside	11
Malvidin-6-acetyl- 3-glucoside	5
Summation Groups	
Total Anthocyanins	1
All Delphinidins	1
All Malvidins	1
All Petunidins	1
All Delphinidin Derivatives	0
All Cyanidins	3
All Cyanidin Derivatives	1
Total Glucosides	0
Total Galactosides	0
Total Arabinosides	0
Total Acetyl-Glucosides	11

Table 3.18 – Summary of significant QTLs genome wide for anthocyanin ratios from DAD-detection by HPLC-QTOFMS targeted profiling.

Anthocyanin (DAD) Ratios	Total QTLs
Anthocyanidin Core Ratios	
All Delphinidin Derivatives / Total Anthocyanins	2
All Delphinidins / Total Anthocyanins	1
All Cyanidin Derivatives / Total Anthocyanins	3
All Cyanidins / Total Anthocyanins	2
All Petunidins / All Delphinidins	1
Delphinidin-Glucoside / Petunidin-Glucoside	8

Table 3.18 – (continued).

Delphinidin-AGluc / Petunidin-AGluc	4
Delphinidin-Glucoside + -AGluc / Petunidin-Glucoside + -AGluc	8
Delphinidin-Arabinoside / Petunidin-Arabinoside	1
Petunidin-Glucoside / Malvidin-Glucoside	1
Petunidin-AGluc / Malvidin-AGluc	4
Petunidin-Glucoside + -AGluc / Malvidin-Glucoside + -AGluc	1
Malvidin-AGluc / Delphinidin-AGluc	6
Cyanidin-AGluc / Total Acetyl-Glucosides	15
Peonidin-Galactoside / Total Galactosides	1
Peonidin-Galactoside / Cyanidin-Galactoside	7
Peonidin + Cyanidin -Galactosides / Total Galactosides	3
Sugar Moiety: Glucoside and Acetyl-Glucoside Specific Ratios	
Total Acetyl-Glucosides / Total Anthocyanins	10
Total Acetyl-Glucosides / Total Glucosides	5
Cyanidin-Glucoside + -AGluc	7
Delphinidin-AGluc / All Delphinidins	8
Petunidin-AGluc / All Petunidins	6
Malvidin-AGluc / All Malvidins	3
Cyanidin-AGluc / All Cyanidins	7
Delphinidin-AGluc / Delphinidin-Glucoside	8
Petunidin-AGluc / Petunidin-Glucoside	4
Malvidin-AGluc / Malvidin-Glucoside	7
Cyanidin-AGluc / Cyanidin-Glucoside	6
Sugar Moiety: Differentiation Ratios	
Total Arabinosides / Total Glucosides	12
Total Galactosides / Total Glucosides	13
Total Arabinosides + Galactosides / Total Glucosides + AGluc	14
Total Galactosides / Total Arabinosides	1
Cyanidin-Arabinoside / All Cyanidins	3
Cyanidin-Galactoside / All Cyanidins	1
Delphinidin-Arabinoside / Delphinidin-Glucoside	1
Petunidin-Arabinoside / Petunidin-Glucoside	1
Malvidin-Arabinoside / Malvidin-Glucoside	5
Cyanidin-Arabinoside / Cyanidin Glucoside	10
Petunidin-Galactoside / Petunidin-Glucoside	1
Malvidin-Galactoside / Malvidin-Glucoside	4
Cyanidin-Galactoside / Cyanidin-Glucoside	11
Delphinidin-Arabinoside / Delphinidin-Galactoside	1
Petunidin-Arabinoside / Petunidin-Galactoside	1
Cyanidin-Arabinoside / Cyanidin-Galactoside	7
Malvidin-Arabinoside + -Galactoside / Malvidin-Glucoside + -AGluc	1
Cyanidin-Arabinoside + -Galactoside / Cyanidin-Glucoside + -AGluc	11

-AGluc represents the Acetyl-Glucoside sugar moiety

Table 3.19 – A subset of significant QTLs with overlapping genetic regions for DAD-detected individual anthocyanins, summation groups, and ratios from HPLC-QTOFMS targeted profiling.

LG	Position (cM)	Anthocyanin (DAD)	LOD	% Variation Explained
1	8-15	Total Acetyl-Glucosides	5.59	14.45
		Delphinidin-Acetyl-Glucoside	6.69	17.03
		Petunidin-Acetyl-Glucoside	7.74	19.43
		Cyanidin-Acetyl-Glucoside	14.20	32.73
		Cyanidin-Glucoside	6.35	16.24
		Cyanidin-Glucoside + -AGluc	6.60	16.82
		Total Acetyl-Glucosides / Total Anthocyanins	4.70	12.29
		Delphinidin-AGluc / All Delphinidins	4.32	11.37
		Petunidin-AGluc / All Petunidins	3.26	8.70
		Malvidin-AGluc / All Malvidins	3.99	10.53
		Cyanidin-AGluc / All Cyanidins	5.70	14.70
		Total Acetyl-Glucoside / Total Glucoside	4.55	11.93
		Delphinidin-AGluc / Delphinidin-Glucoside	3.14	8.39
		Petunidin-AGluc / Petunidin-Glucoside	39.41	66.71
		Malvidin-AGluc / Malvidins-Glucoside	8.75	21.67
Cyanidin-AGluc / Cyanidin-Glucoside	7.20	18.20		
1	8-19	Delphinidin-AGluc / Petunidin-AGluc	47.81	73.67
		Cyanidin-AGluc / Total Acetyl-Glucosides	34.29	61.60
1	14-19	Cyanidin-Arabinoside / Cyanidin-Galactoside	4.96	12.93
		Cyanidin-Arabinoside / All Cyanidins	3.94	10.40
		Peonidin-Galactoside / Cyanidin-Galactoside	4.00	10.56
1	30-32	Cyanidin-Glucoside	9.42	23.12
		Cyanidin-Acetyl-Glucoside	7.29	18.41
		Cyanidin-Glucoside + -AGluc	8.26	20.60
		Cyanidin-AGluc / Total Acetyl-Glucoside	5.51	14.26
		Cyanidin-Arabinoside / Cyanidin-Galactoside	4.15	10.93
		Peonidin-Galactoside / Cyanidin-Galactoside	4.43	11.64
1	47	All Delphinidins	3.14	8.40
		All Petunidins	3.38	9.01
1	52	Cyanidin-Arabinoside / Cyanidin-Galactoside	3.73	9.90
		Peonidin-Galactoside / Cyanidin-Galactoside	3.01	8.07
1	63	Total Acetyl-Glucoside	4.34	11.40
		Delphinidin-Acetyl-Glucoside	5.95	15.30
		Petunidin-Acetyl-Glucoside	6.45	16.46
		Cyanidin-Glucoside	5.23	13.59
		Cyanidin-Acetyl-Glucoside	7.67	19.26
		Cyanidin-Glucoside + -AGluc	5.96	15.34
		Total Acetyl-Glucosides / Total Anthocyanins	3.29	8.77
		Cyanidin-AGluc / Total Acetyl-Glucoside	13.70	31.78
		Cyanidin-AGluc / All Cyanidins	5.31	13.77

Table 3.19 – (continued).

2	25	Total Acetyl-Glucoside	11.12	26.69
		Total Acetyl-Glucoside / Total Glucoside	4.44	11.65
		Malvidin-Acetyl-Glucoside	6.77	17.21
		Petunidin-Acetyl-Glucoside	10.10	24.56
2	25	Petunidin-AGluc / Delphinidin-AGluc	46.44	72.64
		Petunidin-AGluc / Malvidin-AGluc	24.98	50.20
		Malvidin-AGluc / Delphinidin-AGluc	16.90	37.60
2	32	Total Galactosides / Total Glucosides	13.07	30.56
		Total Arabinosides / Total Glucosides	16.43	36.78
		Total Galactosides + Arabinosides / Total Glucosides + AGLuc	13.67	31.72
2	32	Delphinidin-Glucoside + -AGluc / Petunidin-Glucoside + -AGluc	30.70	57.55
		Delphinidin-Glucoside / Petunidin-Glucoside	32.42	59.54
		Peonidin-Galactoside / Cyanidin-Galactoside	3.29	8.78
2	37-41	Petunidin-Acetyl-Glucoside	6.12	15.69
		Cyanidin-Glucoside	5.20	13.51
		Cyanidin-Acetyl-Glucoside	5.09	13.25
		Cyanidin-Glucoside + -AGluc	5.17	13.45
		Total Acetyl-Glucosides / Total Anthocyanins	3.10	8.29
		Petunidin-AGluc / All Petunidins	4.35	11.43
		Malvidin-AGluc / All Malvidins	3.09	8.27
		Delphinidin-AGluc / Delphinidin-Glucosides	4.47	11.73
		Petunidin-AGluc / Petunidin-Glucoside	39.03	66.36
2	37-41	Cyanidin-AGluc / Cyanidin-Glucoside	7.27	18.37
		Cyanidin-AGluc / Total Acetyl-Glucosides	3.01	8.05
		Cyanidin-Galactoside + -Arabinoside / Cyanidin-Glucoside + -AGluc	29.81	56.49
		Cyanidin-Galactoside / Cyanidin-Glucoside	26.54	52.32
2	57-59	Cyanidin-Arabinoside / Cyanidin-Glucoside	25.32	50.68
		Petunidin-AGluc / Petunidin-Glucoside	40.31	67.54
2	65	Malvidin-AGluc / Malvidin-Glucoside	7.68	19.28
		Total Galactosides / Total Glucosides	9.23	22.70
2	63-67	Total Arabinosides / Total Glucosides	12.08	28.62
		Total Galactosides + Arabinosides / Total Glucosides + AGLuc	9.71	23.73
		Malvidin-Galactoside / Malvidin-Glucoside	23.82	48.57
		Malvidin-Arabinoside / Malvidin-Glucoside	9.53	23.35
		Delphinidin-Glucoside + -AGluc / Petunidin-Glucoside + -AGluc	25.45	50.85
2	83	Delphinidin-Glucoside / Petunidin-Glucoside	26.10	51.73
		Peonidin-Galactoside / Cyanidin-Galactoside	3.40	9.04
		Total Galactosides / Total Glucosides	8.78	21.73
		Total Arabinosides / Total Glucosides	11.26	26.97

Table 3.19 – (continued).

		Total Galactosides + Arabinosides / Total Glucosides + AGLuc	9.09	22.41
		Cyanidin-AGluc / Total Acetyl-Glucosides	20.18	43.06
3	28	Cyanidin-Galactoside	3.34	8.89
		All Cyanidins	3.17	8.46
		Cyanidin-Arabinoside / Cyanidin-Galactoside	3.09	8.25
3	33	Malvidin-Glucoside	3.44	9.16
3	36	Cyanidin-Galactoside / Cyanidin-Glucoside	18.89	40.97
		Cyanidin-Arabinoside / Cyanidin-Glucoside	17.13	38.00
		Cyanidin-Galactoside + -Arabinoside / Cyanidin-Glucoside + -AGluc	20.91	44.21
3	49	Total Acetyl-Glucoside / Total Glucoside	3.04	8.13
		Cyanidin-AGluc	3.97	10.48
		Cyanidin-AGluc / Total Acetyl-Glucoside	3.06	8.19
3	122	Malvidin-Galactoside / Malvidin-Glucoside	31.69	58.70
		Malvidin-Arabinoside / Malvidin-Glucoside	9.70	23.72
4	14-20	Total Galactosides / Total Glucosides	8.80	21.77
		Total Arabinosides / Total Glucosides	12.12	28.69
		Total Galactosides + Arabinosides / Total Glucosides + AGLuc	9.38	23.04
		Malvidin-AGluc / Malvidin-Glucoside	7.26	18.34
		Cyanidin-Galactoside / Cyanidin-Glucoside	35.20	62.56
		Cyanidin-Arabinoside / Cyanidin-Glucoside	32.62	59.77
		Cyanidin-Galactoside + -Arabinoside / Cyanidin-Glucoside + -AGluc	37.44	64.83
4	18	Delphinidin-Glucoside + -AGluc / Petunidin-Glucoside + -AGluc	28.59	54.97
		Delphinidin-Glucoside / Petunidin-Glucoside	30.30	57.07
4	29	Peonidin-Galactoside / Cyanidin-Galactoside	6.81	17.31
4	31	Total Galactosides / Total Glucosides	9.00	22.21
		Total Arabinosides / Total Glucosides	12.36	29.18
		Total Galactosides + Arabinosides / Total Glucosides + AGLuc	9.34	22.94
		Malvidin-AGluc / Malvidin-Glucoside	8.53	21.18
4	43	Delphinidin-Glucoside + -AGluc / Petunidin-Glucoside + -AGluc	8.02	20.05
		Delphinidin-Glucoside / Petunidin-Glucoside	8.31	20.71
4	43	Total Arabinoside / Total Glucosides	6.37	16.28
4	127-132	Total Acetyl-Glucosides	12.97	30.37
		Delphinidin-Acetyl-Glucoside	12.84	30.13
		Petunidin-Acetyl-Glucoside	11.39	27.23
		Malvidin-Acetyl-Glucoside	6.20	15.90
		Cyanidin-Acetyl-Glucoside	18.61	40.51
		Total Acetyl-Glucosides / Total Anthocyanins	11.85	28.16

Table 3.19 – (continued).

		Delphinidin-AGluc / All Delphinidins	8.59	21.31
		Petunidin-AGluc / All Petunidins	11.65	27.75
		Malvidin-AGluc / All Malvidins	6.36	16.26
		Cyanidin-AGluc / All Cyanidins	23.95	48.75
		Delphinidin-AGluc / Delphinidin-Glucoside	17.59	38.80
		Cyanidin-AGluc / Cyanidin-Glucoside	14.69	33.63
4	127	Delphinidin-AGluc / Malvidin-AGluc	15.86	35.77
		Delphinidin-Glucoside / Petunidin-Glucoside	22.39	46.47
		Cyanidin-AGluc / Total Acetyl-Glucoside	37.48	64.87
4	127-132	Total Arabinosides / Total Glucosides	6.94	17.61
		Total Galactosides / Total Glucosides	4.16	10.96
		Total Galactosides + Arabinosides / Total Glucosides + AGLuc	5.65	14.60
		Cyanidin-Arabinoside / Cyanidin-Glucoside	33.32	60.54
		Cyanidin-Galactoside / Cyanidin-Glucoside	36.09	63.48
		Cyanidin-Galactoside + -Arabinoside / Cyanidin-Glucoside + -AGluc	38.39	65.75
5	71-73	All Delphinidin Derivatives / Total Anthocyanins	4.38	11.50
		Petunidin-Glucoside / Malvidin-Glucoside	3.45	9.19
		Petunidin-Glucoside + -AGluc / Malvidin-Glucoside + -AGluc	3.27	8.71
		All Cyanidin Derivatives	5.87	15.10
		Cyanidin-Arabinoside	5.08	13.22
		Cyanidin-Galactoside	6.21	15.91
		All Cyanidins	4.76	12.43
		Peonidin-Galactoside	5.37	13.91
		All Cyanidin Derivatives / Total Anthocyanins	4.00	10.56
		Peonidin-Galactoside / Total Galactosides	3.58	9.50
		Peonidin + Cyanidin -Galactosides / Total Galactosides	4.00	10.56
		Total Arabinosides / Total Glucosides	3.33	8.88
		Total Galactosides / Total Arabinosides	4.20	11.05
		Total Galactosides / Total Glucosides	3.40	9.05
		Total Galactosides + Arabinosides / Total Glucosides + AGLuc	3.30	8.80
		Delphinidin-Arabinoside / Delphinidin-Galactoside	3.10	8.28
		Petunidin-Arabinoside / Petunidin-Galactoside	3.88	10.26
		Petunidin-Galactoside / Petunidin-Arabinoside	3.34	8.90
5	108	Cyanidin-Arabinoside	3.09	8.27
6	43	Total Arabinoside / Total Glucosides	13.90	32.16

Table 3.19 – (continued).

		Total Galactosides / Total Glucosides	10.54	25.48
		Total Galactosides + Arabinosides / Total Glucosides + AGLuc	11.14	26.72
		Cyanidin-Arabinoside / Cyanidin-Galactoside	3.24	8.64
6	41-43	Delphinidin-Glucoside / Petunidin-Glucoside	32.91	60.08
		Delphinidin-Glucoside + -AGluc / Petunidin-Glucoside + -AGluc	31.41	58.38
6.5	28-32	Total Arabinoside / Total Glucosides	7.48	18.85
		Total Galactosides / Total Glucosides	6.08	15.60
		Total Galactosides + Arabinosides / Total Glucosides + AGLuc	6.29	16.11
		Delphinidin-Arabinoside / Delphinidin-Glucoside	12.54	29.53
		Petunidin-Arabinoside / Petunidin-Glucoside	8.93	22.07
		Petunidin-Galactoside / Petunidin-Glucoside	28.59	54.97
		Cyanidin-AGluc / All Cyanidins	23.03	47.41
8	87-93	Total Acetyl-Glucosides	3.40	9.06
		Delphinidin-Acetyl-Glucoside	3.75	9.94
		Petunidin-Acetyl-Glucoside	3.24	8.65
		Malvidin-Acetyl-Glucoside	3.07	8.21
		Cyanidin-Acetyl-Glucoside	3.11	8.32
		Total Acetyl-Glucosides / Total Anthocyanins	3.45	9.17
		Delphinidin-AGluc / All Delphinidins	4.11	10.84
		Petunidin-AGluc / All Petunidins	3.53	9.39
		Delphinidin-AGluc / Delphinidin-Glucoside	4.25	11.18
8	93	Delphinidin-AGluc / Petunidin-AGluc	3.79	10.03
		Petunidin-AGluc / Malvidin-AGluc	3.21	8.57
		Cyanidin-AGluc / Total Acetyl-Glucosides	3.48	9.24
8	107	Cyanidin-Acetyl-Glucoside	4.18	11.01
		Cyanidin-AGluc / Total Acetyl-Glucosides	3.17	8.47
9	18	All Delphinidins / Total Anthocyanins	3.10	8.28
		Delphinidin-Arabinoside / Petunidin-Arabinoside	3.14	8.39
9	27	Total Acetyl-Glucosides	11.29	27.03
		Delphinidin-Acetyl-Glucoside	10.62	25.65
		Petunidin-Acetyl-Glucoside	12.83	30.10
		Malvidin-Acetyl-Glucoside	6.76	17.20
		Cyanidin-Acetyl-Glucoside	12.12	28.69
		Total Acetyl-Glucosides / Total Anthocyanins	9.61	23.53
		Delphinidin-AGluc / All Delphinidins	6.38	16.32
		Petunidin-AGluc / All Petunidins	8.55	21.23
		Malvidin-AGluc / All Malvidins	6.94	17.62
		Cyanidin-AGluc / All Cyanidins	9.27	22.79
		Total Acetyl-Glucoside / Total Glucoside	7.20	18.21

Table 3.19 – (continued).

		Delphinidin-AGluc / Delphinidin-Glucoside	5.86	15.09
		Malvidin-AGluc / Malvidin-Glucoside	8.09	20.21
		Cyanidin-AGluc / Cyanidin-Glucoside	9.53	23.36
		Malvidin-AGluc / Delphinidin-AGluc	4.38	11.50
		Cyanidin-AGluc / Total Acetyl-Glucosides	12.99	30.41
		Cyanidin-Arabinoside / Cyanidin-Galactoside	4.00	10.57
10	0-10	Total Acetyl-Glucosides	14.02	32.38
		Delphinidin-Acetyl-Glucoside	13.88	32.11
		Petunidin-Acetyl-Glucoside	12.55	29.55
		Malvidin-Acetyl-Glucoside	9.49	23.28
		Cyanidin-Acetyl-Glucoside	18.34	40.06
		Cyanidin-Glucoside	7.47	18.83
		Cyanidin-Glucoside + -AGluc	7.72	19.38
		Total Acetyl-Glucosides / Total Anthocyanins	10.59	25.58
		Delphinidin-AGluc / All Delphinidins	7.52	18.93
		Petunidin-AGluc / All Petunidins	10.80	26.02
		Total Acetyl-Glucoside / Total Glucoside	7.80	19.57
		Delphinidin-AGluc / Delphinidin-Glucoside	15.87	35.79
		Malvidin-AGluc / Malvidin-Glucoside	3.81	10.10
		Delphinidin-Galactoside	6.02	15.45
		Petunidin-Galactoside	3.86	10.21
		Malvidin-Arabinoside / Malvidin-Glucoside	25.02	50.25
		Malvidin-Galactoside / Malvidin-Glucoside	46.90	72.99
		Malvidin-Galactoside + -Arabinoside / Malvidin-Glucoside + -AGluc	37.84	65.22
		Cyanidin-Arabinoside / Cyanidin-Glucoside	27.04	52.98
		Cyanidin-Galactoside / Cyanidin-Glucoside	32.82	59.99
		Cyanidin-Galactoside + -Arabinoside / Cyanidin-Glucoside + -AGluc	34.17	61.47
		Delphinidin-AGluc / Petunidin-AGluc	56.15	79.14
		Petunidin-AGluc / Malvidin-AGluc	30.80	57.67
		Malvidin-AGluc / Delphinidin-AGluc	22.08	46.01
		Cyanidin-AGluc / Total Acetyl-Glucosides	36.39	63.78
10	44-47	Malvidin-Galactoside	3.54	9.40
		Malvidin-Glucoside / Malvidin-Galactoside	3.12	8.34
11	37-40	Cyanidin-Arabinoside / All Cyanidins	7.22	18.26
		Cyanidin-Arabinoside / Cyanidin-Glucoside	16.36	36.66
		Cyanidin-Galactoside / Cyanidin-Glucoside	12.48	29.42
		Cyanidin-Arabinoside / Cyanidin-Galactoside	3.70	9.81
		Cyanidin-Galactoside + -Arabinoside / Cyanidin-Glucoside + -AGluc	13.63	31.64
		Cyanidin-AGluc / Total Acetyl-Glucosides	3.07	8.21
11	53-60	Malvidin-Galactoside	3.18	8.48
		All Malvidins	3.25	8.66

Table 3.19 – (continued).

		Malvidin-AGluc / Delphinidin-AGluc	3.38	9.00
11	113	All Cyanidin Derivatives / Total Anthocyanins	3.13	8.36
		All Cyanidins / Total Anthocyanins	3.09	8.26
11	129	Total Anthocyanins	3.25	8.67
11	136	Cyanidin-Arabinoside	3.12	8.33
		All Cyanidins	3.19	8.53
		All Cyanidins / Total Anthocyanins	3.24	8.65
		All Cyanidin Derivatives / Total Anthocyanins	3.23	8.61
		All Delphinidin Derivatives / Total Anthocyanins	3.77	9.99
		Peonidin + Cyanidin -Galactosides / Total Galactosides	3.22	8.61
12	10-18	Total Acetyl-Glucosides	6.75	17.18
		Delphinidin-Acetyl-Glucoside	8.72	21.60
		Petunidin-Acetyl-Glucoside	10.05	24.46
		Cyanidin-Acetyl-Glucoside	4.03	10.63
		Cyanidin-Glucoside	5.26	13.66
		Cyanidin-Glucoside + -AGluc	5.78	14.91
		Total Acetyl-Glucosides / Total Anthocyanins	5.90	15.19
		Delphinidin-AGluc / All Delphinidins	4.59	12.02
		Delphinidin-AGluc / Delphinidin-Glucoside	6.78	17.24
		Delphinidin-AGluc / Petunidin-AGluc	3.05	8.17
		Petunidin-AGluc / Malvidin-AGluc	3.61	9.59
		Cyanidin-AGluc / Total Acetyl-Glucosides	13.47	31.34
12	25	Total Arabinoside / Total Glucosides	7.42	18.70
		Total Galactosides / Total Glucosides	8.21	20.48
		Total Galactosides + Arabinosides / Total Glucosides + AGluc	7.89	19.76
12	25	Delphinidin-Glucoside / Petunidin-Glucoside	8.51	21.14
		Delphinidin-Glucoside + -AGluc / Petunidin-Glucoside + -AGluc	7.76	19.46
		Petunidin-AGluc / Petunidin-Glucoside	39.42	66.72
12	35-37	Peonidin-Galactoside	4.82	12.59
		Peonidin-Galactoside / Cyanidin-Galactoside	5.02	13.08
		Cyanidin-Arabinoside / Cyanidin-Galactoside	5.79	14.92
		Cyanidin-Galactoside + -Arabinoside / Cyanidin-Glucoside + -AGluc	8.51	21.15
		Cyanidin-AGluc / Total Acetyl-Glucosides	8.87	21.92
12	49	Cyanidin-Arabinoside / Cyanidin-Glucoside	14.22	32.76
		Cyanidin-Galactoside / Cyanidin-Glucoside	15.42	34.97
		Cyanidin-Galactoside + -Arabinoside / Cyanidin-Glucoside + -AGluc	15.04	34.27
12	52	Cyanidin-Arabinoside / Cyanidin-Glucoside	9.74	23.81
		Cyanidin-Galactoside / Cyanidin-Glucoside	11.67	27.79

Table 3.19 – (continued).

		Cyanidin-Galactoside + -Arabinoside / Cyanidin-Glucoside + -AGluc	11.46	27.37
12	59	Cyanidin-Arabinoside / Cyanidin-Glucoside	31.55	58.55
		Cyanidin-Galactoside / Cyanidin-Glucoside	34.12	61.42
		Cyanidin-Galactoside + -Arabinoside / Cyanidin-Glucoside + -AGluc	37.19	64.58
		Malvidin-Arabinoside / Malvidin-Glucoside	3.93	10.38
		Malvidin-Galactoside / Malvidin-Glucoside	3.02	8.07
12	70-74	Total Acetyl-Glucosides	4.00	10.57
		Cyanidin-Acetyl-Glucoside	7.79	19.54
		Total Acetyl-Glucosides / Total Anthocyanins	6.23	15.95
		Delphinidin-AGluc / All Delphinidins	5.12	13.31
		Petunidin-AGluc / All Petunidins	4.81	12.57
		Malvidin-AGluc / All Malvidins	5.41	14.01
		Cyanidin-AGluc / All Cyanidins	4.88	12.73
		Delphinidin-AGluc / Delphinidins-Glucoside	6.65	16.94
12	72	Cyanidin-AGluc / Cyanidin-Glucoside	5.37	13.92
		Total Arabinoside / Total Glucosides	11.37	27.20
		Total Galactosides / Total Glucosides	7.94	19.87
12	70-74	Total Galactosides + Arabinosides / Total Glucosides + AGluc	8.63	21.40
		Delphinidin-Glucoside + -AGluc / Petunidin-Glucoside + -AGluc	15.93	35.89
		Delphinidin-Glucoside / Petunidin-Glucoside	16.91	37.63
		Malvidin-AGluc / Delphinidin-AGluc	7.82	19.62
		Cyanidin-AGluc / Total Acetyl-Glucosides	15.49	35.11

LG represents linkage group

LOD represents logarithm of odds value

-AGluc represents the Acetyl-Glucoside sugar moiety

3.4.5. Putative Candidate Gene Analysis of Significant QTL Regions

3.4.5.1. ¹H NMR Known Metabolites and DPPH-Antioxidant Capacity

The annotated metabolites were grouped together for summations and results description because they are part of the same pathway, which focused the putative candidate gene analysis to genes that are involved in and play an important role in the pathway. Table 3.20 reports some of significant QTLs for each TCA acid and amino acid metabolites and the putative candidate genes found within the genetic region. Table 3.21 focuses on significant QTLs for the sugar metabolites and the putative candidate genes found within the region. Table 3.22 summarizes significant QTLs and

putative candidate genes within the genetic regions for the phenolic acids and ascorbic acid, while DPPH-antioxidant capacity is summarized in Table 3.23.

Table 3.20 – A subset of significant QTLs for TCA acids and amino acids from ¹H NMR non-targeted profiling with corresponding putative candidate genes found within the genetic region.

LG	Position (cM)	Trait	LOD	% Variation Explained	Putative Candidate Genes
1	19	Citric Acid	48.37	52.29	-Malate Dehydrogenase
1	14	Alanine	7.30	10.56	-Pyruvate kinase
		Leucine	14.25	19.59	
		Valine	13.34	18.46	
1	30	Threonine	8.54	12.23	-Serine hydroxymethyltransferase
2	32	Aspartate	55.16	60.00	-Aspartate semialdehyde dehydrogenase
		Asparagine	79.86	70.53	
2	32	Citric Acid	33.40	40.01	-Phosphoenolpyruvate carboxylase
	37	Malic Acid	18.67	24.84	-Pyruvate dehydrogenase complex (Subunit 2)
2	37	GABA	60.87	60.60	-Glutamate decarboxylase
3	29	Aspartate	4.099	6.08	-Aspartokinase -Homoserine dehydrogenase
3	34	Arginine	3.33	4.97	-Acetylornithine deacetylase
3	34	Succinic Acid +Others	9.42	13.42	-Aconitate hydratase/Aconitase
	36	Citric Acid	34.45	40.97	-Isocitrate lyase
3	36	Alanine	6.35	9.26	-Alanine-glyoxylate aminotransferase
3	59	Citric Acid	35.37	41.79	-Phosphoenolpyruvate carboxylase -Malate dehydrogenase
3	59	Arginine	3.48	9.21	-Carbamoyl-phosphate synthase
3	84	Arginine	3.38	8.95	-Carbamoyl-phosphate synthase
	88	GABA	10.77	15.19	-Succinate semialdehyde dehydrogenase
		Succinic Acid +Others	12.33	17.20	
3	115	Threonine	3.43	5.12	-Serine Hydroxymethyltransferase
3	117	Aspartate	3.792	11.35	-Asparagine synthase
4	27	Malic Acid	24.72	31.49	-ATP-citrate synthase
4	27	Glutamine	8.01	11.53	-Glutamate-glyoxylate aminotransferase
4	27	Alanine	9.68	13.77	-Alanine aminotransferase
4	29	Citric Acid	7.08	10.27	-Pyruvate dehydrogenase Complex (Subunit 1)

Table 3.20 – (continued).

4	43	Citric Acid	26.05	32.87	-Malate synthase
4	43	Isoleucine	18.84	25.05	-Branched-chain amino-acid aminotransferase
		Leucine	31.36	38.11	
		Valine	24.29	31.04	
5	68	Threonine	3.03	4.53	-Serine hydroxymethyltransferase
5	107	Isoleucine	3.34	4.98	-Branched chain alpha-keto dehydrogenase complex (Subunits 1&3) -3-isopropylmalate dehydrogenase
		Valine	3.27	4.87	
		Leucine	3.14	4.70	
6	55	Isoleucine	3.13	4.67	-Acetolactate synthase
		Threonine	3.80	5.64	
6	100	Threonine	3.45	10.37	-Serine Hydroxymethyltransferase
6	101	Arginine	3.06	4.57	-Ornithine carbamoyltransferase
8	107	GABA	9.96	14.13	-Gamma-aminobutyrate transaminase -Glutamate dehydrogenase
9	25	Glutamine	10.95	15.54	-Glutamate synthase (ferredoxin-dependent) (GOGAT)
9	25	GABA	58.22	58.97	-Glutamate dehydrogenase
9	25	Alanine	5.19	7.64	-Pyruvate kinase
		Citric Acid	10.77	15.19	
9	25	Succinic Acid +Others	17.49	23.48	-2-oxoglutarate dehydrogenase
		Malic Acid	24.52	31.28	
10	35	Alanine	3.18	5.23	-Pyruvate kinase -Enolase
12	10	Citric Acid	11.74	16.44	-Pyruvate dehydrogenase complex (Subunits 1&3)
	12	Alanine	21.17	27.66	
12	12	Threonine	13.36	18.48	-Acetolactate synthase
		Isoleucine	15.27	20.83	
12	12	GABA	18.97	25.19	-Succinate semialdehyde dehydrogenase
		Succinic Acid +Others	20.24	26.63	
		Malic Acid	24.93	31.71	

Table 3.20 – (continued).

12	49	Aspartate	11.20	15.75	-Aspartokinase
		Asparagine	40.15	45.90	
12	49	Isopropylmalic Acid	4.79	7.06	-3-isopropylmalate dehydrogenase
		Leucine	21.60	28.14	
		Valine	21.81	28.37	
12	49	Glutamine	4.69	6.92	-Isocitrate Dehydrogenase (NADP)
12	49	Citric Acid	9.08	12.97	-Pyruvate dehydrogenase complex (Subunit 1) -ATP citrate synthase
12	59	Leucine	50.68	53.94	-3-isopropylmalate dehydrogenase
		Valine	29.55	36.37	
12	61	Alanine	5.82	8.53	-Alanine-glyoxylate aminotransferase
12	61	Threonine	13.02	18.06	-Threonine aldolase
12	61	Arginine	7.46	10.79	-N ² -acetylornithine aminotransferase
12	61	Glutamine	19.97	26.32	-Isocitrate dehydrogenase (NAD)
12	61	GABA	20.00	26.36	-Succinate semialdehyde dehydrogenase
		Succinic Acid +Others	12.96	17.98	
		Malic Acid	15.82	21.50	
12	74	Citric Acid	20.23	26.62	-Malate dehydrogenase
		Malic Acid	17.28	23.23	

LG represents linkage group

LOD represents logarithm of odds value

Table 3.21 – A subset of significant QTLs for sugars from ¹H NMR non-targeted profiling with corresponding putative candidate genes found within the genetic region.

LG	Position (cM)	Trait	LOD	% Variation Explained	Putative Candidate Genes
1	30	Fructose	14.96	20.41	-Phosphoglucomutase -Ribose-5-phosphate isomerase
1	30	Sucrose	22.85	29.50	-UTP-G1P uridylyltransferase
2	32	Glucose	4.49	13.29	-Phosphoglucomutase
4	20	Fructose	5.74	16.65	-Triosephosphate isomerase -G6P dehydrogenase
4	27	Sucrose	21.08	27.57	-T6P synthase (TPS)
4	107	Glucose-Fructose Ratio	3.34	4.98	-Fructokinase/Hexokinase -Sucrose phosphatase
5	120	Fructose-Sucrose Ratio	4.30	6.37	-ATP-dependent phosphofructokinase -UTP-G1P uridylyltransferase
		Glucose-Sucrose Ratio	3.55	5.28	-TPS -Trehalose-phosphate phosphatase (TPP)
6	41	Sucrose	25.41	32.21	-Fructokinase/hexokinase
6	41	Maltose	21.95	28.52	-G6P dehydrogenase
9	25	Glucose	19.04	25.27	-G6P dehydrogenase
9	25	Fructose	17.65	23.66	-Cell wall INV -Beta-fructofuranosidase
9	25	Sucrose	24.39	31.14	-TPP
10	8	Sucrose	13.54	18.71	-Cell wall INV
	8	Glucose	3.06	8.15	-Beta-fructofuranosidase
	14	Fructose	3.29	8.72	
10	86	Fructose-Glucose Ratio	4.35	6.43	-Cell wall INV -Beta-fructofuranosidase -ATP-dependent phosphofructokinase
12	12	Fructose	17.30	23.25	-Transaldolase -Ribose-5-phosphate isomerase -Glyceraldehyde-3-phosphate dehydrogenase
12	12	Glucose	15.25	20.81	-G6P dehydrogenase

Table 3.21 – (continued).

12	49	Sucrose	8.79	12.58	-TPS
12	68	Fructose	3.61	10.82	-Fructose-1,6-bisphosphatase -Fructose-1,6-bisphosphate aldolase
1	14	Maltose	11.19	15.73	-Beta-Amylase -ADP-glucose pyrophosphorylase
1	30	Glucose	17.49	23.48	-Beta-glucosidase
1	32	Maltose	18.67	24.85	-Beta-amylase
2	32	Maltose	21.35	27.87	-Glucan beta-glucosidase
		Glucose+Maltose	3.15	9.52	
4	27	Maltose	17.68	23.70	-Beta-amylase
		Glucose	18.12	24.22	-Beta-glucosidase
9	25	Maltose	19.15	25.40	-Beta-glucosidase
12	37	Maltose	9.88	14.03	-Beta-glucosidase
4	20	Maltitol	11.69	16.38	-Galactinol synthase
4	130	Maltitol	4.33	6.41	-Sorbitol-6-phosphate dehydrogenase (NADP-dependent)
12	49	Maltitol	5.35	7.86	-Aldose reductase -Sorbitol-6-phosphate dehydrogenase (NADP-dependent)
12	61	Maltitol	8.71	12.47	-Galactinol synthase
12	74	Maltitol	4.03	5.98	-Galactinol synthase
1	18	Galactose	9.06	12.94	-GDP-mannose-3,5-epimerase
	14	Other Sugars	14.47	19.85	
2	23	Galactose	8.41	12.07	-Polygalacturonase -UDP-glucuronate 4-epimerase
2	59	Other Sugars	5.11	7.52	-Polygalacturonase
2	89	Other Sugars	3.03	9.18	-UDP-glucose 4-epimerase -Trehalase
3	124	Galactose	7.89	11.37	-UDP-glucose 4-epimerase -UDP-glucuronate 4-epimerase

Table 3.21 – (continued).

4	16	Galactose	12.90	17.91	-Polygalacturonase
6	41	Other Sugars	21.58	28.12	-Mannose-1-phosphate guanyltransferase
9	27	Galactose	12.90	17.92	-Alpha-galactosidase
	25	Other Sugars	20.17	26.55	
12	49	Galactose	7.60	10.97	-Polygalacturonase
12	74	Other Sugars	12.25	17.09	-Polygalacturonase
1	30	Xylose	22.35	28.97	-Xyloglucan endotransglucosylase/hydrolase (XTH)
3	36	Xylose	10.33	14.62	-XTH
3	124	Xylose	9.73	13.83	-UDP-arabinose 4-epimerase
4	18	Arabinose +Others	4.27	6.33	-UDP-glucose dehydrogenase
	27	Xylose	20.15	26.53	-XTH
6	55	Arabinose +Others	5.48	8.04	-UDP-glucose dehydrogenase
		Xylose	5.24	7.70	-Beta-xylosidase
6.5	18	Xylose	3.36	5.01	-Beta-xylosidase
		Arabinose +Others	3.97	5.89	
8	107	Arabinose +Others	12.27	17.11	-Trifunctional RHM1 -Bifunctional UDP-glucose 4-epimerase/UDP-xylose 4-epimerase -UDP-glucuronic acid decarboxylase -UDP-glucuronate 4-epimerase
11	54	Xylose	5.85	16.99	-UDP-arabinose 4-epimerase
12	54	Xylose	17.23	23.17	-UDP-glucuronic acid decarboxylase
		Arabinose +Others	5.59	8.20	

LG represents linkage group

LOD represents logarithm of odds value

Table 3.22 – A subset of significant QTLs for phenolic and ascorbic acid from ¹H NMR non-targeted profiling with corresponding putative candidate genes found within the genetic region.

LG	Position (cM)	Trait	LOD	% Variation Explained	Putative Candidate Genes
1	14	Quinic Acid	30.49	37.28	-3-dehydroquinate dehydratase
	18	Gallic Acid	3.74	5.55	-Quinate/Shikimate dehydrogenase
1	15	Epicatechin	20.55	26.98	-Naringenin-chalcone synthase (CHS) -F3'H -F3'5'H -Anthocyanidin synthase (ANS)
1	32	Quinic Acid	41.21	46.76	-Arogenate/prephenate dehydratase
		Chlorogenic	10.92	15.38	
1	32	Epicatechin	29.87	36.68	-F3'H -F3'5'H
2	23	Epicatechin	15.88	21.57	-Anthocyanidin 3-O-glucosyltransferase -Acylsugar acyltransferase
2	25	Gallic Acid	11.58	16.23	-6-phosphogluconolactonase -6-phosphogluconate dehydrogenase
2	25	Chlorogenic	20.66	27.10	-p-coumaroyl-CoA ligase -Hydroxycinnamoyl-CoA Shikimate/Quinate hydroxycinnamoyltransferase (HCT)
2	34	Epicatechin	15.88	21.57	-Flavonol synthase (FLS) -F3'H -F3'5'H -ANS -Anthocyanidin 3-O-glucosyltransferase
2	81	Caffeic Acid+ Others	3.19	4.77	Caffeoyl-shikimate Esterase
3	88	Chlorogenic	10.05	14.25	-p-coumaroyl-CoA ligase -HCT
3	122	Chlorogenic	9.73	13.84	-HCT
3	122	Epicatechin	10.88	15.34	-Acylsugar Acyltransferase -Anthocyanin Acyltransferase
4	20	Epicatechin	18.94	25.16	-CHS

Table 3.22 – (continued).

4	22	Caffeic Acid+ Others	25.96	32.78	-HCT
	27	Quinic Acid	38.55	44.56	
	27	Chlorogenic	26.17	32.99	
4	92	Caffeic Acid+ Others	3.94	5.85	-Prephenate/Phenylpyruvate Aminotransferase
4	127	Quinic Acid	29.64	36.46	-Cinnamate 4-hydroxylase (C4H) -HCT
4	125	Epicatechin	3.03	4.54	-Chalcone-flavanone Isomerase (CHI) -F3'H -F3'5'H
4	132	Epicatechin	26.34	33.17	-CHS -F3'H -F3'5'H -Dihydroflavonol 4-reductase (DFR) -ANS
6	39	Caffeic Acid+ Others	25.16	31.95	-p-coumaroyl-CoA ligase
	43	Chlorogenic	23.28	29.97	
6	41	Epicatechin	21.31	27.82	-F3'H -F3'5'H
6	41	Quinic Acid	42.01	47.41	-3-dehydroquinate dehydratase -Quinate/shikimate dehydrogenase -3-dehydroshikimate dehydrogenase
	45	Gallic Acid	13.33	18.45	
6.5	18	Quinic Acid	3.28	4.89	-HCT
		Chlorogenic	10.91	15.37	
8	107	Quinic Acid	12.52	17.44	-3-deoxy-7-phosphoheptulonate synthase
		Chlorogenic	43.79	48.83	
		Caffeic Acid+ Others	13.55	18.72	
9	25	Epicatechin	14.69	20.13	-Anthocyanidin 3-O-glucosyltransferase
9	25	Quinic Acid	36.64	42.93	-p-coumaroyl-CoA ligase -HCT
	25	Chlorogenic	31.07	37.84	
	27	Caffeic Acid+ Others	5.93	8.67	
9	27	Gallic Acid	9.55	13.60	-G6P dehydrogenase

Table 3.22 – (continued).

10	10	Epicatechin	17.79	23.83	-F3'H -F3'5'H
11	37	Gallic Acid	8.01	11.53	-C4H -HCT
		Quinic Acid	20.48	26.90	-F3'H -F3'5'H
		Epicatechin	19.55	25.85	-Acylsugar Acyltransferase -Anthocyanin Acyltransferase -Acetyl-CoA Acetyltransferase
11	54	Quinic Acid	5.96	8.71	-C4H -HCT
11	54	Epicatechin	21.65	28.20	-F3'H -F3'5'H -Acylsugar acyltransferase -Anthocyanin acyltransferase
11.5	21	Quinic Acid	21.10	27.59	-3-dehydroquininate dehydratase
	34	Chlorogenic	10.02	14.21	-Quinate/Shikimate dehydrogenase
	36	Caffeic Acid+ Others	4.70	6.94	
12	12	Caffeic Acid +Others	6.81	9.90	-Caffeoyl-shikimate esterase
12	12	Epicatechin	22.65	29.29	-FLS -F3'H -F3'5'H -ANS
12	14	Chlorogenic	39.15	45.07	-C4H -p-coumaroyl-CoA ligase -HCT
12	49	Gallic Acid	15.99	21.70	-Arogenate/prephenate dehydratase
		Quinic Acid	6.13	8.95	-Phenylalanine Amino Lyase (PAL)
		Chlorogenic	25.22	32.01	-HCT
		Caffeic Acid+ Others	5.08	7.47	

Table 3.22 – (continued).

12	49	Epicatechin	15.59	21.23	-CHS -FLS -F3'H -F3'5'H -ANS -Anthocyanidin 3-O-glucosyltransferase -Acylsugar acyltransferase -Anthocyanin acyltransferase
12	55	Epicatechin	27.08	33.92	-Anthocyanidin 3-O-glucosyltransferase
12	61	Chlorogenic	14.53	19.93	-HCT
12	61	Epicatechin	10.03	14.22	-DFR -Anthocyanidin reductase (ANR)
12	74	Chlorogenic	15.06	20.58	-C4H
12	81	Epicatechin	8.82	12.62	-ANS
1	19	Ascorbic +Others	3.14	4.69	-Glutathione Reductase (GR) -Glutathione-S-Transferase (GST)
1	52	Ascorbic +Others	4.53	6.69	-Ascorbate Peroxidase (APX) -Ascorbate oxidase
6	41	Ascorbic +Others	3.53	5.26	-APX -Catalase (CAT)
6	55	Ascorbic +Others	4.60	6.80	-Monodehydroascorbate reductase (NADH) (MDAR)
9	25	Ascorbic +Others	3.80	5.64	-Dehydroascorbate reductase (DHAR) -GST
12	55	Ascorbic +Others	3.32	4.95	-APX -Ascorbate oxidase

LG represents linkage group

LOD represents logarithm of odds value

Table 3.23– A subset of significant QTLs for DPPH-antioxidant capacity with corresponding putative candidate genes found within the genetic region.

LG	Position (cM)	Trait	LOD	% Variation Explained	Putative Candidate Genes
5	107	DPPH	3.06	4.50	-3-deoxy-7-phosphoheptulonate synthase -Prephenate/phenylpyruvate aminotransferase -p-coumaroyl-CoA ligase -F3'H -F3'5'H -Anthocyanidin 3-O-glucosyltransferase -Anthocyanidin 3-O-glucoside 2'''-O-xylosyltransferase
6	45	DPPH	3.63	5.32	-3-dehydroquinate dehydratase -Quinate/shikimate dehydrogenase -p-coumaroyl-CoA ligase -F3'H -F3'5'H -CAT -APX -Ascorbate oxidase -GST

LG represents linkage group

LOD represents logarithm of odds value

3.5. Discussion

The Draper x Jewel (DxJ) mapping population represents a cross between two commercial blueberries grown in the US, and represent northern highbush (NHB) and southern high bush (SHB) blueberries (Draper & Hancock, 2003; Hancock et al., 2018). A greater understanding of the diversity of metabolites within the blueberries will provide valuable information about not only anthocyanins, but also primary and other specialized metabolites that contribute to blueberry nutritional benefits and may affect the anthocyanin biosynthesis or stability (He et al., 2010; Howard, Brownmiller, Mauromoustakos, & Prior, 2016; Jeong et al., 2010; Oh, Yu, Chung, Chea, & Lee, 2018; Overall et al., 2017; Silva et al., 2018; Wahyuningsih et al., 2017; Yonekura-Sakakibara, 2009). Since blueberries are potent antioxidants and have been associated with other health benefits, understanding what other compounds may contribute to the health benefits and what potential regulatory genes could regulate their accumulation will be vital to improving the stability and potency of metabolites involved in the health benefits. One of the main research objectives was to conduct metabolite profiling and annotate important metabolite features in the DxJ mapping population. The other research objective was to utilize the metabolite features annotated through the previous objective for biparental association mapping (BiPAM) to identify QTL regions and putative candidate genes that can be utilized in future research to develop blueberry cultivars with improve metabolite diversity and enhanced health benefits.

DxJ blueberry samples from two locations over two years were frozen, dried, and only extracted with acidified methanol to aid in stabilizing the anthocyanins. The blueberry extract samples are considered a relatively crude extract for metabolite profiling as filtering consisted of centrifuge separation and simple cellulose syringe filters. The metabolite profiling utilized both ¹H NMR and HPLC-QTOFMS to detect a large diversity of metabolites. The ¹H NMR method was a non-targeted approach to detect many different metabolite features. This method detects and annotates metabolite features with relatively large abundances, compared to the sensitivity of a HPLC-QTOFMS. The non-targeted ¹H NMR usually identifies metabolite features with large accumulations that are subsequently annotated as primary metabolites. This non-targeted ¹H NMR profiling also identified multiple different sugars and phenolic acids.

Even though profiling a broad blueberry extract like the acidified extraction utilized in this research provides a better representation of the metabolites in fresh blueberries, the metabolite feature annotation and analysis becomes much more difficult as multiple metabolites overlap with others and may not be distinguished without further purification or targeted quantification.

3.5.1. Metabolite Profiling with ^1H NMR Analysis

The ^1H NMR profiling analysis across both years putatively annotated 192 metabolite features that compile into 34 known metabolites. Tables 3.4, 3.5, and 3.6 summarize 29 of the 34 known metabolite peaks that were annotated with greater confidence due to clean, isolated or characteristic peak couplings. There are 4 of the 29 metabolite peaks that are annotated as “+ others” because that peak contained a distinct known metabolite peak along with other indistinguishable metabolite peaks (Tables 3.4, 3.5, and 3.6). The 4 “+ others” metabolites were included with this research as the majority of the peak contained the known metabolite. As described previously, the ^1H NMR metabolites are categorized into TCA acids, amino acids, sugars, and phenolic acids.

Of the TCA metabolites, citric acid constituted the vast majority (89.78%), which also resulted in a very strong correlation ($R^2 = 0.982$) (Table 3.4 and Figure 3.6). The lack of correlation with citric acid and weak, but positive correlation to total TCA acids could indicate that the pathways branching off of the TCA cycle separating citric acid from succinic acid and malic acid, glycolysis and glutamine synthesis, greatly affect the metabolite pools TCA acids.

Of the total amino acids, the aspartate branch represents the majority (69.39%) and the aspartate branch shows a very strong correlation ($R^2 = 0.887$) with the total, but shows a narrow-split pattern (Table 3.4 and Figure 3.10). The glutamine branch represented only 24.40% of the total amino acids and showed a distinct split pattern when correlated with the total (Table 3.4 and Figure 3.8). When the branches are correlated with each other, the correlation between the aspartate and glutamine branches also shows a distinct two split pattern (Figure 3.7). The branch-chain branch represents only a small percentage (6.21%) of total amino acids and shows a split pattern when correlated with total amino acids, aspartate branch, and glutamine branch

(Table 3.4 and Figures 3.7 and 3.9). The relative accumulations of the aspartate, glutamine, and branch-chain branches are different from the relative accumulations of published literature (Hernández-Orte, Cacho, & Ferreira, 2002; USDA, 2018; Hua Zhang et al., 2014). The discrepancy could be due to the different measurement and annotation methods as this research used non-targeted profiling and annotated only nine amino acids, while the published literature uses targeted profiling to annotate all 20 amino acids (Hernández-Orte et al., 2002; USDA, 2018; Hua Zhang et al., 2014). Further elucidation of the amino acid composition in the DxJ population needs targeted profiling and annotation of all the amino acids, which was outside the budget plan of this research. The correlation results with total amino acids indicates two groups within the DxJ population: one group shows an increase in both the total and specific branch accumulation, while the other group increases in only total amino acid accumulation. The correlation results between the branches shows very wide split patterns, which also suggests two groups within the DxJ population, but the increases in accumulation are more distinct: one group increases in branch-chain amino acids with little increase in aspartate branch, whereas the other group increases in aspartate branch amino acids with little increase in branch-chains.

The amino acid GABA accounted for 44.77% of the total glutamine branch and showed a strong positive correlation (Figure 3.8). Whereas, GABA showed a two split pattern when correlated with glutamine and arginine (Figure 3.8). This two split pattern is also seen when glutamine and arginine are correlated with total glutamine branch (Figure 3.8). These two split patterns concur with the branching in the glutamine branch biosynthesis pathway: GABA biosynthesis branches at glutamate with catabolism feeding into the TCA cycle, whereas glutamine and arginine synthesis also branch at glutamate with catabolism cycling back towards glutamate (Kanehisa et al., 2017; T. Kim et al., 2017). Aspartate and asparagine show strong correlations with total aspartate branch, which supports aspartate and asparagine accounting for 48.36% and 40.12% of total aspartate branch as well as being the initial metabolites in the aspartate branch pathway (Figure 3.10). Threonine and alanine show two split patterns when correlated with aspartate and asparagine, which concurs with the multiple branches in the aspartate catabolism pathway and with the other pathways that also contribute to

threonine and alanine accumulation (Figure 3.10) (Kanehisa et al., 2017; T. Kim et al., 2017).

Since glucose and fructose account for 51.84% and 47.14%, respectively, of total sugars, they show a strong correlation with total sugars as well as each other (Table 3.5 and Figures 3.11 and 3.12). This is supported in the literature as fructose and glucose are vital hexoses for signaling and synthesis of other hexose and polysaccharides (Buchanan et al., 2012; Couée, Sulmon, Gouesbet, & El Amrani, 2006; O'Hara, Paul, & Wingler, 2013; Rosa et al., 2009; Tsai & Gazzarrini, 2014; Wingler, 2017). The two split pattern seen in the correlations of glucose with galactose and xylose concurs with the hexose sugar interconversion pathway (Figure 3.12). Galactose is a glucose epimer and xylose is a glucose derivative through glucuronic acid, therefore, the glucose pool can be utilized for galactose or xylose synthesis as represented by the split pattern (Buchanan et al., 2012; Granot, David-Schwartz, & Kelly, 2013; Rosa et al., 2009). Arabinose +others also shows a two split pattern when correlated with glucose, which concurs with arabinose synthesis from xylose and supports the strong correlation between xylose and arabinose +others ($R^2 = 0.615$) (Figure 3.12) (Buchanan et al., 2012; Kong et al., 2015; Paulina Aguilera-Alvarado & Sanchez-Nieto, 2017).

The positive correlations of total phenolics acids with gallic acid, quinic acid, chlorogenic acid and epicatechin suggests each of those phenolic acids contributes to the accumulation of total phenolic acids (Figure 3.13). The positive correlations between gallic acid, chlorogenic acid, and epicatechin indicates that an increase in one will positively affect the accumulation of the others, possibly through inducing specific genes or through increasing substrate production (Figure 3.13) (Ali Ghasemzadeh, 2011; Castrejón, Eichholz, Rohn, Kroh, & Huyskens-Keil, 2008; Colak et al., 2017; Forney et al., 2012; He et al., 2010; Kraujalyte et al., 2015; Mattila, Hellström, & Törrönen, 2006; Prencipe et al., 2014; Routray & Orsat, 2014). Correlations of the other phenolic acids with caffeic acid +others shows a wide two split pattern, which suggests two groups within the DxJ population: one group accumulates both the phenolic acid and caffeic acid +others, while the other group accumulates the phenolic acid with very little caffeic acid +other accumulation (Figure 3.13). This pattern concurs with the branching of caffeic acid biosynthesis from phenylpropanoid acid synthesis (Kanehisa et al., 2017; T.

Kim et al., 2017). The positive correlations between total phenolic acids and the individuals is generally consistent with the published literature because this research measured multiple phenolic acids while other research did not measure as many (Brito, Areche, Sepúlveda, Kennelly, & Simirgiotis, 2014; Colak et al., 2017; Grace et al., 2018; D. Li et al., 2017; Montecchiarini et al., 2018; Oancea, Moiseenco, & Traldi, 2013; Routray & Orsat, 2014; Scalzo et al., 2015; H. Wang et al., 2017).

3.5.2. Metabolite Profiling with HPLC-QTOFMS Analysis

Due to the plethora of health benefits associated with blueberries and linked to their anthocyanins, anthocyanins were annotated and analyzed through targeted metabolite profiling using HPLC-QTOFMS. Anthocyanins are usually measured with HPLC using a UV detector at 520nm because anthocyanins have a UV absorbance (Barnes, Nguyen, Shen, & Schug, 2009; Khoo et al., 2017; D. Li, Meng, & Li, 2016; Lila et al., 2016; Ongkowijoyo, Luna-Vital, & Gonzalez de Mejia, 2018; Routray & Orsat, 2011; Silva et al., 2018; Skates et al., 2018). As mentioned previously, anthocyanins are stabilized as a flavylum ion when in acidic conditions (Khoo et al., 2017; Overall et al., 2017; Sasaki et al., 2014; Stevenson & Scalzo, 2012; Wahyuningsih et al., 2017). Therefore, acidified extractions and HPLC methods are commonly utilized when separating and quantifying that anthocyanin composition. Most HPLC methods for anthocyanins use acidic conditions and a variety of gradients to separate the anthocyanin metabolites while a UV detector like a DAD measures the anthocyanin metabolite (Barnes et al., 2009; Grace et al., 2018; Horbowicz et al., 2008; Ma et al., 2018; Overall et al., 2017; Routray & Orsat, 2011; Scalzo et al., 2015; Zifkin et al., 2012). Unfortunately, the DAD detector cannot separate the metabolite peaks that elute at the same time or detect anthocyanins in small quantities (Jaakola, 2002; Ongkowijoyo et al., 2018; Timmers, Grace, Yousef, & Lila, 2017; Shaoli Wang et al., 2017). These acidic HPLC methods, like the 5% formic acid in water method utilized in this research, is too caustic for injection into an MS instrument, thus researchers usually utilize either HPLC or MS to detect and annotate anthocyanins (Barnes et al., 2009; Ongkowijoyo et al., 2018; Ronald L Prior, Lazarus, Cao, Muccitelli, & Hammerstone, 2001). To utilize an MS for detecting anthocyanins, the extract or anthocyanins must be neutralized to a higher pH before injection (Barnes et al., 2009; Ongkowijoyo et al.,

2018; Ronald L Prior et al., 2001). The benefit of MS detection is that it can differentiate multiple peaks that elute at the same time and is very sensitive to low abundant metabolites with exact masses and EIC (Grace et al., 2018; Jaakola, 2002; Shaoli Wang et al., 2017). In order to utilize the benefits of the HPLC and the MS, the metabolite profiling method for this research used the acidic separation methods of HPLC and then used an auxiliary pump to dilute the HPLC sample output to 1% formic acid before injection into the QTOFMS.

With this optimized method, the anthocyanins were first detected by the DAD UV detector in the HPLC. The DAD measured 17 peaks that were annotated as 17 different anthocyanins (Table 3.7 and Figure 3.36) (Bornsek et al., 2012; Grace et al., 2018; Pertuzatti et al., 2016; Ronald L Prior et al., 2001; Reque et al., 2014; Routray & Orsat, 2011; Stevenson & Scalzo, 2012). The most abundant individual anthocyanin detected with DAD in these extracts is delphinidin-galactoside, which is not consistent with, but is one of the top five highest accumulating in the published literature (Table 3.9) (Brown, Murch, & Shipley, 2012; Castañeda-Ovando, Pacheco-Hernández, Páez-Hernández, Rodríguez, & Galán-Vidal, 2009; Grace et al., 2018; Howard et al., 2016; Lohachoompol, Mulholland, Szrednicki, & Craske, 2008; Montecchiarini et al., 2018; Routray & Orsat, 2011). The least abundant individual anthocyanin is cyanidin-acetylglucoside, which is consistent with the published literature (Table 3.9) (Brito et al., 2014; Bunea et al., 2013; Kalt, McDonald, Ricker, & Lu, 1999; D. Li et al., 2017; Ma et al., 2018; Oancea et al., 2013; Ronald L Prior et al., 2001; Stevenson & Scalzo, 2012; Zifkin et al., 2012; Zorenc et al., 2017). The most abundant anthocyanidin core is delphinidins, whereas the cyanidin anthocyanidin core was the least abundant (Table 3.8). Galactosides are the most abundant sugar moiety detected, whereas acetylglucosides were the least abundant (Table 3.8). These summation group results are consistent with the published literature (Brito et al., 2014; Grace et al., 2018; Howard et al., 2016; D. Li et al., 2017; Ma et al., 2018; Montecchiarini et al., 2018; Timmers et al., 2017; Zorenc et al., 2017).

When the anthocyanins were correlated with each other to gain some insight into their accumulation patterns, the glucosides showed a consistent “2-group” pattern that exhibited two distinct correlations (Figures 3.20 and 3.21). One correlation shows both

compounds increasing, while the other correlation showed only one compound increasing while the other shows very little accumulation change. For example, the correlation between total glucosides and total galactoside shows one correlation where both increase proportionally, whereas the other correlation shows only total galactoside increasing (Figure 3.21). A simplistic hypothesis for this “2-group” pattern is that the DxJ population contains two subsets of individuals. Each population subset contains specific genes that differentially regulate the accumulation of the sugar moieties. One subset of individuals has genes that allow for both glucosides and galactoside to accumulate, indicated with the red line in Figure 3.21. The other subset of individuals has different genes that allow for only the accumulation of galactoside or arabinoside and very little to no accumulation of glucosides, indicated with the green line in Figure 3.21. The different genes described in the example could consist of different gene alleles for functional and non-functional enzymes, different isozymes that exhibit different specificities, or different gene sets that could regulate multiple aspects of sugar moiety accumulation or modification (Castellarin & Di Gaspero, 2007; Jaakola, 2002; Khoo et al., 2017; W. Li et al., 2015; Muleke et al., 2017; Pinu et al., 2018; Rinaldo et al., 2015; Routray & Orsat, 2011; Sasaki et al., 2014; Yonekura-Sakakibara, 2009; Zorenc et al., 2017).

A very similar “2-group” pattern is seen in the correlation between total glucosides and total arabinosides, as well as with the correlation between the combinations of glucoside + acetyl-glucoside and galactoside + arabinoside (Figure 3.21). This strongly suggests that within the population, one subset of individuals (subset T) contains genes that allow for the accumulation of all four sugar moieties, whereas the other subset (subset A) has different genes that allow for the accumulation of only galactosides and arabinosides. When total anthocyanins were correlated with total glucosides and total glucosides + acetyl-glucoside, the correlation showed the same “2-group” pattern, which further suggests the population is separated into two subset groups (Figure 3.20). The correlations with total arabinosides showed a strong positive correlation ($R^2 = 0.607$), while the total galactosides and the combination of total galactosides + arabinosides correlations showed a narrow “2-group” pattern (Figure 3.20). One group accumulates more total anthocyanins than total galactosides + arabinosides, while the other group proportionally accumulates total anthocyanins and

total galactosides + arabinosides, which supports the two subset groups described for comparison of sugar combinations (Figure 3.21) (Castellarin & Di Gaspero, 2007; Jaakola, 2002; Khoo et al., 2017; W. Li et al., 2015; Muleke et al., 2017; Pinu et al., 2018; Rinaldo et al., 2015; Routray & Orsat, 2011; Sasaki et al., 2014; Yonekura-Sakakibara, 2009; Zorenc et al., 2017).

The hierarchical clustering of the individual DAD anthocyanins further supported the correlation results (Figure 3.22). Delphinidin derivative anthocyanidins clustered together in clusters A, C, and D. Cyanidin anthocyanidins clustered together in cluster B, as well as remained separate from the delphinidin derivatives within clusters C and D. The clustering of galactosides and arabinosides, clusters A and B, separate from the glucosides and acetyl-glucosides, clusters C and D, supports the distinct separation between glucoside derivatives and galactosides-arabinosides.

The optimized method in this research also allowed for anthocyanins to be measured using the MS detector. The exact mass (m/z) of known anthocyanins was utilized for EIC to annotate 23 different anthocyanins in the blueberry extracts (Table 3.10 and Figure 3.36) (Bornsek et al., 2012; Grace et al., 2018; Pertuzatti et al., 2016; Ronald L Prior et al., 2001; Reque et al., 2014; Routray & Orsat, 2011; Stevenson & Scalzo, 2012). The most abundant individual anthocyanin is malvidin-galactoside, whereas the least abundant is cyanidin-acetyl-galactoside (Table 3.12). The most abundant anthocyanidin is malvidins, whereas peonidin was the least abundant (Table 3.11). Galactosides are the most abundant sugar moiety detected, whereas acetyl-galactosides were the least abundant (Table 3.11). These individual anthocyanins and summation groups results are consistent with the published literature (Brito et al., 2014; Grace et al., 2018; Howard et al., 2016; Lohachoompol et al., 2008; Ma et al., 2018; Montecchiarini et al., 2018; Oancea et al., 2013; Routray & Orsat, 2011; Stevenson & Scalzo, 2012; Timmers et al., 2017; Zorenc et al., 2017). When the individual anthocyanins are correlated together, the glucosides show a very similar “2-group” pattern when correlated with galactosides or arabinosides (Figures 3.24 and 3.25). Similarly, glucosides with acetyl-glucosides correlated with the combined galactosides, acetyl-galactosides, and arabinosides also shows the “2-group” pattern (Figure 3.25).

The hierarchical clustering of the individual EIC anthocyanins supports the correlation patterns (Figure 3.26). Delphinidin derivative anthocyanidins cluster together in clusters B, C, D, and E. Cyanidin anthocyanidins clustered together in cluster A, while also remaining separated within cluster C, D, and E. The clustering of galactosides and arabinosides together, clusters A and B, supports the strong positive correlation between the sugars. The cluster of acetyl-galactosides separate, but linked to the galactoside-arabinoside clusters indicates a relationship. The clustering of the glucosides and acetyl-glucosides separate from the others, clusters D and E, further supports the correlations that glucoside derivatives and galactoside derivatives-arabinosides are distinguished by specific alleles in the different population subsets.

Therefore, the correlations and hierarchical clustering results both indicate the DxJ population is divided into two population subsets based on the accumulation of glucoside anthocyanins. One subset, subset T, consists of the 110 individuals that accumulate a substantial amount of glucosides, clusters 1-8 for both the DAD and EIC anthocyanins, with 67.3% of those individuals also accumulating acetyl-glucosides (Figures 3.22 and 3.26). The individuals in subset T also accumulate galactosides and arabinosides (Figures 3.21, 3.24, 3.25). The other subset, subset A, consists of 100 individuals that accumulate a very minimal amount of glucosides and acetyl-glucosides, while accumulating a large amount of galactosides and arabinosides (Figures 3.21, 3.24, 3.25). The accumulations of galactosides and arabinosides in subset A are greater than the accumulations in subset T (Figures 3.21, 3.24, 3.25). This suggests subset A favors a greater accumulation of galactosides or arabinosides, than glucosides. This could possibly occur through an increase in enzyme activity that transfers or converts the anthocyanin sugar moieties to galactosides or arabinosides (He et al., 2010; Overall et al., 2017; Routray & Orsat, 2011; Sasaki et al., 2014; Yonekura-Sakakibara et al., 2009). This is supported by the means of % of total anthocyanin for subset A for galactoside and arabinoside showing an increase when compared to subset T (15% to 24%, and 9% to 11%, respectively). Conversely, the mean of % of total anthocyanin for subset A for glucoside shows a decrease when compared to subset T (4% to 0.6%). To better understand the anthocyanin composition and diversification in blueberries, further elucidation of the pathway dynamics and enzyme kinetics regulating anthocyanin sugar

moiety modification should be a focus, especially glucoside and galactoside transferases.

The HPLC-QTOFMS profiling analysis annotated 17 anthocyanins using the DAD detector, while 23 anthocyanins were detected using EIC (Figure 3.36). The results show that there were overlapping anthocyanin peaks within the peaks detected using DAD (Figure 3.36). The results also suggest that some of the acetyl-glucosides and all the acetyl-galactosides may have been under the detection limit of the DAD detector. The EIC annotated six more anthocyanins because exact masses for peonidin-glucoside, peonidin-arabinoside, and acetyl-galactosides differentiated these compounds from within other peaks that the DAD could not distinguish and is more sensitive to small amounts (Figure 3.36). Both peonidin-glucoside and malvidin-galactoside show peak elution accumulation on average between 15.89 to 16.01 mins. This resulted in the peaks overlapping and preventing DAD detection from distinguishing them, as indicated in Figure 36 as peaks labeled A and 11, respectively. Since their m/z are very different, detection using EIC allowed for the peaks to be integrated separately (Figure 3.36). Malvidin-glucoside eluted on average around 16.54mins, as seen as peak 12 in Figure 36. Right after 16.54mins, peonidin-arabinoside and delphinidin-acetyl-galactoside also eluted at 16.70mins and 16.60mins, as indicated as peaks labeled D and B respectively (Figure 3.36). The DAD was not able to distinguish two other metabolites, whereas EIC detection could distinguish using the different m/z . Cyanidin-acetyl-galactoside (17.68mins) eluted within the tail-end of the malvidin-arabinoside peak (17.35mins) as indicated by peaks labeled 13 and C, respectively (Figure 3.36). Similarly, petunidin-acetyl-galactoside (18.39mins) eluted right at the end of the delphinidin acetyl-glucoside peak (18.26mins), while malvidin-acetyl-galactoside (19.61mins) eluted at the end of cyanidin-acetyl-glucoside (19.33mins), as indicated by peaks labeled 14 and P, and 15 and M respectively (Figure 3.36). The DAD detector also did not integrate or annotate the acetyl-galactosides due to the very small accumulation and limited sensitivity. The limited sensitivity is also seen with the acetyl-glucosides as DAD-acetyl-glucosides accounted for 0.89% of total anthocyanins, whereas EIC-acetyl-glucosides accounted for 2.04% of total anthocyanins.

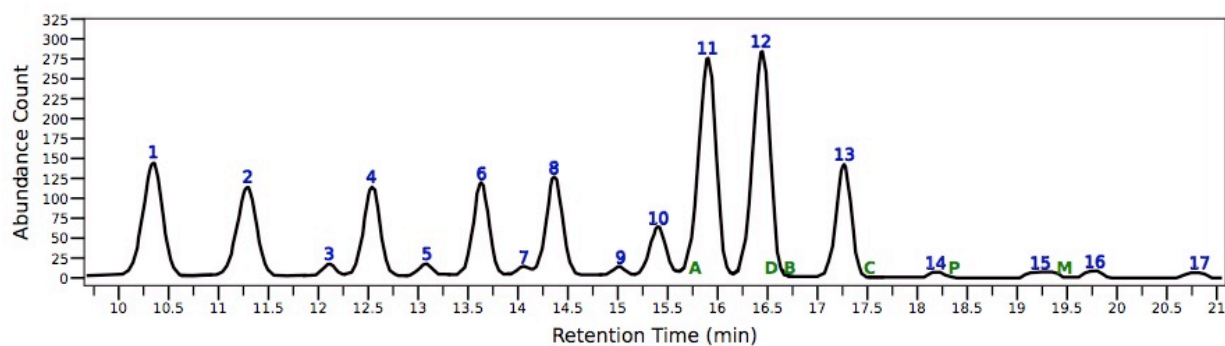


Figure 3.36 – Anthocyanin spectra from the HPLC-QTOFMS with peaks representing the relative locations of DAD-detected individual anthocyanins. Blue numbers indicate the 17 anthocyanins detected using DAD. The green letters indicate the additional six anthocyanins and relative elution times that were detected using EIC.

Overall, the correlations between DAD-anthocyanins and EIC-anthocyanins show a mediocre positive correlation with some showing stronger correlations than others (Figures 3.27, 3.28, 3.29, 3.30, and 3.31). The correlation between total arabinosides as well as the individual correlations for three of the anthocyanidin-arabinosides exhibited the weakest correlations (Figures 3.27, 3.28, 3.29, 3.30, and 3.31). The vast majority of anthocyanin annotation research utilizes either HPLC-UV/Vis detectors like DAD, or MS-exact mass detectors through EIC, therefore, there is a lack of previously published literature investigating possible detection differences for anthocyanins or flavonoids (Brito et al., 2014; Brown et al., 2012; Grace et al., 2018; Howard et al., 2016; Lohachoompol et al., 2008; Ma et al., 2018; Montecchiarini et al., 2018; Ronald L Prior et al., 2001; Routray & Orsat, 2011; Stevenson & Scalzo, 2012; Zifkin et al., 2012). Since MS-EIC detection is more sensitive than HPLC-DAD detection, the discrepancy could be the MS-EIC detecting individuals with low accumulation the HPLC-DAD did not detect (Bingol, 2018; Matsuda, 2016; Pinasseau et al., 2017; Scalbert et al., 2009; Sumner et al., 2015; Theodoridis et al., 2008). The higher sensitivity of MS-EIC could also detect small differences in an individual's accumulation that the HPLC-DAD could not detect, which could lead to more variation across the population (Bingol, 2018; Matsuda, 2016; Pinasseau et al., 2017; Scalbert et al., 2009; Sumner et al., 2015; Theodoridis et al., 2008). Further research and repeat profiling is necessary to elucidate this discrepancy. The total anthocyanin correlation between DAD and EIC shows a

positive trend ($R^2 = 0.333$) (Figures 3.33 and 3.34). The glucosides and acetyl-glucosides showed the best correlations between the detection methods, while cyanidin derivatives showed the strongest correlations between the detection methods for the anthocyanidins.

The BiPAM of the 17 anthocyanins detected with the DAD detector revealed 56 significant QTL regions, while the 11 different summation groups revealed 19 significant QTL regions (Table 3.17). To further investigate the specific anthocyanin composition, ratios between the five anthocyanidin cores as well as four sugar moieties were also mapped with BiPAM (Table 3.18). On linkage group five between positions 71cM and 73cM, there are multiple significant QTLs for both delphinidin and cyanidin anthocyanidin core accumulation and ratios, and for different sugar moiety ratios like total galactosides to total glucosides (Table 3.19). This suggests the genetic region for these overlapping QTLs contains multiple candidate genes involved in overall anthocyanin biosynthesis or in differentiating the specific anthocyanidin cores and different sugar moiety modifications (Castellarin & Di Gaspero, 2007; He et al., 2010; Khoo et al., 2017; W. Li et al., 2015; Muleke et al., 2017; Pinu et al., 2018; Rinaldo et al., 2015; Sasaki et al., 2014; Seymour, Chapman, Chew, & Rose, 2013; Yonekura-Sakakibara, 2009). The large number of diverse significant QTLs for different anthocyanidin cores and sugar moieties overlapping in the same genetic region was also found on linkage group 10 between positions 0cM and 15cM (Table 3.19). On linkage group 11 between positions 129cM and 136cM, there are significant QTLs for not only total anthocyanins and delphinidin derivative ratio, but also multiple cyanidin derivative accumulations and ratios (Table 3.19). This suggests the genetic region may contain candidate genes involved in overall anthocyanin synthesis as well as cyanidin derivative specific accumulation like enzymes involved in the branching of the flavonoid pathway (He et al., 2010; Kanehisa et al., 2017; Khoo et al., 2017; T. Kim et al., 2017).

The structure of the five anthocyanidin cores found in blueberries: delphinidin, petunidin, malvidin, cyanidin, and peonidin, are different from each other due to methylation of the hydroxyl group (Figure 3.1). On linkage group one at position 47cM, significant QTLs for the summations of all delphinidins and all petunidins have overlapping regions, which suggests the genetic region may contain candidate genes

involved in delphinidin derivative synthesis (Table 3.19). Significant QTLs for delphinidin derivative synthesis and diversification were also found overlapping in the genetic region on linkage group nine at position 18cM, and on linkage group 11 between positions 53cM and 60cM (Table 3.19). These overlapping QTLs suggest the genetic region may contain candidate genes also involved in delphinidin derivative synthesis as well as delphinidin anthocyanidin core diversification with methylation (Castellarin & Di Gaspero, 2007; He et al., 2010; Kanehisa et al., 2017; T. Kim et al., 2017; W. Li et al., 2015; Yonekura-Sakakibara et al., 2009; Zifkin et al., 2012). Significant QTLs for anthocyanidin core diversification also overlapped on linkage group one between positions 8cM and 15cM, on linkage group two at position 32cM, on linkage group two between positions 63cM and 67cM, on linkage group four at positions 18cM, 29cM, and 43cM, on linkage group four between positions 127cM and 132cM, on linkage group six at position 43cM, on linkage group eight between positions 87cM and 93cM, on linkage group 12 at positions 18cM and 25cM, and on linkage group 12 between positions 70cM and 74cM (Table 3.19). This suggests the genetic regions may contain candidate genes involved in methylation of the different anthocyanidin cores (Castellarin & Di Gaspero, 2007; He et al., 2010; Kanehisa et al., 2017; T. Kim et al., 2017; W. Li et al., 2015; Yonekura-Sakakibara et al., 2009; Zifkin et al., 2012).

Of the 75 total significant QTL regions, 64% of the QTL regions are significant for anthocyanins with acetyl-glucoside sugar moieties (Tables 3.17 and 3.18). On linkage group one between 8cM-15cM, there are significant QTLs for multiple acetyl-glucoside anthocyanins as well as multiple acetyl-glucoside ratios like total acetyl-glucosides to total anthocyanins or total acetyl-glucosides to total glucosides (Table 3.19). There are also very similar overlapping significant QTLs on linkage group one at position 63cM, on linkage group two between positions 37cM and 41cM, on linkage group four between positions 127cM and 132cM, on linkage group eight between positions 87cM and 93cM, on linkage group nine at position 27cM, on linkage group 12 between positions 10cM and 18cM, and on linkage group 12 between positions 70cM and 74cM (Table 3.19). This suggests the genetic regions for each overlapping region may contain candidate genes involved in the synthesis of glucoside and acetyl-glucoside anthocyanins. On linkage group two at position 25cM, there are several significant QTLs for acetyl-

glucoside anthocyanins, primarily with delphinidin derivative anthocyanidin cores, which suggests the genetic region containing candidate genes involved in acetyl-glucoside sugar modification with specificity for delphinidin derivative anthocyanidin cores (Table 3.19). On linkage group eight at position 107cM, there are overlapping significant QTLs for cyanidin-acetyl-glucoside accumulation and ratio, which suggests the genetic may contain a candidate gene for acetyl-glucoside sugar modification with specificity for cyanidin core anthocyanidins (Table 3.19).

The distinctive “2-group” pattern seen from correlations of galactoside and arabinoside with glucoside and acetyl-glucoside strongly suggested the ratio between the different sugar moieties should be BiPAM mapped. As a result, there were multiple significant QTLs for the different sugar moiety ratios (Table 3.18). On linkage group two at position 32cM, there are significant QTLs for the different sugar moiety ratios that have overlapping genetic regions (Table 3.19). There are also very similar overlapping significant QTLs on linkage group two at positions 65cM and 83cM, on linkage group three at position 122cM, on linkage group four between positions 14cM and 20cM, on linkage group four at position 31cM, on linkage group six at position 43cM, scaffold 6.5 between positions 28cM and 32cM, on linkage group 12 at positions 25cM and 59cM, and on linkage group 12 between positions 70cM and 74cM (Table 3.19). Since the overlapping QTLs are primarily the ratios between galactoside-glucoside, arabinoside-glucoside, and the combinations of galactoside-arabinoside to glucoside-acetyl-glucoside, the genetic region may contain candidate genes involved in specifically adding different sugar moieties, like a UDP-sugar transferase that specifically transfers galactosides or arabinosides (Castellarin & Di Gaspero, 2007; Grace et al., 2018; Sasaki et al., 2014; Yonekura-Sakakibara, 2009). On linkage group one between positions 8cM and 15cM, there are multiple significant QTLs for the different sugar moiety ratios with cyanidin derivative anthocyanidin cores that have overlapping genetic regions (Table 3.19). Similar significant QTLs for cyanidin derivative sugar moiety ratios were also found overlapping in genetic regions on linkage group one between positions 30cM and 32cM, on linkage group one at position 52cM, on linkage group two between positions 37cM and 41cM, on linkage group three between positions 28cM and 36cM, on linkage group three at position 49cM, on linkage group four between positions

127cM and 132cM, on linkage group 11 between positions 37cM and 40cM, and on linkage group 12 at positions 37cM, 49cM, and 52cM (Table 3.19). This suggests that the genetic region may contain similar candidate genes that affect the transfer of specific sugar moieties, but may also exhibit further specificity towards cyanidin derivative anthocyanidin cores (Castellarin & Di Gaspero, 2007; Grace et al., 2018; Routray & Orsat, 2011; Sasaki et al., 2014; Yonekura-Sakakibara, 2009)..

In summary, the acidified extraction and method for targeted metabolite profiling of blueberries using HPLC successfully separated 17 anthocyanin peaks that were detected by the HPLC UV-DAD detector (Table 3.7). The dilution of the high-acid solutions from this HPLC method before injection into the TOFMS allowed for the successful detection of six additional anthocyanins through EIC detection as these six anthocyanins co-eluted within other anthocyanin peaks (Figure 3.36 Table 3.10). This optimized methodology that allowed for injection into the MS is an important initial step towards improving anthocyanin diversity detection. But this methodology should be continually optimized for a diversity of fruits and consistency through replicate profiling and sampling so that the diversity of anthocyanins can be appropriately determined (Barnes et al., 2009; Grace et al., 2018; Oancea et al., 2013; Ongkowitzo et al., 2018; Pertuzatti et al., 2016; Pinu et al., 2018; Ronald L Prior et al., 2001; Shouchuang Wang et al., 2017). Both the DAD and EIC detected anthocyanins showed a similar “2-group” pattern that separated the DxJ population into two subsets. One subset accumulates the four different sugar moieties, while the other subset accumulates significantly more galactosides and arabinosides over glucosides (Figures 3.21, 3.24, and 3.25). The BiPAM results revealed multiple significant QTLs with many of the significant QTLs for anthocyanidin core diversification, acetyl-glucoside specific ratios, and sugar moiety differentiation ratios overlapping in the same genetic region, which strongly suggests those genetic regions may have important candidate genes involved in specific aspects of anthocyanin diversification (Tables 3.17, 3.18, and 3.19). Further elucidation of the anthocyanin synthesis and modification pathway will provide a greater understanding of anthocyanin diversity and regulation, especially when anthocyanin sugar modifications affect the different sugars available for energy conversion, signaling, or cell wall matrix modifications (Buchanan et al., 2012; Castañeda-Ovando et al., 2009; Grace et al.,

2018; Khoo et al., 2017; Posé, Nieves, Quesada, & Mercado, 2011; Tsai & Gazzarrini, 2014; Yonekura-Sakakibara et al., 2009). It is important for future research on anthocyanin composition and diversity that a similar method, directly injecting the HPLC separated anthocyanins into the MS through diluting the acidic extract before injection, be utilized so that better annotation of low abundant or co-eluting anthocyanins can occur and potentially identify novel anthocyanins.

3.5.3. DPPH Assay for Antioxidant Capacity

The DPPH-antioxidant capacity assay is a quick, cost-effective, and reproducible assay that measures the ROS-RNS radical scavenging ability of a solution (Colak et al., 2016; Correia, Grace, Esposito, & Lila, 2017; Himamura et al., 2014; Huang et al., 2005; Mishra et al., 2012; Moharram & Youssef, 2014; O. P. Sharma & Bhat, 2009). Each of the blueberry extracts were replicated at least 10 times between three individuals, which revealed the necessity of preparing fresh DPPH stock everyday as well as meticulous pipetting skills. Multiple extracts and plates were repeated multiple times due to the cold acidified-methanol extracts losing tension in the tip. Allowing the extracts to come to room temperature aided in minimizing this dilemma. The resulting DPPH-antioxidant capacity values were correlated to individual anthocyanins as well as summation groups (Figures 3.33 and 3.34). DPPH-antioxidant capacity correlated strongly with the DAD-total anthocyanins ($R^2 = 0.791$), while the EIC-total anthocyanins exhibited a modest correlation ($R^2 = 0.472$) (Figures 3.33 and 3.34). This overall positive correlation for total anthocyanins and DPPH-antioxidant capacity is supported by previously published literature from multiple different researchers (Aurelia Magdalena Pisoschi et al., 2016; Colak et al., 2017; Galano et al., 2016; D. Li et al., 2017; Neto, 2007). The DPPH-antioxidant capacity and NMR known metabolites correlations utilized the merged years datasets. These correlations revealed that gallic acid, chlorogenic acid, and epicatechin show a positive correlation with DPPH-antioxidant capacity (Figure 3.35). This supports the published literature that anthocyanins play an important role in DPPH-antioxidant capacity, as well as other published literature in other fruits indicate that other phenolic acids contribute to the antioxidant capacity (Colak et al., 2016; Correia et al., 2017; Himamura et al., 2014; Mishra et al., 2012; O. P. Sharma & Bhat, 2009).

Overall, the acidified blueberry extracts exhibited a strong antioxidant capacity when measured with the DPPH-scavenging assay (Table 3.13) (Colak et al., 2017; D. Li et al., 2017, 2016; Neto, 2007). The correlations between DPPH-antioxidant capacity and metabolites annotated from the metabolite profiling showed no strong correlations with individual metabolites (Figures 3.33, 3.34, and 3.35). This suggests the strong antioxidant capacity of blueberries is a result of a combination of metabolites acting synergistically (Aurelia Magdalena Pisoschi et al., 2016; Colak et al., 2017; Galano et al., 2016; D. Li et al., 2017; Neto, 2007). Overall, the moderate positive correlation in this research supports the strong association of antioxidant capacity and anthocyanins, while also suggesting other metabolites contributing to the potency (Figure 3.36) (Aurelia Magdalena Pisoschi et al., 2016; Colak et al., 2017; Galano et al., 2016; D. Li et al., 2017; Neto, 2007). More thorough metabolite profiling of a variety of blueberry extracts will further elucidate the other metabolites that are contributing to blueberry antioxidant capacity (Chiva-Blanch & Visioli, 2012; Lobo et al., 2010; Moharram & Youssef, 2014; Niki, 2011). Future blueberry extract research should also investigate the biological antioxidant capacity through cell culture assays to determine the antioxidant capacity and effectiveness within a biological system (Ahmadinejad et al., 2017; Aurelia Magdalena Pisoschi et al., 2016; N. Singh & Ghosh, 2019).

3.5.4. TCA Cycle and Amino Acid Significant QTLs and Putative Candidate Genes

3.5.4.1. TCA Cycle Pathway

The TCA acids were grouped with amino acids during QTL and candidate gene analysis because the TCA cycle provides the starting substrates and the multiple amino acid pathways branch off at certain points of the TCA cycle (Kanehisa et al., 2017; T. Kim et al., 2017). Pyruvate not only feeds into the TCA cycle with its conversion to acetyl-CoA, but also is utilized in multiple amino acid biosynthesis pathways. Pyruvate is converted to acetyl-CoA by the pyruvate dehydrogenase complex. The first subunit, pyruvate dehydrogenase, is the rate-limiting step that binds together pyruvate and thiamine pyrophosphate to create an unstable intermediate that rearranges into a lipoate-thioester. The second and third subunits, dihydrolipoamide acetyltransferase and dehydrogenase, transfers the acetyl group to Coenzyme-A and regenerates the lipoamide and produces NADPH. The first subunit, pyruvate dehydrogenase, was found

in the QTL regions, on linkage group four at positions 27cM, and linkage group 12 at position 49cM, which contained significant markers for malic acid and citric acid (Table 3.20). The second subunit, dihydrolipoamide acetyltransferase, was found within the QTL region on linkage group two a position 32cM and 37cM where there are significant markers for citric acid and malic acid, respectively (Table 3.20). Along with the first subunit, the third subunit, dihydrolipoamide dehydrogenase, was also found in the QTL region on linkage group 12 at position 10cM and 12cM, where there are significant markers for citric acid and malic acid (Table 3.20).

The first step within the TCA cycle is the conversion of acetyl-CoA into citrate by citrate synthase, which requires oxaloacetate (Buchanan et al., 2012; Kanehisa et al., 2017; T. Kim et al., 2017). The putative candidate gene ATP-citrate synthase was also found within the QTL region on linkage group four at position 29cM and linkage group 12 at position 49cM, both with significant markers for citric acid, thus indicating the QTL regions may be important in regulating the start of TCA cycle (Table 3.20). Since ATP-citrate synthase needs oxaloacetate, its production from malic acid by malate dehydrogenase also plays an important role in the TCA cycle. Malate dehydrogenase was found as a putative candidate gene within the QTL regions on linkage group one at position 19cM for citric acid marker, linkage group three at position 59cM for a significant citric acid marker, and linkage group 12 at position 74cM with significant markers for citric and malic acid (Table 3.20). Oxaloacetate can also be synthesized from phosphoenolpyruvate by phosphoenolpyruvate carboxylase. Phosphoenolpyruvate carboxylase was found as another important putative candidate gene in the QTL regions on linkage group two at position 32cM and 37cM for citric and malic acid, and on linkage group three at position 59cM for citric acid (Table 3.20).

The next step in the TCA cycle utilizes aconitase to interconvert citrate to isocitrate (Kanehisa et al., 2017; T. Kim et al., 2017). Aconitase was found as a putative candidate gene in the QTL region on linkage group three at position 36cM with a significant marker for citric acid (Table 3.20). The next step of the TCA cycle is very important as it provides a vital substrate utilized by multiple amino acid pathways. Isocitrate dehydrogenase converts isocitrate to 2-oxoglutarate. Isocitrate dehydrogenase was found in multiple QTL regions with significant markers for

metabolites further discussed in the glutamine branch pathway section as 2-oxoglutarate is the branch point for the glutamine branch pathway (Table 3.20). In the next step of the TCA cycle, 2-oxoglutarate is converted to succinyl-CoA by the oxoglutarate dehydrogenase complex, which closely resembles the pyruvate dehydrogenase complex with three major subunits. The first subunit, 2-oxoglutarate dehydrogenase and rate-limiting enzyme in the complex, was found as a putative candidate gene in the QTL region on linkage group nine at position 25cM with a significant marker for succinic acid +others and malic acid (Table 3.20). Although the enzyme that converts succinyl-CoA to succinic acid, succinyl-CoA synthase, was not found as a putative candidate gene within the significant QTLs, it does not indicate that succinyl-CoA synthase does not play an important role in the TCA cycle, but that the DxJ population might not have variation for this enzyme that would result in significant QTLs. Since succinic acid accumulation did show variation throughout the population, there are probably other enzymes, that affect succinic acid accumulation. Succinate semialdehyde dehydrogenase can affect succinic acid accumulation as it converts succinate semialdehyde to succinic acid. Succinate semialdehyde dehydrogenase was found as a putative candidate gene in the QTL regions on linkage group three at position 88cM for succinic acid +others, on linkage group 12 at position 12cM for succinic acid +others and malic acid, and on linkage group 12 at position 61cM for succinic acid +others and malic acid (Table 3.20).

Other pathways also produce TCA acids to provide substrates for the TCA cycle, especially interconversions with glyoxylate (Kanehisa et al., 2017; T. Kim et al., 2017). Isocitrate lyase interconverts isocitrate with glyoxylate and succinic acid, skipping 2-oxoglutarate and succinyl-CoA. On linkage group three at position 34cM and 36cM, there is a QTL region with significant markers for succinic acid +others and citric acid with the putative candidate gene isocitrate lyase (Table 3.20). Malate synthase is another enzyme that utilizes glyoxylate as well as acetyl-CoA to produce malic acid and free coenzyme-A. On linkage group four at position 43cM, there is a QTL region with a significant marker for citric acid and the putative candidate gene malate synthase (Table 3.20).

In summary, the non-targeted profiling using ^1H NMR annotated three acid metabolites important in the TCA cycle, citric acid, succinic acid, and malic acid (Table 3.4). Even though citric acid is the prominent acidic metabolite, citric acid did not correlate with succinic or malic acid, but succinic and malic acid correlated with each other (Table 3.4, Figure 3.6). The BiPAM of the TCA acids revealed multiple, significant QTL regions with putative candidate genes involved in multiple steps of the TCA cycle (Table 3.20) (Buchanan et al., 2012; Kanehisa et al., 2017; T. Kim et al., 2017). The most significant citric acid QTL region contains malate dehydrogenase as a putative candidate gene, which regulates the production of oxaloacetate, a vital substrate for citric acid synthesis, from malic acid (Table 3.20). The very significant, overlapping QTLs for succinic acid and malic acid contain the putative candidate genes for the 2-oxoglutarate dehydrogenase complex, which is a vital regulator of TCA cycle progression to succinic and malic acid synthesis (Table 3.20). The identification of significant QTLs and putative candidate genes regulating TCA acid accumulation provides important foundational information for blueberry-specific TCA cycle genes and will aid in further elucidation of other TCA cycle genes. These QTLs and putative candidate gene results can be used in future breeding strategies to improve TCA acid accumulation and potentially increase the overall amino acid accumulation (Buchanan et al., 2012; Ufaz & Galili, 2008; G. Wang, Xu, Wang, & Galili, 2017).

3.5.4.2. Glutamine Branch Pathway

The glutamine branch pathway group consists of the NMR annotated metabolite peaks for glutamine, γ -aminobutyric acid (GABA), and arginine because their synthesis begins with 2-oxoglutarate converting to glutamic acid by the glutamate dehydrogenase complex (Buchanan et al., 2012; Kanehisa et al., 2017; T. Kim et al., 2017). Recent research has tentatively suggested that additional consumption of GABA may positively affect neuron and brain function (Boonstra et al., 2015; Bown & Shelp, 2016; Diana, Quílez, & Rafecas, 2014; Ramesh et al., 2015). The pools of 2-oxoglutarate, glutamate, and glutamine are essential to the biosynthesis of multiple different amino acids, thus enzymes that regulate interconversion between 2-oxoglutarate, glutamate, and glutamine are important for overall amino acid (Buchanan et al., 2012; Kanehisa et al., 2017; T. Kim et al., 2017). Therefore, identifying significant QTLs with putative

candidate genes involved in glutamine branch biosynthesis is important for gaining a greater understanding of amino acid biosynthesis for future breeding strategies. As mentioned previously, 2-oxoglutarate is synthesized from isocitrate by isocitrate dehydrogenase (Kanehisa et al., 2017; T. Kim et al., 2017). Isocitrate dehydrogenase was found as a putative candidate gene in two QTL regions both on linkage group 12 at positions 49cM and 61cM with two corresponding significant markers for glutamine (Table 3.20). Glutamate is interconverted with glutamine and 2-oxoglutarate by glutamate synthase (ferredoxin-dependent), which was found as a putative candidate gene in the QTL region with a significant marker for glutamine on linkage group nine at position 25cM (Table 3.20) (Kanehisa et al., 2017; T. Kim et al., 2017).

Glutamate dehydrogenase, the first subunit and rate-limiting enzyme in the glutamate dehydrogenase complex, interconverts 2-oxoglutarate with glutamate, similarly to pyruvate dehydrogenase complex (Kanehisa et al., 2017; T. Kim et al., 2017). Glutamate dehydrogenase was found as a putative candidate gene in the QTL regions with significant markers for GABA on linkage group eight at position 107cM and linkage group nine at position 25cM (Table 3.20). Glutamate is the substrate for GABA synthesis as glutamate decarboxylase, the first committing step, converts glutamate to GABA. Glutamate decarboxylase was found as a putative candidate gene on linkage group two at position 37cM with a significant marker for GABA (Table 3.20). In the QTL region on linkage group eight at position 108cM for GABA, there was also the putative candidate gene for gamma-aminobutyrate transaminase, which interconverts GABA with succinate semialdehyde (Table 3.20). The GABA pathway completes when succinate semialdehyde is converted to succinic by succinic semialdehyde dehydrogenase, as mentioned previously, and significant markers for GABA were also found in those QTL regions on linkage group three at position 88cM, on linkage group 12 at position 12cM, and on linkage group 12 at position 61cM (Table 3.20).

The glutamate pool can also be contributed to when glutamate-glyoxylate aminotransferase converts glycine and 2-oxoglutarate to glutamate (Kanehisa et al., 2017; T. Kim et al., 2017). Glutamate-glyoxylate aminotransferase was found in the QTL region with a significant marker for glutamine on linkage group four at position 27cM (Table 3.20). Arginine is another amino acid that is part of the glutamine branch as its

biosynthesis starts with both glutamine and glutamate. As one of the first steps towards arginine synthesis, glutamine is converted to carbamoyl-phosphate by carbamoyl-phosphate synthase, which was found as a putative candidate gene in two QTL regions with significant markers for arginine both on linkage group three at positions 59cM and 84cM (Table 3.20). Arginine synthesis utilizes ornithine, which is synthesized from N-acetyl-glutamate semialdehyde by N2-acetylornithine aminotransferase to produce N-acetyl-ornithine, which is then converted to ornithine by acetylornithine deacetylase. In QTL regions with significant markers for arginine, N2-acetylornithine aminotransferase was found on linkage group 12 at position 61cM, and acetylornithine deacetylase was found on linkage group three at position 34cM (Table 3.20). Carbamoyl-phosphate and ornithine are condensed together by ornithine carbamoyltransferase to produce citrulline, which is rapidly converted to arginine through multiple pathways. Ornithine carbamoyltransferase was found as a putative candidate gene in a QTL region on linkage group six at position 101cM with a significant marker for arginine (Table 3.20).

In summary, the non-targeted profiling using ¹H NMR annotated three amino acids that are part of the glutamine branch biosynthesis pathway, glutamine, GABA, and arginine (Table 3.4). The glutamine branch amino acids constitute 24.4% of the total amino acids and shows a narrow-split correlation pattern with the total amino acids (Table 3.4, Figure 3.8). The BiPAM of the glutamine branch amino acids revealed multiple, significant QTL regions with putative candidate genes involved in regulating the glutamate-glutamine interconversion and GABA synthesis (Table 3.20). The very significant glutamine QTL region contains ferredoxin-dependent glutamate synthase, which regulates the interconversion between glutamate and glutamine (Table 3.20) (Buchanan et al., 2012; Kanehisa et al., 2017; T. Kim et al., 2017).. The most significant GABA QTL region contains glutamate decarboxylase, the committing step that converts glutamate to GABA (Table 3.20) (Buchanan et al., 2012; Kanehisa et al., 2017; T. Kim et al., 2017). Since glutamate and glutamine are important substrates for synthesis of many other amino acids, identifying significant QTLs and putative candidate genes will provide important regulatory knowledge for improving overall production of amino acids (Buchanan et al., 2012; Kanehisa et al., 2017; T. Kim et al., 2017; G. Wang et al., 2017). In addition, elucidating blueberry-specific genes regulating GABA synthesis will

provide foundational information that will aid in future improvements in GABA accumulation, thus improved blueberry health benefits (Boonstra et al., 2015; Bown & Shelp, 2016; Diana et al., 2014).

3.5.4.3. Branched-Chain Branch Pathway

Another important amino acid biosynthesis pathway is the branch-chain branch pathway because it includes the biosynthetic enzymes for isoleucine, valine, isopropylmalic acid, and leucine synthesis (Kanehisa et al., 2017; T. Kim et al., 2017). Isoleucine, valine, and leucine are essential amino acids, which are important for human health, thus identifying QTLs and putative regulatory candidate genes will aid in gaining a greater understanding of their biosynthesis (Peng, Uygun, Shiu, & Last, 2015; Ufaz & Galili, 2008; G. Wang et al., 2017). These results will also aid in future breeding strategies to produce blueberry cultivars with improved essential amino acid accumulation, which will further enhance the health benefits of blueberries (Buchanan et al., 2012; Ufaz & Galili, 2008; G. Wang et al., 2017). Valine and leucine synthesis starts with pyruvate, with isopropylmalic acid as an intermediate metabolite in leucine synthesis after its divergence from valine (Kanehisa et al., 2017; T. Kim et al., 2017). Pyruvate kinase catalyzes the last step in glycolysis, converting phosphoenolpyruvate into pyruvate. Pyruvate kinase was found as a putative candidate gene in the QTL region with a significant marker for leucine and valine on linkage group one at position 14cM (Table 3.20). Although isoleucine synthesis starts with threonine, isoleucine and valine synthesis pathways use very similar biosynthesis enzymes.

The first committing step in branch-chain amino acid synthesis is acetolactate synthase producing acetolactate for isoleucine, valine, and leucine biosynthesis (Kanehisa et al., 2017; T. Kim et al., 2017). Acetolactate synthase was found as a putative candidate gene in the QTL regions on linkage group six at position 55cM and on linkage group 12 at position 12cM, with both having significant markers for isoleucine and threonine (Table 3.20). The last step in isoleucine, valine, and leucine synthesis is catalyzed by branch-chain amino acid aminotransferase. Branch-chain amino acid aminotransferase was found as a putative candidate gene in QTL regions significant for isoleucine, valine, and leucine on linkage group four at position 43cM (Table 3.20).

The enzyme, 3-isopropylmalate dehydrogenase, catalyzes the conversion of isopropylmalic acid to 4-methyl-2-oxopentanoate, which is utilized by the branch-chain amino acid aminotransferase to produce leucine (Kanehisa et al., 2017; T. Kim et al., 2017). 3-isopropylmalate dehydrogenase was found in two QTL regions both on linkage group 12 at positions 49cM with significant markers for isopropylmalic acid, leucine and valine, and at position 59cM with significant markers for leucine and valine (Table 3.20). 3-isopropylmalic acid was also found in the QTL region with significant markers for isoleucine, valine, and leucine on linkage group five at position 107cM along with putative candidate genes for the branched-chain alpha-keto dehydrogenase complex subunits 1 and 3 (Table 3.20). The branch-chain alpha-keto dehydrogenase complex is very similar to the pyruvate complex subunits as it catalyzes the catabolism of branch-chain amino acids.

In summary, the ¹H NMR non-targeted profiling annotated the three branch-chain amino acids, isoleucine, leucine, and valine, along with the leucine biosynthesis intermediate, isopropylmalic acid (Table 3.4). The branch-chain branch metabolites constituted only 6% of the total amino acid content with valine accounted for 41% of the branch-chain branch metabolites (Table 3.4). Isoleucine, leucine, and valine all showed strong correlations with each other (Figure 3.9). Isopropylmalic acid showed a wide-split pattern when correlated with leucine, thus indicating part of isopropylmalic acid accumulation is affected by another pathway (Figure 3.9). The BiPAM of branch-chain branch amino acids revealed multiple significant QTLs containing putative candidate genes involved in catalyzing important steps in the pathway (Table 3.20). The most significant isoleucine, leucine, and valine QTLs overlapped in the same region and contained the branch-chain amino acid aminotransferase putative candidate genes that catalyzes the final biosynthesis step (Table 3.20) (Buchanan et al., 2012; Kanehisa et al., 2017; T. Kim et al., 2017). Since isoleucine, leucine, and valine are essential amino acids, elucidating the synthesis and degradation genes in blueberry will aid in future breeding to improve essential amino acid accumulation and health benefits (Buchanan et al., 2012; Kanehisa et al., 2017; T. Kim et al., 2017; Ufaz & Galili, 2008; G. Wang et al., 2017).

3.5.4.4. Aspartate Branch Pathway

The other important amino acid synthesis branch pathway in this research is the aspartate branch. The aspartate, asparagine, threonine, and alanine metabolite peaks are part of the aspartate branch because their biosynthesis begins with aspartate synthesis from the TCA cycle (Jander & Joshi, 2009; Kanehisa et al., 2017; T. Kim et al., 2017). Aspartate biosynthesis begins with either fumarate conversion by aspartate oxidase, or oxaloacetate conversion by aspartate transaminase (Kanehisa et al., 2017; T. Kim et al., 2017). Aspartate can then be interconverted to asparagine or converted to aspartate-4-phosphate by aspartokinase. Asparagine synthase was found as a putative candidate gene in the QTL region with a significant marker for aspartate on linkage group three at position 117cM (Table 3.20). Aspartokinase was found as a putative candidate gene in a QTL region on linkage group 12 at position 49cM with a significant marker for aspartate and asparagine (Table 3.20). Aspartokinase was also found in the QTL region with a significant marker for aspartate on linkage group three at position 29cM (Table 3.20). Aspartate-4-phosphate is converted to aspartate-4-semialdehyde by aspartate semialdehyde dehydrogenase. Aspartate semialdehyde dehydrogenase was found as a putative candidate gene in the QTL region on linkage group two at position 32cM with a significant marker for aspartate and asparagine (Table 3.20). Homoserine dehydrogenase catalyzes the conversion of aspartate semialdehyde to homoserine, which begins cysteine and threonine biosynthesis pathways. Homoserine dehydrogenase was found as a putative candidate gene on linkage group three at position 29cM for an aspartate significant marker (Table 3.20).

Threonine has two biosynthesis pathways that contribute to overall threonine accumulation, one from homoserine and the other from glycine (Kanehisa et al., 2017; T. Kim et al., 2017). From homoserine, homoserine kinase and then threonine synthase produces threonine. Threonine aldolase catalyzes the production of threonine from glycine, and was found as a putative candidate gene on linkage group 12 at position 61cM with a significant marker for threonine (Table 3.20). Maintaining and regulating the glycine pool will affect not only threonine accumulation, but also glutamine and other amino acids as glycine is readily converted to glyoxylate. Glycine is synthesized from serine by serine hydroxymethyltransferase. Serine hydroxymethyltransferase was found

as a putative candidate gene in QTL regions with significant markers for threonine on linkage group one at position 30cM, on linkage group three at position 115cM, on linkage group five at position 68cM, and on linkage group six at position 100cM (Table 3.20).

Alanine biosynthesis occurs through either alanine-glyoxylate aminotransferase activity or by alanine aminotransferase activity (Kanehisa et al., 2017; T. Kim et al., 2017). Alanine-glyoxylate aminotransferase produces alanine and glyoxylate from pyruvate and glycine. Alanine aminotransferase produces alanine and 2-oxoglutarate from pyruvate and glutamate. Alanine-glyoxylate aminotransferase was found as a putative candidate gene in QTL regions with significant markers for alanine on linkage group three at position 36cM and on linkage group 12 at position 61cM (Table 3.20). Alanine aminotransferase was found as a putative candidate gene in the QTL region on linkage group four at position 27cM with a significant marker for alanine (Table 3.20). Since alanine synthesis is dependent on pyruvate, the regulation of the pyruvate pool, particularly through pyruvate kinase may be an important regulator of the TCA cycle, branch-chain amino acids, and alanine accumulation. Pyruvate kinase was found as a putative candidate gene in QTL regions on linkage group one at position 14cM with significant markers for alanine, citric acid, leucine and valine, on linkage group nine at position 25cM with significant markers for alanine and citric acid, and on linkage group 10 at position 35cM with a significant marker for alanine as well as the enzyme gene for phosphoenolpyruvate synthesis, enolase (Table 3.20).

In summary, the ¹H NMR non-targeted profiling annotated four amino acids within the aspartate branch biosynthesis pathway, aspartate, asparagine, threonine, and alanine (Table 3.4). The aspartate branch metabolites accounted for over 69% of the total amino acids with aspartate constituting 48% (Table 3.4). The aspartate branch metabolites show a strong narrow-split pattern when correlated with total amino acids (Figure 3.7). Aspartate showed a narrow-split pattern when correlated with asparagine, which supports the pathway branching from aspartate to either asparagine or other metabolites in the pathway (Figure 3.10) (Buchanan et al., 2012; Kanehisa et al., 2017; T. Kim et al., 2017). The BiPAM results for the aspartate branch metabolites revealed multiple significant QTLs with putative candidate genes for enzymes catalyzing

aspartate catabolism towards homoserine synthesis, and genes for the different biosynthesis pathways for alanine (Table 3.20). The two most significant QTL regions for aspartate and asparagine contain the putative candidate genes, aspartokinase and aspartate semialdehyde dehydrogenase, which commits the aspartate branch pathway to the biosynthesis of other amino acids and important metabolites (Table 3.20). The most significant alanine QTL has the alanine aminotransferase putative candidate gene that catalyzes the interconversion of pyruvate and alanine, while two other very significant alanine QTLs contain alanine-glyoxylate transaminase, which also synthesizes alanine from pyruvate (Table 3.21). The aspartate branch pathway also contains the biosynthesis pathways of many other amino acids that were not directly annotated in this research, thus future research and metabolite profiling should focus on specifically annotating amino acids like lysine, cysteine, serine, and glycine. The identification of QTLs and putative candidate genes for parts of the aspartate branch pathway provides vital foundational knowledge for future research to continue elucidating the pathway as well as improve synthesis of multiple amino acids important for human health (Buchanan et al., 2012; Kanehisa et al., 2017; T. Kim et al., 2017; Ufaz & Galili, 2008; G. Wang et al., 2017).

3.5.5. Sugar Significant QTLs and Putative Candidate Genes

Sugars are not only important for fruit quality and consumer acceptance, but also vital as carbon energy sources, and substrates for biosynthesis and modification of other metabolites (Buchanan et al., 2012; Kanehisa et al., 2017; T. Kim et al., 2017). Photosynthesis consists of two distinct processes, the light reactions and Calvin cycle, that utilize CO₂, water, light energy to produce 3-carbon sugars, O₂, and water. The 3-carbon sugar, 3-phosphoglycerate, is essential for the major metabolic pathways, including glycolysis and the pentose phosphate pathway (PPP) (Buchanan et al., 2012).

3.5.5.1. Fructose and Glucose

In the PPP, the 3-carbon sugars, glyceraldehyde 3-phosphate (GAP) and dihydroxyacetone phosphate (DHAP), are condensed by fructose-1,6-bisphosphate aldolase into fructose -1,6-phosphate, an important 6-carbon sugar (Kanehisa et al., 2017; T. Kim et al., 2017). The metabolite pools of GAP and DHAP are regulated and maintained through triosephosphate isomerase as it readily converts between the two

metabolites. Triosephosphate isomerase was found as a putative candidate gene in the QTL regions with significant markers for fructose on linkage group four at position 20cM (Table 3.21). Fructose-1,6-bisphosphate aldolase was found as a putative candidate gene in the QTL regions with significant fructose markers on linkage group 12 at position 68cM (Table 3.21). Fructose-1,6-bisphosphate interconversion with F6P, one of the main hexose-phosphate substrates, is regulated by three different enzymes, pyrophosphate-dependent phosphofructokinase, fructose-1,6-bisphosphatase, and ATP-dependent phosphofructokinase (Buchanan et al., 2012; Kanehisa et al., 2017; T. Kim et al., 2017). Fructose-1,6-bisphosphatase was also found in the QTL region on linkage group 12 at position 68cM (Table 3.21). ATP-dependent phosphofructokinase was found as a putative candidate gene on linkage group 10 at position 86cM with a significant marker for the fructose-glucose ratio and on linkage group five at position 120 with significant markers for fructose-sucrose and glucose-sucrose ratio (Table 3.21). The PPP is also essential because it not only regenerates F6P and GAP for further carbon condensation, but also provides important multi-carbon sugar substrates for other biosynthesis pathways through ribose-5-phosphate isomerase, transketolase, and transaldolase enzymes. On linkage group 12 at position 12cM there is a QTL region with a significant marker for fructose with the putative candidate genes ribose-5-phosphate isomerase, transaldolase and glyceraldehyde-3-phosphate dehydrogenase, which generates GAP in gluconeogenesis (Table 3.21). These putative candidate genes suggest that this QTL is an important regulator of the PPP, which could regulate sugar diversity synthesis and energy conversion (Buchanan et al., 2012; Kanehisa et al., 2017; T. Kim et al., 2017).

Through F6P, the hexose-phosphates are readily interconverted to regulate and maintain the hexose-phosphate pools, F6P, G6P, and G1P, as they are vital substrates for a multitude of processes and pathways (Buchanan et al., 2012; Kanehisa et al., 2017; T. Kim et al., 2017). G6P is utilized in the PPP by G6P dehydrogenase to produce NADPH reducing energy, which is vital for many other pathways. G6P dehydrogenase was found in the QTL regions on linkage group six at position 41cM with a significant glucose marker, on linkage group nine at position 25cM with a glucose significant marker, and on linkage group 12 at position 12cM with a significant maltose marker

(Table 3.21). G1P is the main hexose-phosphate utilized for synthesis of sucrose, cell wall components, and starch. Therefore, the interconversion between G6P and G1P is important balance to regulate the synthesis of energy and metabolites or polysaccharides (Buchanan et al., 2012). Phosphoglucomutase catalyzes the interconversion between G6P and G1P. Phosphoglucomutase was found in the QTL region on linkage group one at position 30cM with a significant marker for fructose and on linkage group two at position 32cM with a significant marker for glucose (Table 3.21).

3.5.5.2. Sucrose, Maltose, and Maltitol

Sucrose is a disaccharide consisting of a glucose and fructose, whereas trehalose and maltose are disaccharides consisting of glucose (Buchanan et al., 2012; Kanehisa et al., 2017; T. Kim et al., 2017). F6P and UDP-glucose are used to synthesize sucrose. UDP-glucose is produced from G1P by UTP-G1P uridylyltransferase, which was found as a putative candidate gene in the QTLs on linkage group one at position 30cM with a significant marker for sucrose, and on linkage group five at position 120cM with a significant marker for fructose-sucrose and glucose-sucrose ratio (Table 3.21). Sucrose synthesis occurs through either sucrose synthase, or sucrose phosphate synthase and sucrose phosphatase converting it to sucrose-6-phosphate then sucrose glucose. Sucrose phosphatase was found as a putative candidate gene in the QTL region with a significant marker for glucose-fructose ratio on linkage group four at position 107cM (Table 3.21). Also within this QTL region, the putative candidate gene hexokinase or fructokinase was also found (Table 3.21). Hexokinase or fructokinase catalyze the phosphorylation of free hexose sugars, like fructose or glucose, so that they can contribute to the hexose-phosphate pools. On linkage group six at position 41cM, hexokinase/fructokinase were also found in the QTL region with a significant marker for sucrose (Table 3.21). Free hexose like fructose and glucose are produced primarily through the degradation of sucrose by invertases like cell-wall invertase (CWINV) or beta-fructofuranosidase. CWINV and beta-fructofuranosidase were both found as putative candidate genes in QTLs on linkage group nine at position 25cM and linkage group 10 at positions 8cM and 14cM both with a significant marker for sucrose, fructose, and glucose (Table 3.21). Both candidate

genes were also found on linkage group 10 at position 86cM with the significant marker for fructose-glucose ratio (Table 3.21).

Sucrose is a vital sugar signaling and transport metabolite in plants (Buchanan et al., 2012). Recent research has shown that trehalose-6-phosphate (T6P) is also a very important signaling sugar metabolite (Lunn, Delorge, Figueroa, Van Dijck, & Stitt, 2014; O'Hara et al., 2013; Tsai & Gazzarrini, 2014). Trehalose is a disaccharide composed of two glucoses attached by a 1,1-glycosidic bond. T6P and sucrose are proposed to be highly correlated and work together to signal the energy resources and status throughout the plant (Kulik, Wawer, Krzywińska, Bucholc, & Dobrowolska, 2011; Lunn et al., 2014; O'Hara et al., 2013; Tsai & Gazzarrini, 2014). T6P synthesis occurs through the condensation of UDP-glucose and G6P by T6P synthase (TPS) (Kanehisa et al., 2017; T. Kim et al., 2017). Trehalose-phosphate phosphatase (TPP) interconverts T6P and trehalose. TPS was found as a putative candidate gene in the QTL regions with a sucrose significant marker on linkage group four at position 27cM and on linkage group 12 at position 49cM (Table 3.21). TPP was found in the QTL on linkage group nine at position 25cM where there is a significant marker for sucrose, fructose and glucose (Table 3.21). Both TPS and TPP were found as putative candidate genes in the QTL region on linkage group five at position 120cM with significant markers for fructose-sucrose and glucose-sucrose ratios (Table 3.21).

G1P can also be converted to ADP-glucose, the main component for cell wall component and starch synthesis (Buchanan et al., 2012; Kanehisa et al., 2017; T. Kim et al., 2017). ADP-glucose pyrophosphorylase catalyzes G1P conversion to ADP-glucose. ADP-glucose pyrophosphorylase was found as a putative candidate gene in the QTL on linkage group one at position 14cM with a significant marker for maltose (Table 3.21). Starch and cell wall polysaccharides with glycosidic bonds are broken by either amylase or glucosidases. Beta-amylases release maltose, whereas beta-glucosidases release glucose. The disaccharide maltose is composed of two glucoses attached by a 1,4-glycosidic bond. Beta-amylase was found as a putative candidate gene in the QTLs with significant maltose markers on linkage group one at position 14cM, on linkage group one at position 32cM, and on linkage group four at position 27cM (Table 3.21). Beta-glucosidase was found as a putative candidate gene in the

QTLs on linkage group one at position 30cM for glucose, on linkage group two at position 32cM with glucose+maltose and maltose significant markers, on linkage group four at position 27cM with glucose, on linkage group nine at position 25cM for maltose, and on linkage group 12 at position 37cM for maltose (Table 3.21).

Maltitol is the sugar alcohol of maltose with very little characterization of endogenous genes in the synthesis pathway (Kanehisa et al., 2017; T. Kim et al., 2017; Rapaille, Goosens, & Heume, 2003; Sengupta, Mukherjee, Basak, & Majumder, 2015; Sengupta, Mukherjee, Parween, & Majumder, 2012). Fortunately, the sorbitol pathway was been partially elucidated because it is the sugar alcohol of glucose and utilized as a sugar substitute sweetener (Kanehisa et al., 2017; H. Y. Kim et al., 2015; T. Kim et al., 2017; Rapaille et al., 2003; Schwab, Davidovich-Rikanati, & Lewinsohn, 2008). The galactinol pathway was also been partially elucidated because it is the sugar alcohol of galactose and has been proposed to be an important stress signaling metabolite in plants (Kanehisa et al., 2017; T. Kim et al., 2017; Rapaille et al., 2003; Sengupta et al., 2015, 2012). Although the putative candidate genes found within the significant maltitol QTL genetic regions are annotated with sorbitol or galactinol genes, these putative candidate genes will still provide insight into potential genes for further characterization of sugar alcohol synthesis in blueberries or maltitol specific synthesis (Kanehisa et al., 2017; H. Y. Kim et al., 2015; T. Kim et al., 2017; Rapaille et al., 2003; Sengupta et al., 2015, 2012). Aldose reductase reduces glucose into sorbitol and sorbitol-6-phosphate dehydrogenase (NADP-dependent) interconverts sorbitol-6-phosphate with G6P (Kanehisa et al., 2017; T. Kim et al., 2017). Sorbitol-6-phosphate dehydrogenase (NADP-dependent) was found in a significant maltitol QTL region on linkage group four at position 130cM, and on linkage group 12 at position 49cM along with an aldolase reductase gene (Table 3.21). Galactinol synthase interconverts UDP-galactose and myoinositol with galactinol. Galactinol synthase was found in a significant maltitol QTL region on linkage group four at position 20cM, on linkage group 12 at position 61cM, and on linkage group 12 at position 74cM (Table 3.21) (Buchanan et al., 2012; Kanehisa et al., 2017; T. Kim et al., 2017).

In summary, the non-targeted profiling using ¹H NMR annotated fructose, glucose, sucrose, maltose and maltitol metabolites (Table 3.5). Of the total sugar

metabolites, glucose accounted for 52% while fructose accounted for 47% (Table 3.5). Glucose and fructose correlate very strongly, while glucose shows a strong narrow-split pattern when correlated with maltose (Figure 3.12). The BiPAM revealed multiple significant QTLs with regions containing putative candidate genes involved in the PPP, sugar interconversions, or polysaccharide degradation (Table 3.21) (Buchanan et al., 2012; Kanehisa et al., 2017; T. Kim et al., 2017). The most significant fructose QTL contains three putative candidate genes involved in regenerating some of the sugar-phosphates in the PPP for continued cycling (Table 3.21). The most significant glucose QTL has G6P dehydrogenase as a putative candidate gene, which further supports the importance of PPP in sugar regulation and signaling (Table 3.21). In the QTL region with overlapping significant markers for sucrose, glucose, fructose, the putative candidate gene invertase was found, thus indicating the importance of sucrose through regulating its degradation and subsequent hexose pools supply (Table 3.21). The very significant and overlapping QTLs for glucose and maltose contain beta-glucosidase and beta-amylase putative candidate genes, which indicates the degradation of glucan polysaccharides is an important factor in regulating sugar accumulation (Table 3.21) (Buchanan et al., 2012; Kanehisa et al., 2017; T. Kim et al., 2017; Paniagua et al., 2014; Posé et al., 2011; Rosa et al., 2009). The identified QTLs and putative candidate genes will improve our foundational knowledge of blueberry sugar regulation, which will have an effect on the sweet taste and consumer fruit quality of blueberries (Barrett et al., 2010; Gilbert et al., 2014; Pagliarini, Laureati, & Gaeta, 2013; Posé et al., 2011; Serrano et al., 2017; Seymour, Østergaard, Chapman, Knapp, & Martin, 2013). This information can be utilized in future breeding strategies to improve firmness through reducing cell wall component degradation, and improve taste through differentially regulating the sugars and sugar alcohols (Cappai et al., 2018; Castellarin et al., 2016; Kyriacou & Rouphael, 2018; Paniagua et al., 2014).

3.5.5.3. Galactose, Xylose, and Arabinose

The monosaccharides, galactose and mannose, are epimers of glucose. Xylose and arabinose synthesis occur after glucose is converted to glucuronic acid. Galactose, xylose, and arabinose provide the backbone and branching functional groups important for the synthesis of cell wall matrix components, hemicellulose and pectin (Buchanan et

al., 2012). These monosaccharides are also important sugar moieties for diversification of metabolites like anthocyanins (Buchanan et al., 2012; Kanehisa et al., 2017; T. Kim et al., 2017; Overall et al., 2017). Galactose can be utilized as a sugar modification, like in anthocyanins, or as a sugar side-chain, like for hemicellulose xyloglucans. Galactose is an important sidechain on xyloglucans, and alpha-galactosidases remove galactose residues from xyloglucans. Alpha-galactosidase was found as a putative candidate gene on linkage group nine at position 25cM and 27cM with significant markers for other sugars and galactose (Table 3.21).

Galactose synthesis occurs from either GDP-glucose or UDP-glucose (Kanehisa et al., 2017; T. Kim et al., 2017). GDP-glucose is first converted to GDP-mannose by a GDP-glucose-2-epimerase, which is then converted to GDP-galactose by GDP-mannose-3,5-epimerase. GDP-mannose-3,5-epimerase was found as a putative candidate gene in a QTL region on linkage group one at positions 14cM and 18cM with significant markers for other sugars and galactose (Table 3.21). GDP-mannose can also be synthesized from F6P when F6P is converted to mannose-6-phosphate, and then to mannose-1-phosphate, which can then be converted to GDP-mannose by mannose-1-phosphate guanylyltransferase. Mannose-1-phosphate guanylyltransferase was found as a putative candidate gene in a significant “other sugars” QTL on linkage group six at position 41cM (Table 3.21). On linkage group two at position 89cM, there is a significant QTL for “other sugars” with the putative candidate genes trehalase, which catalyzes the cleavage of trehalose into two free glucoses, and UDP-glucose 4-epimerase, which interconverts UDP-glucose to UDP-galactose, thus indicating this QTL may regulate glucose and galactose production (Table 3.21).

Galactose is closely related to galacturonic acid, the main component of the pectin backbone. Polygalacturonase cleaves the 1,4-glycosidic bond that links galacturonic acids together, which forms the pectin backbone (Buchanan et al., 2012; Kanehisa et al., 2017; T. Kim et al., 2017). Polygalacturonase was found in QTL regions on linkage group two at position 59cM for other sugars, on linkage group four at position 16cM for galactose, on linkage group 12 at position 49cM for galactose, and on linkage group 12 at position 74cM for other sugars (Table 3.21). Polygalacturonase was also found in a significant galactose QTL on linkage group two at position 23cM along with

the putative candidate gene UDP-glucuronate 4-epimerase, which interconverts UDP-glucuronate and UDP-galacturonate (Table 3.21). UDP-glucuronate 4-epimerase was also found in another significant galactose QTL on linkage group three at position 124cM along with UDP-glucose 4-epimerase, which supports the close relation of galactose with galacturonic acid (Table 3.21).

Xylose synthesis starts with the conversion of UDP-glucose by UDP-glucose dehydrogenase to UDP-glucuronate, which can then be converted to UDP-xylose by UDP-glucuronic acid decarboxylase (Buchanan et al., 2012; Kanehisa et al., 2017; T. Kim et al., 2017). UDP-xylose can then be converted to UDP-arabinose by UDP-xylose-4-epimerase. UDP-glucose dehydrogenase was found as a putative candidate gene in significant QTL regions for arabinose +others and xylose on linkage group six at position 55cM and on linkage group four at position 18cM and 27cM (Table 3.21). On linkage group 12 at position 54cM, there is significant QTL for arabinose +others and xylose that contains the putative candidate gene, UDP-glucuronic acid decarboxylase (Table 3.21). UDP-arabinose 4-epimerase was found as a putative candidate gene in significant xylose QTLs on linkage group three at position 124cM and on linkage group 11 at position 54cM (Table 3.21). On linkage group eight at position 107cM, there is a significant arabinose +others QTL that contains multiple candidate genes for the synthesis of multiple different sugars, which all play a role in hemicellulose and pectin synthesis (Table 3.21). The RHM1 gene is a trifunctional enzyme, which catalyzes the same reactions as UDP-glucose-4,6-dehydratase, UDP-4-keto-6-deoxy-glucose-3,5-epimerase, and UDP-4-rhamnose-reductase, which overall converts UDP-glucose to UDP-rhamnose, an important component of pectin. The bifunctional UDP-glucose 4-epimerase/UDP-xylose 4-epimerase enzyme was also found and catalyzes the interconversion of UDP-glucose with UDP-galactose as well as UDP-xylose with UDP-arabinose (Kanehisa et al., 2017; T. Kim et al., 2017). UDP-glucuronic acid decarboxylase catalyzes UDP-xylose synthesis from UDP-glucuronic acid. UDP-glucuronic acid 4-epimerase catalyzes the interconversion of UDP-glucuronic acid with UDP-galacturonic acid (Buchanan et al., 2012; Kanehisa et al., 2017; T. Kim et al., 2017). The putative candidate genes in this region indicate that this QTL is an important

regulator of sugar synthesis that could affect not only the integrity of the wall components, but also potentially the anthocyanin diversity.

Xylose is also an important sugar utilized in the backbone for hemicellulose xyloglucans and pectin xylogalacturonans (Buchanan et al., 2012). Xyloglucan endotransglucosylase/hydrolase (XTH) transfers or adds xylosyl residues onto glucose residues in a glucan, especially for hemicellulose (Buchanan et al., 2012; Kanehisa et al., 2017; T. Kim et al., 2017). XTH was found as a putative candidate gene in QTL regions on linkage group one at position 30cM for xylose, on linkage group three at position 36cM for xylose, and on linkage group four at position 18cM and 27cM for arabinose +others and xylose (Table 3.21). Xylose residues or sidechains can be completely removed from hemicellulose or pectin by beta-xylosidase. Beta-xylosidase was found on linkage group fragment 6.5 at position 18cM in a significant QTL for xylose and arabinose +others, as well as in another QTL region significant for xylose and arabinose +others on linkage group six at position 55cM (Table 3.21).

In summary, the ¹H NMR profiling also annotated galactose, xylose, and arabinose metabolites (Table 3.5). While galactose, xylose, and arabinose show split correlations with total sugar, they show positive correlations with each other (Figure 3.12). The BiPAM revealed multiple significant QTLs with regions containing putative candidate genes involved in polysaccharide degradation or sugar interconversions (Table 3.21). The most significant galactose QTL contains the polygalacturonase putative candidate gene that degrades pectin or hemicellulose backbones (Table 3.21) (Buchanan et al., 2012; Chen et al., 2015; Kanehisa et al., 2017; T. Kim et al., 2017; Prasanna et al., 2007). Another significant galactose QTL contains putative candidate genes for galactose and galacturonate synthesis from glucose and glucuronate, respectively (Table 3.21) (Buchanan et al., 2012; Kanehisa et al., 2017; T. Kim et al., 2017). The most significant xylose QTL has the XTH putative candidate gene, which modifies polysaccharides in the primary cell wall (Table 3.21) (Buchanan et al., 2012; Kanehisa et al., 2017; T. Kim et al., 2017; Yoshizawa, Shimizu, Hirano, Sato, & Hashimoto, 2012). Another significant xylose QTL contains the xylose and arabinose synthesis putative candidate gene, UDP-arabinose 4-epimerase (Table 3.21) (Buchanan et al., 2012; Kanehisa et al., 2017; T. Kim et al., 2017; Yoshizawa et al.,

2012). Identifying important QTLs and putative candidate genes aids in elucidating the synthesis and regulation of galactose, xylose, and arabinose, which can be integrated with anthocyanin diversity regulation to improve sugar moiety modifications (Cappai et al., 2018; He et al., 2010; Jeong et al., 2010; Montecchiarini et al., 2018; Overall et al., 2017; Pinu et al., 2018; Routray & Orsat, 2011; Sasaki et al., 2014; Yonekura-Sakakibara, 2009). A greater understanding of galactose, xylose, and arabinose pathways will also improve the regulation of sidechain modifications of cell wall matrix components like hemicellulose and pectin, which can be utilized to improve blueberry firmness and texture (Castellarin et al., 2016; Giongo, Poncetta, Loretta, & Costa, 2013; Leiva-Valenzuela, Lu, & Aguilera, 2013; Paniagua et al., 2014; Seymour, Østergaard, et al., 2013; Vicente et al., 2007).

3.5.6. Phenolic Acid Pathway Significant QTLs and Putative Candidate Genes

3.5.6.1. Shikimic Acid Pathway and Phenylalanine Synthesis

The shikimic acid pathway branches off of and utilizes the products of the PPP to produce gallic acid, shikimic acid, and quinic acid (Ali Ghasemzadeh, 2011; Buchanan et al., 2012; Herrmann, 1995; Kanehisa et al., 2017; T. Kim et al., 2017; Mattila et al., 2006; Raskin I, Yousef GG, 2013; Stalikas, 2007). The shikimic acid pathway progresses into phenylalanine biosynthesis, which begins the phenylpropanoid acid biosynthesis pathway (Buchanan et al., 2012; Kanehisa et al., 2017; T. Kim et al., 2017; Mattila et al., 2006; Raskin I, Yousef GG, 2013; Stalikas, 2007). Annotating putative candidate genes in the phenolic acid pathway, especially phenylalanine synthesis, will provide valuable foundational knowledge to improve the nutritional qualities of blueberries through upregulating the essential amino acid phenylalanine and upregulating downstream biosynthesis pathways of phenylpropanoids and flavonoids (Buchanan et al., 2012; Kanehisa et al., 2017; T. Kim et al., 2017; Prencipe et al., 2014; Ufaz & Galili, 2008).

Many of the reactions in the phenolic acid biosynthesis pathway require NADPH energy for metabolite structure modification or rearrangement, especially for gallic acid, quinic acid, and shikimic acid synthesis (Buchanan et al., 2012; Herrmann, 1995; Kanehisa et al., 2017; T. Kim et al., 2017; Lin et al., 2016). As mentioned previously, the oxidative reactions in the PPP produce NADPHs while converting G6P to ribulose-5-

phosphate with the enzymes, G6P dehydrogenase, 6-phosphogluconolactonase, and 6-phosphogluconate dehydrogenase (Buchanan et al., 2012; Kanehisa et al., 2017; T. Kim et al., 2017). On linkage group nine at position 27cM, the gallic acid significant QTL contains the putative candidate gene, G6P dehydrogenase (Table 3.22). 6-phosphogluconolactonase and 6-phosphogluconate dehydrogenase were both found as putative candidate genes on linkage group two at position 25cM in the QTL region significant for gallic acid (Table 3.22).

The first committing step towards phenolic acid synthesis from the PPP and the start of the shikimic acid pathway occurs with 3-deoxy-7-phosphoheptulonate synthase (DHAP synthase) condensing phosphoenolpyruvate and erythrose 4-phosphate to 3-deoxy-arabinoheptulosonate 7-phosphate (Buchanan et al., 2012; Kanehisa et al., 2017; T. Kim et al., 2017). On linkage group eight at position 107cM, DHAP synthase was found within the QTL region significant for quinic acid, chlorogenic acid, and caffeic acid +others (Table 3.22). 3-deoxy-arabinoheptulosonate 7-phosphate is converted by 3-dehydroquinate synthase to 3-dehydroquinate, which is followed by its conversion to either quinic acid by quinate dehydrogenase, or 3-dehydroshikimate by 3-dehydroquinate dehydratase. Both enzymes were found in the QTL regions on linkage group one at position 18cM and 14cM with significant markers for gallic acid and quinic acid, on linkage group six at position 45cM and 41cM with significant markers for gallic acid and quinic acid, and on linkage group fragment 11.5 at positions 21cM, 34cM, and 36cM with significant markers for quinic acid, chlorogenic acid, and caffeic acid +others (Table 3.22). 3-dehydroshikimate can then be converted to either shikimic acid by shikimate dehydrogenase, or 3,5-didehydroshikimate by 3-dehydroshikimate dehydrogenase, which will then spontaneously rearrange to gallic acid. 3-dehydroshikimate dehydrogenase was found in the QTL on linkage group six at position 45cM with a significant marker for gallic acid (Table 3.22).

Although there are multiple steps along the shikimic acid pathway that led up to phenylalanine synthesis, the overall conversion of prephenate to phenylalanine is very important in regulating phenylalanine accumulation (Buchanan et al., 2012; Kanehisa et al., 2017; T. Kim et al., 2017; Prencipe et al., 2014; Ufaz & Galili, 2008). The prephenate conversion can occur through either prephenate aminotransferase and

arogenate dehydratase activity, or prephenate dehydratase and phenylpyruvate aminotransferase activity (Kanehisa et al., 2017; T. Kim et al., 2017).

Arogenate/prephenate dehydratase was found as a putative candidate gene in QTLs on linkage group one at position 32cM with a significant quinic acid marker and on linkage group 12 at position 49cM with a significant marker for gallic acid, quinic acid, and chlorogenic acid (Table 3.22). Prephenate/phenylpyruvate aminotransferase was found as a putative candidate gene in a significant caffeic acid +others QTL on linkage group four at position 92cM (Table 3.22).

In summary, the ¹H NMR non-targeted profiling annotated in total five phenolic acids with two synthesized from the shikimate pathway, gallic acid and quinic acid (Table 3.6). With the exception of caffeic acid exhibiting a wide-split pattern when correlated with any of the phenolic acids, the other four phenolic acids showed positive correlations with each other (Figure 3.13). The BiPAM revealed a QTL region with the most significant QTLs for gallic and quinic acid overlapping and containing three putative candidate genes involved in both gallic and quinic acid synthesis (Table 3.22) (Buchanan et al., 2012; Kanehisa et al., 2017; T. Kim et al., 2017). Identifying important QTLs and putative candidate genes for gallic, shikimic, and quinic acids provides regulatory information that can be utilized to improve accumulation of the essential amino acid, phenylalanine, which will consequently improve phenylpropanoid and flavonoid biosynthesis (Buchanan et al., 2012; Kanehisa et al., 2017; T. Kim et al., 2017; Prencipe et al., 2014; Ufaz & Galili, 2008). Future research can build upon this information to further elucidate regulation of the shikimic pathway as well as develop breeding strategies for improving phenylalanine accumulation as this will enhance the overall health benefits of blueberries (Buchanan et al., 2012; Kanehisa et al., 2017; T. Kim et al., 2017; Lila et al., 2016; Prencipe et al., 2014; Silva et al., 2018; Ufaz & Galili, 2008).

3.5.6.2. Phenylpropanoid Pathway

The phenylpropanoid pathway starts with phenylalanine ammonia lyase (PAL) converting phenylalanine to cinnamic acid (Kanehisa et al., 2017; T. Kim et al., 2017). On linkage group 12 at position 49cM, PAL was a putative candidate gene for the QTL with significant markers for quinic acid, chlorogenic acid and caffeic acid +others (Table

3.22). The next step is the conversion of cinnamic acid into p-coumaric acid by cinnamate-4-hydroxylase (C4H). C4H was found in QTLs as a putative candidate gene on linkage group four at position 127cM with a significant quinic acid marker, on linkage group 11 at position 37cM for gallic acid and quinic acid, on linkage group 11 at position 54cM for quinic acid, on linkage group 12 at position 14cM for chlorogenic, and on linkage group 12 at position 74cM for chlorogenic acid (Table 3.22). p-coumaroyl-CoA ligase (4CL) converts p-coumaric acid to p-coumaroyl-CoA, which is the branching point for either phenylpropanoid synthesis or flavonoid synthesis. The putative candidate gene 4CL was found in QTLs on linkage group two at position 25cM for chlorogenic acid, on linkage group three at position 88cM for chlorogenic acid, on linkage group six at position 43cM and 39cM for chlorogenic acid and caffeic acid +others, linkage group nine at position 25cM and 27cM for chlorogenic acid and caffeic acid, and on linkage group 12 at position 14cM for chlorogenic acid (Table 3.22).

Hydroxycinnamoyl-CoA shikimate/quinic acid hydroxycinnamoyltransferase (HCT) activity commits the phenylpropanoid pathway to phenylpropanoid acid synthesis (Kanehisa et al., 2017; T. Kim et al., 2017). HCT catalyzes two similar reactions: 1) interconversion of p-coumarate-CoA with p-coumaroyl-quinic acid or with p-coumaroyl-shikimate, and 2) interconversion of caffeoyl-quinic acid or caffeoyl-shikimate with caffeoyl-CoA, respectively. Caffeoyl-quinic acid is better known as chlorogenic acid (Buchanan et al., 2012; Kanehisa et al., 2017; T. Kim et al., 2017). For reaction 1) HCT utilizes quinic acid or shikimate along with p-coumaroyl-CoA to produce p-coumaroyl-quinic acid or p-coumaroyl-shikimate, while giving off CoA. For reaction 2), HCT catalyzes the conversion of chlorogenic acid or caffeoyl-shikimate to caffeoyl-CoA while giving off quinic acid or shikimate acid, respectively. HCT was found in multiple QTL regions as a putative candidate gene on linkage group two at position 25cM for chlorogenic acid, on linkage group three at position 88cM for chlorogenic acid, on linkage group three at position 122cM for chlorogenic acid, on linkage group four at position 27cM and 22cM for quinic acid, chlorogenic acid, and caffeic acid +others, on linkage group four at position 127cM for quinic acid, on linkage group fragment 6.5 at position 18cM for quinic acid and chlorogenic acid, on linkage group nine at position 25cM and 27cM for quinic acid, chlorogenic acid, and caffeic acid +others, on linkage group 11 at position 37cM

for quinic acid, on linkage group 11 at position 54cM for quinic acid, on linkage group 12 at position 14cM for chlorogenic acid, on linkage group 12 at position 49cM for quinic acid and chlorogenic acid, and on linkage group 12 at position 61cM for chlorogenic acid (Table 3.22). Caffeoyl-shikimate esterase converts caffeoyl-shikimate to caffeic acid and was found as a putative candidate gene in caffeic acid +others significant QTLs on linkage group two at position 81cM and on linkage group 12 at position 12cM (Table 3.22).

In summary, the ¹H NMR profiling also annotated two phenolic acids in the phenylpropanoid acid pathway, chlorogenic and caffeic acid (Table 3.6). Of the total phenolic acids, quinic acid and chlorogenic acid accounted for 34% and 36%, respectively (Table 3.6). The BiPAM showed a QTL region with the most significant QTLs for chlorogenic and caffeic acid, and very significant QTL for quinic acid overlapped with the putative candidate gene, HCT (Table 3.22) (Ali Ghasemzadeh, 2011; Buchanan et al., 2012; Kanehisa et al., 2017; T. Kim et al., 2017; Mattila et al., 2006; Villalobos-González, Peña-Neira, Ibáñez, & Pastenes, 2016; Shouchuang Wang et al., 2017). HCT along with p-coumaroyl-CoA ligase were found as putative candidate genes in another region with very significant QTLs overlapping for quinic, chlorogenic, and caffeic acids (Table 3.22) (Buchanan et al., 2012; Kanehisa et al., 2017; T. Kim et al., 2017; Lin et al., 2016). This supports the important role HCT plays in regulating the synthesis and usage of quinic, chlorogenic, and caffeic acid (Ghan et al., 2017; Inostroza-Blancheteau et al., 2014; Karppinen, Zoratti, Nguyenquynh, Häggman, & Jaakola, 2016; Serrano et al., 2017; Villalobos-González et al., 2016; Zhu et al., 2018; Zifkin et al., 2012; Zorenc et al., 2017). The identification of important QTLs and putative candidate genes for chlorogenic, quinic, and caffeic acids provides additional information about the phenylpropanoid pathway to aid in regulating and improving accumulation (Buchanan et al., 2012; Ghan et al., 2017; Kanehisa et al., 2017; Karppinen et al., 2016; T. Kim et al., 2017; Serrano et al., 2017; Zhu et al., 2018; Zifkin et al., 2012). Future research towards improving phenylpropanoid accumulation will aid in increasing the acidity and stability of anthocyanins as well as antioxidant capacity, thus enhancing the health benefits of blueberries.

3.5.6.3. Flavonoid Pathway

Flavonoids consist of a multi-ring structure that allows for a plethora of different modifications, thus there are the most diverse group of specialized metabolites (Buchanan et al., 2012; Kanehisa et al., 2017; T. Kim et al., 2017; Nabavi et al., 2018; Routaboul et al., 2012). The flavonoid pathway begins with the conversion of p-coumaroyl-CoA to chalcone by naringenin-chalcone synthase (CHS) (Kanehisa et al., 2017; T. Kim et al., 2017). CHS was found in epicatechin significant QTLs on linkage group one at position 15cM, on linkage group four at position 20cM, on linkage group four at position 132cM, and on linkage group 12 at position 49cM (Table 3.22). Chalcone is then converted to naringenin by chalcone-flavanone isomerase (CHI), which was found as a putative candidate gene in the epicatechin significant QTL on linkage group four at position 124cM (Table 3.22).

Flavonoid 3'-hydroxylase (F3'H) regulates two reactions: 1) naringenin to dihydrokaempferol, and 2) eriodictyol to dihydroquercetin (Kanehisa et al., 2017; T. Kim et al., 2017). Flavonoid 3',5'-hydroxylase (F3'5'H) regulates three similar reactions: 1) naringenin to eriodictyol, 2) dihydrokaempferol to dihydroquercetin, and 3) dihydroquercetin to dihydromyricetin. Flavonol synthase (FLS) also regulates three reactions: 1) dihydrokaempferol to kaempferol, 2) dihydroquercetin to quercetin, and 3) dihydromyricetin to myricetin. Both F3'H and F3'5'H were found as putative candidate genes in multiple QTLs with a significant marker for epicatechin on linkage group one at position 15cM, on linkage group one at position 32cM, on linkage group two at position 34cM along with the FLS gene, on linkage group four at position 125cM, on linkage group four at position 132cM, on linkage group six at position 41cM, on linkage group 10 at position 10cM, on linkage group 11 at position 37cM, on linkage group 11 at position 54cM, on linkage group 12 at position 12cM along with the FLS gene, and on linkage group 12 at position 49cM along with the FLS gene (Table 3.22).

An important step in epicatechin and anthocyanin synthesis is the production of leucoanthocyanidins, which are either leucocyanidin or leucodelphinidin in blueberries (Kanehisa et al., 2017; T. Kim et al., 2017; Nabavi et al., 2018). Dihydroflavonol 4-reductase (DFR) can catalyze two reactions: 1) dihydroquercetin to leucocyanidin and 2) dihydromyricetin to leucodelphinidin (Kanehisa et al., 2017; T. Kim et al., 2017). In

QTLs significant for epicatechin, the putative candidate gene, DFR, was found on linkage group four at position 132cM and on linkage group 12 at position 61cM (Table 3.22). The leucoanthocyanidins are then utilized by anthocyanidin synthase (ANS) to produce the respective anthocyanidins, leucocyanidin to cyanidin and leucodelphinidin to delphinidin. The anthocyanidins can either be converted to a flavan-3-ol, or converted to anthocyanins (Bujor, Le Bourvellec, Volf, Popa, & Dufour, 2016; Grace et al., 2018; Jenks & Bebeli, 2011; Kanehisa et al., 2017; T. Kim et al., 2017; Ronald L Prior et al., 2001). Anthocyanidin reductase (ANR) catalyzes the conversion of the anthocyanidins, cyanidin and delphinidin, into flavan-3-ols, epicatechin and epigallocatechin, respectively (Kanehisa et al., 2017; T. Kim et al., 2017). In QTLs significant for epicatechin, ANR was found as a putative candidate gene on linkage group 12 at position 61cM (Table 3.22). ANS was found as a putative candidate gene in QTLs significant for epicatechin on linkage group one at position 15cM, on linkage group two at position 34cM, on linkage group four at position 132cM, on linkage group 12 at position 12cM, on linkage group 12 at position 49cM, and on linkage group 12 at position 81cM (Table 3.22).

In the public databases, the anthocyanin synthesis pathway begins with a glucoside sugar moiety attached to the anthocyanidin by anthocyanidin 3-O-glucosyltransferase (Horbowicz et al., 2008; Karppinen et al., 2016; Rinaldo et al., 2015; Serrano et al., 2017; Stebbins et al., 2016; Sun et al., 2017; Yonekura-Sakakibara, 2009; Zifkin et al., 2012; Zorenc et al., 2017). The anthocyanidin-glucoside can then undergo sugar moiety interchanges or further modifications like acylation (Karppinen et al., 2016; Rinaldo et al., 2015; Serrano et al., 2017; Stebbins et al., 2016; Yonekura-Sakakibara et al., 2009; Zorenc et al., 2017). The putative candidate gene anthocyanidin 3-O-glucosyltransferase was found in QTL regions significant for epicatechin on linkage group two at position 34cM, on linkage group nine at position 25cM, and on linkage group 12 at position 55cM (Table 3.22). Other anthocyanin modification genes like acylsugar and anthocyanin-specific acyltransferase were found as putative candidate genes in QTL regions significant for epicatechin on linkage group three at position 122cM, and on linkage group 11 at position 37cM along with an acetyl-CoA acetyltransferase (Table 3.22). On linkage group 12 at position 49cM, the QTL

significant for epicatechin contains the anthocyanidin 3-O-glucosyltransferase, along with both the acylsugar and anthocyanin-specific acyltransferase putative candidate genes.

In summary, the ^1H NMR profiling also annotated the flavonoid, epicatechin, as it accounted for over 14% of the total phenolic acids (Table 3.6). The BiPAM revealed multiple significant QTLs with putative candidate genes involved in multiple steps of flavonoid biosynthesis (Table 3.22). The most significant epicatechin QTL contained the F3'H and F3'5'H putative candidate genes that regulate flavonoid diversity (Table 3.22) (Buchanan et al., 2012; Kanehisa et al., 2017; T. Kim et al., 2017; Nabavi et al., 2018). Another very significant epicatechin QTL also contained F3'H and F3'5'H along with CHS, the committing step from phenylpropanoid acids towards flavonoid biosynthesis, and DFR and ANS, which regulate final synthesis of epicatechin (Table 3.22) (Table 3.22) (Buchanan et al., 2012; Kanehisa et al., 2017; T. Kim et al., 2017; Nabavi et al., 2018). Identifying significant QTLs and putative candidate genes provides important additional knowledge about synthesis and regulation of the flavonoid pathway, which will aid future work towards improving flavonoid and anthocyanin accumulation (He et al., 2010; Montecchiarini et al., 2018; Nabavi et al., 2018; Pinu et al., 2018; Routray & Orsat, 2011; Stevenson & Scalzo, 2012; Yonekura-Sakakibara et al., 2009). Future research can utilize this information to elucidate different enzymes that regulate the diversity of flavonoids and anthocyanins, which breeding programs can use to develop improved strategies to enhance the antioxidant capacity and health benefits in blueberry (Gowd et al., 2017; Khoo et al., 2017; Nabavi et al., 2018; Routray & Orsat, 2011; Silva et al., 2018).

Ascorbic acid and glutathione are the main ROS-RNS radical scavenging enzymes (Buchanan et al., 2012; Kanehisa et al., 2017; T. Kim et al., 2017). Ascorbate biosynthesis begins with galactose, but is recycled and regenerated for radical scavenging with glutathione. When H_2O_2 and other ROS-RNS cause oxidative stress or damage, ascorbate and APX interact to produce water and monodehydroascorbate radical. APX was found in significant ascorbic +others QTLs as a putative candidate gene on linkage group one at position 52cM, on linkage group 12 at position 55cM, and on linkage group six a position 41cM along with another peroxidase, CAT (Table 3.22).

When two monodehydroascorbate radicals are present, MDAR catalyzes the regeneration of two ascorbates using NADH. MDAR was found in the ascorbic acid +others significant QTL on linkage group six at position 55cM as a putative candidate gene (Table 3.22). If the two monodehydroascorbate radicals are not quenched quickly, they will spontaneously convert to ascorbate and dehydroascorbate. The dehydroascorbate is reduced to ascorbate by DHAR, but requires the oxidation of glutathione. DHAR was found as a putative candidate gene in the significant ascorbic +others QTL region on linkage group nine at position 25cM (Table 3.22).

GR uses NADPH to convert oxidized glutathione (GSSG) to reduced glutathione (GSH), so the reduced glutathione can continue functioning as an antioxidant elsewhere (Kanehisa et al., 2017; T. Kim et al., 2017). GR was found as a putative candidate gene in an ascorbic +others significant QTL on linkage group one at position 19cM (Table 3.22). Alternatively, ascorbate oxidase utilizes two dehydroascorbates and water to regenerate two ascorbates and oxygen. Ascorbate oxidase was found as a putative candidate gene in QTL regions with a significant marker for ascorbic +others on linkage group one at position 52cM and on linkage group 12 at position 55cM (Table 3.22). Glutathione S-transferase (GST) is a potent antioxidant and detoxification enzyme as it joins a reduced-glutathione to a reactive compound to prevent any further binding or interactions with other compounds, and signal for appropriate degradation or secretion (Ahmadinejad et al., 2017; Cocetta et al., 2012; Foyer & Noctor, 2011; Huan et al., 2016; Xi et al., 2017). Multiple glutathione S-transferase putative candidate genes were also found in the QTL regions with significant ascorbic +others markers on linkage group one at position 19cM and on linkage group nine at position 25cM (Table 3.22).

In summary, ascorbic acid was also annotated through ¹H NMR (Table 3.6). The BiPAM revealed multiple significant QTLs with putative candidate genes involved in multiple steps in the ascorbate-glutathione pathway (Table 3.22) (Buchanan et al., 2012; Foyer & Noctor, 2011; Kanehisa et al., 2017; T. Kim et al., 2017). The identification of significant QTLs and putative candidate genes involved in the ascorbate-glutathione cycle pathway provides valuable information about other pathways contributing to the potent antioxidant capacity exhibited by blueberries (Aurelia Magdalena Pisoschi et al., 2016; Foyer & Noctor, 2011; Lobo et al., 2010;

Routray & Orsat, 2014; Xi et al., 2017). Future research can build upon this knowledge to further elucidate blueberry-specific regulation of the ascorbate-glutathione cycle as well as contribution to the antioxidant capacity so that breeding strategies can implement an improved antioxidant capacity.

3.5.7. DPPH – Antioxidant Capacity Assay Significant QTLs and Putative Candidate Genes

The antioxidant capacity of an extract is the ability of the metabolites in solution to scavenge and quench free radicals. Biological systems have multiple pathways to regulate the balance of free radicals to antioxidants as an overabundance of free radicals frequently leads to oxidative stress (Himamura et al., 2014; Lobo et al., 2010; López-Alarcón & Denicola, 2013; Moharram & Youssef, 2014). Among the many antioxidant capacity assays available, the DPPH assay was utilized to quantify the antioxidant capacity of the DxJ blueberry extracts because it is efficient and cost-effective (Himamura et al., 2014; Kedare & Singh, 2011; O. P. Sharma & Bhat, 2009; S. Singh & Singh, 2008). The first significant DPPH-antioxidant capacity QTL region is on linkage group five at position 107cM (Table 3.23). Multiple putative candidate genes from multiple stages in phenolic acid synthesis were found within the genetic region. DHAP synthase and prephenate/phenylpyruvate aminotransferase are important enzymes in the shikimate and phenylalanine synthesis pathways (Kanehisa et al., 2017; T. Kim et al., 2017). In the phenylpropanoid pathway, p-coumaroyl-CoA ligase is an important enzyme as the pathway branches at this point to either hydroxycinnamoyl acids or flavonoids. From the flavonoid pathway, F3'H and F3'5'H regulate the divergence and synthesis of multiple dihydroflavonols. From the anthocyanin pathway, anthocyanidin 3-O-glucosyltransferase and anthocyanidin 3-O-glucoside 2''-O-xylosyltransferase were found within the region, which suggests anthocyanins rather than anthocyanidins contribute more to DPPH-antioxidant capacity (Brown et al., 2012; Ma et al., 2018; Sasaki et al., 2014; You et al., 2011; Zifkin et al., 2012).

The second significant DPPH-antioxidant capacity QTL region is on linkage group six at position 45cM (Table 3.23). The putative candidate genes found within the genetic region are involved in both phenolic acid synthesis and the ascorbic acid-glutathione cycle (Foyer & Noctor, 2011; Herrmann, 1995; Kanehisa et al., 2017; T. Kim

et al., 2017; Nabavi et al., 2018). From the shikimate pathway, both 3-dehydroquinate dehydratase and quinate/shikimate dehydrogenase catalyze gallic acid, quinic acid, and shikimic acid synthesis, and were found (Table 3.23) (Herrmann, 1995; Kanehisa et al., 2017; T. Kim et al., 2017). The putative candidate genes, p-coumaroyl-CoA ligase, F3'H, and F3'5'H, were also found, thus indicating the flavonoid synthesis pathway also contributes to antioxidant capacity (Table 3.23) (Kanehisa et al., 2017; T. Kim et al., 2017; Nabavi et al., 2018). The putative candidate genes, APX, CAT, and ascorbate oxidase, were also found, which strongly suggests ascorbate-glutathione cycle plays an important role with antioxidant capacity (Table 3.23) (Foyer & Noctor, 2011; Kanehisa et al., 2017; T. Kim et al., 2017; S. Y. Wang & Jiao, 2000). The putative candidate gene, GST, was also found, further indicating other antioxidants contribute to the overall antioxidant capacity of blueberries (Table 3.23). Within this QTL region for DPPH-antioxidant capacity, the significant markers and QTL regions for gallic acid, quinic acid, chlorogenic acid, caffeic acid +others, epicatechin, and ascorbic +others also overlapped, thus suggesting these metabolites contribute to antioxidant capacity.

In summary, the DPPH scavenging assay quantified the antioxidant capacity for two years of blueberry extracts (Table 3.13). The DPPH-antioxidant capacity showed overall positive correlations with the HPLC-TOFMS annotated anthocyanins, and the total anthocyanins correlation exhibited the strongest correlation (Figures 3.33 and 3.34). For the ¹H NMR annotated metabolites, the DPPH-antioxidant capacity showed positive correlations with only gallic acid, chlorogenic acid, and epicatechin (Figure 3.35). The BiPAM revealed two significant QTL regions with both containing multiple putative candidate genes for the phenolic acid pathway (Table 3.23) (Buchanan et al., 2012; Herrmann, 1995; Kanehisa et al., 2017; T. Kim et al., 2017; Nabavi et al., 2018). One of the QTLs also contained putative candidate genes involved in the ascorbate-glutathione pathway (Table 3.23). This suggests that even though ascorbic acid and DPPH-antioxidant capacity did not show a good correlation, the ascorbate-glutathione pathway still plays a role in antioxidant capacity within blueberries (Himamura et al., 2014; Kedare & Singh, 2011; O. P. Sharma & Bhat, 2009; S. Singh & Singh, 2008). The identification of important QTLs along with putative candidate genes for antioxidant capacity supports the association between blueberries, anthocyanins, and potent

antioxidant capacity (Bornsek et al., 2012; De Souza et al., 2014; Gowd et al., 2017; Grace et al., 2018; Khoo et al., 2017; D. Li et al., 2017; Silva et al., 2018; Yousuf, Gul, Wani, & Singh, 2016). This research also provides additional knowledge concerning other metabolites that may contribute to antioxidant capacity (Ahmadinejad et al., 2017; Chiva-Blanch & Visioli, 2012; Foyer & Noctor, 2011; Herrmann, 1995; Lin et al., 2016; Lobo et al., 2010; Nabavi et al., 2018). Future research can continue to elucidate the specific and synergistic metabolites affecting antioxidant capacity so that future breeding strategies can utilize the information to develop blueberries with improved antioxidant capacity and enhanced health benefits.

3.6. Conclusion

Blueberries exhibit a plethora of health benefits, primarily due to their potent antioxidant properties (Bornsek et al., 2012; Bunea et al., 2013; De Souza et al., 2014; Gowd et al., 2017; Horbowicz et al., 2008; Khoo et al., 2017; Silva et al., 2018; Yousuf et al., 2016). Blueberry extracts have been shown to reduce oxidative stress, reduce inflammation, lessen neurological degeneration, and decrease cancer cell growth (Bunea et al., 2013; Giacalone et al., 2011; Gowd et al., 2017; Horbowicz et al., 2008; Khoo et al., 2017; D. Li et al., 2017; Ma et al., 2018; McNamara et al., 2018; N. Singh & Ghosh, 2019; Subash et al., 2014). As mentioned previously, many of the phenolic acids have been shown to play a role in antioxidant capacity (Bornsek et al., 2012; Bunea et al., 2013; Gowd et al., 2017; Herrmann, 1995; Khoo et al., 2017; D. Li et al., 2017; Nabavi et al., 2018; Silva et al., 2018; Yousuf et al., 2016). The anthocyanins found in blueberry have been strongly associated with potent antioxidant properties (Bunea et al., 2013; De Souza et al., 2014; Horbowicz et al., 2008; Khoo et al., 2017; Silva et al., 2018; Yousuf et al., 2016). Apart from anthocyanins, very little information concerning metabolite composition has been elucidated in blueberries. Determining the metabolite composition within blueberry will aid in understanding signaling pathways during fruit development and metabolite contribution to flavor and antioxidant capacity. The research goals of this chapter were to conduct metabolic profiling on blueberry extracts to provide foundational metabolic resources for blueberries, and to utilize the

annotated metabolites, along with DPPH-antioxidant capacity data, for biparental association mapping to identify important QTL regions and putative candidate genes.

Metabolite profiling measures and potentially annotates metabolite features either through targeted or non-targeted approaches. Targeted profiling focuses on a specific type of metabolite for detailed characterization, whereas non-targeted profiling focuses on a broad sampling of a diversity of compounds (Bingol, 2018; Carreno-Quintero et al., 2013; T. Kim et al., 2017; Matsuda, 2016; Pinu et al., 2018; Saito & Matsuda, 2010; Scalbert et al., 2009; Sumner et al., 2015; Wolfender et al., 2015). Profiling with ^1H NMR measures and annotates metabolites based on the chemical shifts of hydrogen atoms within the metabolites (Bingol, 2018; Buchanan et al., 2012; Sumner et al., 2015). Profiling with HPLC-QTOFMS measures and annotates metabolites based on their mass-to-charge ratio (m/z) effecting the time it takes the metabolite to reach the detector (Grace et al., 2018; Kai et al., 2017; Matsuda, 2016). Non-targeted profiling with ^1H NMR usually detects and measures high-abundance metabolites, which are mainly primary metabolites (Bingol, 2018; Buchanan et al., 2012; Sumner et al., 2015). Targeted profiling with HPLC-QTOFMS usually detects and annotates specific metabolites at either high or low abundance as the separation and detection methods can vary greatly (Grace et al., 2018; Kai et al., 2017; Matsuda, 2016).

The non-targeted profiling of blueberry extracts with ^1H NMR identified 943 metabolite features, with 192 annotated peaks condensing into 29 known metabolites and 751 unknowns (Table 3.3). The profiling measured and annotated three TCA cycle acids and 11 amino acids that represent three major amino acid synthesis pathways that branch from pyruvate or TCA cycle (Table 3.4) (Buchanan et al., 2012; Kanehisa et al., 2017; T. Kim et al., 2017). Among the annotated amino acids, four of the nine essential amino acids were annotated in the blueberry extracts. This suggests that future research and breeding strategies could produce blueberry cultivars with enhanced health benefits through improving essential amino acid accumulation and other phytochemical accumulation (Table 3.4) (Buchanan et al., 2012; Ufaz & Galili, 2008; G. Wang et al., 2017). The total aspartate branch accounted for 69.39% of the total amino acids while the total branch-chain branch account for only 6.21% of the total

(Table 3.4). The non-targeted profiling also measured and annotated eight different sugars, consisting of five monosaccharides that are important for signaling and other synthesis pathways, and three disaccharides that are important for energy storage (Table 3.5) (Buchanan et al., 2012; Castellarin et al., 2016; Choi, Wiersma, Toivonen, & Kappel, 2002; Paniagua et al., 2014; Posé et al., 2011; Tsai & Gazzarrini, 2014; Wingler, 2017). Glucose constituted over half, 51.84%, of the total sugars with fructose as a close second, 47.14%, while galactose accounted for only 0.02% of the total (Table 3.5). The profiling also measured and annotated five phenolic acids that not only effect the extract's acidity, but have also been implicated in contributing to antioxidant capacity (Table 3.6) (Ahmadinejad et al., 2017; Chiva-Blanch & Visioli, 2012; Foyer & Noctor, 2011; Herrmann, 1995; Lin et al., 2016; Lobo et al., 2010; Nabavi et al., 2018). Chlorogenic acid accounted for 36.17% of total phenolic acids, whereas caffeic acid accounts for 6.62% (Table 3.6). The non-targeted profiling annotated many important primary and specialized metabolites that contribute to multiple aspects of consumer-based fruit quality like taste, texture, and appearance (Bingol, 2018; Capitani et al., 2014; Gilbert et al., 2014; Kyriacou & Rouphael, 2018; McGinn, 2015; Rolin, Teyssier, Hong, & Gallusci, 2015; Tieman et al., 2012; Wolfender et al., 2015; Zhu et al., 2018).

The targeted profiling of the blueberry extracts with HPLC-QTOFMS annotated 23 anthocyanin metabolites using an optimized method that diluted the high acid HPLC solvent after separating the individual anthocyanins, but before injection into the QTOFMS (Tables 3.7 and 3.10). The HPLC UV detector, DAD, at wavelength 520nm detected 17 individual anthocyanins, while the QTOFMS detector used specific m/z for EIC to annotate the same 17 anthocyanins from DAD as well as an additional six anthocyanins resulting in a total of 23 (Tables 3.7 and 3.10). The DAD detected only 17 anthocyanins because some of the anthocyanins eluted at the same time as others, and the acetyl-galactosides had very low accumulation (Tables 3.7 and 3.10, and Figure 3.36). Using the specific m/z for the different anthocyanins, the EIC can differentiate multiple metabolites within the same elution peak, as well as detects low accumulating metabolites (Tables 3.7 and 3.10, and Figure 3.36).

Overall, the comparisons between DAD and EIC anthocyanins show a positive correlation (Figures 3.27, 3.28, 3.29, 3.30, and 3.31). For both the anthocyanins

annotated using DAD and EIC, the anthocyanins with anthocyanidin cores derived from delphinidin constitute over 80% of the total anthocyanins (Tables 3.8 and 3.11). For both the anthocyanins annotated using DAD and EIC, the anthocyanins with the galactoside sugar moiety constitute the largest percentage of total anthocyanins, 53.77% and 49.54% respectively (Tables 3.8 and 3.11). The arabinoside correlations show no or very weak correlations when compared between the two detection methods. The correlation patterns for the glucosides of both DAD and EIC anthocyanins show a similar “2-group” pattern when compared to the other sugar moieties (Figures 3.21, 3.24, and 3.25). One correlation, indicated by the red line, shows a subset of the population (subset T) with a strong positive correlation between glucosides with acetyl-glucosides and galactosides with arabinosides, thus indicating an allele allowing the accumulation of all types of sugar moieties. The other correlation, indicated by the green line, shows the other population subset (subset A) with a correlation that shows no to extremely little changes in glucoside with acetyl-glucoside accumulation, while galactosides with arabinosides increase, thus suggesting an allele with specificity to only galactosides and arabinosides. Identifying the different alleles for sugar moiety specificity requires further research to elucidate the specificity and regulatory mechanisms within anthocyanin synthesis.

The antioxidant capacity and health benefits of blueberries are mainly attributed to the high accumulation of anthocyanins in the skin (Bornsek et al., 2012; De Souza et al., 2014; Gowd et al., 2017; Grace et al., 2018; Khoo et al., 2017; D. Li et al., 2017; Silva et al., 2018; Yousuf et al., 2016). The accumulation of other acidic metabolites like citric or phenolic acids may increase the acidity of the blueberry, thus improving the stability of the anthocyanins (Ahmadinejad et al., 2017; Chiva-Blanch & Visioli, 2012; Foyer & Noctor, 2011; Herrmann, 1995; Howard et al., 2016; Lin et al., 2016; Lobo et al., 2010; Nabavi et al., 2018; Wahyuningsih et al., 2017). Therefore, the antioxidant capacity was analyzed for the DxJ blueberry extracts to provide insight into variation across the population and potential metabolites that contribute to antioxidant capacity. The DPPH assay was chosen because it is quick, simple, sensitive, and cost-effective, which made it a great project for the Plant Pathways Elucidation Project undergraduate summer internship students (Himamura et al., 2014; Kedare & Singh, 2011; O. P.

Sharma & Bhat, 2009; S. Singh & Singh, 2008). When the DPPH results were correlated with the anthocyanins, there was an overall positive correlation, but DAD detected anthocyanins showed a much stronger correlation than EIC anthocyanins (Figures 3.33 and 3.34). When DPPH results were correlated with other phenolic acids, there is a positive correlation with gallic acid, chlorogenic acid, and epicatechin (Figure 3.35).

Overall, both metabolite profiling approaches identified 11 amino acids, eight sugars, five phenolic acids, and 17 anthocyanins. Association mapping of the annotated metabolite peaks will provide vital information through the significant QTLs and putative candidate genes that may play a role in regulating the annotated metabolites. The association mapping of the 17 anthocyanins revealed eight significant QTL regions were at least three of the four individual acetyl-glucoside anthocyanin have a significant QTL overlap in the region (Table 3.17). This suggests those genetic regions may contain a putative candidate gene regulating the acetyl-glucoside modification rather than the anthocyanidin core synthesis. The DAD-anthocyanin association mapping also revealed eight QTL regions significant for the ratio of glucosides with acetyl-glucosides, and galactosides with arabinosides (Table 3.17). This suggests those genetic regions may contain putative candidate genes regulating the addition of either a glucoside, or a galactoside or arabinoside, which would support the “2-group” correlation pattern (Figures 3.21, 3.24, and 3.25). Further putative candidate gene analysis and functional characterization of anthocyanidin synthesis and anthocyanin modification enzymes will aid in elucidating anthocyanin diversification enzymes as well as blueberry-specific enzymes.

Association mapping of the glutamine branch metabolites resulted in 26 total significant QTLs with many of those genetic regions containing important synthesis or regulatory genes as putative candidate genes (Tables 3.14 and 3.18). A vital gene for regulating the interconversion between glutamate and glutamine, glutamate synthase (ferredoxin-dependent), was found as a putative candidate gene for the most significant glutamine QTL (Table 3.20) (Kanehisa et al., 2017; T. Kim et al., 2017). The three main genes regulating gamma-aminobutyrate (GABA) synthesis and catabolism were found in the genetic regions of significant GABA QTLs on linkage group two, eight, and 12 at

positions 37cM, 107cM, and 12cM, respectively (Table 3.20). The BiPAM results for branch-chain branch amino acids indicates that the final synthesis enzyme, branch-chain amino-acid transferase, is an important enzyme as it was a putative candidate gene in a QTL region significant for the essential amino acids, isoleucine, valine, and leucine (Table 3.20). The significant aspartate branch QTLs indicate that aspartate degradation towards other amino acid biosynthesis pathways is important as aspartokinase and aspartate semialdehyde dehydrogenase were found as putative candidate genes in multiple aspartate QTLs (Table 3.20). The BiPAM results for threonine indicate that the multiple threonine biosynthesis pathways may contribute to and regulate overall threonine accumulation (Table 3.20). The identified QTLs and putative candidate genes for important TCA and amino acids can be utilized for future research to further annotate and elucidate regulatory pathways of essential amino acids so that breeding strategies can be developed to apply and improve the health benefits of blueberries.

The BiPAM results for the sugars revealed the PPP, cell wall component polysaccharide degradation, and sugar interconversions are important pathways (Table 3.21). Significant fructose QTLs consistently had putative candidate genes from the PPP in the genetic regions (Table 3.21). The INV enzyme breaks down sucrose into glucose and fructose and was found as a putative candidate gene in three significant QTLs for sucrose, fructose, and glucose (Table 3.21) (Buchanan et al., 2012; Kanehisa et al., 2017; T. Kim et al., 2017). Amylases and glucosidases cleave 1,4-glycosidic bonds in polysaccharides to release free maltose or glucose, respectively, and were found as putative candidate genes for multiple maltose and glucose significant QTLs (Table 3.21). The other monosaccharide sugars like galactose, xylose, and arabinose are derivatives of UDP-glucose and the enzymes catalyzing the different interconversions were found as putative candidate genes across multiple significant QTLs (Table 3.21). Galactose and xylose are also important components for the backbones and branches of cell wall matrix polysaccharides like hemicellulose and pectin (Buchanan et al., 2012; Giongo et al., 2013; Paniagua et al., 2014; Posé et al., 2011). Degradation or modification of hemicellulose and pectin by enzymes like polygalacturonase or XTH not only effects the monosaccharides accumulation, but also

effects the integrity of the cell wall matrix, which can lead to fruit softening (Giongo et al., 2013; Paniagua et al., 2014; Posé et al., 2011). Those degradation enzymes were also found as putative candidate genes across multiple significant QTLs (Table 3.21). Identifying QTLs and putative candidate genes for multiple, different sugars is important foundational knowledge that future research can build upon to regulate their accumulation and improve berry development, sweet taste, berry firmness, and anthocyanin diversity through developing breeding strategies.

The BiPAM results for the phenolic acids revealed over 40 significant QTL regions (Table 3.22). Gallic acid and quinic acid synthesis occurs within the shikimic pathway, and then ends in phenylalanine synthesis (Kanehisa et al., 2017; T. Kim et al., 2017). Quinate dehydrogenase and 3-dehydrpquinate dehydratase are important committing steps in the shikimate pathway that were both found as putative candidate genes for multiple significant QTLs for gallic acid and quinic acid (Table 3.22). The last synthesis step for phenylalanine synthesis, arogenate/prephenate dehydratase, and PAL, the first committed step towards phenylpropanoid acid synthesis, were found as putative candidate genes within a significant QTL region for gallic, quinic, chlorogenic, and caffeic acid, thus indicating phenylalanine is vital for the phenolic acid pathway progression (Table 3.22). HCT catalyzes the two important steps in phenylpropanoid acid synthesis, especially breaking down chlorogenic acid to caffeoyl-CoA and release of quinic acid. HCT was found as a putative candidate gene across multiple QTL regions significant for chlorogenic and quinic acid (Table 3.22).

The BiPAM results for epicatechin reveals putative multiple putative candidate genes at multiple steps in the flavonoid pathway (Table 3.22) (Kanehisa et al., 2017; T. Kim et al., 2017). CHS catalyzes the committing step towards flavonoid synthesis by converting p-coumaroyl-CoA to naringenin-chalcone, and was found as a putative candidate gene for multiple significant epicatechin QTLs (Table 3.22). Diversification of flavonoids occurs with the activity of F3'H and F3'5'H to produce dihydroquercetin and dihydromyricetin, which can then be converted to leucocyanidin and leucodelphinidin, respectively, by DFR. ANS converts the leucoanthocyanidins to anthocyanidins, which can then be either converted to epicatechin by ANR, or progress to further anthocyanin diversification. Although F3'H, F3'5'H, DFR, ANS, and ANR were found as putative

candidate genes across multiple significant QTLs, F3'H and F3'5'H putative candidate genes were found in over 60% of the significant epicatechin QTLs (Table 3.22). This indicates that diversification of flavonoids is important to epicatechin accumulation (Ali Ghasemzadeh, 2011; Horbowicz et al., 2008; Howard et al., 2016; Khoo et al., 2017; D. Li et al., 2017; Ma et al., 2018; Montecchiarini et al., 2018; Ronald L Prior et al., 2001; Routray & Orsat, 2011; Scalzo et al., 2015; You et al., 2011). The identified QTLs and putative candidate genes provide additional knowledge on the phenolic acid pathway, which can be utilized to elucidate the regulation of phenolic acid diversification (Herrmann, 1995; Kanehisa et al., 2017; T. Kim et al., 2017; Lin et al., 2016; Nabavi et al., 2018). A greater understanding of phenolic acid diversification will improve the differential accumulation of shikimic pathway acids, phenylpropanoids, and flavonoids, which will not only affect the sour-tart taste of blueberries, but also the blue coloration through stabilizing anthocyanins (Kader, 2008; Khoo et al., 2017; McGinn, 2015; Pagliarini et al., 2013; Tieman et al., 2012; Yonekura-Sakakibara et al., 2009).

Along with mapping the metabolites from non-targeted and targeted profiling, the antioxidant capacity measured through the DPPH assay was also mapped. The BiPAM results revealed two significant QTLs, one on linkage group five at position 107cM and the another on linkage group six at position 45cM (Table 3.23). Both significant QTLs contained the putative candidate genes, p-coumaroyl-CoA ligase, F3'H, and F3'5'H, indicating phenylpropanoid and flavonoid synthesis pathway and metabolites contribute to antioxidant capacity (Table 3.23) (Kanehisa et al., 2017; T. Kim et al., 2017). Both QTL regions also contain important, but different enzymes in the shikimic pathway, suggesting the shikimic pathway also plays an important role in antioxidant capacity (Table 3.23). In the DPPH QTL on linkage group five at position 107cM, putative candidate genes for anthocyanin diversification were also found, which supports the strong association between anthocyanins and antioxidant capacity (Table 3.23) (Bornsek et al., 2012; De Souza et al., 2014; Gowd et al., 2017; Grace et al., 2018; Khoo et al., 2017; D. Li et al., 2017; Silva et al., 2018; Yousuf et al., 2016). In the DPPH QTL on linkage group six at position 45cM, there are also putative candidate genes for catalase and the ascorbate-glutathione cycling pathway, which indicates that enzymatic antioxidants may also contribute to the antioxidant capacity found in blueberries (Table

3.23). Identifying the QTLs and putative candidate genes for antioxidant capacity provides additional support for associating phenolic acids with antioxidant capacity as well as suggesting the antioxidant potency may be a synergistic interaction between multiple metabolites in blueberries (Bornsek et al., 2012; De Souza et al., 2014; Gowd et al., 2017; Khoo et al., 2017; D. Li et al., 2017; Silva et al., 2018; Yousuf et al., 2016). Future research will utilize this knowledge to elucidate the diversity, combination, and potency of different metabolites that improve the antioxidant capacity in blueberries, like phenylpropanoids, which not only can stabilize anthocyanins and improve their antioxidant capacity, but also can act as antioxidants to further improve antioxidant capacity. Through identifying multiple significant QTLs and putative candidate genes for metabolites that contribute to the diversity of health benefits of blueberries, breeders can utilize multiple QTLs in breeding strategies to develop blueberries with enhanced health benefits.

3.7. Acknowledgments

This work was supported by both the Plant Pathways Elucidation Project through Dr. Lila and Dr. Li, and the NCSU faculty start-up funds from Dr. Li. A special thank you to Dr. Hancock, Dr. Finn, and Dr. Olmstead for coordinating and harvesting the DxJ blueberries from GA and OR for both 2015 and 2016. Thank you to Dr. Kevin Knagge and his metabolomics-analytic science research team at the David H. Murdock Research Institute (DHMRI) at the NCRC for assisting with running and software analysis of the ¹H NMR non-targeted profiling of blueberry extracts. Thank you to the Li-Lab members for teaching the intricacies of running and troubleshooting issues on the HPLC-QTOFMS. Thank you to the Lila-Lab members for providing assistance and space for extracting and conducting the DPPH-antioxidant capacity assay for the hundreds of blueberry samples. A special thank you to the P²EP summer undergraduate interns - Ashley Wagoner, Jordan Hunt, Bryan Morris, Estefania Castro-Vazquez; Accola Hudson, Roa Saleh, Alexa Marcy, and Angeli Gupta - for working with me to conduct the DPPH assay as well as perform the biparental association mapping for all the hundreds of metabolites from both the targeted and non-targeted profiling.

REFERENCES

- Ahmadinejad, F., Geir Møller, S., Hashemzadeh-Chaleshtori, M., Bidkhor, G., & Jami, M.-S. (2017). Molecular Mechanisms behind Free Radical Scavengers Function against Oxidative Stress. *Antioxidants*, 6(3), 51.
- Alam, M. N., Bristi, N. J., & Rafiquzzaman, M. (2013). Review on in vivo and in vitro methods evaluation of antioxidant activity. *Saudi Pharmaceutical Journal*, 21(2), 143–152.
- Ali Ghasemzadeh. (2011). Flavonoids and phenolic acids: Role and biochemical activity in plants and human. *Journal of Medicinal Plants Research*, 5(31), 6697–6703.
- Alonso, A., Marsal, S., & JuliÀ, A. (2015). Analytical Methods in Untargeted Metabolomics: State of the Art in 2015. *Frontiers in Bioengineering and Biotechnology*, 3.
- An, C., & Mou, Z. (2011). Salicylic Acid and its Function in Plant ImmunityF: Defense Signal Molecule Salicylic Acid. *Journal of Integrative Plant Biology*, 53(6), 412–428.
- Aqil, F., Jeyabalan, J., Kausar, H., Munagala, R., Singh, I. P., & Gupta, R. (2016). Lung cancer inhibitory activity of dietary berries and berry polyphenolics. *Journal of Berry Research*, 6(2), 105–114.
- Aurelia Magdalena Pisoschi, Aneta Pop, Carmen Cimpeanu, & Gabriel Predoi. (2016). Antioxidant Capacity Determination in Plants and Plant-Derived Products: A Review. *Oxidative Medicine and Cellular Longevity*, 2016(9130976), 36.
- Barnes, J. S., Nguyen, H. P., Shen, S., & Schug, K. A. (2009). General method for extraction of blueberry anthocyanins and identification using high performance liquid chromatography–electrospray ionization-ion trap-time of flight-mass spectrometry. *Journal of Chromatography A*, 1216(23), 4728–4735.
- Barrett, D. M., Beaulieu, J. C., & Shewfelt, R. (2010). Color, flavor, texture, and nutritional quality of fresh-cut fruits and vegetables: Desirable levels, instrumental and sensory measurement, and the effects of processing. *Critical Reviews in Food Science and Nutrition*, 50(5), 369–389.
- Bernardo, R. (2008). Molecular markers and selection for complex traits in plants: Learning from the last 20 years. *Crop Science*, 48(5), 1649–1664.
- Bingol, K. (2018). Recent Advances in Targeted and Untargeted Metabolomics by NMR and MS/NMR Methods. *High-Throughput*, 7(2), 9.
- Blueberry, L., Aiton, V., Grace, M. H., Ribnicky, D. M., Kuhn, P., Poulev, A., ... Ann, M. (2010). Hypoglycemic activity of a novel Anthoxyanin-rich formulation from Lowbush Blueberry, *Vaccinium angustifolium ai*, 16(5), 406–415.
- Boonstra, E., de Kleijn, R., Colzato, L. S., Alkemade, A., Forstmann, B. U., & Nieuwenhuis, S. (2015). Neurotransmitters as food supplements: The effects of GABA on brain and behavior. *Frontiers in Psychology*, 6(OCT), 6–11.
- Bornsek, S. M., Ziberna, L., Polak, T., Vanzo, A., Ulrich, N. P., Abram, V., ... Passamonti, S. (2012). Bilberry and blueberry anthocyanins act as powerful intracellular antioxidants in mammalian cells. *Food Chemistry*, 134(4), 1878–1884.
- Bown, A. W., & Shelp, B. J. (2016). Plant GABA: Not Just a Metabolite. *Trends in Plant Science*, 21(10), 811–813.
- Brito, A., Areche, C., Sepúlveda, B., Kennelly, E. J., & Simirgiotis, M. J. (2014). Anthocyanin characterization, total phenolic quantification and antioxidant features of some chilean edible berry extracts. *Molecules*, 19(8), 10936–10955.

- Brown, P. N., Murch, S. J., & Shipley, P. (2012). Phytochemical diversity of cranberry (*Vaccinium macrocarpon* Aiton) cultivars by anthocyanin determination and metabolomic profiling with chemometric analysis. *Journal of Agricultural and Food Chemistry*, 60(1), 261–271.
- Buchanan, B. B., Grissem, W., & Jones, R. L. (2012). *Biochemistry & Molecular Biology of Plants*. American Society of Plant Biologists: 15501 Monona Drive, Rockville, MD 20855-2768 USA: Markono Print Media Pte Ltd.
- Bujor, O. C., Le Bourvellec, C., Volf, I., Popa, V. I., & Dufour, C. (2016). Seasonal variations of the phenolic constituents in bilberry (*Vaccinium myrtillus* L.) leaves, stems and fruits, and their antioxidant activity. *Food Chemistry*, 213, 58–68.
- Bunea, A., Rugină, D., Sconța, Z., Pop, R. M., Pinte, A., Socaciu, C., ... VanCamp, J. (2013). Anthocyanin determination in blueberry extracts from various cultivars and their antiproliferative and apoptotic properties in B16-F10 metastatic murine melanoma cells. *Phytochemistry*, 95, 436–444.
- Butt, M. S., & Sultan, M. T. (2011). Ginger and its health claims: Molecular aspects. *Critical Reviews in Food Science and Nutrition*, 51(5), 383–393.
- Capitani, D., Sobolev, A. P., Delfini, M., Vista, S., Antiochia, R., Proietti, N., ... Mannina, L. (2014). NMR methodologies in the analysis of blueberries: General. *ELECTROPHORESIS*, 35(11), 1615–1626.
- Cappai, F., Benevenuto, J., Ferrão, L., & Munoz, P. (2018). Molecular and Genetic Bases of Fruit Firmness Variation in Blueberry—A Review. *Agronomy*, 8(9), 174.
- Carreno-Quintero, N., Bouwmeester, H. J., & Keurentjes, J. J. B. (2013). Genetic analysis of metabolome–phenotype interactions: from model to crop species. *Trends in Genetics*, 29(1), 41–50.
- Castañeda-Ovando, A., Pacheco-Hernández, M. de L., Páez-Hernández, M. E., Rodríguez, J. A., & Galán-Vidal, C. A. (2009). Chemical studies of anthocyanins: A review. *Food Chemistry*, 113(4), 859–871.
- Castellarin, S. D., & Di Gaspero, G. (2007). Transcriptional control of anthocyanin biosynthetic genes in extreme phenotypes for berry pigmentation of naturally occurring grapevines. *BMC Plant Biology*, 7, 1–10.
- Castellarin, S. D., Gambetta, G. A., Wada, H., Krasnow, M. N., Cramer, G. R., Peterlunger, E., ... Matthews, M. A. (2016). Characterization of major ripening events during softening in grape: Turgor, sugar accumulation, abscisic acid metabolism, colour development, and their relationship with growth. *Journal of Experimental Botany*, 67(3), 709–722.
- Castrejón, A. D. R., Eichholz, I., Rohn, S., Kroh, L. W., & Huyskens-Keil, S. (2008). Phenolic profile and antioxidant activity of highbush blueberry (*Vaccinium corymbosum* L.) during fruit maturation and ripening. *Food Chemistry*, 109(3), 564–572.
- Chae, L., Kim, T., Nilo-Poyanco, R., & Rhee, S. Y. (2014). Genomic Signatures of Specialized Metabolism in Plants. *Science*, 344(May), 510–513.
- Chen, H., Cao, S., Fang, X., Mu, H., Yang, H., Wang, X., ... Gao, H. (2015). Changes in fruit firmness, cell wall composition and cell wall degrading enzymes in postharvest blueberries during storage. *Scientia Horticulturae*, 188, 44–48.
- Chiva-Blanch, G., & Visioli, F. (2012). Polyphenols and health: Moving beyond antioxidants. *Journal of Berry Research*, 2(2), 63–71.

- Choi, C., Wiersma, P. A., Toivonen, P., & Kappel, F. (2002). Fruit growth, firmness and cell wall hydrolytic enzyme activity during development of sweet cherry fruit treated with gibberellic acid (GA3). *Journal of Horticultural Science and Biotechnology*, 77(5), 615–621.
- Cocetta, G., Karppinen, K., Suokas, M., Hohtola, A., Häggman, H., Spinardi, A., ... Jaakola, L. (2012). Ascorbic acid metabolism during bilberry (*Vaccinium myrtillus* L.) fruit development. *Journal of Plant Physiology*, 169(11), 1059–1065.
- Colak, N., Primetta, A. K., Riihinen, K. R., Jaakola, L., Grúz, J., Strnad, M., ... Ayaz, F. A. (2017). Phenolic compounds and antioxidant capacity in different-colored and non-pigmented berries of bilberry (*Vaccinium myrtillus* L.). *Food Bioscience*, 20(May), 67–78.
- Colak, N., Torun, H., Gruz, J., Strnad, M., Hermosín-Gutiérrez, I., Hayirlioglu-Ayaz, S., & Ayaz, F. A. (2016). Bog bilberry phenolics, antioxidant capacity and nutrient profile. *Food Chemistry*, 201, 339–349.
- Collard, B. C. Y., Jahufer, M. Z. Z., Brouwer, J. B., & Pang, E. C. K. (2005). An introduction to markers, quantitative trait loci (QTL) mapping and marker-assisted selection for crop improvement: The basic concepts. *Euphytica*, 142(1–2), 169–196.
- Correia, R., Grace, M. H., Esposito, D., & Lila, M. A. (2017). Wild blueberry polyphenol-protein food ingredients produced by three drying methods: Comparative physico-chemical properties, phytochemical content, and stability during storage. *Food Chemistry*, 235, 76–85.
- Couée, I., Sulmon, C., Gouesbet, G., & El Amrani, A. (2006). Involvement of soluble sugars in reactive oxygen species balance and responses to oxidative stress in plants. *Journal of Experimental Botany*, 57(3), 449–459.
- De Souza, V. R., Pereira, P. A. P., Da Silva, T. L. T., De Oliveira Lima, L. C., Pio, R., & Queiroz, F. (2014). Determination of the bioactive compounds, antioxidant activity and chemical composition of Brazilian blackberry, red raspberry, strawberry, blueberry and sweet cherry fruits. *Food Chemistry*, 156, 362–368.
- Diana, M., Quílez, J., & Rafecas, M. (2014). Gamma-aminobutyric acid as a bioactive compound in foods: A review. *Journal of Functional Foods*, 10, 407–420.
- Draper, A., & Hancock, J. F. (2003). Florida 4B: Native Blueberry with Exceptional Breeding Value. *Journal of the American Pomological Society*, 57(4), 138–141.
- Edirisinghe, I., & Burton-Freeman, B. (2016). Anti-diabetic actions of Berry polyphenols - Review on proposed mechanisms of action. *Journal of Berry Research*, 6(2), 237–250.
- Eklund, B. (2016). *2016 Blueberry Statistics - USDA*. Trenton.
- Feenstra, B. (2006). Mapping Quantitative Trait Loci by an Extension of the Haley-Knott Regression Method Using Estimating Equations. *Genetics*, 173(4), 2269–2282.
- Fernie, A. R., & Schauer, N. (2009). Metabolomics-assisted breeding: a viable option for crop improvement? *Trends in Genetics*, 25(1), 39–48.
- Ferreira, V., Castro, I., Carrasco, D., Pinto-Carnide, O., & Arroyo-García, R. (2018). Molecular characterization of berry skin color reversion on grape somatic variants. *Journal of Berry Research*, 8(3), 147–162.
- Forney, C. F., Kalt, W., Jordan, M. A., Vinqvist-Tymchuk, M. R., & Fillmore, S. A. E. (2012). Blueberry and cranberry fruit composition during development. *Journal of*

- Berry Research*, 2(3), 169–177.
- Foyer, C. H., & Noctor, G. (2011). Ascorbate and Glutathione: The Heart of the Redox Hub. *Plant Physiology*, 155(1), 2–18.
- French, K. E., Harvey, J., & McCullagh, J. S. O. (2018). Targeted and Untargeted Metabolic Profiling of Wild Grassland Plants identifies Antibiotic and Anthelmintic Compounds Targeting Pathogen Physiology, Metabolism and Reproduction. *Scientific Reports*, 8(1), 1–10.
- Galano, A., Mazzone, G., Alvarez-Diduk, R., Marino, T., Alvarez-Idaboy, J. R., & Russo, N. (2016). Food Antioxidants: Chemical Insights at the Molecular Level. *Annual Review of Food Science and Technology*, 7(1), 335–352.
- Ghan, R., Petereit, J., Tillett, R. L., Schlauch, K. A., Toubiana, D., Fait, A., & Cramer, G. R. (2017). The common transcriptional subnetworks of the grape berry skin in the late stages of ripening. *BMC Plant Biology*, 17(1), 1–21.
- Giacalone, M., Di Sacco, F., Traupe, I., Topini, R., Forfori, F., & Giunta, F. (2011). Antioxidant and neuroprotective properties of blueberry polyphenols: a critical review. *Nutritional Neuroscience*, 14(3), 119–125.
- Gilbert, J. L., Olmstead, J. W., Colquhoun, T. A., Levin, L. A., Clark, D. G., & Moskowitz, H. R. (2014). Consumer-assisted selection of blueberry fruit quality traits. *HortScience*, 49(7), 864–873.
- Giongo, L., Poncetta, P., Loretto, P., & Costa, F. (2013). Texture profiling of blueberries (*Vaccinium* spp.) during fruit development, ripening and storage. *Postharvest Biology and Technology*, 76, 34–39.
- Gowd, V., Jia, Z., & Chen, W. (2017). Anthocyanins as promising molecules and dietary bioactive components against diabetes – A review of recent advances. *Trends in Food Science and Technology*, 68, 1–13.
- Grace, M. H., Xiong, J., Esposito, D., Ehlenfeldt, M., & Lila, M. A. (2018). Simultaneous LC-MS quantification of anthocyanins and non-anthocyanin phenolics from blueberries with widely divergent profiles and biological activities. *Food Chemistry*.
- Granot, D., David-Schwartz, R., & Kelly, G. (2013). Hexose Kinases and Their Role in Sugar-Sensing and Plant Development. *Frontiers in Plant Science*, 4(March), 1–17.
- Gul, K., Tak, A., Singh, A. K., Singh, P., Yousuf, B., & Wani, A. A. (2015). Chemistry, encapsulation, and health benefits of B-carotene - A review. *Cogent Food & Agriculture*, 1(1), 1–12.
- Hackett, C. A., Bradshaw, J. E., & McNicol, J. W. (2001). Interval mapping of quantitative trait loci in autotetraploid species. *Genetics*, 159(4), 1819–1832.
- Halkier, B. A., & Gershenzon, J. (2006). Biology and biochemistry of glucosinolates. *Annu. Rev. Plant Biol.*, 57, 303–333.
- Hancock, J. F., Olmstead, J. W., Iltle, R. A., Callow, P. W., Neils-Kraft, S., Wheeler, E. J., ... Finn, C. E. (2018). Performance of an elite, hybrid family of a northern × southern highbush cross ('Draper' × 'Jewel'). *Euphytica*, 214(6), 1–16.
- He, F., Mu, L., Yan, G. L., Liang, N. N., Pan, Q. H., Wang, J., ... Duan, C. Q. (2010). Biosynthesis of anthocyanins and their regulation in colored grapes. *Molecules*, 15(12), 9057–9091.
- Hernández-Orte, P., Cacho, J. F., & Ferreira, V. (2002). Relationship between varietal amino acid profile of grapes and wine aromatic composition. Experiments with model solutions and chemometric study. *Journal of Agricultural and Food*

- Chemistry*, 50(10), 2891–2899.
- Hernández-Sotomayor, S., Siddiqui, K., Guerriero, G., Abdel-Salam, E., Hausman, J.-F., Cai, G., ... Qahtan, A. (2018). Production of Plant Secondary Metabolites: Examples, Tips and Suggestions for Biotechnologists. *Genes*, 9(6), 309.
- Herrmann, K. M. (1995). The shikimate pathway: early steps in the biosynthesis of aromatic compounds. *The Plant Cell*, 7(7), 907.
- Himamura, T. S., Umikura, Y. S., Amazaki, T. Y., Ada, A. T., Ashiwagi, T. K., Shikawa, H. I., ... Keda, H. U. (2014). Applicability of the DPPH Assay for Evaluating the Antioxidant Capacity of Food Additives - Inter-laboratory Evaluation Study. *Analytical Sciences*, 30(July), 717–721.
- Hirai, M. Y., Klein, M., Fujikawa, Y., Yano, M., Goodenowe, D. B., Yamazaki, Y., ... Kitayama, M. (2005). Elucidation of Gene-to-Gene and Metabolite-to-Gene Networks in Arabidopsis by Integration of Metabolomics and Transcriptomics. *Journal of Biological Chemistry*, 280(27), 25590–25595.
- Horbowicz, M., Grzesiuk, A., DEBski, H., & Kosson, R. (2008). Anthocyanins of Fruits and Vegetables - Their Occurrence, Analysis and Role in Human. *Vegetable Crops Research Bulletin*, 68, 5–22.
- Howard, L. R., Brownmiller, C., Mauromoustakos, A., & Prior, R. L. (2016). Improved stability of blueberry juice anthocyanins by acidification and refrigeration. *Journal of Berry Research*, 6(2), 189–201.
- Huan, C., Jiang, L., An, X., Yu, M., Xu, Y., Ma, R., & Yu, Z. (2016). Potential role of reactive oxygen species and antioxidant genes in the regulation of peach fruit development and ripening. *Plant Physiology and Biochemistry*, 104, 294–303.
- Huang, D., Ou, B., & Prior, R. L. (2005). The Chemistry behind Antioxidant Capacity Assays. *Journal of Agricultural and Food Chemistry*, 53, 1841–1856.
- Inostroza-Blancheteau, C., Reyes-Díaz, M., Arellano, A., Latsague, M., Acevedo, P., Loyola, R., ... Alberdi, M. (2014). Effects of UV-B radiation on anatomical characteristics, phenolic compounds and gene expression of the phenylpropanoid pathway in highbush blueberry leaves. *Plant Physiology and Biochemistry*, 85, 85–95.
- Iorizzo, M., Bostan, H., Aryal, R., Rowland, L. J., Zalapa, J., & Ashrafi, H. (2018). Towards Developing a Chromosome Scale Reference Genome Sequence of Blueberry. In *Plant & Animal Genome Conference XXVI - Fruit/Nuts Workshops* (p. 1). San Diego: Plant & Animal Genome Conference XXVI.
- Jaakola, L. (2002). Expression of Genes Involved in Anthocyanin Biosynthesis in Relation to Anthocyanin, Proanthocyanidin, and Flavonol Levels during Bilberry Fruit Development. *PLANT PHYSIOLOGY*, 130(2), 729–739.
- Jander, G., & Joshi, V. (2009). Aspartate-Derived Amino Acid Biosynthesis in *Arabidopsis thaliana*. *The Arabidopsis Book*, 7, e0121.
- Jenks, M. A., & Bebeli, P. J. (2011). *Breeding for Fruit Quality*. West Sussex: John Wiley & Sons, Inc.
- Jeong, S.-W., Das, P. K., Jeoung, S. C., Song, J.-Y., Lee, H. K., Kim, Y.-K., ... Park, Y.-I. (2010). Ethylene Suppression of Sugar-Induced Anthocyanin Pigmentation in Arabidopsis. *Plant Physiology*, 154(3), 1514–1531.
- Kader, A. A. (2008). Flavor quality of fruits and vegetables. *Journal of the Science of Food and Agriculture*, 88(11), 1863–1868.

- Kai, H., Kinoshita, K., Harada, H., Uesawa, Y., Maeda, A., Suzuki, R., ... Matsuno, K. (2017). Establishment of a Direct-Injection Electron Ionization-Mass Spectrometry Metabolomics Method and Its Application to Lichen Profiling. *Analytical Chemistry*, 89(12), 6408–6414.
- Kalt, W., McDonald, J. E., Ricker, R. D., & Lu, X. (1999). Anthocyanin content and profile within and among blueberry species. *Canadian Journal of Plant Science*, 79(4), 617–623.
- Kanehisa, M., Furumichi, M., Tanabe, M., Sato, Y., & Morishima, K. (2017). KEGG: New perspectives on genomes, pathways, diseases and drugs. *Nucleic Acids Research*, 45(D1), D353–D361.
- Kang, M. S. (2002). *Quantitative genetics, genomics and plant breeding*. New York: CABI Publishing.
- Kao, C.-H. (2000). On The Differences Between Maximum Likelihood and Regression Interval Mapping in the Analysis of Quantitative Trait Loci. *Genetics*, 156, 855–865.
- Karppinen, K., Zoratti, L., Nguyenquynh, N., Häggman, H., & Jaakola, L. (2016). On the Developmental and Environmental Regulation of Secondary Metabolism in *Vaccinium* spp. Berries. *Frontiers in Plant Science*, 7(May), 1–9.
- Kedare, S. B., & Singh, R. P. (2011). Genesis and development of DPPH method of antioxidant assay. *Journal of Food Science and Technology*, 48(4), 412–422.
- Khoo, H. E., Azlan, A., Tang, S. T., & Lim, S. M. (2017). Anthocyanidins and anthocyanins: colored pigments as food, pharmaceutical ingredients, and the potential health benefits. *Food & Nutrition Research*, 61(1), 1–21.
- Kim, H. Y., Faruq, M., Cohen, Y., Crisosto, C., Sadka, A., & Blumwald, E. (2015). Non-climacteric ripening and sorbitol homeostasis in plum fruits. *Plant Science*, 231, 30–39.
- Kim, T., Banf, M., Kahn, D., Bernard, T., Dreher, K., Chavali, A. K., ... Zhang, P. (2017). Genome-Wide Prediction of Metabolic Enzymes, Pathways, and Gene Clusters in Plants. *Plant Physiology*, 173(4), 2041–2059.
- Klessig, D. F., & Malamy, J. (1994). The Salicylic acid signal in plants, 26, 1439–1458.
- Klimis-Zacas, D., Vendrame, S., & Kristo, A. S. (2016). Wild blueberries attenuate risk factors of the metabolic syndrome. *Journal of Berry Research*, 6(2), 225–236.
- Kong, Y., Peña, M. J., Renna, L., Avci, U., Pattathil, S., Tuomivaara, S. T., ... O'Neill, M. A. (2015). Galactose-Depleted Xyloglucan Is Dysfunctional and Leads to Dwarfism in *Arabidopsis*. *Plant Physiology*, 167(4), 1296–1306.
- Kraujalyte, V., Venskutonis, P. R., Pukalskas, A., Česonienė, L., & Daubaras, R. (2015). Antioxidant properties, phenolic composition and potentiometric sensor array evaluation of commercial and new blueberry (*Vaccinium corymbosum*) and bog blueberry (*Vaccinium uliginosum*) genotypes. *Food Chemistry*, 188, 583–590.
- Kulik, A., Wawer, I., Krzywińska, E., Bucholc, M., & Dobrowolska, G. (2011). SnRK2 Protein Kinases—Key Regulators of Plant Response to Abiotic Stresses. *OMICS: A Journal of Integrative Biology*, 15(12), 859–872.
- Kumar, S., Paul, S., Walia, Y. K., Kumar, A., Singhal, P., & Chowk, N. (2015). Therapeutic Potential of Medicinal Plants : A Review. *J. Biol. Chem. Chron.*, 1(1), 46–54.
- Kyriacou, M. C., & Roupael, Y. (2018). Towards a new definition of quality for fresh fruits and vegetables. *Scientia Horticulturae*, 234(August 2017), 463–469.

- Leiva-Valenzuela, G. A., Lu, R., & Aguilera, J. M. (2013). Prediction of firmness and soluble solids content of blueberries using hyperspectral reflectance imaging. *Journal of Food Engineering*, *115*(1), 91–98.
- Li, D., Li, B., Ma, Y., Sun, X., Lin, Y., & Meng, X. (2017). Polyphenols, anthocyanins, and flavonoids contents and the antioxidant capacity of various cultivars of highbush and half-high blueberries. *Journal of Food Composition and Analysis*, *62*, 84–93.
- Li, D., Meng, X., & Li, B. (2016). Profiling of anthocyanins from blueberries produced in China using HPLC-DAD-MS and exploratory analysis by principal component analysis. *Journal of Food Composition and Analysis*, *47*, 1–7.
- Li, H., Ye, G., & Wang, J. (2006). A Modified Algorithm for the Improvement of Composite Interval Mapping. *Genetics*, *175*(1), 361–374.
- Li, W., Liu, Y., Zeng, S., Xiao, G., Wang, G., Wang, Y., ... Huang, H. (2015). Gene expression profiling of development and anthocyanin accumulation in kiwifruit (*actinidia chinensis*) based on transcriptome sequencing. *PLoS ONE*, *10*(8), 1–19.
- Lila, M. A., Burton-Freeman, B., Grace, M., & Kalt, W. (2016). Unraveling Anthocyanin Bioavailability for Human Health. *Annual Review of Food Science and Technology*, *7*(1), 375–393.
- Lin, D., Xiao, M., Zhao, J., Li, Z., Xing, B., Li, X., ... Chen, S. (2016). An overview of plant phenolic compounds and their importance in human nutrition and management of type 2 diabetes. *Molecules*, *21*(10).
- Lobo, V., Patil, A., Phatak, A., & Chandra, N. (2010). Free radicals, antioxidants and functional foods: Impact on human health. *Pharmacognosy Reviews*, *4*(8), 118.
- Lohachompol, V., Mulholland, M., Szrednicki, G., & Craske, J. (2008). Determination of anthocyanins in various cultivars of highbush and rabbiteye blueberries. *Food Chemistry*, *111*(1), 249–254.
- López-Alarcón, C., & Denicola, A. (2013). Evaluating the antioxidant capacity of natural products: A review on chemical and cellular-based assays. *Analytica Chimica Acta*, *763*, 1–10.
- Lunn, J. E., Delorge, I., Figueroa, C. M., Van Dijck, P., & Stitt, M. (2014). Trehalose metabolism in plants. *The Plant Journal*, *79*(4), 544–567.
- Ma, H., Johnson, S. L., Liu, W., Dasilva, N. A., Meschwitz, S., Dain, J. A., & Seeram, N. P. (2018). Evaluation of Polyphenol Anthocyanin-Enriched Extracts of Blackberry , Black Raspberry , Blueberry , Cranberry , Red Raspberry , and Strawberry for Free Radical Scavenging , Reactive Carbonyl Species Aggregation , and Microglial Neuroprotective Effects. *International Journal of Molecular Sciences*, *19*(461), 1–19.
- Matsuda, F. (2016). Technical Challenges in Mass Spectrometry-Based Metabolomics. *Mass Spectrometry*, *5*(2), S0052–S0052.
- Mattila, P., Hellström, J., & Törrönen, R. (2006). Phenolic acids in berries, fruits, and beverages. *Journal of Agricultural and Food Chemistry*, *54*(19), 7193–7199.
- Matusheski, N. V., Juvik, J. A., & Jeffery, E. H. (2004). Heating decreases epithiospecifier protein activity and increases sulforaphane formation in broccoli. *Phytochemistry*, *65*(9), 1273–1281.
- Mayer, M. (2005). A comparison of regression interval mapping and multiple interval mapping for linked QTL. *Heredity*, *94*(6), 599–605.

- McCallum, S., Graham, J., Jorgensen, L., Rowland, L. J., Bassil, N. V., Hancock, J. F., ... Hackett, C. A. (2016). Construction of a SNP and SSR linkage map in autotetraploid blueberry using genotyping by sequencing. *Molecular Breeding*, 36(4).
- McGinn, C. (2015). The science of taste. *Metaphilosophy*, 46(1), 84–103.
- McNamara, R. K., Kalt, W., Shidler, M. D., McDonald, J., Summer, S. S., Stein, A. L., ... Krikorian, R. (2018). Cognitive response to fish oil, blueberry, and combined supplementation in older adults with subjective cognitive impairment. *Neurobiology of Aging*, 64, 147–156.
- Mishra, K., Ojha, H., & Chaudhury, N. K. (2012). Estimation of antiradical properties of antioxidants using DPPH - assay: A critical review and results. *Food Chemistry*, 130(4), 1036–1043.
- Moharram, H. A., & Youssef, M. M. (2014). Methods for Determining the Antioxidant Activity : A Review. *J. Fd . Sci . & Technol*, 11(1), 31–42.
- Montecchiarini, M. L., Bello, F., Rivadeneira, M. F., Vázquez, D., Podestá, F. E., & Tripodi, K. E. J. (2018). Metabolic and physiologic profile during the fruit ripening of three blueberries highbush (*Vaccinium corymbosum*) cultivars. *Journal of Berry Research*, 8(3), 177–192.
- Muleke, E. M., Fan, L., Wang, Y., Xu, L., Zhu, X., Zhang, W., ... Liu, L. (2017). Coordinated Regulation of Anthocyanin Biosynthesis Genes Confers Varied Phenotypic and Spatial-Temporal Anthocyanin Accumulation in Radish (*Raphanus sativus* L.). *Frontiers in Plant Science*, 8(July), 1–17.
- Mykkänen, O. T., Huotari, A., Herzig, K. H., Dunlop, T. W., Mykkänen, H., & Kirjavainen, P. V. (2014). Wild blueberries (*vaccinium myrtillus*) alleviate inflammation and hypertension associated with developing obesity in mice fed with a high-fat diet. *PLoS ONE*, 9(12), 1–21.
- Nabavi, S. M., Šamec, D., Tomczyk, M., Milella, L., Russo, D., Habtemariam, S., ... Shirooie, S. (2018). Flavonoid biosynthetic pathways in plants: Versatile targets for metabolic engineering. *Biotechnology Advances*, (June).
- Nakayama, T., Suzuki, H., & Nishino, T. (2003). Anthocyanin acyltransferases: Specificities, mechanism, phylogenetics, and applications. *Journal of Molecular Catalysis B: Enzymatic*, 23(2–6), 117–132.
- Neto, C. C. (2007). Cranberry and blueberry: Evidence for protective effects against cancer and vascular diseases. *Molecular Nutrition and Food Research*, 51(6), 652–664.
- Niki, E. (2011). Antioxidant capacity: Which capacity and how to assess it? *Journal of Berry Research*, 1(4), 169–176.
- Nile, S. H., & Park, S. W. (2014). Edible berries: Bioactive components and their effect on human health. *Nutrition*, 30(2), 134–144. h
- O'Hara, L. E., Paul, M. J., & Wingler, A. (2013). How do sugars regulate plant growth and development? new insight into the role of trehalose-6-phosphate. *Molecular Plant*, 6(2), 261–274.
- Oancea, S., Moiseenco, F., & Traldi, P. (2013). Total phenolics and anthocyanin profiles of romanian wild and cultivated blueberries by direct infusion esi-it-ms/ms. *Romanian Biotechnological Letters*, 18(3), 8350–8360.
- Oh, H. D., Yu, D. J., Chung, S. W., Chea, S., & Lee, H. J. (2018). Abscisic acid

- stimulates anthocyanin accumulation in ‘Jersey’ highbush blueberry fruits during ripening. *Food Chemistry*, 244(June 2017), 403–407.
- Okazaki, Y., & Saito, K. (2012). Recent advances of metabolomics in plant biotechnology. *Plant Biotechnology Reports*, 6(1), 1–15.
- Oliver, R. E., Tinker, N. A., Lazo, G. R., Chao, S., Jellen, E. N., Carson, M. L., ... Jackson, E. W. (2013). SNP Discovery and Chromosome Anchoring Provide the First Physically-Anchored Hexaploid Oat Map and Reveal Synteny with Model Species. *PLoS ONE*, 8(3).
- Ongkowiyo, P., Luna-Vital, D. A., & Gonzalez de Mejia, E. (2018). Extraction techniques and analysis of anthocyanins from food sources by mass spectrometry: An update. *Food Chemistry*, 250(January), 113–126.
- Overall, J., Bonney, S. A., Wilson, M., Beermann, A., Grace, M. H., Esposito, D., ... Komarnytsky, S. (2017). Metabolic effects of berries with structurally diverse anthocyanins. *International Journal of Molecular Sciences*, 18(2).
- Pagliarini, E., Laureati, M., & Gaeta, D. (2013). Sensory descriptors, hedonic perception and consumer’s attitudes to Sangiovese red wine deriving from organically and conventionally grown grapes. *Frontiers in Psychology*, 4(NOV), 1–7.
- Pan, P., Huang, Y.-W., Oshima, K., Yearsley, M., Zhang, J., Yu, J., ... Wang, L.-S. (2018). An immunological perspective for preventing cancer with berries. *Journal of Berry Research*, 8(3), 163.
- Pan, P., Skaer, C., Yu, J., Zhao, H., Ren, H., Oshima, K., & Wang, L. S. (2017). Berries and other natural products in pancreatic cancer chemoprevention in human clinical trials. *Journal of Berry Research*, 7(3), 147–161.
- Paniagua, C., Posé, S., Morris, V. J., Kirby, A. R., Quesada, M. A., & Mercado, J. A. (2014). Fruit softening and pectin disassembly: An overview of nanostructural pectin modifications assessed by atomic force microscopy. *Annals of Botany*, 114(6), 1375–1383.
- Paulina Aguilera-Alvarado, G., & Sanchez-Nieto, S. (2017). Plant Hexokinases are Multifaceted Proteins. *Plant and Cell Physiology*, 58(7), 1151–1160.
- Peng, C., Uygun, S., Shiu, S.-H., & Last, R. L. (2015). The Impact of the Branched-Chain Ketoacid Dehydrogenase Complex on Amino Acid Homeostasis in *Arabidopsis*. *Plant Physiology*, 169(November), pp.00461.2015.
- Pertuzatti, P. B., Barcia, M. T., Rebello, L. P. G., Gómez-Alonso, S., Duarte, R. M. T., Duarte, M. C. T., ... Hermosín-Gutiérrez, I. (2016). Antimicrobial activity and differentiation of anthocyanin profiles of rabbiteye and highbush blueberries using HPLC–DAD–ESI–MS and multivariate analysis. *Journal of Functional Foods*, 26, 506–516.
- Pilati, S., Brazzale, D., Guella, G., Milli, A., Ruberti, C., Biasioli, F., ... Moser, C. (2014). The onset of grapevine berry ripening is characterized by ROS accumulation and lipoxygenase-mediated membrane peroxidation in the skin. *BMC Plant Biology*, 14(1), 1–15.
- Pinasseau, L., Vallverdú-Queralt, A., Verbaere, A., Roques, M., Meudec, E., Le Cunff, L., ... Cheynier, V. (2017). Cultivar Diversity of Grape Skin Polyphenol Composition and Changes in Response to Drought Investigated by LC-MS Based Metabolomics. *Frontiers in Plant Science*, 8(October), 1–24.
- Pinu, F., Pinu, & R, F. (2018). Grape and Wine Metabolomics to Develop New Insights

- Using Untargeted and Targeted Approaches. *Fermentation*, 4(4), 92.
- Posé, S., Nieves, J. a G., Quesada, F. P. M. a, & Mercado, J. a. (2011). Strawberry Fruit Softening : Role of Cell Wall Disassembly and its Manipulation in Transgenic Plants. *Genes, Genomes and Genomics*, 5, 40–48.
- Prasanna, V., Prabha, T. N., & Tharanathan, R. N. (2007). Fruit ripening phenomena-an overview. *Critical Reviews in Food Science and Nutrition*, 47(1), 1–19.
- Prencipe, F. P., Bruni, R., Guerrini, A., Rossi, D., Benvenuti, S., & Pellati, F. (2014). Metabolite profiling of polyphenols in *Vaccinium* berries and determination of their chemopreventive properties. *Journal of Pharmaceutical and Biomedical Analysis*, 89, 257–267.
- Prior, R. L., Sintara, M., & Chang, T. (2016). Multi-radical (ORACMR5) antioxidant capacity of selected berries and effects of food processing. *Journal of Berry Research*, 6(2), 159–173.
- Prior, Ronald L, Lazarus, S. A., Cao, G., Muccitelli, H., & Hammerstone, J. F. (2001). Identification of Procyanidins and Anthocyanins in Blueberries and Cranberries (*Vaccinium Spp.*) Using High-Performance Liquid Chromatography/Mass Spectrometry. *Journal of Agricultural and Food Chemistry*, 49(3), 1270–1276.
- Ramesh, S. A., Tyerman, S. D., Xu, B., Bose, J., Kaur, S., Conn, V., ... Gillham, M. (2015). GABA signalling modulates plant growth by directly regulating the activity of plant-specific anion transporters. *Nature Communications*, 6, 1–10.
- Rapaille, A., Goosens, J., & Heume, M. (2003). Sugar Alcohols. *Encyclopedia of Food Sciences and Nutrition*, 5665–5671.
- Raskin I, Yousef GG, G. M. (2013). Distribution of Ingested Berry Polyphenolics. *J Agric Food Chem*, 60(23), 5763–5771.
- Reque, P. M., Steffens, R. S., Jablonski, A., Flôres, S. H., Rios, A. de O., & de Jong, E. V. (2014). Cold storage of blueberry (*Vaccinium spp.*) fruits and juice: Anthocyanin stability and antioxidant activity. *Journal of Food Composition and Analysis*, 33(1), 111–116.
- Rinaldo, A., Cavallini, E., Jia, Y., Moss, S. M. A., McDavid, D. A. J., Hooper, L. C., ... Walker, A. R. (2015). A grapevine anthocyanin acyltransferase, transcriptionally regulated by VvMYBA, can produce most acylated anthocyanins present in grape skins. *Plant Physiology*, 169(November), pp.01255.2015.
- Rodriguez-Mateos, A., Feliciano, R. P., Cifuentes-Gomez, T., & Spencer, J. P. E. (2016). Bioavailability of wild blueberry (poly)phenols at different levels of intake. *Journal of Berry Research*, 6(2), 137–148.
- Rodriguez-Mateos, A., Rendeiro, C., Bergillos-Meca, T., Tabatabaee, S., George, T. W., Heiss, C., & Spencer, J. P. E. (2013). Intake and time dependence of blueberry flavonoid-induced improvements in vascular function: a randomized, controlled, double-blind, crossover intervention study with mechanistic insights into biological activity. *The American Journal of Clinical Nutrition*, 98(5), 1179–1191.
- Rolin, D., Teyssier, E., Hong, Y., & Gallusci, P. (2015). *Tomato fruit quality improvement facing the functional genomics revolution. Applied Plant Genomics and Biotechnology*. Elsevier Ltd.
- Rosa, M., Prado, C., Podazza, G., Interdonato, R., González, J. A., Hilal, M., & Prado, F. E. (2009). Soluble sugars-metabolism, sensing and abiotic stress a complex network in the life of plants. *Plant Signaling and Behavior*, 4(5), 388–393.

- Routaboul, J.-M., Dubos, C., Beck, G., Marquis, C., Bidzinski, P., Loudet, O., & Lepiniec, L. (2012). Metabolite profiling and quantitative genetics of natural variation for flavonoids in *Arabidopsis*. *Journal of Experimental Botany*, *63*(10), 3749–3764.
- Routray, W., & Orsat, V. (2011). Blueberries and Their Anthocyanins: Factors Affecting Biosynthesis and Properties. *Comprehensive Reviews in Food Science and Food Safety*, *10*(6), 303–320.
- Routray, W., & Orsat, V. (2014). Variation of phenolic profile and antioxidant activity of North American highbush blueberry leaves with variation of time of harvest and cultivar. *Industrial Crops and Products*, *62*, 147–155.
- Rungapamestry, V., Duncan, A. J., Fuller, Z., & Ratcliffe, B. (2008). Influence of blanching and freezing broccoli (*Brassica oleracea* var. *italica*) prior to storage and cooking on glucosinolate concentrations and myrosinase activity. *European Food Research and Technology*, *227*(1), 37–44.
- Saban, G. M. (2018). The Benefits of Brassica Vegetables on Human Health. *J Human Health Res*, *1*(1), 104.
- Saito, K., & Matsuda, F. (2010). Metabolomics for Functional Genomics, Systems Biology, and Biotechnology. *Annual Review of Plant Biology*, *61*(1), 463–489.
- Sarkar, Di., Agustinah, W., Woods, F., Coneva, E., Vinson, E., & Shetty, K. (2017). In vitro screening and evaluation of phenolic antioxidant-linked anti-hyperglycemic functions of rabbit-eye blueberry (*Vaccinium ashei*) cultivars. *Journal of Berry Research*, *7*(3), 163–177.
- Sasaki, N., Nishizaki, Y., Ozeki, Y., & Miyahara, T. (2014). The role of acyl-glucose in anthocyanin modifications. *Molecules*, *19*(11), 18747–18766.
- Scalbert, A., Brennan, L., Fiehn, O., Hankemeier, T., Kristal, B. S., van Ommen, B., ... Wopereis, S. (2009). Mass-spectrometry-based metabolomics: Limitations and recommendations for future progress with particular focus on nutrition research. *Metabolomics*, *5*(4), 435–458.
- Scalzo, J., Stevenson, D., & Hedderley, D. (2013). Blueberry estimated harvest from seven new cultivars: Fruit and anthocyanins. *Food Chemistry*, *139*(1–4), 44–50.
- Scalzo, J., Stevenson, D., & Hedderley, D. (2015). Polyphenol compounds and other quality traits in blueberry cultivars. *Journal of Berry Research*, *5*(3), 117–130.
- Schwab, W., Davidovich-Rikanati, R., & Lewinsohn, E. (2008). Biosynthesis of plant-derived flavor compounds. *Plant Journal*, *54*(4), 712–732.
- Sengupta, S., Mukherjee, S., Basak, P., & Majumder, A. L. (2015). Significance of galactinol and raffinose family oligosaccharide synthesis in plants. *Frontiers in Plant Science*, *6*(August), 1–11.
- Sengupta, S., Mukherjee, S., Parween, S., & Majumder, A. L. (2012). Galactinol synthase across evolutionary diverse taxa: Functional preference for higher plants? *FEBS Letters*, *586*(10), 1488–1496.
- Serrano, A., Espinoza, C., Armijo, G., Inostroza-Blancheteau, C., Poblete, E., Meyer-Regueiro, C., ... Arce-Johnson, P. (2017). Omics Approaches for Understanding Grapevine Berry Development: Regulatory Networks Associated with Endogenous Processes and Environmental Responses. *Frontiers in Plant Science*, *8*(September), 1–15.
- Seymour, G. B., Chapman, N. H., Chew, B. L., & Rose, J. K. C. (2013). Regulation of

- ripening and opportunities for control in tomato and other fruits. *Plant Biotechnology Journal*, 11(3), 269–278.
- Seymour, G. B., Østergaard, L., Chapman, N. H., Knapp, S., & Martin, C. (2013). Fruit Development and Ripening. *Annual Review of Plant Biology*, 64(1), 219–241.
- Sharma, K. D., Karki, S., Thakur, N. S., & Attri, S. (2012). Chemical composition, functional properties and processing of carrot-a review. *Journal of Food Science and Technology*, 49(1), 22–32. h
- Sharma, O. P., & Bhat, T. K. (2009). DPPH Antioxidant Assay Revisited. *Food Chemistry*, 113, 1202–1205.
- Silva, S., Costa, E. M., Veiga, M., Morais, R. M., & Pintado, M. (2018). Health promoting properties of blueberries : a review. *Critical Reviews in Food Science and Nutrition*, 0(0), 1–20.
- Singh, N., & Ghosh, K. K. (2019). Recent Advances in the Antioxidant Therapies for Alzheimer's Disease: Emphasis on Natural Antioxidants. In S. Singh & N. Joshi (Eds.), *Pathology, Prevention, and Therapeutics of Neurodegenerative Disease* (pp. 253–263).
- Singh, Sudhakar, & Singh, R. P. (2008). In vitro methods of assay of antioxidants: An overview. *Food Reviews International*.
- Skates, E., Overall, J., DeZego, K., Wilson, M., Esposito, D., Lila, M. A., & Komarnytsky, S. (2018). Berries containing anthocyanins with enhanced methylation profiles are more effective at ameliorating high fat diet-induced metabolic damage. *Food and Chemical Toxicology*, 111(November 2017), 445–453.
- Sønderby, I. E., Geu-Flores, F., & Halkier, B. A. (2010). Biosynthesis of glucosinolates – gene discovery and beyond. *Trends in Plant Science*, 15(5), 283–290.
- Song, L., & Thornalley, P. J. (2007). Effect of storage, processing and cooking on glucosinolate content of Brassica vegetables. *Food and Chemical Toxicology*, 45(2), 216–224.
- Stalikas, C. D. (2007). Extraction, separation, and detection methods for phenolic acids and flavonoids. *Journal of Separation Science*, 30(18), 3268–3295.
- Stebbins, N. B., Howarda, L. R., Prior, R. L., Brownmiller, C., Liyanage, R., Lay, J. O., ... Qian, S. Y. (2016). Ascorbic acid-catalyzed degradation of cyanidin-3-O- β -glucoside: Proposed mechanism and identification of a novel hydroxylated product. *Journal of Berry Research*, 6(2), 175–187.
- Stevenson, D., & Scalzo, J. (2012). Anthocyanin composition and content of blueberries from around the world. *Journal of Berry Research*, 2(4), 179–189.
- Subash, S., Essa, M. M., Al-adawi, S., Memon, M. A., Manivasagam, T., & Akbar, M. (2014). Neuroprotective effects of berry fruits on neurodegenerative diseases. *Neural Regeneration Research*, 9(16), 1557–1566.
- Sumner, L. W., Lei, Z., Nikolau, B. J., & Saito, K. (2015). Modern plant metabolomics: Advanced natural product gene discoveries, improved technologies, and future prospects. *Natural Product Reports*, 32(2), 212–229.
- Sun, R.-Z., Cheng, G., Li, Q., He, Y.-N., Wang, Y., Lan, Y.-B., ... Wang, J. (2017). Light-induced Variation in Phenolic Compounds in Cabernet Sauvignon Grapes (*Vitis vinifera* L.) Involves Extensive Transcriptome Reprogramming of Biosynthetic Enzymes, Transcription Factors, and Phytohormonal Regulators. *Frontiers in Plant Science*, 8(April), 1–18.

- Suzuki, N., Koussevitzky, S., Mittler, R., & Miller, G. (2012). ROS and redox signalling in the response of plants to abiotic stress. *Plant, Cell and Environment*, 35(2), 259–270.
- Theodoridis, G., Gika, H. G., & Wilson, I. D. (2008). LC-MS-based methodology for global metabolite profiling in metabonomics/metabolomics. *TrAC Trends in Analytical Chemistry*, 27(3), 251–260.
- Tieman, D., Bliss, P., McIntyre, L. M. M., Blandon-Ubeda, A., Bies, D., Odabasi, A. Z. Z., ... Klee, H. J. J. (2012). The chemical interactions underlying tomato flavor preferences. *Current Biology*, 22(11), 1035–1039.
- Timmers, M. A., Grace, M. H., Yousef, G. G., & Lila, M. A. (2017). Inter- and intra-seasonal changes in anthocyanin accumulation and global metabolite profiling of six blueberry genotypes. *Journal of Food Composition and Analysis*, 59, 105–110.
- Traka, M., & Mithen, R. (2009). Glucosinolates, isothiocyanates and human health. *Phytochemistry Reviews*, 8(1), 269–282.
- Tsai, A. Y.-L., & Gazzarrini, S. (2014). Trehalose-6-phosphate and SnRK1 kinases in plant development and signaling: the emerging picture. *Frontiers in Plant Science*, 5(April), 1–11.
- Ufaz, S., & Galili, G. (2008). Improving the Content of Essential Amino Acids in Crop Plants: Goals and Opportunities. *Plant Physiology*, 147(3), 954–961.
- USDA. (2018). *Blueberries, Raw - National Nutrient Database for Standard Reference*.
- Van Eylen, D., Oey, I., Hendrickx, M., & Van Loey, A. (2007). Kinetics of the Stability of Broccoli (*Brassica oleracea* Cv. Italica) Myrosinase and Isothiocyanates in Broccoli Juice during Pressure/Temperature Treatments. *Journal of Agricultural and Food Chemistry*, 55(6), 2163–2170.
- Vicente, A. R., Ortugno, C., Rosli, H., Powell, A. L. T., Greve, L. C., & Labavitch, J. M. (2007). Temporal sequence of cell wall disassembly events in developing fruits. 2. Analysis of blueberry (*Vaccinium* species). *Journal of Agricultural and Food Chemistry*, 55(10), 4125–4130.
- Villalobos-González, L., Peña-Neira, A., Ibáñez, F., & Pastenes, C. (2016). Long-term effects of abscisic acid (ABA) on the grape berry phenylpropanoid pathway: Gene expression and metabolite content. *Plant Physiology and Biochemistry*, 105, 213–223.
- Vlot, A. C., Dempsey, D. A., & Klessig, D. F. (2009). Salicylic Acid, a Multifaceted Hormone to Combat Disease. *Annual Review of Phytopathology*, 47(1), 177–206.
- Wahyuningsih, S., Wulandari, L., Wartono, M. W., Munawaroh, H., & Ramelan, A. H. (2017). The Effect of pH and Color Stability of Anthocyanin on Food Colorant. *IOP Conference Series: Materials Science and Engineering*, 193(1), 12047.
- Wang, G., Xu, M., Wang, W., & Galili, G. (2017). Fortifying horticultural crops with essential amino acids: A review. *International Journal of Molecular Sciences*, 18(6).
- Wang, H., Guo, X., Hu, X., Li, T., Fu, X., & Liu, R. H. (2017). Comparison of phytochemical profiles, antioxidant and cellular antioxidant activities of different varieties of blueberry (*Vaccinium* spp.). *Food Chemistry*, 217, 773–781.
- Wang, S. Y., Chen, H., Camp, M. J., & Ehlenfeldt, M. K. (2012). Genotype and growing season influence blueberry antioxidant capacity and other quality attributes. *International Journal of Food Science and Technology*, 47(7), 1540–1549.
- Wang, S. Y., & Jiao, H. (2000). Scavenging capacity of berry crops on superoxide

- radicals, hydrogen peroxide, hydroxyl radical's, and singlet oxygen. *Journal of Agricultural and Food Chemistry*, 48(11), 5677–5684.
- Wang, Shaoli, Chu, Z., Ren, M., Jia, R., Zhao, C., Fei, D., ... Ding, X. (2017). Identification of anthocyanin composition and functional analysis of an anthocyanin activator in solanum nigrum fruits. *Molecules*, 22(6), 1–14.
- Wang, Shouchuang, Yang, C., Tu, H., Zhou, J., Liu, X., Cheng, Y., ... Xu, J. (2017). Characterization and Metabolic Diversity of Flavonoids in Citrus Species. *Scientific Reports*, 7(1), 1–10.
- Weng, J. K. (2014). The evolutionary paths towards complexity: A metabolic perspective. *New Phytologist*, 201(4), 1141–1149.
- Whyte, A. R., Schafer, G., & Williams, C. M. (2016). Cognitive effects following acute wild blueberry supplementation in 7- to 10-year-old children. *European Journal of Nutrition*, 55(6), 2151–2162.
- Willig, J. A. (2009). the Effect of Anthocyanin Acylation on the Inhibition of Ht-29 Colon Cancer Cell Proliferation. *Presented in Partial Fulfillment of the Requirements for the Degree Master of Science in the Graduate School of The Ohio State University*, 90.
- Wingler, A. (2017). Transitioning to the next phase: the role of sugar signaling throughout the plant life cycle. *Plant Physiology*, 176(February), pp.01229.2017.
- Wolfender, J. L., Marti, G., Thomas, A., & Bertrand, S. (2015). Current approaches and challenges for the metabolite profiling of complex natural extracts. *Journal of Chromatography A*, 1382, 136–164.
- Xi, F. F., Guo, L. L., Yu, Y. H., Wang, Y., Li, Q., Zhao, H. L., ... Guo, D. L. (2017). Comparison of reactive oxygen species metabolism during grape berry development between 'Kyoho' and its early ripening bud mutant 'Fengzao.' *Plant Physiology and Biochemistry*, 118, 634–642.
- Xu, Y. (2010). *Molecular Blant Breeding*. New York: CABI Publishing.
- Yonekura-Sakakibara, K. (2009). Functional genomics of family 1 glycosyltransferases in Arabidopsis. *Plant Biotechnology*, 26(3), 267–274.
- Yonekura-Sakakibara, K., Nakayama, T., Yamazaki, M., & Saito, K. (2009). Modification and Stabilization of Anthocyanins. In C. S. Winefield, K. Davies, & K. Gould (Eds.), *Anthocyanins* (pp. 169–190). New York: Springer Science+Business Media.
- Yoshizawa, T., Shimizu, T., Hirano, H., Sato, M., & Hashimoto, H. (2012). Structural Basis for Inhibition of Xyloglucan-specific Endo- -1,4-glucanase (XEG) by XEG-Protein Inhibitor. *Journal of Biological Chemistry*, 287(22), 18710–18716.
- You, Q., Wang, B., Chen, F., Huang, Z., Wang, X., & Luo, P. G. (2011). Comparison of anthocyanins and phenolics in organically and conventionally grown blueberries in selected cultivars. *Food Chemistry*, 125(1), 201–208.
- Yousuf, B., Gul, K., Wani, A. A., & Singh, P. (2016). Health Benefits of Anthocyanins and Their Encapsulation for Potential Use in Food Systems: A Review. *Critical Reviews in Food Science and Nutrition*, 56(13), 2223–2230.
- Zhang, Hengyou, Mittal, N., Leamy, L. J., Barazani, O., & Song, B. H. (2017). Back into the wild—Apply untapped genetic diversity of wild relatives for crop improvement. *Evolutionary Applications*, 10(1), 5–24.
- Zhang, Hua, Wang, Z. Y., Yang, X., Zhao, H. T., Zhang, Y. C., Dong, A. J., ... Wang, J. (2014). Determination of free amino acids and 18 elements in freeze-dried

- strawberry and blueberry fruit using an Amino Acid Analyzer and ICP-MS with micro-wave digestion. *Food Chemistry*, 147, 189–194.
- Zhu, G., Wang, S., Huang, Z., Zhang, S., Liao, Q., Zhang, C., ... Huang, S. (2018). Rewiring of the Fruit Metabolome in Tomato Breeding. *Cell*, 172(1–2), 249–255.e12.
- Zifkin, M., Jin, A., Ozga, J. A., Zaharia, L. I., Schernthaner, J. P., Gesell, A., ... Constabel, C. P. (2012). Gene expression and metabolite profiling of developing highbush blueberry fruit indicates transcriptional regulation of flavonoid metabolism and activation of abscisic acid metabolism. *Plant Physiology*, 158(1), 200–224.
- Zorenc, Z., Veberic, R., Slatnar, A., Koron, D., Miosic, S., Chen, M. H., ... Mikulic-Petkovsek, M. (2017). A wild 'albino' bilberry (*Vaccinium myrtillus* L.) from Slovenia shows three bottlenecks in the anthocyanin pathway and significant differences in the expression of several regulatory genes compared to the common blue berry type. *PLoS ONE*, 12(12), 1–14.

**Chapter 4. Identification of QTLs and Putative Candidate Genes Associated with
Agronomic Traits in *Brassica oleracea* var. *italica***

4.1. Abstract

Vegetable consumption and research has increased in the past decade due to societal interest in plant-based nutrition as well as research implicating plant metabolites greatly affecting human health and nutrition. Vegetables in the *Brassica* genus have received substantial attention as their unique, specialized metabolites, glucosinolates, have been associated with health benefits like antioxidant capacity and detoxification. Broccoli in particular has been associated with potent anticarcinogenic properties due to broccoli accumulating the largest amount of the specific glucosinolate, glucoraphanin. Improving the agronomic production of broccoli while maintaining glucosinolate metabolite diversity will allow for more consumers to benefit from the nutritious qualities. Agronomic traits important for broccoli production are harvest season and pathogen resistance. To elucidate the genetic regulation of complex traits like agronomic harvest and pathogen resistance, association mapping studies were conducted to determine genetic regions that most likely contain regulatory putative candidate genes. With a broccoli diversity panel representing global and industry varieties, a genome-wide association mapping study (GWAS) was conducted for over 20 different agronomic traits. The significant genetic regions from the GWAS were further analyzed through a text-mining method optimized with natural-language processing to identify putative candidate genes. The putative candidate genes found within regions significant for the harvest trait were involved in photoperiodism and floral meristem transition pathways. The putative candidate genes found within regions significant for pathogen-related traits represented multiple steps in the pathogen resistance signaling pathway. Specifically, there were putative candidate genes from pathogen recognition receptors, signal transduction through calcium and transcription factors, and physiological responses through resistance genes or hypersensitive response. The GWAS and putative candidate gene results can be utilized by future broccoli breeding strategies to develop broccoli lines with improved harvest time and enhanced pathogen resistance.

4.2. Introduction

Consumption and research in *Brassica oleracea* var. *italica*, broccoli, has dramatically increased in the past decade as broccoli has been shown as a functional food with numerous health benefits (Mithen et al., 2003; M. Traka & Mithen, 2009; Y. Zhang, Talalay, Cho, & Posner, 1992). According to the recommended serving size, raw broccoli provides 27% of the total dietary fiber, 7% of the iron, 10% of the potassium, 176% of the vitamin C, 14% of the riboflavin, 20% of the vitamin B-6, 23% of the folate, and 143% of the vitamin K recommended for an average adult's proper nutrition (USDA, 2018). The incorporation of broccoli into a daily diet will provide a great source for not only the previously mentioned vitamins and minerals, but also other nutrients important for human health. Furthermore, broccoli has been repeatedly shown through epidemiological studies to exhibit potent anti-cancer effects (Armah et al., 2013; Brown et al., 2002; Cornblatt et al., 2007; Dinkova-Kostova et al., 2010; Fahey et al., 2002; Li, Hullar, Beresford, & Lampe, 2011; Mithen et al., 2003; Nho & Jeffery, 2001; Staack, Kingston, Wallig, & Jeffery, 1998; Yanaka et al., 2009).

The health benefits are attributed to isothiocyanates, breakdown products of glucosinolates, a class of specialized metabolites characteristic of broccoli and other Brassicaceae plants (Dinkova-Kostova et al., 2010, 2006; Fahey et al., 2002; Fahey, Zhang, & Talalay, 1997; Mithen et al., 2003; Nho & Jeffery, 2001; Staack et al., 1998; Tawfiq et al., 1995; M. Traka & Mithen, 2009; Y. Zhang et al., 1992). Sulforaphane is the isothiocyanate derived from glucoraphanin, the highest accumulating glucosinolate in broccoli (Araki et al., 2013; Baik et al., 2003; Cole, 1976; Farnham, Stephenson, & Fahey, 2005; Kushad et al., 1999; M. H. Traka et al., 2013). Sulforaphane has been shown to drastically inhibit growth of cancerous cell cultures and inhibit angiogenesis in developing tumors (Armah et al., 2013; Cornblatt et al., 2007; Dinkova-Kostova et al., 2010; Mithen et al., 2003; Tawfiq et al., 1995; Y. Zhang et al., 1992). Isothiocyanates have also been shown to inhibit phase I detoxification enzymes and induce phase II detoxification enzymes (Nho & Jeffery, 2001; Staack et al., 1998). Due to the great health benefits of broccoli, demand for broccoli will continue to rise, thus the production of broccoli will need to be improved through agronomics.

Improving the broccoli crop supply requires a greater understanding of broccoli agronomics, specifically, the factors regulating harvest and productivity (Franzke, Lysak, Al-Shehbaz, Koch, & Mummenhoff, 2011; Jones, Faragher, & Winkler, 2006; Lan & Paterson, 2000; Metwali & Al-Maghrabi, 2012; Parkin et al., 2014; Pék et al., 2012; Rangkadilok et al., 2004; Saban, 2018; Wagner et al., 2012; Walley et al., 2012). The length of the growing season greatly affects the crop's harvest timing as only efficient growth stores enough energy and nutrients to allow for vegetative maturation and the subsequent transition to reproductive life stage and harvest (Albani & Coupland, 2010; Amasino & Michaels, 2010; Bennett, Roberts, & Wagstaff, 2012; Conti, 2017; Moghaddam & Ende, 2013; Molinero-Rosales, Latorre, JAMILENA, & Lozano, 2004; Wingler, 2017; Yadav, 2010). Improving overall growth pathways will aid broccoli in reaching vegetative maturity quickly, which will transition broccoli into the reproductive life stage sooner, thus shortens a growing season for multiple harvests. Broccoli agronomic harvest and productivity is usually determined by the size and weight of the broccoli reproductive head, which is separated into smaller broccoli florets for markets (Brown, Jeffery, & Juvik, 2007; Couée, Sulmon, Gouesbet, & El Amrani, 2006; Jenks & Bebeli, 2011; Keunen, Peshev, Vangronsveld, Van Den Ende, & Cuypers, 2013; Walley et al., 2012; Zoratti, Karppinen, Luengo Escobar, HÅggman, & Jaakola, 2014). Although broccoli research and breeding has selected for more compact heads for increased floret production per plant, the compactness has decreased air circulation, increased humidity, and decreased pesticide access, which has resulted in an increase in pathogen and disease instances (Brown et al., 2007; Conrath, Beckers, Langenbach, & Jaskiewicz, 2015; Couée et al., 2006; Freeman & Beattie, 2008; Jenks & Bebeli, 2011; Jones et al., 2006; Keunen et al., 2013; Walley et al., 2012; Zoratti et al., 2014).

The susceptibility of broccoli plants to pathogens and diseases has been increasing gradually because of not only the increased compactness, but also the decrease in endogenous metabolites (Brown et al., 2014; Buchanan, GUISSEM, & Jones, 2012; Ionescu, Møller, & Sánchez-Pérez, 2016; Kyriacou & Rouphael, 2018; H. Zhang, Mittal, Leamy, Barazani, & Song, 2017). Many crop species, including broccoli, have shown a decrease in specialized metabolite accumulation (Buchanan et al., 2012; Kyriacou & Rouphael, 2018; H. Zhang et al., 2017). The specialized metabolites in

broccoli aid in pathogen and disease resistance through interacting with signaling cascades to induce resistance, and through directly interacting with the pathogen or disease to inhibit damage, infection, or spread (Bellostas, Sørensen, & Sørensen, 2007; Brown et al., 2002; Buchanan et al., 2012; Clay, Adio, Denoux, Jander, & Ausubel, 2009; Grubb & Abel, 2006; Halkier & Gershenzon, 2006; Jones et al., 2006). Improving the accumulation of the endogenous specialized metabolites in broccoli will increase production and profit because biomass loss from damage will be less and costs for pesticides will be less. In short, a greater understanding of the genetic control of agronomic traits in broccoli is essential for increasing the supply of broccoli florets.

4.2.1. Genome-Wide Association Mapping

Agronomic traits like height and yield are often quantitative traits regulated by multiple genes across the genome (Gibson, 2018; Körber et al., 2016; Korte & Farlow, 2013; Riedelsheimer et al., 2012; Visscher, Brown, McCarthy, & Yang, 2012; Visscher et al., 2017; H. Zhang et al., 2017). Historically, the association of genetic regions and quantitative traits has been identified through genetic mapping using a biparental mapping population (Borevitz & Chory, 2004; Gibson, 2018; Hospital, 2009; M. S. Kang, 2002; Rafalski, 2010; Winter & Kahl, 1995; Y. Xu, 2010). Crop breeders and researchers are incorporating diverse cultivars and multiple populations into an overall association mapping study to decrease linkage disequilibrium and account for different genetic background effects (Gibson, 2018; H M Kang et al., 2008; Hyun Min Kang et al., 2010; M. S. Kang, 2002; Körber et al., 2016; Korte & Farlow, 2013; Passam, Karapanos, Bebeli, & Savvas, 2007). With crop research expanding to crops with restricted interbreeding or long-life cycles, a genome wide association study (GWAS) has become a powerful genetic mapping tool, as GWAS does not require a structured population (Gibson, 2018; H M Kang et al., 2008; Hyun Min Kang et al., 2010; Körber et al., 2016; Korte & Farlow, 2013; Visscher et al., 2012, 2017). A GWAS not only decreases linkage disequilibrium through a multi-generational analysis of historical recombination events, but also accounts for genetic background bias through a large population of diverse individuals (Gibson, 2018; H M Kang et al., 2008; Hyun Min Kang et al., 2010; M. S. Kang, 2002; Körber et al., 2016; Korte & Farlow, 2013; Passam et al., 2007). The relatedness of individuals as well as of markers may cause false

associations, but kinship relation and population structure, K and Q, respectively, are incorporated within the GWAS to reduce false positives (Gibson, 2018; H M Kang et al., 2008; Hyun Min Kang et al., 2010; M. S. Kang, 2002; Körber et al., 2016; Korte & Farlow, 2013; Passam et al., 2007; J. Yu et al., 2006). Individuals that have been genotyped together and phenotypes replicated across years or environments strengthen the GWAS results, similarly to replicates improving biparental association mapping statistical power (Borevitz & Chory, 2004; Gibson, 2018; Hospital, 2009; M. S. Kang, 2002; Rafalski, 2010; Winter & Kahl, 1995; Y. Xu, 2010).

GWAS have been successfully performed on many different plant species (Atwell et al., 2010; Körber et al., 2016; Lu et al., 2013; Meyer & Purugganan, 2013; Riedelsheimer et al., 2012; Schönhals et al., 2017; Visscher et al., 2012, 2017; H. Zhang et al., 2017; Zhu et al., 2018). GWAS has been successfully conducted in *Arabidopsis thaliana* to elucidate extremely complex traits since the genomic resource is very robust (Atwell et al., 2010; Seren et al., 2012; Vandepoele, 2002). Specifically, gene annotations and putative cell cycle regulators were identified using GWAS (Vandepoele, 2002). GWAS has also been conducted in maize, oat, and other crop species to understand disease resistance and specific metabolite regulatory genes (Asoro, Newell, Scott, Beavis, & Jannink, 2013; Kump et al., 2011; Riedelsheimer et al., 2012; Song & Zhang, 2009). With the potent health benefits found in broccoli, there is increasing interest in the genes that regulate agronomic traits to improve growth and productivity. The objectives of this research are to identify QTL regions associated with agronomic traits, and identify candidate genes for select traits of interest, using genome wide association mapping on *Brassica oleracea* var. *italica*.

4.3. Materials and Methods

4.3.1. Plant Population Material

In this research, 110 lines of broccoli (*Brassica oleracea* var. *italica*) from General Mills' global diversity panel were chosen for the first year of analysis, and a subset of 60 were replicated for a second year. The varieties, representing a global diversity from six major seed companies and 28 different countries, were grown in Irapuato, Mexico.

4.3.2. Phenotypic Data

For each line, more than 20 different traits were measured and collected over two years by General Mills Crop Biosciences. Agronomic traits related to plant growth include % floret, height(in), width(in), % leaves, pedicle, % side shoots, % stalk, and % unharvested plants. Harvest quality traits include compact score, color score, color (A,B,L), days to harvest, head weight (lbs), and yield (kg/ha). Pathogen related traits include % black stem/leg, % brown bead, % hollow stem heads, % mechanical damage, and % Xanthomonas damage. Each phenotype was analyzed for normal distribution and outliers that increased the skewness and kurtosis values outside of +/- 1.0 of each other were removed.

4.3.3. Genotypic Data and Genetic Map

The genotypic information was obtained from a *Brassica oleracea* var. *italica* mapping population, previously described in Brown, et al., 2014 (Brown et al., 2014). In brief, genomic DNA extracted with CTAB procedure was hybridized to Illumina Infinium iSelect array (Brassica60k_Cons_ParkinAAFC), and scanned with Illumina iSCAN (Brown et al., 2014). The SNPs and genotypes were called using Genotyping Module v.1.9.5 of Illumina GenomeStudio software. The genotypic information for the diversity population was obtained using the same method and analysis as Brown et al., 2014 (Brown et al., 2014).

A genetic linkage map was developed using the genotypic information from the mapping population. The methodology for constructing the high-density linkage map is described in detail in Chaffin et al., 2016. Since there was only one population, this consensus linkage map was constructed from only the initial part of the consensus strategy, component mapping. In brief, multiple individuals built separate linkage maps solutions in the MultiPoint package (MultiQTL Ltd., Haifa, Israel) (Chaffin et al., 2016). The reliability of marker order was checked through jackknife re-sampling; the probability of marker order was estimated based on 10 to 30 calculations, each one resulting from 90% of the population being sampled without replacement. Markers were removed iteratively when neighborhoods of unstable marker order occurred. The ordering and marker removal sequence was iterated until the given linkage group showed stable marker order. Multiple linkage groups were merged together by

incrementally increasing rf by 0.05 up to a final rf of 0.3. Due to the flexibility provided by the decision-making process in MultiPoint, and the potential for variable outcomes, a community-based mapping procedure was used. Following initial mapping, a team of five people evaluated the linkage groups from the individually constructed maps and chose the linkage groups that represented the consensus of the team. These selections were based on quality (length of linkage groups) and the frequency with which that solution was derived (winner-takes-all approach) (Chaffin et al., 2016).

4.3.4. Genome-Wide Association Mapping

The genome wide association study was conducted using JMP Genomics 7 (JMP®, SAS Institute Inc.). The genotypic information was filtered using an Asymptotic Hardy-Weinberg Equilibrium test set to a $-\log_{10}$ p-value of 15, a minor allele frequency (MAF) cutoff of 0.05, and proportion of missing genotypes cutoff of 0.35. The phenotypic data was filtered for outliers outside of the normal distribution in a normal quantile-quantile plot. If all phenotypes in a trait did not follow normal distribution, the data was log transformed. The linkage disequilibrium was calculated to determine the distance at which linkage equilibrium decays. A spline (λ of 25,000,000) was fit to determine the resolution power of the population and ideal genetic map. Multiple studies have shown that association mapping is susceptible to bias when population structure is not properly accounted for (Korte & Farlow, 2013; J. Yu et al., 2006). A principle component analysis (PCA) was conducted to determine the variables that account for population structure. A relationship matrix was developed, using an identity by state parameter, to determine the kinship variables that account for population structure. The identity by state parameter allows the matrix to represent both recent relationships and historical relationships. A multivariate analysis comparing the variables from PCA and relationship matrix analyses was conducted to determine if the two sets of variables accounted for the same or different population structure factors. The results indicated that the appropriate model necessary to account for the population's structure is a Q-K mixed model. A Q-K mixed model uses the population structure from both PCA and relationship matrix analyses to determine associations.

4.3.5. Quantitative Trait Loci and Putative Candidate Gene Identification

The significant QTLs were determined by p-value significance 0.001, and the significant QTL region was determined by a linkage disequilibrium of 8.46 cM on either side of the significant marker. The linkage disequilibrium indicates the distance at which linkage between markers decays. The most significant markers within a single QTL region was chosen as the QTL region representative, and all other significant markers within that QTL region were considered linked. The sequence tags for the markers were obtained by comparing the genotypic information to previously published genotypes of the same population (Brown et al., 2014). The unique pattern of genotype calls across the population from the new high-density genetic map for each marker was aligned to the previously published genetic map using a custom Perl script to obtain surrounding sequence information (Brown et al., 2014).

Of the more than 20 agronomic traits analyzed, the days to harvest trait was chosen for further candidate gene identification analysis because regulating the timing of broccoli floret maturation will aid in improving growth and harvest. Broccoli floret growth and harvest can also be improved by reducing the energy and biomass lost due to pathogens. The pathogen-related traits, consisting of black stem, brown bead, % hollow stem heads, mechanical damage, and % *Xanthomonas* damage, were chosen for further candidate gene identification analysis. The procedure for candidate gene identification analysis is summarized in Figure 4.1. For each significant QTL region of the above-mentioned traits, a custom Perl script extracted nucleotide sequences and gene annotations from the published *Brassica oleracea* var. *capitata* draft genome. The gene annotations included Bol- gene-identification numbers, associated nucleotide positions, and short descriptions of possible gene functions. A preliminary keyword list describing the six traits was generated through a cursory literature review and manual curation of extracted gene annotations. The preliminary keyword list was used as a starting point for text-mining queries, described below.

Text mining and BLAST were used to assist in developing a putative list of genes responsible for regulating particular agronomic traits of interest. Text-mining was performed with I2E, a natural-language processing (NLP)-based text-mining software from Linguamatics (I2E, Linguamatics [www.linguamatics.com]; United Kingdom),

which extracts semantic information at high throughput from large document collections (Milward et al., 2005). Text mining queries were iteratively developed by combining experienced knowledge with ontologies for genes, plants, and phenotypes. Ontologies included the Gene Ontology, Entrez Gene, NCBI Taxonomy, Plant Ontology, Plant Trait Ontology, Medical Subject Headings, and the National Agricultural Library Thesaurus. These queries were applied to over 30 million abstracts from MEDLINE and Agricola to extract semantic relationships describing how genes in *Arabidopsis thaliana* and *Brassica oleracea* var. *italica* may regulate the six agronomic traits of interest in this study (MEDLINE/PubMed, [<http://www.ncbi.nlm.nih.gov/pubmed/>], Agricola, [<http://agricola.nal.usda.gov/>]). Genes extracted from text-mining were used to generate a putative list containing genes of interest, along with literature supporting the identified relationship between gene and trait. The putative gene list underwent iterative manual curation and refinement to filter out irrelevant genes.

Nucleotide sequence associated with text-mined genes from the refined, putative list were downloaded identified using ESearch, EPost, ELink, and EFetch methods in the NCBI Entrez Programming Utilities (E-Utilities) application programming interface (API) (Sayers & Wheeler, 2004). These sequences were used for comparison against the nucleotide sequences and gene annotations extracted for the significant QTLs of the six traits. A series of scripts, written in the Perl programming language, were developed to link nucleotide sequences to text-mined genes and download them for use in BLAST. The BLAST algorithm, implemented by NCBI through the command line, was used to align nucleotide sequences associated with putative, text mined genes to the publicly available draft genome of *Brassica oleracea* var. *capitata* (Camacho et al., 2009). In order to perform this alignment, a custom BLAST database of the publicly available *Brassica oleracea* var. *capitata* draft genome and gene coding DNA sequence (CDS) was created. BLAST was run, with default parameters, using FASTA files generated from NCBI E-Utilities as input, and the custom *Brassica oleracea* var. *capitata* as the reference database, resulting in tab separated files of BLAST highest scoring pairs (HSPs) for each of the six agronomic traits of interest.

Scripts were developed in the Python programming language to parse BLAST result files and filter HSPs based on alignment length, percent identity, and query

sequence length. Filtering on query sequence length was performed to eliminate HSPs found from alignment of entire chromosomes from *Arabidopsis thaliana* to multiple genes in *Brassica oleracea* var. *capitata*. Alignment positions to the draft genome and corresponding gene annotation identification codes (Bol-IDs) for those positions were also parsed from BLAST results for comparison to the candidate gene list from the GWAS analysis. Bol-IDs from BLAST HSPs of text-mined genes were matched to candidate genes from the candidate gene list using a custom python script. Genes found in common between the gene candidate lists along with their positions, BLAST HSP information, and text-mined information were output to tab delimited files for manual review and comparison. Discovering homology between *Arabidopsis thaliana* and Bol-ID genes from this study serves as evidence and a basis for further investigation of their involvement in specific agronomic traits of interest.

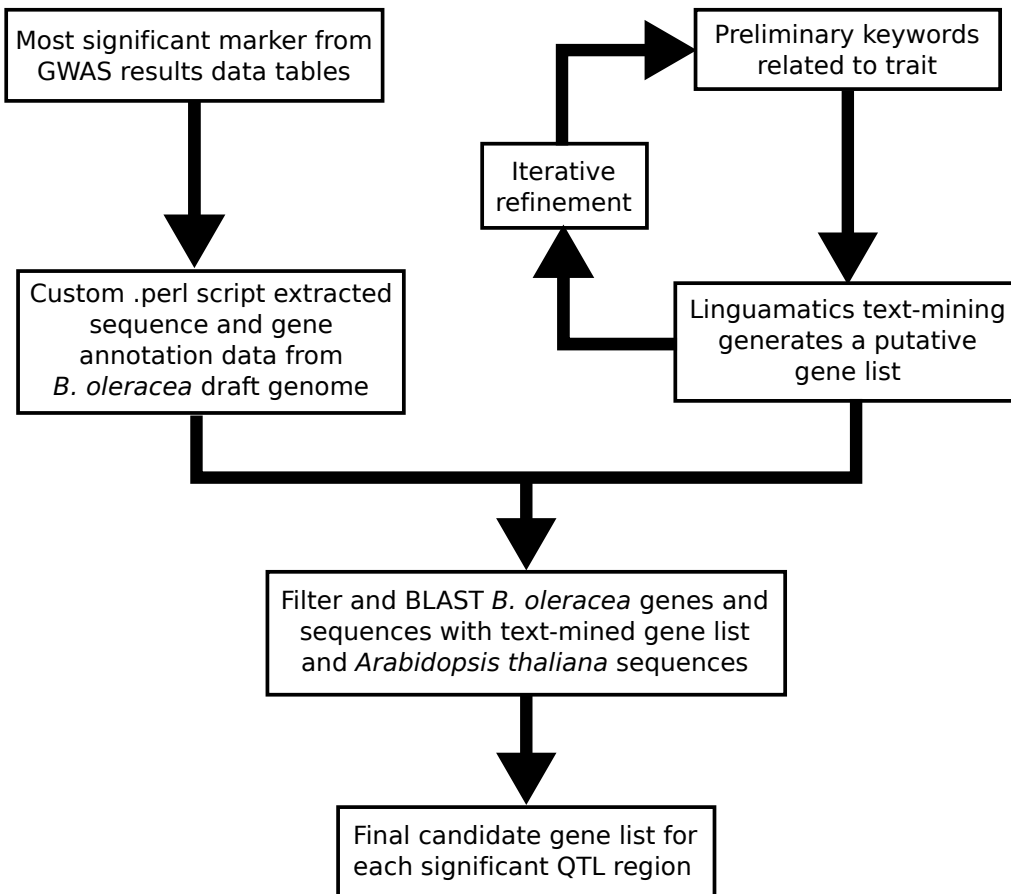


Figure 4.1 – Flow diagram outlining the putative candidate gene identification process.

4.4. Results

4.4.1. Genetic Map

A *de novo* high-density genetic map was constructed for *Brassica oleracea* var. *italica* (Figure 4.2) using the community-based component mapping strategy (Chaffin et al., 2016). The number of linkage groups (nine) and total length (1406.84 cM) is similar to previously published genetic maps of *Brassica oleracea* (Brown et al., 2014). Across the whole genetic map, the average density is 3.05 cM per locus and average gap size is 1.07 cM. There is only one gap greater than 20 cM. Linkage group four contains the greatest number of markers, 304, and the smallest average density of 2.02 cM per locus. Linkage group seven contains the least number of markers, 66, and the second greatest average density of 3.53 cM per locus. Further summary statistics of individual linkage groups are in Table 1. Genotypic SNP data from the DNA Landmark custom SNP array for *Brassica* resulted in 1,375 markers. The filtering of genetic markers in JMP Genomics 7 excluded 66 markers, resulting in 1,309 markers remaining for GWAS. The heterozygosity and polymorphism of the genetic markers is represented by the polymorphic information content (PIC) value, and 75% of the SNPs in each linkage group had PIC values over 0.25 (Figure 4.2).

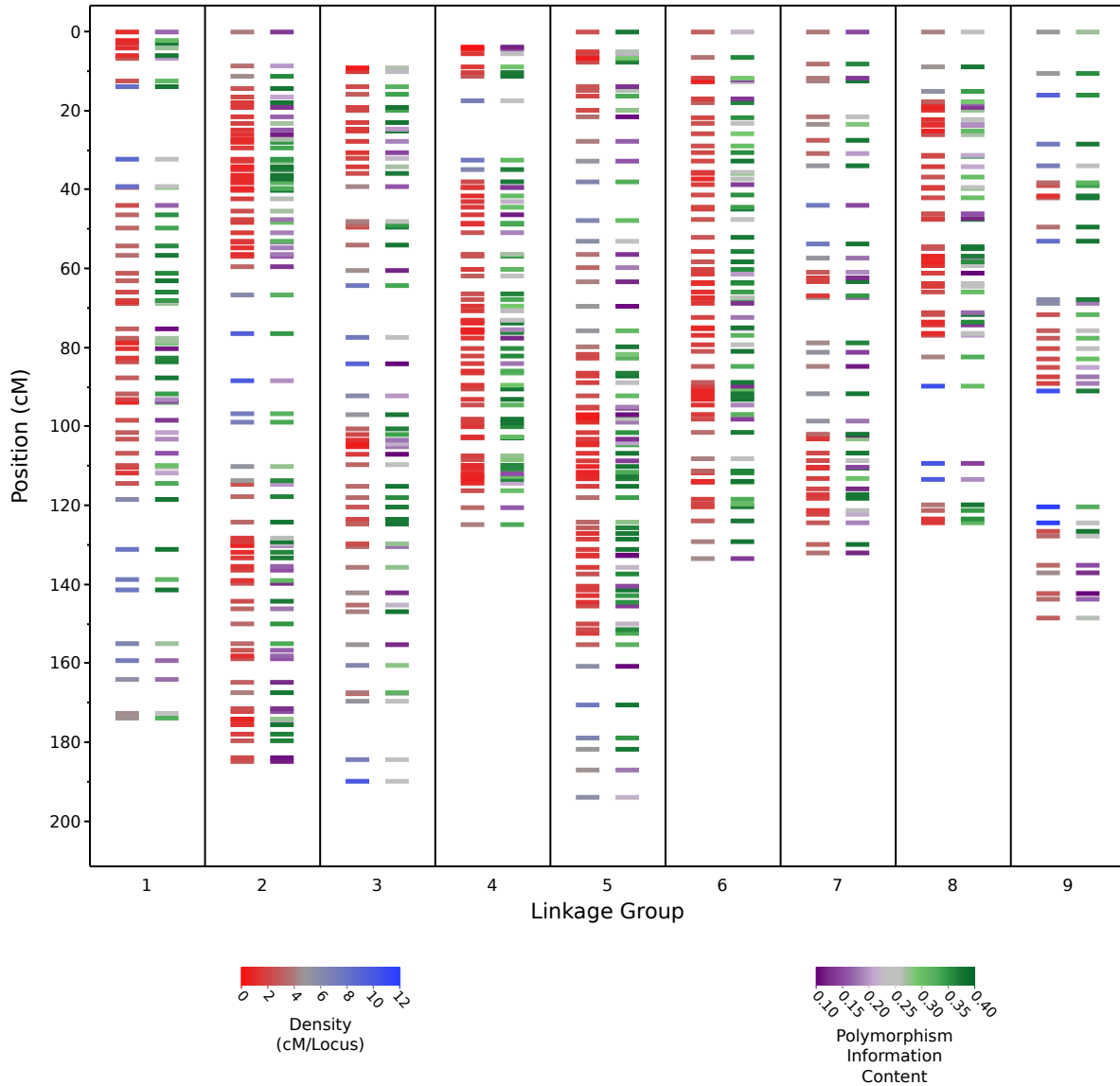


Figure 4.2 - The high-density genetic linkage map of *Brassica oleracea* var. *italica* represented by horizontal dashes. Each dash is one of the 1,309 SNP markers grouped into two sets of 9 broccoli linkage groups. The distance between dashes is scaled in Kosambi centiMorgans. Within each group, the left set of dashes (colored red to blue) represent density in cM/locus. Within each group, the right set of dashes (colored purple to green) represents the polymorphism information content.

Table 4.1 - Summary statistics of individual linkage groups for the broccoli high-density genetic map.

Linkage Group	Markers	Total Distance	Average Density (cM/Locus)	Average Gap (cM)	Gaps >7.5	Gaps >10	Gaps >15	Gaps >20
1	118	174.02	3.44	1.49	5	3	1	0
2	141	185.06	2.56	1.31	5	2	0	0
3	140	189.9	3.51	1.29	5	2	0	0
4	304	124.97	2.02	0.40	1	1	0	0
5	176	194.03	2.70	1.10	3	0	0	0
6	127	133.69	2.08	1.05	0	0	0	0
7	66	132.11	3.53	2.00	5	2	0	0
8	149	124.51	2.74	0.84	2	1	1	0
9	89	148.55	4.83	1.67	4	4	2	1

4.4.2. Agronomic Phenotypes

The 20+ agronomic phenotypes are summarized in Table 4.2 and were filtered for normal distribution. The phenotypes of brown bead and % GII for both years were log transformed so that the distribution followed a normal distribution. Outliers were removed in Color L and Color A phenotypes for year one and compact and %GI for year two. The distributions for the days to harvest trait and pathogen-related traits are shown in Figures 4.3 and 4.4.

Table 4.2 – Summary statistics for broccoli agronomic phenotypes.

Trait	Year	N	Mean	Standard Error Mean	Maximum	Minimum
Black Stem	1	95	0.009	0.001	0.04	0
	2	55	0.009	0.002	0.06	0
Brown Bead	1	95	0.23	0.02	0.8	0
	2	55	0.08	0.02	0.8	0
Color A	1	95	6.92	0.27	10.1	-8.8
Color B	1	95	11.93	0.42	27.1	3.7
Color L	1	95	33.77	0.29	42	20.3
Compact	1	93	3.52	0.08	4.5	1
	2	55	4.32	0.05	5	3
Days to Harvest	1	95	72.71	0.72	90	54
	2	56	76.86	0.64	86	68
% Floret	1	94	70.40	0.55	90	55
	2	55	69.46	0.83	82.6	52.6

Table 4.2 – (continued).

% GI	1	95	65.48	2.02	94	15
	2	55	73.45	1.85	91.8	6.8
% GII	1	95	6.16	0.47	26	0
	2	55	2.94	0.36	11.8	0.4
Head Weight (lbs)	1	95	0.90	0.02	1.8	0.04
	2	55	1.02	0.02	1.3	0.6
Height (in)	1	110	28.99	0.39	45	19
	2	56	26.91	0.52	35	20
% Hollow Stems Heads	1	95	50.75	3.04	100	0
	2	55	53.56	4.07	100	0
% Leaves	1	64	21.69	0.43	29	12
	2	57	20.53	0.35	29	16
Mechanical Damage	1	95	0.02	0.002	0.08	0
	2	57	0.05	0.004	0.1	0
Pedicle	1	93	3.36	0.07	4.5	1
	2	55	4.06	0.07	5	3
% Side Shoots	1	110	33.47	3.47	91	0
	2	55	39.33	4.47	97	0
% Stalk	1	94	29.73	0.54	45	10
	2	55	30.54	0.83	47.4	17.4
% Unharvested Plants	1	95	24.67	1.13	50	0
	2	57	25.56	1.59	52	3
Width (in)	1	110	27.37	0.28	35	20
	2	56	22.07	0.31	26	16
% Xanthomonas Damage	1	95	43.14	2.08	100	3
Yield (kg/ha)	1	95	13018.8	507.9	23187	2713
	2	55	16121.6	655.8	24265	1748

-N – indicates the total number of individuals with phenotype data

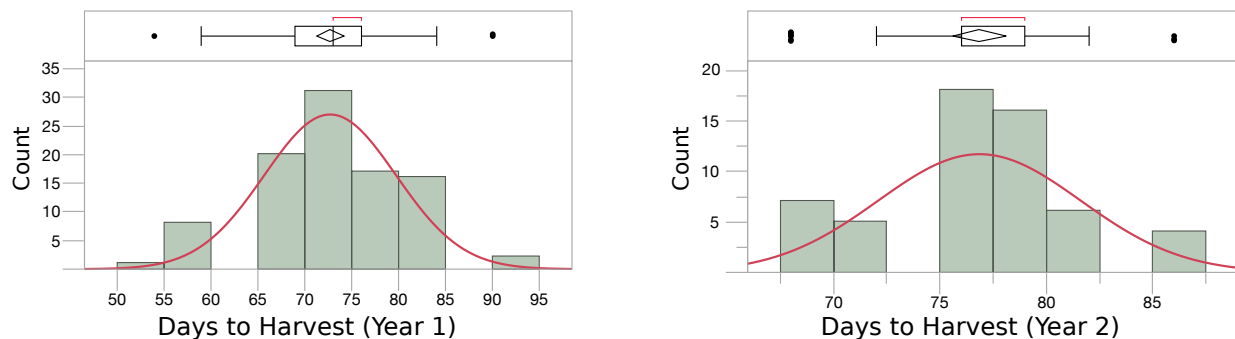


Figure 4.3 – Distribution histograms for the days to harvest trait for both years. The red line indicates a normal distribution. The box plot shows the mean, quartiles, and interquartile range, as well as possible outliers as dots.

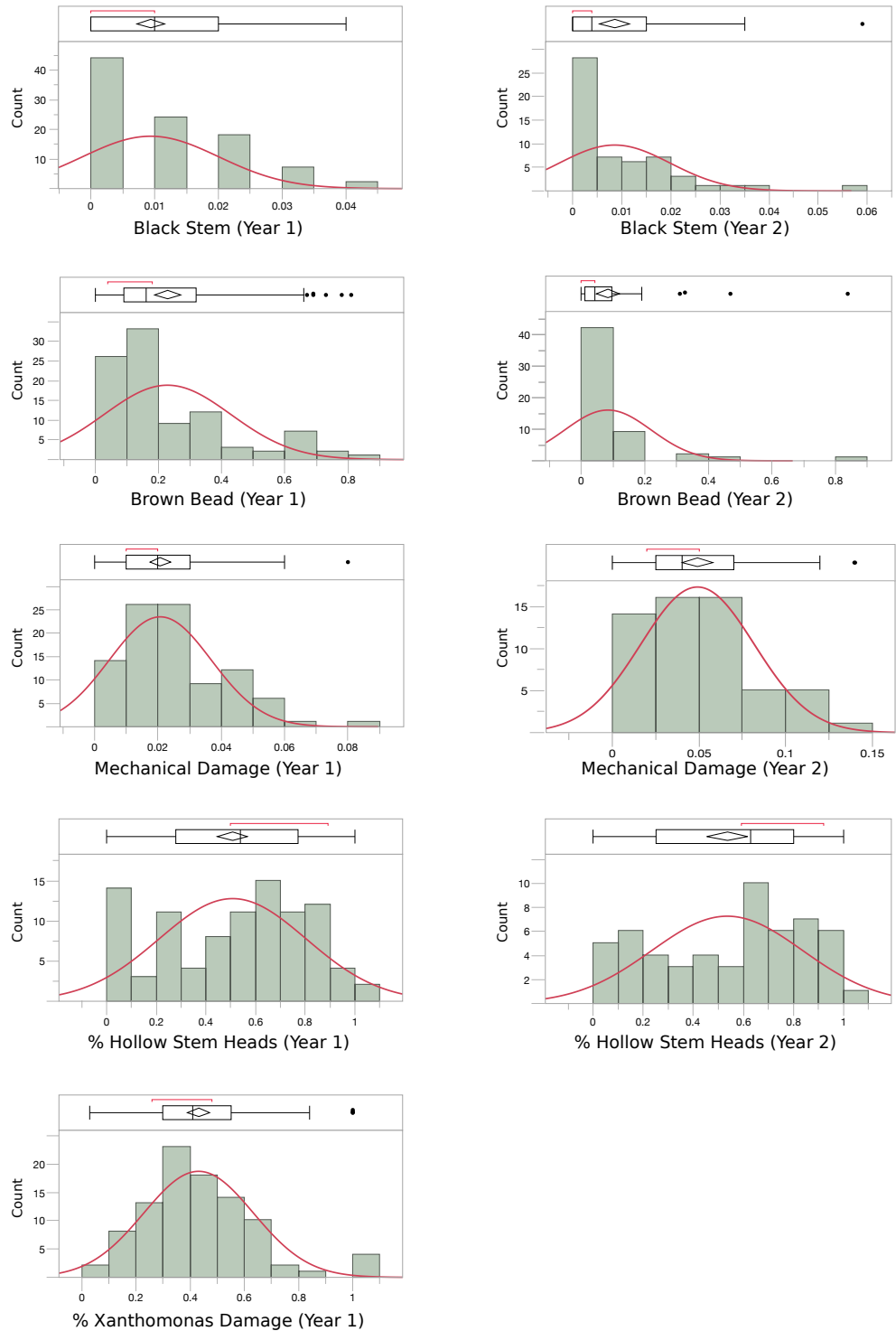


Figure 4.4 – Distribution histograms for the pathogen-related traits for both years, black stem, brown bead, mechanical damage, and % hollow stem heads. % Xanthomonas damage only had data for year 1. The red line indicates a normal distribution. The box plot shows the mean, quartiles, and interquartile range, as well as possible outliers as dots.

4.4.3. Linkage Disequilibrium

In the entire collection, 66,999 (~59%) of the 112,931 intra-chromosomal pairs showed a significant level of linkage disequilibrium ($\text{proChi} < 0.05$). The average R^2 for all pairs was 0.1545. With an R^2 of 0.2, the linkage disequilibrium decays on average in the diversity population at 8.46cM (Figure 4.5).

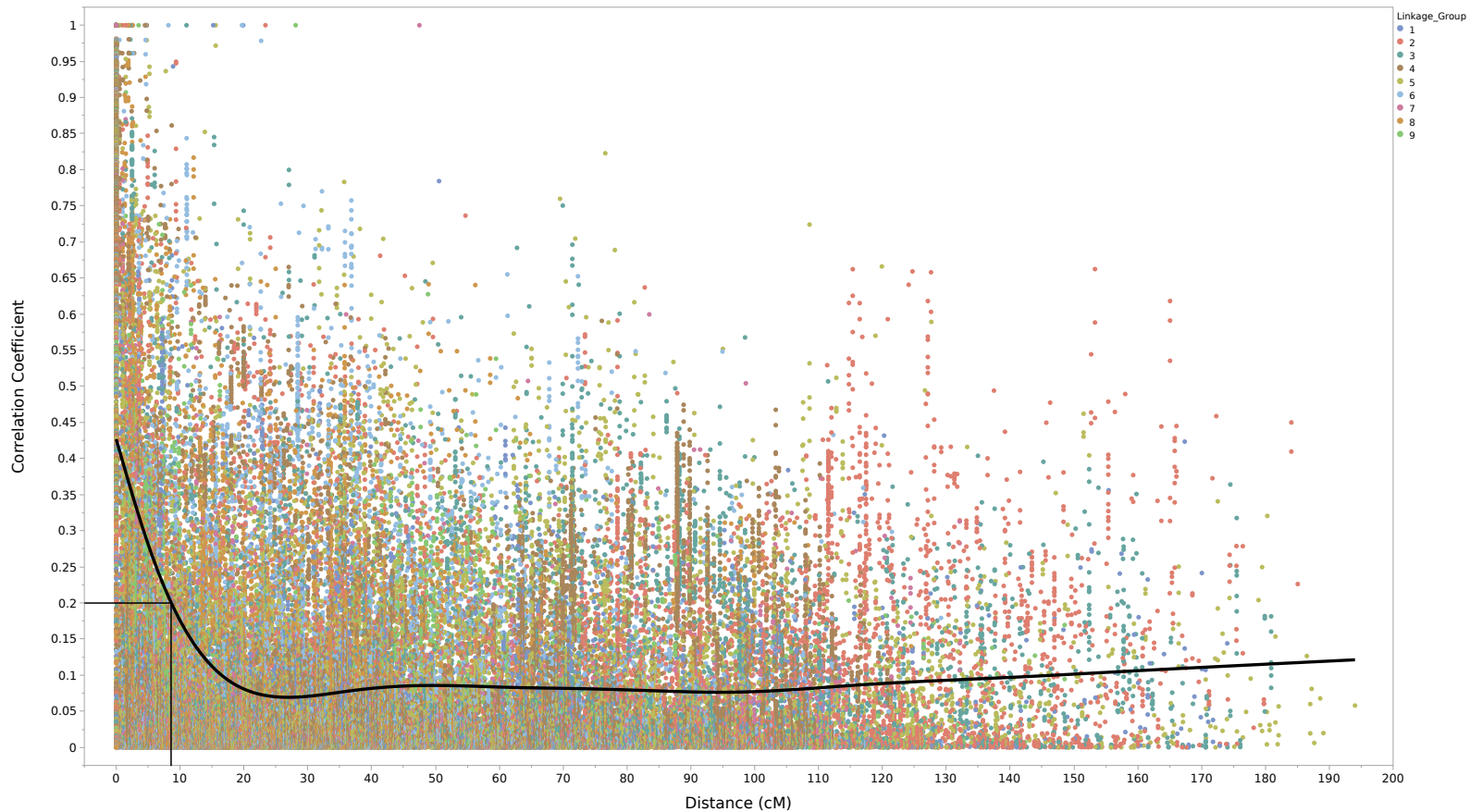


Figure 4.5 - Waterfall scatterplot representing linkage disequilibrium (R^2) as a function of map distance of 1,309 genetic markers in a set of 110 diversity broccoli varieties.

4.4.4. Principal Component Analysis

A principle component analysis accounts for population structure through variance clustering (Korte & Farlow, 2013; J. Yu et al., 2006). The principle component analysis indicates that the first PC accounts for 46.9% of the variance. The percent of variance accounted for by the second PC is 11.9%. The third PC accounts for 8.2% of the variance. The first three PC account for 67%% of the variance. This indicates that only the first three PC are enough to account for the majority of population structure. The first five PC were incorporated into further analyses to account for 79.3% of the variance (Figure 4.6).

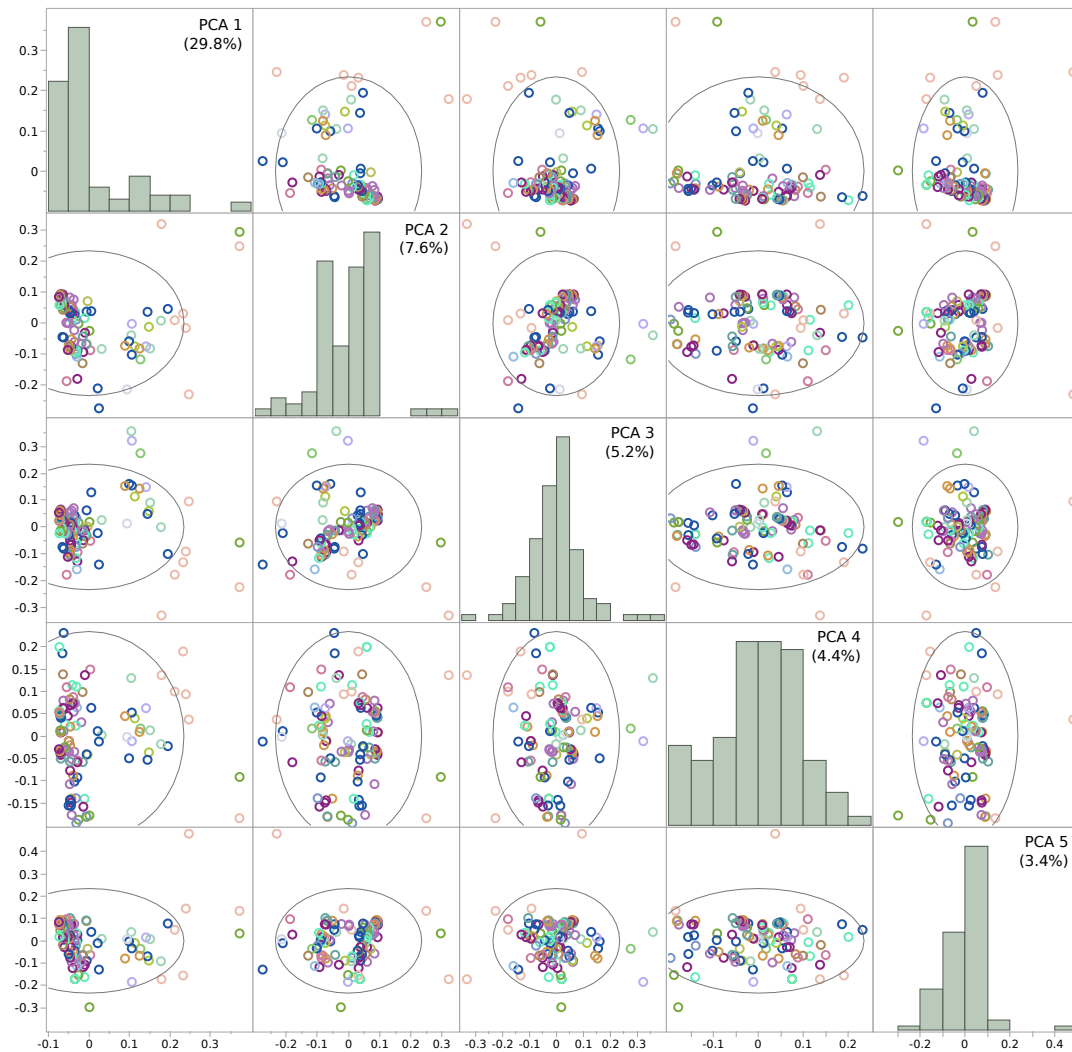


Figure 4.6 - Scatterplots and histograms representing each pairwise comparison of the first five principal components as well as the overall distribution.

4.4.5. Kinship Analysis and Relationship Matrix

Kinship clustering accounts for population structure through finding historical recombination events (Korte & Farlow, 2013; J. Yu et al., 2006). Hierarchical cluster using Ward's method shows that the diversity population clusters into 14 different sub-clusters (SC) (Figure 4.7). SC-1 groups 15 lines together, accounting for 13.4% of relatedness. SC-2 groups 2 lines together, accounting for 1.8% of relatedness. SC-3 groups 13 lines together, accounting for 11.6% of relatedness. SC-4 groups 6 lines together, accounting for 5.4% of relatedness. SC-5 groups 8 lines together, accounting for 7.1% of relatedness. SC-6 groups 6 lines together, accounting for 5.4% of relatedness. SC-7 groups 11 lines together, accounting for 9.8% of relatedness. SC-8 groups 5 lines together, accounting for 4.5% of relatedness. SC-9 groups 17 lines together, accounting for 15.2% of relatedness. SC-10 groups 7 lines together, accounting for 6.3% of relatedness. SC-11 groups 8 lines together, accounting for 7.1% of relatedness. SC-12 groups 6 lines together, accounting for 5.4% of relatedness. SC-13 groups 2 lines together, accounting for 1.8% of relatedness. SC-14 groups 6 lines together, accounting for 5.4% of relatedness.

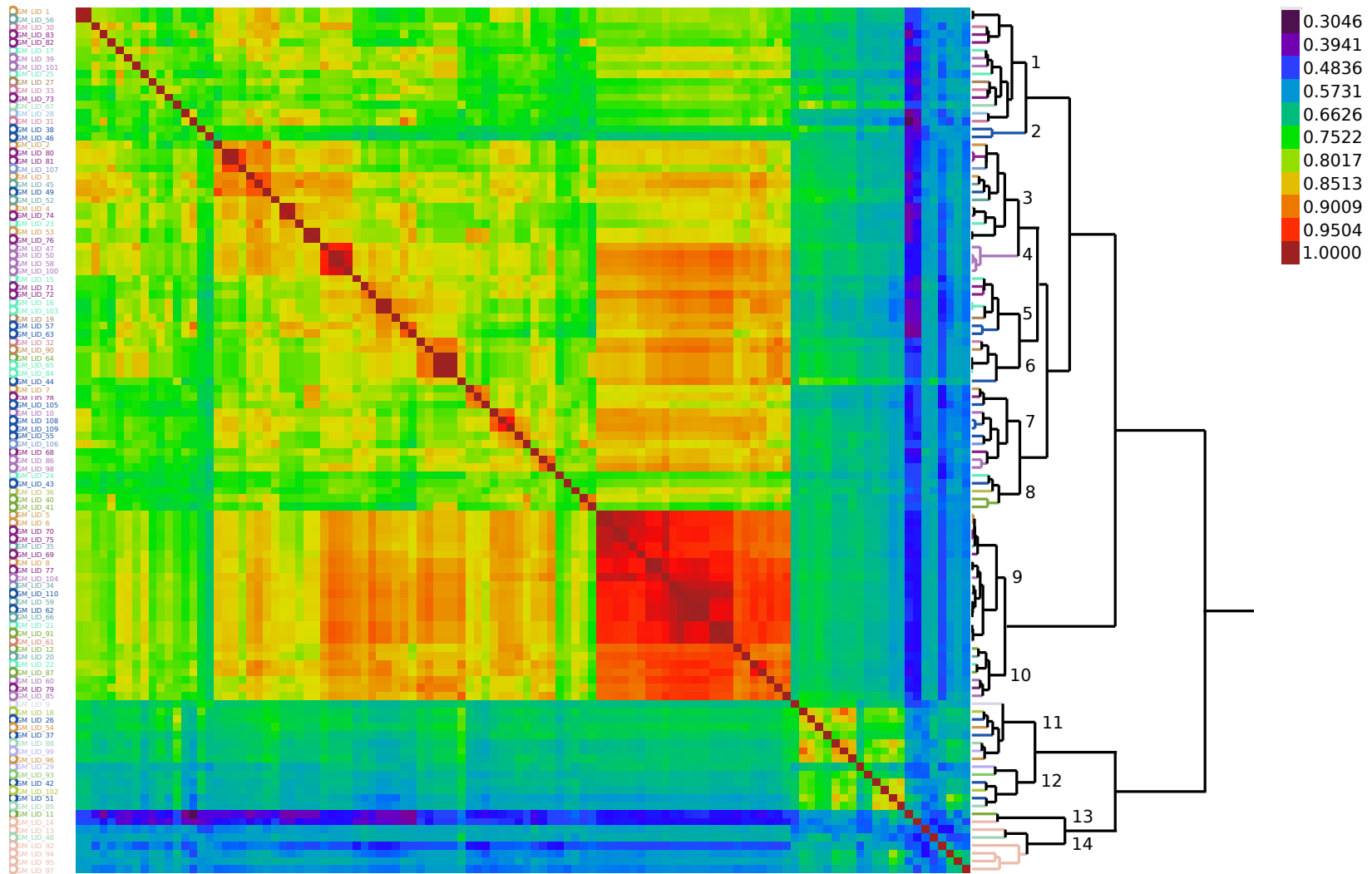


Figure 4.7 - Heat map representing the hierarchal clustering analysis of 112 broccoli lines from the diversity population based on a pair-wise identity by state similarity matrix. The lines cluster into 14 different sub-clusters.

The principle component analysis results of the relationship matrix indicate that the percent of variance accounted for by the first PC is 75.3%. The percent of variance accounted for by the second PC is 11.1%. The third PC accounts for 4.9% of the variance. The first three PC account for 91.3% of the variance. The first five PC were incorporated into further analyses to account for 95.6% of the variance. In the final analysis, the whole relationship matrix was used to account for the variation due to kinship in the population structure (Figure 4.8).

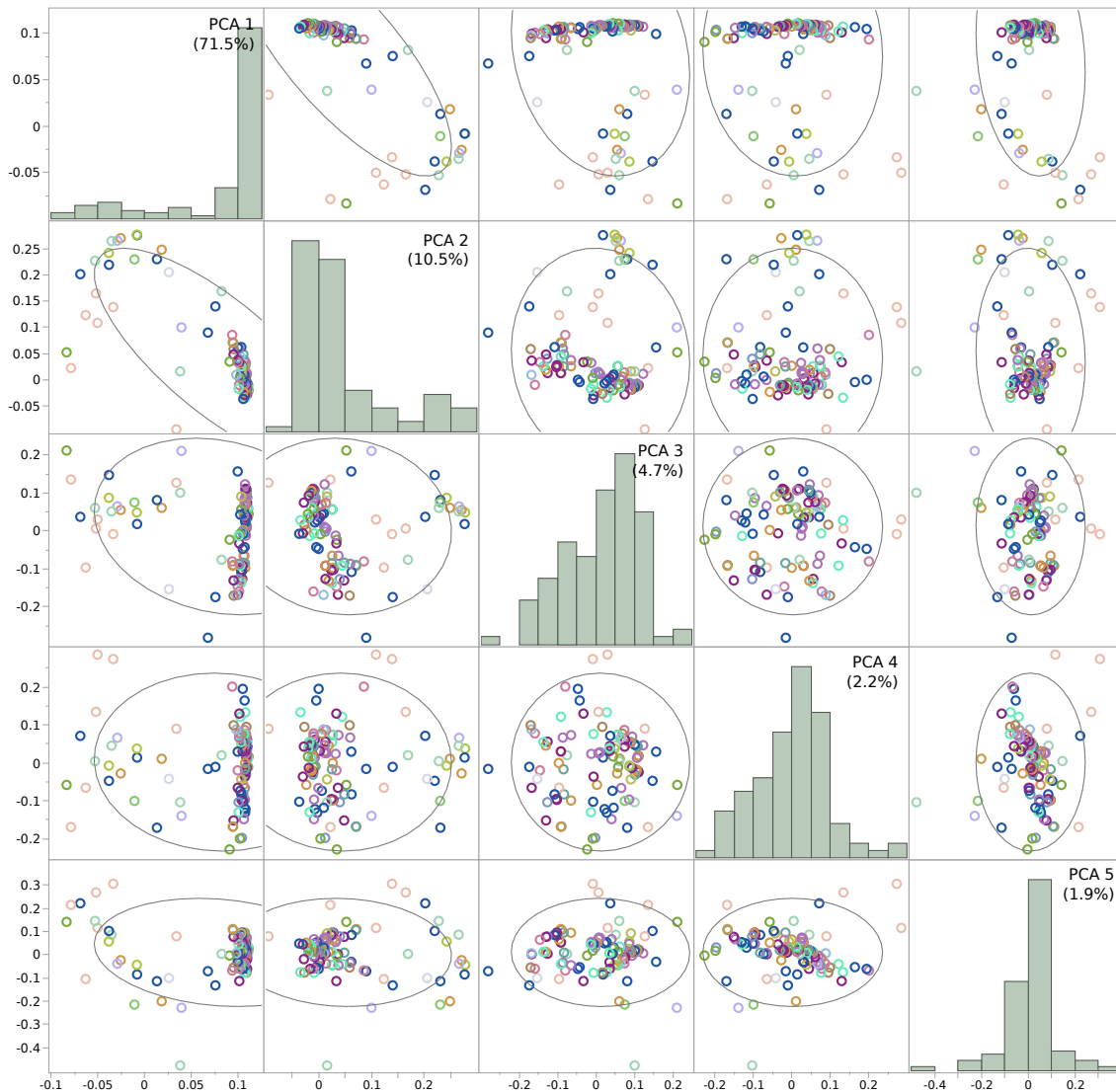


Figure 4.8 - Scatterplots and histograms representing each pairwise comparison of the first five principle components due to kinship, as well as the overall distribution.

4.4.6. Multivariate Correlation

A multivariate analysis of the PCA and kinship analyses determined the similarity of the modeled population structures. Although there was some similarity between PCA and kinship components (Table 4.3), it was not consistent that one population structure completely accounted for the other. To account for as much population structure as possible, thus reduce false positives, a Q-K mixed model approach that incorporates both PCA and kinship population structures was used for the GWAS analysis.

Table 4.3 - Correlation statistics for the multivariate analysis of PCA and Kinship population structure variables.

	PCA1	PCA2	PCA3	PCA4	PCA5
Kinship1	-0.96	0.056	-0.093	-0.046	-0.055
Kinship2	0.65	-0.47	0.32	0.016	-0.078
Kinship3	0.15	0.81	0.51	0.088	0.033
Kinship4	-0.021	0.048	-0.28	0.88	0.042
Kinship5	0.17	0.29	-0.598	-0.403	0.17

-Darker blue shading indicates a greater correlation

4.4.7. Quantitative Trait Loci from Association Mapping

The results of Q-K mixed model association mapping revealed multiple QTLs for every trait. The significant QTLs above the threshold of $-\log_{10}(\text{p-value } 0.001)$ or an LOD 3 for year 1 and year 2 are summarized in Table 4.4. Due to the small population size, the relatively low power of the association mapping would be compromised with multiple testing correction. Therefore, an uncorrected p-value (0.001) or LOD 3 was used as the significant threshold for QTLs detection. Of the more than 20 agronomic traits analyzed, the days to harvest trait was chosen for further analyses as regulating broccoli floret maturation will improve harvest productivity. The four significant QTLs for the days to harvest trait were aligned to the high-density genetic map to determine which of the significant QTL regions for further putative candidate gene analysis. The four significant QTLs for the days to harvest trait are on linkage group four, two on linkage group eight, and one on linkage group nine (Figures 4.9, 4.10, and 4.11).

The pathogen-related traits, consisting of black stem, brown bead, % hollow stem heads, and mechanical damage were chosen for further analyses and grouped together as pathogen resistance. All of the significant QTLs for the pathogen resistance traits are aligned to the high-density genetic map to identify pathogen resistance 'hotspots'. A pathogen-resistance 'hotspot' was chosen when the region contained both overlapping QTLs for replicate years of at least one pathogen-related trait, and overlapping QTLs for two or more pathogen-related traits. The specific Manhattan plots for the pathogen-related 'hotspots' that were chosen for further putative candidate gene analysis are on linkage group two, four, and eight (Figures 4.12, 4.13, and 4.14).

The manhattan plot for linkage group two shows overlapping, significant QTLs for both years of the mechanical damage trait at 77.4cM as well as a significant QTL for year 2 for the hollow stem heads trait at 89.0cM (Figure 4.12). The manhattan plot for linkage group four shows two sets of overlapping QTLs: one 'hotspot' shows overlapping QTLs at 10.3cM for both years of hollow stem heads and year 1 for black stem, while the second 'hotspot' shows a QTLs at 49.9cM for year 1 of brown bead as well as overlapping QTLs at 56.8cM for year 1 of hollow stem heads and year 2 of mechanical damage (Figure 4.13). The manhattan plot for linkage group eight shows significant QTLs at position 54.5cM for year 2 of black stem and at position 66.4cM for year 2 of hollow stem heads (Figure 4.14).

Table 4.4 - Summary of significant QTLs (genome-wide) for year 1 and 2 GWAS.

Trait	QTL Regions - Year 1	QTL Regions - Year 2
Black Stem	1	2
Brown Bead	1	1
Color A	1	-
Color B	5	-
Color L	2	-
Compact	0	0
Days to Harvest	2	2
% Floret	1	0
% GI	1	16
% GII	4	5
Head Weight (lbs)	4	1
Height (in)	0	4
% Hollow Stems Heads	3	3
% Leaves	5	1
Mechanical Damage	1	1
Pedicle	3	1
% Side Shoots	0	0
% Stalk	1	0
% Unharvested Plants	2	0
Width (in)	1	0
% Xanthomonas Damage	0	-
Yield (kg/ha)	1	10

- A second year of data was not collected for Color A, B, or L, and % Xanthomonas Damage

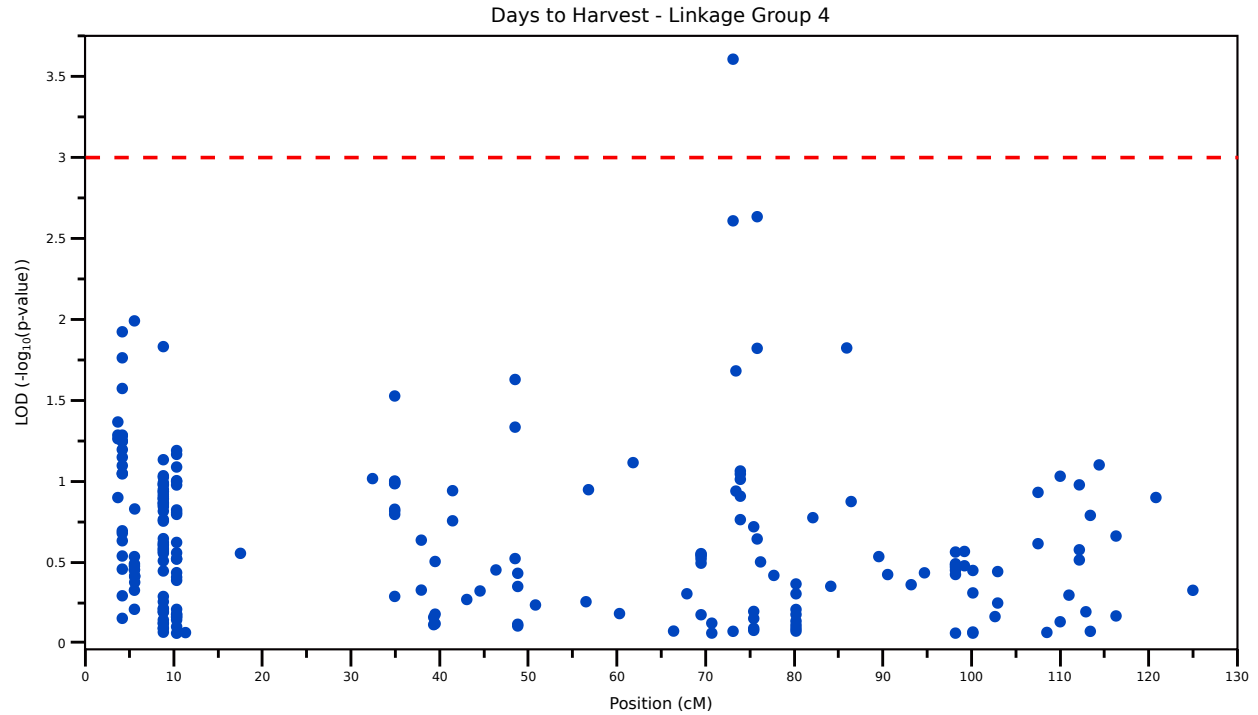


Figure 4.9 – Manhattan plot of the days to harvest trait (Year 2) for linkage group four. The red dashed line indicates the significance threshold of LOD 3.

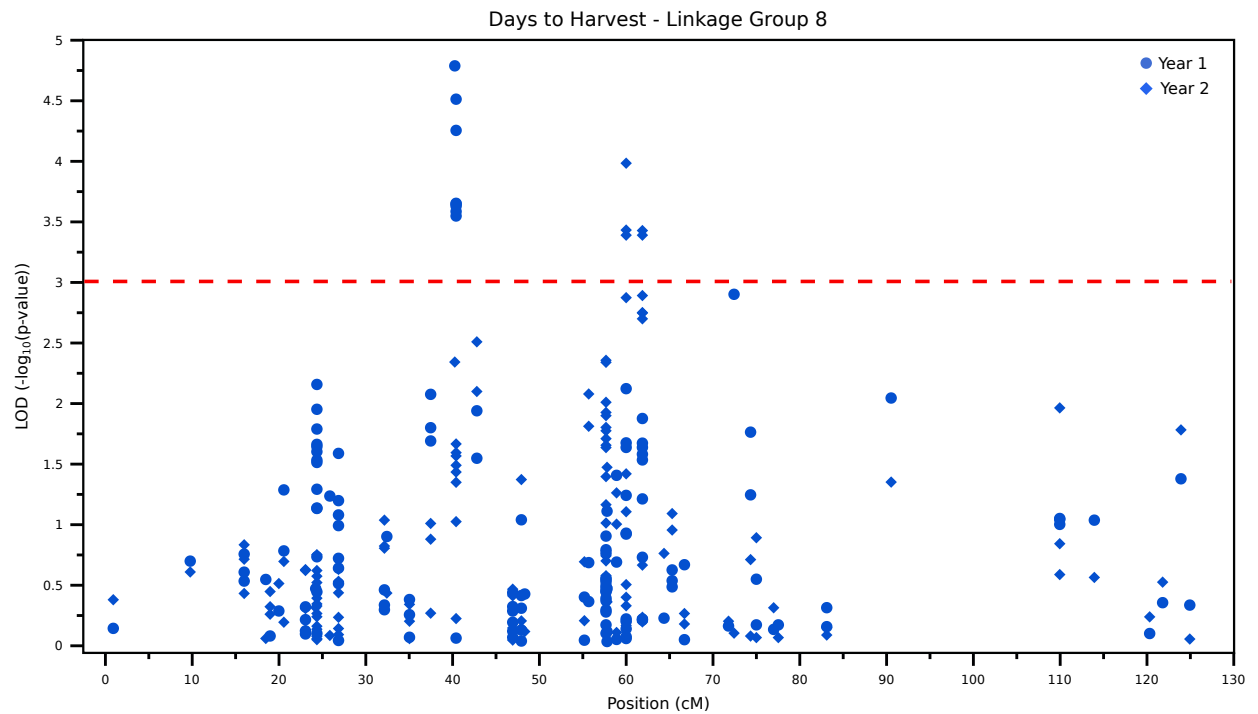


Figure 4.10 – Manhattan plot of the days to harvest trait for both years for linkage group eight. There are two separate significant QTLs. The red dashed line indicates the significance threshold of LOD 3.

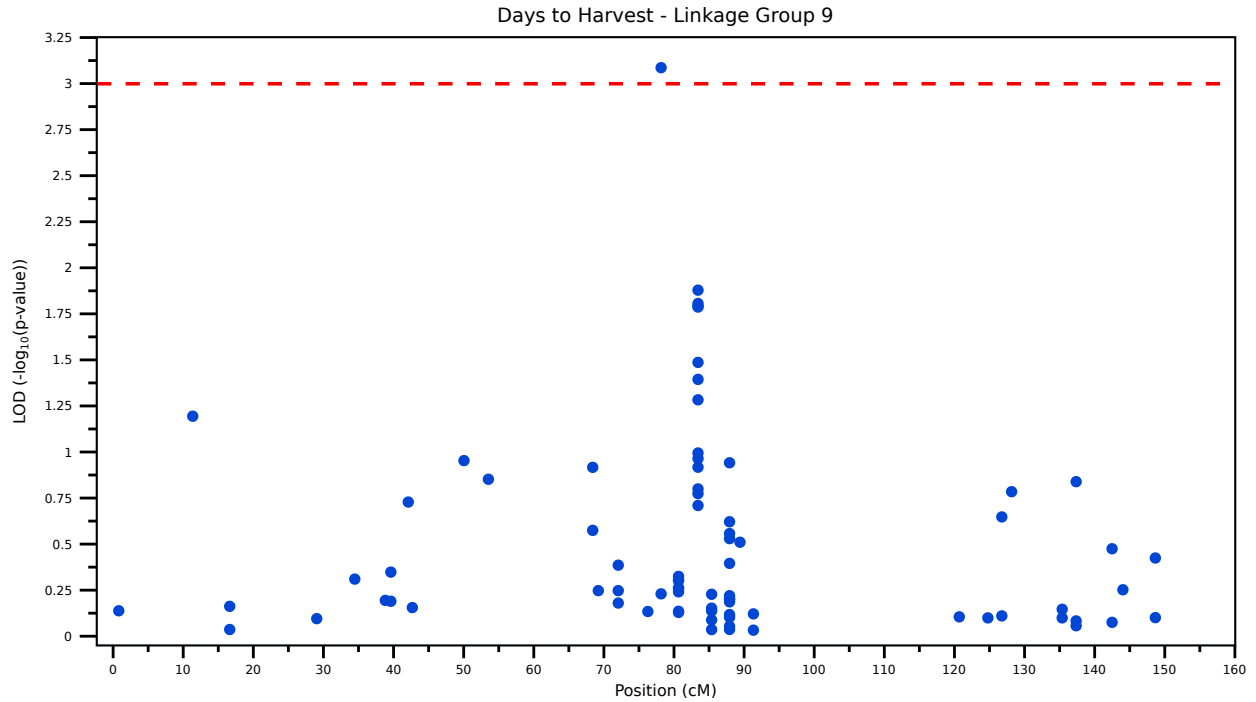


Figure 4.11 – Manhattan plot of the days to harvest trait (Year 1) for linkage group nine. The red dashed line indicates the significance threshold of LOD 3

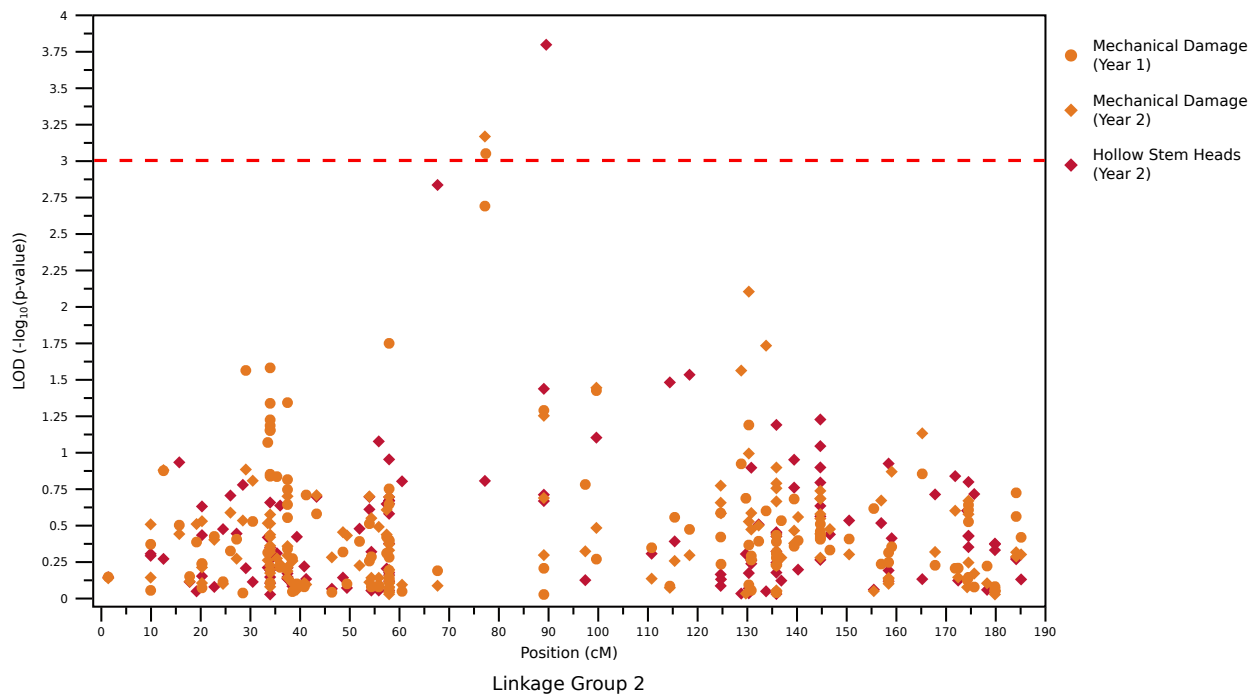


Figure 4.12 – Manhattan plot of multiple pathogen-related traits for both years for linkage group two. The red dashed line indicates the significance threshold of LOD 3.

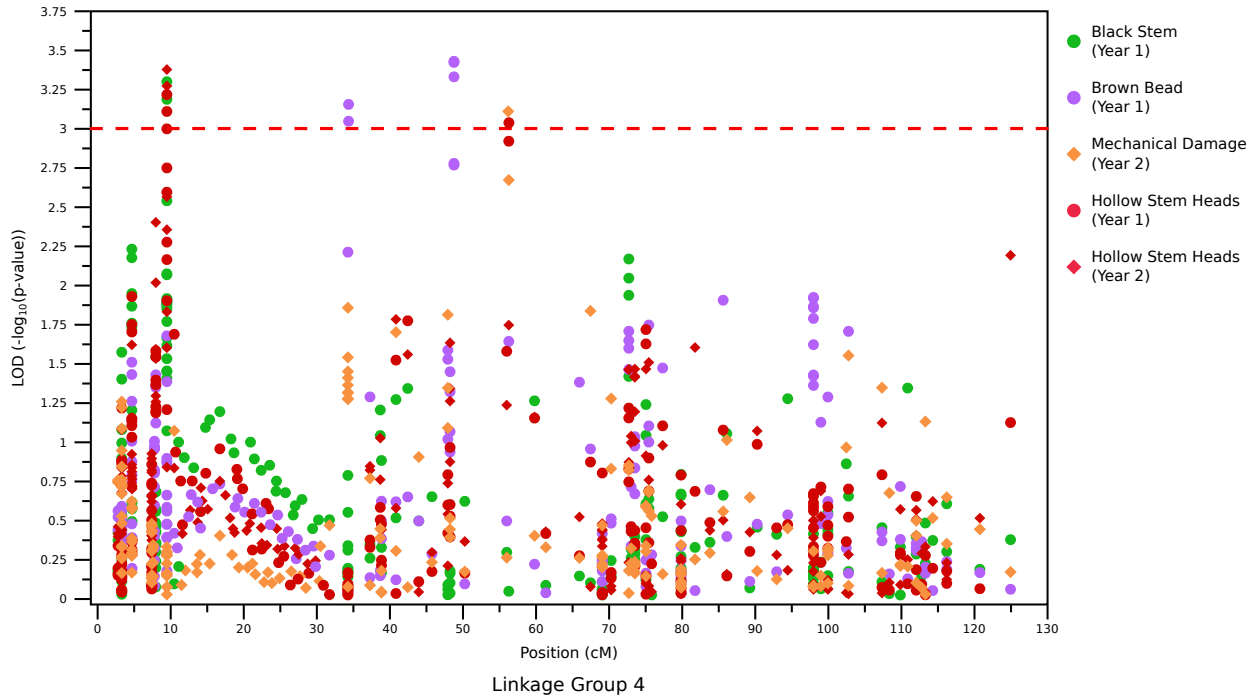


Figure 4.13 – Manhattan plot of multiple pathogen-related traits for both years for linkage group four. Although there are three significant overlapping QTLs, only two QTLs were chosen for further candidate gene analysis. The red dashed line indicates the significance threshold of LOD 3.

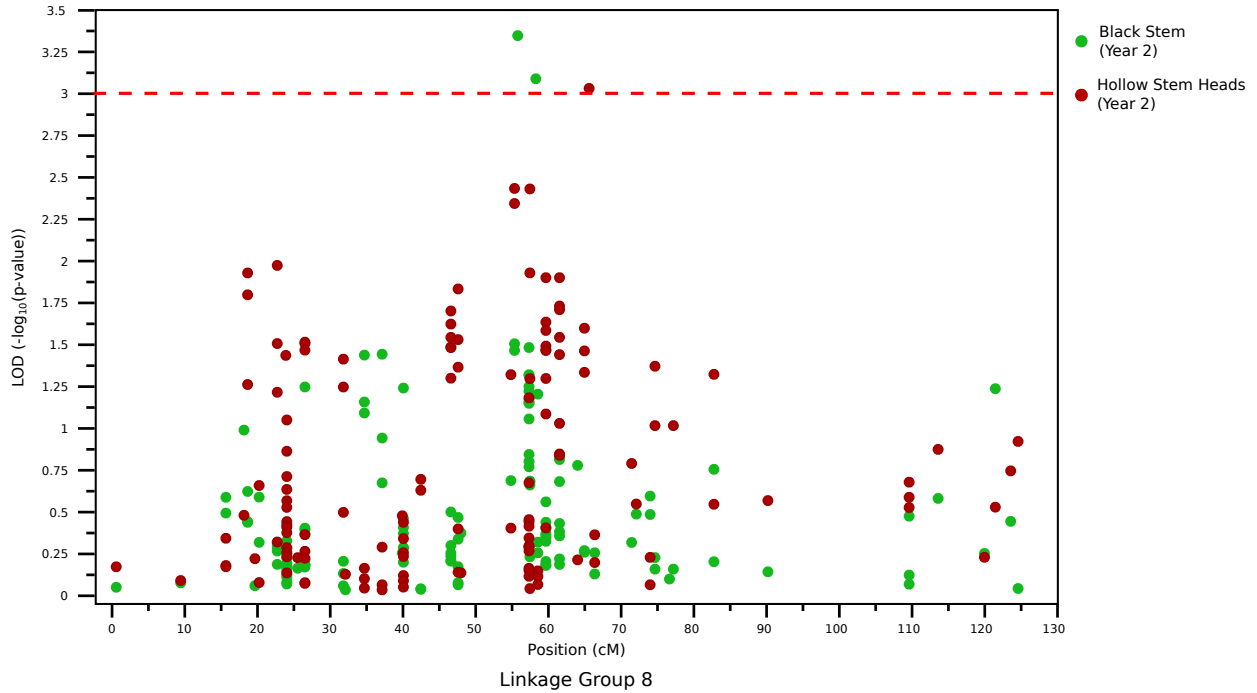


Figure 4.14 – Manhattan plot of multiple pathogen-related traits for year 2 for linkage group eight. The red dashed line indicates the significance threshold of LOD 3.

4.4.8. Putative Candidate Gene Identification

The significant QTLs from year 1 and year 2 for all the 'focus' traits were used in candidate gene identification. Within the database AGRICOLA, Linguamatics extracted 2,223 hits, or unique matches to the query, from 635 journal articles. From the database MEDLINE, Linguamatics extracted 3,076 hits from 861 journal articles. Manually identified candidate genes were combined with Linguamatic results to produce candidate gene lists for each significant QTL regions for the days to harvest trait and pathogen-related traits. The candidate gene lists reported for the days to harvest trait are QTL regions with a p-value below an alpha value of 0.001 with year 1 QTLs shown in Table 4.5 and year 2 QTLs shown in Table 4.6.

The candidate gene list reported for the pathogen-related traits is a selection of the putative candidates found within the pathogen-resistance 'hotspots' (Table 4.7). The 'hotspot' on linkage group two has overlapping QTL regions for the traits hollow stem head during year 2 and mechanical damage for both years. There are two 'hotspots' on linkage group four. The one 'hotspot' at position 10.3cM, designated 4A, has overlapping QTL regions for the traits black stem during year 1 and hollow steam heads for both years. The second 'hotspot' between 49.9cM and 56.8cM, designated 4B, has overlapping QTL regions for the traits brown bead year 1, hollow stem heads for year 1, and mechanical damage for year 2. The 'hotspot' on linkage group eight between 54.5cM and 66.4cM has overlapping QTL regions for the traits black stem for year 2 and hollow stem heads for year 2.

Table 4.5 – Putative candidate genes for days to harvest (year 1) significant QTLs.

QTL: Linkage Group 8 – 39.5cM		
Gene	Function Summary	BLAST e-value
TAP46	Phosphatase 2A regulatory A subunit PP2A	2.00E-28
PYR	Abscisic acid receptor 3	3.00E-64
FAR	Far-Red light sensing protein-like	0
QTL: Linkage Group 9 – 77.7cM		
Gene	Function Summary	BLAST e-value
CLV3	Clavata3/ESR-RELATED 41 – Meristem maintenance (x2)	6.00E-71
GF14	14-3-3-like protein	1.00E-34
SYD/BRM	SWI/SNF2 Chromatin-remodeling ATPase	7.00E-167
PFT	Phytochrome and flowering time regulatory protein	0
RCN1	Phosphatase 2A regulatory A subunit PP2A	0
CO	Zinc Finger CONSTANS with CCT domain	0

(x#) indicates multiple copies of the same gene found in the QTL region

Table 4.6 – Putative candidate genes for days to harvest (year 2) significant QTLs.

QTL: Linkage Group 4 – 73.1cM		
Gene	Function Summary	BLAST e-value
CLV3	Clavata3/ESR-RELATED 41 – Meristem maintenance	6.00E-71
NPH3	Phototropic-responsive NPH3 protein (x2)	0
TCP20	Transcription factor associated with circadian clock	2.00E-180
EDM2	Enhanced Downy Mildew 2-like protein	4.00E-29
CO	Zinc Finger CONSTANS with CCT domain	1.00E-7
FRI	FRIGIDA-like protein	0
QTL: Linkage Group 8 – 59.3-61.2cM		
Gene	Function Summary	BLAST e-value
TFL2	Terminal Flower 2	0
PIF	Phytochrome Interacting Factor (x2)	1.00E-94
NPH3	Phototropic-responsive NPH3	0
GAI	GAI-like protein/RGA-like protein 3	0
AP2	APETALA2-like ethylene-responsive transcription factor	4.00E-37
PSI	Photosystem I P700 chlorophyll a apoprotein A2 PsaA/PsaB protein	0
FT	Flowering Locus T	0-R
TIC	Time for Coffee protein	2.00E-19
FRI	Truncated FRIGIDA-like protein 1 (x2)	02
FAR	Far-Red light sensing protein-like (x2)	1.00E-60
SPL	SQUAMOSA promoter binding protein like 7	1.00E-127

(x#) indicates multiple copies of the same gene found in the QTL region

Table 4.7 – Putative candidate genes for multiple pathogen-related traits for a subset of overlapping, significant QTLs called pathogen-related ‘hotspots’.

Gene	Function	BLAST E-value	QTL Linkage Group	QTL Region (cM)
PL/ PeL	Pectin lyase-like/ Pectate lyase (x6)	0	2	76.4– 99.0
			4B	34.9 – 56.7
			8	54.5 – 76.4
PG	Polygalacturonase (x4)	3.24E-141	4B	34.9 – 56.7
			8	54.5 – 76.4
PMEI	Pectin methylesterase inhibitor/ Pectinesterase (x8)	0	4B	34.9 – 56.7
			8	54.5 – 76.4
XEGIP/ EDGP	Xyloglucan-specific endoglucanase inhibitor (x4)	~	8	54.5 – 76.4
KPI	Serine protease inhibitor Kazal-type	6.19E-84	2	76.4– 99.0
TNL -RPS4 -TAO1	Disease resistance receptor protein (TIR-NBS-LRR class) (x18) -Specific for <i>P. syringae</i> (x2) -Target of AvrB Operation (x2)	0	4B	34.9 – 56.7
			8	54.5 – 76.4
CNL -RPP8 -ADR1	Disease resistance receptor (CC-NBS-LRR) -Resistance to <i>Peronospora parasitica</i> protein 8 -Activated disease resistance 1 gene	4.23E-117	4B	34.9 – 56.7
			8	54.5 – 76.4
AIG2L	Avirulence Induced gene 2-like protein	1.80E-21	4B	34.9 – 56.7
TRAF	Tumor necrosis factor receptor-associated factor-like protein (x12)	2.05E-29	2	76.4– 99.0
			4B	34.9 – 56.7
			8	54.5 – 76.4
RIN -RIN4	RPM1-interacting protein (x2) -RPM1-interacting protein 4-like	~	4A	1.9 – 18.8
			4B	34.9 – 56.7
ACA	Autoinhibited Ca ²⁺ -ATPase (x2)	3.71E-34	4B	34.9 – 56.7
			8	54.5 – 76.4
VCX	Vacuolar cation/proton exchanger (x4)	0	4B	34.9 – 56.7
CaX	Ca ²⁺ exchanger	~	4A	1.9 – 18.8
CNGC	Cyclic nucleotide-gated channel	0	2	76.4– 99.0

Table 4.7 – (continued).

IQD	IQ domain-containing protein (x2)	8.99E-143	2	76.4– 99.0
			4B	34.9 – 56.7
PCAP	Plasma-membrane associated cation-binding	~	8	54.5 – 76.4
MATE	Multidrug and toxic compound extrusion protein/efflux protein (x8)	0	4A	1.9 – 18.8
			4B	34.9 – 56.7
			8	54.5 – 76.4
VDAC	Voltage-dependent anion channel	9.83E-81	2	76.4– 99.0
RALF	Rapid alkalization factor-like protein (x3)	4.27E-70	4A	1.9 – 18.8
			4B	34.9 – 56.7
CaBP	Ca ²⁺ -binding protein (x3)	4.10E-121	2	76.4– 99.0
			8	54.5 – 76.4
CaM	Calmodulin (x2)	~	4B	34.9 – 56.7
CaML	Calmodulin-like protein	0	4B	34.9 – 56.7
CaMBP	Calmodulin-binding protein (x4)	4.07E-136	2	76.4– 99.0
CBL	Calcineurin B-like protein	3.63E-24	4B	34.9 – 56.7
CDPK	Ca ²⁺ -dependent protein kinase (x6)	1.49E-145	4B	34.9 – 56.7
			8	54.5 – 76.4
CIPK	Calcineurin B-like interacting protein kinase (x2)	0	8	54.5 – 76.4
CaLB	Ca ²⁺ -dependent lipid-binding protein (x4)	0	2	76.4– 99.0
			4B	34.9 – 56.7
PLD	Phospholipase D/ C2 Ca ²⁺ -lipid binding phospholipase (x4)	0	2	76.4– 99.0
			4B	26.5 – 81.6
RBOHD	Respiratory burst oxidase homolog protein D	0	4B	34.9 – 56.7
ERD5	Early responsive to dehydration 5	0	4B	34.9 – 56.7
PAD4	Phytoalexin deficient (x3)	0	4B	34.9 – 56.7
NIMIN2	NIM1-interacting 2	9.50E-87	4B	34.9 – 56.7
WRKY	WRKY transcription factor (x5)	1.48E-180	2	76.4– 99.0
			4B	34.9 – 56.7
			8	54.5 – 76.4
ELP1	Enhanced Downy Mildew 2-like protein 1	3.67E-29	4B	34.9 – 56.7

Table 4.7 – (continued).

MAPK	Mitogen-activated protein kinase (x3)	6.47E-123	2	76.4– 99.0
			8	54.5 – 76.4
PDF1.2	Plant Defensin	6.00E-147	8	13.8 – 67.8
DEFL	Defensin-like protein (x7)	7.52E-31	4B	34.9 – 56.7
			8	54.5 – 76.4
AP2 -ERF -EREBP	AP2-like transcription factors -Ethylene-responsive transcription factor (x7) -Ethylene-responsive element-binding factor-like protein (x6)	0	2	76.4– 99.0
			4A	1.9 – 18.8
			4B	34.9 – 56.7
			8	54.5 – 76.4
EDR2	Enhanced Disease Resistance 2	3.09E-29	8	54.5 – 76.4
GLIP	GDSL-like lipase/GDSL esterase/lipase (x8)	0	2	76.4– 99.0
			4B	34.9 – 56.7
			8	54.5 – 76.4
GH18	Chitinase/Glycosyl hydrolase family protein	9.31E-26	2	76.4– 99.0
NUDT	Nudix-hydrolase protein (x2)	0	4A	1.9 – 18.8
			4B	34.9 – 56.7
NUDTL	Nudix-hydrolase-like protein (x3)	2.30E-35	4B	34.9 – 56.7
			8	54.5 – 76.4
PR5	Pathogenesis-related protein 5 (x2)	~	4B	34.9 – 56.7
			8	54.5 – 76.4
ATG	Autophagy-related protein (x3)	1.85E-68	2	76.4– 99.0
			4B	34.9 – 56.7
CYC	Cyclin	1.14E-09	4B	34.9 – 56.7
CDKI	Cyclin-dependent kinase inhibitor	~	4B	34.9 – 56.7
FZR1	Fizzy-related 1/Cell cycle switch protein 52A2	9.53E-78	4B	34.9 – 56.7
RAD1	Cell cycle checkpoint protein	1.26E-29	4B	34.9 – 56.7
CDC45	Cell division cycle 45	0	4A	1.9 – 18.8
MAD2	Mitotic spindle checkpoint protein	~	4B	34.9 – 56.7
CRL	Cullin	1.16E-68	8	54.5 – 76.4

Table 4.7 – (continued).

FBD1	FBD-associated F-box protein (x5)	3.62E-66	4B	34.9 – 56.7
			8	54.5 – 76.4
AIF	Apoptosis-inducing factor	~	8	54.5 – 76.4
HIR	Hypersensitive-induced response protein/ HR-like lesion-inducing protein (x2)	1.89E-77	2	76.4– 99.0
HAUS	HAUS/augmin-like complex	~	4B	34.9 – 56.7
MAP	Microtubule-associated protein (x2)	2.40E-20	4B	34.9 – 56.7
			8	54.5 – 76.4
TUB4	Tubulin beta	0	8	54.5 – 76.4
TUA5	Tubulin alpha (x2)	0	8	54.5 – 76.4
ARP	Actin-related protein	9.33E-32	4B	34.9 – 56.7
FH2	Actin-binding Formin homology 2 protein	2.09E-41	4B	34.9 – 56.7
VLN	Villin (x2)	6.98E-32	8	54.5 – 76.4
MYA	Myosin heavy-chain-associated protein/Myosin XI (x12)	1.40E-30	4A	1.9 – 18.8
			4B	34.9 – 56.7
			8	54.5 – 76.4
ATM1	Myosin-like protein/Myosin VII (x3)	1.63E-25	4B	34.9 – 56.7
DCD	Development and Cell Death protein	3.46E-35	4B	34.9 – 56.7

(x#) indicates multiple copies of the same gene found in the QTL region

~ indicates BLAST comparison of *Brassica oleracea* var. *italica* sequence to *Arabidopsis thaliana* only returned hypothetical or un-annotated proteins

4.5. Discussion

The diversity population analyzed in this research represents the global diversity of *Brassica oleracea* var. *italica*. The higher density genetic map developed and used for this study allowed for decreased linkage disequilibrium regions, thus smaller QTL regions for candidate gene investigation. The higher density of markers retained in the genetic map increased the resolution of GWAS, but the resolution would be further increased if a larger population was used for mapping. The candidate gene identification was performed on a select few traits to support the confidence of GWAS analysis. In this work, we focused on traits important for increasing harvest and productivity.

4.5.1. Broccoli Traits with Putative Candidate Genes for Improving Harvest and Productivity

One of the 'focus' traits is days to harvest as shortening the growth and maturation time has implications to adding a third harvest to the growing season, which would increase the supply of broccoli available for the consumer. Understanding the regulatory genes behind the days to harvest will also improve the synchronization of heading, thus more broccoli heads at the appropriate maturation stage can be harvested at once. Of the four total significant QTL regions found for the days to harvest trait, two QTL regions on linkage group eight and nine were significant for year 1 and two other regions on linkage group four and eight were significant for year 2 (Table 4.5 and 4.6). Candidate genes related to photoperiodism sensing, signaling, and floral meristem transition regulation were found nearby the above-mentioned QTL regions (Tables 4.5 and 4.6).

Photoperiodism, the sensing of day length, is an important regulator of flowering time to ensure the delicate flora buds develop at the appropriate time (Batschauer, 1998; Conti, 2017; Park et al., 1999; Schaart, van de Wiel, Lotz, & Smulders, 2016). The first step of photoperiodism requires the appropriate sensing of light by specific proteins (Cerdan & Chory, 2003; Conti, 2017; Hudson, Ringli, Boylan, & Quail, 1999; R. Lin, 2004). When light is sensed by photoreceptors like phytochromes, the phytochrome undergoes a conformational change into its active state (Batschauer, 1998; Hudson et al., 1999; Lau & Deng, 2010; L. Lin, Liu, & Yin, 2018). Once in the activate state, transcription factors like phytochrome interacting factors (PIF) interact

with the phytochrome and start the signal cascade by interacting with other proteins (Batschauer, 1998; Cerdan & Chory, 2003; Jang, Henriques, Seo, Nagatani, & Chua, 2010; L. Lin et al., 2018; Willige et al., 2007). Two copies of PIFs were found within the QTL on linkage group eight (Table 4.6). Although the exact mechanism is unknown, the far-red impaired response (FAR1) protein interacts with the activated phytochromes and other transcription factors as a coactivator to enhance far-red signal transduction (Hudson et al., 1999; R. Lin, 2004). The FAR1 protein was found in the QTL on linkage group eight at position 39.5cM (Table 5) as well as multiple copies in the QTL on linkage group eight at positions 59.3cM-71.8cM (Table 4.6). An important component of signal transduction is the transfer of the signal through membranes by proteins like non-phototropic hypocotyl 3 (NPH3), which multiple copies were found in the QTL on linkage group four as well as a copy in the QTL on linkage group eight (Table 4.6) (Pedmale & Liscum, 2007).

Plant hormones regulate a multitude of growth and developmental processes (Buchanan et al., 2012). Gibberellin, one of nine plant hormones, regulates shoot elongation, senescence, seed germination, and flowering (Buchanan et al., 2012). GA regulates flowering through the degradation DELLA proteins, and any mutations in the DELLA motif cause GA insensitivity, thus a delay in flowering (Cheng, 2004; Conti, 2017; S. Lee et al., 2002; Mutasa-Gottgens & Hedden, 2009; S. Yu et al., 2012). A GA-insensitive (GAI)-like DELLA gene was found in the QTL on linkage group eight (Table 4.6). DELLA proteins directly bind to SQUAMOSA promoter binding-like proteins (SPL), which prevents the SPLs from activating flowering time regulators like miR172, LEAFY (LFY), and APETELLA2 (AP2), thus causing a delay in flowering (Conti, 2017; Ionescu et al., 2016; Teotia & Tang, 2015; S. Yu et al., 2012). A SPL gene was also found in the same QTL on linkage group eight as well as the GAI gene (Table 4.6). Abscisic acid, another plant hormone, regulates bud dormancy, stomata closing, seed germination, and flowering (Buchanan et al., 2012). ABA signaling requires the four basic components: receptors, phosphatase 2 (PP2), SNF1-related kinase 2 (SnRK2), and transcription factors (Hu, Zhu, Shen, & Zhang, 2014; Vishwakarma et al., 2017). The ABA receptor PYR was found in the QTL on linkage group eight (Table 4.5). Two copies

of a regulatory phosphatase 2A, TAP46 and RCN1, were found in QTLs on linkage group eight and nine (Table 4.5) (Hu et al., 2014; Tseng & Briggs, 2010).

Signal transduction pathways link multiple different regulatory pathways to coordinate a specific response to a specific signal, usually an environmental stimulus (Buchanan et al., 2012). Through a variety of receptors and signals, usually secondary messenger compounds, signal transduction pathways amplify and relay the signal to other receptors at different locations or regulation proteins that induce differential expression of response genes (Buchanan et al., 2012). Transcription factors are often involved at the later stages of signal transduction to differentially regulate the expression of other transcription factors and response genes (Buchanan et al., 2012). For photoperiodism, transcription factors like phytochrome and flowering time (PFT) interact with the Flowering Locus T (FT) (Cerdan & Chory, 2003; Conti, 2017; Ionescu et al., 2016). A copy of PFT was found in the QTL on linkage group nine (Table 4.5). For the circadian rhythm, the time for coffee (TIC) gene not only interacts with many of the circadian rhythm genes, but also with photoperiodism genes (Conti, 2017; Hall, 2003; Ionescu et al., 2016). A copy of the TIC gene was found in the QTL on linkage group eight (Table 6). Another transcription factor that regulates the circadian rhythm and photoperiodism genes is teosinte branched 1 (TCP20) as it transcriptionally regulates PIF and CAA1 (Giraud et al., 2010). A copy of TCP20 was found in the QTL on linkage group four (Table 4.6).

Another environmental signal incorporated into flowering time is vernalization, or prolonged exposure to cold temperatures (Buchanan et al., 2012; Helliwell, Robertson, Finnegan, Buzas, & Dennis, 2011; D.-H. Kim & Sung, 2014; I. Lee & Amasino, 1995). The FRIGIDA gene increases the flowering repressor Flowering Locus C (FLC) through forming a complex (K. Choi et al., 2011; Helliwell et al., 2011; D.-H. Kim & Sung, 2014; I. Lee & Amasino, 1995). Vernalization suppresses FRI and FLC through chromatin remodeling (K. Choi et al., 2011; Helliwell et al., 2011; D.-H. Kim & Sung, 2014; I. Lee & Amasino, 1995). A copy of FRI was found in the QTL on linkage group four, as well as multiple copies in the QTL on linkage group eight (Table 4.6). One of the major transcription factors regulating flowering is the CONSTANS (CO) gene as it activates FT and other flowering time genes (Castillejo & Pelaz, 2008; Conti, 2017; Putterill, Robson,

Lee, Simon, & Coupland, 1995). A copy of the CO gene was found in the QTL on linkage group four and five (Table 4.6).

The FT protein is a vital response protein that is transported to accumulate in the shoot apical meristem where it interacts with other transcription factors to upregulate APETELLA1 (AP1) and other floral meristem identity genes (Kotake, Takada, Nakahigashi, Ohto, & Goto, 2003; Wickland & Hanzawa, 2015). A copy of the FT gene was found in the QTL on linkage group eight (Table 4.6). An important part to flowering time is the meristem transition from vegetative to floral (Buchanan et al., 2012). The differential expression of meristem genes like CLAVATA maintain the meristem population (Clark, Running, & Meyerowitz, 1995; Durbak & Tax, 2011). Multiple copies of the CLV gene were found in the QTLs on linkage group nine and four (Table 4.5 and 4.6). Along with CLV, FT, and CO, many other genes need to be activated to appropriately transition and establish the floral meristem (Buchanan et al., 2012; Conti, 2017; Ionescu et al., 2016). AP2 associates with AP1, LFY, and cauliflower (CAL) for the establishment of the floral meristem (Conti, 2017; Jofuku, Den Boer, Van Montagu, & Okamoto, 1994). A copy of AP2 was found in the second QTL on linkage group eight (Table 4.6). Some research suggests a dual role for enhanced downy mildew 2-like protein 1 (ELP1) gene because when it interacts with WNK8, there is a suppression of FLC expression (Tsuchiya & Eulgem, 2010). A copy of ELP1 was found in the QTL on linkage group four (Table 6). After the establishment of the floral meristem, there needs to be differential regulation of other genes to terminate the meristem activity so floral organ identity genes can be upregulated to produce the organs. The terminal flower locus 2 (TFL2) is a negative regulator of FT expression, thus indirectly down regulates the other meristem genes (Kotake et al., 2003). A copy of TFL2 was found in the second QTL on linkage group eight (Table 6). Chromatin remodeling through SWI2/SNF2 chromatin remodeling ATPases SPLAYED and BRAHMA (SYD/BRM) is another way to transcriptional regulate the termination for floral meristem genes to transition to floral organ identity gene (Wu et al., 2012). A copy of SYD/BRM was found in the QTL on linkage group nine (Table 4.5). The presence of more key photoperiodism genes as well as important floral meristem differentiation genes in the QTL region provides confidence in the identified QTL as an important regulator of the days to

harvest trait. The identification of these QTLs and candidate genes could aid in breeding for reduced growing season, where broccoli can head and differentiate to floral buds more quickly, thus increasing annual yield.

4.5.2. Broccoli Pathogen-Related Traits for Improving Pathogen Resistance

The pathogen-related traits focused on for candidate gene investigation are black stem, brown bead, hollow stem heads, and mechanical damage as they are all related to pathogens, thus can confer resistance. Black stem, the dark discoloration of the floret stalk, may be caused by either *Xanthomonas campestris* or *Bacillus campestris* (Williams, 2007). The bacteria *Xanthomonas campestris* is a devastating pathogen causing vast amounts of damage to broccoli crop every year. Brown bead is the discoloration, abortion, and necrosis of floral buds starting in the center of the floret (Jenni, Dutilleul, Yamasaki, & Tremblay, 2001; Williams, 2007). The hollow stem head is when the floret stalk splits and hollows from the center outwards (Belec, Villeneuve, Coulombe, & Tremblay, 2001; Jenni et al., 2001). Researchers are still unsure whether brown bead and hollow stem heads are caused by a bacterial infection or a nutrient imbalance that makes the broccoli floret more susceptible to infection (Belec et al., 2001; Jenni et al., 2001). A better understanding of the genetic regulation of pathogen resistance is important for developing more pathogen resistant broccoli florets. Improving natural pathogen resistances from within broccoli florets will aid in increasing growth productivity and in reducing pesticide application, as valuable biomass will not be lost to bacteria, fungi, insects, or necrosis. Of the multitude of significant QTLs associated with each pathogen-related trait, there were some QTLs that were replicated across different pathogen-related traits and across the two years, thus a pathogen resistance 'hotspot'. Every aspect of recognizing, signaling, and responding to a pathogen attack is represented in the 'hot spots' identified through the GWAS.

4.5.2.1. Pathogen Recognition Putative Candidate Genes

The complex interaction between pathogen and host is often described as an 'arms race' as one side is always working to gain the advantageous adaptation that will defeat the other (Buchanan et al., 2012; H. Zhang et al., 2017). A pathogen constantly adapts its virulence factors to either more efficiently degrade the host's barriers or avoid recognition of the pathogen's elicitor proteins by host's receptors (Malinovsky, Fangel, &

Willats, 2014; McHale, Tan, Koehl, & Michelmore, 2006; H. Zhang et al., 2017). Concurrently, the host also constantly adapts its resistance factors to either more quickly inhibit the pathogen's enzymes or appropriately recognize the pathogen's elicitor proteins (Malinovsky et al., 2014; McHale et al., 2006; H. Zhang et al., 2017). Since the first barrier of a plant cell is the cell wall, the pathogen might secrete enzymes to degrade the cell wall and provide nutrients for growth, like pectin methylesterase (PME), pectin lyase-like (PL), polygalacturonases (PG), xyloglucan-specific endoglucanase, or cysteine proteases (Bellincampi, Cervone, & Lionetti, 2014; D'Ovidio, Mattei, Roberti, & Bellincampi, 2004; Figueiredo, Monteiro, & Sebastiana, 2014; J.-Y. Kim et al., 2009; Lionetti et al., 2007; Vogel, 2002; Yoshizawa, Shimizu, Hirano, Sato, & Hashimoto, 2012). In turn, the plant would have multiple inhibitors located within the cell wall to block any degradation. Pectin methylesterase inhibitors (PMEI) and xyloglucan-specific endoglucanase inhibitor (XEGIP/EDGP) inhibit cell wall degradation, and serine protease inhibitor Kazal-type (KPI), subtilase (SBT), and cystatin (CYS) block the accumulation of nutrients so the pathogen cannot grow from cell wall degradation products (Belenghi et al., 2003; Bellincampi et al., 2014; D'Ovidio et al., 2004; Figueiredo et al., 2014; J.-Y. Kim et al., 2009; Lionetti et al., 2007; Pariani et al., 2016; Tornero, Conejero, & Vera, 1996, 1997; Vogel, 2002; Yoshizawa et al., 2012). Multiple copies of pathogen secretion motifs and plant inhibitor enzymes were found in multiple 'hotspot' QTLs (Table 4.7). The presence of important pathogen recognition genes provides support that the QTL regions play a role in regulating pathogen resistance. The first stage of pathogen resistance is the recognition of attack. It is vital that recognition is efficient and accurate in order to start the signal transduction and differential regulation of resistance genes (Buchanan et al., 2012; H. Zhang et al., 2017).

The recognition of attack depends on receptors interacting with specific proteins, elicitors, from the pathogen (Buchanan et al., 2012). These receptors are usually embedded in and span the cell wall or plasma membrane (Buchanan et al., 2012). The first class of receptors associated with pathogen recognition is the toll/interleukin-1(TIR)-nucleotide-binding site (NBS)-leucine rich repeat (LRR) receptors (TNL) (Meyers, Morgante, & Michelmore, 2002; Torii, 2004; Z.-S. Xu et al., 2009). The gene resistant to *Pseudomonas syringae* 4 (RPS4) is a TNL that recognizes AvrRps4 elicitor

from the pathogen (Gassmann, Hinsch, & Staskawicz, 1999). Since pathogens can secrete multiple effectors, it is vital the plant have multiple receptors to interact with each effector in order to accurately recognize the pathogen. The bacteria, *P. syringae*, also secretes AvrB, therefore there is the TNL target of AvrB operation (TAO1) that interacts with AvrB (Eitas, Nimchuk, & Dangl, 2008). Multiple general TNLs, RPS4, and TAO1 were found in multiple 'hotspot' QTLs (Table 4.7). To ensure pathogen resistance signal transduction cascades are not redundantly activated when it may be unnecessary, some receptors have interacting factors that regulate activation (Buchanan et al., 2012). For example, tumor necrosis factor receptor-associated factors (TRAF) directly interact with TIR domains to start a kinase cascade (Takatsuna et al., 2003). An example of a specific interaction, RPM1 has an interacting factor, RIN4, that regulates RPM1 activation (Bartsch, 2006; Eitas et al., 2008; Mackey, Holt, Wiig, & Dangl, 2002). Multiple copies of TRAFs and RIN4 were also found in multiple 'hotspot' QTLs (Table 4.7). The presence of important receptors genes and the interacting proteins provides further support that the QTL regions play a role in regulating pathogen resistance. If the pathogen effector is not accurately recognized, then the appropriate signal transduction cascade cannot be initiated, thus the plant becomes susceptible to the pathogen.

4.5.2.2. Pathogen Attack Signal Transduction Putative Candidate Genes

The mechanisms and interacting partners of signal transduction cascades are difficult to elucidate, especially in plants, as many protein functions have partial redundancy with each other (Buchanan et al., 2012). The initiation of a signal transduction cascade usually consists of the production a secondary messenger that can be transported to interact in other signaling pathways or start a kinase/phosphorylation cascade (Buchanan et al., 2012). A common secondary messenger is calcium, Ca^{2+} , concentrations in the cytoplasm (Cheval, Aldon, Galaud, & Ranty, 2013; Poovaiah, Du, Wang, & Yang, 2013; Sanders, Pelloux, Brownlee, & Harper, 2002; Tuteja & Mahajan, 2007). The change in calcium concentration contributes to calcium's secondary messenger role by affecting the transmembrane potential. A Ca^{2+} specific pump, autoinhibited Ca-ATPase (ACA) are responsible for the outward flux of Ca^{2+} (Cheval et al., 2013; Harper, 2001; Hepler, 2005; Kolukisaoglu,

2004; Sanders et al., 2002; Tuteja & Mahajan, 2007). When Ca²⁺-binding is blocked or loss-of-function mutation has occurred in ACA8, there is enhanced susceptibility of Arabidopsis to pathogen (Cheval et al., 2013; Harper, 2001; Hepler, 2005; Kolukisaoglu, 2004; Sanders et al., 2002; Tuteja & Mahajan, 2007). Exchangers and channels also regulate the flux of calcium between membranes. Vacuolar cation/proton exchanger (VCX), Calcium exchanger (CaX), and Cyclic nucleotide-gated channel (CNGC) almost exclusively transport calcium (S. M. Y. Lee et al., 2009; Ma, Smigel, Verma, & Berkowitz, 2009; Sanders et al., 2002). The IQ domain of CNGCs is the binding site for Ca²⁺ bound calmodulin (CaM) to provide feedback regulation of Ca²⁺ flux depending on the CNGC gene member (Abel, Savchenko, & Levy, 2005; Fischer, Kugler, Hoth, & Dietrich, 2013; Sanders et al., 2002). Plasma membrane associated cation-binding protein (PCAP) exhibits some specificity towards Ca²⁺ binding, but still can bind other cations (Ide et al., 2007). Calcium transport may also be regulated through general transporters like the multidrug and toxic compound extrusion proteins (MATE) (Nawrath, 2002; Tiwari, Sharma, Singh, Tripathi, & Trivedi, 2014). The balance of activity between calcium transport and anion transporters like voltage-dependent anion channel (VDAC) and rapid alkalization factor-like (RALF) may also regulate the transmembrane potential signal (S. M. Y. Lee et al., 2009; Sharma et al., 2016). Multiple copies of calcium-related exchangers and channel were found in multiple 'hotspot' QTLs (Table 4.7). The presence of multiple copies of calcium sensing proteins and regulators of flux in multiple 'hotspot' QTLs provides further support that the identified QTL regions regulate pathogen resistance (Table 4.7).

The change in cytoplasmic Ca²⁺ by exchangers and channels is sensed by Ca²⁺-binding proteins (CaBP), calmodulin (CaM), calmodulin-like (CaML), calmodulin-binding proteins (CaMBP), and Calcineurin B-like proteins (CBL) (Cheval et al., 2013; Chiasson, Ekengren, Martin, Dobney, & Snedden, 2005; Kolukisaoglu, 2004; A. S. N. Reddy, Ali, Celesnik, & Day, 2011; V. S. Reddy, Ali, & Reddy, 2003; Sanders et al., 2002; Tuteja & Mahajan, 2007; Vadassery & Oelmüller, 2009). Multiple copies of these calcium sensors were found in multiple 'hotspot' QTLs (Table 4.7). The Ca²⁺ sensors do not contain catalytic domains, therefore they complex with other enzymes to transfer the signal to another signaling pathway (Cheval et al., 2013; Harper, 2001; Hepler, 2005;

Kolukisaoglu, 2004; A. S. N. Reddy et al., 2011; Sanders et al., 2002; Tuteja & Mahajan, 2007; Vadassery & Oelmüller, 2009). More research needs to be conducted to further identify the interacting enzymes with which the multitude of Ca^{2+} sensors binds too. Some Ca^{2+} sensors have been shown to interact with multiple enzymes like EDS1 and certain WRKY proteins, thus transferring the signal to the salicylic acid pathway (Cheval et al., 2013; Hepler, 2005; A. S. N. Reddy et al., 2011; Sanders et al., 2002; Tuteja & Mahajan, 2007; Vadassery & Oelmüller, 2009). The Ca^{2+} signal may also be sensed through Ca^{2+} responders, which contain a catalytic domain (Cheval et al., 2013; A. S. N. Reddy et al., 2011; Tuteja & Mahajan, 2007). The Ca^{2+} responders Ca^{2+} -dependent protein kinases (CDPK) and CBL-interacting protein kinases (CIPK) have been shown to interacting with ethylene responsive transcription factors (ERFs) and plant defensin (PDF1.2), thus transferring the signal to the jasmonic acid (JA) and ET signaling pathway (Cheval et al., 2013; Kolukisaoglu, 2004; Ludwig et al., 2005; Matschi, Hake, Herde, Hause, & Romeis, 2015; Nie et al., 2012).

The Ca^{2+} signal may also interact with lipid secondary messengers (Cheval et al., 2013; A. S. N. Reddy et al., 2011; Sanders et al., 2002). Lipid signals, like phospholipids are produced from degradation of membranes and cell wall components by pathogen secreted enzymes as mentioned previously (de Silva, Laska, Brown, Sederoff, & Khodakovskaya, 2011; Maldonado, Doerner, Dixon, Lamb, & Cameron, 2002; Shah, 2005). The Ca^{2+} -dependent lipid-binding proteins (CaLB) and C2 Ca^{2+} -lipid binding phospholipase D (PLD) convert phospholipids into phosphatidic acid (PA) another secondary messenger for signal transduction (Canonne, Froidure-Nicolas, & Rivas, 2011; Carman & Han, 2009; Craddock, Adams, Bryant, Kurup, & Eastmond, 2015; de Silva et al., 2011; Ide et al., 2007; Nakano et al., 2013; Racapé et al., 2005). The Ca^{2+} signal may also be transferred to the ROS signaling pathway through interacting with respiratory burst oxidase homolog protein D (RBOHD) (Cheval et al., 2013; Fabro, Rizzi, & Alvarez, 2016; Ludwig et al., 2005; A. S. N. Reddy et al., 2011; Sanders et al., 2002; Torres, Jones, & Dangl, 2005). Some isoforms of RBOHD are directly activated by CDPK (Boudsocq et al., 2010; Cheval et al., 2013; Dixit & Jayabaskaran, 2012; Ludwig et al., 2005; Matschi et al., 2015; Nie et al., 2012). Early responsive to dehydration 5 (ERD5) has been shown to enhance RBOHD (Cheval et al., 2013; Fabro

et al., 2016; Ludwig et al., 2005; A. S. N. Reddy et al., 2011; Sanders et al., 2002; Torres et al., 2005). The presence of multiple genes related to calcium signaling and transduction to other signaling pathways in multiple 'hotspot' QTLs provides further support for the identified QTL regions regulating pathogen resistance (Table 4.7).

The SA and JA/ET signaling pathways are the two main hormone signaling pathways that regulate downstream pathogen resistance genes (Buchanan et al., 2012). Enhanced disease susceptibility 1 (EDS1) has been shown to directly interact with TNL receptors and SA pathway (Feys, Moisan, Newman, & Parker, 2001; Heidrich et al., 2011; Rustérucchi, Aviv, Holt, Dangl, & Parker, 2001; Yun et al., 2003). EDS1 interacts with phytoalexin deficient (PAD4) to upregulate the SA pathway as well as induce hypersensitive response (HR) (Feys et al., 2001; Heidrich et al., 2011; Rustérucchi et al., 2001; Yun et al., 2003). The accumulation of SA regulates non-expresser of PR gene 1 (NPR1)/NIM1 (Bowling, Clarke, Liu, Klessig, & Dong, 1997; Boyle et al., 2009; Després, DeLong, Glaze, Liu, & Fobert, 2000). NPR1/NIM1, and its interacting partner, NIMIN2, bind to the promoter region of TGA2 to activate transcription of pathogenesis-related protein 1 (PR1) and systematic acquired resistance (SAR) (Bowling et al., 1997; Boyle et al., 2009; Després et al., 2000; Friedrich et al., 2001). The presence of multiple copies of genes regulating the SA pathway in multiple 'hotspot' QTLs provides even further support for the identified QTL regions regulating pathogen resistance (Table 4.7).

In the JA/ET signaling pathway, the enhanced downy mildew 2 (EDM2) and EDM2-like (ELP1) protein has been shown to interact with CNL receptors and JA/ET pathway (Eulgem et al., 2007). Mitogen-activated protein kinases (MAPK) are important signal transducers as they have been shown to regulate ethylene-responsive transcription factors (ERF) and some WRKY transcription factors, as well as negatively regulate the accumulation of SA (Brodersen et al., 2006; Lassowskat, Bottcher, Eschen-Lippold, Scheel, & Lee, 2014; Pandey & Somssich, 2009; Sarris, Cevik, Dagdas, Jones, & Krasileva, 2016; Sarris et al., 2015; Schweighofer et al., 2007; Zhao, Mehrabi, & Xu, 2007). The activation of SAR by JA/ET is mediated through PDF1.2 activation (de Oliveira Carvalho & Moreira Gomes, 2011; Manners et al., 1998; Shafee, Lay, Hulett, & Anderson, 2016). The activation mechanism of plant defensin-like genes (DEFL)

requires more research to elucidate the interacting proteins (de Oliveira Carvalho & Moreira Gomes, 2011; Manners et al., 1998; Shafee et al., 2016). The presence of multiple genes regulating the JA/ET signaling pathway in multiple 'hotspot' QTLs further indicates the identified QTL regions regulate pathogen resistance (Table 4.7).

The interaction of multiple secondary messengers and regulators of plant hormones further transduces and confers specificity to the pathogen attack signal (Buchanan et al., 2012). In the SA pathway, enhanced disease resistance 2 (EDR2) interacts with phospholipids and SA to activate programmed cell death (Tang, Ade, Frye, & Innes, 2005). In the JA/ET pathway, GDSL-like lipases (GLIP) and chitinases (GH18) have been shown to hydrolyze fungal cell walls as well as promote SAR through ET, ERF, and PAD1.2 signaling (Kwon et al., 2009; Langner & Göhre, 2016; Son et al., 2012). Also within the JA/ET pathway, some ERF gene members regulate RBOHD activity and increase ROS (Grennan, 2008; Licausi, Ohme-Takagi, & Perata, 2013; Sewelam et al., 2013; Son et al., 2012). Nudix hydrolases (NUDT) and NUDT-like (NUDTL) enzymes regulate the oxidation state, thus can 'prime' plant for quicker induction of pathogen resistance genes through oxidative stress sensitivity (Bartsch, 2006; X Ge et al., 2007; Xiaochun Ge & Xia, 2008). The presence of multiple genes regulating multiple secondary messengers and hormones in multiple 'hotspot' QTLs further indicates the identified QTL regions regulate pathogen resistance (Table 4.7). The result of pathogen resistance signal transduction cascades is the differential regulation of resistance genes that change the plant's physiology (Buchanan et al., 2012).

4.5.2.3. Pathogen Resistance Response Putative Candidate Genes

The physiological response exhibited by plants in response to pathogen attack is programmed cell death (PCD) so the pathogen does not obtain more resources for further infection (Coll, Epple, & Dangl, 2011; Heath, 1998; Reape, Molony, & McCabe, 2008; Yamada, Ichimura, Kanekatsu, & van Doorn, 2009). PCD is the systematic interference with the cell cycle and regulation of autophagy (Coll et al., 2011; Heath, 1998; Reape et al., 2008; Yamada et al., 2009). Autophagy is the recycling of cellular components with autophagy-related proteins (ATG) (Lai, Wang, Zheng, Fan, & Chen, 2011; Pečenková, Sabol, Kulich, Ortmannová, & Žárský, 2016; Tsai, Koo, Delk, Gehl, &

Braam, 2013). Cyclins (CYC) and cyclin-dependent kinase inhibitors (CDKI) are important in the G1/S and S/G2 transitions (Bao, Yang, & Hua, 2013; Eichmann & Schäfer, 2015; Gutierrez, 2009; Hamdoun et al., 2016; Nielsen & Thordal-Christensen, 2012; Parker, 2014; Reitz, Gifford, & Schafer, 2015; Scofield, Jones, & Murray, 2014; Vandepoele, 2002). The Fizzy-related 1/Cell cycle switch protein 52A2 (FZR1) interacts with other proteins to degrade CYCs at the transition G2/M (Bao et al., 2013; Eichmann & Schäfer, 2015; Gutierrez, 2009; Parker, 2014; Reitz et al., 2015; Scofield et al., 2014; Vandepoele, 2002). There are checkpoint proteins like RAD1, cell division cycle 45 (CDC45), and mitotic spindle (MAD2) that ensure DNA damage does not get propagated to the next cell (Bao et al., 2013; Eichmann & Schäfer, 2015; Fang, Yu, & Kirschner, 1998; Gutierrez, 2009; Nielsen & Thordal-Christensen, 2012; Parker, 2014; Reitz et al., 2015; Scofield et al., 2014; Vandepoele, 2002). Cullin proteins (CRL) and FBD-associated F-box proteins (FBD1) interfere with the cell cycle when upregulated as they have been shown to degrade CYCs and CDKs (Békés & Drag, 2012; Catala et al., 2007; C. M. Choi, Gray, Mooney, & Hellmann, 2014; Kuroda, Yanagawa, Takahashi, Horii, & Matsui, 2012). The presence of multiple genes regulating PCD in multiple 'hotspot' QTLs provides further support that the identified QTL regions regulate pathogen resistance (Table 4.7).

Hypersensitive response (HR) is rapid PCD and is usually induced by rapid accumulation of ROS. The apoptosis-inducing factor (AIF) and hypersensitive-induced response protein (HIR) produce and amplify ROS accumulation (Belenghi et al., 2003; Heath, 1998; Qi et al., 2011; Racapé et al., 2005; Rolli et al., 2010; Sevrioukova, 2011). Over accumulation of ROS can cause damage to DNA and proteins, thus further perturbing the progression of the cell cycle. During PCD and HR, there is also an upregulation of cytoskeleton-related proteins. The improper regulation of cytokinesis through HAUS/augmin-like complex (HAUS), Microtubule-associated proteins (MAP), and tubulins beta and alpha (TUB and TUA) causes PCD (Caillaud et al., 2008; Hotta et al., 2012; Huesmann et al., 2012; Smertenko, 2004; Yemets, Sheremet, & Blume, 2005). The rearrangement of actin filaments and myosin motors through actin-related proteins (ARP), formin homology (FH2), villin proteins (VLN), myosin XI and VII (MYA and ATM1) allows for transfer nutrients during autophagy, neighboring cell wall

reinforcement, and transport of pathogen inhibitors described previously (Deeks, Hussey, & Davies, 2002; Henty-Ridilla et al., 2013; Huang, 2005; Klahre, Friederich, Kost, Louvard, & Chua, 2000; Yang et al., 2014; Yokota & Shimmen, 2011; Yun et al., 2003). The presence of multiple genes regulating HR and cytoskeleton remodeling in multiple ‘hotspot’ QTLs provides even further support that the identified QTL regions regulate pathogen resistance (Table 4.7).

Overall, the pathogen-resistance ‘hotspots’ identified multiple candidate genes from each step of multiple pathogen resistance pathways. The multitude of recognition receptor proteins and regulators of secondary messengers indicates the necessity of accurate and efficient signaling. The QTLs and candidate genes identified through this GWAS research are great candidates for future functional genomic work to increase the natural pathogen resistance present in broccoli florets.

4.6. Conclusion

Broccoli, *Brassica oleracea* var. *italica*, is an important vegetable crop that is gaining research attention due to multiple studies strongly associating broccoli extracts with potent anticarcinogenic properties (Armah et al., 2013; Cornblatt et al., 2007; Li et al., 2011; Oliviero, Verkerk, & Dekker, 2012; Saban, 2018; M. Traka & Mithen, 2009; Yanaka et al., 2009). Improving consumer consumption of broccoli may be difficult due to the bitter taste most commonly linked to glucosinolate or isothiocyanate compounds, commonly found in the *Brassica* genus (Drewnowski & Gomez-Carneros, 2000; Fenwick, Griffiths, & Heaney, 1983; Kader, 2008; van Doorn et al., 1998). Unfortunately, reducing glucosinolates or isothiocyanates accumulation in broccoli would reduce its anticarcinogenic qualities (Cornblatt et al., 2007; Dinkova-Kostova et al., 2006; Saban, 2018; Tawfiq et al., 1995; M. Traka & Mithen, 2009; Vallejo, García-Viguera, & Tomás-Barberán, 2003). Multiple studies show that when the specific glucosinolate, glucoraphanin, is converted by myrosinase to its isothiocyanate, sulforaphane, it exhibits anticarcinogenic properties very similar to current anticarcinogenic drugs (Cornblatt et al., 2007; Kanehisa, Furumichi, Tanabe, Sato, & Morishima, 2017; T. Kim et al., 2017; Ludikhuyze, Rodrigo, & Hendrickx, 2000; Saban, 2018; Vallejo et al., 2003; Van Eylen, Oey, Hendrickx, & Van Loey, 2007). Glucoraphanin and sulforaphane

accumulation is highest in broccoli, therefore, improving agronomic traits will aid in providing more broccoli to consumers and allow more consumers access to its health benefits (Baik et al., 2003; Brown et al., 2002; Farnham et al., 2005; M. H. Traka et al., 2013; Yanaka et al., 2009). The research goals of this chapter were to identify important QTL regions for broccoli agronomics using a genome-wide association study, with a focus on investigating harvest and pathogen resistance.

Broccoli is grown and harvested for two seasons, an early spring crop and mid-fall crop, due to some cold tolerance in *Brassica* crops (Brown et al., 2007; Farnham & Harrison, 2003; Farnham et al., 2005; Greenhalgh & Mitchell, 1976; Jenni et al., 2001; Rangkadilok et al., 2004; Sones, Heaney, & Fenwick, 1984). Extending the broccoli season would allow for three harvests instead of two, which would result in an increase in broccoli production. Improving broccoli's cold-tolerance would allow for the season to extend into the winter. Unfortunately, this may increase the risk of broccoli floret damage if temperatures drop too quickly (D.-H. Kim & Sung, 2014; S. Sanghera, H. Wani, Hussain, & B. Singh, 2011; Zuther, Juszczyk, Ping Lee, Baier, & Hinch, 2015). Broccoli growth and maturation time could also be shortened through promoting faster growth and quicker transition to reproductive maturity. Photoperiodism is the sensing and responding to changes in daylength, usually through phytochromes starting a signal transduction cascade as the daylength shortens (I. Lee & Amasino, 1995; Bobin Liu et al., 2016; Park et al., 1999; Soy, Leivar, & Monte, 2014; Wilkie, Sedgley, & Olesen, 2008). The signal transduction cascade induces the shoot apical meristem to transition for floral and reproductive meristems so that the broccoli floret can start developing (I. Lee & Amasino, 1995; Bobin Liu et al., 2016; Park et al., 1999; Soy et al., 2014; Wilkie et al., 2008). Utilizing genetic association mapping for a complex trait like harvest season allows for identification of QTLs that may regulate multiple pathways within the signal transduction cascade. The association mapping of the days to harvest trait revealed two significant QTLs. Within the genetic regions for these QTLs, there were two photoperiodism, three floral meristem, and five signal transduction putative candidate genes. These results indicate that the days to harvest QTLs most likely play a role in regulating floral meristem transition in broccoli.

Due to the close proximity to the ground and compact foliage, broccoli is affected by many pathogens and pests (Farnham & Harrison, 2003; Farnham et al., 2005; Greenhalgh & Mitchell, 1976; Jenni et al., 2001; Rangkadilok et al., 2004; Sones et al., 1984). Broccoli pathogens consist primarily of fungi and bacteria that thrive in the compact, sheltered florets (Greenhalgh & Mitchell, 1976; Hopkins, van Dam, & van Loon, 2009; Ignatov, Kuginuki, & Hida, 1999; Jenni et al., 2001; Lan & Paterson, 2000; Nault, Reiners, Hsu, & Hoepting, 2010; Williams, 2007). Broccoli exhibits less biomass loss from pests like insects and invertebrates than tissue loss from pathogen damage due to glucosinolates and isothiocyanates acting as endogenous pesticides that inhibit pest gastrointestinal function (Bones & Rossiter, 2006; Fahey, Zalcmann, & Talalay, 2001; Greenhalgh & Mitchell, 1976; Hopkins et al., 2009; Ignatov et al., 1999; Lionetti et al., 2007; Rimmer & van den Berg, 1992). Thus, investigating pathogen resistance through genetic association mapping will identify important QTL regions and putative candidate genes that may play a role in specific or non-specific pathogen resistance.

In general, pathogen resistance consists of pathogen recognition, signal transduction, and resistance response (Buchanan et al., 2012; Gardner, Heinz, Wang, & Mitchum, 2017; Hanson et al., 2016; Klink & Matthews, 2009; Miedaner & Korzun, 2012; Mitchum, 2016). Pathogen recognition consists of membrane-bound plant receptors that recognize specific degradation products from pathogen enzymes trying to degrade cell wall components (Conrath et al., 2015; Dodds & Rathjen, 2010; Fu & Dong, 2013; Howe & Jander, 2007). There is a constant “arms-race” between pathogen and plant to evolve infiltration mechanisms that plant has no receptors to and evolve receptors capable of recognizing specific or novel mechanisms (Conrath et al., 2015; Dodds & Rathjen, 2010; Fu & Dong, 2013; Howe & Jander, 2007). Once the pathogen attack signal is recognized, it is transduced through multiple pathways in order to induce an appropriate resistance response (Buchanan et al., 2012; Conrath et al., 2015; Dodds & Rathjen, 2010; Fu & Dong, 2013; Howe & Jander, 2007). The regulation of Ca^{2+} across membranes is one of the earliest signals to transduce the pathogen attack signal (Buchanan et al., 2012; Cheval et al., 2013; Conrath et al., 2015; Dodds & Rathjen, 2010; Fu & Dong, 2013; Howe & Jander, 2007; Kolukisaoglu, 2004; Vadassery & Oelmüller, 2009). Once the signal is appropriately transduced, the resulting pathogen

resistance responses are up-regulated to prevent further spread of the pathogen (Buchanan et al., 2012; Conrath et al., 2015; Dodds & Rathjen, 2010; Fu & Dong, 2013; Howe & Jander, 2007). The genetic association mapping of pathogen-related traits revealed five pathogen resistance hotspots where multiple pathogen-related traits have overlapping QTL regions. Multiple calcium binding and signaling putative candidate genes were found in each of the 'hot-spots'. Other signaling transducers like PDF and PAD4 as well as known pathogen-resistance transcription factors were found within the significant QTL regions (de Oliveira Carvalho & Moreira Gomes, 2011; Feys et al., 2001; Rust rucci et al., 2001; Shafee et al., 2016). Overall, the majority of putative candidate genes found within the significant pathogen-resistance 'hot-spot' QTLs are involved in signal transduction to differential transcription, indicating that efficient signaling of the pathogen attack is vital to mounting an appropriate pathogen resistance response.

4.7. Acknowledgments

This work was supported by both the Plant Pathways Elucidation Project through Dr. Lila and Dr. Li, and the NCSU faculty start-up funds from Dr. Li. A special thank you to Dr. Eric Jackson, Dr. Jaime Sheridan, and Dr. Corey Scott from General Mills for providing the agronomic and genotypic data, and for guiding the genetic map developing. Thank you to Dr. Allen Brown from the Horticulture Department at NCSU for imparting your broccoli wisdom and inspiration. A special thank you to the P²EP summer undergraduate interns – Kevon Stanford, Kiristin Klement, Amber Williamson, Jordan Hartman, Tamara Marlowe, and Christian Krzykwa, Titus Hunt, Fernando Guerrero-Nava, Daniel Sanchez, Stephany Daniel-Lopez, Austin Gibbs, Alexis Brown, Doriane Taylor, Zjanazja Cornwall, Jonathan Fabish, and James Lohr – for working with me to organize and conduct the genetic map development and genome-wide association mapping for all the agronomic traits.

REFERENCES

- Abel, S., Savchenko, T., & Levy, M. (2005). Genome-wide comparative analysis of the IQD gene families in *Arabidopsis thaliana* and *Oryza sativa*. *BMC Evolutionary Biology*, 5(1), 1.
- Albani, M. C., & Coupland, G. (2010). Comparative analysis of flowering in annual and perennial plants. *Current Topics in Developmental Biology*, 91(C), 323–348.
- Amasino, R. M., & Michaels, S. D. (2010). The Timing of Flowering. *Plant Physiology*, 154(2), 516–520.
- Araki, R., Hasumi, A., Nishizawa, O. I., Sasaki, K., Kuwahara, A., Sawada, Y., ... Hirai, M. Y. (2013). Novel bioresources for studies of *Brassica oleracea*: identification of a kale MYB transcription factor responsible for glucosinolate production. *Plant Biotechnology Journal*,
- Armah, C. N., Traka, M. H., Dainty, J. R., Defernez, M., Janssens, A., Leung, W., ... Mithen, R. F. (2013). A diet rich in high-glucoraphanin broccoli interacts with genotype to reduce discordance in plasma metabolite profiles by modulating mitochondrial function. *American Journal of Clinical Nutrition*, 98(3), 712–722.
- Asoro, F. G., Newell, M. A., Scott, M. P., Beavis, W. D., & Jannink, J.-L. (2013). Genome-wide Association Study for Beta-glucan Concentration in Elite North American Oat. *Crop Science*, 53(2), 542–553.
- Atwell, S., Huang, Y. S., Vilhjálmsson, B. J., Willems, G., Horton, M., Li, Y., ... Nordborg, M. (2010). Genome-wide association study of 107 phenotypes in *Arabidopsis thaliana* inbred lines. *Nature*, 465(7298), 627–631.
- Baik, H.-Y., Juvik, J. A., Jeffery, E. H., Wallig, M. A., Kushad, M., & Klein, B. P. (2003). Relating glucosinolate content and flavor of broccoli cultivars. *Journal of Food Science*, 68(3), 1043–1050.
- Bao, Z., Yang, H., & Hua, J. (2013). Perturbation of cell cycle regulation triggers plant immune response via activation of disease resistance genes. *Proceedings of the National Academy of Sciences*, 110(6), 2407–2412.
- Bartsch, M. (2006). Salicylic Acid-Independent ENHANCED DISEASE SUSCEPTIBILITY1 Signaling in *Arabidopsis* Immunity and Cell Death Is Regulated by the Monooxygenase FMO1 and the Nudix Hydrolase NUDT7. *THE PLANT CELL ONLINE*, 18(4), 1038–1051.
- Batschauer, A. (1998). Photoreceptors of higher plants. *Planta*, 206(4), 479–492.
- Békés, M., & Drag, M. (2012). Trojan Horse Strategies Used by Pathogens to Influence the Small Ubiquitin-Like Modifier (SUMO) System of Host Eukaryotic Cells. *Journal of Innate Immunity*, 4(2), 159–167.
- Belec, C., Villeneuve, S., Coulombe, J., & Tremblay, N. (2001). Influence of nitrogen fertilization on yield, hollow stem incidence and sap nitrate concentration in broccoli. *Canadian Journal of Plant Science*, 81(4), 765–772.
- Belenghi, B., Acconcia, F., Trovato, M., Perazzolli, M., Bocedi, A., Polticelli, F., ... Delledonne, M. (2003). AtCYS1, a cystatin from *Arabidopsis thaliana*, suppresses hypersensitive cell death. *European Journal of Biochemistry*, 270(12), 2593–2604.
- Bellincampi, D., Cervone, F., & Lionetti, V. (2014). Plant cell wall dynamics and wall-related susceptibility in plant–pathogen interactions. *Frontiers in Plant Science*, 5.
- Bellostas, N., Sørensen, J. C., & Sørensen, H. (2007). Profiling glucosinolates in vegetative and reproductive tissues of four *Brassica* species of the U-triangle for

- their biofumigation potential. *Journal of the Science of Food and Agriculture*, 87(8), 1586–1594.
- Bennett, E., Roberts, J. A., & Wagstaff, C. (2012). Manipulating resource allocation in plants. *Journal of Experimental Botany*, 63(9), 3391–3400.
- Bones, A., & Rossiter, J. (2006). The enzymic and chemically induced decomposition of glucosinolates. *Phytochemistry*, 67(11), 1053–1067.
- Borevitz, J. O., & Chory, J. (2004). Genomics tools for QTL analysis and gene discovery. *Current Opinion in Plant Biology*, 7(2), 132–136.
- Boudsocq, M., Willmann, M. R., McCormack, M., Lee, H., Shan, L., He, P., ... Sheen, J. (2010). Differential innate immune signalling via Ca²⁺ sensor protein kinases. *Nature*, 464(7287), 418–422.
- Bowling, S. A., Clarke, J. D., Liu, Y., Klessig, D. F., & Dong, X. (1997). The cpr5 mutant of *Arabidopsis* expresses both NPR1-dependent and NPR1-independent resistance. *The Plant Cell*, 9(9), 1573–1584.
- Boyle, P., Le Su, E., Rochon, A., Shearer, H. L., Murmu, J., Chu, J. Y., ... Després, C. (2009). The BTB/POZ domain of the *Arabidopsis* disease resistance protein NPR1 interacts with the repression domain of TGA2 to negate its function. *The Plant Cell*, 21(11), 3700–3713.
- Brodersen, P., Petersen, M., Bjørn Nielsen, H., Zhu, S., Newman, M.-A., Shokat, K. M., ... Mundy, J. (2006). *Arabidopsis* MAP kinase 4 regulates salicylic acid- and jasmonic acid/ethylene-dependent responses via EDS1 and PAD4. *The Plant Journal*, 47(4), 532–546.
- Brown, A. F., Jeffery, E. H., & Juvik, J. A. (2007). A polymerase chain reaction-based linkage map of broccoli and identification of quantitative trait loci associated with harvest date and head weight. *Journal of the American Society for Horticultural Science*, 132(4), 507–513.
- Brown, A. F., Yousef, G. G., Chebrolu, K. K., Byrd, R. W., Everhart, K. W., Thomas, A., ... Jackson, E. W. (2014). High-density single nucleotide polymorphism (SNP) array mapping in *Brassica oleracea*: identification of QTL associated with carotenoid variation in broccoli florets. *Theoretical and Applied Genetics*, 127(9), 2051–2064.
- Brown, A. F., Yousef, G. G., Jeffery, E. H., Klein, B. P., Wallig, M. A., Kushad, M. M., & Juvik, J. A. (2002). Glucosinolate Profiles in Broccoli: Variation in Levels and Implications in Breeding for Cancer Chemoprotection. *Journal of American Soci and Horticulture Science*, 127(5), 807–813.
- Buchanan, B. B., Gruissem, W., & Jones, R. L. (2012). *Biochemistry & Molecular Biology of Plants*. American Society of Plant Biologists: 15501 Monona Drive, Rockville, MD 20855-2768 USA: Markono Print Media Pte Ltd.
- Caillaud, M.-C., Lecomte, P., Jammes, F., Quentin, M., Pagnotta, S., Andrio, E., ... Favery, B. (2008). MAP65-3 Microtubule-Associated Protein Is Essential for Nematode-Induced Giant Cell Ontogenesis in *Arabidopsis*. *THE PLANT CELL ONLINE*, 20(2), 423–437.
- Camacho, C., Coulouris, G., Avagyan, V., Ma, N., Papadopoulos, J., Bealer, K., & Madden, T. L. (2009). BLAST+: architecture and applications. *BMC Bioinformatics*, 10(1), 421.
- Canonne, J., Froidure-Nicolas, S., & Rivas, S. (2011). Phospholipases in action during

- plant defense signaling. *Plant Signaling & Behavior*, 6(1), 13–18.
- Carman, G. M., & Han, G.-S. (2009). Phosphatidic Acid Phosphatase, a Key Enzyme in the Regulation of Lipid Synthesis. *Journal of Biological Chemistry*, 284(5), 2593–2597.
- Castillejo, C., & Pelaz, S. (2008). The Balance between CONSTANS and TEMPRANILLO Activities Determines FT Expression to Trigger Flowering. *Current Biology*, 18(17), 1338–1343.
- Catala, R., Ouyang, J., Abreu, I. A., Hu, Y., Seo, H., Zhang, X., & Chua, N.-H. (2007). The Arabidopsis E3 SUMO Ligase SIZ1 Regulates Plant Growth and Drought Responses. *THE PLANT CELL ONLINE*, 19(9), 2952–2966.
- Cerdan, P. D., & Chory, J. (2003). Regulation of Flowering Time by Light Quality. *Nature*, 423(6942), 881–885.
- Chaffin, A. S., Huang, Y.-F., Smith, S., Bekele, W. A., Babiker, E., Gnanesh, B. N., ... Tinker, N. A. (2016). A Consensus Map in Cultivated Hexaploid Oat Revealed Conserved Grass Synteny with Substantial Sub-Genome Rearrangement. *The Plant Genome*, 9(2), 0.
- Cheng, H. (2004). Gibberellin regulates Arabidopsis floral development via suppression of DELLA protein function. *Development*, 131(5), 1055–1064.
- Cheval, C., Aldon, D., Galaud, J.-P., & Ranty, B. (2013). Calcium/calmodulin-mediated regulation of plant immunity. *Biochimica et Biophysica Acta (BBA) - Molecular Cell Research*, 1833(7), 1766–1771.
- Chiasson, D., Ekengren, S. K., Martin, G. B., Dobney, S. L., & Snedden, W. A. (2005). Calmodulin-like Proteins from Arabidopsis and Tomato are Involved in Host Defense Against *Pseudomonas syringae* pv. tomato. *Plant Molecular Biology*, 58(6), 887–897.
- Choi, C. M., Gray, W. M., Mooney, S., & Hellmann, H. (2014). Composition, Roles, and Regulation of Cullin-Based Ubiquitin E3 Ligases. *The Arabidopsis Book*, 12, e0175.
- Choi, K., Kim, J., Hwang, H.-J., Kim, S. Y., Park, C., Kim, S. Y., & Lee, I. (2011). The FRIGIDA Complex Activates Transcription of *FLC*, a Strong Flowering Repressor in *Arabidopsis*, by Recruiting Chromatin Modification Factors. *The Plant Cell*, 23(1), 289–303.
- Clark, S. E., Running, M. P., & Meyerowitz, E. M. (1995). CLAVATA3 is a specific regulator of shoot and floral meristem development affecting the same processes as CLAVATA1. *Development*, 121(7), 2057–2067.
- Clay, N. K., Adio, A. M., Denoux, C., Jander, G., & Ausubel, F. M. (2009). Glucosinolate Metabolites Required for an Arabidopsis Innate Immune Response. *Science*, 323(5910), 95–101.
- Cole, R. A. (1976). Isothiocyanates, Nitriles, and Thiocyanates as Products of Autolysis of Glucosinolates in Cruciferae. *Phytochemistry*, 15, 759–762.
- Coll, N. S., Epple, P., & Dangl, J. L. (2011). Programmed cell death in the plant immune system. *Cell Death & Differentiation*, 18(8), 1247–1256.
- Conrath, U., Beckers, G. J. M., Langenbach, C. J. G., & Jaskiewicz, M. R. (2015). Priming for Enhanced Defense. *Annual Review of Phytopathology*, 53(1), 97–119.
- Conti, L. (2017). Hormonal control of the floral transition: Can one catch them all? *Developmental Biology*, 430(2), 288–301.
- Cornblatt, B. S., Ye, L., Dinkova-Kostova, A. T., Erb, M., Fahey, J. W., Singh, N. K., ...

- Visvanathan, K. (2007). Preclinical and clinical evaluation of sulforaphane for chemoprevention in the breast. *Carcinogenesis*, 28(7), 1485–1490.
- Couée, I., Sulmon, C., Gouesbet, G., & El Amrani, A. (2006). Involvement of soluble sugars in reactive oxygen species balance and responses to oxidative stress in plants. *Journal of Experimental Botany*, 57(3), 449–459.
- Craddock, C. P., Adams, N., Bryant, F. M., Kurup, S., & Eastmond, P. J. (2015). PHOSPHATIDIC ACID PHOSPHOHYDROLASE Regulates Phosphatidylcholine Biosynthesis in Arabidopsis by Phosphatidic Acid-Mediated Activation of CTP:PHOSPHOCHOLINE CYTIDYLYLTRANSFERASE Activity. *The Plant Cell*, 27(4), 1251–1264.
- D'Ovidio, R., Mattei, B., Roberti, S., & Bellincampi, D. (2004). Polygalacturonases, polygalacturonase-inhibiting proteins and pectic oligomers in plant–pathogen interactions. *Biochimica et Biophysica Acta (BBA) - Proteins and Proteomics*, 1696(2), 237–244.
- de Oliveira Carvalho, A., & Moreira Gomes, V. (2011). Plant Defensins and Defensin-Like Peptides - Biological Activities and Biotechnological Applications. *Current Pharmaceutical Design*, 17(38), 4270–4293.
- de Silva, K., Laska, B., Brown, C., Sederoff, H. W., & Khodakovskaya, M. (2011). Arabidopsis thaliana calcium-dependent lipid-binding protein (AtCLB): a novel repressor of abiotic stress response. *Journal of Experimental Botany*, 62(8), 2679–2689.
- Deeks, M. J., Hussey, P. J., & Davies, B. (2002). Formins: intermediates in signal-transduction cascades that affect cytoskeletal reorganization. *Trends in Plant Science*, 7(11), 492–498.
- Després, C., DeLong, C., Glaze, S., Liu, E., & Fobert, P. R. (2000). The Arabidopsis NPR1/NIM1 protein enhances the DNA binding activity of a subgroup of the TGA family of bZIP transcription factors. *The Plant Cell*, 12(2), 279–290.
- Dinkova-Kostova, A. T., Fahey, J. W., Benedict, A. L., Jenkins, S. N., Ye, L., Wehage, S. L., & Talalay, P. (2010). Dietary glucoraphanin-rich broccoli sprout extracts protect against UV radiation-induced skin carcinogenesis in SKH-1 hairless mice. *Photochemical & Photobiological Sciences*, 9(4), 597.
- Dinkova-Kostova, A. T., Jenkins, S. N., Fahey, J. W., Ye, L., Wehage, S. L., Liby, K. T., ... Talalay, P. (2006). Protection against UV-light-induced skin carcinogenesis in SKH-1 high-risk mice by sulforaphane-containing broccoli sprout extracts. *Cancer Letters*, 240(2), 243–252.
- Dixit, A. K., & Jayabaskaran, C. (2012). Phospholipid Mediated Activation of Calcium Dependent Protein Kinase 1 (CaCDPK1) from Chickpea: A New Paradigm of Regulation. *PLoS ONE*, 7(12), e51591.
- Dodds, P. N., & Rathjen, J. P. (2010). Plant immunity: Towards an integrated view of plant–pathogen interactions. *Nature Reviews Genetics*, 11(8), 539–548.
- Drewnowski, A., & Gomez-Carneros, C. (2000). Bitter taste, phytonutrients, and the consumer: a review. *The American Journal of Clinical Nutrition*, 72(6), 1424–1435.
- Durbak, A. R., & Tax, F. E. (2011). CLAVATA Signaling Pathway Receptors of Arabidopsis Regulate Cell Proliferation in Fruit Organ Formation as well as in Meristems. *Genetics*, 189(1), 177–194.
- Eichmann, R., & Schäfer, P. (2015). Growth versus immunity—a redirection of the cell

- cycle? *Current Opinion in Plant Biology*, 26, 106–112.
- Eitas, T. K., Nimchuk, Z. L., & Dangl, J. L. (2008). Arabidopsis TAO1 is a TIR-NB-LRR protein that contributes to disease resistance induced by the *Pseudomonas syringae* effector AvrB. *Proceedings of the National Academy of Sciences*, 105(17), 6475–6480.
- Eulgem, T., Tsuchiya, T., Wang, X.-J., Beasley, B., Cuzick, A., Tör, M., ... Dangl, J. L. (2007). EDM2 is required for RPP7-dependent disease resistance in Arabidopsis and affects RPP7 transcript levels: EDM2-mediated disease resistance. *The Plant Journal*, 49(5), 829–839.
- Fabro, G., Rizzi, Y. S., & Alvarez, M. E. (2016). Arabidopsis proline dehydrogenase contributes to flagellin-mediated PAMP-triggered immunity by affecting RBOHD. *Molecular Plant-Microbe Interactions*, 29(8), 620–628.
- Fahey, J. W., Haristoy, X., Dolan, P. M., Kensler, T. W., Scholtus, I., Stephenson, K. K., ... Lozniewski, A. (2002). Sulforaphane inhibits extracellular, intracellular, and antibiotic-resistant strains of *Helicobacter pylori* and prevents benzo [a] pyrene-induced stomach tumors. *Proceedings of the National Academy of Sciences*, 99(11), 7610–7615.
- Fahey, J. W., Zalcmann, A. T., & Talalay, P. (2001). The Chemical Diversity and Distribution of Glucosinolates and Isothiocyanates Among Plants. *Phytochemistry*, 56, 5–51.
- Fahey, J. W., Zhang, Y., & Talalay, P. (1997). Broccoli sprouts: an exceptionally rich source of inducers of enzymes that protect against chemical carcinogens. *Proceedings of the National Academy of Sciences*, 94(19), 10367–10372.
- Fang, G., Yu, H., & Kirschner, M. W. (1998). The checkpoint protein MAD2 and the mitotic regulator CDC20 form a ternary complex with the anaphase-promoting complex to control anaphase initiation. *Genes & Development*, 12(12), 1871–1883.
- Farnham, M. W., & Harrison, H. F. (2003). Using Self-compatible Inbreds of Broccoli as Seed Producers. *Horticulture Science*, 38(1), 85–87.
- Farnham, M. W., Stephenson, K. K., & Fahey, J. W. (2005). Glucoraphanin Level in Broccoli Seed is Largely Determined by Genotype. *Horticulture Science*, 40(1), 50–53.
- Fenwick, G. R., Griffiths, N. M., & Heaney, R. K. (1983). Bitterness in Brussels sprouts (*Brassica oleracea* L. var. *gemmifera*): the role of glucosinolates and their breakdown products. *Journal of the Science of Food and Agriculture*, 34(1), 73–80.
- Feys, B. J., Moisan, L. J., Newman, M.-A., & Parker, J. E. (2001). Direct interaction between the Arabidopsis disease resistance signaling proteins, EDS1 and PAD4. *The EMBO Journal*, 20(19), 5400–5411.
- Figueiredo, A., Monteiro, F., & Sebastiana, M. (2014). Subtilisin-like proteases in plant pathogen recognition and immune priming: a perspective. *Frontiers in Plant Science*, 5.
- Fischer, C., Kugler, A., Hoth, S., & Dietrich, P. (2013). An IQ Domain Mediates the Interaction with Calmodulin in a Plant Cyclic Nucleotide-Gated Channel. *Plant and Cell Physiology*, 54(4), 573–584.
- Franzke, A., Lysak, M. A., Al-Shehbaz, I. A., Koch, M. A., & Mummenhoff, K. (2011). Cabbage family affairs: the evolutionary history of Brassicaceae. *Trends in Plant Science*, 16(2), 108–116.

- Freeman, B. C., & Beattie, G. A. (2008). An Overview of Plant Defenses against Pathogens and Herbivores. *Iowa State University - Plant Pathology and Microbiology Publications*, 1–12.
- Friedrich, L., Lawton, K., Dietrich, R., Willits, M., Cade, R., & Ryals, J. (2001). NIM1 overexpression in *Arabidopsis* potentiates plant disease resistance and results in enhanced effectiveness of fungicides. *Molecular Plant-Microbe Interactions*, *14*(9), 1114–1124.
- Fu, Z. Q., & Dong, X. (2013). Systemic Acquired Resistance: Turning Local Infection into Global Defense. *Annual Review of Plant Biology*, *64*(1), 839–863.
- Gardner, M., Heinz, R., Wang, J., & Mitchum, M. G. (2017). Genetics and Adaptation of Soybean Cyst Nematode to Broad Spectrum Soybean Resistance. *G3; Genes|Genomes|Genetics*, *7*(3), 835–841.
- Gassmann, W., Hinsch, M. E., & Staskawicz, B. J. (1999). The *Arabidopsis* RPS4 bacterial-resistance gene is a member of the TIR-NBS-LRR family of disease-resistance genes. *The Plant Journal*, *20*(3), 265–277.
- Ge, X, Li, G.-J., Wang, S.-B., Zhu, H., Zhu, T., Wang, X., & Xia, Y. (2007). AtNUDT7, a Negative Regulator of Basal Immunity in *Arabidopsis*, Modulates Two Distinct Defense Response Pathways and Is Involved in Maintaining Redox Homeostasis. *PLANT PHYSIOLOGY*, *145*(1), 204–215.
- Ge, Xiaochun, & Xia, Y. (2008). The role of AtNUDT7, a Nudix hydrolase, in the plant defense response. *Plant Signaling & Behavior*, *3*(2), 119–120.
- Gibson, G. (2018). Population genetics and GWAS: A primer. *PLoS Biology*, *16*(3), 1–6.
- Giraud, E., Ng, S., Carrie, C., Duncan, O., Low, J., Lee, C. P., ... Whelan, J. (2010). TCP Transcription Factors Link the Regulation of Genes Encoding Mitochondrial Proteins with the Circadian Clock in *Arabidopsis thaliana*. *The Plant Cell*, *22*(12), 3921–3934.
- Greenhalgh, J. R., & Mitchell, N. D. (1976). The Involvement of Flavour Volatiles in the Resistance to Downy Mildew of Wild and Cultivated Forms of *Brassica oleracea*, *77*, 391–398.
- Grennan, A. K. (2008). Ethylene response factors in jasmonate signaling and defense response. *Plant Physiology*, *146*(4), 1457–1458.
- Grubb, C. D., & Abel, S. (2006). Glucosinolate metabolism and its control. *Trends in Plant Science*, *11*(2), 89–100.
- Gutierrez, C. (2009). The *Arabidopsis* Cell Division Cycle. *The Arabidopsis Book*, *7*, e0120.
- Halkier, B. A., & Gershenzon, J. (2006). Biology and biochemistry of glucosinolates. *Annu. Rev. Plant Biol.*, *57*, 303–333.
- Hall, A. (2003). The TIME FOR COFFEE Gene Maintains the Amplitude and Timing of *Arabidopsis* Circadian Clocks. *THE PLANT CELL ONLINE*, *15*(11), 2719–2729.
- Hamdoun, S., Zhang, C., Gill, M., Kumar, N., Churchman, M., Larkin, J. C., ... Lu, H. (2016). Differential Roles of Two Homologous Cyclin-Dependent Kinase Inhibitor Genes in Regulating Cell Cycle and Innate Immunity in *Arabidopsis*. *Plant Physiology*, *170*(1), 515–527.
- Hanson, P., Lu, S. F., Wang, J. F., Chen, W., Kenyon, L., Tan, C. W., ... Yang, R. Y. (2016). Conventional and molecular marker-assisted selection and pyramiding of genes for multiple disease resistance in tomato. *Scientia Horticulturae*, *201*, 346–

- Harper, J. F. (2001). Dissecting calcium oscillators in plant cells. *Trends in Plant Science*, 6(9), 395–397.
- Heath, M. C. (1998). Apoptosis, programmed cell death and the hypersensitive response. *European Journal of Plant Pathology*, 104(2), 117–124.
- Heidrich, K., Wirthmueller, L., Tasset, C., Pouzet, C., Deslandes, L., & Parker, J. E. (2011). Arabidopsis EDS1 Connects Pathogen Effector Recognition to Cell Compartment-Specific Immune Responses. *Science*, 334, 1401–1404.
- Helliwell, C. A., Robertson, M., Finnegan, E. J., Buzas, D. M., & Dennis, E. S. (2011). Vernalization-Repression of Arabidopsis FLC Requires Promoter Sequences but Not Antisense Transcripts. *PLoS ONE*, 6(6), e21513.
- Henty-Ridilla, J. L., Shimono, M., Li, J., Chang, J. H., Day, B., & Staiger, C. J. (2013). The Plant Actin Cytoskeleton Responds to Signals from Microbe-Associated Molecular Patterns. *PLoS Pathogens*, 9(4), e1003290.
- Hepler, P. K. (2005). Calcium: a central regulator of plant growth and development. *The Plant Cell*, 17(8), 2142–2155.
- Hopkins, R. J., van Dam, N. M., & van Loon, J. J. A. (2009). Role of Glucosinolates in Insect-Plant Relationships and Multitrophic Interactions. *Annual Review of Entomology*, 54(1), 57–83.
- Hospital, F. (2009). Challenges for effective marker-assisted selection in plants. *Genetica*, 136(2), 303–310.
- Hotta, T., Kong, Z., Ho, C.-M. K., Zeng, C. J. T., Horio, T., Fong, S., ... Liu, B. (2012). Characterization of the *Arabidopsis* Augmin Complex Uncovers Its Critical Function in the Assembly of the Acentrosomal Spindle and Phragmoplast Microtubule Arrays. *The Plant Cell*, 24(4), 1494–1509.
- Howe, G. A., & Jander, G. (2007). Plant Immunity to Insect Herbivores. *Annual Review of Plant Biology*, 59(1), 41–66.
- Hu, R., Zhu, Y., Shen, G., & Zhang, H. (2014). TAP46 Plays a Positive Role in the ABSCISIC ACID INSENSITIVE5-Regulated Gene Expression in Arabidopsis. *PLANT PHYSIOLOGY*, 164(2), 721–734.
- Huang, S. (2005). Arabidopsis VILLIN1 Generates Actin Filament Cables That Are Resistant to Depolymerization. *THE PLANT CELL ONLINE*, 17(2), 486–501.
- Hudson, M., Ringli, C., Boylan, M. T., & Quail, P. H. (1999). The FAR1 locus encodes a novel nuclear protein specific to phytochrome A signaling. *Genes & Development*, 13(15), 2017–2027.
- Huesmann, C., Reiner, T., Hoefle, C., Preuss, J., Jurca, M. E., Domoki, M., ... Huckelhoven, R. (2012). Barley ROP Binding Kinase1 Is Involved in Microtubule Organization and in Basal Penetration Resistance to the Barley Powdery Mildew Fungus. *PLANT PHYSIOLOGY*, 159(1), 311–320.
- Ide, Y., Nagasaki, N., Tomioka, R., Suito, M., Kamiya, T., & Maeshima, M. (2007). Molecular properties of a novel, hydrophilic cation-binding protein associated with the plasma membrane. *Journal of Experimental Botany*, 58(5), 1173–1183.
- Ignatov, A., Kuginuki, Y., & Hida, K. (1999). Vascular Stem Resistance to Black Rot in Brassica oleracea. *Canadian Journal of Botany*, 77(3), 442–446.
- Ionescu, I. A., Møller, B. L., & Sánchez-Pérez, R. (2016). Chemical control of flowering time. *Journal of Experimental Botany*, 68(3), erw427.

- Jang, I.-C., Henriques, R., Seo, H. S., Nagatani, A., & Chua, N.-H. (2010). Arabidopsis PHYTOCHROME INTERACTING FACTOR Proteins Promote Phytochrome B Polyubiquitination by COP1 E3 Ligase in the Nucleus. *THE PLANT CELL ONLINE*, 22(7), 2370–2383.
- Jenks, M. A., & Bebeli, P. J. (2011). *Breeding for Fruit Quality*. West Sussex: John Wiley & Sons, Inc.
- Jenni, S., Dutilleul, P., Yamasaki, S., & Tremblay, N. (2001). Brown bead of broccoli. I. Response of the physiological disorder to management practices. *HortScience*, 36(7), 1224–1227.
- Jofuku, K. D., Den Boer, B. G., Van Montagu, M., & Okamoto, J. K. (1994). Control of Arabidopsis flower and seed development by the homeotic gene APETALA2. *The Plant Cell*, 6(9), 1211–1225.
- Jones, R. B., Faragher, J. D., & Winkler, S. (2006). A review of the influence of postharvest treatments on quality and glucosinolate content in broccoli (*Brassica oleracea* var. *italica*) heads. *Postharvest Biology and Technology*, 41(1), 1–8.
- Kader, A. A. (2008). Flavor quality of fruits and vegetables. *Journal of the Science of Food and Agriculture*, 88(11), 1863–1868.
- Kanehisa, M., Furumichi, M., Tanabe, M., Sato, Y., & Morishima, K. (2017). KEGG: New perspectives on genomes, pathways, diseases and drugs. *Nucleic Acids Research*, 45(D1), D353–D361.
- Kang, H M, Zaitlen, N. A., Wade, C. M., Kirby, A., Heckerman, D., Daly, M. J., & Eskin, E. (2008). Efficient Control of Population Structure in Model Organism Association Mapping. *Genetics*, 178(3), 1709–1723.
- Kang, Hyun Min, Sul, J. H., Service, S. K., Zaitlen, N. A., Kong, S., Freimer, N. B., ... Eskin, E. (2010). Variance component model to account for sample structure in genome-wide association studies. *Nature Genetics*, 42(4), 348–354.
- Kang, M. S. (2002). *Quantitative genetics, genomics and plant breeding*. New York: CABI Publishing.
- Keunen, E., Peshev, D., Vangronsveld, J., Van Den Ende, W., & Cuypers, A. (2013). Plant sugars are crucial players in the oxidative challenge during abiotic stress: Extending the traditional concept. *Plant, Cell and Environment*, 36(7), 1242–1255.
- Kim, D.-H., & Sung, S. (2014). Genetic and Epigenetic Mechanisms Underlying Vernalization. *The Arabidopsis Book*, 12, e0171.
- Kim, J.-Y., Park, S.-C., Hwang, I., Cheong, H., Nah, J.-W., Hahm, K.-S., & Park, Y. (2009). Protease Inhibitors from Plants with Antimicrobial Activity. *International Journal of Molecular Sciences*, 10(6), 2860–2872.
- Kim, T., Banf, M., Kahn, D., Bernard, T., Dreher, K., Chavali, A. K., ... Zhang, P. (2017). Genome-Wide Prediction of Metabolic Enzymes, Pathways, and Gene Clusters in Plants. *Plant Physiology*, 173(4), 2041–2059.
- Klahre, U., Friederich, E., Kost, B., Louvard, D., & Chua, N.-H. (2000). Villin-like actin-binding proteins are expressed ubiquitously in Arabidopsis. *Plant Physiology*, 122(1), 35–48.
- Klink, V. P., & Matthews, B. F. (2009). Emerging Approaches to Broaden Resistance of Soybean to Soybean Cyst Nematode as Supported by Gene Expression Studies. *Plant Physiology*, 151(3), 1017–1022.
- Kolukisaoglu, U. (2004). Calcium Sensors and Their Interacting Protein Kinases:

- Genomics of the Arabidopsis and Rice CBL-CIPK Signaling Networks. *PLANT PHYSIOLOGY*, 134(1), 43–58.
- Körber, N., Bus, A., Li, J., Parkin, I. A. P., Wittkop, B., Snowdon, R. J., & Stich, B. (2016). Agronomic and Seed Quality Traits Dissected by Genome-Wide Association Mapping in *Brassica napus*. *Frontiers in Plant Science*, 7.
- Korte, A., & Farlow, A. (2013). The advantages and limitations of trait analysis with GWAS: a review. *Plant Methods*, 9(1), 1.
- Kotake, T., Takada, S., Nakahigashi, K., Ohto, M., & Goto, K. (2003). Arabidopsis TERMINAL FLOWER 2 gene encodes a heterochromatin protein 1 homolog and represses both FLOWERING LOCUS T to regulate flowering time and several floral homeotic genes. *Plant and Cell Physiology*, 44(6), 555–564.
- Kump, K. L., Bradbury, P. J., Wisser, R. J., Buckler, E. S., Belcher, A. R., Oropeza-Rosas, M. A., ... Holland, J. B. (2011). Genome-wide association study of quantitative resistance to southern leaf blight in the maize nested association mapping population. *Nature Genetics*, 43(2), 163–168.
- Kuroda, H., Yanagawa, Y., Takahashi, N., Horii, Y., & Matsui, M. (2012). A Comprehensive Analysis of Interaction and Localization of Arabidopsis SKP1-LIKE (ASK) and F-Box (FBX) Proteins. *PLoS ONE*, 7(11), e50009.
- Kushad, M. M., Brown, A. F., Kurilich, A. C., Juvik, J. A., Klein, B. P., Wallig, M. A., & Jeffery, E. H. (1999). Variation of Glucosinolates in Vegetable Crops of *Brassica oleracea*. *Journal of Agricultural and Food Chemistry*, 47(4), 1541–1548.
- Kwon, S. J. S. II, Jin, H. C., Lee, S., Nam, M. H., Chung, J. H., Kwon, S. J. S. II, ... Park, O. K. (2009). GDSL lipase-like 1 regulates systemic resistance associated with ethylene signaling in Arabidopsis. *The Plant Journal*, 58(2), 235–245.
- Kyriacou, M. C., & Roupael, Y. (2018). Towards a new definition of quality for fresh fruits and vegetables. *Scientia Horticulturae*, 234(August 2017), 463–469.
- Lai, Z., Wang, F., Zheng, Z., Fan, B., & Chen, Z. (2011). A critical role of autophagy in plant resistance to necrotrophic fungal pathogens: Autophagy in plant disease resistance. *The Plant Journal*, 66(6), 953–968.
- Lan, T.-H., & Paterson, A. H. (2000). Comparative mapping of quantitative trait loci sculpting the curd of *Brassica oleracea*. *Genetics*, 155(4), 1927–1954.
- Langner, T., & Göhre, V. (2016). Fungal chitinases: function, regulation, and potential roles in plant/pathogen interactions. *Current Genetics*, 62(2), 243–254.
- Lassowskat, I., Bottcher, C., Eschen-Lippold, L., Scheel, D., & Lee, J. (2014). Sustained mitogen-activated protein kinase activation reprograms defense metabolism and phosphoprotein profile in Arabidopsis thaliana. *Frontiers in Plant Science*, 5.
- Lau, O. S., & Deng, X. W. (2010). Plant hormone signaling lightens up: integrators of light and hormones. *Current Opinion in Plant Biology*, 13(5), 571–577.
- Lee, I., & Amasino, R. M. (1995). Effect of vernalization, photoperiod, and light quality on the flowering phenotype of Arabidopsis plants containing the FRIGIDA gene. *Plant Physiology*, 108(1), 157–162.
- Lee, S., Cheng, H., King, K. E., Wang, W., He, Y., Hussain, A., ... Peng, J. (2002). Gibberellin regulates Arabidopsis seed germination via RGL2, a GAI/RGA-like gene whose expression is up-regulated following imbibition. *Genes & Development*, 16(5), 646–658.
- Lee, S. M. Y., Hoang, M. H. T., Han, H. J., Kim, H. S., Lee, K., Kim, K. E., ... Chung, W.

- S. (2009). Pathogen inducible voltage-dependent anion channel (AtVDAC) isoforms are localized to mitochondria membrane in Arabidopsis. *Molecules and Cells*, 27(3), 321–327.
- Li, F., Hullar, M. A. J., Beresford, S. A. A., & Lampe, J. W. (2011). Variation of glucoraphanin metabolism in vivo and ex vivo by human gut bacteria. *British Journal of Nutrition*, 106(03), 408–416.
- Licausi, F., Ohme-Takagi, M., & Perata, P. (2013). APETALA2/Ethylene Responsive Factor (AP2/ERF) transcription factors: mediators of stress responses and developmental programs. *New Phytologist*, 199(3), 639–649.
- Lin, L., Liu, X., & Yin, R. (2018). PIF3 Integrates Light and Low Temperature Signaling. *Trends in Plant Science*, 23(2), 93–95.
- Lin, R. (2004). Arabidopsis FHY3/FAR1 Gene Family and Distinct Roles of Its Members in Light Control of Arabidopsis Development. *PLANT PHYSIOLOGY*, 136(4), 4010–4022.
- Lionetti, V., Raiola, A., Camardella, L., Giovane, A., Obel, N., Pauly, M., ... Bellincampi, D. (2007). Overexpression of pectin methylesterase inhibitors in Arabidopsis restricts fungal infection by Botrytis cinerea. *Plant Physiology*, 143(4), 1871–1880.
- Liu, Bobin, Yang, Z., Gomez, A., Liu, B., Lin, C., & Oka, Y. (2016). Signaling mechanisms of plant cryptochromes in Arabidopsis thaliana. *Journal of Plant Research*, 129(2), 137–148.
- Lu, F., Lipka, A. E., Glaubitz, J., Elshire, R., Cherney, J. H., Casler, M. D., ... Costich, D. E. (2013). Switchgrass Genomic Diversity, Ploidy, and Evolution: Novel Insights from a Network-Based SNP Discovery Protocol. *PLoS Genetics*, 9(1), e1003215.
- Ludikhuyze, L., Rodrigo, L., & Hendrickx, M. (2000). The activity of myrosinase from broccoli (*Brassica oleracea* L. cv. Italica): Influence of intrinsic and extrinsic factors. *Journal of Food Protection*, 63(3), 400–403.
- Ludwig, A. A., Saitoh, H., Felix, G., Freymark, G., Miersch, O., Wasternack, C., ... Romeis, T. (2005). Ethylene-mediated cross-talk between calcium-dependent protein kinase and MAPK signaling controls stress responses in plants. *Proceedings of the National Academy of Sciences of the United States of America*, 102(30), 10736–10741.
- Ma, W., Smigel, A., Verma, R., & Berkowitz, G. A. (2009). Cyclic Nucleotide Gated Channels and Related Signaling Components in Plant Innate Immunity. *Plant Signaling & Behavior*, 4(4), 277–282.
- Mackey, D., Holt, B. F., Wiig, A., & Dangl, J. L. (2002). RIN4 interacts with *Pseudomonas syringae* type III effector molecules and is required for RPM1-mediated resistance in Arabidopsis. *Cell*, 108(6), 743–754.
- Maldonado, A. M., Doerner, P., Dixon, R. A., Lamb, C. J., & Cameron, C. K. (2002). A Putative Lipid Transfer Protein Involved in Systemic Resistance Signalling in Arabidopsis. *Nature*, 419, 399–403.
- Malinovsky, F. G., Fangel, J. U., & Willats, W. G. T. (2014). The role of the cell wall in plant immunity. *Frontiers in Plant Science*, 5.
- Manners, J. M., Penninckx, I. A. M. A., Vermaere, K., Kazan, K., Brown, R. L., Morgan, A., ... Broekaert, W. F. (1998). The promoter of the plant defensin gene PDF1. 2 from Arabidopsis is systemically activated by fungal pathogens and responds to methyl jasmonate but not to salicylic acid. *Plant Molecular Biology*, 38(6), 1071–

1080.

- Matschi, S., Hake, K., Herde, M., Hause, B., & Romeis, T. (2015). The Calcium-Dependent Protein Kinase CPK28 Regulates Development by Inducing Growth Phase-Specific, Spatially Restricted Alterations in Jasmonic Acid Levels Independent of Defense Responses in Arabidopsis. *The Plant Cell*, 27(3), 591–606.
- McHale, L., Tan, X., Koehl, P., & Michelmore, R. W. (2006). Plant NBS-LRR proteins: adaptable guards. *Genome Biol*, 7(4), 212.
- Metwali, E. M. R., & Al-Maghrabi, O. A. (2012). Effectiveness of tissue culture media components on the growth and development of cauliflower (*Brassica oleracea* var. *Botrytis*) seedling explants in vitro. *African Journal of Biotechnology*, 11(76), 14069–14076.
- Meyer, R. S., & Purugganan, M. D. (2013). Evolution of crop species: Genetics of domestication and diversification. *Nature Reviews Genetics*, 14(12), 840–852.
- Meyers, B. C., Morgante, M., & Michelmore, R. W. (2002). TIR-X and TIR-NBS proteins: two new families related to disease resistance TIR-NBS-LRR proteins encoded in Arabidopsis and other plant genomes. *The Plant Journal*, 32(1), 77–92.
- Miedaner, T., & Korzun, V. (2012). Marker-Assisted Selection for Disease Resistance in Wheat and Barley Breeding. *Phytopathology*, 102(6), 560–566.
- Milward, D., Bjäreland, M., Hayes, W., Maxwell, M., Öberg, L., Tilford, N., ... Barnes, J. (2005). Ontology-based interactive information extraction from scientific abstracts. *Comparative and Functional Genomics*, 6(1–2), 67–71.
- Mitchum, M. G. (2016). Soybean resistance to the soybean cyst nematode *Heterodera glycines*: an update. *Phytopathology*, 106(12), 1–29.
- Mithen, R., Faulkner, K., Magrath, R., Rose, P., Williamson, G., & Marquez, J. (2003). Development of isothiocyanate-enriched broccoli, and its enhanced ability to induce phase 2 detoxification enzymes in mammalian cells. *Theoretical and Applied Genetics*, 106(4), 727–734.
- Moghaddam, M. R. B., & Ende, W. Van den. (2013). Sugars, the clock and transition to flowering. *Frontiers in Plant Science*, 4(February), 1–6.
- Molinero-Rosales, N., Latorre, A., Jamilena, M., & Lozano, R. (2004). SINGLE FLOWER TRUSS regulates the transition and maintenance of flowering in tomato. *Planta*, 218(3), 427–434.
- Mutasa-Gottgens, E., & Hedden, P. (2009). Gibberellin as a factor in floral regulatory networks. *Journal of Experimental Botany*, 60(7), 1979–1989.
- Nakano, M., Nishihara, M., Yoshioka, H., Takahashi, H., Sawasaki, T., Ohnishi, K., ... Kiba, A. (2013). Suppression of DS1 Phosphatidic Acid Phosphatase Confirms Resistance to *Ralstonia solanacearum* in *Nicotiana benthamiana*. *PLoS ONE*, 8(9), e75124.
- Nault, B., Reiners, S., Hsu, C., & Hoepfing, C. (2010). Black Rot Resistance Breeding Brassica, 1–7.
- Nawrath, C. (2002). EDS5, an Essential Component of Salicylic Acid-Dependent Signaling for Disease Resistance in Arabidopsis, Is a Member of the MATE Transporter Family. *THE PLANT CELL ONLINE*, 14(1), 275–286.
- Nho, C., & Jeffery, E. H. (2001). The Synergistic Upregulation of Phase II Detoxification Enzymes by Glucosinolate Breakdown Products in Cruciferous Vegetables. *Toxicology and Applied Pharmacology*, 174(2), 146–152.

- Nie, H., Zhao, C., Wu, G., Wu, Y., Chen, Y., & Tang, D. (2012). SR1, a Calmodulin-Binding Transcription Factor, Modulates Plant Defense and Ethylene-Induced Senescence by Directly Regulating NDR1 and EIN3. *PLANT PHYSIOLOGY*, 158(4), 1847–1859.
- Nielsen, M. E., & Thordal-Christensen, H. (2012). Recycling of Arabidopsis plasma membrane PEN1 syntaxin. *Plant Signaling & Behavior*, 7(12), 1541–1543.
- Oliviero, T., Verkerk, R., & Dekker, M. (2012). Effect of water content and temperature on glucosinolate degradation kinetics in broccoli (*Brassica oleracea* var. *italica*). *Food Chemistry*, 132(4), 2037–2045.
- Pandey, S. P., & Somssich, I. E. (2009). The Role of WRKY Transcription Factors in Plant Immunity. *PLANT PHYSIOLOGY*, 150(4), 1648–1655.
- Pariani, S., Contreras, M., Rossi, F. R., Sander, V., Corigliano, M. G., Simón, F., ... Clemente, M. (2016). Characterization of a novel Kazal-type serine proteinase inhibitor of Arabidopsis thaliana. *Biochimie*, 123, 85–94.
- Park, D. H., Somer, D. E., Kim, Y. S., Choy, Y. H., Lim, H. K., Soh, M. S., ... Nam, H. G. (1999). Control of Circadian Rhythms and Photoperiodic Flowering by the Arabidopsis GIGANTEA Gene, 285, 1579–1582.
- Parker, J. E. (2014). Co-opting the Cell-Cycle Machinery for Plant Immunity. *Cell Host & Microbe*, 16(6), 707–709.
- Parkin, I. A. P., Koh, C., Tang, H., Robinson, S. J., Kagale, S., Clarke, W. E., ... others. (2014). Transcriptome and methylome profiling reveals relics of genome dominance in the mesopolyploid Brassica oleracea. *Genome Biology*, 15(6), R77.
- Passam, H. C., Karapanos, I. C., Bebeli, P. J., & Savvas, D. (2007). A review of recent research on tomato nutrition, breeding and post-harvest technology with reference to fruit quality. *The European Journal of Plant Science and Biotechnology*, 1 (1), 1–21.
- Pečenková, T., Sabol, P., Kulich, I., Ortmannová, J., & Žárský, V. (2016). Constitutive Negative Regulation of R Proteins in Arabidopsis also via Autophagy Related Pathway? *Frontiers in Plant Science*, 7.
- Pedmale, U. V., & Liscum, E. (2007). Regulation of Phototropic Signaling in Arabidopsis via Phosphorylation State Changes in the Phototropin 1-interacting Protein NPH3. *Journal of Biological Chemistry*, 282(27), 19992–20001.
- Pék, Z., Daood, H., Nagyné, M. G., Berkí, M., Tóthné, M. M., Neményi, A., & Helyes, L. (2012). Yield and phytochemical compounds of broccoli as affected by temperature, irrigation, and foliar sulfur supplementation. *HortScience*, 47(11), 1646–1652.
- Poovaiah, B. W., Du, L., Wang, H., & Yang, T. (2013). Recent Advances in Calcium/Calmodulin-Mediated Signaling with an Emphasis on Plant-Microbe Interactions. *PLANT PHYSIOLOGY*, 163(2), 531–542.
- Putterill, J., Robson, F., Lee, K., Simon, R., & Coupland, G. (1995). The CONSTANS Gene of Arabidopsis Promotes Flowering and Encodes a Protein Showing Similarities to Zinc Finger Transcription Factor, 80, 847–857.
- Qi, Y., Tsuda, K., Nguyen, L. V., Wang, X., Lin, J., Murphy, A. S., ... Katagiri, F. (2011). Physical Association of Arabidopsis Hypersensitive Induced Reaction Proteins (HIRs) with the Immune Receptor RPS2. *Journal of Biological Chemistry*, 286(36), 31297–31307.

- Racapé, J., Belbahri, L., Engelhardt, S., Lacombe, B., Lee, J., Lochman, J., ... others. (2005). Ca²⁺-dependent lipid binding and membrane integration of PopA, a harpin-like elicitor of the hypersensitive response in tobacco. *Molecular Microbiology*, 58(5), 1406–1420.
- Rafalski, J. A. (2010). Association genetics in crop improvement. *Current Opinion in Plant Biology*, 13(2), 174–180.
- Rangkadilok, N., Nicolas, M. E., Bennett, R. N., Eagling, D. R., Premier, R. R., & Taylor, P. W. J. (2004). The Effect of Sulfur Fertilizer on Glucoraphanin Levels in Broccoli (*B. oleracea* L. var. *italica*) at Different Growth Stages. *Journal of Agricultural and Food Chemistry*, 52(9), 2632–2639.
- Reape, T. J., Molony, E. M., & McCabe, P. F. (2008). Programmed cell death in plants: distinguishing between different modes. *Journal of Experimental Botany*, 59(3), 435–444.
- Reddy, A. S. N., Ali, G. S., Celesnik, H., & Day, I. S. (2011). Coping with Stresses: Roles of Calcium- and Calcium/Calmodulin-Regulated Gene Expression. *The Plant Cell*, 23(6), 2010–2032.
- Reddy, V. S., Ali, G. S., & Reddy, A. S. N. (2003). Characterization of a pathogen-induced calmodulin-binding protein: Mapping of four Ca²⁺-dependent calmodulin-binding domains, 52, 143–159.
- Reitz, M. U., Gifford, M. L., & Schafer, P. (2015). Hormone activities and the cell cycle machinery in immunity-triggered growth inhibition. *Journal of Experimental Botany*, 66(8), 2187–2197.
- Riedelsheimer, C., Lisec, J., Czedik-Eysenberg, A., Sulpice, R., Flis, A., Grieder, C., ... Melchinger, A. E. (2012). Genome-wide association mapping of leaf metabolic profiles for dissecting complex traits in maize. *Proceedings of the National Academy of Sciences*, 109(23), 8872–8877.
- Rimmer, S. R., & van den Berg, C. G. J. (1992). Resistance of oilseed *Brassica* spp. to blackleg caused by *Leptosphaeria maculans*. *Canadian Journal of Plant Pathology*, 14(1), 56–66.
- Rolli, J., Loukili, N., Levrard, S., Rosenblatt-Velin, N., Rignault-Clerc, S., Waeber, B., ... Liaudet, L. (2010). Bacterial flagellin elicits widespread innate immune defense mechanisms, apoptotic signaling, and a sepsis-like systemic inflammatory response in mice. *Critical Care*, 14(4), 1.
- Rustérucci, C., Aviv, D. H., Holt, B. F., Dangl, J. L., & Parker, J. E. (2001). The disease resistance signaling components EDS1 and PAD4 are essential regulators of the cell death pathway controlled by LSD1 in Arabidopsis. *The Plant Cell*, 13(10), 2211–2224.
- S. Sanghera, G., H. Wani, S., Hussain, W., & B. Singh, N. (2011). Engineering Cold Stress Tolerance in Crop Plants. *Current Genomics*, 12(1), 30–43.
- Saban, G. M. (2018). The Benefits of Brassica Vegetables on Human Health. *J Human Health Res*, 1(1), 104.
- Sanders, D., Pelloux, J., Brownlee, C., & Harper, J. F. (2002). Calcium at the crossroads of signaling. *The Plant Cell*, 14(suppl 1), S401–S417.
- Sarris, P. F., Cevik, V., Dagdas, G., Jones, J. D. G., & Krasileva, K. V. (2016). Comparative analysis of plant immune receptor architectures uncovers host proteins likely targeted by pathogens. *BMC Biology*, 14(1).

- Sarris, P. F., Duxbury, Z., Huh, S. U., Ma, Y., Segonzac, C., Sklenar, J., ... Jones, J. D. G. (2015). A Plant Immune Receptor Detects Pathogen Effectors that Target WRKY Transcription Factors. *Cell*, *161*(5), 1089–1100.
- Sayers, E., & Wheeler, D. (2004). Building customized data pipelines using the entrez programming utilities (eUtils).
- Schaart, J. G., van de Wiel, C. C. M., Lotz, L. A. P., & Smulders, M. J. M. (2016). Opportunities for Products of New Plant Breeding Techniques. *Trends in Plant Science*, *21*(5), 438–449.
- Schönhals, E. M., Ding, J., Ritter, E., Paulo, M. J., Cara, N., Tacke, E., ... Gebhardt, C. (2017). Physical mapping of QTL for tuber yield, starch content and starch yield in tetraploid potato (*Solanum tuberosum* L.) by means of genome wide genotyping by sequencing and the 8.3 K SolCAP SNP array. *BMC Genomics*, *18*(1).
- Schweighofer, A., Kazanaviciute, V., Scheickl, E., Teige, M., Doczi, R., Hirt, H., ... Meskiene, I. (2007). The PP2C-Type Phosphatase AP2C1, Which Negatively Regulates MPK4 and MPK6, Modulates Innate Immunity, Jasmonic Acid, and Ethylene Levels in Arabidopsis. *THE PLANT CELL ONLINE*, *19*(7), 2213–2224.
- Scofield, S., Jones, A., & Murray, J. A. H. (2014). The plant cell cycle in context. *Journal of Experimental Botany*, *65*(10), 2557–2562.
- Seren, U., Vilhjalmsson, B. J., Horton, M. W., Meng, D., Forai, P., Huang, Y. S., ... Nordborg, M. (2012). GWAPP: A Web Application for Genome-Wide Association Mapping in Arabidopsis. *The Plant Cell*, *24*(12), 4793–4805.
- Sevrioukova, I. F. (2011). Apoptosis-inducing factor: structure, function, and redox regulation. *Antioxidants & Redox Signaling*, *14*(12), 2545–2579.
- Sewelam, N., Kazan, K., Thomas-Hall, S. R., Kidd, B. N., Manners, J. M., & Schenk, P. M. (2013). Ethylene Response Factor 6 Is a Regulator of Reactive Oxygen Species Signaling in Arabidopsis. *PLoS ONE*, *8*(8), e70289.
- Shafee, T. M. A., Lay, F. T., Hulett, M. D., & Anderson, M. A. (2016). The Defensins Consist of Two Independent, Convergent Protein Superfamilies. *Molecular Biology and Evolution*, *33*(9), 2345–2356.
- Shah, J. (2005). Lipids, Lipases, and Lipid-Modifying Enzymes in Plant Disease Resistance. *Annual Review of Phytopathology*, *43*, 229–260.
- Sharma, A., Hussain, A., Mun, B.-G., Imran, Q. M., Falak, N., Lee, S.-U., ... Yun, B.-W. (2016). Comprehensive analysis of plant rapid alkalization factor (RALF) genes. *Plant Physiology and Biochemistry*, *106*, 82–90.
- Smertenko, A. P. (2004). The Arabidopsis Microtubule-Associated Protein AtMAP65-1: Molecular Analysis of Its Microtubule Bundling Activity. *THE PLANT CELL ONLINE*, *16*(8), 2035–2047.
- Son, G. H., Wan, J., Kim, H. J., Nguyen, X. C., Chung, W. S., Hong, J. C., & Stacey, G. (2012). Ethylene-responsive element-binding factor 5, ERF5, is involved in chitin-induced innate immunity response. *Molecular Plant-Microbe Interactions*, *25*(1), 48–60.
- Sones, K., Heaney, R. K., & Fenwick, G. R. (1984). An estimate of the mean daily intake of glucosinolates from cruciferous vegetables in the UK. *Journal of the Science of Food and Agriculture*, *35*(6), 712–720.
- Song, X., & Zhang, T. (2009). Quantitative trait loci controlling plant architectural traits in cotton. *Plant Science*, *177*(4), 317–323.

- Soy, J., Leivar, P., & Monte, E. (2014). PIF1 promotes phytochrome-regulated growth under photoperiodic conditions in *Arabidopsis* together with PIF3, PIF4, and PIF5. *Journal of Experimental Botany*, 65(11), 2925–2936.
- Staack, R., Kingston, S., Wallig, M. A., & Jeffery, E. H. (1998). A Comparison of the Individual and Collective Effects of Four Glucosinolate Breakdown Products from Brussels Sprouts on Induction of Detoxification Enzymes. *Toxicology and Applied Pharmacology*, 149, 17–23.
- Takatsuna, H., Kato, H., Gohda, J., Akiyama, T., Moriya, A., Okamoto, Y., ... Inoue, J. - i. (2003). Identification of TIFA as an Adapter Protein That Links Tumor Necrosis Factor Receptor-associated Factor 6 (TRAF6) to Interleukin-1 (IL-1) Receptor-associated Kinase-1 (IRAK-1) in IL-1 Receptor Signaling. *Journal of Biological Chemistry*, 278(14), 12144–12150.
- Tang, D., Ade, J., Frye, C. A., & Innes, R. W. (2005). Regulation of plant defense responses in *Arabidopsis* by EDR2, a PH and START domain-containing protein. *The Plant Journal*, 44(2), 245–257.
- Tawfiq, N., Heaney, R. K., Plumb, J. A., Fenwick, G. R., Musk, S. R. R., & Williamson, G. (1995). Dietary glucosinolates as blocking agents against carcinogenesis: glucosinolate breakdown products assessed by induction of quinone reductase activity in murine hepa1c1c7 cells. *Carcinogenesis*, 16(5), 1191–1194.
- Teotia, S., & Tang, G. (2015). To bloom or not to bloom: Role of micrnas in plant flowering. *Molecular Plant*, 8(3), 359–377.
- Tiwari, M., Sharma, D., Singh, M., Tripathi, R. D., & Trivedi, P. K. (2014). Expression of OsMATE1 and OsMATE2 alters development, stress responses and pathogen susceptibility in *Arabidopsis*. *Scientific Reports*, 4.
- Torii, K. U. (2004). Leucine-rich repeat receptor kinases in plants: structure, function, and signal transduction pathways. *International Review of Cytology*, 234, 1–46.
- Tornero, P., Conejero, V., & Vera, P. (1996). Primary structure and expression of a pathogen-induced protease (PR-P69) in tomato plants: similarity of functional domains to subtilisin-like endoproteases. *Proceedings of the National Academy of Sciences*, 93(13), 6332–6337.
- Tornero, P., Conejero, V., & Vera, P. (1997). Identification of a new pathogen-induced member of the subtilisin-like processing protease family from plants. *Journal of Biological Chemistry*, 272(22), 14412–14419.
- Torres, M. A., Jones, J. D. G., & Dangl, J. L. (2005). Pathogen-induced, NADPH oxidase-derived reactive oxygen intermediates suppress spread of cell death in *Arabidopsis thaliana*. *Nature Genetics*, 37(10), 1130–1134.
- Traka, M. H., Saha, S., Huseby, S., Kopriva, S., Walley, P. G., Barker, G. C., ... Mithen, R. F. (2013). Genetic regulation of glucoraphanin accumulation in Beneforté® broccoli. *New Phytologist*, 198(4), 1085–1095.
- Traka, M., & Mithen, R. (2009). Glucosinolates, isothiocyanates and human health. *Phytochemistry Reviews*, 8(1), 269–282.
- Tsai, Y.-C., Koo, Y., Delk, N. A., Gehl, B., & Braam, J. (2013). Calmodulin-related CML24 interacts with ATG4b and affects autophagy progression in *Arabidopsis*. *The Plant Journal*, 73(2), 325–335.
- Tseng, T.-S., & Briggs, W. R. (2010). The *Arabidopsis* rcn1-1 Mutation Impairs Dephosphorylation of Phot2, Resulting in Enhanced Blue Light Responses. *The*

- Plant Cell*, 22(2), 392–402.
- Tsuchiya, T., & Eulgem, T. (2010). The Arabidopsis defense component EDM2 affects the floral transition in an FLC-dependent manner: EDM2 promotes the floral transition. *The Plant Journal*, 62(3), 518–528.
- Tuteja, N., & Mahajan, S. (2007). Calcium signaling network in plants: an overview. *Plant Signaling & Behavior*, 2(2), 79–85.
- USDA. (2018). *Broccoli, Raw - National Nutrient Database for Standard Reference*.
- Vadassery, J., & Oelmüller, R. (2009). Calcium signaling in pathogenic and beneficial plant microbe interactions: what can we learn from the interaction between *Piriformospora indica* and *Arabidopsis thaliana*. *Plant Signaling & Behavior*, 4(11), 1024–1027.
- Vallejo, F., García-Viguera, C., & Tomás-Barberán, F. A. (2003). Changes in Broccoli (*Brassica oleracea* L. Var. *italica*) Health-Promoting Compounds with Inflorescence Development. *Journal of Agricultural and Food Chemistry*, 51(13), 3776–3782.
- van Doorn, H. E., van der Kruk, G. C., van Holst, G. J., Raaijmakers-Ruijs, N. C. M. E., Postma, E., Groeneweg, B., & Jongen, W. H. F. (1998). The Glucosinolates Sinigrin and Progoitrin are Important Determinants for Taste Preference and Bitterness of Brussels Sprouts, 78, 30–38.
- Van Eylen, D., Oey, I., Hendrickx, M., & Van Loey, A. (2007). Kinetics of the Stability of Broccoli (*Brassica oleracea* Cv. *Italica*) Myrosinase and Isothiocyanates in Broccoli Juice during Pressure/Temperature Treatments. *Journal of Agricultural and Food Chemistry*, 55(6), 2163–2170.
- Vandepoele, K. (2002). Genome-Wide Analysis of Core Cell Cycle Genes in *Arabidopsis*. *THE PLANT CELL ONLINE*, 14(4), 903–916.
- Vishwakarma, K., Upadhyay, N., Kumar, N., Yadav, G., Singh, J., Mishra, R. K., ... Sharma, S. (2017). Abscisic Acid Signaling and Abiotic Stress Tolerance in Plants: A Review on Current Knowledge and Future Prospects. *Frontiers in Plant Science*, 08(February), 1–12.
- Visscher, P. M., Brown, M. A., McCarthy, M. I., & Yang, J. (2012). Five years of GWAS discovery. *American Journal of Human Genetics*, 90(1), 7–24.
- Visscher, P. M., Wray, N. R., Zhang, Q., Sklar, P., McCarthy, M. I., Brown, M. A., & Yang, J. (2017). 10 Years of GWAS Discovery: Biology, Function, and Translation. *American Journal of Human Genetics*, 101(1), 5–22.
- Vogel, J. P. (2002). PMR6, a Pectate Lyase-Like Gene Required for Powdery Mildew Susceptibility in *Arabidopsis*. *THE PLANT CELL ONLINE*, 14(9), 2095–2106.
- Wagner, G., Charton, S., Lariagon, C., Laperche, A., Lugan, R., Hopkins, J., ... Gravot, A. (2012). Metabotyping: a new approach to investigate rapeseed (*Brassica napus* L.) genetic diversity in the metabolic response to clubroot infection. *Molecular Plant-Microbe Interactions*, 25(11), 1478–1491.
- Walley, P. G., Carder, J., Skipper, E., Mathas, E., Lynn, J., Pink, D., & Buchanan-Wollaston, V. (2012). A new broccoli × broccoli immortal mapping population and framework genetic map: Tools for breeders and complex trait analysis. *Theoretical and Applied Genetics*, 124(3), 467–484.
- Wickland, D. P., & Hanzawa, Y. (2015). The FLOWERING LOCUS T/TERMINAL FLOWER 1 Gene Family: Functional Evolution and Molecular Mechanisms. *Molecular Plant*, 8(7), 983–997.

- Wilkie, J. D., Sedgley, M., & Olesen, T. (2008). Regulation of floral initiation in horticultural trees. *Journal of Experimental Botany*, *59*(12), 3215–3228.
- Williams, P. H. (2007). Black rot. *Compendium of Brassica Diseases*, 60–62.
- Willige, B. C., Ghosh, S., Nill, C., Zourelidou, M., Dohmann, E. M. N., Maier, A., & Schwechheimer, C. (2007). The DELLA Domain of GA INSENSITIVE Mediates the Interaction with the GA INSENSITIVE DWARF1A Gibberellin Receptor of Arabidopsis. *THE PLANT CELL ONLINE*, *19*(4), 1209–1220.
- Wingler, A. (2017). Transitioning to the next phase: the role of sugar signaling throughout the plant life cycle. *Plant Physiology*, *176*(February), pp.01229.2017.
- Winter, P., & Kahl, G. (1995). Molecular Marker Technologies for Plant Improvement. *World Journal of Microbiology & Biotechnology*, *11*(4), 438–448.
- Wu, M.-F., Sang, Y., Bezhani, S., Yamaguchi, N., Han, S.-K., Li, Z., ... Wagner, D. (2012). SWI2/SNF2 chromatin remodeling ATPases overcome polycomb repression and control floral organ identity with the LEAFY and SEPALLATA3 transcription factors. *Proceedings of the National Academy of Sciences*, *109*(9), 3576–3581.
- Xu, Y. (2010). *Molecular Blant Breeding*. New York: CABI Publishing.
- Xu, Z.-S., Xiong, T.-F., Ni, Z.-Y., Chen, X.-P., Chen, M., Li, L.-C., ... Ma, Y.-Z. (2009). Isolation and identification of two genes encoding leucine-rich repeat (LRR) proteins differentially responsive to pathogen attack and salt stress in tobacco. *Plant Science*, *176*(1), 38–45.
- Yadav, S. K. (2010). Cold stress tolerance mechanisms in plants. A review. *Agronomy for Sustainable Development*, *30*(3), 515–527.
- Yamada, T., Ichimura, K., Kanekatsu, M., & van Doorn, W. G. (2009). Homologs of Genes Associated with Programmed Cell Death in Animal Cells are Differentially Expressed During Senescence of Ipomoea nil Petals. *Plant and Cell Physiology*, *50*(3), 610–625.
- Yanaka, A., Fahey, J. W., Fukumoto, A., Nakayama, M., Inoue, S., Zhang, S., ... Yamamoto, M. (2009). Dietary Sulforaphane-Rich Broccoli Sprouts Reduce Colonization and Attenuate Gastritis in Helicobacter pylori-Infected Mice and Humans. *Cancer Prevention Research*, *2*(4), 353–360.
- Yang, L., Qin, L., Liu, G., Peremyslov, V. V., Dolja, V. V., & Wei, Y. (2014). Myosins XI modulate host cellular responses and penetration resistance to fungal pathogens. *Proceedings of the National Academy of Sciences*, *111*(38), 13996–14001.
- Yemets, A., Sheremet, Y., & Blume, Y. B. (2005). Does tubulin phosphorylation correlate with cell death in plant cells? *BMC Plant Biology*, *5*(Suppl 1), S36.
- Yokota, E., & Shimmen, T. (2011). Plant Myosins. In Bo Liu (Ed.), *The Plant Cytoskeleton* (pp. 33–56). New York, NY: Springer New York.
- Yoshizawa, T., Shimizu, T., Hirano, H., Sato, M., & Hashimoto, H. (2012). Structural Basis for Inhibition of Xyloglucan-specific Endo- -1,4-glucanase (XEG) by XEG-Protein Inhibitor. *Journal of Biological Chemistry*, *287*(22), 18710–18716.
- Yu, J., Pressoir, G., Briggs, W. H., Vroh Bi, I., Yamasaki, M., Doebley, J. F., ... Buckler, E. S. (2006). A unified mixed-model method for association mapping that accounts for multiple levels of relatedness. *Nature Genetics*, *38*(2), 203–208.
- Yu, S., Galvao, V. C., Zhang, Y.-C., Horrer, D., Zhang, T.-Q., Hao, Y.-H., ... Wang, J.-W. (2012). Gibberellin Regulates the Arabidopsis Floral Transition through miR156-

- Targeted SQUAMOSA PROMOTER BINDING-LIKE Transcription Factors. *The Plant Cell*, 24(8), 3320–3332.
- Yun, B.-W., Atkinson, H. A., Gaborit, C., Greenland, A., Read, N. D., Pallas, J. A., & Loake, G. J. (2003). Loss of actin cytoskeletal function and EDS1 activity, in combination, severely compromises non-host resistance in Arabidopsis against wheat powdery mildew. *The Plant Journal*, 34(6), 768–777.
- Zhang, H., Mittal, N., Leamy, L. J., Barazani, O., & Song, B. H. (2017). Back into the wild—Apply untapped genetic diversity of wild relatives for crop improvement. *Evolutionary Applications*, 10(1), 5–24.
- Zhang, Y., Talalay, P., Cho, C.-G., & Posner, G. H. (1992). A major inducer of anticarcinogenic protective enzymes from broccoli: isolation and elucidation of structure. *Proceedings of the National Academy of Sciences*, 89(6), 2399–2403.
- Zhao, X., Mehrabi, R., & Xu, J.-R. (2007). Mitogen-Activated Protein Kinase Pathways and Fungal Pathogenesis. *Eukaryotic Cell*, 6(10), 1701–1714.
- Zhu, G., Wang, S., Huang, Z., Zhang, S., Liao, Q., Zhang, C., ... Huang, S. (2018). Rewiring of the Fruit Metabolome in Tomato Breeding. *Cell*, 172(1–2), 249–255.e12.
- Zoratti, L., Karppinen, K., Luengo Escobar, A., Håggman, H., & Jaakola, L. (2014). Light-controlled flavonoid biosynthesis in fruits. *Frontiers in Plant Science*, 5(October), 1–16.
- Zuther, E., Juszczak, I., Ping Lee, Y., Baier, M., & Hinch, D. K. (2015). Time-dependent deacclimation after cold acclimation in Arabidopsis thaliana accessions. *Scientific Reports*, 5, 1–10.

**Chapter 5. Improving Our Understanding of Agronomic, Fruit Quality, and
Metabolic Traits in Blueberry and Broccoli**

Nutrition and health are growing concerns to society and researchers as the global population continues to quickly increase and the agriculture industry tries to supply enough food (Barrett, Beaulieu, & Shewfelt, 2010; Betoret, Betoret, Vidal, & Fito, 2011; Biltekoff, 2010; Kearney, 2010; Klee, 2010; Kyriacou & Roupael, 2018; Matas, Gapper, Chung, Giovannoni, & Rose, 2009; Sam Saguy, 2011). Plants provide all the vital carbohydrates, lipids, minerals, vitamins, and amino acids vital for proper human nutrition (Barrett et al., 2010; Betoret et al., 2011; Biltekoff, 2010; Buchanan, Gruissem, & Jones, 2012; Kearney, 2010; Kyriacou & Roupael, 2018; Sam Saguy, 2011; Ufaz & Galili, 2008; G. Wang, Xu, Wang, & Galili, 2017). In addition, plants have evolved a plethora of specialized metabolites that not only enhance their own pathogen defense and reproductive fitness, but also potentially improve human health and treat disease (Buchanan et al., 2012; Okazaki & Saito, 2012; Sumner, Lei, Nikolau, & Saito, 2015; Weng, 2014; Wolfender, Marti, Thomas, & Bertrand, 2015; H. Zhang, Mittal, Leamy, Barazani, & Song, 2017).

Some of the domesticated crops contain specialized compounds. For example, carrots synthesize β -carotene to function as a light and free radical protectant, and when consumed by humans, provides a vital source of provitamin A (Gul et al., 2015; K. D. Sharma, Karki, Thakur, & Attri, 2012; Toivonen & Brummell, 2008). Unfortunately, only a few currently cultivated crops accumulate health-promoting, specialized compounds because the intense selective breeding in the past has focused on improving yield, shelf-life, and size (Gul et al., 2015; Klee, 2010; Konarska, 2015; Matas et al., 2009; Sam Saguy, 2011; K. D. Sharma et al., 2012; Toivonen & Brummell, 2008). In particular, selecting for yield, shelf-life, and size along with intense pesticide and herbicide use shifted the selection pressures and resource allocations away from specialized metabolite diversity and towards primary metabolite growth and storage (Bennett, Roberts, & Wagstaff, 2012; Y. Kang, Khan, & Ma, 2009; Klee, 2010; Konarska, 2015; E. A. Lee & Tollenaar, 2007; Matas et al., 2009; O. Sadras & F. Denison, 2009; Sam Saguy, 2011). For example, the use of pesticides and herbicides on crops eliminated the majority of biotic stresses, like pest damage or weed competition; therefore, there was no selection pressure to maintain a robust innate immune system of pathways synthesizing specialized metabolites (Boudsocq et al.,

2010; Buchanan et al., 2012; Denancé, Sánchez-Vallet, Goffner, & Molina, 2013; Freeman & Beattie, 2008; Fu & Dong, 2013). Similarly, since fertilization or self-fertilization became guaranteed in monoculture fields, the selection pressure to maintain production and storage of specialized volatile and pigment metabolites became irrelevant as there was no need to entice pollinators (Bennett et al., 2012; Buchanan et al., 2012; Howe & Jander, 2007; Karppinen, Zoratti, Nguyenquynh, Häggman, & Jaakola, 2016; O. Sadras & F. Denison, 2009; Ogden & van Iersel, 2009; Tieman et al., 2012).

Fortunately, the genetic diversity for restoring and producing more specialized metabolites exists in the appropriate germplasm (Heslot, Yang, Sorrells, & Jannink, 2012; Tester & Langridge, 2010; Winter & Kahl, 1995; H. Zhang et al., 2017). Developing breeding strategies to improve the specialized metabolites in current crops is complex, as it cannot sacrifice yield or fruit quality and cannot significantly increase cost to farmers or consumers, all while increasing specialized metabolite synthesis when little is known about specialized metabolite regulation (Al-Khayri, Jain, & Johnson, 2015; Fernie & Schauer, 2009; E. A. Lee & Tollenaar, 2007; Palmgren et al., 2015; H. Zhang et al., 2017). Accordingly, a greater understanding of the genetic and metabolic regulatory networks involved in agronomic, fruit quality, and metabolic traits is necessary to developing new breeding strategies and crop varieties with improved nutrition.

5.1. Blueberry Agronomic Growth, Dormancy, and Fruit Quality Traits Associated with Multiple Genetic Regions

Blueberries, *Vaccinium corymbosum*, are an important fresh fruit crop given the recent publicity of blueberries as a “super fruit” due to potent antioxidant properties (Betoret et al., 2011; Gowd, Jia, & Chen, 2017; McNamara et al., 2018; Pan et al., 2017; N. Singh & Ghosh, 2019; Subash et al., 2014; Whyte, Schafer, & Williams, 2016). The antioxidant capacity of blueberries has been shown to reduce the oxidative stress of free radicals that increase the onset and progression of inflammation, heart disease, diabetes, neurological degeneration, and cancer (Gowd et al., 2017; McNamara et al., 2018; Morita, Naito, Yoshikawa, & Niki, 2017; Pan et al., 2017; N. Singh & Ghosh, 2019; Subash et al., 2014; Whyte et al., 2016). The polyphenols in blueberries, including the

blue pigment metabolites, the anthocyanins, have been consistently attributed to the antioxidant properties of blueberries (Gowd et al., 2017; McNamara et al., 2018; Pan et al., 2017; N. Singh & Ghosh, 2019; Subash et al., 2014; Whyte et al., 2016). The current commercial breeding and production of blueberries has decreased polyphenol accumulation and diversity, especially in the high-yield cultivars (P. Liu et al., 2014; Prencipe et al., 2014; Routray & Orsat, 2011; Scalzo, Stevenson, & Hedderley, 2013, 2015; S. Y. Wang, Chen, Camp, & Ehlenfeldt, 2012). Gaining a greater understanding of the different networks contributing to agronomic productivity will aid in fine-tuning selection for possibility greater fruit production and longer harvest seasons. The advancements in bioinformatics computing allows for utilization of genomic datasets and statistics for genetic association mapping (Chae, Kim, Nilo-Poyanco, & Rhee, 2014; Kanehisa, Furumichi, Tanabe, Sato, & Morishima, 2017; T. Kim et al., 2017). Genetic association mapping links variation in a trait to variation in a genetic marker (Borevitz & Chory, 2004; Collard, Jahufer, Brouwer, & Pang, 2005; M. S. Kang, 2002). This determines genetic regions or QTLs that are associated to differences in a quantitative trait like bud density or fruit color because the genetic regions contain possible regulatory genes (Borevitz & Chory, 2004; Collard et al., 2005; M. S. Kang, 2002). The goal of this research was to identify significant QTLs associated with agronomic growth, dormancy, and fruit quality traits with a focus on improving fruit production and quality through enhancing floral bud break efficiency and fruit quality production.

The DxJ mapping population provides a valuable resource for investigating agronomic growth, dormancy, and fruit quality characteristics because the Draper and Jewel cultivars are diverse commercial cultivars for NHB and SHB blueberries. Since Draper and Jewel cultivars are adapted to different environmental conditions, the DxJ progeny exhibit a wide range of growth traits, including leafing strength, floral bud density, and vigor. Plant growth regulation is a complex network of interacting signals, like hormones and sugars, that coordinate processes like cell proliferation, cell differentiation, and resource allocation (Bennett et al., 2012; Buchanan et al., 2012; Del Pozo, Lopez-Matas, Ramirez-Parra, & Gutierrez, 2005; O. Sadras & F. Denison, 2009; Takatsuka & Umeda, 2014; van der Schoot & Rinne, 2011; Xing et al., 2015). The availability and signaling of resources is also very important in bud differentiation

regulation as a depletion of resources results in the premature termination of the tissue (Bennett et al., 2012; Buchanan et al., 2012; Moghaddam & Ende, 2013; O'Hara, Paul, & Wingler, 2013; Ruan, 2014; Tsai & Gazzarrini, 2014; Wingler, 2017). The signaling and regulation of resource availability is essential for perennial plants because bud formation and differentiation as well as preparations for dormancy induction occurs after fruiting (Beauvieux, Wenden, & Dirlewanger, 2018; Considine & Considine, 2016; Cooke, Eriksson, & Junttila, 2012; J. Li et al., 2018; Lloret, Badenes, & Ríos, 2018; Malyshev, Shelyakin, & Golovko, 2016; Shim et al., 2014; Zheng et al., 2015).

The association mapping of the eight growth traits identified many significant QTLs using CIM and multiple different analyses for vegetative meristem growth, bud meristem differentiation, and plant vigor traits. The comparison of all the significant QTLs from all the different analyses revealed 43 overlapping QTL regions that contained at least three significant QTLs. While 12 of the 43 overlapping QTL regions are associated with vegetative meristem growth, 15 regions are associated specifically with bud meristem differentiation between vegetative and floral buds. Of the eight individual growth traits, the vigor rating trait identified the most overlapping QTL regions. Specifically the 16 overlapping QTL regions for this trait represents overall plant growth and efficient resource allocation after fruiting to prepare for dormancy (Bennett et al., 2012; Díaz-Riquelme, Grimplet, Martínez-Zapater, & Carmona, 2012; J. Li et al., 2018; O. Sadras & F. Denison, 2009; Xing et al., 2015).

To explore how the growth traits relate to one another, the overlapping QTL regions were analyzed further for multiple overlapping traits, which revealed seven multi-trait overlapping QTL regions. Three of the seven multi-trait regions contain significant QTLs for vegetative meristem growth, which indicates this region may regulate the induction of shoot apical and axillary meristem growth and rapid cell differentiation and expansion into new vegetative tissue (Bar & Ori, 2014; Bennett et al., 2012; Considine & Considine, 2016; Signorelli, Agudelo-Romero, Meitha, Foyer, & Considine, 2018; van der Schoot & Rinne, 2011). Two of the seven multi-trait regions contain significant QTLs for bud meristem differentiation between vegetative and floral, which indicates these regions are most likely involved in signaling differentiation and resource availability signals as well as floral meristem identity genes (Bennett et al.,

2012; Costes et al., 2014; Mohamed et al., 2010; Molinero-Rosales, Latorre, Jamilena, & Lozano, 2004; O. Sadras & F. Denison, 2009; O'Hara et al., 2013; van der Schoot & Rinne, 2011; Wingler, 2017). Further gene research within the genetic regions corresponding to the QTL regions associated with bud density and growth will provide important foundational knowledge for bud formation and differentiation (Costes et al., 2014; Meitha et al., 2018; Mert, Barut, & Ipek, 2013; Mohamed et al., 2010; Molinero-Rosales et al., 2004; van der Schoot & Rinne, 2011). Future breeding strategies can utilize this information and the identified QTL regions to improve meristem differentiation and floral bud density, which will subsequently improve blueberry yield per plant.

Since blueberries are woody, perennial shrubs, blueberry floral buds must overwinter and efficiently burst in early spring to produce blueberry fruit (Draper & Hancock, 2003; Lyrene, Journal, & Society, 2002; Trehane, 2004; Williamson & Lyrene, 2004). Appropriately coordinating floral bud burst for different environments is the main issue inhibiting blueberry habitat expansion and productivity, because poor timing leads to meristem tissue damage and termination (J F Hancock et al., 2008; Trehane, 2004). The coordination of floral bud dormancy break is a complex network that is essential for subsequent yield (Anderson, 2015; Beauvieux et al., 2018; Considine & Considine, 2016; Cooke et al., 2012; Die, Arora, & Rowland, 2016; Lloret et al., 2018; Z. Zhang et al., 2018). The low oxygen and low carbon environment within the floral bud suggests the oxidative-ROS signaling and regulation pathways plays an important role in floral bud burst and flowering (Beauvieux et al., 2018; Lloret et al., 2018; Meitha et al., 2018; Signorelli et al., 2018). Sugar metabolism and signaling is another important pathway for dormancy break and flowering as the availability of carbon and energy is essential for a successful developmental transition to reproduction (Anderson, 2015; Beauvieux et al., 2018; Malyshev et al., 2016; Pagter, Andersen, & Andersen, 2015; Z. Zhang et al., 2018).

The association mapping of the eight dormancy break and flowering traits identified many significant QTLs using CIM and multiple different analyses. The comparison of all the significant QTLs from all the different analyses revealed four overlapping QTL regions that contained at least three significant QTLs. Of those four overlapping QTL regions, two of the overlapping QTL regions address dormancy break

for vegetative buds, while the other two overlapping QTL regions address dormancy break for floral buds. The corresponding genetic regions for the four overlapping QTL regions should be further investigated for regulatory genes in pathways like oxidative signaling, sugar signaling, or hormone regulation because multiple studies indicate they are vital in regulating bud dormancy break across a variety of environmental conditions (Beauvieux et al., 2018; Considine & Considine, 2016; Cooke et al., 2012; Díaz-Riquelme et al., 2012; J. Li et al., 2018; Lloret et al., 2018; Malyshev et al., 2016; van der Schoot & Rinne, 2011; Vergara, Noriega, Aravena, Prieto, & Pérez, 2017; Z. Zhang et al., 2018; Zheng et al., 2015). The many other significant QTLs for the eight dormancy break and flowering traits are also important for future gene research as the many indicate that the environmental variation strongly impacts the regulation of dormancy break and flowering regulation (Arora, Rowland, & Tanino, 2003; Basler & Körner, 2012, 2014; Beauvieux et al., 2018; Cooke et al., 2012; Ghelardini, Santini, Black-Samuelsson, Myking, & Falusi, 2009; Horvath, Anderson, Chao, & Foley, 2003; Malyshev et al., 2016; Rohde & Bhalerao, 2007; Shim et al., 2014; R. K. Singh, Svystun, AIDahmash, Jonsson, & Bhalerao, 2017). Utilizing these dormancy break and flowering QTLs for future breeding strategies will aid in narrowing the QTL and genetic regions through fine-mapping and in improving the efficiency of dormancy break and floral maturation to increase blueberry's yield and productive growth range (Arora et al., 2003; Ehlenfeldt, 2012; Jim F Hancock, 2008; Kovaleski, Williamson, Olmstead, & Darnell, 2015; G. A. Lobos & Hancock, 2015; Melke, 2015; Rowland, Ogden, Ehlenfeldt, & Arora, 2008; Trehane, 2004).

The traditional breeding of fruits and vegetables for storage and shelf-life has led to many fruits and vegetables becoming too firm and tasteless, which increased consumer awareness to the discrepancies of fruit quality perception (Betoret et al., 2011; Bilttekoff, 2010; Grunert, 2005; Kader, 2008; Kearney, 2010; Kyriacou & Roupheal, 2018; Tieman et al., 2012). The slower ripening process selected for by industry most likely differentially regulates the development and onset of ripening, which results in very firm fruits that improve the fruit's resistance to tissue damage and reduces product loss (Barrett et al., 2010; Gilbert et al., 2014; Giongo, Poncetta, Loretti, & Costa, 2013; X. Li, Xu, Korban, & Chen, 2010; Matas et al., 2009; Prasanna, Prabha,

& Tharanathan, 2007; Sam Saguy, 2011). For blueberries, good fruit quality characteristics from the consumer perspective consist of firm, juicy, sweet, and blue colored berries (Barrett et al., 2010; Cappai, Benevenuto, Ferrão, & Munoz, 2018; Gilbert et al., 2014; Giongo et al., 2013; Kader, 2008; Leiva-Valenzuela, Lu, & Aguilera, 2013; Matas et al., 2009; Saftner, Polashock, Ehlenfeldt, & Vinyard, 2008). Before the onset of non-climacteric blueberry ripening, the fruit undergoes extensive cell proliferation to support fruit growth, and undergoes sugar and precursor metabolite accumulation to prepare for ripening (Castellarin et al., 2016; Coombe & McCarthy, 2000; Godoy, Monterubbianesi, & Tognetti, 2008; Serrano et al., 2017). During fruit ripening, multiple pathways like auxin, ABA, and GA mediate the cross-talk and regulation of multiple pathways to induce rapid growth with acidic cell expansion, soluble sugar accumulation, turgor pressure, and pigment accumulation (Cappai et al., 2018; Giovannoni, 2004; Huan et al., 2016; Jia et al., 2017; Osorio, Scossa, & Fernie, 2013; Prasanna et al., 2007; Seymour, Østergaard, Chapman, Knapp, & Martin, 2013). In order to investigate the multiple different pathways involved in fruit development and ripening, the 14 fruit quality traits in this research represent consumer-driven fruit quality characteristics like firmness, color, taste, and nutrition, while also representing the above-mentioned ripening regulatory pathways (Cappai et al., 2018; Gilbert et al., 2015, 2014; Saftner et al., 2008; J. L. Silva, Marroquin, Matta, Garner, & Stojanovic, 2005).

The association mapping of the 14 fruit quality traits identified many significant QTLs for fruit development, ripening, and quality using CIM and multiple different mapping analyses. The comparison of all the significant QTLs from all the different analyses revealed 51 overlapping QTL regions that contained at least three significant QTLs. Of the 51 overlapping QTL regions, 25 overlapping regions are specifically associated with firmness and turgor pressure traits. The other 25 overlapping QTL regions are associated with the pH, SS, TA, SS:TA ratio, and total anthocyanin traits, which can contribute to regulating color, firmness, turgor, or flavor (Castellarin et al., 2016; Forney, Kalt, Jordan, Vinqvist-Tymchuk, & Fillmore, 2012; Gilbert et al., 2015, 2014; T. E. Lobos et al., 2018; Montecchiarini et al., 2018). When the overlapping QTL regions were analyzed further for multiple overlapping traits, eight multi-trait overlapping QTL regions were revealed. One multi-trait region contained significant QTLs for TA,

SS:TA ratio, and total anthocyanin content, which indicates this region may regulate anthocyanin accumulation as acidity and sugars induce anthocyanin diversity synthesis (Howard, Brownmiller, Mauromoustakos, & Prior, 2016; Jia et al., 2017; Karppinen et al., 2013; Oh, Yu, Chung, Chea, & Lee, 2018; Wahyuningsih, Wulandari, Wartono, Munawaroh, & Ramelan, 2017). Four of the eight multi-trait regions contained significant QTLs for at least two traits involved in regulating firmness and turgor pressure, which strongly suggests that blueberry firmness and turgor pressure are closely associated within the DxJ population. Since there is limited information on the regulation of berry firmness and fruit turgor pressure, further gene research within the genetic regions of these QTL regions will provide foundational knowledge for berry firmness regulation (Castellarin et al., 2016; Giongo et al., 2013; Gould et al., 2013; Konarska, 2015; Montecchiarini et al., 2018; A. C. Paniagua, East, Hindmarsh, & Heyes, 2013; Yadav & Singh, 2014). Future breeding strategies can utilize this information and the identified QTL regions to improve berry firmness and turgor pressure while concurrently improving color, texture, flavor, and nutrition fruit quality.

The goal of this research was to identify important QTLs for different agronomic growth, dormancy break and flowering, and fruit quality traits. Improving the vegetative and floral bud growth along with the efficiency of bud dormancy break will increase bud density and reduce bud tissue damage. This will subsequently improve blueberry productivity and growth range. Through investigating the different fruit quality traits, future gene research can elucidate regulatory information while future breeding strategies can utilize the QTL regions to improve blueberry ripening along with fruit quality characteristics preferred by both industry and consumers. Overall, the results provide valuable foundational knowledge for blueberry resources to develop specific markers and breeding strategies for specific agronomic or fruit quality traits. As a result, more blueberries will be produced that more consumers will want to eat, and will benefit from their potent nutritious qualities.

5.2. Blueberry metabolic profiling and associated genetic regions containing possible regulatory genes

Blueberries exhibit a plethora of health benefits, primarily due to their potent antioxidant properties (Bornsek et al., 2012; Bunea et al., 2013; De Souza et al., 2014;

Gowd et al., 2017; Khoo, Azlan, Tang, & Lim, 2017; D. Li et al., 2017; S. Silva, Costa, Veiga, Morais, & Pintado, 2018; Yousuf, Gul, Wani, & Singh, 2016). Blueberry extracts have been shown to reduce oxidative stress, reduce inflammation, lessen neurological degeneration, and decrease cancer cell growth (Giacalone et al., 2011; Horbowicz, Grzesiuk, DĘBski, & Kosson, 2008; Khoo et al., 2017; D. Li et al., 2017; Ma et al., 2018; McNamara et al., 2018; N. Singh & Ghosh, 2019; Subash et al., 2014). As mentioned previously, many of the phenolic acids have been shown to play a role in antioxidant capacity (Bornsek et al., 2012; Bunea et al., 2013; Gowd et al., 2017; Herrmann, 1995; Khoo et al., 2017; D. Li et al., 2017; Nabavi et al., 2018; S. Silva et al., 2018; Yousuf et al., 2016). The anthocyanins found in blueberry have been strongly associated with potent antioxidant properties (Bornsek et al., 2012; Bunea et al., 2013; De Souza et al., 2014; Gowd et al., 2017; Horbowicz et al., 2008; Khoo et al., 2017; D. Li et al., 2017; S. Silva et al., 2018; Yousuf et al., 2016). Apart from anthocyanins, very little information concerning metabolite composition has been elucidated in blueberries. Determining the metabolite composition within blueberry will aid in understanding signaling pathways during fruit development and metabolite contribution to flavor and antioxidant capacity. The research goals of this chapter were to conduct metabolic profiling on blueberry extracts to provide foundational metabolic resources for blueberries, and to utilize the annotated metabolites, along with DPPH-antioxidant capacity data, for biparental association mapping to identify important QTL regions and putative candidate genes.

Metabolite profiling quantifies and potentially annotates metabolite features either through targeted or non-targeted approaches (Carreno-Quintero, Bouwmeester, & Keurentjes, 2013; T. Kim et al., 2017; Matsuda, 2016; Pinu, Pinu, & R, 2018; Saito & Matsuda, 2010; Scalbert et al., 2009; Sumner et al., 2015; Wolfender et al., 2015). Targeted profiling focuses on a specific type of metabolite for detailed characterization, whereas non-targeted profiling focuses on a broad sampling of a diversity of compounds (Bingol, 2018; Matsuda, 2016; Pinu et al., 2018; Scalbert et al., 2009; Sumner et al., 2015). Profiling with ¹H NMR quantifies metabolites based on the chemical shifts of hydrogen atoms within the metabolites (Bingol, 2018; Buchanan et al., 2012; Sumner et al., 2015). Profiling with HPLC-QTOFMS quantifies metabolites based on their mass-to-charge ratio (m/z) effecting the time it takes the metabolite to reach the

detector (Grace, Xiong, Esposito, Ehlenfeldt, & Lila, 2018; Kai et al., 2017; Matsuda, 2016). Non-targeted profiling with ^1H NMR usually quantifies high-abundance metabolites, which is mainly primary metabolites (Bingol, 2018; Buchanan et al., 2012; Sumner et al., 2015). Targeted profiling with HPLC-QTOFMS usually quantifies specific metabolites at either high or low abundance as the separation and detection methods can vary greatly (Grace et al., 2018; Kai et al., 2017; Matsuda, 2016).

The non-targeted profiling of blueberry extracts with ^1H NMR identified 943 metabolite features, with 192 annotated peaks condensing into 29 known metabolites and 751 unknowns (Table 3.3). The profiling quantified three TCA cycle acids and 11 amino acids that represent three major amino acid synthesis pathways that branch from pyruvate or TCA cycle (Table 3.4) (Buchanan et al., 2012; Kanehisa et al., 2017; T. Kim et al., 2017). Among these, four of the nine essential amino acids were quantified, indicating blueberry consumption can provide some of the essential amino acids along with the benefits of other phytochemicals (Table 3.4) (Buchanan et al., 2012; Ufaz & Galili, 2008; G. Wang et al., 2017). The total aspartate branch accounted for 69.39% of the total amino acids while the total branch-chain branch accounted for only 6.21% of the total (Table 3.4). The non-targeted profiling also quantified eight different sugars, consisting of five monosaccharides that are important for signaling and other synthesis pathways, and three disaccharides that are important for energy storage (Table 3.5) (Buchanan et al., 2012; Castellarin et al., 2016; Choi, Wiersma, Toivonen, & Kappel, 2002; C. Paniagua et al., 2014; Posé, Nieves, Quesada, & Mercado, 2011; Tsai & Gazzarrini, 2014; Wingler, 2017). Glucose constituted over half, 51.84%, of the total sugars with fructose as a close second, 47.14%, while galactose accounted for only 0.02% of the total (Table 3.5). The profiling also quantified five phenolic acids that not only effect the extract's acidity, but have also been implicated in contributing to antioxidant capacity (Table 3.6) (Ahmadinejad, Geir Møller, Hashemzadeh-Chaleshtori, Bidkhorji, & Jami, 2017; Chiva-Blanch & Visioli, 2012; Foyer & Noctor, 2011; Herrmann, 1995; Lin et al., 2016; Lobo, Patil, Phatak, & Chandra, 2010; Nabavi et al., 2018). Chlorogenic acid accounted for 36.17% of total phenolic acids, whereas caffeic acid accounts for 6.62% (Table 3.6). The non-targeted profiling annotated many important primary and specialized metabolites that contribute to multiple aspects of consumer-

based fruit quality like taste, texture, and appearance (Bingol, 2018; Capitani et al., 2014; Gilbert et al., 2014; Kyriacou & Roupael, 2018; McGinn, 2015; Rolin, Teyssier, Hong, & Gallusci, 2015; Tieman et al., 2012; Wolfender et al., 2015; Zhu et al., 2018).

The targeted profiling of the blueberry extracts with HPLC-QTOFMS annotated 23 anthocyanin metabolites using an optimized method that diluted the high acid HPLC solvent after separating the individual anthocyanins, but before injection into the QTOFMS (Tables 3.7 and 3.10). The HPLC UV detector, DAD, at wavelength 520nm detected 17 individual anthocyanins, while the QTOFMS detector used specific m/z for EIC to annotate the same 17 anthocyanins from DAD as well as an additional six anthocyanins resulting in a total of 23 (Tables 3.7 and 3.10). The DAD quantified only 17 anthocyanins because some of the anthocyanins eluted at the same time as others, and the acetyl-galactosides had very low accumulation (Tables 3.7 and 3.10, and Figure 3.36). Using the specific m/z for the different anthocyanins, the EIC can differentiate multiple metabolites within the same elution peak, as well as detects low accumulating metabolites (Tables 3.7 and 3.10, and Figure 3.36).

Overall, the comparisons between DAD and EIC anthocyanins show a positive correlation (Figures 3.27, 3.28, 3.29, 3.30, and 3.31). For both the anthocyanins annotated using DAD and EIC, the anthocyanins with anthocyanidin cores derived from delphinidin constitute over 80% of the total anthocyanins (Tables 3.8 and 3.11). For both the anthocyanins annotated using DAD and EIC, the anthocyanins with the galactoside sugar moiety constitute the largest percentage of total anthocyanins, 53.77% and 49.54% respectively (Tables 3.8 and 3.11). The arabinoside correlations show no or very weak correlations when compared between the two detection methods. The correlation patterns for the glucosides of both DAD and EIC anthocyanins show a similar “2-group” pattern when compared to the other sugar moieties (Figures 3.21, 3.24, and 3.25). One correlation, indicated by the red line, shows a subset of the population (subset T) with a strong positive correlation between glucosides with acetyl-glucosides and galactosides with arabinosides, thus indicating an allele allowing the accumulation of all types of sugar moieties. The other correlation, indicated by the green line, shows the other population subset (subset A) with a correlation that shows no to extremely little changes in glucoside with acetyl-glucoside accumulation, while

galactosides with arabinosides increase, thus suggesting an allele with specificity to only galactosides and arabinosides. Identifying the different alleles for sugar moiety specificity requires further research to elucidate the specificity and regulatory mechanisms within anthocyanin synthesis.

The antioxidant capacity and health benefits of blueberries are mainly attributed to the high accumulation of anthocyanins in the skin (Bornsek et al., 2012; De Souza et al., 2014; Gowd et al., 2017; Grace et al., 2018; Khoo et al., 2017; D. Li et al., 2017; S. Silva et al., 2018; Yousuf et al., 2016). The accumulation of other acidic metabolites like citric or phenolic acids may increase the acidity of the blueberry, thus improving the stability of the anthocyanins (Ahmadinejad et al., 2017; Chiva-Blanch & Visioli, 2012; Foyer & Noctor, 2011; Howard et al., 2016; Lin et al., 2016; Lobo et al., 2010; Nabavi et al., 2018; Wahyuningsih et al., 2017). Therefore, the antioxidant capacity was analyzed for the DxJ blueberry extracts to provide insight into variation across the population and potential metabolites that contribute to antioxidant capacity. The DPPH assay was chosen because it is quick, simple, sensitive, and cost-effective, which made it a great project for the Plant Pathways Elucidation Project undergraduate summer internship students (Himamura et al., 2014; Kedare & Singh, 2011; O. P. Sharma & Bhat, 2009; Sudhakar Singh & Singh, 2008). When the DPPH results were correlated with the anthocyanins, there was an overall positive correlation, but DAD detected anthocyanins showed a much stronger correlation than EIC anthocyanins (Figures 3.33 and 3.34). When DPPH results were correlated with other phenolic acids, there is a positive correlation with gallic acid, chlorogenic acid, and epicatechin (Figure 3.35).

Overall, both metabolite profiling approaches identified 11 amino acids, eight sugars, five phenolic acids, and 17 anthocyanins. Association mapping of the annotated metabolite peaks will provide vital information through the significant QTLs and putative candidate genes that may play a role in regulating the annotated metabolites. The association mapping of the 17 anthocyanins revealed eight significant QTL regions where at least three of the four individual acetyl-glucoside anthocyanins have a significant QTL that overlaps in the region (Table 3.17). This suggests those genetic regions may contain a putative candidate gene regulating the acetyl-glucoside modification rather than the anthocyanidin core synthesis. The DAD-anthocyanin

association mapping also revealed eight QTL regions significant for the ratio of glucosides with acetyl-glucosides, and galactosides with arabinosides (Table 3.17). This suggests those genetic regions may contain putative candidate genes regulating the addition of either a glucoside, or a galactoside or arabinoside, which would support the “2-group” correlation pattern (Figures 3.21, 3.24, and 3.25). Further putative candidate gene analysis and functional characterization of anthocyanidin synthesis and anthocyanin modification enzymes will aid in elucidating anthocyanin diversification enzymes as well as blueberry-specific enzymes.

Association mapping of the glutamine branch metabolites resulted in 26 total significant QTLs with many of those genetic regions containing important synthesis or regulatory genes as putative candidate genes (Tables 3.14 and 3.18) (Kanehisa et al., 2017; T. Kim et al., 2017). A vital gene for regulating the interconversion between glutamate and glutamine, glutamate synthase (ferredoxin-dependent), was found as a putative candidate gene for the most significant glutamine QTL (Table 3.18). The three main genes regulating gamma-aminobutyrate (GABA) synthesis and catabolism were found in the genetic regions of significant GABA QTLs on linkage group two, eight, and 12 at positions 37cM, 107cM, and 12cM, respectively (Table 3.18). The BiPAM results for branch-chain amino acids indicates that the final synthesis enzyme, branch-chain amino-acid transferase, is an important enzyme as it was a putative candidate gene in a QTL region significant for the essential amino acids, isoleucine, valine, and leucine (Table 3.18). The significant aspartate branch QTLs indicate that aspartate degradation towards other amino acid biosynthesis pathways is important as aspartokinase and aspartate semialdehyde dehydrogenase were found as putative candidate genes in multiple aspartate QTLs (Table 3.18). The BiPAM results for threonine indicate that the multiple threonine biosynthesis pathways may contribute to and regulate overall threonine accumulation (Table 3.18). The identified QTLs and putative candidate genes for important TCA and amino acids can be utilized for future research to further annotate and elucidate regulatory pathways of essential amino acids so that breeding strategies can be developed to apply and improve the health benefits of blueberries.

The BiPAM results for the sugars revealed the PPP, cell wall component polysaccharide degradation, and sugar interconversions are important pathways (Table 3.19) (Buchanan et al., 2012; Kanehisa et al., 2017; T. Kim et al., 2017). Significant fructose QTLs consistently had putative candidate genes from the PPP in the genetic regions (Table 3.19). The INV enzyme breaks down sucrose into glucose and fructose and was found as a putative candidate gene in three significant QTLs for sucrose, fructose, and glucose (Table 3.19). Amylases and glucosidases cleave 1,4-glycosidic bonds in polysaccharides to release free maltose or glucose, respectively, and were found as putative candidate genes for multiple maltose and glucose significant QTLs (Table 3.19). The other monosaccharide sugars like galactose, xylose, and arabinose are derivatives of UDP-glucose and the enzymes catalyzing the different interconversions were found as putative candidate genes across multiple significant QTLs (Table 3.19). Galactose and xylose are also important components for the backbones and branches of cell wall matrix polysaccharides like hemicellulose and pectin (Buchanan et al., 2012; Giongo et al., 2013; C. Paniagua et al., 2014; Posé et al., 2011). Degradation or modification of hemicellulose and pectin by enzymes like polygalacturonase or XTH not only effects the monosaccharides accumulation, but also effects the integrity of the cell wall matrix, which can lead to fruit softening (Giongo et al., 2013; C. Paniagua et al., 2014; Posé et al., 2011). Those degradation enzymes were also found as putative candidate genes across multiple significant QTLs (Table 3.19). Identifying QTLs and putative candidate genes for multiple, different sugars is important foundational knowledge that future research can build upon to regulate their accumulation and improve berry development, sweet taste, berry firmness, and anthocyanin diversity through developing breeding strategies.

The BiPAM results for the phenolic acids revealed over 40 significant QTL regions (Table 3.20) (Kanehisa et al., 2017; T. Kim et al., 2017). Gallic acid and quinic acid synthesis occurs within the shikimic pathway, and then ends in phenylalanine synthesis. Quinate dehydrogenase and 3-dehydrpquinate dehydratase are important committing steps in the shikimate pathway that were both found as putative candidate genes for multiple significant QTLs for gallic acid and quinic acid (Table 3.20). The last synthesis step for phenylalanine synthesis, arogenate/prephenate dehydratase, and

PAL, the first committed step towards phenylpropanoid acid synthesis, were found as putative candidate genes within a significant QTL region for gallic, quinic, chlorogenic, and caffeic acid, thus indicating phenylalanine is vital for the phenolic acid pathway progression (Table 3.20). HCT catalyzes the two important steps in phenylpropanoid acid synthesis, especially breaking down chlorogenic acid to caffeoyl-CoA and release of quinic acid. HCT was found as a putative candidate gene across multiple QTL regions significant for chlorogenic and quinic acid (Table 3.20).

The BiPAM results for epicatechin reveals multiple putative candidate genes at multiple steps in the flavonoid pathway (Table 3.20) (Kanehisa et al., 2017; T. Kim et al., 2017). CHS catalyzes the committing step towards flavonoid synthesis by converting p-coumaroyl-CoA to naringenin-chalcone, and was found as a putative candidate gene for multiple significant epicatechin QTLs (Table 3.20). Diversification of flavonoids occurs with the activity of F3'H and F3'5'H to produce dihydroquercetin and dihydromyricetin, which can then be converted to leucocyanidin and leucodelphinidin, respectively, by DFR. ANS converts the leucoanthocyanidins to anthocyanidins, which can then be either converted to epicatechin by ANR, or progress to further anthocyanin diversification. Although F3'H, F3'5'H, DFR, ANS, and ANR were found as putative candidate genes across multiple significant QTLs, F3'H and F3'5'H putative candidate genes were found in over 60% of the significant epicatechin QTLs (Table 3.20). This indicates that diversification of flavonoids is important to epicatechin accumulation (Ali Ghasemzadeh, 2011; Horbowicz et al., 2008; Howard et al., 2016; Khoo et al., 2017; D. Li et al., 2017; Ma et al., 2018; Montecchiarini et al., 2018; Routray & Orsat, 2011; Scalzo et al., 2015; You et al., 2011). The identified QTLs and putative candidate genes provides additional knowledge on the phenolic acid pathway, which can be utilized to elucidate the regulation of phenolic acid diversification (Herrmann, 1995; Kanehisa et al., 2017; T. Kim et al., 2017; Lin et al., 2016; Nabavi et al., 2018). A greater understanding of phenolic acid diversification will improve the differential accumulation of shikimic pathway acids, phenylpropanoids, and flavonoids, which will not only affect the sour-tart taste of blueberries, but also the blue coloration through stabilizing anthocyanins (Kader, 2008; Khoo et al., 2017; McGinn, 2015; Pagliarini, Laureati, &

Gaeta, 2013; Tieman et al., 2012; Yonekura-Sakakibara, Nakayama, Yamazaki, & Saito, 2009).

Along with mapping the metabolites from non-targeted and targeted profiling, the antioxidant capacity measured through the DPPH assay was also mapped. The BiPAM results revealed two significant QTLs, one on linkage group five at position 107cM and the another on linkage group six at position 45cM (Table 3.21). Both significant QTLs contained the putative candidate genes, p-coumaroyl-CoA ligase, F3'H, and F3'5'H, indicating phenylpropanoid and flavonoid synthesis pathway and metabolites contribute to antioxidant capacity (Table 3.21) (Kanehisa et al., 2017; T. Kim et al., 2017). Both QTL regions also contain important, but different enzymes in the shikimic pathway, suggesting the shikimic pathway also plays an important role in antioxidant capacity (Table 3.21) (Kanehisa et al., 2017; T. Kim et al., 2017). In the DPPH QTL on linkage group five at position 107cM, putative candidate genes for anthocyanin diversification were also found, which supports the strong association between anthocyanins and antioxidant capacity (Table 3.21) (Bornsek et al., 2012; De Souza et al., 2014; Gowd et al., 2017; Grace et al., 2018; Khoo et al., 2017; D. Li et al., 2017; S. Silva et al., 2018; Yousuf et al., 2016). In the DPPH QTL on linkage group six at position 45cM, there are also putative candidate genes for catalase and the ascorbate-glutathione cycling pathway, which indicates that enzymatic antioxidants may also contribute to the antioxidant capacity found in blueberries (Table 3.21). Identifying the QTLs and putative candidate genes for antioxidant capacity provides additional support for associating phenolic acids with antioxidant capacity as well as suggesting the antioxidant potency may be a synergistic interaction between multiple metabolites in blueberries (Bornsek et al., 2012; De Souza et al., 2014; Gowd et al., 2017; Khoo et al., 2017; D. Li et al., 2017; S. Silva et al., 2018; Yousuf et al., 2016). Future research will utilize this knowledge to elucidate the diversity, combination, and potency of different metabolites that improve the antioxidant capacity in blueberries, like phenylpropanoids not only can stabilize anthocyanins and improve their antioxidant capacity, but also can act as antioxidants to further improve antioxidant capacity (Bornsek et al., 2012; De Souza et al., 2014; Gowd et al., 2017; Khoo et al., 2017; D. Li et al., 2017; S. Silva et al., 2018; Yousuf et al., 2016). Through identifying multiple significant QTLs and putative candidate genes for

metabolites that contribute to the diversity of health benefits of blueberries, breeders can utilize multiple QTLs in breeding strategies to develop blueberries with enhanced health benefits.

5.3. Broccoli agronomic associated genetic regions containing possible regulatory genes

Broccoli, *Brassica oleracea* var. *italica*, is an important vegetable crop that is gaining research attention due to multiple studies strongly associating broccoli extracts with potent anticarcinogenic properties (Armah et al., 2013; Cornblatt et al., 2007; F. Li, Hullar, Beresford, & Lampe, 2011; Oliviero, Verkerk, & Dekker, 2012; Saban, 2018; M. Traka & Mithen, 2009; Yanaka et al., 2009). Improving consumer consumption of broccoli may be difficult due to the bitter taste most commonly linked to glucosinolate or isothiocyanate compounds, commonly found in the *Brassica* genus (Drewnowski & Gomez-Carneros, 2000; Fenwick, Griffiths, & Heaney, 1983; Kader, 2008; van Doorn et al., 1998). Unfortunately, reducing glucosinolates or isothiocyanates accumulation in broccoli would reduce its anticarcinogenic qualities (Cornblatt et al., 2007; Dinkova-Kostova et al., 2006; Saban, 2018; Tawfiq et al., 1995; M. Traka & Mithen, 2009; Vallejo, García-Viguera, & Tomás-Barberán, 2003). Multiple studies show that when the specific glucosinolate, glucoraphanin, is converted by myrosinase to its isothiocyanate, sulforaphane, it exhibits anticarcinogenic properties very similar to current anticarcinogenic drugs (Cornblatt et al., 2007; Dinkova-Kostova et al., 2006; Kanehisa et al., 2017; T. Kim et al., 2017; Saban, 2018; M. Traka & Mithen, 2009; Vallejo et al., 2003; Van Eylen, Oey, Hendrickx, & Van Loey, 2007). Glucoraphanin and sulforaphane accumulation is highest in broccoli, therefore, improving agronomic traits will aid in providing more broccoli to consumers and allow more consumers access to its health benefits (Baik et al., 2003; Brown et al., 2002; Farnham, Stephenson, & Fahey, 2005; M. H. Traka et al., 2013; Yanaka et al., 2009). The research goals of this chapter were to identify important QTL regions for broccoli agronomics using a genome-wide association study, with a focus on investigating harvest and pathogen resistance.

Broccoli is grown and harvested for two seasons, an early spring crop and mid-fall crop, due to some cold tolerance in *Brassica* crops (Brown, Jeffery, & Juvik, 2007; Farnham & Harrison, 2003; Farnham et al., 2005; Greenhalgh & Mitchell, 1976; Jenni,

Dutilleul, Yamasaki, & Tremblay, 2001; Sones, Heaney, & Fenwick, 1984). Extending the broccoli season would allow for three harvests instead of two, which would result in an increase in broccoli production. Improving broccoli's cold-tolerance would allow for the season to extend into the winter. Unfortunately, this may increase the risk of broccoli floret damage if temperatures drop too quickly (D.-H. Kim & Sung, 2014; S. Sanghera, H. Wani, Hussain, & B. Singh, 2011; Zuther, Juszczak, Ping Lee, Baier, & Hinch, 2015). Broccoli growth and maturation time could also be shortened through promoting faster growth and quicker transition to reproductive maturity. Photoperiodism is the sensing and responding to changes in daylength, usually through phytochromes starting a signal transduction cascade as the daylength shortens (I. Lee & Amasino, 1995; B. Liu et al., 2016; Park et al., 1999; Soy, Leivar, & Monte, 2014; Wilkie, Sedgley, & Olesen, 2008). The signal transduction cascade induces the shoot apical meristem to transition for floral and reproductive meristems so that the broccoli floret can start developing (I. Lee & Amasino, 1995; B. Liu et al., 2016; Park et al., 1999; Soy et al., 2014; Wilkie et al., 2008). Utilizing genetic association mapping for a complex trait like harvest season allows for identification of QTLs that may regulate multiple pathways within the signal transduction cascade. The association mapping of the days to harvest trait revealed two significant QTLs. Within the genetic regions for these QTLs, there were two photoperiodism, three floral meristem, and five signal transduction putative candidate genes. These results indicate that the days to harvest QTLs most likely play a role in regulating floral meristem transition in broccoli.

Due to the close proximity to the ground and compact foliage, broccoli is affected by many pathogens and pests (Farnham & Harrison, 2003; Farnham et al., 2005; Greenhalgh & Mitchell, 1976; Jenni et al., 2001; Rangkadilok et al., 2004; Sones et al., 1984). Broccoli pathogens consists primarily of fungi and bacteria that thrive in the compact, sheltered florets (Bones & Rossiter, 2006; Hopkins, van Dam, & van Loon, 2009; Ignatov, Kuginuki, & Hida, 1999; Jenni et al., 2001; Lan & Paterson, 2000; Nault, Reiners, Hsu, & Hoeping, 2010; Rimmer & van den Berg, 1992; Williams, 2007). Broccoli exhibits less biomass loss from pests like insects and invertebrates than tissue loss from pathogen damage due to glucosinolates and isothiocyanates acting as endogenous pesticides that inhibit pest gastrointestinal function (Fahey, Zalcmann, &

Talalay, 2001; Greenhalgh & Mitchell, 1976; Lionetti et al., 2007; Rimmer & van den Berg, 1992). Thus, investigating pathogen resistance through genetic association mapping will identify important QTL regions and putative candidate genes that may play a role in specific or non-specific pathogen resistance.

In general, pathogen resistance consists of pathogen recognition, signal transduction, and resistance response (Buchanan et al., 2012; Gardner, Heinz, Wang, & Mitchum, 2017; Hanson et al., 2016; Klink & Matthews, 2009; Miedaner & Korzun, 2012; Mitchum, 2016). Pathogen recognition consists of membrane-bound plant receptors that recognize specific degradation products from pathogen enzymes trying to degrade cell wall components (Conrath, Beckers, Langenbach, & Jaskiewicz, 2015; Dodds & Rathjen, 2010; Fu & Dong, 2013; Howe & Jander, 2007). There is a constant “arms-race” between pathogen and plant to evolve infiltration mechanisms that plant has no receptors to and evolve receptors capable of recognizing specific or novel mechanisms (Conrath et al., 2015; Dodds & Rathjen, 2010; Fu & Dong, 2013; Howe & Jander, 2007). Once the pathogen attack signal is recognized, it is transduced through multiple pathways in order to induce an appropriate resistance response (Buchanan et al., 2012; Conrath et al., 2015; Dodds & Rathjen, 2010; Fu & Dong, 2013; Howe & Jander, 2007). The regulation of Ca^{2+} across membranes is one of the earliest signals to transduce the pathogen attack signal (Buchanan et al., 2012; Cheval, Aldon, Galaud, & Ranty, 2013; Conrath et al., 2015; Dodds & Rathjen, 2010; Fu & Dong, 2013; Howe & Jander, 2007; Kolukisaoglu, 2004; Vadassery & Oelmüller, 2009). Once the signal is appropriately transduced, the resulting pathogen resistance responses are up-regulated to prevent further spread of the pathogen (Buchanan et al., 2012; Conrath et al., 2015; Dodds & Rathjen, 2010; Fu & Dong, 2013; Howe & Jander, 2007). The genetic association mapping of pathogen-related traits revealed five pathogen resistance hotspots where multiple pathogen-related traits have overlapping QTL regions. Multiple calcium binding and signaling putative candidate genes were found in each of the ‘hot-spots’. Other signaling transducers like PDF and PAD4 as well as known pathogen-resistance transcription factors were found within the significant QTL regions (de Oliveira Carvalho & Moreira Gomes, 2011; Feys, Moisan, Newman, & Parker, 2001; Rustérucci, Aviv, Holt, Dangl, & Parker, 2001; Shafee, Lay, Hulett, & Anderson, 2016). Overall, the

majority of putative candidate genes found within the significant pathogen-resistance 'hot-spot' QTLs are involved in signal transduction to differential transcription, indicating that efficient signaling of the pathogen attack is vital to mounting an appropriate pathogen resistance response.

REFERENCES

- Ahmadinejad, F., Geir Møller, S., Hashemzadeh-Chaleshtori, M., Bidkhor, G., & Jami, M.-S. (2017). Molecular Mechanisms behind Free Radical Scavengers Function against Oxidative Stress. *Antioxidants*, 6(3), 51.
- Al-Khayri, J. M., Jain, S. M., & Johnson, D. V. (2015). *Advances in Plant Breeding Strategies: Breeding, Biotechnology and Molecular Tools*. Cham: Springer International Publishing.
- Ali Ghasemzadeh. (2011). Flavonoids and phenolic acids: Role and biochemical activity in plants and human. *Journal of Medicinal Plants Research*, 5(31), 6697–6703.
- Anderson, J. V. (2015). *Advances in plant dormancy*. (J. V. Anderson, Ed.). New York, NY: Springer Science+Business Media.
- Armah, C. N., Traka, M. H., Dainty, J. R., Defernez, M., Janssens, A., Leung, W., ... Mithen, R. F. (2013). A diet rich in high-glucoraphanin broccoli interacts with genotype to reduce discordance in plasma metabolite profiles by modulating mitochondrial function. *American Journal of Clinical Nutrition*, 98(3), 712–722.
- Arora, R., Rowland, L. J., & Tanino, K. (2003). Induction and release of bud dormancy in woody perennials: A science comes of age. *HortScience*, 38(5), 911–921.
- Baik, H.-Y., Juvik, J. A., Jeffery, E. H., Wallig, M. A., Kushad, M., & Klein, B. P. (2003). Relating glucosinolate content and flavor of broccoli cultivars. *Journal of Food Science*, 68(3), 1043–1050.
- Bar, M., & Ori, N. (2014). Leaf development and morphogenesis. *Development*, 141(22), 4219–4230.
- Barrett, D. M., Beaulieu, J. C., & Shewfelt, R. (2010). Color, flavor, texture, and nutritional quality of fresh-cut fruits and vegetables: Desirable levels, instrumental and sensory measurement, and the effects of processing. *Critical Reviews in Food Science and Nutrition*, 50(5), 369–389.
- Basler, D., & Körner, C. (2012). Photoperiod sensitivity of bud burst in 14 temperate forest tree species. *Agricultural and Forest Meteorology*, 165, 73–81.
- Basler, D., & Körner, C. (2014). Photoperiod and temperature responses of bud swelling and bud burst in four temperate forest tree species. *Tree Physiology*, 34(4), 377–388.
- Beauvieux, R., Wenden, B., & Dirlwanger, E. (2018). Bud Dormancy in Perennial Fruit Tree Species: A Pivotal Role for Oxidative Cues. *Frontiers in Plant Science*, 9(May), 1–13.
- Bennett, E., Roberts, J. A., & Wagstaff, C. (2012). Manipulating resource allocation in plants. *Journal of Experimental Botany*, 63(9), 3391–3400.
- Betoret, E., Betoret, N., Vidal, D., & Fito, P. (2011). Functional foods development: Trends and technologies. *Trends in Food Science and Technology*, 22(9), 498–508.
- Biltekoff, C. (2010). Consumer response: The paradoxes of food and health. *Annals of the New York Academy of Sciences*, 1190, 174–178.
- Bingol, K. (2018). Recent Advances in Targeted and Untargeted Metabolomics by NMR and MS/NMR Methods. *High-Throughput*, 7(2), 9.
- Bones, A., & Rossiter, J. (2006). The enzymic and chemically induced decomposition of glucosinolates. *Phytochemistry*, 67(11), 1053–1067.
- Borevitz, J. O., & Chory, J. (2004). Genomics tools for QTL analysis and gene

- discovery. *Current Opinion in Plant Biology*, 7(2), 132–136.
- Bornsek, S. M., Ziberna, L., Polak, T., Vanzo, A., Ulrich, N. P., Abram, V., ... Passamonti, S. (2012). Bilberry and blueberry anthocyanins act as powerful intracellular antioxidants in mammalian cells. *Food Chemistry*, 134(4), 1878–1884.
- Boudsocq, M., Willmann, M. R., McCormack, M., Lee, H., Shan, L., He, P., ... Sheen, J. (2010). Differential innate immune signalling via Ca²⁺ sensor protein kinases. *Nature*, 464(7287), 418–422.
- Brown, A. F., Jeffery, E. H., & Juvik, J. A. (2007). A polymerase chain reaction-based linkage map of broccoli and identification of quantitative trait loci associated with harvest date and head weight. *Journal of the American Society for Horticultural Science*, 132(4), 507–513.
- Brown, A. F., Yousef, G. G., Jeffery, E. H., Klein, B. P., Wallig, M. A., Kushad, M. M., & Juvik, J. A. (2002). Glucosinolate Profiles in Broccoli: Variation in Levels and Implications in Breeding for Cancer Chemoprotection. *Journal of American Soci and Horticulture Science*, 127(5), 807–813.
- Buchanan, B. B., Gruissem, W., & Jones, R. L. (2012). *Biochemistry & Molecular Biology of Plants*. American Society of Plant Biologists: 15501 Monona Drive, Rockville, MD 20855-2768 USA: Markono Print Media Pte Ltd.
- Bunea, A., Rugină, D., Sconța, Z., Pop, R. M., Pinte, A., Socaciu, C., ... VanCamp, J. (2013). Anthocyanin determination in blueberry extracts from various cultivars and their antiproliferative and apoptotic properties in B16-F10 metastatic murine melanoma cells. *Phytochemistry*, 95, 436–444.
- Capitani, D., Sobolev, A. P., Delfini, M., Vista, S., Antiochia, R., Proietti, N., ... Mannina, L. (2014). NMR methodologies in the analysis of blueberries: General. *ELECTROPHORESIS*, 35(11), 1615–1626. h
- Cappai, F., Benevenuto, J., Ferrão, L., & Munoz, P. (2018). Molecular and Genetic Bases of Fruit Firmness Variation in Blueberry—A Review. *Agronomy*, 8(9), 174.
- Carreno-Quintero, N., Bouwmeester, H. J., & Keurentjes, J. J. B. (2013). Genetic analysis of metabolome–phenotype interactions: from model to crop species. *Trends in Genetics*, 29(1), 41–50.
- Castellarin, S. D., Gambetta, G. A., Wada, H., Krasnow, M. N., Cramer, G. R., Peterlunger, E., ... Matthews, M. A. (2016). Characterization of major ripening events during softening in grape: Turgor, sugar accumulation, abscisic acid metabolism, colour development, and their relationship with growth. *Journal of Experimental Botany*, 67(3), 709–722. h
- Chae, L., Kim, T., Nilo-Poyanco, R., & Rhee, S. Y. (2014). Genomic Signatures of Specialized Metabolism in Plants. *Science*, 344(May), 510–513.
- Cheval, C., Aldon, D., Galaud, J.-P., & Ranty, B. (2013). Calcium/calmodulin-mediated regulation of plant immunity. *Biochimica et Biophysica Acta (BBA) - Molecular Cell Research*, 1833(7), 1766–1771.
- Chiva-Blanch, G., & Visioli, F. (2012). Polyphenols and health: Moving beyond antioxidants. *Journal of Berry Research*, 2(2), 63–71.
- Choi, C., Wiersma, P. A., Toivonen, P., & Kappel, F. (2002). Fruit growth, firmness and cell wall hydrolytic enzyme activity during development of sweet cherry fruit treated with gibberellic acid (GA3). *Journal of Horticultural Science and Biotechnology*, 77(5), 615–621.

- Collard, B. C. Y., Jahufer, M. Z. Z., Brouwer, J. B., & Pang, E. C. K. (2005). An introduction to markers, quantitative trait loci (QTL) mapping and marker-assisted selection for crop improvement: The basic concepts. *Euphytica*, *142*(1–2), 169–196.
- Conrath, U., Beckers, G. J. M., Langenbach, C. J. G., & Jaskiewicz, M. R. (2015). Priming for Enhanced Defense. *Annual Review of Phytopathology*, *53*(1), 97–119.
- Considine, M. J., & Considine, J. A. (2016). On the language and physiology of dormancy and quiescence in plants. *Journal of Experimental Botany*, *67*(11), 3189–3203.
- Cooke, J. E. K., Eriksson, M. E., & Junttila, O. (2012). The dynamic nature of bud dormancy in trees: environmental control and molecular mechanisms. *Plant, Cell & Environment*, *35*(10), 1707–1728. h
- Coombe, B. G., & McCarthy, M. G. (2000). Dynamics of grape growth and physiology of ripening. *Australian Journal of Grape and Wine Research*, *6*(2), 131–135.
- Cornblatt, B. S., Ye, L., Dinkova-Kostova, A. T., Erb, M., Fahey, J. W., Singh, N. K., ... Visvanathan, K. (2007). Preclinical and clinical evaluation of sulforaphane for chemoprevention in the breast. *Carcinogenesis*, *28*(7), 1485–1490.
- Costes, E., Crespel, L., Denoyes, B., Morel, P., Demene, M.-N., Lauri, P.-E., & Wenden, B. (2014). Bud structure, position and fate generate various branching patterns along shoots of closely related Rosaceae species: a review. *Frontiers in Plant Science*, *5*(December), 1–11.
- de Oliveira Carvalho, A., & Moreira Gomes, V. (2011). Plant Defensins and Defensin-Like Peptides - Biological Activities and Biotechnological Applications. *Current Pharmaceutical Design*, *17*(38), 4270–4293.
- De Souza, V. R., Pereira, P. A. P., Da Silva, T. L. T., De Oliveira Lima, L. C., Pio, R., & Queiroz, F. (2014). Determination of the bioactive compounds, antioxidant activity and chemical composition of Brazilian blackberry, red raspberry, strawberry, blueberry and sweet cherry fruits. *Food Chemistry*, *156*, 362–368.
- Del Pozo, J. C., Lopez-Matas, M. A., Ramirez-Parra, E., & Gutierrez, C. (2005). Hormonal control of the plant cell cycle. *Physiologia Plantarum*, *123*(2), 173–183.
- Denancé, N., Sánchez-Vallet, A., Goffner, D., & Molina, A. (2013). Disease resistance or growth: the role of plant hormones in balancing immune responses and fitness costs. *Frontiers in Plant Science*, *4*.
- Díaz-Riquelme, J., Grimplet, J., Martínez-Zapater, J. M., & Carmona, M. J. (2012). Transcriptome variation along bud development in grapevine (*Vitis vinifera* L.). *BMC Plant Biology*, *12*.
- Die, J. V., Arora, R., & Rowland, L. J. (2016). Global patterns of protein abundance during the development of cold hardiness in blueberry. *Environmental and Experimental Botany*, *124*, 11–21.
- Dinkova-Kostova, A. T., Jenkins, S. N., Fahey, J. W., Ye, L., Wehage, S. L., Liby, K. T., ... Talalay, P. (2006). Protection against UV-light-induced skin carcinogenesis in SKH-1 high-risk mice by sulforaphane-containing broccoli sprout extracts. *Cancer Letters*, *240*(2), 243–252.
- Dodds, P. N., & Rathjen, J. P. (2010). Plant immunity: Towards an integrated view of plant-pathogen interactions. *Nature Reviews Genetics*, *11*(8), 539–548.
- Draper, A., & Hancock, J. F. (2003). Florida 4B: Native Blueberry with Exceptional

- Breeding Value. *Journal of the American Pomological Society*, 57(4), 138–141.
- Drewnowski, A., & Gomez-Carneros, C. (2000). Bitter taste, phytonutrients, and the consumer: a review. *The American Journal of Clinical Nutrition*, 72(6), 1424–1435.
- Ehlenfeldt, M. (2012). Cold-hardiness, acclimation, and deacclimation among diverse blueberry genotypes. *Journal of the ...*, 137(1), 31–37.
- Fahey, J. W., Zalcmann, A. T., & Talalay, P. (2001). The Chemical Diversity and Distribution of Glucosinolates and Isothiocyanates Among Plants. *Phytochemistry*, 56, 5–51.
- Farnham, M. W., & Harrison, H. F. (2003). Using Self-compatible Inbreds of Broccoli as Seed Producers. *Horticulture Science*, 38(1), 85–87.
- Farnham, M. W., Stephenson, K. K., & Fahey, J. W. (2005). Glucoraphanin Level in Broccoli Seed is Largely Determined by Genotype. *Horticulture Science*, 40(1), 50–53.
- Fenwick, G. R., Griffiths, N. M., & Heaney, R. K. (1983). Bitterness in Brussels sprouts (*Brassica oleracea* L. var. *gemmifera*): the role of glucosinolates and their breakdown products. *Journal of the Science of Food and Agriculture*, 34(1), 73–80.
- Fernie, A. R., & Schauer, N. (2009). Metabolomics-assisted breeding: a viable option for crop improvement? *Trends in Genetics*, 25(1), 39–48.
- Feys, B. J., Moisan, L. J., Newman, M.-A., & Parker, J. E. (2001). Direct interaction between the *Arabidopsis* disease resistance signaling proteins, EDS1 and PAD4. *The EMBO Journal*, 20(19), 5400–5411.
- Forney, C. F., Kalt, W., Jordan, M. A., Vinqvist-Tymchuk, M. R., & Fillmore, S. A. E. (2012). Blueberry and cranberry fruit composition during development. *Journal of Berry Research*, 2(3), 169–177.
- Foyer, C. H., & Noctor, G. (2011). Ascorbate and Glutathione: The Heart of the Redox Hub. *Plant Physiology*, 155(1), 2–18.
- Freeman, B. C., & Beattie, G. A. (2008). An Overview of Plant Defenses against Pathogens and Herbivores. *Iowa State University - Plant Pathology and Microbiology Publications*, 1–12.
- Fu, Z. Q., & Dong, X. (2013). Systemic Acquired Resistance: Turning Local Infection into Global Defense. *Annual Review of Plant Biology*, 64(1), 839–863.
- Gardner, M., Heinz, R., Wang, J., & Mitchum, M. G. (2017). Genetics and Adaptation of Soybean Cyst Nematode to Broad Spectrum Soybean Resistance. *G3: Genes|Genomes|Genetics*, 7(3), 835–841.
- Ghelardini, L., Santini, A., Black-Samuelsson, S., Myking, T., & Falusi, M. (2009). Bud dormancy release in elm (*Ulmus* spp.) clones - A case study of photoperiod and temperature responses. *Tree Physiology*, 30(2), 264–274.
- Giacalone, M., Di Sacco, F., Traupe, I., Topini, R., Forfori, F., & Giunta, F. (2011). Antioxidant and neuroprotective properties of blueberry polyphenols: a critical review. *Nutritional Neuroscience*, 14(3), 119–125.
- Gilbert, J. L., Guthart, M. J., Gezan, S. A., de Carvalho, M. P., Schwieterman, M. L., Colquhoun, T. A., ... Olmstead, J. W. (2015). Identifying breeding priorities for blueberry flavor using biochemical, sensory, and genotype by environment analyses. *PLoS One*, 10(9), 1–21.
- Gilbert, J. L., Olmstead, J. W., Colquhoun, T. A., Levin, L. A., Clark, D. G., & Moskowitz, H. R. (2014). Consumer-assisted selection of blueberry fruit quality traits.

- HortScience*, 49(7), 864–873.
- Giongo, L., Poncetta, P., Loretto, P., & Costa, F. (2013). Texture profiling of blueberries (*Vaccinium* spp.) during fruit development, ripening and storage. *Postharvest Biology and Technology*, 76, 34–39.
- Giovannoni, J. J. (2004). Genetic Regulation of Fruit Development and Ripening. *The Plant Cell*, 16, S170–S180.
- Godoy, C., Monterubbianesi, G., & Tognetti, J. (2008). Analysis of highbush blueberry (*Vaccinium corymbosum* L.) fruit growth with exponential mixed models. *Scientia Horticulturae*, 115(4), 368–376.
- Gould, N., Morrison, D. R., Clearwater, M. J., Ong, S., Boldingh, H. L., & Minchin, P. E. H. (2013). Elucidating the sugar import pathway into developing kiwifruit berries (*Actinidia deliciosa*). *New Zealand Journal of Crop and Horticultural Science*, 41(4), 189–206.
- Gowd, V., Jia, Z., & Chen, W. (2017). Anthocyanins as promising molecules and dietary bioactive components against diabetes – A review of recent advances. *Trends in Food Science and Technology*, 68, 1–13.
- Grace, M. H., Xiong, J., Esposito, D., Ehlenfeldt, M., & Lila, M. A. (2018). Simultaneous LC-MS quantification of anthocyanins and non-anthocyanin phenolics from blueberries with widely divergent profiles and biological activities. *Food Chemistry*.
- Greenhalgh, J. R., & Mitchell, N. D. (1976). The Involvement of Flavour Volatiles in the Resistance to Downy Mildew of Wild and Cultivated Forms of *Brassica oleracea*, 77, 391–398.
- Grunert, K. G. (2005). Food quality and safety: Consumer perception and demand. *European Review of Agricultural Economics*, 32(3), 369–391.
- Gul, K., Tak, A., Singh, A. K., Singh, P., Yousuf, B., & Wani, A. A. (2015). Chemistry, encapsulation, and health benefits of B-carotene - A review. *Cogent Food & Agriculture*, 1(1), 1–12.
- Hancock, J F, Lyrene, P., Finn, C. E., Vorsa, N., Lobos, G. A., Building, S. S., ... Agronomia, D. (2008). Blueberries and Cranberries. In James F. Hancock (Ed.), *Temperate Fruit Crop Breeding: Germplasm to Genomics* (pp. 1–31). Dordrecht, The Netherlands: Springer, Kluwer Academic Publishers.
- Hancock, Jim F. (2008). *Temperate fruit crop breeding: germplasm to genomics*. (James F. Hancock, Ed.), *Temperate fruit crop. Germoplasm to genomics*. Springer Science+Business Media. h
- Hanson, P., Lu, S. F., Wang, J. F., Chen, W., Kenyon, L., Tan, C. W., ... Yang, R. Y. (2016). Conventional and molecular marker-assisted selection and pyramiding of genes for multiple disease resistance in tomato. *Scientia Horticulturae*, 201, 346–354.
- Herrmann, K. M. (1995). The shikimate pathway: early steps in the biosynthesis of aromatic compounds. *The Plant Cell*, 7(7), 907.
- Heslot, N., Yang, H.-P., Sorrells, M. E., & Jannink, J.-L. (2012). Genomic Selection in Plant Breeding: A Comparison of Models. *Crop Science*, 52(1), 146.
- Himamura, T. S., Umikura, Y. S., Amazaki, T. Y., Ada, A. T., Ashiwagi, T. K., Shikawa, H. I., ... Keda, H. U. (2014). Applicability of the DPPH Assay for Evaluating the Antioxidant Capacity of Food Additives - Inter-laboratory Evaluation Study. *Analytical Sciences*, 30(July), 717–721.

- Hopkins, R. J., van Dam, N. M., & van Loon, J. J. A. (2009). Role of Glucosinolates in Insect-Plant Relationships and Multitrophic Interactions. *Annual Review of Entomology*, 54(1), 57–83.
- Horbowicz, M., Grzesiuk, A., DEBski, H., & Kosson, R. (2008). Anthocyanins of Fruits and Vegetables - Their Occurrence, Analysis and Role in Human. *Vegetable Crops Research Bulletin*, 68, 5–22.
- Horvath, D. P., Anderson, J. V., Chao, W. S., & Foley, M. E. (2003). Knowing when to grow: Signals regulating bud dormancy. *Trends in Plant Science*, 8(11), 534–540.
- Howard, L. R., Brownmiller, C., Mauromoustakos, A., & Prior, R. L. (2016). Improved stability of blueberry juice anthocyanins by acidification and refrigeration. *Journal of Berry Research*, 6(2), 189–201.
- Howe, G. A., & Jander, G. (2007). Plant Immunity to Insect Herbivores. *Annual Review of Plant Biology*, 59(1), 41–66.
- Huan, C., Jiang, L., An, X., Yu, M., Xu, Y., Ma, R., & Yu, Z. (2016). Potential role of reactive oxygen species and antioxidant genes in the regulation of peach fruit development and ripening. *Plant Physiology and Biochemistry*, 104, 294–303.
- Ignatov, A., Kuginuki, Y., & Hida, K. (1999). Vascular Stem Resistance to Black Rot in Brassica oleracea. *Canadian Journal of Botany*, 77(3), 442–446.
- Jenni, S., Dutilleul, P., Yamasaki, S., & Tremblay, N. (2001). Brown bead of broccoli. I. Response of the physiological disorder to management practices. *HortScience*, 36(7), 1224–1227.
- Jia, H., Xie, Z., Wang, C., Shangguan, L., Qian, N., Cui, M., ... Fang, J. (2017). Abscisic acid, sucrose, and auxin coordinately regulate berry ripening process of the Fujiminori grape. *Functional and Integrative Genomics*, 17(4), 441–457.
- Kader, A. A. (2008). Flavor quality of fruits and vegetables. *Journal of the Science of Food and Agriculture*, 88(11), 1863–1868.
- Kai, H., Kinoshita, K., Harada, H., Uesawa, Y., Maeda, A., Suzuki, R., ... Matsuno, K. (2017). Establishment of a Direct-Injection Electron Ionization-Mass Spectrometry Metabolomics Method and Its Application to Lichen Profiling. *Analytical Chemistry*, 89(12), 6408–6414.
- Kanehisa, M., Furumichi, M., Tanabe, M., Sato, Y., & Morishima, K. (2017). KEGG: New perspectives on genomes, pathways, diseases and drugs. *Nucleic Acids Research*, 45(D1), D353–D361.
- Kang, M. S. (2002). *Quantitative genetics, genomics and plant breeding*. New York: CABI Publishing.
- Kang, Y., Khan, S., & Ma, X. (2009). Climate change impacts on crop yield, crop water productivity and food security - A review. *Progress in Natural Science*, 19(12), 1665–1674.
- Karppinen, K., Hirvelä, E., Nevala, T., Sipari, N., Suokas, M., & Jaakola, L. (2013). Changes in the abscisic acid levels and related gene expression during fruit development and ripening in bilberry (*Vaccinium myrtillus* L.). *Phytochemistry*, 95, 127–134.
- Karppinen, K., Zoratti, L., Nguyenquynh, N., Häggman, H., & Jaakola, L. (2016). On the Developmental and Environmental Regulation of Secondary Metabolism in *Vaccinium* spp. Berries. *Frontiers in Plant Science*, 7(May), 1–9.
- Kearney, J. (2010). Food consumption trends and drivers. *Philosophical Transactions of*

- the Royal Society B: Biological Sciences*, 365(1554), 2793–2807.
- Kedare, S. B., & Singh, R. P. (2011). Genesis and development of DPPH method of antioxidant assay. *Journal of Food Science and Technology*, 48(4), 412–422.
- Khoo, H. E., Azlan, A., Tang, S. T., & Lim, S. M. (2017). Anthocyanidins and anthocyanins: colored pigments as food, pharmaceutical ingredients, and the potential health benefits. *Food & Nutrition Research*, 61(1), 1–21.
- Kim, D.-H., & Sung, S. (2014). Genetic and Epigenetic Mechanisms Underlying Vernalization. *The Arabidopsis Book*, 12, e0171.
- Kim, T., Banf, M., Kahn, D., Bernard, T., Dreher, K., Chavali, A. K., ... Zhang, P. (2017). Genome-Wide Prediction of Metabolic Enzymes, Pathways, and Gene Clusters in Plants. *Plant Physiology*, 173(4), 2041–2059.
- Klee, H. J. (2010). Improving the flavor of fresh fruits: Genomics, biochemistry, and biotechnology. *New Phytologist*, 187(1), 44–56.
- Klink, V. P., & Matthews, B. F. (2009). Emerging Approaches to Broaden Resistance of Soybean to Soybean Cyst Nematode as Supported by Gene Expression Studies. *Plant Physiology*, 151(3), 1017–1022.
- Kolukisaoglu, U. (2004). Calcium Sensors and Their Interacting Protein Kinases: Genomics of the Arabidopsis and Rice CBL-CIPK Signaling Networks. *PLANT PHYSIOLOGY*, 134(1), 43–58.
- Konarska, A. (2015). Development of fruit quality traits and comparison of the fruit structure of two *Vaccinium corymbosum* (L.) cultivars. *Scientia Horticulturae*, 194, 79–90.
- Kovaleski, A. P., Williamson, J. G., Olmstead, J. W., & Darnell, R. L. (2015). Inflorescence Bud Initiation, Development, and Bloom in Two Southern Highbush Blueberry Cultivars. *Journal of American Soci and Horticulture Science*, 140(1), 38–44.
- Kyriacou, M. C., & Roupael, Y. (2018). Towards a new definition of quality for fresh fruits and vegetables. *Scientia Horticulturae*, 234(August 2017), 463–469.
- Lan, T.-H., & Paterson, A. H. (2000). Comparative mapping of quantitative trait loci sculpting the curd of *Brassica oleracea*. *Genetics*, 155(4), 1927–1954.
- Lee, E. A., & Tollenaar, M. (2007). Physiological basis of successful breeding strategies for maize grain yield. *Crop Science*, 47(SUPPL. DEC.).
- Lee, I., & Amasino, R. M. (1995). Effect of vernalization, photoperiod, and light quality on the flowering phenotype of *Arabidopsis* plants containing the FRIGIDA gene. *Plant Physiology*, 108(1), 157–162.
- Leiva-Valenzuela, G. A., Lu, R., & Aguilera, J. M. (2013). Prediction of firmness and soluble solids content of blueberries using hyperspectral reflectance imaging. *Journal of Food Engineering*, 115(1), 91–98.
- Li, D., Li, B., Ma, Y., Sun, X., Lin, Y., & Meng, X. (2017). Polyphenols, anthocyanins, and flavonoids contents and the antioxidant capacity of various cultivars of highbush and half-high blueberries. *Journal of Food Composition and Analysis*, 62, 84–93.
- Li, F., Hullar, M. A. J., Beresford, S. A. A., & Lampe, J. W. (2011). Variation of glucoraphanin metabolism in vivo and ex vivo by human gut bacteria. *British Journal of Nutrition*, 106(03), 408–416.
- Li, J., Xu, Y., Niu, Q., He, L., Teng, Y., & Bai, S. (2018). Abscisic acid (ABA) promotes

- the induction and maintenance of pear (*Pyrus pyrifolia* white pear group) flower bud endodormancy. *International Journal of Molecular Sciences*, 19(1).
- Li, X., Xu, C., Korban, S. S., & Chen, K. (2010). Regulatory mechanisms of textural changes in ripening fruits. *Critical Reviews in Plant Sciences*, 29(4), 222–243.
- Lin, D., Xiao, M., Zhao, J., Li, Z., Xing, B., Li, X., ... Chen, S. (2016). An overview of plant phenolic compounds and their importance in human nutrition and management of type 2 diabetes. *Molecules*, 21(10).
- Lionetti, V., Raiola, A., Camardella, L., Giovane, A., Obel, N., Pauly, M., ... Bellincampi, D. (2007). Overexpression of pectin methylesterase inhibitors in *Arabidopsis* restricts fungal infection by *Botrytis cinerea*. *Plant Physiology*, 143(4), 1871–1880.
- Liu, B., Yang, Z., Gomez, A., Liu, B., Lin, C., & Oka, Y. (2016). Signaling mechanisms of plant cryptochromes in *Arabidopsis thaliana*. *Journal of Plant Research*, 129(2), 137–148.
- Liu, P., Lindstedt, A., Markkinen, N., Sinkkonen, J., Suomela, J. P., & Yang, B. (2014). Characterization of metabolite profiles of leaves of bilberry (*Vaccinium myrtillus* L.) and lingonberry (*Vaccinium vitis-idaea* L.). *Journal of Agricultural and Food Chemistry*, 62(49), 12015–12026.
- Lloret, A., Badenes, M. L., & Ríos, G. (2018). Modulation of Dormancy and Growth Responses in Reproductive Buds of Temperate Trees. *Frontiers in Plant Science*, 9(September), 1368.
- Lobo, V., Patil, A., Phatak, A., & Chandra, N. (2010). Free radicals, antioxidants and functional foods: Impact on human health. *Pharmacognosy Reviews*, 4(8), 118.
- Lobos, G. A., & Hancock, J. F. (2015). Breeding blueberries for a changing global environment: a review. *Frontiers in Plant Science*, 6.
- Lobos, T. E., Retamales, J. B., Ortega-Farías, S., Hanson, E. J., López-Olivari, R., & Mora, M. L. (2018). Regulated deficit irrigation effects on physiological parameters, yield, fruit quality and antioxidants of *Vaccinium corymbosum* plants cv. Brigitta. *Irrigation Science*, 36(1), 49–60.
- Lyrene, P., Journal, P., & Society, A. P. (2002). Development of Highbush Blueberry Cultivars Adapted to Florida. *Journal of the American Pomological Society*, 56(2), 79–85.
- Ma, H., Johnson, S. L., Liu, W., Dasilva, N. A., Meschwitz, S., Dain, J. A., & Seeram, N. P. (2018). Evaluation of Polyphenol Anthocyanin-Enriched Extracts of Blackberry , Black Raspberry , Blueberry , Cranberry , Red Raspberry , and Strawberry for Free Radical Scavenging , Reactive Carbonyl Species Aggregation , and Microglial Neuroprotective Effects. *International Journal of Molecular Sciences*, 19(461), 1–19.
- Malyshev, R. V., Shelyakin, M. A., & Golovko, T. K. (2016). Bud dormancy breaking affects respiration and energy balance of bilberry shoots in the initial stage of growth. *Russian Journal of Plant Physiology*, 63(3), 409–416.
- Matas, A. J., Gapper, N. E., Chung, M. Y., Giovannoni, J. J., & Rose, J. K. (2009). Biology and genetic engineering of fruit maturation for enhanced quality and shelf-life. *Current Opinion in Biotechnology*, 20(2), 197–203.
- Matsuda, F. (2016). Technical Challenges in Mass Spectrometry-Based Metabolomics. *Mass Spectrometry*, 5(2), S0052–S0052.
- McGinn, C. (2015). The science of taste. *Metaphilosophy*, 46(1), 84–103.

- McNamara, R. K., Kalt, W., Shidler, M. D., McDonald, J., Summer, S. S., Stein, A. L., ... Krikorian, R. (2018). Cognitive response to fish oil, blueberry, and combined supplementation in older adults with subjective cognitive impairment. *Neurobiology of Aging*, *64*, 147–156.
- Meitha, K., Agudelo-Romero, P., Signorelli, S., Gibbs, D. J., Considine, J. A., Foyer, C. H., & Considine, M. J. (2018). Developmental control of hypoxia during bud burst in grapevine. *Plant Cell and Environment*, *41*(5), 1154–1170.
- Melke, A. (2015). The Physiology of Chilling Temperature Requirements for Dormancy Release and Bud-break in Temperate Fruit Trees Grown at Mild Winter Tropical Climate. *Journal of Plant Studies*, *4*(2), 110–156.
- Mert, C., Barut, E., & Ipek, A. (2013). Variation in Flower Bud Differentiation and Progression of Floral Organs with Respect to Crop Load in Olive. *Notulae Botanicae Horti Agrobotanici Cluj-Napoca*, *41*(1), 79–85.
- Miedaner, T., & Korzun, V. (2012). Marker-Assisted Selection for Disease Resistance in Wheat and Barley Breeding. *Phytopathology*, *102*(6), 560–566.
- Mitchum, M. G. (2016). Soybean resistance to the soybean cyst nematode *Heterodera glycines*: an update. *Phytopathology*, *106*(12), 1–29.
- Moghaddam, M. R. B., & Ende, W. Van den. (2013). Sugars, the clock and transition to flowering. *Frontiers in Plant Science*, *4*(February), 1–6.
- Mohamed, R., Wang, C. T., Ma, C., Shevchenko, O., Dye, S. J., Puzey, J. R., ... Brunner, A. M. (2010). *Populus* CEN/TFL1 regulates first onset of flowering, axillary meristem identity and dormancy release in *Populus*. *Plant Journal*, *62*(4), 674–688.
- Molinero-Rosales, N., Latorre, A., Jamilena, M., & Lozano, R. (2004). SINGLE FLOWER TRUSS regulates the transition and maintenance of flowering in tomato. *Planta*, *218*(3), 427–434.
- Montecchiarini, M. L., Bello, F., Rivadeneira, M. F., Vázquez, D., Podestá, F. E., & Tripodi, K. E. J. (2018). Metabolic and physiologic profile during the fruit ripening of three blueberries highbush (*Vaccinium corymbosum*) cultivars. *Journal of Berry Research*, *8*(3), 177–192.
- Morita, M., Naito, Y., Yoshikawa, T., & Niki, E. (2017). Antioxidant capacity of blueberry extracts: Peroxyl radical scavenging and inhibition of plasma lipid oxidation induced by multiple oxidants. *Journal of Berry Research*, *7*(1), 1–9.
- Nabavi, S. M., Šamec, D., Tomczyk, M., Milella, L., Russo, D., Habtemariam, S., ... Shirooie, S. (2018). Flavonoid biosynthetic pathways in plants: Versatile targets for metabolic engineering. *Biotechnology Advances*, (June).
- Nault, B., Reiners, S., Hsu, C., & Hoepting, C. (2010). Black Rot Resistance Breeding Brassica, 1–7.
- O. Sadras, V., & F. Denison, R. (2009). Do plant parts compete for resources? An evolutionary viewpoint. *New Phytologist*, *183*(3), 565–574.
- O'Hara, L. E., Paul, M. J., & Winkler, A. (2013). How do sugars regulate plant growth and development? new insight into the role of trehalose-6-phosphate. *Molecular Plant*, *6*(2), 261–274.
- Ogden, A. B., & van Iersel, M. W. (2009). Southern highbush Blueberry production in High Tunnels: Temperatures, development, yield, and fruit quality during the establishment years. *HortScience*, *44*(7), 1850–1856.
- Oh, H. D., Yu, D. J., Chung, S. W., Chea, S., & Lee, H. J. (2018). Abscisic acid

- stimulates anthocyanin accumulation in 'Jersey' highbush blueberry fruits during ripening. *Food Chemistry*, 244(June 2017), 403–407.
- Okazaki, Y., & Saito, K. (2012). Recent advances of metabolomics in plant biotechnology. *Plant Biotechnology Reports*, 6(1), 1–15.
- Oliviero, T., Verkerk, R., & Dekker, M. (2012). Effect of water content and temperature on glucosinolate degradation kinetics in broccoli (*Brassica oleracea* var. *italica*). *Food Chemistry*, 132(4), 2037–2045.
- Osorio, S., Scossa, F., & Fernie, A. R. (2013). Molecular regulation of fruit ripening. *Frontiers in Plant Science*, 4(June 2013).
- Pagliarini, E., Laureati, M., & Gaeta, D. (2013). Sensory descriptors, hedonic perception and consumer's attitudes to Sangiovese red wine deriving from organically and conventionally grown grapes. *Frontiers in Psychology*, 4(NOV), 1–7.
- Pagter, M., Andersen, U. B., & Andersen, L. (2015). Winter warming delays dormancy release, advances budburst, alters carbohydrate metabolism and reduces yield in a temperate shrub. *AoB PLANTS*, 7(1), 1–15.
- Palmgren, M. G., Edenbrandt, A. K., Vedel, S. E., Andersen, M. M., Landes, X., Østerberg, J. T., ... Pagh, P. (2015). Are we ready for back-to-nature crop breeding? *Trends in Plant Science*, 20(3), 155–164.
- Pan, P., Skaer, C., Yu, J., Zhao, H., Ren, H., Oshima, K., & Wang, L. S. (2017). Berries and other natural products in pancreatic cancer chemoprevention in human clinical trials. *Journal of Berry Research*, 7(3), 147–161.
- Paniagua, A. C., East, A. R., Hindmarsh, J. P., & Heyes, J. A. (2013). Moisture loss is the major cause of firmness change during postharvest storage of blueberry. *Postharvest Biology and Technology*, 79, 13–19.
- Paniagua, C., Posé, S., Morris, V. J., Kirby, A. R., Quesada, M. A., & Mercado, J. A. (2014). Fruit softening and pectin disassembly: An overview of nanostructural pectin modifications assessed by atomic force microscopy. *Annals of Botany*, 114(6), 1375–1383.
- Park, D. H., Somer, D. E., Kim, Y. S., Choy, Y. H., Lim, H. K., Soh, M. S., ... Nam, H. G. (1999). Control of Circadian Rhythms and Photoperiodic Flowering by the *Arabidopsis* GIGANTEA Gene, 285, 1579–1582.
- Pinu, F., Pinu, & R, F. (2018). Grape and Wine Metabolomics to Develop New Insights Using Untargeted and Targeted Approaches. *Fermentation*, 4(4), 92.
- Posé, S., Nieves, J. a G., Quesada, F. P. M. a, & Mercado, J. a. (2011). Strawberry Fruit Softening : Role of Cell Wall Disassembly and its Manipulation in Transgenic Plants. *Genes, Genomes and Genomics*, 5, 40–48.
- Prasanna, V., Prabha, T. N., & Tharanathan, R. N. (2007). Fruit ripening phenomena-an overview. *Critical Reviews in Food Science and Nutrition*, 47(1), 1–19.
- Prencipe, F. P., Bruni, R., Guerrini, A., Rossi, D., Benvenuti, S., & Pellati, F. (2014). Metabolite profiling of polyphenols in *Vaccinium* berries and determination of their chemopreventive properties. *Journal of Pharmaceutical and Biomedical Analysis*, 89, 257–267.
- Rangkadilok, N., Nicolas, M. E., Bennett, R. N., Eagling, D. R., Premier, R. R., & Taylor, P. W. J. (2004). The Effect of Sulfur Fertilizer on Glucoraphanin Levels in Broccoli (*B. oleracea* L. var. *italica*) at Different Growth Stages. *Journal of Agricultural and Food Chemistry*, 52(9), 2632–2639.

- Rimmer, S. R., & van den Berg, C. G. J. (1992). Resistance of oilseed *Brassica* spp. to blackleg caused by *Leptosphaeria maculans*. *Canadian Journal of Plant Pathology*, 14(1), 56–66.
- Rohde, A., & Bhalerao, R. P. (2007). Plant dormancy in the perennial context. *Trends in Plant Science*, 12(5), 217–223.
- Rolin, D., Teyssier, E., Hong, Y., & Gallusci, P. (2015). *Tomato fruit quality improvement facing the functional genomics revolution*. *Applied Plant Genomics and Biotechnology*. Elsevier Ltd.
- Routray, W., & Orsat, V. (2011). Blueberries and Their Anthocyanins: Factors Affecting Biosynthesis and Properties. *Comprehensive Reviews in Food Science and Food Safety*, 10(6), 303–320.
- Rowland, L. J., Ogden, E. L., Ehlenfeldt, M. K., & Arora, R. (2008). Cold tolerance of blueberry genotypes throughout the dormant period from acclimation to deacclimation. *HortScience*, 43(7), 1970–1974.
- Ruan, Y.-L. (2014). Sucrose Metabolism: Gateway to Diverse Carbon Use and Sugar Signaling. *Annual Review of Plant Biology*, 65(1), 33–67.
- Rustérucci, C., Aviv, D. H., Holt, B. F., Dangl, J. L., & Parker, J. E. (2001). The disease resistance signaling components EDS1 and PAD4 are essential regulators of the cell death pathway controlled by LSD1 in Arabidopsis. *The Plant Cell*, 13(10), 2211–2224.
- S. Sanghera, G., H. Wani, S., Hussain, W., & B. Singh, N. (2011). Engineering Cold Stress Tolerance in Crop Plants. *Current Genomics*, 12(1), 30–43.
- Saban, G. M. (2018). The Benefits of Brassica Vegetables on Human Health. *J Human Health Res*, 1(1), 104.
- Saftner, R., Polashock, J., Ehlenfeldt, M., & Vinyard, B. (2008). Instrumental and sensory quality characteristics of blueberry fruit from twelve cultivars. *Postharvest Biology and Technology*, 49(1), 19–26.
- Saito, K., & Matsuda, F. (2010). Metabolomics for Functional Genomics, Systems Biology, and Biotechnology. *Annual Review of Plant Biology*, 61(1), 463–489.
- Sam Saguy, I. (2011). Paradigm shifts in academia and the food industry required to meet innovation challenges. *Trends in Food Science and Technology*, 22(9), 467–475.
- Scalbert, A., Brennan, L., Fiehn, O., Hankemeier, T., Kristal, B. S., van Ommen, B., ... Wopereis, S. (2009). Mass-spectrometry-based metabolomics: Limitations and recommendations for future progress with particular focus on nutrition research. *Metabolomics*, 5(4), 435–458.
- Scalzo, J., Stevenson, D., & Hedderley, D. (2013). Blueberry estimated harvest from seven new cultivars: Fruit and anthocyanins. *Food Chemistry*, 139(1–4), 44–50.
- Scalzo, J., Stevenson, D., & Hedderley, D. (2015). Polyphenol compounds and other quality traits in blueberry cultivars. *Journal of Berry Research*, 5(3), 117–130.
- Serrano, A., Espinoza, C., Armijo, G., Inostroza-Blancheteau, C., Poblete, E., Meyer-Regueiro, C., ... Arce-Johnson, P. (2017). Omics Approaches for Understanding Grapevine Berry Development: Regulatory Networks Associated with Endogenous Processes and Environmental Responses. *Frontiers in Plant Science*, 8(September), 1–15.
- Seymour, G. B., Østergaard, L., Chapman, N. H., Knapp, S., & Martin, C. (2013). Fruit

- Development and Ripening. *Annual Review of Plant Biology*, 64(1), 219–241.
- Shafee, T. M. A., Lay, F. T., Hulett, M. D., & Anderson, M. A. (2016). The Defensins Consist of Two Independent, Convergent Protein Superfamilies. *Molecular Biology and Evolution*, 33(9), 2345–2356.
- Sharma, K. D., Karki, S., Thakur, N. S., & Attri, S. (2012). Chemical composition, functional properties and processing of carrot-a review. *Journal of Food Science and Technology*, 49(1), 22–32.
- Sharma, O. P., & Bhat, T. K. (2009). DPPH Antioxidant Assay Revisited. *Food Chemistry*, 113, 1202–1205.
- Shim, D., Ko, J.-H. H., Kim, W.-C. C., Wang, Q., Keathley, D. E., & Han, K.-H. H. (2014). A molecular framework for seasonal growth-dormancy regulation in perennial plants. *Horticulture Research*, 1(1), 1–9.
- Signorelli, S., Agudelo-Romero, P., Meitha, K., Foyer, C. H., & Considine, M. J. (2018). Roles for Light, Energy, and Oxygen in the Fate of Quiescent Axillary Buds. *Plant Physiology*, 176(2), 1171–1181.
- Silva, J. L., Marroquin, E., Matta, F. B., Garner, J. O., & Stojanovic, J. (2005). Physicochemical, carbohydrate and sensory characteristics of highbush and rabbiteye blueberry cultivars. *Journal of the Science of Food and Agriculture*, 85(11), 1815–1821.
- Silva, S., Costa, E. M., Veiga, M., Morais, R. M., & Pintado, M. (2018). Health promoting properties of blueberries : a review. *Critical Reviews in Food Science and Nutrition*, 0(0), 1–20.
- Singh, N., & Ghosh, K. K. (2019). Recent Advances in the Antioxidant Therapies for Alzheimer's Disease: Emphasis on Natural Antioxidants. In S. Singh & N. Joshi (Eds.), *Pathology, Prevention, and Therapeutics of Neurodegenerative Disease* (pp. 253–263).
- Singh, R. K., Svystun, T., AlDahmash, B., Jonsson, A. M., & Bhalerao, R. P. (2017). Photoperiod- and temperature-mediated control of phenology in trees – a molecular perspective. *New Phytologist*, 213(2), 511–524.
- Singh, Sudhakar, & Singh, R. P. (2008). In vitro methods of assay of antioxidants: An overview. *Food Reviews International*.
- Sones, K., Heaney, R. K., & Fenwick, G. R. (1984). An estimate of the mean daily intake of glucosinolates from cruciferous vegetables in the UK. *Journal of the Science of Food and Agriculture*, 35(6), 712–720.
- Soy, J., Leivar, P., & Monte, E. (2014). PIF1 promotes phytochrome-regulated growth under photoperiodic conditions in Arabidopsis together with PIF3, PIF4, and PIF5. *Journal of Experimental Botany*, 65(11), 2925–2936.
- Subash, S., Essa, M. M., Al-adawi, S., Memon, M. A., Manivasagam, T., & Akbar, M. (2014). Neuroprotective effects of berry fruits on neurodegenerative diseases. *Neural Regeneration Research*, 9(16), 1557–1566.
- Sumner, L. W., Lei, Z., Nikolau, B. J., & Saito, K. (2015). Modern plant metabolomics: Advanced natural product gene discoveries, improved technologies, and future prospects. *Natural Product Reports*, 32(2), 212–229.
- Takatsuka, H., & Umeda, M. (2014). Hormonal control of cell division and elongation along differentiation trajectories in roots. *Journal of Experimental Botany*, 65(10), 2633–2643.

- Tawfiq, N., Heaney, R. K., Plumb, J. A., Fenwick, G. R., Musk, S. R. R., & Williamson, G. (1995). Dietary glucosinolates as blocking agents against carcinogenesis: glucosinolate breakdown products assessed by induction of quinone reductase activity in murine hepa1c1c7 cells. *Carcinogenesis*, *16*(5), 1191–1194.
- Tester, M., & Langridge, P. (2010). Breeding Technologies to Increase Crop Production in a Changing World. *Science*, *327*(5967), 818–822.
- Tieman, D., Bliss, P., McIntyre, L. M. M., Blandon-Ubeda, A., Bies, D., Odabasi, A. Z. Z., ... Klee, H. J. J. (2012). The chemical interactions underlying tomato flavor preferences. *Current Biology*, *22*(11), 1035–1039.
- Toivonen, P. M. A. A., & Brummell, D. A. (2008). Biochemical bases of appearance and texture changes in fresh-cut fruit and vegetables. *Postharvest Biology and Technology*, *48*(1), 1–14.
- Traka, M. H., Saha, S., Huseby, S., Kopriva, S., Walley, P. G., Barker, G. C., ... Mithen, R. F. (2013). Genetic regulation of glucoraphanin accumulation in Beneforté[®] broccoli. *New Phytologist*, *198*(4), 1085–1095.
- Traka, M., & Mithen, R. (2009). Glucosinolates, isothiocyanates and human health. *Phytochemistry Reviews*, *8*(1), 269–282.
- Trehane, J. (2004). *Blueberries, Cranberries, and Other Vacciniums*. Portland, OR: Royal Horticultural Society.
- Tsai, A. Y.-L., & Gazzarrini, S. (2014). Trehalose-6-phosphate and SnRK1 kinases in plant development and signaling: the emerging picture. *Frontiers in Plant Science*, *5*(April), 1–11.
- Ufaz, S., & Galili, G. (2008). Improving the Content of Essential Amino Acids in Crop Plants: Goals and Opportunities. *Plant Physiology*, *147*(3), 954–961.
- Vadassery, J., & Oelmüller, R. (2009). Calcium signaling in pathogenic and beneficial plant microbe interactions: what can we learn from the interaction between *Piriformospora indica* and *Arabidopsis thaliana*. *Plant Signaling & Behavior*, *4*(11), 1024–1027.
- Vallejo, F., García-Viguera, C., & Tomás-Barberán, F. A. (2003). Changes in Broccoli (*Brassica oleracea* L. Var. *italica*) Health-Promoting Compounds with Inflorescence Development. *Journal of Agricultural and Food Chemistry*, *51*(13), 3776–3782.
- van der Schoot, C., & Rinne, P. L. H. (2011). Dormancy cycling at the shoot apical meristem: Transitioning between self-organization and self-arrest. *Plant Science*, *180*(1), 120–131.
- van Doorn, H. E., van der Kruk, G. C., van Holst, G. J., Raaijmakers-Ruijs, N. C. M. E., Postma, E., Groeneweg, B., & Jongen, W. H. F. (1998). The Glucosinolates Sinigrin and Progoitrin are Important Determinants for Taste Preference and Bitterness of Brussels Sprouts, *78*, 30–38.
- Van Eylen, D., Oey, I., Hendrickx, M., & Van Loey, A. (2007). Kinetics of the Stability of Broccoli (*Brassica oleracea* Cv. *Italica*) Myrosinase and Isothiocyanates in Broccoli Juice during Pressure/Temperature Treatments. *Journal of Agricultural and Food Chemistry*, *55*(6), 2163–2170. h
- Vergara, R., Noriega, X., Aravena, K., Prieto, H., & Pérez, F. J. (2017). ABA Represses the Expression of Cell Cycle Genes and May Modulate the Development of Endodormancy in Grapevine Buds. *Frontiers in Plant Science*, *8*(May), 1–10.
- Wahyuningsih, S., Wulandari, L., Wartono, M. W., Munawaroh, H., & Ramelan, A. H.

- (2017). The Effect of pH and Color Stability of Anthocyanin on Food Colorant. *IOP Conference Series: Materials Science and Engineering*, 193(1), 12047.
- Wang, G., Xu, M., Wang, W., & Galili, G. (2017). Fortifying horticultural crops with essential amino acids: A review. *International Journal of Molecular Sciences*, 18(6).
- Wang, S. Y., Chen, H., Camp, M. J., & Ehlenfeldt, M. K. (2012). Genotype and growing season influence blueberry antioxidant capacity and other quality attributes. *International Journal of Food Science and Technology*, 47(7), 1540–1549.
- Weng, J. K. (2014). The evolutionary paths towards complexity: A metabolic perspective. *New Phytologist*, 201(4), 1141–1149.
- Whyte, A. R., Schafer, G., & Williams, C. M. (2016). Cognitive effects following acute wild blueberry supplementation in 7- to 10-year-old children. *European Journal of Nutrition*, 55(6), 2151–2162.
- Wilkie, J. D., Sedgley, M., & Olesen, T. (2008). Regulation of floral initiation in horticultural trees. *Journal of Experimental Botany*, 59(12), 3215–3228.
- Williams, P. H. (2007). Black rot. *Compendium of Brassica Diseases*, 60–62.
- Williamson, J. G., & Lyrene, P. M. (2004). Blueberry varieties for Florida (HS967), 1–9.
- Wingler, A. (2017). Transitioning to the next phase: the role of sugar signaling throughout the plant life cycle. *Plant Physiology*, 176(February), pp.01229.2017.
- Winter, P., & Kahl, G. (1995). Molecular Marker Technologies for Plant Improvement. *World Journal of Microbiology & Biotechnology*, 11(4), 438–448.
- Wolfender, J. L., Marti, G., Thomas, A., & Bertrand, S. (2015). Current approaches and challenges for the metabolite profiling of complex natural extracts. *Journal of Chromatography A*, 1382, 136–164.
- Xing, L. B., Zhang, D., Li, Y. M., Shen, Y. W., Zhao, C. P., Ma, J. J., ... Han, M. Y. (2015). Transcription profiles reveal sugar and hormone signaling pathways mediating flower induction in apple (*Malus domestica* Borkh.). *Plant and Cell Physiology*, 56(10), 2052–2068.
- Yadav, A. K., & Singh, S. V. (2014). Osmotic dehydration of fruits and vegetables: a review. *Journal of Food Science and Technology*, 51(9), 1654–1673.
- Yanaka, A., Fahey, J. W., Fukumoto, A., Nakayama, M., Inoue, S., Zhang, S., ... Yamamoto, M. (2009). Dietary Sulforaphane-Rich Broccoli Sprouts Reduce Colonization and Attenuate Gastritis in Helicobacter pylori-Infected Mice and Humans. *Cancer Prevention Research*, 2(4), 353–360.
- Yonekura-Sakakibara, K., Nakayama, T., Yamazaki, M., & Saito, K. (2009). Modification and Stabilization of Anthocyanins. In C. S. Winefield, K. Davies, & K. Gould (Eds.), *Anthocyanins* (pp. 169–190). New York: Springer Science+Business Media.
- You, Q., Wang, B., Chen, F., Huang, Z., Wang, X., & Luo, P. G. (2011). Comparison of anthocyanins and phenolics in organically and conventionally grown blueberries in selected cultivars. *Food Chemistry*, 125(1), 201–208.
- Yousuf, B., Gul, K., Wani, A. A., & Singh, P. (2016). Health Benefits of Anthocyanins and Their Encapsulation for Potential Use in Food Systems: A Review. *Critical Reviews in Food Science and Nutrition*, 56(13), 2223–2230.
- Zhang, H., Mittal, N., Leamy, L. J., Barazani, O., & Song, B. H. (2017). Back into the wild—Apply untapped genetic diversity of wild relatives for crop improvement. *Evolutionary Applications*, 10(1), 5–24.
- Zhang, Z., Zhuo, X., Zhao, K., Zheng, T., Han, Y., Yuan, C., & Zhang, Q. (2018).

- Transcriptome Profiles Reveal the Crucial Roles of Hormone and Sugar in the Bud Dormancy of *Prunus mume*. *Scientific Reports*, 8(1).
- Zheng, C., Halaly, T., Acheampong, A. K., Takebayashi, Y., Jikumaru, Y., Kamiya, Y., & Or, E. (2015). Abscisic acid (ABA) regulates grape bud dormancy, and dormancy release stimuli may act through modification of ABA metabolism. *Journal of Experimental Botany*, 66(5), 1527–1542.
- Zhu, G., Wang, S., Huang, Z., Zhang, S., Liao, Q., Zhang, C., ... Huang, S. (2018). Rewiring of the Fruit Metabolome in Tomato Breeding. *Cell*, 172(1–2), 249–255.e12.
- Zuther, E., Juszczak, I., Ping Lee, Y., Baier, M., & Hinch, D. K. (2015). Time-dependent deacclimation after cold acclimation in *Arabidopsis thaliana* accessions. *Scientific Reports*, 5, 1–10.